Evidence-Based Complementary and Alternative Medicine

Real-World Big Data Processing and Analysis for Traditional Chinese Medicine

Lead Guest Editor: Xuezhong Zhou
Guest Editors: Baoyan Liu, Josiah Poon, Yonghong Peng, and Jianan Xia

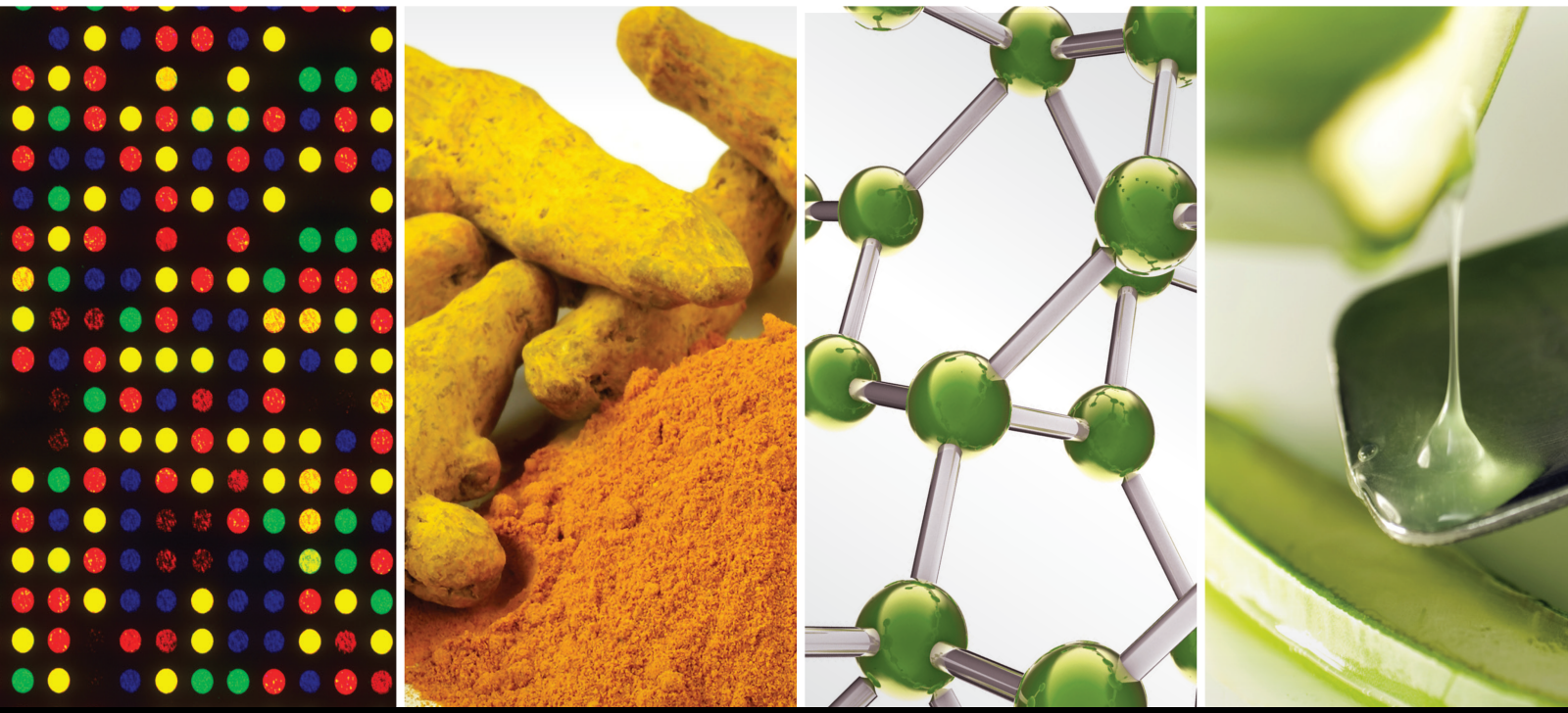

Real-World Big Data Processing and Analysis for Traditional Chinese Medicine

Evidence-Based Complementary and Alternative Medicine

Real-World Big Data Processing and Analysis for Traditional Chinese Medicine

Lead Guest Editor: Xuezhong Zhou
Guest Editors: Baoyan Liu, Josiah Poon, Yonghong Peng, and Jianan Xia

Chief Editor

Associate Editors

Academic Editors

Contents

Contents

Hindawi
Evidence-Based Complementary and Alternative Medicine
Volume 2023, Article ID 9876529, 1 page
https://doi.org/10.1155/2023/9876529

Retraction

Retracted: Network-Based Elaboration of the Efficacy of the Dachangshu (BL25) and Tianshu (ST25) Points in the Treatment of Functional Constipation in Children through Inflammation, Adipocytokine, or Leptin Pathways

Evidence-Based Complementary and Alternative Medicine

Received 26 September 2023; Accepted 26 September 2023; Published 27 September 2023

This article has been retracted by Hindawi following an investigation undertaken by the publisher [1]. This investigation has uncovered evidence of one or more of the following indicators of systematic manipulation of the publication process:

(1) Discrepancies in scope
(2) Discrepancies in the description of the research reported
(3) Discrepancies between the availability of data and the research described
(4) Inappropriate citations
(5) Incoherent, meaningless and/or irrelevant content included in the article
(6) Peer-review manipulation

The presence of these indicators undermines our confidence in the integrity of the article's content and we cannot, therefore, vouch for its reliability. Please note that this notice is intended solely to alert readers that the content of this article is unreliable. We have not investigated whether authors were aware of or involved in the systematic manipulation of the publication process.

Wiley and Hindawi regrets that the usual quality checks did not identify these issues before publication and have since put additional measures in place to safeguard research integrity.

We wish to credit our own Research Integrity and Research Publishing teams and anonymous and named external researchers and research integrity experts for contributing to this investigation.

The corresponding author, as the representative of all authors, has been given the opportunity to register their agreement or disagreement to this retraction. We have kept a record of any response received.

References

[1] Y. Xu, H. Xu, X. Wang et al., "Network-Based Elaboration of the Efficacy of the Dachangshu (BL25) and Tianshu (ST25) Points in the Treatment of Functional Constipation in Children through Inflammation, Adipocytokine, or Leptin Pathways," *Evidence-Based Complementary and Alternative Medicine*, vol. 2022, Article ID 5315927, 13 pages, 2022.

Hindawi
Evidence-Based Complementary and Alternative Medicine
Volume 2023, Article ID 9876529, 1 page
https://doi.org/10.1155/2023/9876529

Retraction

Retracted: Network-Based Elaboration of the Efficacy of the Dachangshu (BL25) and Tianshu (ST25) Points in the Treatment of Functional Constipation in Children through Inflammation, Adipocytokine, or Leptin Pathways

Evidence-Based Complementary and Alternative Medicine

Received 26 September 2023; Accepted 26 September 2023; Published 27 September 2023

This article has been retracted by Hindawi following an investigation undertaken by the publisher [1]. This investigation has uncovered evidence of one or more of the following indicators of systematic manipulation of the publication process:

(1) Discrepancies in scope
(2) Discrepancies in the description of the research reported
(3) Discrepancies between the availability of data and the research described
(4) Inappropriate citations
(5) Incoherent, meaningless and/or irrelevant content included in the article
(6) Peer-review manipulation

The presence of these indicators undermines our confidence in the integrity of the article's content and we cannot, therefore, vouch for its reliability. Please note that this notice is intended solely to alert readers that the content of this article is unreliable. We have not investigated whether authors were aware of or involved in the systematic manipulation of the publication process.

Wiley and Hindawi regrets that the usual quality checks did not identify these issues before publication and have since put additional measures in place to safeguard research integrity.

We wish to credit our own Research Integrity and Research Publishing teams and anonymous and named external researchers and research integrity experts for contributing to this investigation.

The corresponding author, as the representative of all authors, has been given the opportunity to register their agreement or disagreement to this retraction. We have kept a record of any response received.

References

[1] Y. Xu, H. Xu, X. Wang et al., "Network-Based Elaboration of the Efficacy of the Dachangshu (BL25) and Tianshu (ST25) Points in the Treatment of Functional Constipation in Children through Inflammation, Adipocytokine, or Leptin Pathways," *Evidence-Based Complementary and Alternative Medicine*, vol. 2022, Article ID 5315927, 13 pages, 2022.

Hindawi
Evidence-Based Complementary and Alternative Medicine
Volume 2022, Article ID 5315927, 13 pages
https://doi.org/10.1155/2022/5315927

Research Article

Network-Based Elaboration of the Efficacy of the Dachangshu (BL25) and Tianshu (ST25) Points in the Treatment of Functional Constipation in Children through Inflammation, Adipocytokine, or Leptin Pathways

Yan Xu,[1,2] **Hanying Xu**,[3] **Xinna Wang**,[3] **Hongjuan Wen**,[3] **Huifang Guan**,[3] **Fa Gao**,[3] **Hang Xu**,[3] **Wei Jing**,[3] **Jing Li**,[3] **Yan Mei**,[4] **Weibin Li**,[4] **Qixiong Chen**,[4] **Fang Liu**,[4] **and Hongtao Cui**[4]

[1]*School of Pediatrics, Henan University of Chinese Medicine, Zhengzhou, Henan 450000, China*
[2]*The First Affiliated Hospital of Henan University of Chinese Medicine, Zhengzhou, Henan 450000, China*
[3]*Changchun University of Chinese Medicine, Changchun, Jilin 130117, China*
[4]*Chongqing Hospital Of Traditional Chinese Medicine, Chongqing 400021, China*

Correspondence should be addressed to Weibin Li; cqlwb1969@163.com, Qixiong Chen; 13193039866@126.com, Fang Liu; 892677702@qq.com, and Hongtao Cui; dr.cuihongtao@qq.com

Received 28 January 2022; Revised 4 August 2022; Accepted 8 September 2022; Published 6 December 2022

Academic Editor: Jianan Xia

Constipation commonly occurs during childhood, and more than 95% of cases are classified as functional constipation. If not effectively treated, 20% of patients with childhood constipation can continue to exhibit symptoms into adulthood, which seriously affects their mental health and quality of life. The main feature of acupuncture or acupoint stimulation, a special branch of traditional Chinese medicine, is the selection of different acupoints for different diseases, and many worthy guidelines have been established for matching acupoints. The back-shu and front-mu point combination adheres to an important acupoint compatibility law that has been used since its proposal 2,500 years ago but has not yet been verified by the modern evidence-based experiments. This study focused on the back-shu and front-mu point combination using the Dachangshu (BL25) and Tianshu (ST25) points as examples to explore possible research methods for network acupoint-based stimulation based on existing evidence and to elucidate the mechanisms induced by BL25 and ST25 in the treatment of functional constipation in children (FCC). The study found that BL25 and ST25 have 20 common targets, namely, AQP8, DRD2, VIP, TAC1, IL6R, TNF, FOS, KIT, CHAT, HTR3A, GAS8, SOD3, TRPV1, MPO, CALCA, IL1B, P2RX7, NPY2R, IL10RA, and TPH1, and these targets may provide a strategy for the combined usage of BL25 and ST25. In addition, BL25 and ST25 can affect FCC treatment through inflammation-relatedTh17-cell differentiation, the NF-kappa B signaling pathway, and the Toll-like receptor signaling pathway. Adipocytokines or leptin may also comprise the mechanism through which BL25 and ST25 regulate FCC. In addition, BL25 and ST25 regulate FCC through 13 core targets, namely, NFKBIA, RELA, TNF, IKBKB, IRAK1, TLR4, MYD88, TNFRSF1A, IL1R1, TLR2, IL1B, TRAF6, and TNFRSF1B. In short, this study provides new ideas and methods for studying the mechanism of acupuncture points.

1. Background

Constipation commonly occurs during childhood, with an incidence ranging from 3% to 30%, and more than 95% of all cases are classified as functional constipation [1]. The median age of constipation onset in children is 2.3 years, and the ages at the 25th and 75th percentiles are 0.8 and 4.8 years, respectively [2]. If not effectively treated, 20% of patients with childhood constipation continue to exhibit symptoms into adulthood, which seriously affects their mental health and quality of life [3]. Therefore, early intervention for functional constipation in children

(FCC) is necessary to reduce the impacts on mental health and quality of life in adulthood.

The traditional Chinese medicine (TCM) theory has gradually developed over a long period based on medical practices guided by ancient simple Chinese material principles and dialectics of nature and includes complex theoretical systems and treatment methods. Acupuncture or acupoint stimulation is a special branch of TCM. The selection of different points for different diseases is the main feature of acupuncture or acupoint stimulation, and many important laws have been established for matching acupoints. A typical method is the back-shu and front-mu point combination, which has been considered the classic acupoint combination applied in the clinic since its proposal in the "Classic of Questioning" 2500 years ago and is still used today. Simply, the back-shu and front-mu point combination is based on the yin and yang theory in Chinese medicine. The abdomen (which belongs to yin according to the TCM theory) and the back (which belongs to yang according to the TCM theory) are selected as acupoint stimulation targets to balance yin and yang and thereby regulate visceral functions. Some studies have investigated the regulatory mechanisms of the back-shu and front-mu points, including the Feishu point (back-shu point) and the Zhongfu point (front-mu), which can reduce inflammatory exudation and inflammatory cell infiltration in the lung tissues of asthmatic mice [4]. The Weishu point (back-shu point) and Zhongwan point (front-mu) can regulate gastric motility and are closely related to the thalamus, limbic system, and some brain areas of the default network [5]. The Dachangshu point (BL25, back-shu point) and Tianshu point (ST25, front-mu point) regulate the expression of c-kit and TRPV1 to improve diarrhea in rats with an irritable bowel syndrome [6]. However, most studies are limited to the investigation of a single mechanistic change after acupoint stimulation and cannot explain the complex multimechanistic and multifunctional changes that subsequently occur in the human body. To more specifically explain the relatively complex mechanistic changes that occur after acupuncture point stimulation, we assessed the combination of BL25 (back-shu point) and ST25 (front-mu) in the treatment of FCC and explored the complex mechanism induced by acupoint stimulation based on existing evidence.

BL25 was selected as the research object because it belongs to the bladder meridian of foot-taiyang, which is also the dorsal point of the large intestine. BL25 is located at the same level as the inferior border of the spinous process of the fourth lumbar vertebra (L4), 1.5 B-cun lateral to the posterior median line. According to the TCM theory, targeting BL25 can cure abdominal pain, bloating, diarrhea, and constipation, among other ailments. Previous studies have provided ample information about BL25, and the evidence shows that targeting this point can enhance jejunal movement in rats with constipation and diarrhea [7], that moxibustion at BL25 can reduce visceral hyperalgesia [8] and that electroacupuncture at BL25 can be used to treat inflammatory bowel disease (IBD) in mice [9]. ST25 belongs to the stomach meridian of foot-yangming, the front-mu acupoint of the large intestine. ST25 is located on the upper abdomen, 2 B-cun lateral to the center of the umbilicus. ST25 can be used to treat many of the same ailments as BL25, including abdominal pain, bloating, diarrhea, and constipation. Previous studies on ST25 have revealed that this acupoint can be targeted to treat functional constipation [10], that acupuncture at ST25 is safe and effective for the treatment of functional constipation [11] and that the moxibustion of ST25 can exert its effect on TNBS-induced colitis rats by triggering the degranulation of local mast cells [12], among other effects. Some clinical evidence, including the results from Zhu Qi's clinical research on stimulating BL25 and other back-shu points to treat senile constipation through warm needling moxibustion, demonstrates that the total effective rate of stimulating back-shu points to treat senile constipation is higher than that of ordinary acupuncture [13]. Guifang and Yuejuan used iontophoresis to stimulate ST25 and BL25 in a clinical study of stroke patients and found that the improvement rate in the symptom score obtained through stimulation at ST25 combined with BL25 was higher than that obtained with conventional treatment [14]. Hui et al.'s clinical observation of 40 patients with functional constipation treated with acupuncture at BL25 and ST25 also found that the number of stools from patients treated with BL25 and ST25 was significantly increased [15]. In addition, some studies have investigated FCC. For example, Niansong et al. used pediatric massage combined with acupoint stimulation (including ST25) to treat 75 cases of FCC and found that the symptom score decreased after treatment, which showed that pediatric massage combined with acupoint stimulation can significantly improve the clinical symptoms of FCC [16]. Although the above-mentioned studies showed that BL25 and ST25 can be widely used in the treatment of intestinal diseases, no comprehensive or systematic evidence-based analyses of these two acupoints in the treatment of FCC have been performed.

In brief, this study aimed to assess the back-shu and front-mu point combination using BL25 and ST25 as examples to explore network acupoint research methods based on existing evidence and to elucidate the mechanisms induced by stimulation at BL25 and ST25 in the treatment of FCC. The results of this study should provide new ideas and methods for acupuncture research. The research route is shown in Figure 1.

2. Materials and Methods

2.1. Retrieval of Information on BL25 and ST25 Targets. We manually searched the CNKI, Wanfang, VIP, PubMed, and Web of Science databases to collect information on targets of BL25 and ST25, and the search time was from the time of database creation to July 1, 2021. Using a search method involving subject headings and free words and taking a PubMed search based on BL25 as an example, the search formula was ((((((((((((((((((((((((((Acupuncture Points [MeSH Terms])) OR (Electroacupuncture [MeSH Terms])) OR (Moxibustion [MeSH Terms])) OR (Acupuncture Therapy [MeSH Terms])) OR (Acupuncture Point)) OR (Point, Acupuncture)) OR (Points, Acupuncture)) OR (Acupoints)) OR (Acupoint)) OR (Acupuncture Treatment)) OR (Acupuncture Treatments)) OR (Treatment, Acupuncture)) OR (Therapy, Acupuncture)) OR

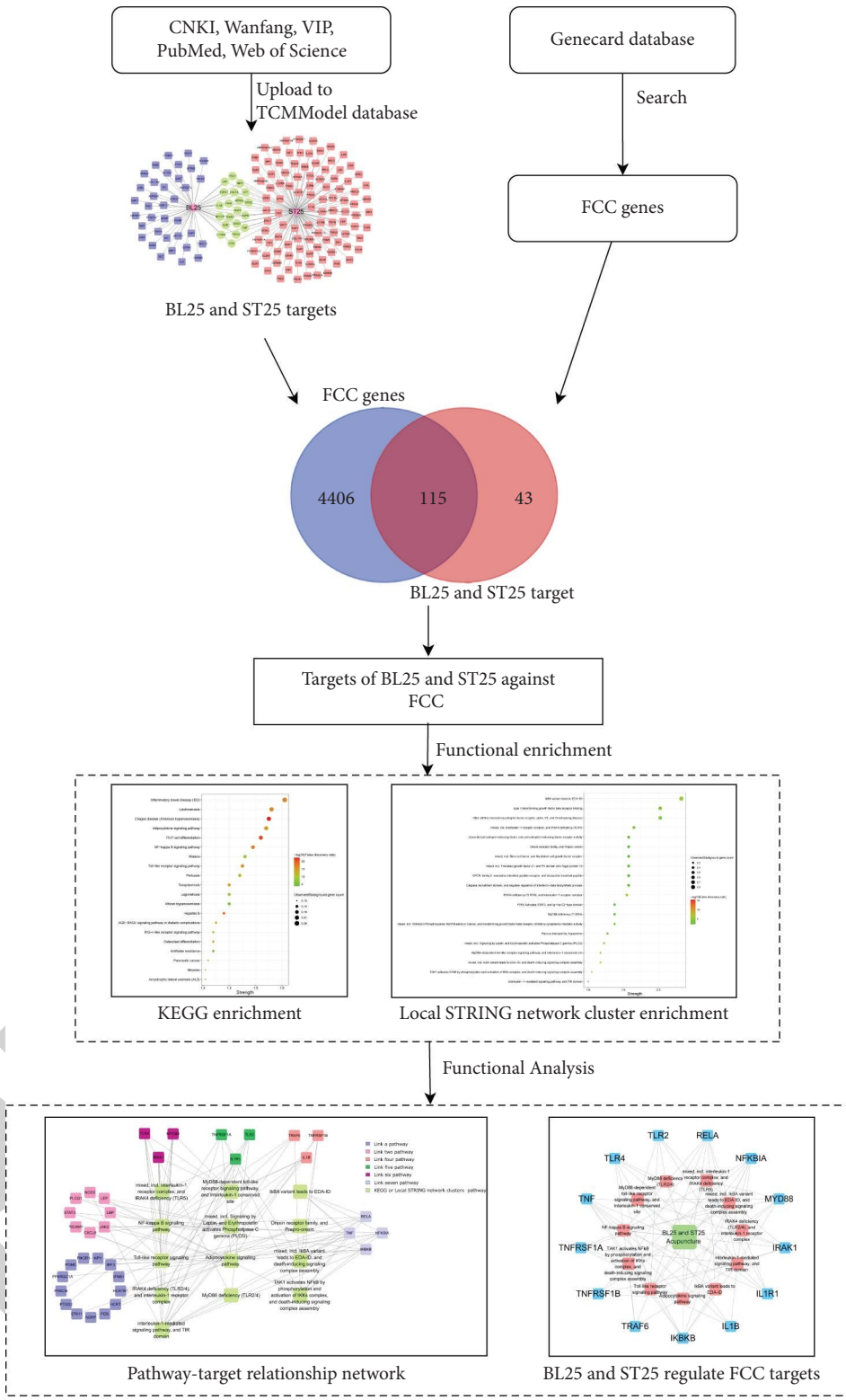

Figure 1: Workflow for the regulation of FCC by BL25 and ST25.

(Pharmacoacupuncture Treatment)) OR (Treatment, Pharmacoacupuncture)) OR (Pharmacoacupuncture Therapy)) OR (Therapy, Pharmacoacupuncture)) OR (Acupotomy)) OR (Acupotomies)) AND (((BL25) OR (B25)) OR (Dachangshu)). Reexamination, debugging, double-checking, and omission repair were performed by special personnel.

2.2. Correction of BL25 and ST25 Target Names. The two acupoint targets were entered separately into the UniProt database (https://www.UniProt.org/) for correction and conversion into gene names. UniProt is a nonredundant protein sequence database with the most complete sequence data and the richest annotation information in the world. Since its establishment at the beginning of this century, this database has provided valuable resources for the field of life sciences. More than 500,000 sequences in the Swiss-Prot sublibrary were manually reviewed and annotated, and all corrected data in this study were obtained from the Swiss-Prot sublibrary. The target information for the two acupoints was then uploaded to the website (https://www.tcmmodel.com).

2.3. FCC-Related Genes. The key phrase "functional constipation in children" was searched in the GeneCards database (https://www.genecards.org) to identify disease-related genes, and those related to both the acupoint targets and FCC were retained. Cytoscape 3.8.2 software was then used to prepare the figure.

2.4. KEGG and Local STRING Network Enrichment Analysis. The above-described genes were inputted into the String (https://string-db.org/) database, and their functional enrichment was assessed based on Kyoto Encyclopedia of Genes and Genomes (KEGG) and local STRING network clusters. A bioinformatics website (https://www.bioinformatics.com.cn) was then used to prepare the figure.

In the KEGG and local STRING network clusters, the strength was directly associated with the substantiality of the enrichment effect. The false discovery rate indicated the significance of the enrichment, and the p values for each category were subjected to multiple-testing correction using the Benjamini–Hochberg procedure.

The local STRING network cluster enrichment analysis included precomputed protein clusters derived from a hierarchical clustering of the full STRING network using an average linkage algorithm. The cluster names were derived automatically based on the consensus protein annotations from the GO, KEGG, Reactome, UniProt, Pfam, SMART, and InterPro databases. All clusters and their hierarchical tree are available for download in the download section of STRING (https://string-db.org/cgi/download.pl). In brief, local STRING network clusters were reenriched based on the STRING, GO, KEGG, Reactome, UniProt, Pfam, SMART, and InterPro databases, which may provide a more comprehensive description of the gene enrichment status. Therefore, we selected the local STRING network clusters for reenrichment.

We also used the following principles to select the enriched pathways: (1) pathways that have been proven to be directly or indirectly related to FCC; (2) pathways with the same or similar mechanisms present in both the enrichment methods; and (3) multiple pathways with the same or a similar meaning.

3. Results

3.1. BL25 and ST25 Target Information. After retrieval, removal of redundant data, and correction based on the UniProt database, a total of 56 BL25 targets and 122 ST25 targets were obtained, as shown in Figure 2. Twenty targets were shared between BL25 and ST25: AQP8, DRD2, VIP, TAC1, IL6R, TNF, FOS, KIT, CHAT, HTR3A, GAS8, SOD3, TRPV1, MPO, CALCA, IL1B, P2RX7, NPY2R, IL10RA, and TPH1.

3.2. FCC and Intersection Genes. After removing the redundancy among the BL25 and ST25 targets, an analysis of the FCC genes from the GeneCards database that intersected with the abovementioned targets revealed 115 targets that were related to the two acupoints and diseases. Detailed information is provided in Supplementary Material 1 and shown in Figure 3.

3.3. KEGG Enrichment Analysis. The abovementioned targets were entered into the STRING website, and the analysis function was used to obtain enrichment information for 141 KEGG pathways. Detailed information is provided in Supplementary Material 2. The strength values were sorted from high to low, and the first 20 pathways were selected for analysis (Figure 4). IBD, which mainly includes ulcerative colitis and Crohn's disease, was identified as the most important enriched item. IBD is a chronic nonspecific inflammatory disease involving the gastrointestinal tract that is recurring and difficult to treat [17]. In addition, the adipocytokine signaling pathway [18, 19], Th17-cell differentiation [20], NF-kappa B signaling pathway [21], and Toll-like receptor signaling pathway [22] may also be closely related to FCC.

3.4. Local STRING Network Cluster Enrichment Analysis. A total of 59 local STRING network cluster enrichment items were obtained, as shown in Supplementary Material 3. As shown in Figure 5, the IκBA variant leads to EDA-ID; the IκBA variant leads to EDA-ID and death-inducing signaling complex assembly; TAK1 activates NF-κB by phosphorylation and activation of the IKK complex; and death-inducing signaling complex assemblies are closely related to the NF-κB signaling pathway. The enrichment of local STRING network clusters also revealed that the NF-κB signaling pathway is correlated with acupoints and FCC.

The enrichment analysis of the local STRING network clusters also showed several pathways that are related to inflammation, such as the interleukin-1 receptor complex and IRAK4 deficiency (TLR5); IRAK4 deficiency (TLR2/4) and interleukin-1 receptor complex; interleukin-1-mediated signaling pathway and TIR domain; MyD88 deficiency (TLR2/4); and MyD88-dependentToll-like receptor signaling pathway and interleukin-1 conserved site pathways. All of these pathways are related to IL-1 or MyD88; IL-1 is a well-known proinflammatory factor [23], and MyD88 is a key linker molecule in the Toll-like receptor signaling pathway. MyD88-dependentToll-like receptor signaling and the interleukin-1 conserved site pathway are closely related to the Toll-like receptor signaling pathway, which was found to be enriched by the KEGG analysis. Both IL-1 and MyD88

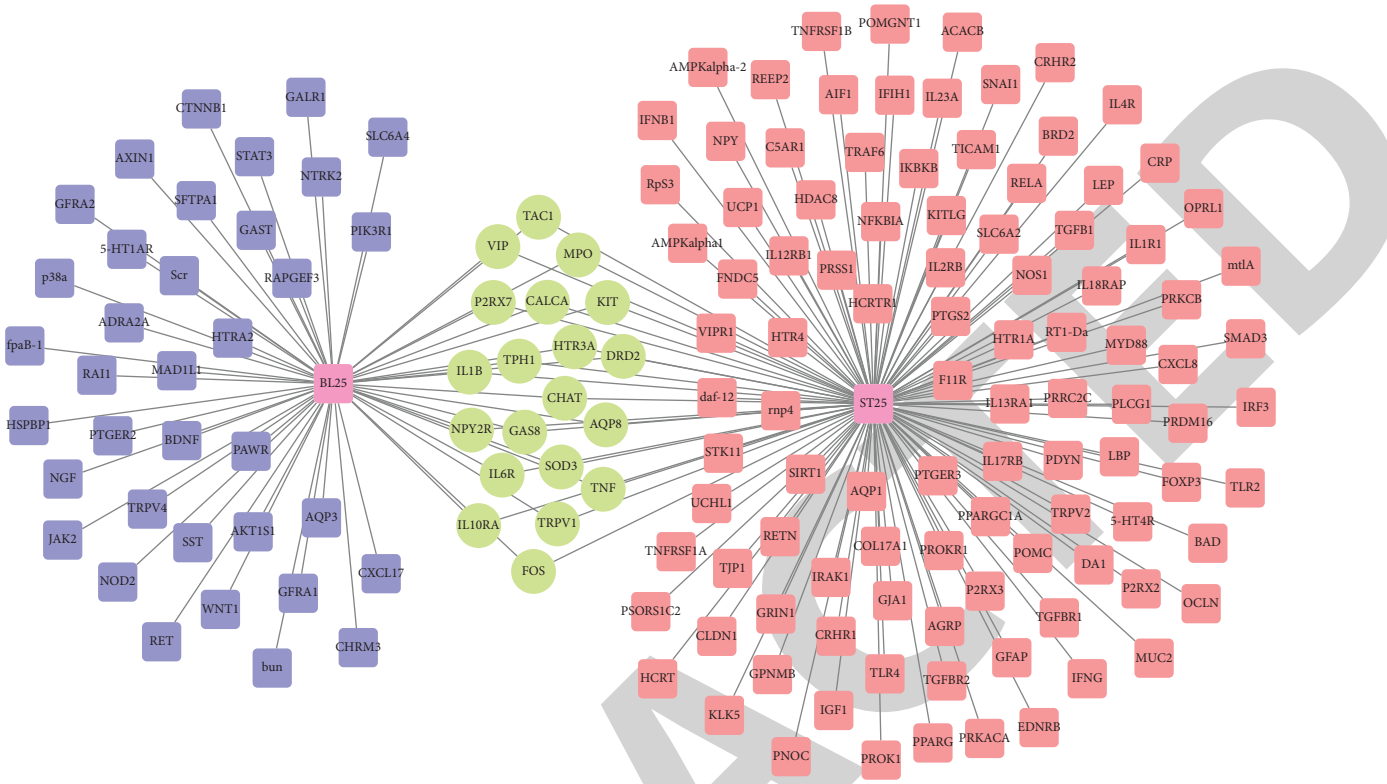

Figure 2: BL25 and ST25 target information. The BL25 targets are shown in light purple, the ST25 targets are shown in wine red, and the common BL25 and ST25 targets are shown in lime green.

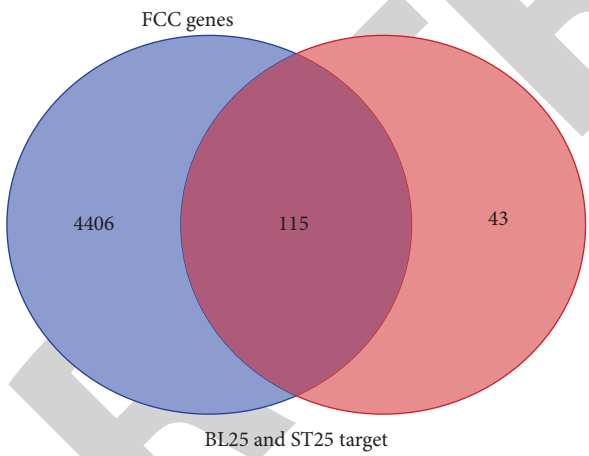

Figure 3: Venn diagram of FCC genes and acupoint targets.

are closely related to rectal diseases [24], and MyD88 can mediate the proliferation, migration, and invasion of rectal cancer cells via the NF-κB signaling pathway [25]. In addition, the orexin receptor family, prepro-orexin, leptin signaling, and erythropoietin activate phospholipase C gamma (PLCG) pathways and appear to have functions similar to that of the adipocytokine signaling pathway in the KEGG database, and these pathways function by regulating the neuropeptide levels.

In short, enrichment analyses of the KEGG and local STRING network clusters revealed two important points. First, the potential mechanisms through which the two acupoints regulate FCC appear to be related to inflammatory pathways, including the following: NF-κB signaling, Toll-like receptor signaling, IKBA variant leads to death-inducing signaling complex assembly, TAK1 activation of NF-κB by phosphorylation and activation of the IKK complex and death-inducing signaling complex assembly, interleukin-1 receptor complex, IRAK4 deficiency (TLR5), IRAK4 deficiency (TLR2/4), interleukin-1 receptor complex, interleukin-1-mediated signaling pathway, TIR domain, MyD88 deficiency (TLR2/4), MyD88-dependentToll-like receptor signaling pathway, and interleukin-1 conserved site pathways. Second, adipocytokines and leptin appear to be associated with the acupoint regulation of FCC, including through adipocytokine signaling, the orexin receptor family, prepro-orexin, and leptin signaling, and erythropoietin activates PLCG pathways.

Therefore, we subsequently aimed to analyze the abovementioned 13 signaling pathways to determine commonalities.

3.5. Signaling Pathway-Target Relationship Network. To identify the commonalities among the abovementioned 13 pathways, the pathway-target relationship network was constructed using Cytoscape. As shown in Figure 6, a total of 34 targets were included in the network, and the targets simultaneously participating in 4 or more pathways were considered the core targets. Thirteen targets were included, namely, NFKBIA, RELA, TNF, IKBKB, IRAK1, TLR4,

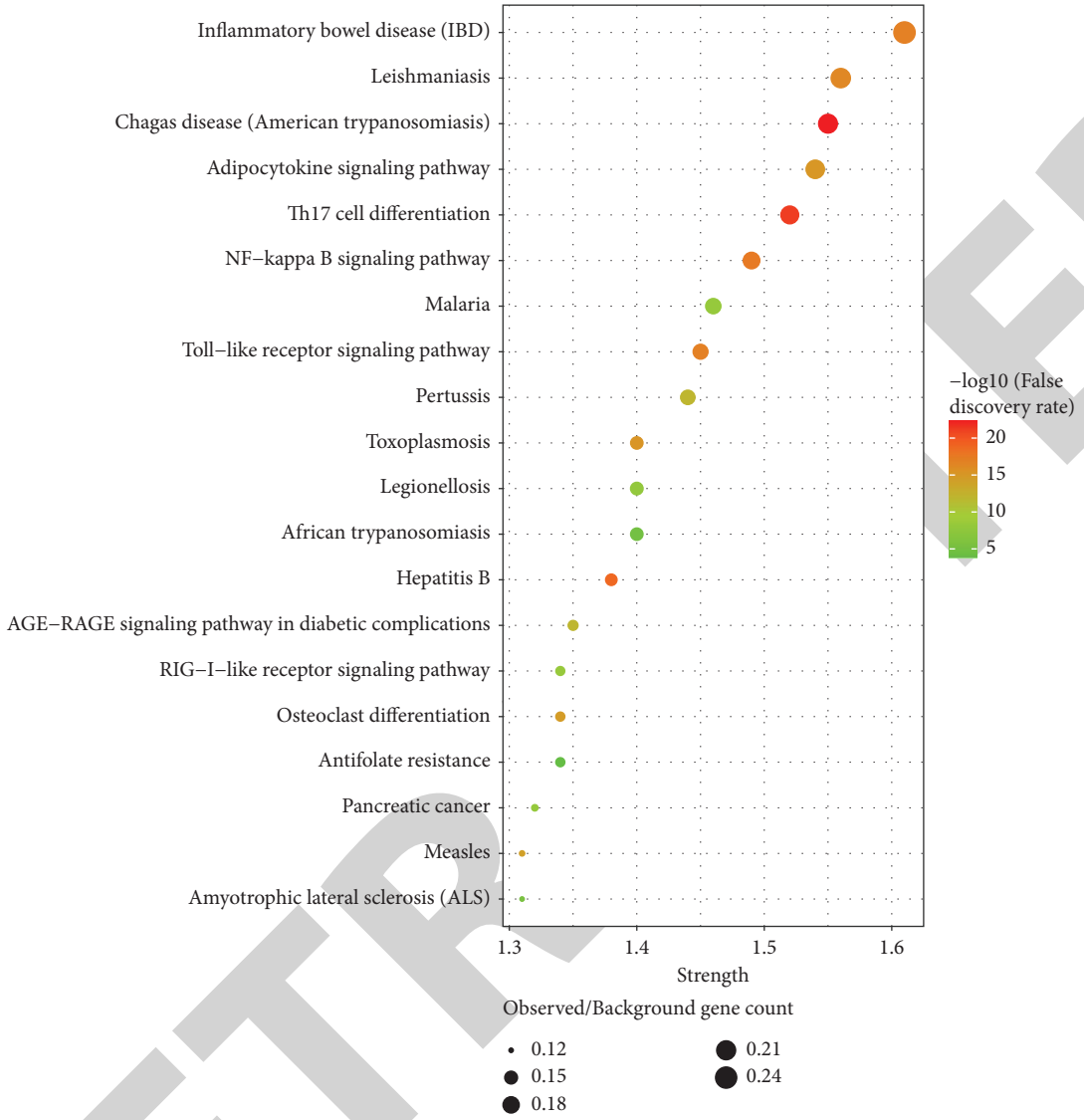

Figure 4: Top 20 terms identified from the KEGG enrichment analysis.

MYD88, TNFRSF1A, IL1R1, TLR2, IL1B, TRAF6, and TNFRSF1B, and these were considered the core targets through which the BL25 and ST25 acupoints can treat FCC.

4. Discussion

4.1. The Combination of BL25 and ST25 May Enhance the Therapeutic Effect of a Single Acupoint. According to the TCM theory, the back-shu point refers to the acupoints at which the energies of the five internal organs and six FCs are inflicted upon the back. In subjects with visceral diseases, the corresponding back-shu points often have abnormal reactions, such as sensitivity and tenderness, and stimulation of these acupoints can be used to treat corresponding visceral diseases. BL25 corresponds to the passage of qi in the large intestine through the back, and stimulation of BL25 can regulate the pathological changes in the large intestine. Front-mu acupoints are those at which the vital energies of the viscera are infused into the chest and abdomen, and "mu" means gathering and confluence. Similar to the back-shu point, when the viscera are diseased, stimulation of the front-mu acupoint usually results in abnormal manifestations such as sensitivity and tenderness. ST25 is also the front-mu acupoint of the large intestine. In clinical treatment, the back-shu and front-mu points are often used in combination due to their similar effects. Despite being used for thousands of years, Chinese researchers have not provided evidence-based experimental results that sufficiently support the effectiveness of this combination therapy. This study aimed to analyze the existing evidence and revealed that BL25 and ST25 have 20 common targets, namely, AQP8, DRD2, VIP, TAC1, IL6R, TNF, FOS, KIT, CHAT, HTR3A, GAS8, SOD3, TRPV1, MPO, CALCA, IL1B, P2RX7, NPY2R, IL10RA, and TPH1. These targets may underlie how BL25 and ST25 can be used together to enhance the therapeutic effect. In addition, because the BL5 and ST25 combination is based on the specific embodiment of back-shu and front-mu points,

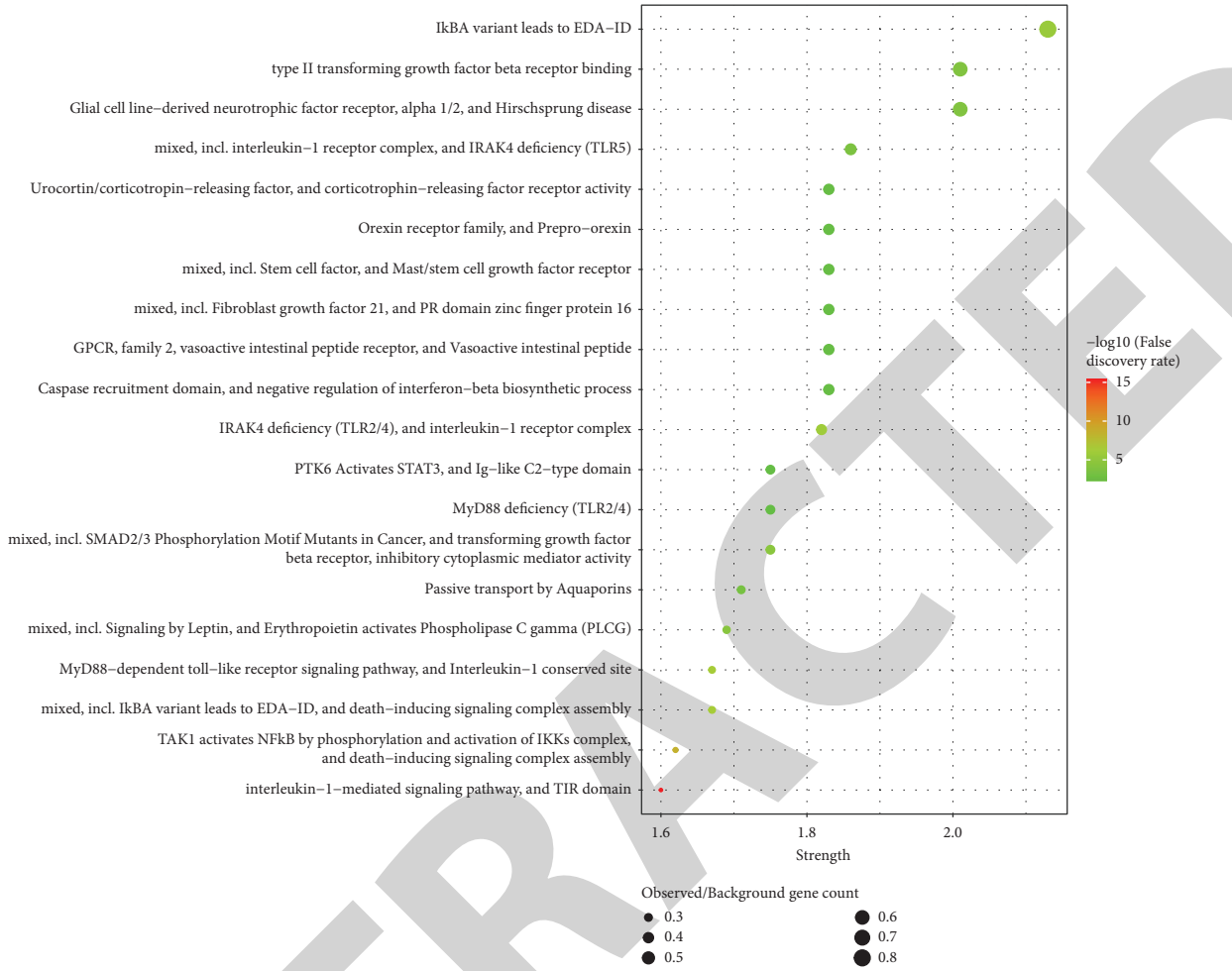

Figure 5: Top 20 items identified by local STRING network cluster enrichment analysis.

other acupoints belonging to the back-shu and front-mu point combination may also have similar matching targets, and this possibility may represent a direction of future research on acupoint compatibility.

4.2. Mechanism through Which BL25 and ST25 Regulate FCC. FCC can be attributed to eating habits (too much milk or too little fiber), changes in the intestinal flora, and psychological and behavioral factors secondary to systemic diseases or drug use, among other factors [26]. Among these factors, the histological changes in the colonic mucosa caused by a milk protein allergy [27] and some diseases, such as colon cancer and IBD [28], are closely related to inflammation. Other diseases, including intestinal diseases, anorectal diseases, metabolic and endocrine diseases, neuropathological diseases, and other systemic diseases, are also causes of FCC [26]. In addition, FCC is more common in children with autism, attention-deficit hyperactivity disorder, anxiety, and depression than in healthy children [29–33].

In this study, KEGG and local STRING network cluster analyses revealed several interesting potential functions of BL25 and ST25.

4.2.1. BL25 and ST25 Regulate FCC through Inflammation. Constipation is a common problem in childhood, affecting approximately 3% of children in the world, and up to 30% of children in some environments suffer from constipation. Constipation is defined as infrequent bowel movements (<2 times per week), reduced bowel frequency, occurrence of fecal incontinence, fecal retention, painful or hard bowel movements, or large-diameter feces [1]. FCC accounts for the vast majority of constipation in children and refers to constipation without a clear cause [34]. The pathogenesis of FCC has not yet been elucidated. At present, it is believed that the etiology of FCC is related to colon and rectal dysmotility, pelvic floor dysfunction, psychosocial factors, and abnormal gastrointestinal regulatory peptides. During the development of FCC, with the accumulation of intestinal feces, water is continuously absorbed. Simultaneously, bacteria in the colon, particularly *Enterococcus, Escherichia* coli, and *Klebsiella* [35], overproliferate and ferment with carbohydrates, resulting in increased gas release, which in turn aggravates the symptoms of abdominal distension, bloating, abdominal discomfort, flatulence, diarrhea, and/or constipation. In severe cases, these bacteria may also cause intestinal villi atrophy, malabsorption, and fat-soluble vitamin deficiency [36]. In this process, bacteria and stool

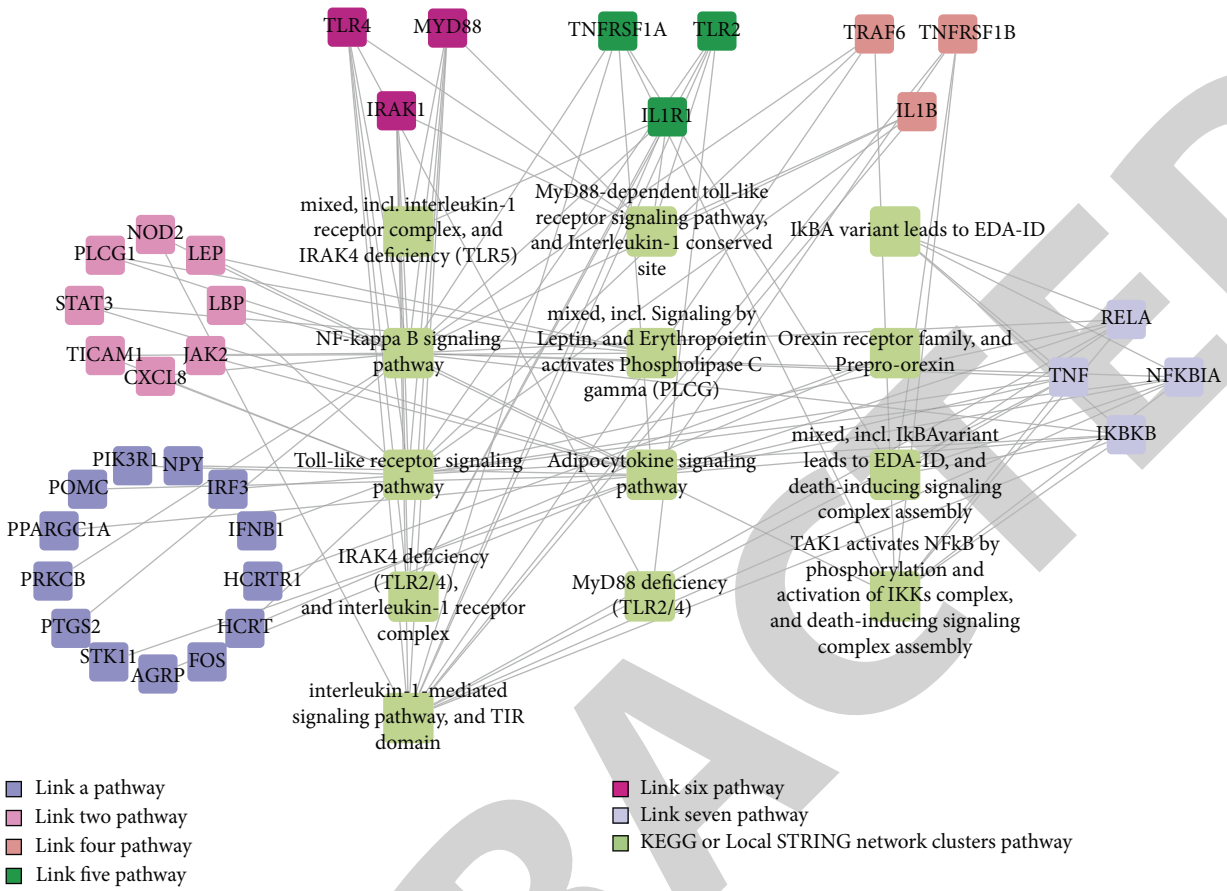

Figure 6: Pathway-target relationship network.

stimulate the intestines to increase in volume, which leads to inflammation, and this occurrence of inflammation will continue to increase the occurrence of constipation and induce the formation of a serious "constipation-inflammation-aggravated constipation" promotion model [36, 37]. Our research found that the stimulation of BL25 and ST25 appears to affect the occurrence of inflammation, as mainly reflected by the enrichment of Th17-cell differentiation, the NF-kappa B signaling pathway and the Toll-like receptor signaling pathway in the KEGG clusters and the inflammatory pathway in the local STRING network clusters.

As one of the CD4+ T-cell subsets, Th17 cells play a dual role in the pathogenesis of inflammation-related bowel disease (mainly proinflammatory). These cells can not only protect the intestinal mucosa by maintaining the balance of the immune microenvironment but also aggravate the intestinal inflammatory response through proinflammatory cytokines. Th17 cells can secrete IL-17, IL-21, and IL-22 and the proinflammatory cytokines IL-1, IL-6, IL-18, and TNF-α [38]. Among these factors, IL-17 is an important cytokine secreted by Th17 cells that can induce inflammation and aggravate tissue damage. The IL-17A subtype of IL-17 can act on a variety of cells (such as epithelial cells and fibroblasts) to secrete chemokines and cytokines. Simultaneously, this subtype can promote the proliferation and maturation of neutrophils, macrophages, and lymphocytes through cell colony-stimulating factors and chemokines [39]. The potential regulatory effect of BL25 and ST25 on Th17-cell differentiation appears to be very important for FCC-induced intestinal inflammation.

In addition, the NF-kappa B signaling pathway has long been regarded as a typical proinflammatory signaling pathway, mainly based on the role of NF-kappa B in the expression of proinflammatory genes, including cytokines, chemokines, and adhesion molecules [21]. Due to the extensive role of the NF-kappa B signaling pathway in cell proliferation, apoptosis, angiogenesis, inflammation, metastasis, and drug resistance [40], the NF-kappa B signaling pathway has also been explored in various diseases, including enteritis [41], ulcerative colitis [42], intestinal flora [43], and rectal cancer [40]. Similar to the NF-kappa B signaling pathway, the Toll-like receptor signaling pathway can also trigger a series of cellular responses and thereby elicits a range of cellular responses, including proliferation, anergy, and apoptosis [44]. The Toll-like receptor signaling pathway can also regulate the enteric nervous system, neurochemical coding, and enteric neuromuscular function to regulate intestinal inflammation [22]. Moreover, the Toll-like receptor signaling pathway can regulate the NF-kappa B signaling pathway and further affect intestinal function [45]. In summary, this study found that BL25 and ST25 exert potential regulatory effects on Th17-cell differentiation, the NF-kappa B signaling pathway and the Toll-like receptor

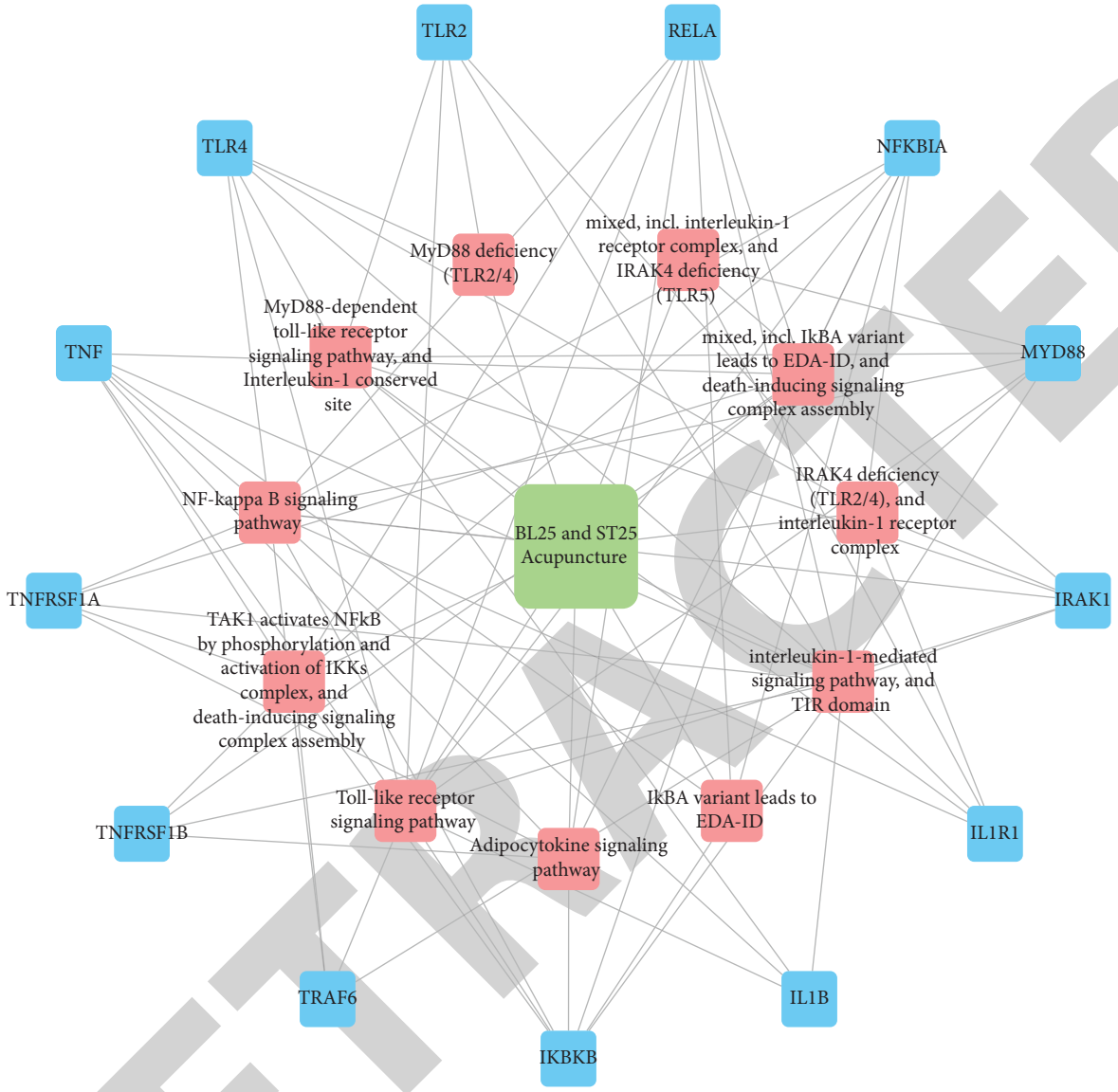

Figure 7: Mechanism of action of BL25 and ST25. The red color indicates the pathways, and the blue color indicates the targets.

signaling pathway, which further affects the "constipation-inflammation-aggravated constipation" model and thereby reduces the degree of FCC aggravation.

4.2.2. BL25 and ST25 Regulate FCC through Adipocytokine or Leptin. Adipocytokines are peptides that signal the functional status of the adipose tissue to the targets in the brain, liver, pancreas, immune system, vasculature, muscle, and other tissues. Adipokines, including leptin, adiponectin, fibroblast growth factor 21, retinol-binding protein 4, dipeptidyl peptidase 4, bone morphogenetic protein-4, BMP-7, vaspin, apelin, and proanulin, play an important role in the function of the adipose tissue and obesity-related diseases. Leptin is a 16-kDa protein composed of 167 amino acids [46]. Leptin is secreted by adipocytes and plays an important role in regulating satiety, appetite, food intake, reproductive function, fertility, puberty, activity, energy expenditure, atherosclerosis [46, 47], and fetal growth [48] through leptin receptors on target cells. In the hypothalamus, leptin can also reduce the synthesis of orexin, which subsequently leads to a decrease in appetite [46]. In addition, leptin may play a role in insulin sensitization and is considered an important regulator of β cells. Due to the ability of recombinant leptin to reduce appetite under normal or low circulating leptin conditions, recombinant leptin has been developed as a weight-loss drug for the treatment of obesity [47, 49].

At present, weight loss is considered an alarm symptom of gastrointestinal disease, but the relationship between obesity and gastrointestinal symptoms is unclear [50]. However, a meta-analysis of gastrointestinal symptoms and obesity (analysis of studies from 1950 to November 2011) found a strong correlation between obesity and incomplete evacuation [50]. Another meta-analysis involving 20 studies showed that obesity is associated with fecal incontinence and diarrhea rates [51]. Although the correlation between obesity

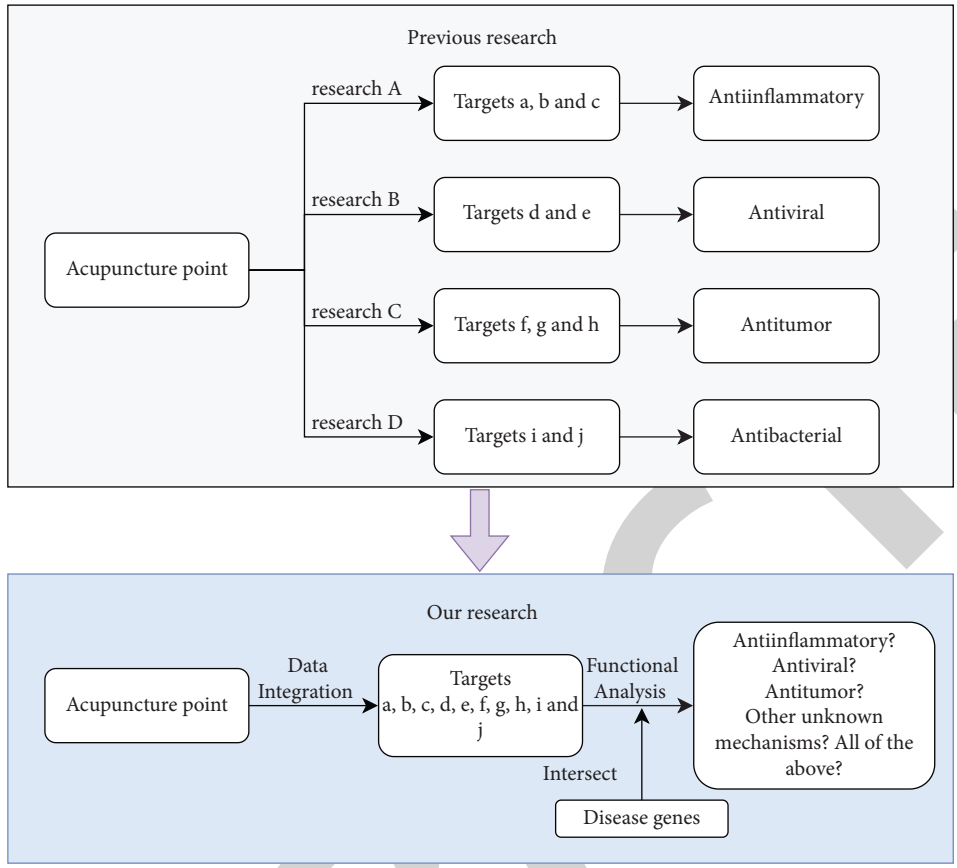

Figure 8: Roadmap for this research.

and constipation cannot be accurately concluded, a close relationship between obesity and gastrointestinal symptoms has been proven. This study found that BL25 and ST25 have the potential to regulate the adipocytokine signaling pathway, orexin receptor family, and prepro-orexin, including signaling by leptin and erythropoietin-mediated activation of phospholipase *C* gamma (PLCG). This finding may indicate that BL25 and ST25 can regulate FCC through adipocytokine or leptin, and although more evidence is needed, this study at least provides a new idea.

4.2.3. BL25 and ST25 Regulate FCC Function and Other Diseases. Approximately less than 5% of children with constipation have organic changes, and these organic changes include anorectal malformations, megacolon, neurological abnormalities, or endocrine and metabolic disorders. More than 95% of children with constipation have no obvious organic causes and are considered to have FCC. However, this study found that leishmaniasis, Chagas disease (American trypanosomiasis), malaria, African trypanosomiasis, toxoplasmosis, hepatitis B, osteoclast differentiation, and measles may be related to FCC, but the relationship between these diseases and FCC is currently poorly understood. However, according to the theory of Chinese medicine, humans should be considered as a whole, and the various tissues and organs of the human body can cooperate with each other to complete various complex physiological functions. Therefore, it does not seem impossible that the occurrence of one disease will eventually cause the occurrence of another disease. Of course, more research is needed on the internal links between these diseases and FCC. We only provide the current results obtained through bioinformatics analysis, and we expect that more scholars will explore and further decipher these findings.

Our PPI analysis also revealed that the proteins involved in the abovementioned regulatory functions are NFKBIA, RELA, TNF, IKBKB, IRAK1, TLR4, MYD88, TNFRSF1A, IL1R1, TLR2, IL1B, TRAF6, and TNFRSF1B, as shown in Figure 7.

4.3. Innovative Attempts for Using BL25 and ST25 for FCC. Any strong or weak external stimulus can alter the physiological functions of the human body. The most basic changes are those related to protein conformation and output caused by gene expression, which result in various positive or negative bodily states. Based on this information, the stimulation of BL25 and ST25 will inevitably change the human body, and exploring the changes in genes or proteins produced after the stimulation of BL25 and ST25 is thus meaningful.

Based on the existing evidence, this study revealed the targets of BL25 and ST25 and performed enrichment analyses, as shown in Figure 8, and the research thus represents

a new attempt to explore the mechanism of acupoints. We hope to provide new ideas and methods for the development of acupuncture strategies.

5. Conclusion

At present, there are many difficulties in acupuncture research, such as the difficulty of determining the targets of acupoints, and the theory of acupoint compatibility has not been effectively proven. This research explored published articles, collected the existing BL25 and ST25 targets for further research, and explored the connotation of combinations of back-shu and front-mu points for TCM. This research draws the following conclusions:

(1) BL25 and ST25 exert a synergistic effect.

(2) The pathway through which BL25 and ST25 regulate FCC is closely related to inflammation and adipocytokine or leptin.

(3) The findings indirectly prove the usability of the method of matching points based on the back-shu and front-mu point combination.

In short, this study provides a new method and idea for exploring the mechanism induced by acupuncture points and provides a new research direction for the modernization of Chinese medicine, particularly acupuncture and moxibustion.

Data Availability

The data used to support the findings of this study are included within the supplementary information files.

Conflicts of Interest

The authors declare that they have no conflicts of interest.

Acknowledgments

This work was supported by China Postdoctoral Science Foundation (2020M673158), Natural Science Foundation of Chongqing (cstc2021jcyj-msxmX0505), Natural Science Foundation of Chongqing for Performance Incentive and Guidance of Scientific Research Institutions (cstc2021jxjl130010), Special funding for postdoctoral research from Chongqing Municipal Human Resources and Social Security Bureau ((2019) no. 298), Chongqing Science and Health Joint Funding Project (2020ZY024084, 2021MSXM317), Chongqing Municipal Health Commission Key Project (2019ZY013201), Natural Science Foundation of Henan Province (202300410251), Henan Province Traditional Chinese Medicine Scientific Research Special Project (2019JDZX2033), Jilin Province Science and Technology Development Plan Project (20190201124JC), 2019 Jilin Province Traditional Chinese Medicine Science and Technology Key Project (2019020), Department of Education of Jilin Province (JJKH20210955) and The 13th Five-Year Science and Technology Research Planning Project of the Education Department of Jilin Province (JJKH20170723KJ) and National Natural Science Foundation of China (82205190).

Supplementary Materials

Supplementary file 1: acupoints and disease-related targets. Supplementary file 2: KEGG enrichment analysis of 141 items. Supplementary file 3: local STRING network cluster enrichment analysis of 59 items. (*Supplementary Materials*)

References

[1] M. Waterham, J. Kaufman, and S. Gibb, "Childhood constipation," *Australian Family Physician*, vol. 46, no. 12, pp. 908–912, 2017.

[2] S. Malowitz, M. Green, A. Karpinski, A. Rosenberg, and P. E. Hyman, "Age of onset of functional constipation," *Journal of Pediatric Gastroenterology and Nutrition*, vol. 62, no. 4, pp. 600–602, 2016.

[3] N. Ranasinghe, N. M. Devanarayana, M. A. Benninga, M. van Dijk, and S. Rajindrajith, "Psychological maladjustment and quality of life in adolescents with constipation," *Archives of Disease in Childhood*, vol. 102, no. 3, pp. 268–273, 2017.

[4] Y. Qiao, H. T. Lei, W. Yi et al., "Effect of moxa-cone moxibustion at lung's back-shu points and front-mu points on Th17/Treg balance in mice with asthma," *Zhongguo Zhen Jiu*, vol. 40, no. 11, pp. 1217–1222, 2020.

[5] R. Cai, Y. Guan, H. Wu et al., "Effects on the regional homogeneity of resting-state brain function in the healthy subjects of gastric distention treated with acupuncture at the front-mu and back-shu points of the stomach, Weishu (BL 21) and Zhongwan (CV 12)," *Zhongguo Zhen Jiu*, vol. 38, no. 4, pp. 379–386, 2018.

[6] L. Kaige, G. Mengwei, T. Lihua et al., "Comparison of effects of electroacupuncture at "Dachangshu" (BL 25) or "Tianshu" (ST 25) on visceral sensitivity, c-kit and TRPV1 of irritable bowel syndrome rats," *Zhongguo Zhen Jiu*, vol. 38, 2018.

[7] Q. G. Qin, X. Y. Gao, K. Liu et al., "Acupuncture at heterotopic acupoints enhances jejunal motility in constipated and diarrheic rats," *World Journal of Gastroenterology*, vol. 20, no. 48, pp. 18271–18283, 2014.

[8] W. Zou, H. Lin, W. Liu et al., "Moxibustion relieves visceral hyperalgesia via inhibition of transient receptor potential vanilloid 1 (TRPV1) and heat shock protein (HSP) 70 expression in rat bone marrow cells," *Acupuncture in Medicine*, vol. 34, no. 2, pp. 114–119, 2016.

[9] T. Hou, H. Xiang, L. Yu et al., "Electroacupuncture inhibits visceral pain via adenosine receptors in mice with inflammatory bowel disease," *Purinergic Signalling*, vol. 15, no. 2, pp. 193–204, 2019.

[10] X. M. Meng and X. T. Liu, "Effect of application of herbal medicine paste to "Tianshu" (ST25) on intestinal mobility and expression of vasoactive intestinal peptide and substance P in colonic myenteric plexus in rats with functional constipation," *Zhen Ci Yan Jiu*, vol. 44, no. 12, pp. 906–910, 2019.

[11] P. Li, Y. Luo, Q. Wang et al., "Efficacy and safety of acupuncture at Tianshu (ST25) for functional constipation: evidence from 10 randomized controlled trials," *Evidence-Based Complementary and Alternative Medicine*, vol. 2020, Article ID 2171587, 14 pages, 2020.

[12] Y. Shi, L. Qi, J. Wang et al., "Moxibustion activates mast cell degranulation at the ST25 in rats with colitis," *World Journal of Gastroenterology*, vol. 17, no. 32, pp. 3733–3738, 2011.

[13] Z. Qi, *Clinical Study on Treatment of Senile Constipation of Yang Deficiency Type of Spleen and Kidney by Warming Needle and Moxibustion at Back Shu Point*, https://www.ncbi.nlm.nih.gov/pmc/articles/PMC2922210/, 2020.

[14] P. Guifang and Z. Yuejuan, "Clinical observation on Tianshu point combined with Dachangshu for treatment of constipation in stroke patients with iontophoresis," *Chinese Community Physician*, vol. 36, pp. 97-98, 2020.

[15] L. Hui, X. Lifei, and N. Wenmin, "Observation on therapeutic effect of 40 cases of functional constipation treated by acupuncture Tianshu and Dachangshu," *Traditional Chinese Medicine Forum*, vol. 36, pp. 42-43, 2021.

[16] K. Niansong, Q. Rong, Z. Juanjuan, L. Suman, S. Weijiong, and M. Weiming, "Clinical observation on treatment of 75 cases of children's functional constipation with pediatric massage and acupoint Application," *Journal of Pediatrics of Traditional Chinese Medicine*, vol. 17, pp. 79–82, 2021.

[17] Y. Hirata, S. Ihara, and K. Koike, "Targeting the complex interactions between microbiota, host epithelial and immune cells in inflammatory bowel disease," *Pharmacological Research*, vol. 113, pp. 574–584, 2016.

[18] C. W. Liew, J. Boucher, J. K. Cheong et al., "Ablation of TRIP-Br2, a regulator of fat lipolysis, thermogenesis and oxidative metabolism, prevents diet-induced obesity and insulin resistance," *Nature Medicine*, vol. 19, no. 2, pp. 217–226, 2013.

[19] J. E. Kim, Y. J. Choi, S. J. Lee et al., "Molecular characterization of constipation disease as novel phenotypes in CRISPR-cas9-generated leptin knockout mice with obesity," *International Journal of Molecular Sciences*, vol. 21, no. 24, p. 9464, 2020.

[20] A. P. Gobert, G. Sagrestani, E. Delmas et al., "The human intestinal microbiota of constipated-predominant irritable bowel syndrome patients exhibits anti-inflammatory properties," *Scientific Reports*, vol. 6, no. 1, Article ID 39399, 2016.

[21] T. Lawrence, "The nuclear factor NF-B pathway in inflammation," *Cold Spring Harbor Perspectives in Biology*, vol. 1, no. 6, Article ID a001651, 2009.

[22] P. Brun, M. C. Giron, M. Qesari et al., "Toll-like receptor 2 regulates intestinal inflammation by controlling integrity of the enteric nervous system," *Gastroenterology*, vol. 145, no. 6, pp. 1323–1333, 2013.

[23] W. Zhang, N. Borcherding, and R. Kolb, "IL-1 signaling in tumor microenvironment," *Advances in Experimental Medicine & Biology*, vol. 1240, pp. 1–23, 2020.

[24] L. Wang, K. Yu, X. Zhang, and S. Yu, "Dual functional roles of the MyD88 signaling in colorectal cancer development," *Biomedicine & Pharmacotherapy*, vol. 107, pp. 177–184, 2018.

[25] G. Zhu, Z. Cheng, Y. Huang et al., "MyD88 mediates colorectal cancer cell proliferation, migration and invasion via NF-κB/AP-1 signaling pathway," *International Journal of Molecular Medicine*, vol. 45, no. 1, pp. 131–140, 2020.

[26] M. H. Vriesman, I. J. N. Koppen, M. Camilleri, C. Di Lorenzo, and M. A. Benninga, "Management of functional constipation in children and adults," *Nature Reviews Gastroenterology & Hepatology*, vol. 17, no. 1, pp. 21–39, 2020.

[27] S. Miceli Sopo, R. Arena, M. Greco, M. Bergamini, and S. Monaco, "Constipation and cow's milk allergy: a review of the literature," *International Archives of Allergy and Immunology*, vol. 164, no. 1, pp. 40–45, 2014.

[28] A. E. Bharucha, J. H. Pemberton, and G. R. Locke, "American Gastroenterological Association technical review on constipation," *Gastroenterology*, vol. 144, no. 1, pp. 218–238, 2013.

[29] C. McKeown, E. Hisle-Gorman, M. Eide, G. H. Gorman, and C. M. Nylund, "Association of constipation and fecal incontinence with attention-deficit/hyperactivity disorder," *Pediatrics*, vol. 132, no. 5, pp. e1210–e1215, 2013.

[30] B. Peeters, I. Noens, E. M. Philips, S. Kuppens, and M. A. Benninga, "Autism spectrum disorders in children with functional defecation disorders," *The Journal of Pediatrics*, vol. 163, no. 3, pp. 873–878, 2013.

[31] M. van Dijk, M. A. Benninga, M. A. Grootenhuis, and B. F. Last, "Prevalence and associated clinical characteristics of behavior problems in constipated children," *Pediatrics*, vol. 125, no. 2, pp. e309–e317, 2010.

[32] S. Dykes, S. Smilgin-Humphreys, and C. Bass, "Chronic idiopathic constipation: a psychological enquiry," *European Journal of Gastroenterology and Hepatology*, vol. 13, no. 1, pp. 39–44, 2001.

[33] T. T. Haug, A. Mykletun, and A. A. Dahl, "Are anxiety and depression related to gastrointestinal symptoms in the general population," *Scandinavian Journal of Gastroenterology*, vol. 37, no. 3, pp. 294–298, 2002.

[34] M. K. H. Auth, R. Vora, P. Farrelly, and C. Baillie, "Childhood constipation," *BMJ*, vol. 345, Article ID e7309, 2012.

[35] W. Takakura and M. Pimentel, "Small intestinal bacterial overgrowth and irritable bowel syndrome-an update," *Frontiers in Psychiatry*, vol. 11, p. 664, 2020.

[36] L. L. Barros, A. Q. Farias, and A. Rezaie, "Gastrointestinal motility and absorptive disorders in patients with inflammatory bowel diseases: prevalence, diagnosis and treatment," *World Journal of Gastroenterology*, vol. 25, no. 31, pp. 4414–4426, 2019.

[37] M. Schmulson, M. V. Bielsa, R. Carmona-Sánchez et al., "Microbiota, gastrointestinal infections, low-grade inflammation, and antibiotic therapy in irritable bowel syndrome: an evidence-based review," *Revista de Gastroenterología de México*, vol. 79, no. 2, pp. 96–134, 2014.

[38] X. Geng and J. Xue, "Expression of Treg/Th17 cells as well as related cytokines in patients with inflammatory bowel disease," *Pakistan Journal of Medical Sciences*, vol. 32, no. 5, pp. 1164–1168, 2016.

[39] A. Luo, S. T. Leach, R. Barres, L. B. Hesson, M. C. Grimm, and D. Simar, "The microbiota and epigenetic regulation of T helper 17/regulatory T cells: in search of a balanced immune system," *Frontiers in Immunology*, vol. 8, p. 417, 2017.

[40] A. Soleimani, F. Rahmani, G. A. Ferns, M. Ryzhikov, A. Avan, and S. M. Hassanian, "Role of the NF-κB signaling pathway in the pathogenesis of colorectal cancer," *Gene*, vol. 726, Article ID 144132, 2020.

[41] M. Zhou, W. Xu, J. Wang et al., "Boosting mTOR-dependent autophagy via upstream TLR4-MyD88-MAPK signalling and downstream NF-κB pathway quenches intestinal inflammation and oxidative stress injury," *EBioMedicine*, vol. 35, pp. 345–360, 2018.

[42] J. Shen, J. Cheng, S. Zhu et al., "Regulating effect of baicalin on IKK/IKB/NF-κB signaling pathway and apoptosis-related proteins in rats with ulcerative colitis," *International Immunopharmacology*, vol. 73, pp. 193–200, 2019.

[43] J. Tang, L. Xu, Y. Zeng, and F. Gong, "Effect of gut microbiota on LPS-induced acute lung injury by regulating the TLR4/NF-κB signaling pathway," *International Immunopharmacology*, vol. 91, Article ID 107272, 2021.

[44] S. Ntoufa, M. G. Vilia, K. Stamatopoulos, P. Ghia, and M. Muzio, "Toll-like receptors signaling: a complex network for NF-κB activation in B-cell lymphoid malignancies," *Seminars in Cancer Biology*, vol. 39, pp. 15–25, 2016.

Hindawi
Evidence-Based Complementary and Alternative Medicine
Volume 2022, Article ID 3860231, 10 pages
https://doi.org/10.1155/2022/3860231

Review Article

Acupuncture Case Registry Study: Rationale, Implementations, and Achievements

Tianyi Zhao,[1] Jia Liu,[1] Yiming Li,[2] Hongjiao Li,[1] Chao Wang,[1] Zhuoxin Yang,[3] Xin Wang,[4] Yanke Ai,[1] Yuning Qin,[1] Xue Cao,[1] Lihong Yue,[1] Zhishan Ge,[1] Shihua Wang,[1] Xiangran Meng,[1] Yanjun Wang,[5] and Liyun He[1]

[1]*Institute of Basic Research in Clinical Medicine, China Academy of Chinese Medical Sciences, Beijing, China*
[2]*Swiviss University of Traditional Chinese Medicine, Hauptstrasse 61, Bad Zurzach 5330, Switzerland*
[3]*Department of Acupuncture and Moxibustion, Shenzhen Traditional Chinese Medicine Hospital, Futian District, Shenzhen, China*
[4]*China Academy of Chinese Medical Sciences, Beijing, China*
[5]*Department of Acupuncture and Moxibustion, The First Affiliated Hospital of Hebei University of Chinese Medicine, Chang'an District, Shijiazhuang, Hebei, China*

Correspondence should be addressed to Yanjun Wang; wangyj8055@sina.com and Liyun He; hely3699@163.com

Received 5 May 2022; Accepted 10 October 2022; Published 21 November 2022

Academic Editor: Xuezhong Zhou

The acupuncture case registry study is focusing on acupuncture therapy data from patient cases. The main objective is to collect real-world data and integrate clinically meaningful outcome evaluation indicators to uncover and evaluate real-world acupuncture efficacy and safety, explore factors affecting acupuncture efficacy, and provide real-world evidence to complement RCTs. Since the International Acupuncture Case Registry data collection system's establishment in 2017, 16 projects have been underway, including two acupuncture specialty therapies and 15 diseases. Data from 3404 patients included extensive information on the diagnosis and treatment of acupuncture and the evaluation of its efficacy. In order to serve as a guide for future studies, this article discusses the value of and rationale for establishing acupuncture case registry studies, how to distinguish them from patient registries, and crucial techniques for implementing registry studies in terms of applications, patient recruitment, costakeholder collaboration, data collection and management, study quality control, and ethics.

1. Introduction

Acupuncture is a technique that is used to stimulate specific body points, usually by inserting fine needles into the skin. Acupuncture has been used in China for 2,500 years and is increasingly used to treat various conditions. The World Health Organization 2019 Global Report [1] revealed that acupuncture is widely used in 183 countries and regions worldwide for 461 symptoms and 972 diseases [2], and some countries have incorporated it into their health insurance and medical regulations. More than 10 million acupuncture treatments are performed annually in the United States [3], and the National Health Service provides over four million acupuncture treatments [4]. An increasing number of randomized controlled trials (RCTs) have been conducted in recent decades in terms of clinical research to study the efficacy and safety of acupuncture. More clinical studies of acupuncture, especially RCTs have increased as evidence-based medicine continuously develops. In the last 10 years, seven acupuncture clinical trial publications have been published in the world's top medical journals [5], including the Annals of Internal Medicine [6] and the Journal of the American Medical Association [7]. These articles document the clinical effectiveness of acupuncture and the quality of clinical studies in China. However, RCTs are limited in themselves

and require strict implementation of randomization and blinding principles. RCTs cannot fully meet the needs of clinical evidence generation in traditional Chinese medicine (TCM). Highlighting the strengths and characteristics of TCM is difficult, resulting in acupuncture therapies that are being determined clinically effective showing negative results in most RCTs.

Therefore, further development of real-world studies of acupuncture is necessary. Rather than operating in a "sterile" environment with a narrowly defined audience, the real-world study assesses the effectiveness and safety of an intervention with a more diverse audience in a real-world setting. Therefore, real-world studies could provide a valid and valuable method for acupuncture assessment [8]. Conducting real-world studies of acupuncture to complement the evidence from RCTs of acupuncture is important.

Registries for evaluating patient outcomes and the real-world evidence they provide are highly valuable to physicians and patients. Registries increase the understanding of treatment effects and the natural history and progression of the disease and allow the observation of large patient populations [9].

Therefore, Prof. Liu, who is the principal investigator of our team, proposed the idea and methodology of an international acupuncture registry study in 2013 [10]. By further design, the first international acupuncture case registry study started in science in 2017, which aimed to establish a worldwide networked data platform for evaluating the clinical efficacy and safety of acupuncture treatments [11].

Registry studies were not clearly classified, and the common names currently used are "patient registry" and "case registry." The term "patient" shows that the registry primarily concerns health information. It is a broad term that can include people with a certain disease, pregnant or lactating women, or people who have a birth defect or a molecular or genomic feature [12]. The term "case" focuses on collecting data on specific eligible illness cases. The "Case Registry" studies are more concerned with public health surveillance or the tracking and documentation of data from studies of eligible patients [13, 14]. Based on our review of previous registry studies and real-world studies of acupuncture, the acupuncture case registry study differs from most existing patient registry studies for a particular disease. Table 1 shows the comparison of the specific differences. The acupuncture patient registry studies primarily aimed to evaluate the clinical efficacy of acupuncture rather than to epidemiologically investigate diseases. Based on this research purpose, the design of the study should reflect the diagnostic and therapeutic characteristics of acupuncture, such as the registration and analysis of acupuncture operational details (e. g., acupuncture site/acupoints, techniques, and the state of the doctor and patient) and acupuncture diagnostic and therapeutic thinking (e. g., identification/diagnosis).

This manuscript outlines the use of key techniques and specific considerations for the implementation and application of acupuncture patient registries.

2. Methods and Implementations

2.1. Objectives and Applications. The acupuncture case registry is a study focusing on acupuncture therapy data from patient cases, making it primarily distinct from a patient registry which is a study designed to collect epidemiological data on the disease [16]. Table 1 shows the difference between the acupuncture case registry and patient registry in terms of study purpose. The acupuncture case registry has a more specific purpose, with efforts focused on collecting data on how acupuncture is used in the clinic and tracking the ongoing impact of acupuncture on patients to uncover the diagnostic and therapeutic patterns of acupuncture. This is different from the primary purpose of a patient registry, which is to describe the natural history of the disease.

Acupuncture registry studies can be conducted for the following applications.

2.1.1. Evaluating the Clinical Efficacy and Cost-Effectiveness of Acupuncture. In contrast to RCTs that require strict inclusion and exclusion criteria, patient registration studies have a relatively broad population, making them suitable for examining the efficacy rather than the efficacy of acupuncture in actual clinical practice. Concurrently, the registration mechanism is more convenient for the study population. Furthermore, the registration mechanism is more suitable for the long-termfollow-up of the study population, long-term efficacy observation of acupuncture, and dynamic change analyses in the treatment process of acupuncture, as well as flexibility in adjusting the study protocol according to the current situation during the study and providing more comprehensive data for efficacy evaluation or related critical factors exploration. Registration mechanisms can be used to evaluate the cost-effectiveness of acupuncture in the real-world. Cost-effectiveness is a way of describing the relative value of the ability of a healthcare product or service to achieve the desired outcome for the given resources spent, thereby comparing costs with measured clinical regression [17]. Cost-effectiveness models are developed to assess the cost-effectiveness of the procedure by collecting data related to the costs and benefits of acupuncture or by linking it to health insurance data during acupuncture case registry studies.

2.1.2. Description of the Acupuncture Application. Describing acupuncture applications in different regions and countries provides a clear picture of the theoretical foundation, methods, prescriptions, acupuncture point selection, techniques, and other essential acupuncture applications in clinical practice. Additionally, it discusses the types of diseases that can be treated by acupuncture, the population that receives acupuncture treatment, and the differences in the basic situation of acupuncture in different regions and countries. Until now, no one has studied and analyzed these basic acupuncture applications. A descriptive study that uses data from a case registry could answer this question. These works can provide preliminary studies to explore the spectrum of acupuncture diseases, dominant diseases, and treatment norms.

Table 1: Differences between a acupuncture case registry study and a patient registry.

Topics	Acupuncture case registry study	Patient registry [15]
Definition	Prospective observational studies that use acupuncture as the primary intervention and collect data uniformly to evaluate clinical efficacy and cost-effectiveness, describe the application of acupuncture therapy, monitor the safety of acupuncture therapy, evaluate the quality of acupuncturists, or conduct epidemiological disease investigation.	Organized system that collects uniform data (clinical and other) to identify specified outcomes for a population defined by a particular disease, condition, or exposure.
Objective	Primary purposes include assessing the clinical efficacy and cost-effectiveness of acupuncture, describing the application of acupuncture techniques, monitoring treatment safety, and evaluating the quality of acupuncturists.	Registry purposes can be broadly described in terms of patient outcomes. Major purposes include describing the natural history of disease, determining clinical and/or cost-effectiveness, and assessing safety or harm.
Patient enrollment	As determined by the study objectives, enrolled patients with a disease/certain symptom or a condition who have had acupuncture therapy from an acupuncturist or other acupoint stimulation interventions; generalisability of the acupuncture data and study results to be documented.	Aimed at enrollment of all patients with a disease or condition; generalisability of registry data to be documented.
Follow-up	Timelines are determined by the specific study objectives as well as the collection/extraction and processing of important study data.	Schedules drive timeliness for data collection and any anticipated data analyses which prompted the registry.
Data collection	Data is collected based on the objective of the registry study. A core set of data elements to be collected is agreed upon, and their definitions, coding systems, and data entry procedures are written down. Data collected for the purpose of a registry study can involve the primary collection of data or the secondary use of data.	
Data quality management	Study-specific data quality management will be defined in advance and executed using a risk-based approach, with a focus on regular surveillance and inspection of registered data.	Quality management is applied consistently to data and processes, with an emphasis on a core set of data elements; data quality management is specified and documented in advance.
	Data management systems to ensure data integrity, completeness, and security	
Analysis plan	Most of the time, detailed statistical considerations are written in a document separate from the study and registry protocols. This document is called a descriptive or hypothesis-driven statistical analysis plan.	Plan for statistical analysis, with analyses often done regularly at regular intervals based on patient accrual or analyses of predefined outcomes at time points described in the registry protocol.

2.1.3. Monitoring and Documentation of Acupuncture Safety. Acupuncturists can promptly record adverse events during treatment [18], such as dizziness, needle breakage, hematoma, etc., in a patient case registry study, and disease-related adverse reactions should be recorded to observe whether acupuncture has reduced the occurrence of disease-related adverse reactions compared to other treatment methods. Specific advantages include: first, increased motivation of physicians to record adverse events and focused follow-up of patients with adverse events, especially for the recording of minor symptoms or easily-ignored acupuncture adverse events, such as bleeding after acupuncture and thick needles; second, the existing electronic medical record lacks records of adverse acupuncture events or has incomplete records and cannot accurately estimate the incidence of adverse events in the total population. The case registry addresses this issue by improving the reporting of the incidence of adverse acupuncture events.

2.1.4. Evaluation of Clinical Treatment Quality and Patient Satisfaction in Acupuncture. Acupuncture's clinical efficacy is influenced by a variety of factors, including the acupuncturist's experience and technical mastery of the consultation and treatment, as well as nonspecific factors like the patient's psychological expectations before acupuncture treatment [19], satisfaction after acupuncture, the patient's psychological treatment environment state [20], comfort while receiving treatment, and the acupuncturist's experience and technical mastery of the consultation and treatment. The consistency of these health services with available expertise and the amount to which individual and population health services increase the chance of expected health regression are used to determine the quality of care. Case registry studies can indirectly aid in improving clinical outcomes and better individualizing acupuncture treatment by including a patient satisfaction survey module, combining data on follow-up rates and the number of follow-up visits, and comparing differences in the quality of care between physicians or providers.

In summary, the most important thing for acupuncture case registry studies at the project stage is to clarify the clinical significance of the project, prioritize clinical studies of acupuncture advantageous diseases or potential advantageous diseases, as well as acupuncture characteristic techniques to conduct registry studies to support clinical evidence from acupuncture RCTs, expand the scope of acupuncture clinical efficacy evaluation studies, and enhance the quality of acupuncture clinical efficacy evaluation studies [8].

2.2. Patient Recruitment and Costakeholder Collaboration in Study Implementation. Personal health information and patient-generated data are becoming increasingly available as vast amounts of data and real-world evidence emerge. Increasingly, individuals and community organizations are seen as research partners as shared decision-making increases, particularly in the design and management of studies involving patient registries [21]. Therefore, the collected data will be more extensive and more authentic if we can consider the enthusiasm of primary care institutions and individuals for registration, and more meaningful results can be produced.

The study implementation should start with the participation of medical institutions (hospitals, associations, etc.) and therefore should include researchers, clinicians, service providers in their industry, and relevant community managers, all of whom can participate in the collaborative study [22]. In an acupuncture case registry study, physician recruitment should be conducted on the platform of a medical institution. The investigator needs to fully consider the international and domestic clinical status of acupuncture, screen the study institution, recruit acupuncturists to participate through multiple channels, and recruit patients through physicians. Additionally, achieving research objectives and participating in acupuncture case registry studies can improve physicians' clinical research skills, standardize acupuncture clinical practice, increase interest in clinical research, increase patient-physician interaction, facilitate the promotion and introduction of acupuncture therapies, and promote acupuncture culture. Finally, a physician recruits patients who participate in the study. The project needs to be centered on a clear research goal at the research initiation stage, with the interests of multiple participants identified and prioritized, to better conduct the work and maintain long-term, stable research [23]. It also needs to assess the conflicts of interest among participants that affect the bias of the study results and try to avoid such conflicts.

Moreover, we attempted to establish an academic community of acupuncture for POI by establishing acupuncture expert studios and professional academic committees in the implementation of the registry research of acupuncture for premature ovarian insufficiency (POI). Nearly 30 acupuncture POI expert workshops have now been established in China. The World Federation of Acupuncture-Moxibustion Societies and the China Association for Acupuncture and Moxibustion have taken the lead in forming an expert committee, which has included experts in acupuncture, evidence-based medicine, clinical epidemiology, statistics, obstetrics and gynecology, and other fields, to discuss acupuncture intervention protocols, efficacy evaluation methods, data management, quality control, and other topics. Experts worldwide attended the meeting. The cross-discipline exchange and learning of these experts improve the quality of case registry studies and deepen clinicians' disease knowledge, which not only ensures the smooth operation of registry studies but also aids clinicians in improving diagnosis and achieving early detection and treatment of POI [11].

2.3. Data Collection and Data Stewardship. The "Framework for FDA's Real-World Evidence Program" recognizes the importance of patient registries as a source of real-world data and emphasizes processes to minimize missing or incomplete data, as well as the collection of rigorous and high-quality data, thereby ensuring that the generated data can be used as evidence in the real world [24]. Fundamental,

structural, semantic, and organizational interoperability techniques must be created and widely embraced, following specific sections of the 21st Century Cures Act, to improve current research and development. The primary and secondary data sources for the registry should be defined because this is a real-world clinical trial. Secondary data is received through external links to electronic medical record systems or medical data systems of other institutions, and primary data is collected on a standardized data platform. Technical steps are adopted to ensure the feasibility of data linkage and thorough quality control of secondary data to limit the dangers of data linkage, assure the accuracy of data, and protect patient privacy [25]. Data was gathered in addition to documenting the general features of the patients and their medical problem information. The researcher should focus on refining the collection of acupuncture-related data when designing the registration form, primarily including (1) information on clinical acupuncture prescription and clinical acupuncture operation should be described in detail, which can be clearly displayed and illustrated using text, pictures, or videos; (2) acupuncture operation information, such as acupuncture point selection, acupuncture tool selection, body position, tonic and diarrheal techniques, stabbing methods, auxiliary acupuncture techniques, needle holding methods, needle entry methods, needle angles, needle directions, needle depths, acupuncture techniques, acupuncture techniques, acupuncture duration, needle retention methods, needle retention times, and records of changes in the method of starting acupuncture; (3) influencing factors on the clinical effect of acupuncture, such as such as the psychological state of the acupuncturist and the patient during the treatment period and the characteristics of the acupuncturist (age, years of practice, and seniority). Furthermore, based on a case registry study of chronic low back pain treated via acupuncture, we found that (1) it is difficult for patients to be visited on the planned data collection date, so key evaluation points should be predetermined during protocol design; (2) compared with patient registry studies, acupuncture case registry studies have shorter observation periods; thus, establishing enough follow-up duration to see the long-term advantages of acupuncture is necessary; (3) Some disease characteristics, such as pain quality, causes of pain aggravation and relief, and pain provoke, are not critical influencing factors in the analysis of the efficacy of acupuncture for low back pain and are nonmandatory data collection, so ignoring the collection of these data can reduce the researcher's workload [26].

We advocate putting in place a more complex data management system before collecting patient data in terms of data governance to ensure that the collected information meets the basic standards and best practices for clinical inquiries. Establishing a data quality assurance program to monitor and manage data attributability, readability, simultaneity, originality, regularity, consistency, completeness, timeliness, accuracy, authenticity, persistence, and accessibility are among the specific needs [27]. A strict data management plan is in place to ensure data quality, with data managers tracking and spot-checking the data regularly, providing timely feedback on quality issues with the entered data, and encouraging researchers to correct them as soon as possible with in-platform alerts and e-mail reminders. Statisticians were involved, and suspect data is constantly queried and processed [28]. The above data spot-checking, query issuing, and response must be completed and recorded within the registration platform.

Our research team has created the International Acupuncture Case Registry Platform for Real-World Study, which is based on the Chinese Academy of Traditional Chinese Medicine's "Research Integration Platform (https://www.amreg.org/)." The platform supports programs that recruit volunteer acupuncturists through the World Federation of Acupuncture-Moxibustion Societies Research Center and records patients who have received acupuncture therapy in the system, with the cooperation of 189 member organizations in 53 countries. This system primarily performs data collection and operation administration. The acupuncture case registry database built on this platform will become a tremendous resource for acupuncturists worldwide with the long-term development of this study, thereby giving comprehensive treatment data. Physicians will be able to use these tools for free to solve clinical problems connected to acupuncture and enhance clinical outcomes, with the permission of the study's expert committees [10].

2.4. Quality Control and Ethics. Acupuncture case registry studies are "multicenter, large sample, and diversified treatment" in nature, which require strong quality control (QC) to assure their scientific validity [29]. Real-time data quality monitoring is necessary to ensure the smooth implementation of high-quality registries because of the large sample size, wide geographic distribution, and long follow-up period [30]. This also determines whether the collected dataset meets the purpose of the study and is of high analytical value [31]. Thus, QC efforts need to be designed from the start of the study design and throughout the study process to ensure that this principle is followed. We have developed a combined remote and on-site quality control methodology during the last 5 years [32], with remote QC as the primary focus and on-site QC as a supplement.

This registration platform was used to undertake remote QC. Each clinical center was expected to conduct online QC by a data monitor for every 2-3 new cases entered during the study period to ensure the quality of subsequent cases. The monitors were then asked to log in to the platform once a week to check the number of cases and to undertake online monitoring every 10–15 cases to provide prompt feedback and recall issues. Online platform QC, telephone interviews, e-mail call-backs, and social networking software call-backs are all examples of remote QC approaches. Online data QC is only one component of the study because the acupuncture case registry study primarily focuses on evaluating an intervention. QC efforts at the study site are also necessary to ensure that acupuncture, as a treatment method, fits specifications during the study and determine the investigator's proficiency in mastering the acupuncture treatment protocol and the completeness of the operational information

recorded. We adopted an audit system of first-level inspection by participating hospitals, second-level monitoring by the lead unit, and third-level supervision by high-level experts to conduct regular audits [33]. We conducted regular monitoring mainly on study data management, physician compliance with the study protocol, patient compliance, acupuncture operation accuracy, and the completeness of registration of acupuncture-related information to ensure a high-level implementation of study procedures.

A case registry must be designed, implemented, and maintained following ethical, legal, social, and privacy considerations for it to be successful [22]. An Institutional Review Board is an independent ethics committee that oversees research studies and ensures that the protocol, governance, protections, and methods are ethical and appropriate [22]. It is required for any study that collects identifiable information from human subjects. In all cases, study participation is entirely voluntary and elective, and participants are free to withdraw at any moment. Participants or their legally authorized representatives must provide informed consent to the collection, storage, and use of their health data once they have been enrolled before sharing any personal data with third parties [34]. They must be evaluated and authorized by an independent ethical committee before starting any acupuncture case registry studies. Multicenter studies should be ethically approved at each participating institution, and each registered patient should be informed, explained, and asked to sign an informed consent form before participating. We have implemented an electronic informed consent feature on our data platform to ensure that patients obtain proper informed consent and to reduce the occurrence of falsely informed circumstances. The patient can request a video call with his or her physician through the internet after completing a question-and-answer session about the study design, process, and patient rights relating to the study. Upon deciding to join, the patient will manually check off several conditions that demonstrate informed consent, such as affirmation that they have read and understood the study information and consent form, as well as certification that any questions they had were well answered. Patients who answered "yes" to all questions will be required to electronically sign and be formally enrolled in the study. The platform is also developed with the need for health information confidentiality in mind, employing technical measures and permission settings to actively preserve patient privacy information, such as eliminating identifiable patient information, from the database [35].

3. Achievements

One of the most important sources of evidence for acupuncture clinical research will be the creation of an international acupuncture case registry research platform and the development of case registry research with acupuncture features. The Acupuncture Case Registry Research Consortium of the China Association for Acupuncture and Moxibustion was officially created on February 11, 2017 [35], and the first initiatives include patient registry research on premature ovarian failure, chronic low back pain, and floating needle therapy. Therefore, the first international real-world acupuncture study was formally formed, with an expert steering committee and an acupuncture patient registration center run by the Clinical Evaluation Center of the Chinese Academy of Traditional Chinese Medicine's Institute of Clinical Basic Medicine.

The acupuncture case registry project is operational in many provinces around China. The registry has significantly grown over the past 9 years, and 3404 patients from 16 studies in 30 provinces have been enrolled as of March 30, 2022 (Figure 1). This study has continued to grow since its initiation and is currently the largest international study of acupuncture patient registries. Table 2 demonstrates the 16 individual research projects that are currently in progress, including two studies of specialty acupuncture techniques, involving 15 diseases. Additionally, the studies now have four officially published research papers. Two-phase analyses have been published since the beginning of acupuncture studies for POI, which examine the differences in the effects of acupuncture with various stimulation intensities on increased sinus follicle counts [36] and the development of a columnar line graph clinical prediction model of the effects of acupuncture on pregnancy outcomes in patients with early-onset ovarian insufficiency (POI) [37]. This indicates that this study is in the phase of clinical data accumulation, and we estimate a successive research output in the last few years.

We presided over the drafting of the Standard for Management of Registry Study on Acupuncture-Moxibustion to better conduct international acupuncture patient registration, and the consultation draft of this specification was made public in the CAAM (https://www.ttbz.org.cn/Home/Show/21183) on January 13, 2021.

4. Looking to the Future

Since their inception, acupuncture case registry studies have significantly contributed to the advancement of clinical acupuncture-moxibustion research. The acupuncture case registry study preserves the individualized characteristics of the syndrome differentiation and acupuncture treatment. Additionally, the open-ended inclusion and exclusion criteria enable greater generalisability of the results of a study. As a result, it will play a significant role in the structure of evidence-based medicine for acupuncture. As the scope of the acupuncture case registry study expands, the Research Integration Platform will need to be modified to ensure the most relevant data are captured. In the future, new technologies may allow for faster and more efficient data aggregation from electronic medical records as well as other sources, such as smartphone app-based patient-reported outcomes or mobile data-logging devices.

In addition, future studies need to consider the registry of individuals receiving long-term acupuncture treatment. Tracing individual patients who receive acupuncture treatment for different reasons is necessary. This is not a traditional medical record data collection, and we will attempt to create a specifically relevant registry study to explore the role of acupuncture in public health.

Table 2: Acupuncture case registry research project and data collection*

Acupuncture therapy	Patients	First patient enrolled	Cases	Published articles
Acupotomy	Lateral epicondylitis	2022.03	3	—
Acupotomy	Subacromial impingement syndrome	2022.03	0	—
Acupotomy	Upper limb spasticity after stroke.	2022.03	4	—
Acupotomy	Calcaneodynia	2022.03	0	—
Acupotomy	Knee osteoarthritis	2022.03	2	—
Acupotomy	Tenovaginitis of flexor digitorum	2022.03	0	—
Acupuncture therapy, not limited to specific types	Premature ovarian insufficiency	2017.06	1319	Clinical prediction model establishment of the influence of acupuncture-moxibustion on pregnancy outcome of patients with premature ovarian insufficiency based on patient registry study and LASSO-Cox model [36]. Effects of acupuncture on antral follicle count in patients with premature ovarian insufficiency based on patient registry study [37]
Acupuncture therapy	Postpartum depression	2018.09	433	—
Acupuncture therapy	Neurogenic urinary retention	2019.08	152	—
Custom blood therapy for acupoints	Urticaria chronica	2019.01	501	—
Acupuncture therapy	Asthenic bulbar paralysis	2022.03	6	—
Acupuncture therapy	Chronic low back pain	2017.06	573	Acupuncture therapy for chronic low back pain: protocol of a prospective, multicenter, registry study [38]
Acupuncture therapy	Prediabetes	2018.03	104	—
Acupuncture therapy	Degenerative osteoarthritis	2018.05	309	—
Acupuncture therapy	Diabetes prevention	2018.03	0	—
Acupuncture therapy	Malignant pleural effusion	2019.04	5	Discussion on registry study of acupuncture-moxibustion for malignant pleural effusion

*The data in the table are up to 2022.3.30.

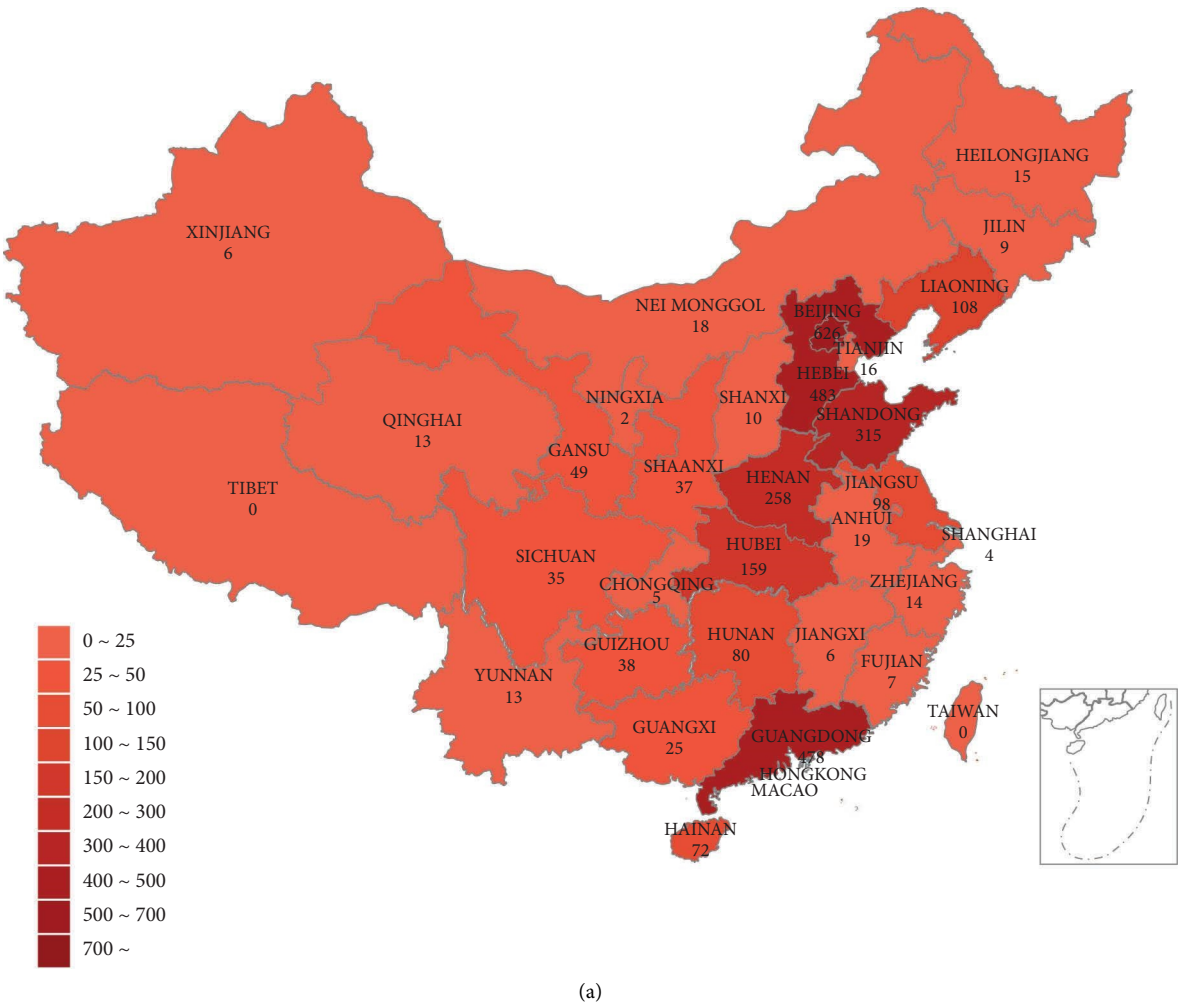

(a)

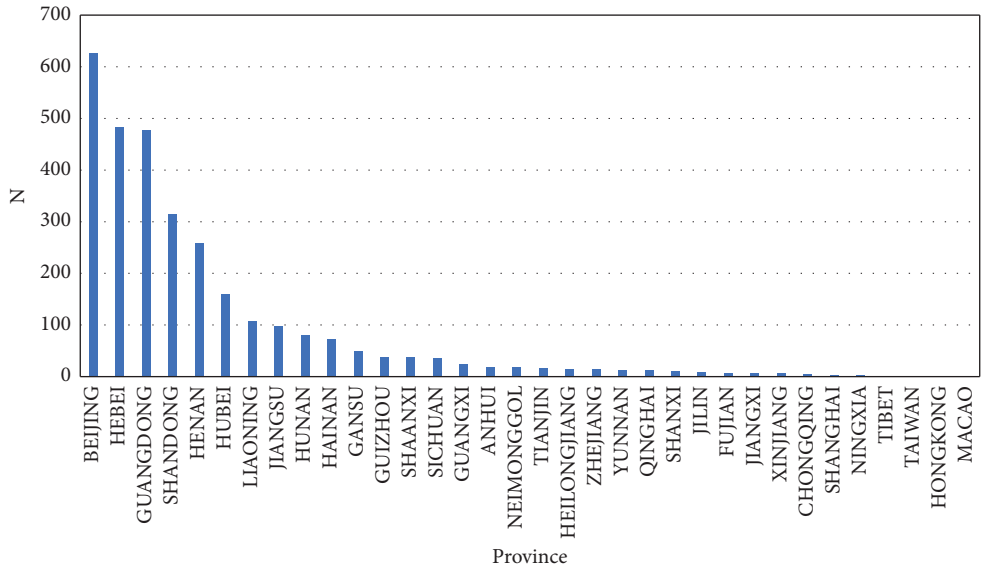

(b)

Figure 1: Key facts about the acupuncture patient registry. (a) The global reach of acupuncture patient registry. Provinces with active acupuncture patients are indicated in red. (b) Ranking chart of the number of registered cases by province.

There is no doubt that case registry studies can be applied to other forms of traditional Chinese medicine (TCM). There are already case registry studies of proprietary Chinese medicines, such as the case registry study of Nao Shuan Tong capsules for the treatment of ischemic stroke based on the theory of "toxic damage to brain collaterals," which began in 2019 and has collected over 5,000 cases (https://www.news.cn/video/2022-08/16/c_1211676629.htm); and the prospective case registry study of Jianpi Sheng Xue tablets/granules for the treatment of iron deficiency anemia during pregnancy, which was conducted in 2017-2018 and included a total of 10,000 patients [39]. Both studies focused on the beneficial population as well as the clinical action features of proprietary Chinese medicines, which can be valuable for clarifying the scope of action and increasing clinical efficacy. In general, the current TCM real-world case registry studies are in their infancy. Our team intends to expand on the experience and platform of the acupuncture registry study to further the Chinese medicine case registry study. Due to the complex characteristics of syndrome differentiation and TCM treatment, collecting data can be challenging. Thus it is feasible to begin the case registry study using proprietary Chinese medicine or Chinese medicine injections [40]. Soon, with the improvement of TCM case registry study methodology and technology maturity and the development of a professional team, it will be possible to conduct a case registry study of Chinese herbal prescriptions in order to collect comprehensive data on TCM characteristics and investigate the clinical benefits of TCM treatments.

5. Conclusions

Acupuncture case registry studies were conducted for >5 years, and the currently collected information on acupuncture interventions and patients treated with acupuncture is greater and more extensive than any other previous clinical study. Our study develops a discussion of the purpose of the acupuncture patient registry, the three aspects of data collection and management, the discussion of common stakeholders in our implementation, and the differences from existing patient-centered registry studies to maximize the clinical value of the study and its value to the clinical development of acupuncture. Finally, this study will help ensure the acupuncture case registry study's understanding, improve the conducted follow-up quality, increase the active participation of the investigators in this study, and facilitate our management of this study.

Abbreviations

QC: Quality control
POI: Premature ovarian insufficiency
CAAM: China association for acupuncture and moxibustion
TCM: Traditional Chinese medicine.

Data Availability

No data were used to support this study.

Conflicts of Interest

The authors declare that there are no conflicts of interest.

Authors' Contributions

Tianyi Zhao and Jia Liu contributed equally to this study.

Acknowledgments

The authors acknowledge Baoyan Liu, PhD, of the China Academy of Chinese Medical Sciences for the presentation of the design of the acupuncture case registry study. The authors are grateful to Shiyan Yan, PhD, Beijing University of Chinese Medicine, for the guidance of statistical analyses of acupuncture case registry studies. Neither was compensated for their contributions. The authors would also like to thank Enago (https://www.enago.cn/) for his contribution to language editing. This work was supported by National Key R&D Program of China (2017YFC1703600), Key technology Research of International Case Registry Platform of Acupuncture-Moxibustion (2017YFC1703601), National Key R&D Program of China (2019YFC1712200), International Standards Research on Clinical Research and Service of Acupuncture-Moxibustion (2019YFC1712205), Innovation Project Project of China Academy of Chinese Medical Sciences (CI2021A0540).

References

[1] W. H. Organization, *WHO Global Report on Traditional and Complementary Medicine 2019*, World Health Organization, Geneva, Switzerland, 2019.
[2] S. Y. Yan, Z. Y. Xiong, X. Y. Liu, C. Z. Liu, and B. Y. Liu, "Review of clinical research in acupuncture and moxibustion from 2010 to 2020 and future prospects," *Zhongguo zhen jiu=Chinese acupuncture & moxibustion*, vol. 42, no. 1, pp. 116–118, 2022.
[3] P. Whittaker, "Laser acupuncture: past, present, and future," *Lasers in Medical Science*, vol. 19, no. 2, pp. 69–80, 2004.
[4] A. K. Hopton, S. Curnoe, M. Kanaan, and H. Macpherson, "Acupuncture in practice: mapping the providers, the patients and the settings in a national cross-sectional survey," *BMJ Open*, vol. 2, no. 1, Article ID e000456, 2012.
[5] B. Liu, B. Chen, Y. Guo, and L. Tian, "Acupuncture-a national heritage of China to the world: international clinical research advances from the past decade," *Acupuncture and Herbal Medicine*, vol. 1, no. 2, pp. 65–73, 2021.
[6] Z. Liu, S. Yan, J. Wu et al., "Acupuncture for chronic severe functional constipation: a randomized trial," *Annals of Internal Medicine*, vol. 165, no. 11, pp. 761–769, 2016.
[7] Z. Liu, Y. Liu, H. Xu et al., "Effect of electroacupuncture on urinary leakage among women with stress urinary incontinence: a randomized clinical trial," *Journal of the American Medical Association*, vol. 317, no. 24, pp. 2493–2501, 2017.
[8] J. Luo, H. Xu, and B. Liu, "Real world research: a complementary method to establish the effectiveness of acupuncture," *BMC Complementary and Alternative Medicine*, vol. 15, no. 1, p. 153, 2015.
[9] B. K. Potter, S. D. Khangura, K. Tingley, P. Chakraborty, and J. Little, "Translating rare-disease therapies into improved

care for patients and families: what are the right outcomes, designs, and engagement approaches in health-systems research?" *Genetics in Medicine*, vol. 18, no. 2, pp. 117–123, 2016.

[10] B. Y. Liu, "International registration system on clinical case of acupuncture and moxibustion: thinking and methods," in *Book of Abstracts of 8th World Conference on Acupuncture WFAS SYDNEY 2013*, 2013.

[11] D. Gao, L. He, Y. Fang et al., "International patient registry on acupuncture therapy for premature ovarian insufficiency: challenges and opportunities," *World Journal of Acupuncture-Moxibustion*, vol. 28, no. 1, pp. 1–3, 2018.

[12] European Medicines Agency, "Patient registries," https://www.ema.europa.eu/en/human-regulatory/post-authorisation/patient-registries.

[13] I. Law, "Case registry definition," https://www.lawinsider.com/dictionary/case-registry.

[14] National Center for Chronic Disease Prevention and Health Promotion, "Division of reproductive health. Maternal and infant health branch," https://stacks.cdc.gov/view/cdc/25614. 10/14/2008.

[15] Agency for Healthcare Research and Quality, "Registries for evaluating patient outcomes: A user's guide effective health care program," https://effectivehealthcare.ahrq.gov/products/registries-guide-4th-edition/users-guide,9/1/2020.

[16] P. Gavin, "The importance of natural histories for rare diseases," *Expert Opinion on Orphan Drugs*, vol. 3, no. 8, pp. 855–857, 2015.

[17] S. J. Stratton, "Research in prehospital and disaster health and medicine: developing a research objective statement," *Prehospital and Disaster Medicine*, vol. 29, no. 4, pp. 341–343, 2014.

[18] C. Wang, B. Liu, Y. Liu, L. He, H. Li, and J. Liu, "Analysis on the concepts related to adverse events and adverse reactions of acupuncture," *Zhongguo zhen jiu=Chinese acupuncture & moxibustion*, vol. 38, no. 1, pp. 87–90, 2018.

[19] Z. Yang, Y. Li, Z. Zou et al., "Does patient's expectation benefit acupuncture treatment?: a protocol for systematic review and meta-analysis," *Medicine*, vol. 100, no. 1, Article ID e24178, 2021.

[20] F. L. Bishop and G. T. Lewith, "A review of psychosocial predictors of treatment outcomes: what factors might determine the clinical success of acupuncture for pain," *Journal of acupuncture and meridian studies*, vol. 1, no. 1, pp. 1–12, 2008.

[21] A. M. O'Connor, H. A. Llewellyn-Thomas, and A. B. Flood, "Modifying unwarranted variations in health care: shared decision making using patient decision aids," *Health affairs*, vol. 6, 2004.

[22] Y. Kodra, M. Posada de la Paz, A. Coi et al., "Data quality in rare diseases registries," *Advances in Experimental Medicine and Biology*, vol. 1031, pp. 149–164, 2017.

[23] J. Flood, M. Minkler, S. Hennessey Lavery, J. Estrada, and J. Falbe, "The collective impact model and its potential for health promotion," *Health Education & Behavior*, vol. 42, no. 5, pp. 654–668, 2015.

[24] Agency for Healthcare Research and Quality, "Registries for evaluating patient outcomes: A user's guideeffective health care program," https://effectivehealthcare.ahrq.gov/products/registries-guide-3rd-edition/research.

[25] M. Gooderham and K. Papp, "Clinical trial and registry data," *Current Problems in Dermatology*, vol. 53, pp. 15–27, 2018.

[26] X. Yang, *Study on the Methods and Key Techniques of Acupuncture Case Registry*, Beijing University of Chinese Medicine, Chaoyang, China, 2018.

[27] R. A. Peppler, C. N. Long, D. L. Sisterson et al., "An overview of ARM program climate research facility data quality assurance," *The Open Atmospheric Science Journal*, vol. 2, no. 1, pp. 192–216, 2008.

[28] B. R. Wang, R. Edwards, E. A. Freiheit et al., "The pulmonary fibrosis foundation patient registry. Rationale, design, and methods," *Annals of the American Thoracic Society*, vol. 17, no. 12, pp. 1620–1628, 2020.

[29] C. S. Zheng, H. S. Yang, Y. G. Fang, M. Z. Hao, S. Y. Liu, and B. Y. Liu, "Discussion on contents and methods of quality control for acupuncture registry study," *Zhongguo zhen jiu=Chinese acupuncture & moxibustion*, vol. 40, no. 7, pp. 773–775, 2020.

[30] O. Lidegaard, C. H. Vestergaard, and M. S. Hammerum, "Quality monitoring based on data from the Danish national patient registry," *Ugeskrift for Laeger*, vol. 171, no. 6, pp. 412–415, 2009.

[31] H. Ahn, C. M. Court-Brown, M. M. McQueen, and E. H. Schemitsch, "The use of hospital registries in orthopaedic surgery," *Journal of Bone and Joint Surgery*, vol. 91, no. Supplement_3, pp. 68–72, 2009.

[32] C. Wang, J. Liu, and H. Li, "Experience of on-site audit work in quality control of registered studies on Acupuncture study and Moxibustion cases in Real World," *World Chinese medicine*, vol. 17, no. 5, pp. 625–629, 2022.

[33] J. Driscoll, G. Stacey, K. Harrison-Dening, C. Boyd, and T. Shaw, "Enhancing the quality of clinical supervision in nursing practice," *Nursing Standard*, vol. 34, no. 5, pp. 43–50, 2019.

[34] V. Boulanger, M. Schlemmer, S. Rossov, A. Seebald, and P. Gavin, "Establishing patient registries for rare diseases: rationale and challenges," *Pharmaceutical Medicine*, vol. 34, no. 3, pp. 185–190, 2020.

[35] L. Jia, L. He, Y. Zhao, and B. Liu, "Key technologies of international patient registry study for acupuncture-moxibustion based on real world," *Modernization of Traditional Chinese Medicine and Materia Medica-World Science and Technology*, vol. 19, no. 12, pp. 1920–1923, 2017.

[36] Y. X. Yang, H. S. Yang, and Y. G. Fang, "Clinical prediction model establishment of the influence of acupuncture-moxibustion on pregnancy outcome of patients with premature ovarian insufficiency based on patient registry study and LASSO-Cox model," *CJTCMP*, vol. 36, no. 04, pp. 1979–1983, 2021.

[37] H. S. Yang, Y. G. Fang, and B. Y. Liu, "Effects of acupuncture on antral follicle count in patients with premature ovarian insufficiency based on patient registry study," *CJTCMP*, vol. 35, no. 05, pp. 2276–2281, 2020.

[38] X. Wei, B. Liu, L. He et al., "Acupuncture therapy for chronic low back pain: protocol of a prospective, multi-center, registry study," *BMC Musculoskeletal Disorders*, vol. 20, no. 1, p. 488, 2019.

[39] S. Wang, L. Feng, and J. Huan, "Clinical value of Jianpishengxue tablets/granules in the treatment of iron deficiency anemia during pregnancy," *Chinese Journal of Practical Gynecology and Obstetrics*, vol. 36, no. 11, pp. 1110–1115, 2020.

[40] S. Zhou, "Comparison of the efficacy of danhong injection in the treatment of acute and convalescence of ischemic stroke," *Chinese Journal of Integrative Medicine on Cardio-Cerebrovascular Disease*, vol. 16, no. 15, pp. 2123–2127, 2018.

Hindawi
Evidence-Based Complementary and Alternative Medicine
Volume 2022, Article ID 7708376, 10 pages
https://doi.org/10.1155/2022/7708376

Research Article

Knowledge-Based Recurrent Neural Network for TCM Cerebral Palsy Diagnosis

Dongmei Li[1,2] **Jintao Qu**[1,2] **Ziwei Tian**[1,2] **Zijun Mou**[3] **Lei Zhang**[4] **and Xiaoping Zhang**[4]

[1]*School of Information Science and Technology, Beijing Forestry University, Beijing 100083, China*
[2]*Engineering Research Center for Forestry-oriented Intelligent Information Processing, National Forestry and Grassland Administration, Beijing 100083, China*
[3]*Shandong University of Traditional Chinese Medicine, Jinan 250355, Shandong, China*
[4]*National Data Center of Traditional Chinese Medicine, China Academy of Chinese Medical Sciences, Beijing 100700, China*

Correspondence should be addressed to Xiaoping Zhang; xiao_ping_zhang@139.com

Received 22 April 2022; Accepted 30 August 2022; Published 12 October 2022

Academic Editor: Huantian Cui

Cerebral palsy is one of the most prevalent neurological disorders and the most frequent cause of disability. Identifying the syndrome by patients' symptoms is the key to traditional Chinese medicine (TCM) cerebral palsy treatment. Artificial intelligence (AI) is advancing quickly in several sectors, including TCM. AI will considerably enhance the dependability and precision of diagnoses, expanding effective treatment methods' usage. Thus, for cerebral palsy, it is necessary to build a decision-making model to aid in the syndrome diagnosis process. While the recurrent neural network (RNN) model has the potential to capture the correlation between symptoms and syndromes from electronic medical records (EMRs), it lacks TCM knowledge. To make the model benefit from both TCM knowledge and EMRs, unlike the ordinary training routine, we begin by constructing a knowledge-based RNN (KBRNN) based on the cerebral palsy knowledge graph for domain knowledge. More specifically, we design an evolution algorithm for extracting knowledge in the cerebral palsy knowledge graph. Then, we embed the knowledge into tensors and inject them into the RNN. In addition, the KBRNN can benefit from the labeled EMRs. We use EMRs to fine-tune the KBRNN, which improves prediction accuracy. Our study shows that knowledge injection can effectively improve the model effect. The KBRNN can achieve 79.31% diagnostic accuracy with only knowledge injection. Moreover, the KBRNN can be further trained by the EMRs. The results show that the accuracy of fully trained KBRNN is 83.12%.

1. Introduction

Cerebral palsy is a leading cause of disability and could be challenging to cure throughout life [1]. The TCM theory plays an active role in the treatment of cerebral palsy. Symptoms are crucial in clinical diagnosis and treatment [2]. During clinical diagnosis, doctors integrate TCM theories to identify the syndrome based on patients' symptoms, which are heavily influenced by the doctor's previous experience. AI-assisted TCM diagnosis relies primarily on digital data obtained by modern electronic instruments, making TCM diagnosis more quantitative, objective, and standardized [3]. Thus, it is necessary to have a computer-aided decision-making model for the diagnosis to balance the uncertainty of human factors.

For the past two decades, owing to advancements in sensor, detector, and transducer technologies, it makes possible for AI to learn from digital information. Thus, AI-assisted TCM diagnosis has become a burgeoning field of research [4]. In earlier research, most AI approaches employed in TCM diagnosis are mostly limited to traditional machine-learning algorithms and their modified forms, such as support vector machine (SVM), random forest (RF), AdaBoost, and decision tree (DT). Wang [5] used a Bayesian classifier to generate the relationships between the human pulse and diagnostic. Zhang et al. [6] studied quantitative

correlations between diseases and the physical appearance of the human tongue. In these conventional machine learning methods, the characteristics are extracted by specialists with extensive TCM clinical expertise. Deep learning technology has grown rapidly in recent years. Unlike the traditional machine learning methods, neurons in deep learning models can acquire diagnostic properties from the initial data set. The deep learning model comprises more complex hierarchical multilayer networks of artificial neurons that can automatically discover valuable features from the original data. Hu et al. [7] proposed a classifier by using the Shannon energy envelope, Hilbert transform, and deep convolutional neural networks (DCNN) for the analysis of the human pulse. Combing the characteristics of basic image processing and deep learning, Fu et al. [8] presented a computerized tongue coating nature diagnosis method using deep neural networks. Hou et al. [9] proposed a neural network for tongue color classification, which is more practical and accurate than the traditional one. Although the previous studies have attained a high level of accuracy, they only considered single-modal data and only a portion of patients' information. Therefore, recent studies are expected to introduce more comprehensive data. Yang et al. [10] developed a novel deep neural network that uses multiview features of the gene data to identify the disease genes. Dai et al. [11] proposed a multimodal deep learning framework based on the four-diagnosis of TCM. These approaches effectively compensate for the information in a single-modal and improve the accuracy of the model.

With the rise of medical digitalization, the hospital information system deposited a considerable volume of EMR data, which completely documents the patients' situation in text form. There is increasing interest in applying machine learning techniques to decision-making models for medical diagnosis and treatment. Liang et al. [12] adopted the deep belief network (DBN) to acquire feature representation from EMR and then combined the SVM for supervised learning on the labeled data. Similarly, various supervised machine learning algorithms such as random forest and logistic regression were used in [13] to build ischemic stroke classifiers. Although these ML-based methods outperform conventional techniques such as rule-based algorithms by using massive datasets, they ignore domain-specific knowledge.

The knowledge graph (KG), once known as ontology in early research, serves as an excellent solution to inject domain-specific knowledge into the ML models. The KG is a multirelational graph composed of entities and relationships containing a large amount of prior knowledge [14, 15]. Gone et al. [16] stood on advances in graph embedding learning techniques, decomposing the medicine recommendation task into a link prediction process, and proposed the safe medicine recommendation framework. Abdelaziz et al. [17] developed a large-scalesimilarly-based framework that predicts drug-drug interactions through text and graph embedding algorithms. These studies fully exploit the domain knowledge in the knowledge graph, but they cannot benefit from the large scale of labeled data. In other words, an exceptional specialist should process not just sound professional knowledge but also extensive experience.

For the TCM cerebral palsy diagnosis model to benefit from both the knowledge graph and the EMR, we propose a two-step model called KBRNN to achieve this purpose. In the first step, we extract evidence-based diagnostic knowledge from cerebral palsy KG by using intelligent optimization algorithms and represent this knowledge as tensors. Then, we inject the knowledge into RNN by converting the tensor to the parameter of the RNN. So far, we have obtained the knowledge-based RNN (KBRNN) that can be trained with the TCM data for fine-tuning.

Our key contributions are listed as follows:

(1) We propose the knowledge-based RNN (KBRNN). Compared with the traditional methods, the KBRNN can be enhanced by the domain knowledge in KG. Also, the performance of KBRNN can be further enhanced by training on the labeled data.

(2) Under the KBRNN proposed, we design an evolutionary algorithm for knowledge extraction and give an ingenious way to represent the knowledge as tensors and inject them into the RNN.

(3) The experiment results show the accuracy of diagnosis of the untrained KBRNN which only with knowledge injections is 79.31%, and is up to 83.12% for the fully trained KBRNN.

2. Related Work

2.1. Knowledge Graph Inference and Its Applications. The knowledge graph contains the amount of prior knowledge [18], which can provide external information for various downstream tasks [19]. For medical tasks, Yang et al. [20] introduced the link prediction for the diagnosis of syndrome by dismantling medical records into multiple symptoms based on the KG. Zheng et al. [21] learned the relational embedding from nodes in KG to access medical knowledge and used them to improve the classifier's performance through the mechanism of medical knowledge attention. Zhang and Che. [22] constructed Parkinson's disease KG and KG completion methods that were leveraged to predict drug candidates. Yang et al. [23] pretrained the embeddings of entities by large-scale domain-specific corpus while learning the knowledge embeddings of entities via a joint TransC-TransE model. Lin et al. [24] combined the context provided by medical entity descriptions with the embeddings of medical entities and relations and user embeddings to learn patient similarities through a convolutional neural network. Lin et al. [25] utilized graph representation learning models to obtain the embedding vectors of the entities, then applied the embeddings to study patient similarities. These works used joint representation to bring entity and word vector space closer. However, for KGs with large numbers of entities, dealing with entities and their relationships leads to higher time complexity.

Furthermore, there is also some research about inference on the KG directly, without embedding the relations and entities. El-Shafai et al. [26] provided a method that simulates syndrome differentiation through Bayes and TF-IDF on a knowledge graph to achieve automated diagnosis in

TCM. Yao et al. [27] presented an ontology-based model that utilized ontology attributes for training the neural network for medicine side-effect prediction. Xie et al. [28] applied the TF-IDF to the TCM KG and proposed a knowledge-based syndrome reasoning model.

2.2. Neural Network with Knowledge Enhance. Lin et al. [29] proposed a trigger matching network, which trains a trigger matching network with additional annotation and uses the output as the attention of the sequence labeler. Luo et al. [30] combined a neural network with regular expressions (RE) to improve supervised learning for natural language processing. Jiang et al. [31] proposed FA-RNN, a recurrent neural network that incorporates the benefits of both neural networks and regular expression rules. Finally, Jiang et al. [32] transformed regular expressions into neural networks to combine the two ways for slot filling.

3. Methods

3.1. Framework Overview. Figure 1 shows a two-step routine to construct a KBRNN, i.e., knowledge extracting and knowledge injecting. In knowledge extraction, an evolutionary algorithm is designed to extract high-scored knowledge from the KG. A part of EMRs is utilized to score knowledge. In knowledge injecting, knowledge is converted to a tensor in the knowledge embedding module. Then, the tensor decompose module decomposes the knowledge tensor as the parameters of RNN. This gives us the KBRNN which incorporates domain knowledge.

3.2. Notation. To focus on diagnosing the syndrome by the patients' symptoms, shown in Figure 2, we reconstruct a sub-KG K based on the KG proposed by [33]. In this sub-KG K, we only retain the symptom and syndrome entities related to this research and exclude other entities such as acupoints, formula, and herb which are not related to diagnosis. For description, we give each symptom a unique and continuous ID starting from 0 and denote the symptom by "SYM"+ID. Similarly, we use "SYN"+ID to refer to a syndrome.

As a KG, K consists of entities E and relations R.

E: a set of entities. $|E| = N$. There are three types of entities (main symptom, additional symptom, and syndrome), $E = E_{\text{main\_sym}} \cup E_{\text{add\_sym}} \cup E_{\text{syn}}$.

R: a set of relations. $|R| = M$.

t: Let $e_i, e_k \in E, r_j \in R, t = (e_i, r_j, e_j)$ is the relationship between entities.

In data processing and knowledge extraction, two common operations on K should be mentioned here.

$E\_\text{Query}(SYNi, E')$: returns a set containing all the entities in E' that are connected to $SYNi$.

$E\_\text{match}(\text{sentence})$: sequential output the alias of entities which appear in sentence.

In this study, each EMR contains two parts: the descriptions of the main symptom and the additional symptom. Via data preprocessing, we splice the two parts of each EMR to get a sentence s and c convert each EMR to a symptom-level sentence by $E\_\text{match}(s)$. The EMR sentence corresponds to the EMR labeled as $SYNi$ is defined as

$$s_{SYNi} = <\text{sym}_1, \text{sym}_2, \ldots \text{sym}_i, \text{sym}_{i+1}, \ldots \text{sym}_n>, \quad (1)$$

where $s_{SYNi}[1, i] \subseteq E_{\text{main\_sym}}$, $s_{SYNi}[i+1, n] \subseteq E_{\text{add\_sym}}$, n is the length of sentence s.

3.3. Extract Knowledge from KG

3.3.1. Definitions and Task Complexity. This section details the thought to treat the knowledge extracting task as an optimization problem.

Above all, we define what the "knowledge" in the KG is. For the $SYN2$ shown in Figure 2, one of the knowledge about $SYN2$ denoted as Knowl_{SYN2} can acquire by (2) and the result as (3).

$$\text{Knowl}_{SYN2} = \left[E\_\text{Query}\left(SYN2, E_{\text{main\_sym}}\right), \left(E\_\text{Query}\left(SYN2, E_{\text{add\_sym}}\right)\right)\right], \quad (2)$$

$$\text{Knowl}_{SYN2} = [[SYM3, SYM4, SYM5], [SYM2, SYM7]]. \quad (3)$$

The (3) can be visually converted to a regular expression (RE) as (4), where "|" is the OR operator, "+" means one or more occurrences.

$$RE_{SYN2} = (SYM3 \mid SYM4 \mid SYM5)^{+} (SYM2 \mid SYM7)^{+}. \quad (4)$$

Obviously, the sentence $s_{SYN2} = <SYM5, SYM3, SYM7, SYN2>$ labeled as $SYN2$ can be recognized by RE_{SYN2}. However, the risk raised with the *REs* is that it may lead to the wrong diagnosis. For example, RE_{SYN2} may also recognize the sentence $s_{SYN3} = <SYM4, SYM2, SYM7>$ labeled as $SYN3$. For this issue, it looks like a feasible method that enumerates the subsets of $E_{\text{main\_sym}}$ and $E_{\text{add\_sym}}$, then, splicing them to generate Knowl_{SYN_i} as candidate solutions and filtering the useful Knowl_{SYNi} with the verification of EMR sentences for each syndrome. But the time complexity is as high as $O(2^{|E_{\text{main\_sym}}|} \times 2^{|E_{\text{add\_sym}}|}) = O(2^{|E_{\text{main\_sym}}|+|E_{\text{add\_sym}}|}) \approx O(2^{|E|}) = O(2^N)$. Fortunately, too much knowledge injection complicates the diagnosis model, which will be discussed further in Section 3.4.2. Thus, for a specific syndrome named $SYNi$ and a Knowl_{SYNi} scoring function V, it is enough to find the "top-k Knowl_{SYNi}" corresponding to the k highest score Knowl_{SYNi} from all the Knowl_{SYNi} of each syndrome.

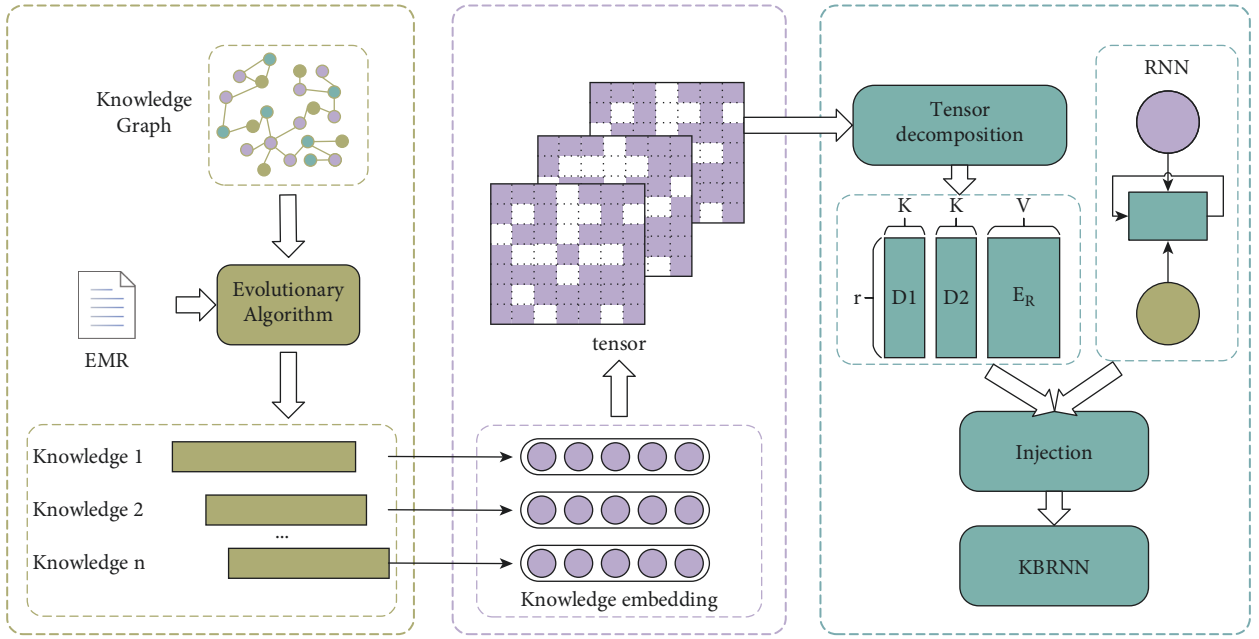

Figure 1: The model structure of KBRNN.

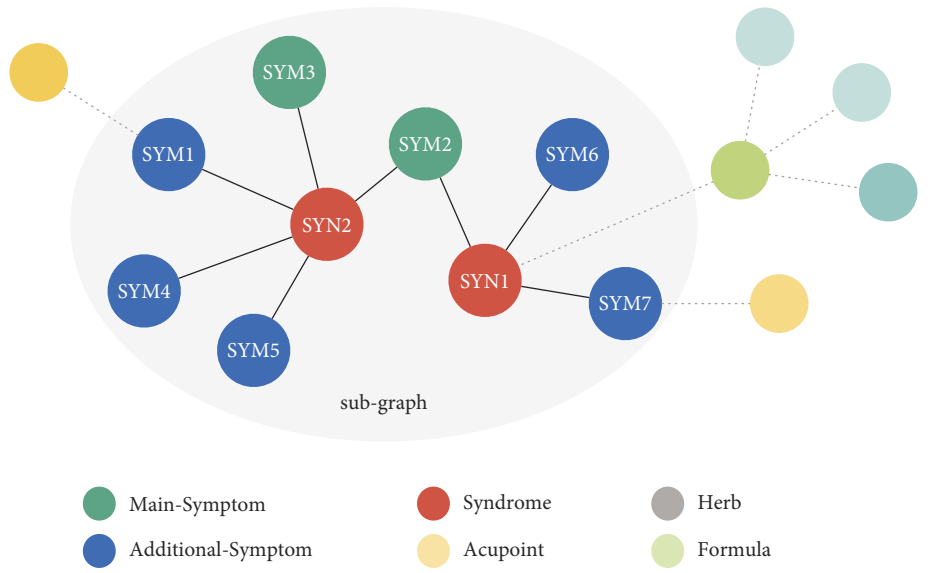

Figure 2: Structure of the knowledge graph.

By the well-performance of the evolutionary algorithm in searching for relative optimal solutions from the large solution space, we design an evolutionary algorithm for knowledge extraction. Figure 3 shows the main steps of the algorithm.

Our knowledge extraction method via evolutionary algorithms is based on the combination of two well-known expansions to the standard genetic strategy. On the one hand, we apply repeated reinitializations of the candidate solution when it reaches a state of stagnation. On the other hand, we utilize parallel computing in the process of evolution. While the former effectively overcomes the evolutionary algorithm's difficulty of falling into local optimal, the latter significantly improves the efficiency by allowing parallel calculation of the score of each solution. Moreover, assigning individuals to different computational cores can be viewed as a strategy for multiple population evolution, optimizing the algorithm's robustness.

There are two problem-specific modules in evolutionary algorithms, i.e., generator and evaluator. The following sections detail their specific implementation.

3.3.2. Generator. The generator module creates the initial set of Knowl_{SYN_i} as candidate solutions for $SYNi$. A candidate

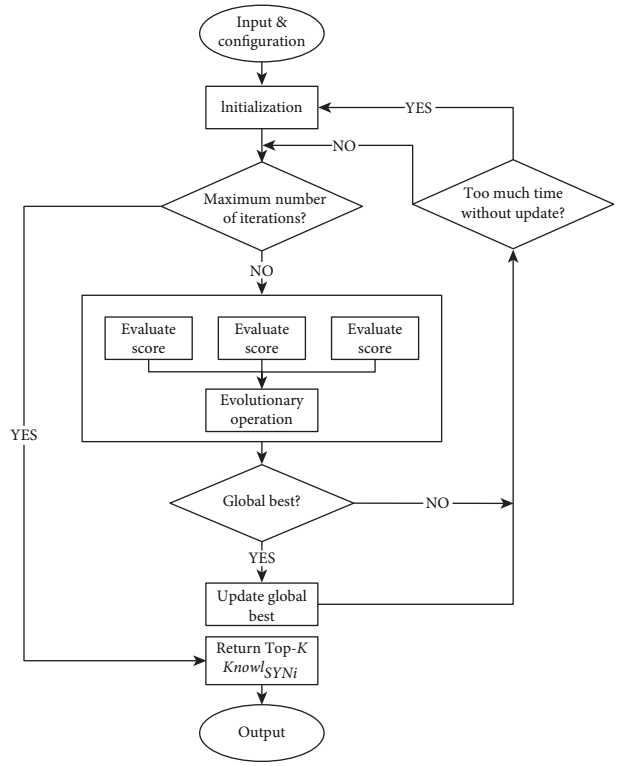

Figure 3: The steps of the evolutionary algorithm.

solution corresponding to a Knowl$_{SYNi}$ can be defined as a triple $\tau = <\varphi, \psi, v>$, let $|E_{\text{main\_sym}} \cup E_{\text{add\_sym}}| = m$.

(i) $\varphi \in \{0,1\}^m$: main symptom vector, $\phi[j] = 1$ if $SYMj$ is selected, else $\phi[j] = 0$.

(ii) $\psi \in \{0,1\}^m$: additional symptom vector, $\psi[j] = 1$ if $SYMj$ is selected, else $\psi[j] = 0$.

(iii) $v \in \mathbb{R}$: the score of such solution, calculated by using the evaluator module. Initialize to 0.

The generator generates a list of $\tau_r = <\phi_r, \psi_r, 0>$ denoted by $\Gamma = [\tau_0, \tau_1, \tau_2, \ldots, \tau_{l-1}]$ by initializing the ϕ_i and ψ_i randomly, where l is the length of Γ, $l > k$, $0 \le r < l$.

3.3.3. Evaluator. The evaluator calculates the score of each τ in Γ. We select n EMR sentences as the test case to compute the score of τ. This section will detail the scoring algorithm.

For a syndrome aliased $SYNi$, the evaluator divides the n EMR sentences into two disjoint sets denoted by EMR_{true} and EMR_{false}, where let $|EMR_{\text{true}}| = a, |EMR_{\text{false}}| = b$, $a + b = n$. A sentence is divided into EMR_{true} if and only if it is labeled as $SYNi$.

By these, variables t_r, f_r, c_r about solution $\tau_r = <\varphi_r, \psi_r, v_r>$ can be defined as follows:

(i) $t_r \in \mathbb{N}$: the number of sentences in EMR_{true} which can be recognized by τ_r

(ii) $f_r \in \mathbb{N}$: the number of sentences in EMR_{false} which can be recognized by τ_r

(iii) $c_r \in \mathbb{N}$: the number of symptoms in τ_r

As explained in Section 3.3.1, a high-score solution corresponding to an RE that recognizes the maximum number of s_{SYNi} while maintaining a minimal number of symptoms. In addition, misrecognition is not allowed. This provides us with the fundamental form of the scoring function equation.

$$V(\tau_r) = \frac{t_r}{c_r} \times 1_{N^+}(f_r), \tag{5}$$

where 1_{N^+} is the indicator function, $1_{N^+}(f_r) = 1$ if $f_r \in N^+$, else $1_{\mathbb{N}^+}(f_r) = 0$.

c_r can be calculated as equation.

$$c_r = \sum_{i=0}^{m-1} \phi[i] + \psi[i]. \tag{6}$$

The following describes the calculation of t_r and f_r. We maintain two matrices TP, FP with the following rules.

(i) $TP \in \{0,1\}^{a \times m}$: $TP[i][j] = 1$ if the $SYMj$ in the ith sentence of EMR_{true}, otherwise $TP[i][j] = 0$

(ii) $TF \in \{0,1\}^{b \times m}$: $TF[i][j] = 1$ if the $SYMj$ in the ith sentence of EMR_{false}, otherwise $TF[i][j] = 1$

Then, we obtain t_r and f_r from equation (7) and equation (8), respectively.

$$t_r = \sum_{i=0}^{a-1} 1_{N^+}\left\{\left[TP[i] - (\phi_r + \psi_r) \circ TP[i]\right] \times A^T\right\}, \quad (7)$$

$$f_r = \sum_{i=0}^{b-1} 1_{N^+}\left\{\left[FP[i] - (\phi_r + \psi_r) \circ FP[i]\right] \times A^T\right\}, \quad (8)$$

where $\circ$ denotes element-wise product and $A \in [1]^m$.

3.4. Convert the Knowledge to KBRNN. By the knowledge extraction algorithm details in Section 3.3, we get the top-k Knowl_{SYNi} for each syndrome. A Knowl_{SYNi} can be converted to an RE as (3)and (4) details in Section 3.3.1. We formally take the syndrome diagnosis task as a text classification problem, i.e., given an EMR sentence as the input of KBRNN, the output is the syndrome corresponding to the sentence.

For this task, as usual, we further process the EMR sentences as follows: we add the "BOS" and "EOS" at both ends of each EMR sentence as the mark of the start and end. We fill the sentence with "PAD"s to make all the sentences of the same length. Accordingly, to ensure that the RE corresponding to the Knowl_{SYNi} can recognize these new sentences, we add the \$* at both ends of RE, while \$ is the wildcard, and * is the Kleene star operator. Take (3) as an example. The equation (4) corresponding to (3) can be rewritten as the following equation:

$$RE_{SYN2} = \$^*(SYM3 \mid SYM4 \mid SYM5)^+ (SYM2 \mid SYM7)^+ \quad (9)$$

In the following section, we illustrate the implementation of the KBRNN, which is generated by injecting Knowl_{SYNi} into RNN.

3.4.1. Embedding the Knowledge via Finite-State Automaton. Finite-State Automaton (FSA) is an abstract model of computation, which can change from one state to another in response to some inputs. The FSA can be used to recognize sentences. Given a sentence $s = <'BOS', \text{sym}_1, \text{sym}_2, \text{sym3}, \ldots, \text{sym}_n, 'EOS'>$, an FSA Λ, we feed the elements of s into Λ in order. Λ recognizes s if and only if the state transition sequence starts from the start state and ends with a final state.

There are two types of FSA: nondeterministic finite automaton (NFA) and deterministic finite automaton (DFA). The "deterministic" indicates that by giving the state an input, there is a unique transition to the next state. With Thompson's construction algorithm [34], an RE can be converted into an NFA. Then, the NFA can be converted to a unique DFA with a minimum number of states called m-DFA by the power set construction algorithm and the DFA minimization algorithm.

For $k \times |E_{syn}|\text{Knowl}_{SYNi}$ obtained by the algorithm in Section 3.3, each Knowl_{SYNi} can be converted to an m-DFA. Then, we merge all the m-DFAs by adding a new start state q_ϵ and adding empty transitions from q_ϵ to all start states of m-DFAs. This new FSA is denoted as $\mathscr{A}$, which can be defined formally as a 5-tuple: $\mathscr{A} = <Q, \Sigma, \delta, q_\varepsilon, F'>$.

Q: a nonempty, finite set of states. Let $|Q| = K$.

Σ: a nonempty, finite set of input vocabulary. Let $|\Sigma| = V$, $V \propto |E_{sym}|$.

δ: transfer function, $\delta(q, \sigma) = p(p, q \in Q, \sigma \in \Sigma)$.

q_ϵ: the start state, $q_\epsilon \in Q$.

F': a nonempty, finite set of final states, $F' \subseteq Q$.

Based on the above definition, we can represent $\mathscr{A}$ equivalently by matrixes T, S, F.

$T \in \{0,1\}^{V \times K \times K}$: the transfer matrix, $T[\sigma, i, j] = 1$ if the state q_i can transit to q_j when input a vocabulary σ, otherwise 0. $(q_i, q_j \in Q, \sigma \in \Sigma)$.

$S \in \{0,1\}^K$: $S[i] = 1$ if q_ϵ can transit to q_i directly, otherwise 0.

$F \in \{0,1\}^K$: $F[i] = 1$ if $q_i \in F'$, otherwise 0.

Now, we obtain the knowledge embedding $\langle T, S, F \rangle$.

3.4.2. Inject the Knowledge Embedding into RNN. For a sentence $s = <s_1, s_2, s_3 \ldots, s_x>$, the $\text{Out}(s)$ denotes the number of s recognized by m-DFAs, which can be expressed as the following equation:

$$\text{Out}(s) = S^T \cdot \left(\prod_{i=1}^{x} T[s_i]\right) \cdot F. \quad (10)$$

Here, we extend the approach in [31], which used canonical polyadic decomposition (CPD) to decompose T into $E_R \in R^{V \times r}, D_1 \in R^{K \times r}, D_2 \in R^{K \times r}$, where r is a hyperparameter. As the study in [31], the decomposition is approximate when the r converges to the rank of T, and if r is too large, it may lead to a higher space complexity. In this work, the rank of T is positive to the number of symptoms in Knowl_{SYNi}. That is why, we must maintain a minimum number of symptoms in Knowl_{SYNi}.

E_R has a dimension equal to the size of the input set Σ, which can be considered as the word embedding of each input word. In this work, we integrate the BERT [35] embedding into E_R. Let w_t be the word embedding of s_t, u_t be the 768-dim word embedding generated by using bert-base-chinese, and v_t be the embedding of s_t in E_r. The BERT embedding can be integrated by equation (11). Here, $\beta \in [0, 1]$ is a hyperparameter, and $G \in R^{D \times r}$ is a trainable matrix.

$$w_t = \beta v_t + (1 - \beta) u_t G. \quad (11)$$

With the CPD result, the equation (10) can be rewritten to the recurrent form similar to the formal definition of RNN as the following equation:

$$\begin{aligned} a &= (h_{t-1} \cdot D_1) \circ w_t, h_0 = S, \\ h_t &= a \cdot D_2^T, \\ \text{Out}(s) &= h_x \cdot F. \end{aligned} \quad (12)$$

So far, we have obtained the RNN injected with knowledge.

4. Experiments and Results

4.1. Datasets. We collect the dataset from a project by the National Key Research and Development Program of the Chinese Academy of Traditional Chinese Medicine, "Chinese Medicine Data Center and Health Cloud Platform Building." The EMR data are mainly from the Hospital Information System (HIS), which includes admission records, course records, discharge summaries, and medical records of cerebral palsy patients within a specific time frame. These data come from clinically valid cases and have been desensitized to protect patients' private information.

The original EMR data has several flaws, including a nonstandard format and diverse expression. A team of professionals is invited to tag the EMR data manually so that it may be organized into structured data for further research. Data tagging assumes the form of two-person cooperation to prevent errors caused by the limited expertise of a single individual. There remain nonstandard data in the structured data after the data tagging process. For instance, a particular symptom may have several distinct expressions. In data standardization, numerous professional words are first standardized and sorted out collaboratively by a group of individuals. Then, a medical specialist induces the standard terms included in the medical records. In the end, the standardization of 988 symptoms and 15 syndromes was achieved. According to traditional Chinese medicine, these symptoms may be further subdivided into main symptoms and additional symptoms. The main symptoms might generally represent the patients' overall condition, but the additional symptoms relate to complications, which is a significant diagnostic criterion for syndrome kinds.

Thus, we obtained 5514 labeled diagnostic records from 1755 patients. Each record has three fields, main symptoms, additional symptoms, and syndrome as the label.

4.2. Experimental Steps. We divide the EMR dataset randomly into the following four parts:

(i) Pre-set (20%): the pretrained dataset that engages in the scoring of knowledge in the knowledge extraction algorithm

(ii) Train-set (50%): train dataset, the dataset used for training models

(iii) Dev-set (20%): validation dataset, a set of examples used to tune hyperparameters

(iv) Test-set (10%): test dataset, a dataset for testing the performance of the trained model

During the knowledge extraction phase, we execute the evolutionary algorithm and utilize pre-set data for knowledge scoring and obtain top-k Knowl_{SYNi} ($k = 6$ in practice) for each syndrome. We removed some Knowl_{SYNi} that scored poorly, which is caused by the insufficiency of the corresponding syndromes' sample sizes.

Table 1: The classification accuracy of the KBRNN and baselines.

	Preset	Preset + 50% train-set	Preset + 100% train-set
KBRNN	79.31	82.03	83.12
RNN	44.28	71.32	78.03
LSTM	45.01	76.04	79.49
GRU	45.19	76.22	79.85
Bi-RNN	44.64	76.59	82.39
Bi-LSTM	45.74	77.13	80.40
Bi-GRU	45.91	79.85	82.58
CNN	47.37	79.67	81.67
DAN	48.09	80.21	81.85

During knowledge embedding and injecting, we obtain an untrained KBRNN that has not been trained on the train-set. We adopt some conventional machine learning models which are frequently used in text classification as baselines and compare them with KBRNN. For each baseline, we feed the hidden representation produced by these models into a multilayer perceptron (MLP) and use the cross-entropy loss as the objective function.

4.3. Experimental Results. We compare KBRNN with RNN [36], LSTM [37], GRU [38], 4-layer CNN [39], 4-layer DAN [40] as well as their bidirectional variants. We use the cross-entropy loss as the objective function and input the hidden representation generated by these models into a 3-layer MLP to obtain the label logits. For each dataset, we tune the learning rates from $[0.01, 0.005, 0.001, 0.0005, 0.0001]$ and the number of hidden states in [50, 100, 150, 200]. Two potential benefits are explored as follows:

(1) The contribution of knowledge extraction to KBRNN: we use the pre-set as the training set of baselines and compare the performance of untrained KBRNN and baselines on the test set

(2) The ability of KBRNN to benefit from labeled data: we utilize both the pre-set and the train-set (50%, 100%) as the training set and fine-tune the untrained KBRNN with the train-set

Table 1 displays the classification accuracy of the KBRNN and baseline models on the test-set after training with varying amounts of training data. The KBRNN can achieve 79.31% diagnostic accuracy with only injecting the knowledge extracted from the KG based on pre-set and rises to 83.12% with sufficient training based on the 100% train-set.

The result shows that the untrained KBRNN outperforms all the other baselines which are only trained on the pre-set. It is also better than some of the baselines trained with 50% of the train-set (Figure 4.). We believe that KBRNN obtains considerable a priori knowledge from the knowledge graph through injection. The classification result on the full samples by using the fully trained KBRNN is shown as the confusion matrix in Figure 5, which provides a good insight into how often samples of each fifteen syndromes are correctly classified or misclassified by the proposed model. We can find that the number of samples varies greatly in each syndrome type, and the true positive rate

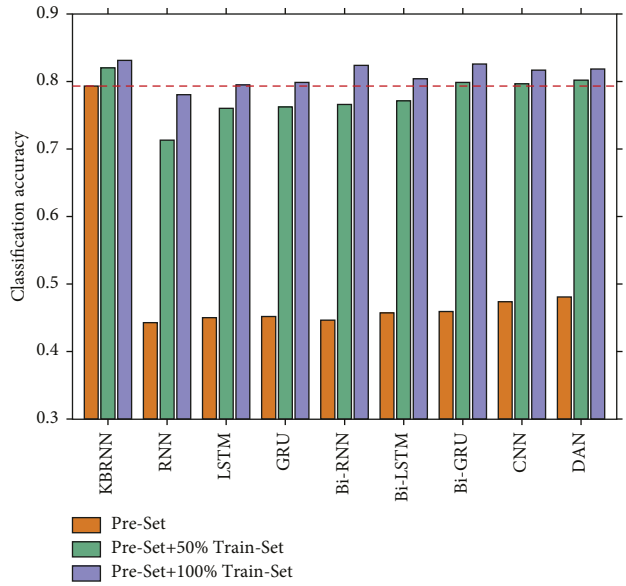

Figure 4: The untrained KBRNN outperforms some of the full-trained baselines.

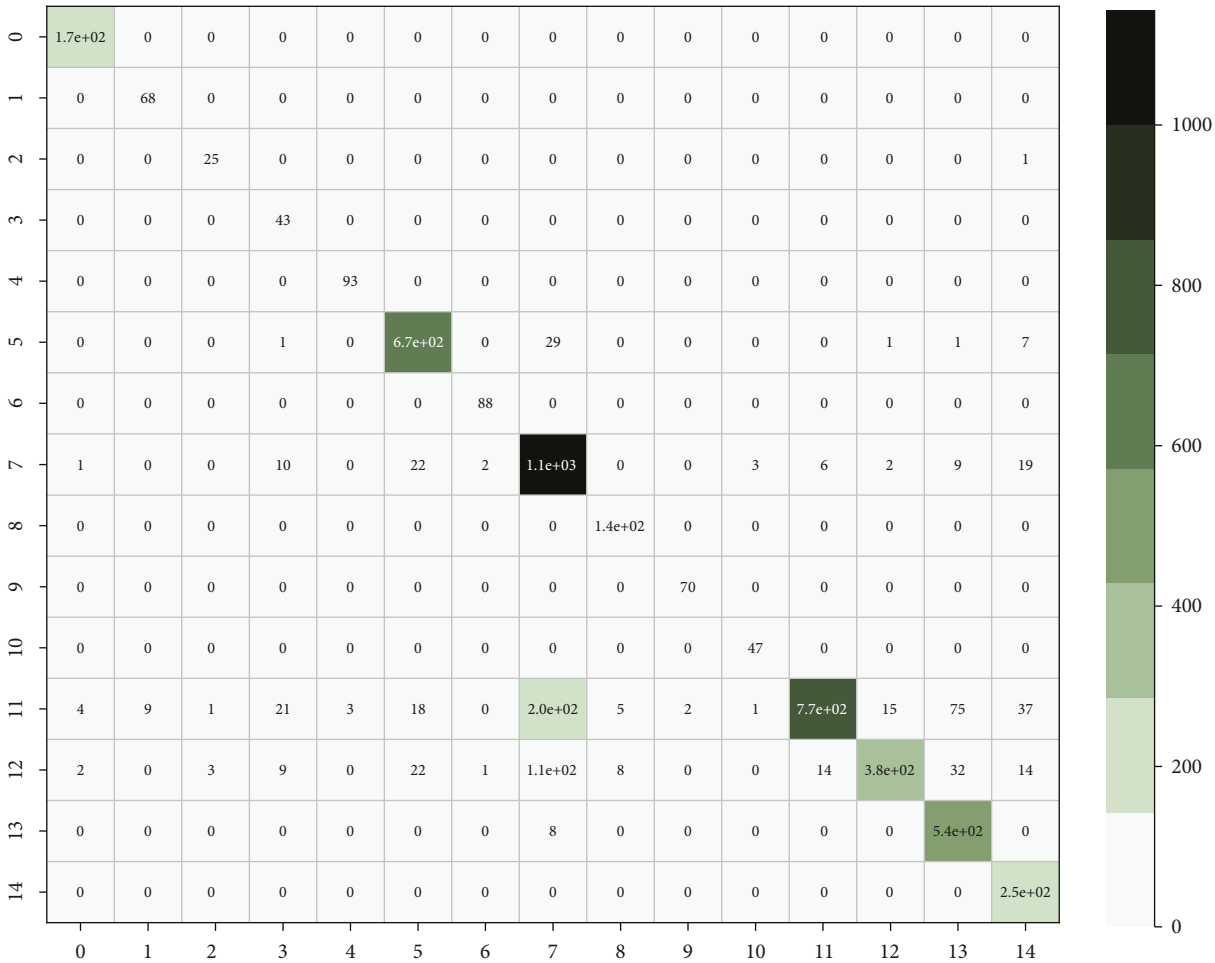

Figure 5: Confusion matrix of the classification result by using the fully trained KBRNN for all the samples.

could be maintained at a high level even for the syndrome with a large number of samples. As with other models, KBRNN can benefit from expanding the training set while keeping accuracy benefits.

5. Discussion and Conclusions

TCM, as a complementary field of medicine outside the modern medicine system, has played a significant role in cerebral palsy syndrome diagnosis. In this work, we propose a knowledge-based RNN (KBRNN) for cerebral palsy syndrome diagnosis. Our major contribution is building an evolutionary algorithm to extract the diagnosis knowledge from the KG. In particular, we also present the method of injecting the TCM knowledge into the RNN. Compared with the simple KG inference or the rule-based methods, as a neural network model, the KBRNN can be further trained by EMR data, which makes the KBRNN more generalized. On the other hand, compared with the traditional neural network model, KBRNN can benefit from TCM knowledge. Specifically, with the help of TCM knowledge, KBRNN outperforms previous neural approaches in the scene where only a few EMRs are available, and it remains competitive in rich-resource settings.

In conclusion, KBRNN can benefit from two aspects, i.e., knowledge extracted from the cerebral palsy knowledge graph and labeled EMR. We show that KBRNN achieves higher accuracy in syndrome diagnostic tasks only with knowledge injection. Moreover, the performance of KBRNN can be further improved after training with a large amount of labeled EMR, which outperforms the current model.

Data Availability

All data included in this study are available upon request by contact with the corresponding author.

Conflicts of Interest

The authors declare that they have no conflicts of interest.

Acknowledgments

This work was supported by the CACMS Innovation Fund (CI2021A00512) and the National Key Research and Development Program of China under grant (2017YFC1703506).

References

[1] H. K. Graham, P. Rosenbaum, and N. Paneth, "Erratum: cerebral palsy," *Nature Reviews Disease Primers*, vol. 2, no. 1, p. 1, 2016.

[2] X. Zhou, J. Menche, A.-L. Barabási, and A. Sharma, "Human symptoms–disease network," *Nature Communications*, vol. 5, no. 1, p. 4212, 2014.

[3] Y. Wang, X. Shi, L. Li, T. Efferth, and D. Shang, "The impact of artificial intelligence on traditional Chinese medicine," *The American Journal of Chinese Medicine*, vol. 49, no. 6, pp. 1297–1314, 2021.

[4] X. Zhou, S. Chen, B. Liu et al., "Development of traditional Chinese medicine clinical data warehouse for medical knowledge discovery and decision support," *Artificial Intelligence in Medicine*, vol. 48, no. 2–3, pp. 139–152, 2010.

[5] H. Wang, "A computerized diagnostic model based on naive bayesian classifier in traditional Chinese medicine," *International Conference on BioMedical Engineering and Informatics*, vol. 1, pp. 474–477, 2008.

[6] D. Zhang, B. Pang, N. Li, K. Wang, and H. Zhang, "Computerized diagnosis from tongue appearance using quantitative feature classification," *The American Journal of Chinese Medicine*, vol. 33, no. 6, pp. 859–866, 2005.

[7] X. Hu, H. Zhu, J. Xu, D. Xu, and J. Dong, "Wrist pulse signals analysis based on deep convolutional neural networks," in *Proceedings of the IEEE Conference on Computational Intelligence in Bioinformatics and Computational Biology*, pp. 1–7, IEEE, Honolulu, HI, USA, 2014.

[8] S. Fu, H. Zheng, and Z. Yang, "Computerized tongue coating nature diagnosis using convolutional neural network," in *Proceedings of the IEEE 2nd International Conference on Big Data Analysis (ICBDA)*, pp. 730–734, IEEE, Piscataway, NY, USA, 2017.

[9] J. Hou, H.-Y. Su, and B. Yan, "Classification of tongue color based on cnn," in *Proceedings of the IEEE 2nd International Conference on Big Data Analysis (ICBDA)*, pp. 725–729, IEEE, Piscataway, NY, USA, 2017.

[10] K. Yang, Y. Zheng, K. Lu et al., "PDGNet: predicting disease genes using a deep neural network with multi-view features," *IEEE/ACM Transactions on Computational Biology and Bioinformatics*, vol. 19, no. 1, pp. 575–584, 2022.

[11] Y. Dai, G. Wang, J. Dai, and O. Geman, "A multimodal deep architecture for traditional Chinese medicine diagnosis," *Concurrency and Computation: Practice and Experience*, vol. 32, no. 19, 2020.

[12] Z. Liang, J. Liu, A. Ou, H. Zhang, Z. Li, and J. X. Huang, "Deep generative learning for automated EHR diagnosis of traditional Chinese medicine," *Computer Methods and Programs in Biomedicine*, vol. 174, pp. 17–23, 2019.

[13] S.-F. Sung, C.-Y. Lin, and Y.-H. Hu, "EMR-Based phenotyping of ischemic stroke using supervised machine learning and text mining techniques," *IEEE Journal of Biomedical and Health Informatics*, vol. 24, no. 10, pp. 2922–2931, 2020.

[14] X. Chen, S. Jia, and Y. Xiang, "A review: knowledge reasoning over knowledge graph," *Expert Systems with Applications*, vol. 141, 2020.

[15] S. Ji, S. Pan, E. Cambria, P. Marttinen, and P. S. Yu, "A survey on knowledge graphs: representation, acquisition, and applications," *IEEE Transactions on Neural Networks and Learning Systems*, vol. 33, no. 2, pp. 494–514, 2022.

[16] F. Gong, M. Wang, H. Wang, S. Wang, and M. Liu, "SMR: medical knowledge graph embedding for safe medicine recommendation," *Big Data Research*, vol. 23, 2021.

[17] I. Abdelaziz, A. Fokoue, O. Hassanzadeh, P. Zhang, and M. Sadoghi, "Large-Scale structural and textual similarity-based mining of knowledge graph to predict drug-drug interactions," *Journal of Web Semantics*, vol. 44, pp. 104–117, 2017.

[18] W. Liu, P. Zhou, Z. Zhao et al., "K-BERT: enabling language representation with knowledge graph," *Proceedings of the AAAI Conference on Artificial Intelligence*, vol. 34, no. 3, pp. 2901–2908, 2020.

[19] H. Wang, H. Ren, and J. Leskovec, "Relational message passing for knowledge graph completion," 2021, https://arxiv.org/abs/2002.06757.

[20] R. Yang, Q. Ye, C. Cheng, S. Zhang, Y. Lan, and J. Zou, "Decision-making system for the diagnosis of syndrome based on traditional Chinese medicine knowledge graph," *Evidence-based Complementary and Alternative Medicine*, vol. 9, 2022.
[21] W. Zheng, L. Yan, C. Gou et al., "Pay attention to doctor–patient dialogues: multi-modal knowledge graph attention image-text embedding for COVID-19 diagnosis," *Information Fusion*, vol. 75, pp. 168–185, 2021.
[22] X. Zhang and C. Che, "Drug repurposing for Parkinson's disease by integrating knowledge graph completion model and knowledge fusion of medical literature," *Future Internet*, vol. 13, no. 1, 2021.
[23] Y. Yang, X. Yin, and H. Yang, *KGSynNet: A Novel Entity Synonyms Discovery Framework with Knowledge Graph*, Springer, New York, NY, USA, 2021.
[24] Z. Lin, D. Yang, and X. Yin, "Patient similarity via joint embeddings of medical knowledge graph and medical entity descriptions," *IEEE Access*, vol. 8, pp. 156663–156676, 2020.
[25] Z. Lin, D. Yang, H. Jiang, and H. Yin, "Learning patient similarity via heterogeneous medical knowledge graph embedding," *IAENG International Journal of Computer Science*, vol. 48, 2021.
[26] W. El-Shafai, A. A Mahmoud, E. S. M El-Rabaie et al., "Traditional Chinese medicine automated diagnosis based on knowledge graph reasoning," *Computers, Materials and Continua*, vol. 71, no. 1, pp. 159–170, 2022.
[27] Y. Yao, Z. Wang, L. Li et al., "An ontology-based artificial intelligence model for medicine side-effect prediction: taking traditional Chinese medicine as an example," *Computational and Mathematical Methods in Medicine*, vol. 7, 2019.
[28] Y. Xie, L. Hu, X. Chen, J. Feng, and D. Zhang, "Auxiliary diagnosis based on the knowledge graph of TCM syndrome," *Computers, Materials and Continua*, vol. 65, no. 1, pp. 481–494, 2020.
[29] B. Y. Lin, D.-H. Lee, and M. Shen, "TriggerNER: learning with entity triggers as explanations for named entity recognition," 2020, https://aclanthology.org/2020.acl-main.752.
[30] B. Luo, Y. Feng, and Z. Wang, "Marrying up regular expressions with neural networks: a case study for spoken language understanding," 2018, https://arxiv.org/abs/1805.05588.
[31] C. Jiang, Y. Zhao, S. Chu, L. Shen, and K. Tu, "Cold-start and interpretability: turning regular expressions into trainable recurrent neural networks," 2020, https://aclanthology.org/2020.emnlp-main.258.
[32] C. Jiang, Z. Jin, and K. Tu, "Neuralizing regular expressions for slot filling," 2021, https://aclanthology.org/2021.emnlp-main.747.
[33] Z. Mou, "Study on the construction of tcm diagnosis and treatment knowledge map and the dominance of tacit knowledge in children with cerebral palsy," *Chinese Academy Of Traditional Chinese Medicine*, vol. 33, 2021.
[34] K. Thompson, "Programming Techniques: regular expression search algorithm," *Communications of the ACM*, vol. 11, no. 6, pp. 419–422, 1968.
[35] J. Devlin, M.-W. Chang, K. Lee, and K. Toutanova, "Bert: pre-training of deep bidirectional transformers for language understanding," 2019, https://arxiv.org/abs/1810.04805.
[36] J. L. Elman, "Finding structure in time," *Cognitive Science*, vol. 14, no. 2, pp. 179–211, 1990.
[37] S. Hochreiter and J. Schmidhuber, "Long short-term memory," *Neural Computation*, vol. 9, no. 8, pp. 1735–1780, 1997.
[38] J. Chung, C. Gulcehre, K. Cho, and Y. Bengio, "Empirical evaluation of gated recurrent neural networks on sequence modeling," 2014, https://arxiv.org/abs/1412.3555.
[39] Y. Kim, "Convolutional neural networks for sentence classification," 2014, https://arxiv.org/abs/1408.5882.
[40] M. Iyyer, V. Manjunatha, J. Boyd-Graber, and H. Daumé, "Deep unordered composition rivals syntactic methods for text classification," 2015, https://aclanthology.org/P15-1162.

Hindawi
Evidence-Based Complementary and Alternative Medicine
Volume 2022, Article ID 6016757, 13 pages
https://doi.org/10.1155/2022/6016757

Review Article

Meta-Analysis on the Efficacy of Traditional Chinese Medicine Decoction in the Treatment of Cardiac Neurosis Complicated with Depression and Anxiety

Linjie Xu,[1,2] **Dazhuo Shi**,[1] **and Ying Zhang**[1]

[1]*National Clinical Research Center for Chinese Medicine Cardiology, Xiyuan Hospital of China Academy of Chinese Medical Sciences, Beijing 100091, China*
[2]*Graduate School of Beijing University of Traditional Chinese Medicine, Beijing 100029, China*

Correspondence should be addressed to Ying Zhang; echo993272@sina.com

Received 8 April 2022; Accepted 30 August 2022; Published 23 September 2022

Academic Editor: Yonghong Peng

Objective. To analyze and evaluate the effectiveness of traditional Chinese medicine decoction (TCMD) in the treatment of cardiac neurosis (CN) complicated with depression and anxiety. *Methods*. Relevant literature on TCMD in the treatment of CN complicated with depression and anxiety was retrieved from Chinese and English databases, and the retrieved literature was included and excluded. The quality of the retrieved literature was evaluated according to the Cochrane system, and the meta-analysis was undertaken with RevMan5.3 software. *Results*. A total of 10 papers were included, including 686 patients and 349 patients in the treatment group (131 males and 218 females), and there were 337 cases in the control group (131 males and 206 females). The results of the meta-analysis showed that compared with the control group, TCMD could significantly improve palpitation (MD = 0.78, 95% CI = 0.55–1.01, $P < 0.00001$), chest tightness/chest pain (MD = 0.53, 95% CI = 0.10–0.97, $P < 0.05$), shortness of breath (MD = 0.60, 95% CI = 0.26–0.93, $P = 0.0005$), and TCM syndrome score (MD = 5.91, 95% CI = 4.32–7.49, $P < 0.00001$), reduce resting heart rate (MD = 13.21, 95% CI = 9.01–17.40, $P < 0.00001$), and could reduce psychological scale scores, such as Zung's self-rating Depression Scale (MD = 7.90, 95% CI = 4.98–10.83, $P < 0.00001$), Zung's self-rating Anxiety Scale (MD = 6.55, 95% CI = 4.25–8.86, $P < 0.00001$), Hamilton Depression Scale (MD = 4.46, 95% CI = 3.00–5.92, $P < 0.00001$), and Hamilton Anxiety Scale (MD = 3.35, 95% CI = 1.85–4.85, $P < 0.0001$). The differences were statistically significant. Tonic drugs were commonly used; *Angelica sinensis*, *Poria cocos*, *Polygala tenuifolia*, Wild jujube kernel, and *Bupleurum* were the most frequently used traditional Chinese medicines. *Conclusion*. TCMD mainly composed of tonic and tranquilizing herbs could significantly improve the clinical symptoms of patients with CN and reduce heart rate, anxiety, and depression scores. However, the evidence grade of the clinical research was limited by the quality of the included literature, and more high-quality clinical trials are still needed for further verification. This trial was registered with PROSPERO: CRD42022312164

1. Introduction

Cardiac neurosis, also known as cardiovascular neurosis, is a psychological and physiological syndrome characterized by circulatory symptoms in the absence of underlying organic disease. The syndrome is characterized by dyspnea, precordial pain, palpitations, and shortness of breath as common symptoms. In recent years, the prevalence of CN has increased significantly, accounting for more than 30% of the total number of patients in cardiology [1, 2]. The study found that most patients with CN are mainly mental workers, and CN is most common in young and middle-aged people and more often in females than males, especially in menopausal women. [1, 3, 4].

At present, the etiology and pathogenesis of CN are not fully understood, and mental state, physical state, nervous system, genetic factors, and external environmental stimuli may all be related to the disease. Clinically, Western medical

treatment is mainly based on antidepressants, antianxiety, neuromodulators, and β-blocker drugs, which have moderate short-term effects but poor long-term efficacy.[5].

The treatment of CN in traditional Chinese medicine had formed its characteristics before modern medicine and has unique insights in clinical practice and rehabilitation methods, which have certain advantages in relieving clinical symptoms, improving quality of life, and improving function. The treatment of CN mainly focuses on clinical symptoms, such as "sleeplessness," "heart palpitation," and "depression," and is aimed at regulating the deficiency of internal organs and the imbalance of Qi mechanisms [5–7]. In this study, we investigated the efficacy of TCMD in the treatment of CN and conducted a systematic Meta-analysis, aiming to provide an evidence-based basis for the treatment of CN.

2. Methods

Our meta-analysis was conducted based on preferred Reporting Items for Systematic Reviews and Meta-Analyses (PRISMA) guidelines. Ethical approval was not required. The study protocol was registered in the PROSPERO international prospective register of systematic review (CRD42022312164).

2.1. Search Strategy. The English search terms "Chinese medicine decoction," "Chinese herb medicine," "medicinal broth," "cardiovascular neurosis," and "cardiac neurosis" were searched in Clinical Trials, MEDLINE, EMBASE, PubMed, and The Cochrane Library of Evidence-Based Medicine. And the Chinese search terms "traditional Chinese medicine decoction," "decoction," "Cardiac neurosis," "Cardiovascular neurosis," etc. were searched in China National Knowledge Internet (CNKI), China Clinical Trials Registry, Wanfang database, VIP database (VIP), and China Biomedical Literature Service. The search time range was from the earliest inclusion in the database to December 2021.

2.2. Inclusion and Exclusion Criteria

2.2.1. Inclusion Criteria. 1 Study type: randomized controlled studies, domestic and foreign studies involving "traditional Chinese medicine decoction (TCMD) for the treatment of cardiac neurosis," and the language of the literature selected for inclusion was Chinese or English. ②The study subjects should be patients with cardiac neurosis, cardiovascular dysfunction, and neurological manifestations and without organic heart disease after the examination. ③ The study subjects should be aged 14–80 years old and the syndrome type in TCM includes Qi stagnation in the heart and chest, Qi depression transforming into the fire, deficiency in the heart and spleen, and Qi and Yin deficiency; the Western medicine diagnosis should refer to the diagnostic criteria of Practical Internal Medicine (15th edition). ④ The treatment group was given TCMD treatment, and various relevant parameters were compared with the control group. ⑤ The result indicators were the Chinese medicine evidence points, heart rate analysis, and psychological scale points analysis [Zung's Depression Self-Rating Scale (SDS), Zung's Anxiety Self-Rating Scale (SAS), Hamilton Depression Scale (HAMD), Hamilton Anxiety Scale (HAMA), Somatization Self-Rating Scale (SSS), etc.].

2.2.2. Exclusion Criteria. Exclusion criteria were as follows: ① clinical trial studies with unclear diagnostic criteria, ② research subjects that do not meet the diagnostic criteria of TCM and Western medicine, and ③ repeatedly published papers with no need for clinical outcome indicators.

2.3. Quality Evaluation Criteria and Data Extraction. In this study, Cochrane systematic evaluation was used to evaluate the quality of the included literature, including eight sequential items such as random sequence generation, allocation concealment, whether to apply blinding, blinded evaluation, withdrawal/missed visit handling, outcome data integrity, selective reporting of study results and other sources of bias, and evaluation summary. Data screening extraction was done by two investigators individually and eventually combined for analysis, and any disagreement was resolved by discussion and negotiation. The main elements of the evaluation information included the following: ① whether the random assignment was used to the research group, ② whether blinded methods were utilized to evaluate treatment subjects and outcomes, ③ whether the study used allocation concealment, ④ whether complete data were reported in the included literature, and ⑤ whether there were other risks of bias.

2.4. Statistical Methods. Meta-Analysis was performed using RevMan5.3 software for the statistical analysis studied in this paper. This analysis was performed using a fixed-effects model if there was statistical homogeneity between studies ($P > 0.05$, $I^2 < 50\%$) and a random-effects model for data analysis when there was statistical heterogeneity between studies ($P < 0.05$, $I^2 > 50\%$).

2.5. Ethical Statement. All study results and data analysis in this study evaluation system were approved by the Medical Ethics Committee, so no further approval from the Medical Ethics Committee or patient consent was required.

3. Results

3.1. Search and Screening Results. In this study, a total of 31 relevant literature in English and Chinese were initially retrieved, and by excluding studies in which the diagnostic criteria did not match those of Chinese and Western medicine, a total of 10 papers with 686 patients were finally included, with 349 cases in the treatment group, including 131 male patients and 218 female patients, and 337 cases in the control group, including 131 male patients and 206 female patients. The literature screening inclusion process was shown in Figure 1, and the basic characteristics of the literature were shown in Table 1.

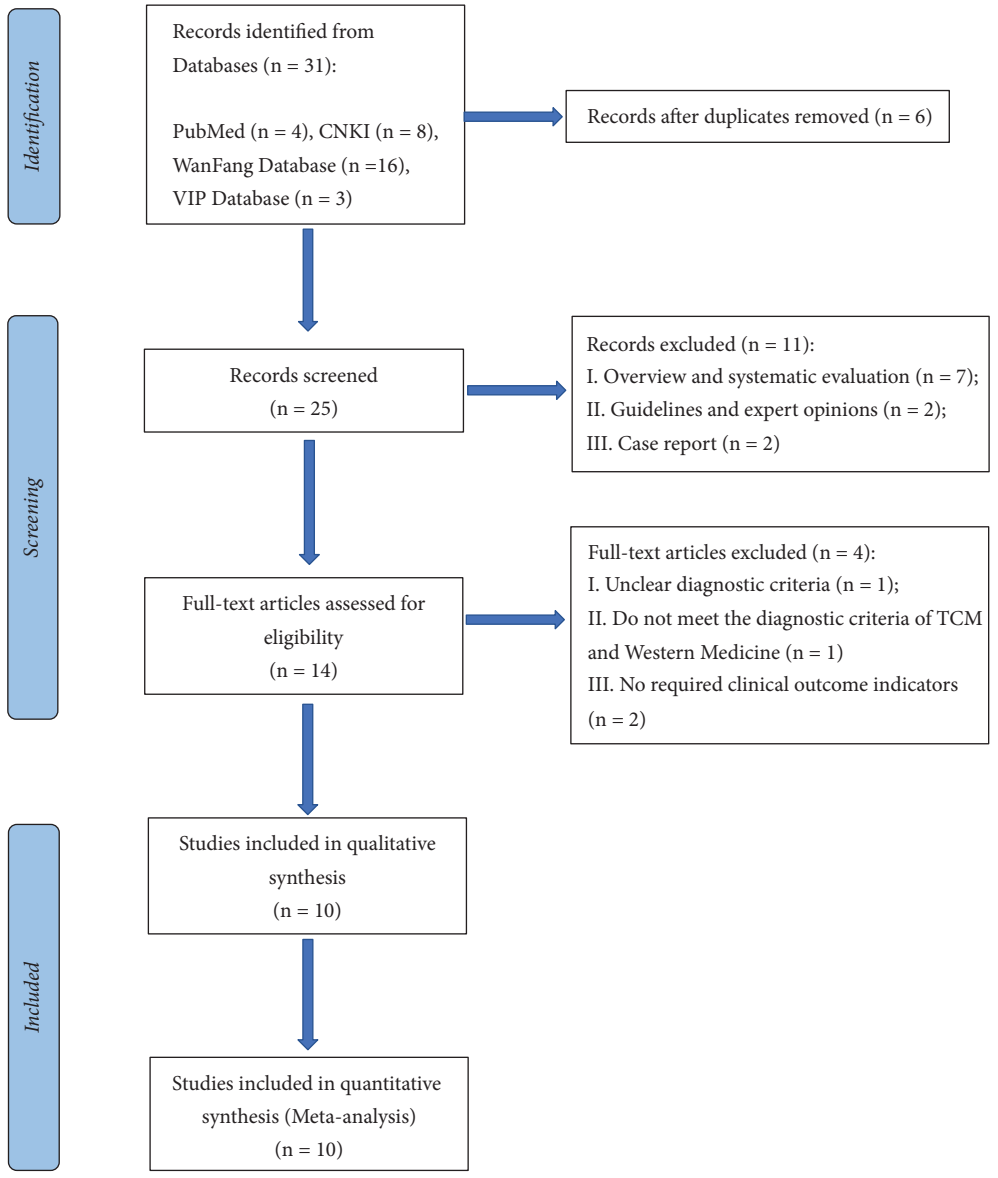

Figure 1: Flow chart of study selection and identification.

3.2. Methodological Quality. A total of 4 included papers [9, 10, 12, 16] used the random number table method, 5 papers [11, 13–15, 17] used the randomized control method, 1 paper [8] grouping method was not described, the results of the included literature were not affected by the blinded method, the results data were complete and free of bias, no allocation concealment and withdrawal from follow-up or missed visits, and 1 [8] paper had selective reporting of study results. The methodological quality of the species included literature was evaluated in Figure 2 and Table 2.

3.3. Meta-Analysis Results

3.3.1. Analysis of TCM Evidence Points

(1) Heart Palpitations. 3 papers were included in this analysis [8, 14, 17], and there was heterogeneity in the findings ($I^2 = 93\%$, $P < 0.00001$), so a random-effects model was used for the combined analysis. The results showed that the treatment group was significantly better than the control group in improving palpitation symptoms, with a statistically significant difference ($MD = 0.78$, 95% $CI = 0.55$–1.01, $P < 0.00001$), as shown in Figure 3.

(2) Chest Tightness/Chest Pain. 3 papers were included in this analysis [8, 14, 17], and there was heterogeneity in the study results ($I^2 = 98\%$, $P < 0.00001$), so a random-effects model was used for the combined analysis. The results showed that the treatment group improved chest tightness/chest pain symptoms significantly better than the control group, with a statistically significant difference ($MD = 0.53$, 95% $CI = 0.10$–0.97, $P = 0.02 < 0.05$), as shown in Figure 4.

(3) Shortness of Breath. 3 papers were included in this analysis [8, 14, 17] and there was heterogeneity in the study results ($I^2 = 98\%$, $P < 0.00001$), so a random-effects model

Table 1: Basic characteristics of the included studies.

Include studies	Years (*Y*)	Total sample/*N*		Treatment strategy		Course of treatment/ Weeks	Adverse reactions
		Treatment group (male/ female)	Control group (male/ female)	Treatment group	Control group		
Li and Jia [8]	2009	52 (20/32)	50 (20/30)	Shugan Ningxin Decoction (1 dose/d, decoct 300 ml of decoction with water and take it twice warmly in the morning and evening)	Sertraline hydrochloride tablets (oral, 50 mg/ once per night)	2/8	Yes (none in the treatment group; 7 cases in the control group)
Jiang and Zhou [9]	2015	30 (16/14)	25 (13/12)	Chaihu guizhi keel oyster Decoction (1 dose/d, add 1.5 g cinnabar to take, take it twice in the morning and evening, decoct twice and combine to obtain 400 ml decoction)	Betaloc (oral, 25 mg/time, once daily)	2/4	None
Yao [10]	2016	32 (9/23)	28 (10/18)	On the basis of the control group, jieyu decoction was added	Sertraline hydrochloride (50 mg, once/ day) + lorazepam tablets (1.0 mg, 3 times/ day) + psychotherapy	2/2	None
Liu [11]	2016	30 (7/23)	30 (5/25)	Yangxin dingji Decoction (1 dose/d, decoct 300 ml of decoction with water and take it twice warmly in the morning and evening)	Oryzanol tablets (oral, 3 times/d, 20 mg each time)	1/4	Yes (none in the treatment group; 2 cases in the control group)
Leng [12]	2018	36 (14/22)	36 (15/21)	Yangxin chaihuan Decoction (Oral, powder, 50–100 ml each time, twice/d)	Patients with high heart rate: Betaloc (oral, 47.5 mg/tablet, 1/d); Patients with insomnia: Right zopiclone tablets (oral, 3 mg/tablet/ time)	Unknown/4	None
Ma [13]	2020	30 (10/20)	30 (9/21)	Jiawei erxian decoction (decocting, taking 1 packet each time, 2 packets/ day)	Flupentixol and melitracen tablets (oral, 2 tablets/day)	1/4	Yes (none in the treatment group; 5 cases in the control group)
Wang [14]	2020	33 (17/16)	33 (18/15)	Shengxian Decoction (Granules, brewing 300 ml with warm water, oral, 2/d, 150 ml/time)	Oryzanol tablets (oral, 3 times/*d*, 20 mg/2 tablets each time)	1/4	None
Dai et al. [15]	2021	30 (9/21)	30 (10/20)	On the basis of the control group, Tianwang Buxin Decoction was added (one dose of 250 ml per day, taken in the morning and evening)	Oryzanol tablets (oral, 3 times/*d*, 20 mg/2 tablets each time)	1/4	None
Tong et al. [16]	2021	43 (16/27)	43 (18/25)	On the basis of the control group, Suanzaogen Decoction was added (decoction, 1 dose per day, taken in the morning and evening)	Oryzanol tablets (oral, 3 times/d, 20 mg/2 tablets each time) + vitamin B1 (oral, 10 mg each time, 3 times/d)	1/4	None
Zhang [17]	2021	33 (13/20)	32 (13/19)	On the basis of the control group, huanglian zhengdan decoction was added (decoction pieces of traditional Chinese medicine, each dose of decoction 300 ml, 150 ml/time, oral, 2/d)	Oryzanol tablets (oral, 3 times/*d*, 20 mg each time) + vitamin B1 (oral, 10 mg each time, 3 times/d) [patients with high heart rate: Betaloc (oral, 23.75–47.5 mg); in case of insomnia, right zopiclone tablets (oral, 2 mg)]	1/4	None

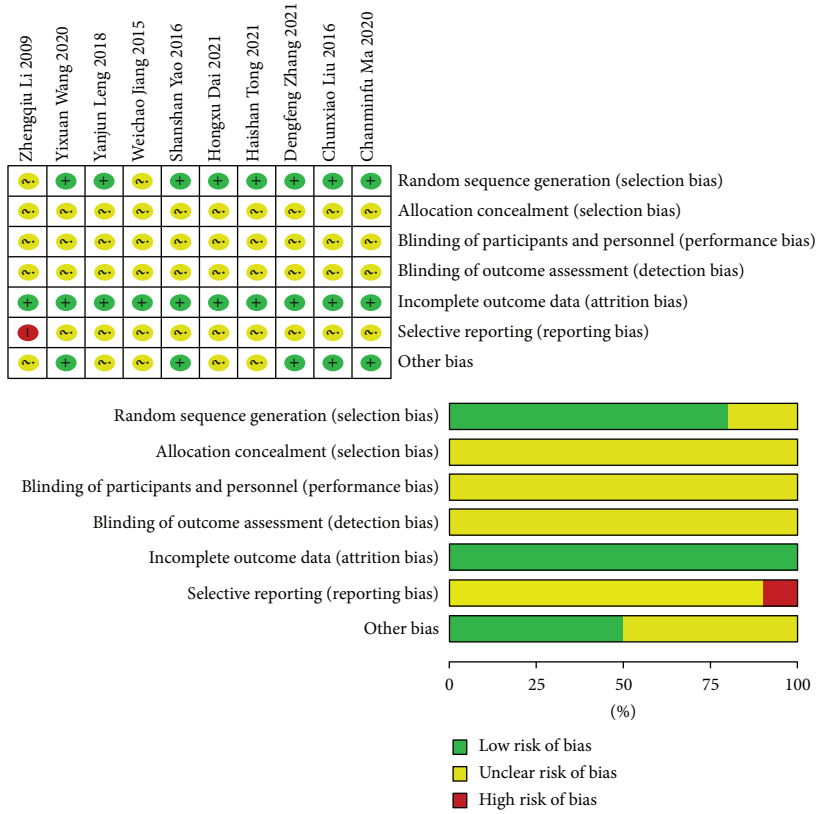

Figure 2: Risk of bias summary and graph.

was used for the combined analysis. The results showed that the treatment group improved shortness of breath symptoms significantly better than the control group, with a statistically significant difference ($MD = 0.60$, 95% $CI = 0.26$–0.93, $P = 0.0005$), as shown in Figure 5.

(4) Total TCM Evidence Score. 6 papers were included in this analysis [10–13, 15, 17] and there was heterogeneity in the study results ($I^2 = 96\%$, $P < 0.00001$), so a random-effects model was used for the combined analysis. The results showed that the treatment group outperformed the control group in terms of improvement of clinical symptoms, with a statistically significant difference ($MD = 5.91$, 95% $CI = 4.32$–7.49, $P < 0.00001$), as shown in Figure 6.

3.4. Heart Rate Analysis. 2 papers were included in this analysis [13, 15], and there was heterogeneity in the study results ($I^2 = 98\%$, $P < 0.00001$), so a random-effects model was used for the combined analysis. The results showed that the treatment group was superior to the control group in reducing resting heart rate, with a statistically significant difference ($MD = 13.21$, 95% $CI = 9.01$–17.40, $P < 0.00001$), as shown in Figure 7.

3.5. Analysis of Psychological Scale Scores

3.5.1. Zung's Self-Rating Scale for Depression (SDS). 4 papers were included in this analysis [9, 15–17], and there was heterogeneity in the findings ($I^2 = 97\%$, $P < 0.00001$), so a random-effects model was used for the combined analysis. The results showed that the treatment group outperformed the control group in terms of self-rated antidepressants, with a statistically significant difference ($MD = 7.90$, 95% $CI = 4.98$–10.83, $P < 0.00001$), as shown in Figure 8.

3.5.2. Zung's Self-Assessment Scale for Anxiety (SAS). 3 papers were included in this analysis [9, 15, 16], and there was heterogeneity in the study results ($I^2 = 93\%$, $P < 0.00001$), so a random-effects model was used for the combined analysis. The results showed that the treatment group outperformed the control group in terms of self-rated anxiolysis, with a statistically significant difference ($MD = 6.55$, 95% $CI = 4.25$–8.86, $P < 0.00001$), as shown in Figure 9.

3.5.3. Hamilton Depression Scale (HAMD). 4 papers were included in this analysis [8, 10, 11, 13], and there was heterogeneity in the study results ($I2 = 100\%$, $P < 0.00001$), so a random-effects model was used for the combined analysis. The results showed that the treatment group was superior to the control group in terms of antidepressants, with a statistically significant difference ($MD = 4.46$, 95% $CI = 3.00$–5.92, $P < 0.00001$), as shown in Figure 10.

3.5.4. Hamilton Anxiety Inventory (HAMA). 6 papers were included in this analysis [8, 10, 11, 13, 14, 17], and there was heterogeneity in the study results ($I^2 = 99\%$,

Table 2: Quality evaluation of research methodology included.

Included literature	Random sequence generation	Allocation concealment	Blind or not	Blind evaluation	Withdraw/ Lost visit handling	Result data integrity	Selective research report	Other sources of bias
Li and Jia [8]	Not described	Not described	Not	Not affected by the blind method	Unknown	Completed	Yes	No significant other bias
Jiang and Zhou [9]	Random number table method	Not described	Not	Not affected by the blind method	Unknown	Completed	No	No significant other bias
Yao [10]	Random number table method	Not described	Not	Not affected by the blind method	Unknown	Completed	No	No significant other bias
Liu [11]	Randomized controlled method	Not described	Not	Not affected by the blind method	Unknown	Completed	No	No significant other bias
Leng [12]	Random number table method	Not described	Not	Not affected by the blind method	Unknown	Completed	No	No significant other bias
Ma [13]	Randomized controlled method	Not described	Not	Not affected by the blind method	Unknown	Completed	No	No significant other bias
Wang [14]	Randomized controlled method	Not described	Not	Not affected by the blind method	Unknown	Completed	No	No significant other bias
Dai HX et al. [15]	Randomized controlled method	Not described	Not	Not affected by the blind method	Unknown	Completed	No	No significant other bias
Tong et al. [16]	Random number table method	Not described	Not	Not affected by the blind method	Unknown	Completed	No	No significant other bias
Zhang [17]	Randomized controlled method	Not described	Not	Not affected by the blind method	Unknown	Completed	No	No significant other bias

Study or Subgroup	Experimental Mean	SD	Total	Control Mean	SD	Total	Weight	Mean Difference IV, Random, 95% CI
Dengfeng Zhang 2021	1.11	0.31	52	0.21	0.01	50	36.4%	0.90 [0.82, 0.98]
Yixuan Wang 2020	2.48	0.06	33	1.87	0.17	32	37.2%	0.61 [0.55, 0.67]
Zhengqiu Li 2009	4.43	0.14	33	3.57	0.72	33	26.4%	0.86 [0.61, 1.11]
Total (95% CI)			*118*			*115*	*100.0%*	*0.78 [0.55, 1.01]*

Heterogeneity: $\tau^2 = 0.04$; $\chi^2 = 30.66$, df = 2 (P < 0.00001); $I^2 = 93\%$
Test for overall effect: Z = 6.63 (P < 0.00001)

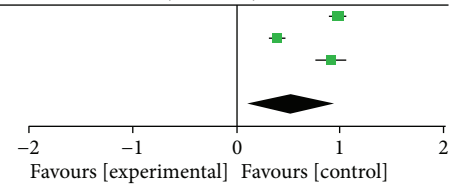

Figure 3: Forest diagram of TCMD on the change value of palpitation score before and after CN treatment.

Study or Subgroup	Experimental Mean	SD	Total	Control Mean	SD	Total	Weight	Mean Difference IV, Random, 95% CI
Dengfeng Zhang 2021	1.45	0.27	52	1.14	0.01	50	34.0%	0.31 [0.24, 0.38]
Zhengqiu Li 2009	3.15	0.54	33	2.79	0.14	33	32.2%	0.36 [0.17, 0.55]
Yixuan Wang 2020	2.48	0.07	33	1.56	0.29	32	33.7%	0.92 [0.82, 1.02]
Total (95% CI)			*118*			*115*	*100.0%*	*0.53 [0.10, 0.97]*

Heterogeneity: $\tau^2 = 0.14$; $\chi^2 = 91.32$, df = 2 (P < 0.00001); $I^2 = 98\%$
Test for overall effect: Z = 2.41 (P = 0.02)

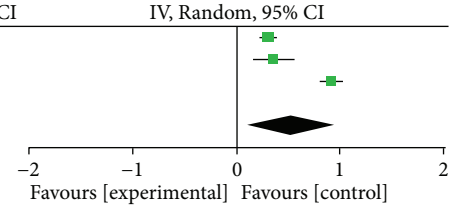

Figure 4: Forest diagram of TCMD on the change value of chest tightness and chest pain scores before and after CN treatment.

Study or Subgroup	Experimental Mean	SD	Total	Control Mean	SD	Total	Weight	Mean Difference IV, Random, 95% CI
Dengfeng Zhang 2021	0.62	0.46	52	0.08	0.01	50	32.8%	0.54 [0.41, 0.67]
Yixuan Wang 2020	1.43	0.09	33	0.56	0.12	32	34.0%	0.87 [0.82, 0.92]
Zhengqiu Li 2009	1.16	0.28	33	0.79	0.12	33	33.2%	0.37 [0.27, 0.47]
Total (95% CI)			*118*			*115*	*100.0%*	*0.60 [0.26, 0.93]*

Heterogeneity: $\tau^2 = 0.09$; $\chi^2 = 82.79$, df = 2 (P < 0.00001); $I^2 = 98\%$
Test for overall effect: Z = 3.46 (P = 0.0005)

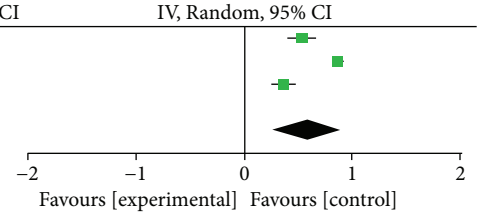

Figure 5: Forest diagram of TCMD on the change value of shortness of breath symptom score before and after CN treatment.

Study or Subgroup	Experimental Mean	SD	Total	Control Mean	SD	Total	Weight	Mean Difference IV, Random, 95% CI
Chanminfu Ma 2020	15.76	1.9	32	9.7	2.99	32	16.3%	6.06 [4.83, 7.29]
Chunxiao Liu 2016	13.61	0.37	36	6.3	1.19	36	17.9%	7.31 [6.90, 7.72]
Dengfeng Zhang 2021	15.92	4.74	30	9.1	2.44	30	14.3%	6.82 [4.91, 8.73]
Hongxu Dai 2021	13.94	0.79	32	9.9	1.42	28	1 7.6%	4.04 [3.45, 4.63]
Shanshan Yao 2016	31.2	2.08	30	23.6	2.64	30	1 6.4%	7.60 [6.40, 8.80]
Yanjun Leng 2018	13.2	1.14	30	9.3	1.4	30	17.5%	3.90 [3.25, 4.55]
Total (95% CI)			*190*			*186*	*100.0%*	*5.91 [4.32, 7.49]*

Heterogeneity: $\tau^2 = 3.62$; $\chi^2 = 129.34$, df = 5 (P < 0.00001); $I^2 = 96\%$
Test for overall effect: Z = 7.30 (P < 0.00001)

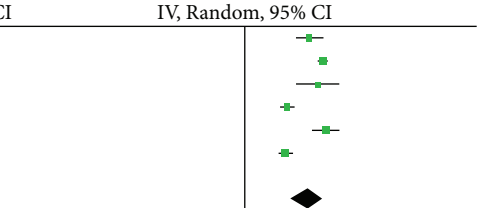

Figure 6: Forest diagram of TCM syndrome integral change value of TCMD before and after CN treatment.

Study or Subgroup	Experimental Mean	SD	Total	Control Mean	SD	Total	Weight	Mean Difference IV, Random, 95% CI
Chanminfu Ma 2020	16.26	2.09	30	5.2	1.64	30	49.8%	11.06 [10.11, 12.01]
Hongxu Dai 2021	28.07	0.91	30	12.73	2.06	30	50.2%	15.34 [14.53, 16.15]
Total (95% CI)			*60*			*60*	*100.0%*	*13.21 [9.01, 17.40]*

Heterogeneity: $\tau^2 = 8.96$; $\chi^2 = 45.31$, df = 1 (P < 0.00001); $I^2 = 98\%$
Test for overall effect: Z = 6.17 (P < 0.00001)

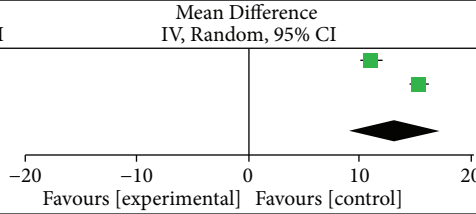

Figure 7: Forest diagram of heart rate change value of TCMD before and after CN treatment.

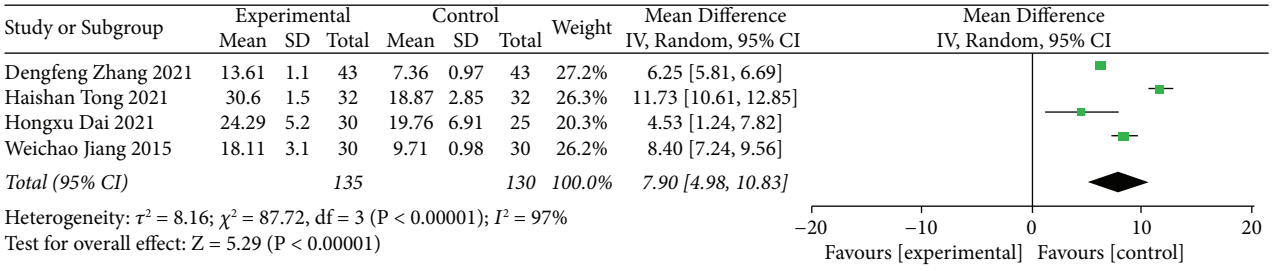

Figure 8: Forest diagram of self-rated antidepressant change value of TCMD before and after CN treatment.

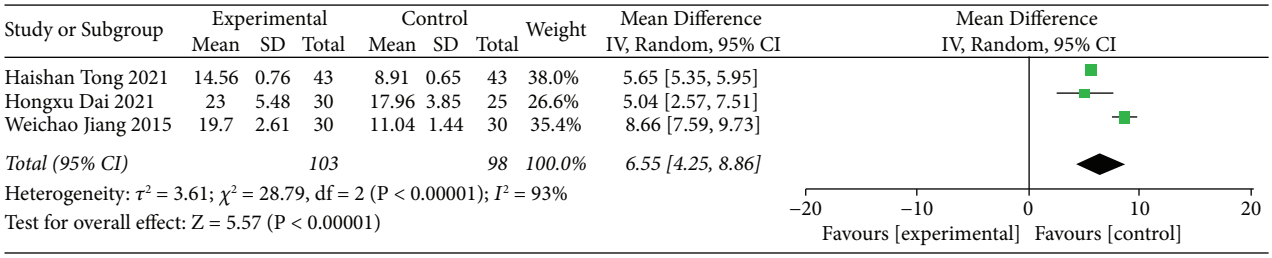

Figure 9: Forest diagram of self-rated antianxiety change value of TCMD before and after CN treatment.

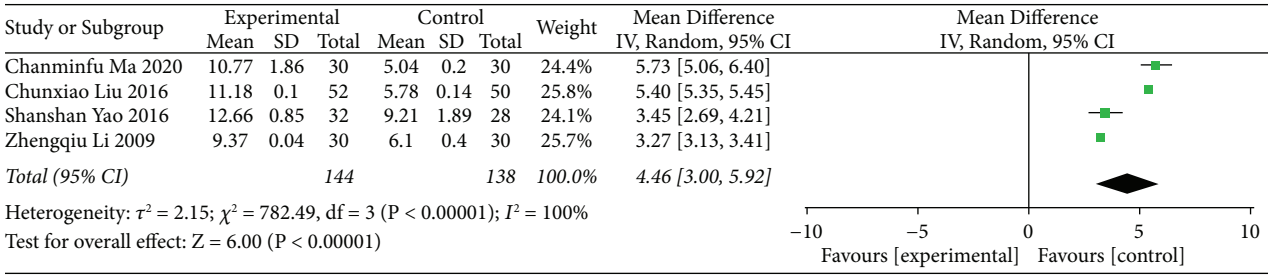

Figure 10: Forest diagram of antidepressant changes of TCMD before and after CN treatment.

$P < 0.00001$), so a random-effects model was used for the combined analysis. The results showed that the treatment group was superior to the control group in terms of anxiolysis, with a statistically significant difference ($MD = 3.35$, 95% $CI = 1.85$–4.85, $P < 0.0001$), as shown in Figure 11.

3.6. Analysis of Traditional Chinese Medicines Use. Among the 10 literature studies included in this study for the treatment of CN, 55 TCMs were used, with a total frequency of 125 times. Among them, 8 TCMs were used 4 times or more, which were *Angelica sinensis* (6, 4.8%), *Poria cocos* (6, 4.8%), *Polygala tenuifolia* (6, 4.8%), Wild jujube kernel (6, 4.8%), *Bupleurum* (6, 4.8%), White peony (5, 4.0%), Chuanxiong (4, 3.2%), Gan song (4, 3.2%), and 23 TCMs were used once, as shown in Table 3. Among them, the most frequently used drugs were tonic drugs, 29 times in total, accounting for 23.2% of the total frequency, followed by tranquilizing drugs (21, 16.8%), antipyretic drugs (14, 11.2%), and surface relieving drugs (12, 9.6%), as shown in Table 4.

4. Discussion

Cardiac neurosis is a typical psychosomatic disease of the circulatory system [18]. With the change in the modern lifestyle and the increase of social and environmental pressure, the transformation of the "Biological-Psychological-Social" medical model and various psychological factors such as anxiety and depression have been gradually emphasized in the development and regression of circulatory system diseases. CN is mainly manifested in heart palpitation, accelerated resting heart rate, chest tightness, chest pain, etc., but there are no signs of organic heart disease [2, 3]. CN mostly occurs in young and middle-aged people, more females than males, especially menopausal women, and mental workers outnumber manual workers [19]. The above somatic symptoms are related to emotion and brain function. Psychological factors are one of the key reasons, patients are usually accompanied by obvious psychological disorders such as anxiety, depression, or neurasthenia. Friedman [20] believes that the hypothalamus may be the site of CN, and the lesions in this area can cause anxiety and affect the functional regulation of many other systems.

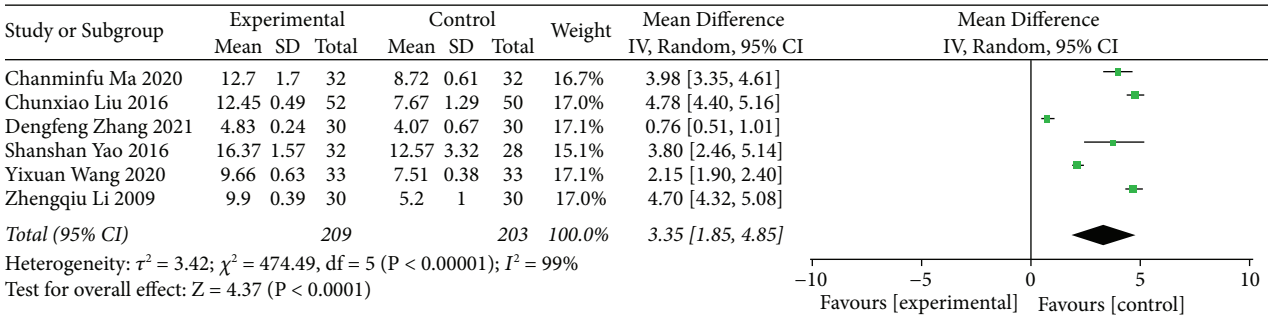

Figure 11: Forest diagram of antianxiety changes of TCMD before and after CN treatment.

Due to the lack of laboratory evidence, CN is generally diagnosed in patients with symptoms, few signs, and no organic heart disease [21]. In recent years, the incidence rate of CN has been increasing. When the psychological burden and mental pain borne by patients due to the disease are serious, it can affect their normal life and work, and the long-term development will further lead to or aggravate organic diseases [22]. At present, there is no effective drug treatment for CN in modern medicine, which mainly depends on psychotherapy combined with corresponding symptomatic treatment, such as oryzanol β-Receptor blockers, etc.; however, the problems such as large side effects, poor patient compliance, and severe relapse are more prominent.

CN mostly belongs to the category of "palpitation," "depression syndrome," and other diseases in TCM. The occurrence of CN is mostly caused by adverse changes such as constitution, diet, and emotion, resulting in the imbalance of Qi, blood, Yin, and Yang in the body, loss of support for the heart, loss of possession of the mind, or tangible solid evil blocking the heart pulse and loss of support for the mind. The occurrence of CN is closely related to the five organs. Tietao Deng [23], a master of TCM, believes that CN is most closely related to the spleen. The methods of regulating the spleen, protecting the heart, tonifying Qi, and removing phlegm are often used to treat the disease. Professor Shi [24] believes that middle-aged women are prone to this disease, which is related to the theory that women are blood-based and that women are born with depression. He believes that the pathogenesis of CN is usually blood deficiency and liver depression. Professor Xian [25] believes that the occurrence of CN is also related to the brain and connected with the heart and brain and advocates the treatment of "simultaneous treatment of heart and brain." Professor Meng [26] believes that the disease is closely related to "Qi depression" and "blood stasis," and Xuefu Zhuyu decoction is often used for treatment.

A number of clinical trials have shown that TCMD, as a traditional Chinese medicine dosage form, can significantly improve the clinical symptoms of patients with CN and has certain advantages in the treatment of CN. Therefore, it is of practical significance to explore the systematic evaluation of TCMD on the curative effect of CN. TCMD represented by *Bupleurum* and longbone oyster decoction, *Bupleurum* Shugan powder, Xiaoyao Powder, Ganmai Dazhao Decoction, and Guipi Decoction are mostly used in the treatment of CN with remarkable curative effect. Moreover, pharmacological studies on TCMD (e.g., Shugan Ningxin Decoction, Chaihu Guizhi Longgu oyster decoction, Jieyu Decoction, etc.) have shown that they have tranquilizing, anticonvulsant, and reducing skeletal muscle excitability effects, which is closely related to the effective treatment of CN [27].

And through the analysis of the 10 literature studies on the treatment of CN included in this study, it was found that 55 kinds of traditional Chinese medicines were used, with a total frequency of 125 times. Among them, *Angelica sinensis*, *Poria cocos*, *Polygala tenuifolia*, Wild jujube kernel, and *Bupleurum* were the most frequently used TCMs. CN is located in the heart and is closely related to the liver, spleen, and kidney. The pathogenesis is the loss of the heart and liver, the depression of the liver and the deficiency of the spleen, or the deficiency of the heart and liver yin, and the deficiency of the liver and kidney yin. The treatment should be based on soothing the liver and strengthening the spleen, nourishing the heart, and calming the mind. If the blood of the heart is blocked, it will lead to chest tightness, chest pain, and palpitation. If the heart is in charge of the spirit, it will lead to worry and anxiety. The liver is in charge of catharsis and regulating emotions. The heart and liver are closely related to mental and emotional diseases while *Angelica sinensis* belongs to the liver, heart, and spleen meridians and has the effect of supplementing blood and activating blood circulation. Modern pharmacological studies have proved that *Angelica sinensis* has the effects of regulating immunity [28], anti-inflammation [29], and promoting blood circulation [30] and has good therapeutic effects on the symptoms of CN such as chest tightness, chest pain, palpitation, and anxiety. *Bupleurum* can soothe the liver and relieve depression, directly reach Shaoyang, help the operation of the cardinal machine, and make the Fu Qi smooth and the spirit tranquil. It has a significant effect in the clinical treatment of sleep disorders and depression. Experimental pharmacological studies have found that *Poria cocos* and Wild jujube kernel play an antianxiety role by making the neuroendocrine-immune regulatory network reach a steady state, while *Poria cocos*, *Polygala tenuifolia,* and Wild jujube kernel nourish the blood, regulate the liver, nourish the heart, and calm mind. In modern clinical applications, they can significantly improve symptoms such as palpitation, insomnia, and anxiety caused by the deficiency of the heart and liver blood in CN.

Table 3: Frequency of TCMs used in the treatment of CN.

TCM	Frequency (n)	TCM	Frequency (n)	TCM	Frequency (n)	TCM	Frequency (n)
Angelica sinensis	6	*Calamus*	3	Rehmannia glutinosa	2	Mother of pearl	1
Poria cocos	6	Licorice	3	Dried tangerine peel	2	Gardenia	1
Polygala tenuifolia	6	Calcined oyster	3	Dalbergia odorifera	2	Perilla stem	1
Wild jujube kernel	6	Curcuma	3	Raw dragon teeth	2	Pueraria lobata	1
Bupleurum	6	Pinellia ternata	3	Cinnamomum cassia	1	Bletilla striata	1
White peony	5	*Cassia* twig	2	*Morinda* officinalis	1	Magnet	1
Chuanxiong	4	Rhizoma Anemarrhenae	2	Motherwort	1	Zhu Ru	1
Gan song	4	Codonopsis pilosula	2	Phellodendron amurense	1	Fructus aurantii	1
Astragalus membranac-eus	3	Albizzia bark	2	Radix polygoni	1	Red ochre	1
Coptis chinensis	3	Figwort	2	Cohosh	1	Festuca arundinacea	1
Ophiopogon japonicus	3	Cypress seed	2	Scutellaria baicalensis	1	Epimedium	1
Schisandra chinensis	3	Ginseng	2	*Asparagus* sprengeri	1	Amber powder	1
Salvia miltiorrhiza	3	Chinese bellflower	2	Rhizoma cyperi	1	Cinnabar	1
Fu Shen	3	Peony bark	2	Mint	1	—	—

Table 4: Classification frequency of TCMs used in the treatment of CN.

Category of TCM	TCM	Frequency (n)	Proportion (%)
Antidote drugs	*Bupleurum*, cassia twig, cohosh, mint, pueraria lobata, perilla stem	12	9.6
Antipyretic drugs	*Coptis chinensis*, rhizoma anemarrhenae, rehmannia glutinosa, Figwort, peony bark, scutellaria baicalensis, gardenia, phellodendron amurense	14	11.2
Diuretic and hygroscopic drugs	*Poria cocos*, fu shen	9	7.2
Warming interior drugs	*Cinnamomum cassia*	1	0.8
Qi regulating drugs	Rhizoma nardostachyos, Dalbergia odorifera, Dried tangerine peel, Rhizoma Cyperi, Fructus aurantii	10	8.0
Hemostatics	Bletilla striata	1	0.8
Promoting blood circulation and removing blood stasis drugs	Chuanxiong, Salvia miltiorrhiza, Curcuma, Motherwort	11	8.8
Antitussive and antiasthmatic drugs for resolving phlegm	Pinellia ternata, Platycodon grandiflorum, Zhu Ru	6	4.8
Calming liver and wind drugs	Calcined oyster, Mother of Pearl, Red ochre	5	4.0
Tonic medicine	Chinses Angelica, Radix paeoniae Alba, Astragalus membranac-eus, Radix liquiritiae、Ophiopogon japonicus, Codonopsis pilosula, Ginseng, Festuca arundinacea、Epimedium, Radix asparagi, Morinda officinalis, Radix polygoni multiflori	29	23.2
Tranquilizer	Wild jujube kernel, High aspiration, Albizzia bark, Cypress seed, Raw dragon teeth, Magnet, Amber powder, Cinnabar	21	16.8
Resuscitation medicine	Calamus	3	2.4
Astringent medicine	Schisandra chinensis	3	2.4

This study finally included 10 papers with 686 patients, 349 in the treatment group, of which 131 were males and 218 were females, and 337 in the control group, of which 131 were males and 206 were females. 9 of the papers [9–17] mentioned the specific randomization method, 1 paper [8] did not describe it, and all of them did not mention the blinding method used, allocation concealment, lost visits, and withdrawal; 1 paper [8] selectively reported the study results; and 3 papers [8, 11, 13] reported adverse effects. Meta-analysis showed that CN, treated with herbal tonics, significantly improved palpitations compared with the control group ($MD = 0.78$, 95% $CI = 0.55$–1.01, $P < 0.00001$), chest tightness/chest pain ($MD = 0.53$, 95% $CI = 0.10$–0.97, $P < 0.05$), shortness of breath symptoms ($MD = 0.60$, 95% $CI = 0.26$–0.93, $P = 0.0005$), and the TCM symptom score ($MD = 5.91$, 95% $CI = 4.32$–7.49, $P < 0.00001$), reduced resting heart rate ($MD = 13.21$, 95% $CI = 9.01$–17.40, $P < 0.00001$), and reduced depression and anxiety symptoms. [SDS ($MD = 7.90$, 95% $CI = 4.98$–10.83, $P < 0.00001$), SAS ($MD = 6.55$, 95% $CI = 4.25$–8.86, $P < 0.00001$), HAMD ($MD = 4.46$, 95% $CI = 3.00$–5.92, $P < 0.00001$), HAMA ($MD = 3.35$, 95% $CI = 1.85$–4.85, $P < 0.00001$)], all with statistically significant differences. According to the analysis of this study, TCMD has a significant effect on improving the common clinical symptoms, depression, and anxiety of CN.

4.1. Limitations. There are some limitations that should be noted. To begin with, due to the high risk of performance bias and detection bias, unclear risk of selection bias, and reporting bias, we only got relatively low-grade evidence for TCMD in the treatment of CN complicated with depression and anxiety, which means further research is very likely to have an important impact on our confidence in the estimate of effects and is likely to change the estimate. What is more, the sample size of the papers was small, and there was a lack of evaluation indicators such as safety analysis and quality of life analysis. Finally, because CN is mainly manifested in physical symptoms and lacks clear laboratory index evidence, we had to evaluate the effectiveness of TCMD in the treatment of CN from the results of TCM syndrome scores and psychological scale scores. Accordingly, further validation of the effectiveness of TCMD in the treatment of CN through large sample, multicenter, scientifically designed, and rigorously implemented clinical trials are still needed in the future.

5. Conclusion

In conclusion, TCMD mainly composed of tonic and tranquilizing drugs could significantly improve the clinical symptoms of cases with CN and reduce heart rate, anxiety, and depression scores. However, the evidence strength of the research results was limited by the quality of the included literature, and more high-quality clinical trials are still needed for further verification.

Data Availability

The data used to support the findings of the study are available at https://www.crd.york.ac.uk/PROSPERO/display_record.php?RecordID=312164.

Conflicts of Interest

The authors declared that they have no conflicts of interest in this work.

Acknowledgments

The authors would like to acknowledge the Special Fund for Basic Scientific Research Business Expenses of Central Public Welfare Scientific Research Institutes (no. ZZ13-YQ-008) and Major Research Project of Scientific and Technological Innovation Project of Chinese Academy of Traditional Chinese Medicine (no. CI2021A03115).

References

[1] J. Rogers, G. Collins, M. Husain, and M. Docherty, "Identifying and managing functional cardiac symptoms," *Clinical Medicine*, vol. 21, no. 1, pp. 37–43, 2021.

[2] C. N. Carmin, P. S. Wiegartz, J. A. Hoff, and G. T. Kondos, "Cardiac anxiety in patients self-referred for electron beam tomography," *Journal of Behavioral Medicine*, vol. 26, no. 1, pp. 67–80, 2003.

[3] S. Conti, G. Savron, G. Bartolucci et al., "Cardiac neurosis and psychopathology," *Psychotherapy and Psychosomatics*, vol. 52, pp. 88–91, 1989.

[4] L. Y. Zuo, Y. U. Hui, and Z. Zhou, "Clinical observation of Chaihu long oyster decoction combined with metoprolol on patients with cardiovascular neurosis," *Abstract of the world's latest medical information*, vol. 15, no. 04, pp. 136-137, 2015.

[5] A. L. Zhang, *Clinical Observation and Meta-Analysis of Chaihu Long Oyster Decoction in the Treatment of Cardiac Neurosis*, Heilongjiang University of Traditional Chinese Medicine, Heilongjiang, China, 2018.

[6] H. Ren, *Clinical Observation of Baihe Buxin Decoction in the Treatment of Cardiac Neurosis of Yin Deficiency and Fire Excess Type*, Changchun University of Traditional Chinese Medicine, Changchun, China, 2018.

[7] Y. Ge, *Clinical Observation of Chaihu Long Oyster Decoction in the Treatment of Cardiac Neurosis of Qi Stagnation and Fire Transformation Type*, Heilongjiang University of Traditional Chinese Medicine, Heilongjiang, China, 2019.

[8] Z. Q. Li and S. Jia, "Clinical observation of shugan Ningxin decoction in the treatment of cardiac neurosis," *Hebei Traditional Chinese Medicine*, vol. 31, pp. 1145-1146, 2009.

[9] W. C. Jiang and Y. Zhou, "Clinical study on modified Chaihu Guizhi Longgu oyster decoction in the treatment of cardiac neurosis," *Chinese medical emergency*, vol. 24, no. 07, pp. 1146–1148, 2015.

[10] S. S. Yao, *Clinical Observation of Jieyu Decoction on Cardiovascular Neurosis of Liver Qi Stagnation Type*, Nanjing University of Traditional Chinese Medicine, Nanjing, China, 2016.

[11] C. X. Liu, *Clinical Observation of Yangxin Dingji Decoction in the Treatment of Cardiac Neurosis of Qi and Blood Deficiency Type*, Heilongjiang University of Traditional Chinese Medicine, Heilongjiang, China, 2016.

[12] Y. J. Leng, *Clinical Observation of Yangxin Chaihuan Decoction in the Treatment of Cardiac Neurosis of Qi and Blood Deficiency and Stagnation Type*, Changchun University of Traditional Chinese Medicine, Changchun, China, 2018.

[13] C. M. F. Ma, *Clinical Observation of Jiawei Erxian Decoction in the Treatment of Cardiac Neurosis of Heart Kidney Disharmony Type*, Hunan University of Traditional Chinese Medicine, Hunan, China, 2020.

[14] Y. X. Wang, *Clinical Observation of Shengkeng Decoction in the Treatment of Cardiac Neurosis of Qi and Blood Deficiency and Stagnation Type*, Changchun University of Traditional Chinese Medicine, Changchun, China, 2020.

[15] H. X. Dai, W. Zhai, and Y. Xiang, "Clinical study of Tianwang Buxin Decoction in the treatment of Cardiac Neurosis of yin deficiency and fire excess type," *China prescription drugs*, vol. 19, no. 09, pp. 154-155, 2021.

[16] H. S. Tong, J. Tian, and Y. Liu, "Clinical observation of suanzaogen decoction in the treatment of cardiac neurosis," *Chinese Folk Therapy*, vol. 29, pp. 64-65, 2021.

[17] D. F. Zhang, *Clinical Study on Modified Huanglian Zhengdan Decoction in the Treatment of Cardiac Neurosis*, Changchun University of Traditional Chinese Medicine, Changchun, China, 2021.

[18] A. W. Serlie, R. Erdman, J. Passchier, R. Trijsburg, and F. ten Cate, "Psychological aspects of non-cardiac chest pain," *Psychotherapy and Psychosomatics*, vol. 64, no. 2, pp. 62–73, 1995.

[19] H. W. Luo, *Systematic Evaluation and Meta-Analysis of the Efficacy of Traditional Chinese Medicine in the Treatment of Cardiac Neurosis*, Beijing University of Chinese Medicine, Beijing, China, 2016.

[20] W. Friedman, "Panic disorder and Pathologic anxiety," *Psychiacl in North Am*, vol. 10, no. 6, pp. 375–377, 1998.

[21] F. Zheng, Y. Duan, J. Li et al., "Somatic symptoms and their association with anxiety and depression in Chinese patients with cardiac neurosis," *Journal of International Medical Research*, vol. 47, no. 10, pp. 4920–4928, 2019.

[22] W. Katon, E. H. Lin, and K. Kroenke, "The association of depression and anxiety with medical symptom burden in patients with chronic medical illness," *General Hospital Psychiatry*, vol. 29, no. 2, pp. 147–155, 2007.

[23] Z. Y. Liu, X. Zou, and Y. Luo, "Summary of clinical experience of Deng Tietao's heart spleen correlation theory in the treatment of palpitation," *Chinese Journal of traditional Chinese medicine information*, vol. 14, no. 7, pp. 82-83, 2007.

[24] D. Z. Shi and L. Ma, "Introduction to Professor Shi Dazhuo's experience in treating cardiac neurosis," *Journal of cardio cerebrovascular disease with integrated traditional Chinese and Western medicine*, vol. 14, no. 18, pp. 2198-2199, 2016.

[25] X. X. Zhou, M. C. Liu, and T. C. Ye, "Introduction to Xian Shaoxiang's academic thought and experience in treating cardiovascular diseases with the theory of simultaneous treatment of heart and brain," *New traditional Chinese medicine*, vol. 49, pp. 206–208, 2017.

[26] J. L. Huang, X. J. Huang, and D. S. Meng, "Professor meng dingshui used Xuefu Zhuyu decoction to treat cardiac neurosis," *National Medical Forum*, vol. 30, pp. 23-24, 2015.

[27] X. Y. Ge, *Clinical Observation of Modified Schisandra Decoction in the Treatment of Cardiac Neurosis with Deficiency of Qi and Yin*, Heilongjiang University of Traditional Chinese Medicine, Heilongjiang, China, 2016.

[28] J. M. Wang, B. L. Ge, Z. H. Li, F. Guan, and F. Li, "Structural analysis and immunoregulation activity comparison of five polysaccharides from Angelica sinensis," *Carbohydrate Polymers*, vol. 140, pp. 6–12, 2016.

[29] M. M. Li, Y. Zhang, J. Wu, and K. P. Wang, "Polysaccharide from Angelica sinensis suppresses inflammation and reverses anemia in complete freund's adjuvant-induced rats," *Curr Med Sci*, vol. 40, no. 2, pp. 265–274, 2020.

[30] Z. W. Yuan, L. J. Zhong, Y. L. Hua et al., "Metabolomics study on promoting blood circulation and ameliorating blood stasis: investigating the mechanism of Angelica sinensis and its processed products," *Biomedical Chromatography*, vol. 33, no. 4, p. e4457, 2019.

Hindawi
Evidence-Based Complementary and Alternative Medicine
Volume 2022, Article ID 5899975, 12 pages
https://doi.org/10.1155/2022/5899975

Research Article

Deep Learning Based Tongue Prickles Detection in Traditional Chinese Medicine

Xinzhou Wang,[1,2] Siyan Luo,[3,4] Guihua Tian,[5] Xiangrong Rao,[3] Bin He,[1] and Fuchun Sun[2]

[1]*College of Electronic and Information Engineering, Tongji University, Shanghai 200092, China*
[2]*Department of Computer Science and Technology, Tsinghua University, Beijing 100084, China*
[3]*Guang'Anmen Hospital, China Academy of Chinese Medical Sciences, Beijing 100053, China*
[4]*Beijing University of Chinese Medicine, Beijing 100029, China*
[5]*Dongzhimen Hospital, Beijing University of Chinese Medicine, Beijing 100700, China*

Correspondence should be addressed to Fuchun Sun; fcsun@tsinghua.edu.cn

Received 21 April 2022; Revised 8 August 2022; Accepted 26 August 2022; Published 22 September 2022

Academic Editor: Jianan Xia

Tongue diagnosis is a convenient and noninvasive clinical practice of traditional Chinese medicine (TCM), having existed for thousands of years. Prickle, as an essential indicator in TCM, appears as a large number of red thorns protruding from the tongue. The term "prickly tongue" has been used to describe the flow of qi and blood in TCM and assess the conditions of disease as well as the health status of subhealthy people. Different location and density of prickles indicate different symptoms. As proved by modern medical research, the prickles originate in the fungiform papillae, which are enlarged and protrude to form spikes like awn. Prickle recognition, however, is subjective, burdensome, and susceptible to external factors. To solve this issue, an end-to-end prickle detection workflow based on deep learning is proposed. First, raw tongue images are fed into the Swin Transformer to remove interference information. Then, segmented tongues are partitioned into four areas: root, center, tip, and margin. We manually labeled the prickles on 224 tongue images with the assistance of an OpenCV spot detector. After training on the labeled dataset, the super-resolutionfaster-RCNN extracts advanced tongue features and predicts the bounding box of each single prickle. We show the synergy of deep learning and TCM by achieving a 92.42% recall, which is 2.52% higher than the previous work. This work provides a quantitative perspective for symptoms and disease diagnosis according to tongue characteristics. Furthermore, it is convenient to transfer this portable model to detect petechiae or tooth-marks on tongue images.

1. Introduction

Based on the clinical practice of doctors, traditional Chinese medicine has been developed for thousands of years and has achieved brilliant results both in the past and in modern times. Tongue diagnosis, as a role of vital importance in TCM clinical diagnosis, is a convenient and noninvasive method based on the health status information carried by the appearance of the tongue [1]. The chromatic features and morphological characteristics of the tongue, the number of prickles and the form of tongue coating reveal the pathological changes of internal organs, as shown in Figure 1 [2, 3]. There have been reports that prickles are associated with tumors, kidney disease, gastric disease, and new crowns [4]. However, traditional tongue diagnosis is an empirical procedure that relies heavily on the personal experience and subjective judgment of TCM doctors. With the assistance of artificial intelligence (AI), tongue diagnosis will be objective and people without medical knowledge can give themselves a preliminary diagnosis of a health condition. In recent years, much effort has been spent on AI-based tongue diagnosis, especially in the field of tongue color recognition [5, 6], tongue shape analysis [7], cracks segmentation [8], thickness, and moisture of tongue coating classification [9, 10].

Prickle, also called red-pointe, appears as a large number of red thorns protruding from the tongue. It indicates blood heat or excess heat in the internal organs. The color and

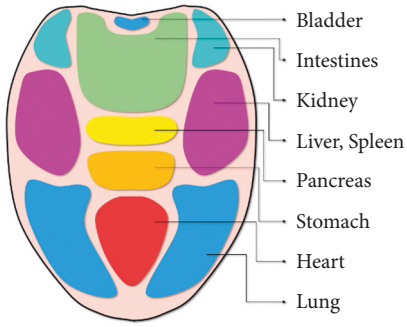

Figure 1: Tongue reflexology chart. Different areas on the tongue reflect the state of different organs.

number of the prickles can help estimate the flow of qi and blood. As proved by the study, the prickles originate in the fungiform papillae, which are enlarged and protrude to form spikes like awn [11]. Shang et al. further analyzed the association of prickles with the gastric sinus [12]. On the one hand, prickles mean increased blood flow and thus congestion. On the other hand, prickles represent thermal burns to blood vessels, resulting in blood spillage and mucosal erythema. The automatic detection of prickles can not only release the burden of doctors but also enable patients without medical knowledge to give themselves a brief examination.

Though AI-based tongue diagnosis has attracted a lot of attention, there is little literature on prickle detection due to its difficulty. In most tongue images, each prickle only occupies a few pixels and has little difference in tongue color under natural light. Moreover, the similarity between prickles and petechiae in both morphological and chromatic characteristics makes it a challenging task to distinguish them. Xu et al. were the first to introduce template feature matching to detect the prickles and petechiae, and then distinguished them based on RGB value range, gray average, and the position of the detected object [13]. Zhang employed the fuzzy C-means color cluster and noise reduction methods to detect prickles in the tongue edge image. Wang et al. used multistep threshold spot detection to detect prickles and petechiae. After extracting the features of spots (including prickles and petechiae), support vector machines and k-means were introduced to distinguish prickles and petechiae [11]. Wang et al. proposed a prickle detection method based on an auxiliary light source and a LOG operator edge detection method [14]. The last two works are most similar to our work, for they provided a quantitative description of prickles.

By eliminating background areas such as the face and lips, the tongue region segmentation can enhance the performance of downstream tasks, including prickle detection. Practice has proved that the neural network is very effective in the task of tongue segmentation. Zhang et al. introduced a DCNN-based tongue segmentation algorithm [15]. Wang et al. designed a coarse-to-fine segmentor based on RsNet and FsNet [16]. Jiangproposed an HSV enhanced CNN to segment the tongue region [17]. Zhang et al. combined superpixel with CNN to increase decoding performance [18].

Though previous researchers put much efforts into prickles and petechiae detection, the existing methods all rely heavily on manual parameter tuning. This not only adds to the burden of researchers but also causes the model to overfit to specific circumstances and equipment. Moreover, there is no end-to-end prickle detection method, which could provide a quantitative description of prickles without manually segmenting the tongue raw images. Finally, most methods only took gray values of the exact pixels into consideration and lose the color information and the context information around the prickles.

The method proposed in this paper solved the question mentioned above from a completely new perspective: Deep Learning. We designed an end-to-end workflow to detect prickle automatically. The entire workflow and intermediate results are depicted in Figure 2.

2. Dataset and Methods

2.1. Dataset Collection. In this paper, the tongue images and segmentation annotations come from the bio-HIT tongue image dataset [19] (https://github.com/BioHit/TongeImageDataset). The tongue images dataset contains 300 RGB images with 576×768 pixels, and the images are obtained by the tongue image acquisition device shown in Figure 3. The device is designed as a semiclosed black box with a camera and illuminated on each side of the camera. The daylight illuminant D50, recommended by CIE (Commission Internationale de lEclairage) [20], was utilized as daylight illumination. According to the guidelines provided by CIE, the angle between the incident and outgoing rays is 45°. We elaborately screened out images with poor quality and got 224 images to train the model. The device has a closed image acquisition environment with an independent stable light source and a head restraint to ensure all the images are sampled to one standard. In addition, the image registration and calibration is not necessary either. Four volunteers in HIT elaborately annotated the image segmentation labels and the best one was chosen [19]. All the images were standardized to meet the standard normal distribution.

2.2. Tongue Segmentation. The AI-assisted tongue diagnosis is based on the information obtained from the tongue image. When concentrated on the tongue, irrelevant elements, including the lips, cheek, and chin, distract I neural network. With interference eliminated and the tongue matted, the contour line of the tongue becomes apparent and the performance of feature extraction is guaranteed. Therefore, it is necessary to segment the tongue before the next step, and we introduced the Swin Transformer [21] as the segmentor. The core concept of the Swin Transformer is self-attention, as shown in equations:

$$\begin{aligned} Q &= XW^{Q}, \\ K &= XW^{K}, \\ V &= XW^{V}, \end{aligned} \tag{1}$$

$$\text{Attention}(Q, K, V) = \text{softmax}\left(\frac{QK^{T}V}{\sqrt{d_k}}\right), \tag{2}$$

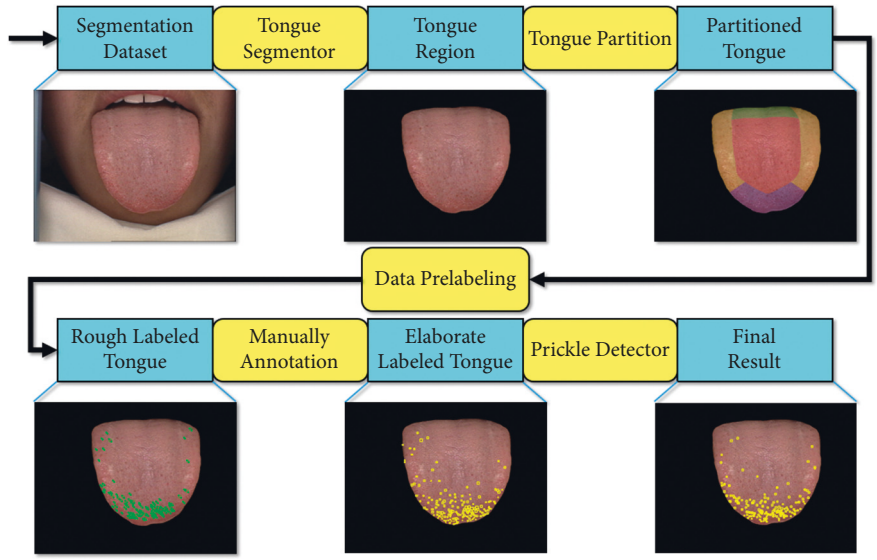

Figure 2: Prickle detection workflow. Blue rectangles represent images, and yellow rectangles represent image processing. First, in tongue segmentor, we introduced Swin Transformer, a state-of-the-art computer vision segmentation neural network, to mat the tongue region out of the raw picture. Second, in tongue partition, the tongue is partitioned into four areas: root, margin, tip, and center. Third, in data prelabeling, a spot detector is applied based on tongue areas. Fourth, elaborate manual annotation is conducted with the help of TCM doctors. Fifth, to fully embody the advantages of the neural network, a super-resolutionfaster-RCNN based detector is deployed to detect the prickles from a matted tongue image.

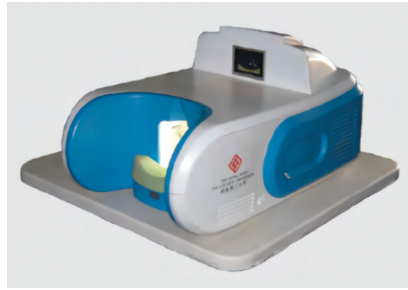

Figure 3: The tongue image acquisition device. The device is designed to obtain tongue images in uniform illumination and facial poses.

where the Q is the query vector, the K is the key vector, and the V is the value vector. W^Q, W^K, W^V are all weight matrices. With the self-attention mechanism, the network can perceive global semantic information. The entire architecture of Swin Transformer is shown in Figure 4, where Z_0, Z_2, Z_4, Z_6, Z_8, and Z_{10} used multihead self-attention with regular windowing (W-MSA) and the others used multihead self-attention with shifted windowing (SW-MSA). Considering the fact that the dataset only contains 224 images, which is insufficient for training a network from scratch, we adopted a paradigmatic strategy in computer vision: pretraining and fine-tuning with data augmentation. Microsoft has trained the model with over 20,000 images on the ADE20K dataset [22], and we fine-tuned the model on the tongue segmentation dataset. The data augmentation pipeline includes flipping, cropping, and photometric distortion. Photometric distortion applies the following transformations with a probability of 0.5: random brightness, random contrast, color space converting, random saturation, random hue, and randomly swapping channels. With data augmentation, the model will be more robust when the illumination or sampling device varies. Though the neural network is able to classify each pixel as tongue or background, there is no guarantee that the segmented tongue region has structural integrity. To address this issue, we analyzed the connected components of each mask, filled the blank areas in the tongue and eliminated the outliers using two-pass connected component analysis [23]. The algorithm is shown in Algorithm 1 and the result is shown in Figure 5.

2.3. Prickles Annotation. Usually, hundreds of prickles appear on the tongue in groups. Therefore, it will be a challenging task if we manually annotate the whole dataset. In this paper, we employed partition spots detection [11] with LAB chromatic aberration filtering to give a primitive annotation of the prickles.

The LAB color space is based on the human eye's perception of color and can represent all colors the human eye can perceive. "L" represents lightness, "A" represents red-

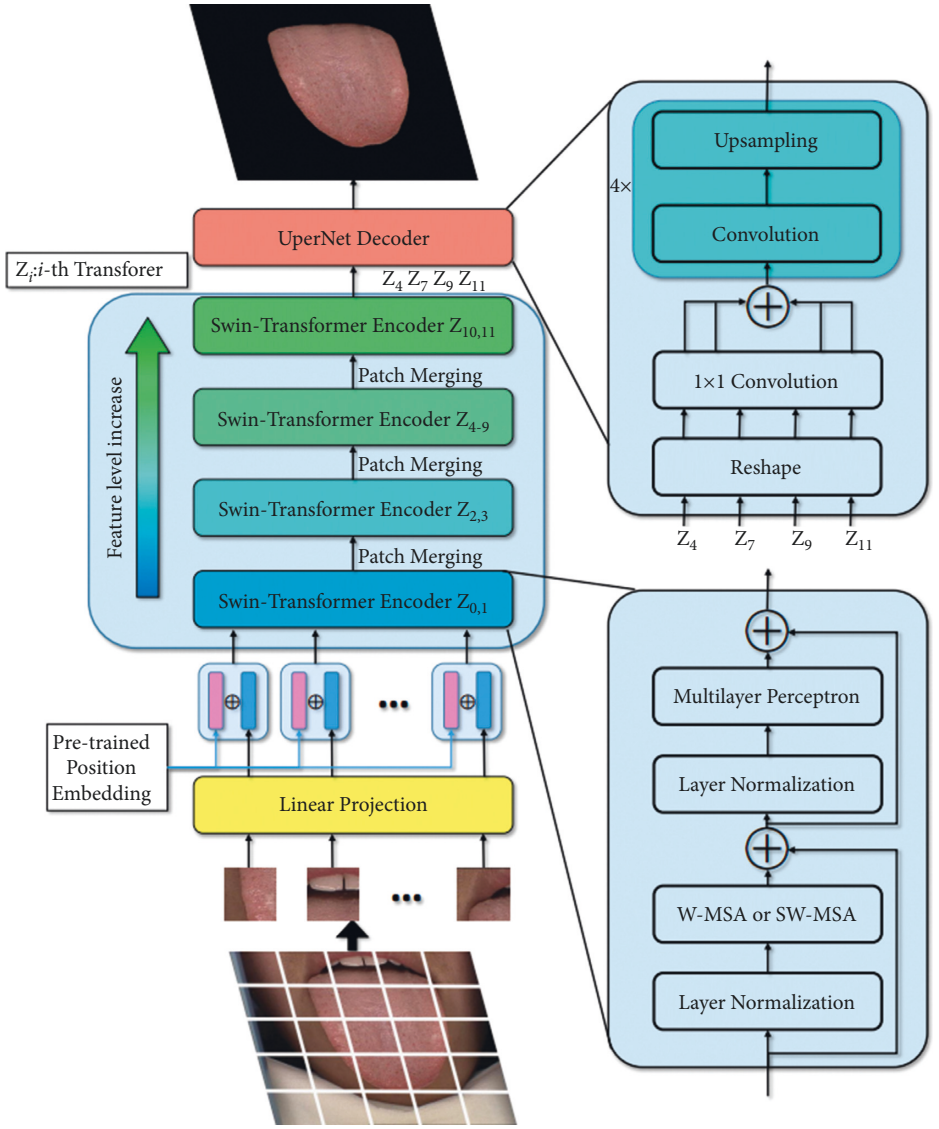

Figure 4: Architecture of tongue segmentor. The tongue image is divided into several patches and then added with position embeddings to retain spatial information. The encoder consists of cascaded Swin Transformers, while UperNet decoder is applied to aggregate multilevel features from encoder.

Figure 5: Mask morphology processing. The connected component with the largest area in black or white will be marked as "1" and other connected components will be eliminated.

green difference, and "B" represents blue-yellow difference. The spot detection algorithm works on gray images and the color information is lost. Therefore, we filtered the spots by the chromatic aberration between the spots and the manually picked prickles. Given an RGB value, an approximate LAB chromatic aberration can be calculated as follows:

Input: Binary tongue mask I width W and height H
Output: Tongue mask with structural integrity
num_label = 0
for $y = 0$ **to** $H - 1$ **do**
  for $x = 0$ **to** $W - 1$ **do**
    N = neighbours ($I[y, x]$)
    if $I[y, x] == 1$ **then**
      if 0 **not in** N **then**
        $I[y, x]$ = *num_label*//Give each mask pixel a label
        num_label+=1
      else if has_mask(N) **then**
        label = min(N)
        $I[y, x]$ = *label*//If neighbours have label, use the minimum one.
        labelSet[*label*].append(N.all_labels())
for $y = 0$ **to** $H - 1$ **do**
  for $x = 0$ **to** $W - 1$ **do**
    $I(y, x)$ = min(*labelSet*[$I(y, x)$])//Unify the label of each component
Select the mask component with largest area as tongue and discard others
Select the background component with largest area and discard others//Fill holes in mask
Return I

Algorithm 1: Mask morphology processing.

$$\begin{aligned}\widetilde{r} &= C_{1,R} + \frac{C_{2,R}}{2},\\ \Delta R &= C_{1,R} - C_{2,R},\\ \Delta G &= C_{1,G} - C_{2,G},\\ \Delta B &= C_{1,B} - C_{2,B},\\ \text{Chromatic Aberration} &= \sqrt{\left(2 + \frac{\widetilde{r}}{256}\right) \times \Delta R^2 + 4 \times \Delta G^2 + \left(2 + \frac{(255 - \widetilde{r})}{256}\right) \times \Delta B^2}.\end{aligned} \tag{3}$$

The tongue is partitioned before detection so that we can elaborately set different detection parameters for different areas. The tongue coating is distributed on the tongue surface, which is usually slightly thicker in the center or root of the tongue, and the prickles covered by the coating have different characteristics from the prickles on the margin and tip. In addition, the cracks on the root and center of the tongue tend to be detected mistakenly by the spot detection algorithm. To solve this problem, we divided the tongue into four areas: root, margin, tip, and center before preliminary annotation. Then we set the threshold of chromatic aberration, area, circularity, and convexity tighter in the root and center than in other areas. This setting avoids the misdetection of cracks while maintaining the detection rate.

The algorithm of annotation is shown in Figure 6. First, the parallel-line method is introduced to build a reference line for tongue partition [14]. Second, the tongue is divided into four areas by the relative thickness compared to the overall scale of the tongue. The result is depicted in Figure 7. Third, a simple blob detector based on OpenCV (Open Source Computer Vision Library) is deployed with different parameters in different tongue regions. Fourth, the detected spots are filtered by LAB chromatic aberration. Finally, a professional TCM doctor revised the roughly annotated bounding boxes with the MIT Labelme annotation tool (https://labelme.csail.mit.edu) and two other TCM doctors checked the result under the same diagnostic criteria on the same monitor [24, 25].

2.4. Prickle Detection. In this paper, we take the Faster-RCNN as the prickle detector. In 2016, Ross B. Girshick proposed a new object detection neural network called Faster-RCNN, which is depicted in Figure 8. The Faster-RCNN first uses a set of basic convolution layers, ReLU function, and pooling layers to extract an image feature map, which is subsequently shared by region proposal networks (RPN) and fully connected layers. The RPN network is designed to generate region proposals with the softmax layer to determine whether the anchors are positive or negative, and then it employs bounding box regression to correct the anchors to obtain accurate proposals. The roi-pooling layer collects the input feature maps and proposals, extracts proposal feature maps after synthesizing the information,

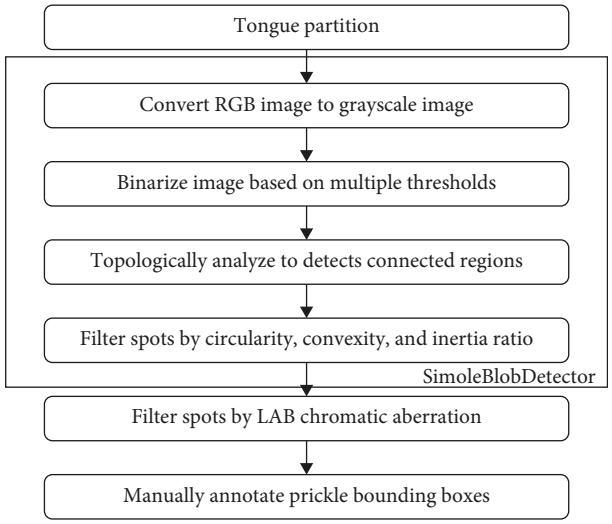

Figure 6: Prickle bounding boxes annotation workflow. Prickle bounding boxes are labeled automatically and then manually adjusted by TCM doctors.

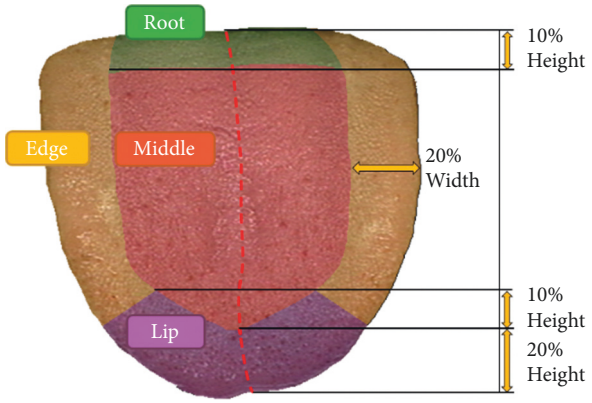

Figure 7: Tongue partition. The tongue is divided into four areas automatically based on the midline and the detection parameters vary with areas adaptively.

and sends them to the subsequent fully connected layer to determine the target category [26].

There are two obstacles that need to be overcome before training the Faster-RCNN. First, insufficient data makes the model hard to train. Therefore, we introduced data augmentation, including flip, crop, scale, translation, and rotation, as shown in Figure 9. In addition, we followed the paradigm of computer vision workflow: we pretrained the model on a general detection dataset and used transfer learning to fine-tune the model on the prickle detection dataset. Second, the Faster-RCNN is designed for the detection of the target on a normal scale. When the target is smaller than 32×32 pixels, the performance of the model will decrease sharply. To address this issue, we used 4× bilinear interpolation for upsampling to improve the model performance. Since the neural network aims to build an end-to-end prickle detection model and it is proven that the color calibration and irrelevant noise filtering may cause a degradation in model performance [27], image registration and filtering are not employed.

2.5. Evaluation Metrics. The segmentation tasks in computer vision field could be considered as a pixel-wise classification, and there are four types of the results: true positive (TP), false positive (FP), true negative (TN), and false negative (FN), as shown in Figure 10. The standard evaluation metrics of segmentation task is intersection over union (IoU), defined as follows:

$$\text{IoU} = \frac{\text{TP}}{(\text{FP} + \text{FN} + \text{TP})}, \tag{4}$$

where TP, FP, and FN are about pixel-wise classification results. We also employed precision and accuracy as metrics to fully demonstrate the performance of the proposed method, which are defined as follows:

$$\begin{aligned} \text{Accuracy} &= \frac{(\text{TP} + \text{TN})}{(\text{TP} + \text{TN} + \text{FP} + \text{FN})}, \\ \text{Precision} &= \frac{\text{TP}}{\text{TP} + \text{FP}}. \end{aligned} \tag{5}$$

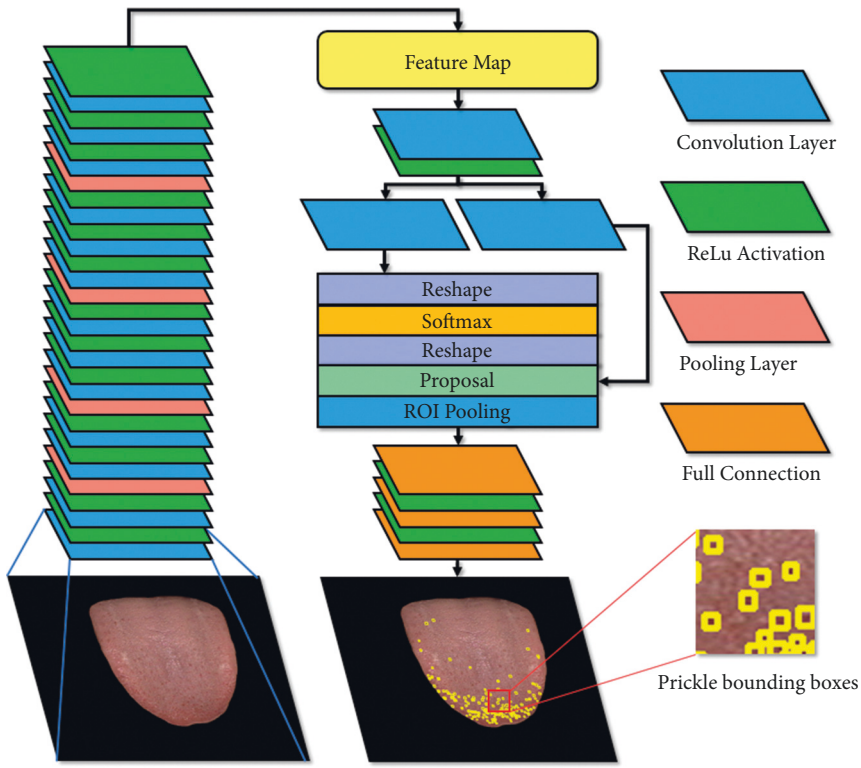

Figure 8: Architecture of prickle detector. CNN encoder extract features from images. Region proposal networks generate region proposals and bounding box regressor modify anchors to predict precise prickle bounding boxes.

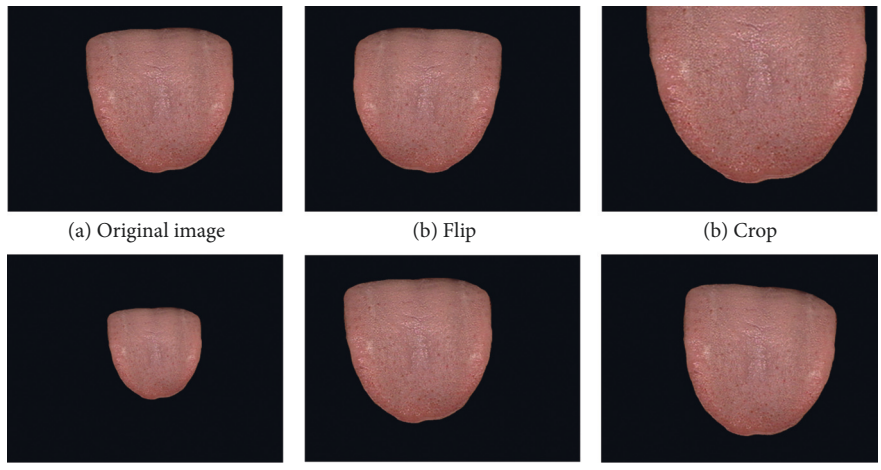

Figure 9: Data augmentation. Super-resolution, flip, crop, scale, translation, and rotation are conducted to increase dataset size and improve network robustness without collecting new data. (a) Original image (b) flip (c) crop (d) scale (e) translation and (f) rotation.

A prickle is classified as detected correctly when the bounding box has IoU over the threshold.

The metrics for prickles detection are precision defined above and recall defined as follows:

$$\text{Recall} = \frac{\text{TP}}{(\text{TP} + \text{FN})}. \tag{6}$$

Where FP is the number of misdetected prickles, TP and FN is the number of manually annotated prickles that were detected and undetected, respectively.

3. Experiments and Results

3.1. Experiment Setting. In our work, the models were trained and tested based on the Python deep-learning

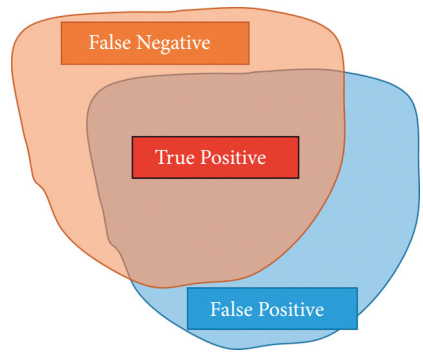

Figure 10: Types of the predicted segmentation. The orange area represents the ground truth, and the blue represents the predicted segmentation.

framework PyTorch (https://pytorch.org) and the computing platform is a Linux server with Intel Xeon (R) E5-2620 CPU, 4 NVIDIA RTX2080Ti GPUs, and 128 GB memory. The total training time is about 2 hours. The parameters of segmentor and detector in the training stage are shown in Table 1.

3.2. Result of Tongue Segmentation. The Swin Transformer is a flexible neural network, which means it requires more training compared to the conventional CNN. To address this issue, we introduced the pretraining model provided by Microsoft (https://github.com/SwinTransformer/Swin-Transformer-Semantic-Segmentation). Microsoft has trained the model with over 20,000 images on ADE20K dataset [16] and we fine-tuned the model on our tongue segmentation dataset. The training set and test set contained 178 and 46 annotated images, respectively. The splitting of the dataset took a cross-validation strategy. After we got the predicted segmentation, we filled the blank areas in the tongue and eliminated the outliers. The result is shown in Table 2 and Figure11(b).

The excellent performance of the Swin Transformer makes the segmentation results basically the same as manual segmentation. Compared to the conventional machine vision segmentation methods, neural network is an end-to-end progress without the requirement of manual tuning parameters. It is also more robust when the illumination or sampling device varies and the result proves the superiority of the transformer architecture in tongue segmentation.

3.3. Prickle Labeling. We employed the simple blob detector with LAB chromatic aberration filtering to detect the prickles coarsely. The simple lob detector is a multistep threshold spot detection method for processing gray images. We took the parameters of the simple blob detector in [11] as the initial value and introduced the grid search to find the optimal parameters for each area. The searching step length is set to 10% of the initial value and the searching range is set from 50% to 150% of the initial value. The parameters of the partitioned simple blob detector are shown in Table 3.

Petechiae are usually found on the center and roots of the tongue. To reduce the probability of misdetection, the constrains of spots in those areas are more stringent. In addition, to take full advantage of the color information, we sampled the RGB value of prickles in different tongues and areas and filtered the detected spots by the LAB chromatic aberration. The automatic annotation result with and without partitioning is shown in Figure 12 to give a clear demonstration of how the partitioning helps the prickle labeling. After automatic annotation, three well-trained TCM doctors manually revised the labels. The annotation is shown in the Figure 11(d).

Table 1: Parameters for training Swin Transformer.

Hyper-parameter	Segmentor	Detector
Epoch	20	100
Batch size	4	4
Optimizer	AdamW	SGD
Learning rate	6e-05	5e-2
Learning rate policy	Polynomial	Step
Weight decay	1e-2	1e-4
Loss function`	Cross entropy	Cross entropy

3.4. Result of Prickle Detection. Object detection is a challenging task requiring a lot of training. We downloaded the pretrained model provided by CUHK and SenseTime (https://github.com/open-mmlab) and fine-tuned it on the prickle detection dataset. The training set and test set contained 178 and 46 annotated images, respectively. The splitting of the dataset took a cross-validation strategy. Compared to the original Faster-RCNN, we employed a 4× bilinear interpolation for upsampling and modified the anchor size to match the prickle detection. To demonstrate the superiority of our modified Faster-RCNN, we took the vanilla Faster-RCNN and other detection algorithms for comparison. The predicted result of the entire dataset is shown in Table 4.

The recall of our method outperformed the existing methods without fine-tuning the parameters manually. We did not choose YOLO because it is a one-stage detection algorithm and the resolution is fixed, which limits the performance of detecting tiny targets. It is worth mentioning that we tried other learning-based algorithms, including DCNv2 [29] and SSD [30], but they were unable to predict

Table 2: The performance of segmentor and previous studies.

Method	IoU (%)	Precision (%)	Accuracy (%)
DCNN [8]	—	97.94	99.41
RsNet and FsNet [9]	—	97.85	99.04
HSV enhanced CNN [10]	—	94.70	97.88
Ours	**99.08**	**99.47**	**99.79**

(a)

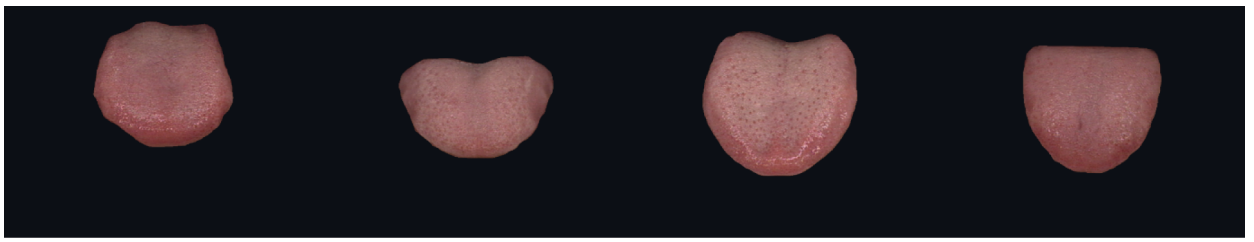

(b)

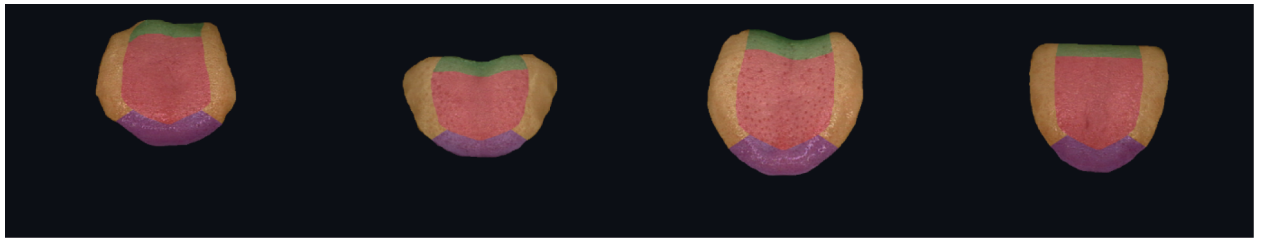

(c)

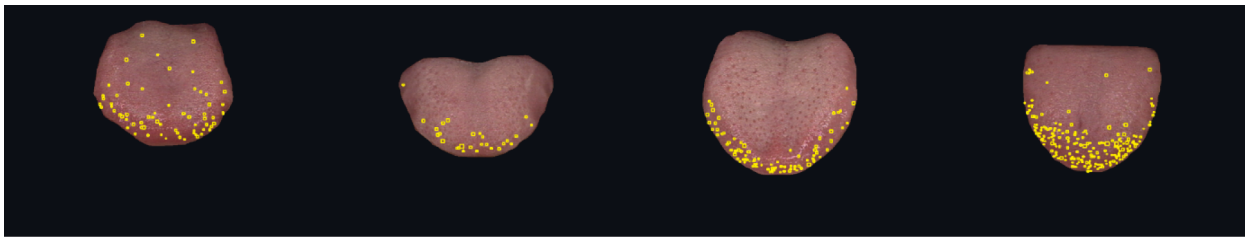

(d)

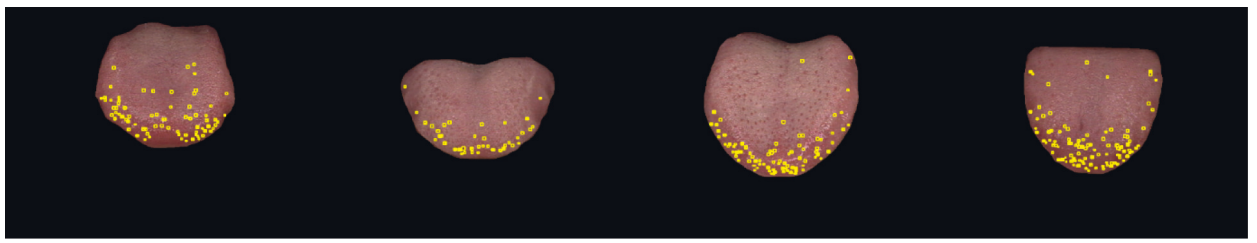

(e)

Figure 11: Continued.

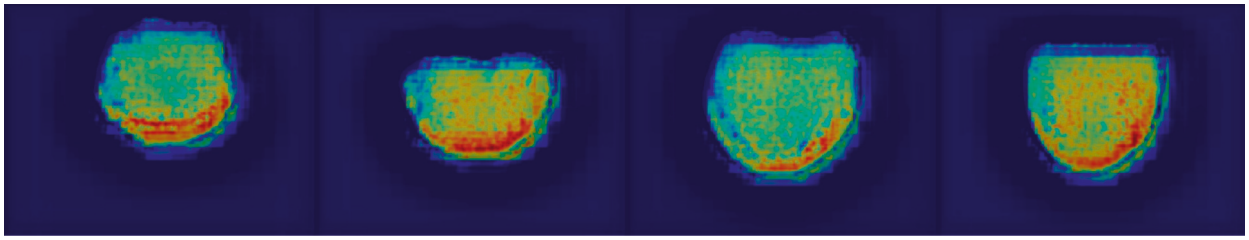

(f)

Figure 11: Prickle detection result. (a) Original images (b) segmentation result (c) partitioned tongues (d) prickle labels (e) prickle detection result and (f) neural network attention map. The intermediate result of the whole workflow is shown (zoom in for better viewing).

Table 3: Parameters of the simple blob detector in different areas.

Parameter	Root and center	Tip	Margin
Min threshold	60	60	60
Max threshold	100	100	100
Threshold step	2	2	2
Min repeatability	8	4	4
Min area	4	2	2
Max area	25	40	40
Min circularity	0.8	0.4	0.4
Min convexity	0.8	0.4	0.4
Min inertia ratio	0.5	0.4	0.4
Max aberration	85	100	100

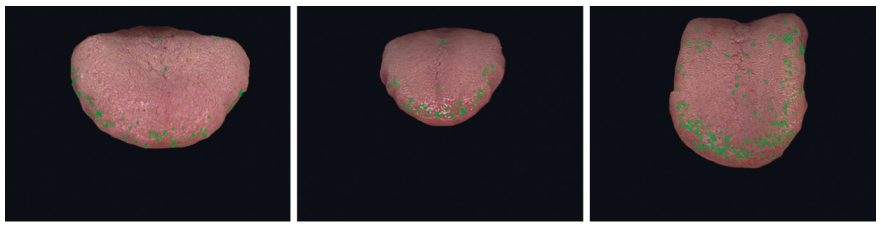

(a)

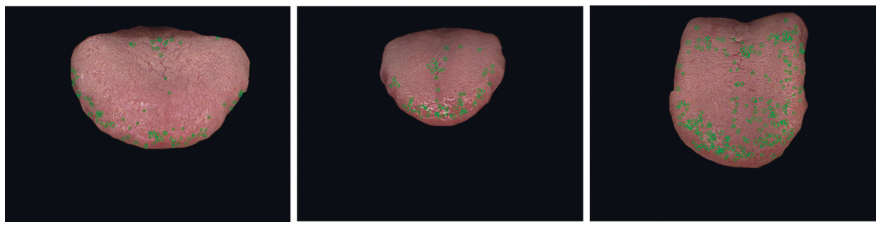

(b)

Figure 12: Automatic annotation results with and without partitioning. (a) Annotation with partitioning. (b) Annotation without partitioning. With annotation parameters differing between areas, the misdetections of center cracks are reduced.

Table 4: Prickle detection results and comparison with previous studies.

Method	Recall				Accuracy
	Root & center (%)	Tip (%)	Margin (%)	Total (%)	Total (%)
LOG [7]	84.97	67.37	84.23	86.95	—
SVM [5]	—	—	—	89.90	—
YOLO [28]	73.28	67.68	65.48	67.95	60.44
Vanilla faster-RCNN [26]	69.43	66.48	61.22	65.58	72.13
Ours w/o segmentation	88.89	89.45	83.34	89.77	86.69
Ours	**98.62**	**89.92**	**94.59**	**92.42**	**88.46**

any bounding box. As shown in Figure 11(e), the detected prickle patterns are similar to the annotation while it tends to detect prickles on the tip. To illustrate the principle of our neural network, we provided an attention heat map of the detector, as shown in Figure 11(f). The neural network had more attention on the edge of the tongue, where the prickles are most likely to appear. This attention is learned by the neural network automatically and has the potential to provide TCM doctors an intuition to distinguish a tongue with prickles. In addition, we fed the raw images into the detector as an ablation experiment to validate the necessity of segmentation, and the result is shown in the 3rd line of Table 4.

4. Discussion

Prickle, as an essential syndrome feature of TCM, can be used to assist in the diagnosis and treatment of subhealthy people. But the ambiguity of prickle recognition and the subjective preferences of doctors limit its further application. Combined with modern AI technology, we proposed an end-to-end computer vision-based prickle detection workflow, which makes prickle detection more precise and objective. This workflow is divided into three main steps. Firstly, Swin Transformer, a state-of-the-art semantic segmentation neural network, was employed to segment the tongue region out of a raw image. The segmented tongues were partitioned into four areas: root, center, tip, and margin to help the parameters setting of follow-up spot detection and prickle detection. Secondly, we manually labeled the prickles on 224 tongue images with the help of a spot detector and fed the result into the Faster-RCNN. Finally, the neural network extracted the features of images at both a texture level and morphological level to detect the prickles on the tongues. The precision of our segmentation is 99.47%, and the recall of our detection is 92.42%, which outperformed the existing methods. The result illustrates that the utilization of transfer learning made it possible to train neural networks on a limited number of images. Compared to previously published studies, it gets rid of the trivial parameters tuning procedure and releases the burden on researchers. Meanwhile, the workflow proposed is more portable, which means you can transfer the model to arbitrary tongue characteristics or image acquisition equipment.

In the context of artificial intelligence and big data, the informatization of TCM diagnosis is an area that urgently needs in-depth research. Our work took full advantage of the deep learning algorithm to implement an intelligent recognition of prickles and provided the possibility of establishing the quantitative association between the tongue image and clinical symptoms. In addition, incorporating a prickle detection model into the smartphone will allow people without medical knowledge to give themselves a simple health status assessment, and a quantitative and objective tongue diagnosis will also benefit the integration of TCM and modern Western medicine. The precise segmentation and feature recognition of the tonguecan also be used for throat swab robot perception.

Though our method is state-of-the-art, there are some aspects for further research. Firstly, the model was trained on the images sampled by a standard acquisition device, which limits its generalization and robustness. A larger dataset consisting of images from different devices would help the model to establish a greater degree of accuracy in this matter. Secondly, our model provides a paradigm for tongue feature detection. With petechiae, cracks, toothmarks, and other TCM features of the tongues labeled, the model has the potential to achieve an acceptable result. Thirdly, most existing learning-based tongue feature detection methods aim to find bounding boxes. It is possible to use a segmentor to classify every single pixel in the image into a kind of TCM tongue feature.

Data Availability

The experimental data and code used to support the findings of this study will be available on https://github.com/zz7379/PrickleDetection or on contacting the authors with reasonable request (wangxinzhou@tongji.edu.cn).

Conflicts of Interest

The authors declare that there are no conflicts of interest.

Authors' Contributions

Xinzhou Wang and Siyan Luo contributed equally to this work.

Acknowledgments

The research in the paper is jointly funded by the Sino-German Collaborative Research Project Crossmodal Learning (NSFC 62061136001/DFG TRR169), Key Technoligies on a Pharyngeal Swab Sampling Robot using Human-Machine Fusion Based on the Prey Mechanism of the Tip of the Chameleon Tongue and its Demonstration Applications (No. 2020GQG0006), and National Science Foundation No. 81973683.

References

[1] L. Zhi, D. Zhang, J. Q. Yan, Q. L. Li, and Q. L. Tang, "Classification of hyperspectral medical tongue images for tongue diagnosis," *Computerized Medical Imaging and Graphics*, vol. 31, no. 8, pp. 672–678, 2007.

[2] B. Zhang, H. Zhang, and G. Li, "Significant geometry features in tongue image analysis," *Evidence-based Complementary and Alternative Medicine*, vol. 2015, Article ID 897580, 8 pages, 2015.

[3] E. Vocaturo and E. Zumpano, "Machine learning opportunities for automatic tongue diagnosis systems," in *Proceedings of the 2020 IEEE International Conference On Bioinformatics and Biomedicine (BIBM)*, pp. 1498–1502, IEEE, Seout, South Korea, 2020.

[4] S. Han, X. Yang, Q. Qi et al., "Potential screening and early diagnosis method for cancer: tongue diagnosis," *International Journal of Oncology*, vol. 48, no. 6, pp. 2257–2264, 2016.

[5] B. Zhang, X. Wang, J. You, and D. Zhang, "Tongue color analysis for medical application," *Evidence-Based Complementary and Alternative Medicine*, vol. 2013, Article ID 264742, 11 pages, 2013.

[6] J. Hou, H. Su, B. Yan, H. Zheng, Z. Sun, and X.-C. Cai, "Classification of tongue color based on cnn," in *Proceedings of the 2017 IEEE 2nd International Conference On Big Data Analysis*, IEEE, Beijing, China, 2017.

[7] B. Huang, J. Wu, D. Zhang, and N. Li, "Tongue shape classification by geometric features," *Information Sciences*, vol. 180, no. 2, pp. 312–324, 2010.

[8] Z. Shi and C. Zhou, "Fissure extraction and analysis of image of tongue," *Computer Technology and Development*, vol. 1, no. 5, pp. 245–248, 2007.

[9] J. Kim, G. J. Han, B. H. Choi et al., "Development of differential criteria on tongue coating thickness in tongue diagnosis," *Complementary Therapies in Medicine*, vol. 20, no. 5, pp. 316–322, 2012.

[10] D. Meng, G. Cao, Y. Duan et al., "Tongue images classification based on constrained high dispersal network," *Evidence-Based Complementary and Alternative Medicine*, vol. 2017, Article ID 7452427, 12 pages, 2017.

[11] S. Wang, K. Liu, and L. Wang, "Tongue spots and petechiae recognition and extraction in tongue diagnosis images," *Computer Engineering and Science*, vol. 39, no. 6, pp. 1126–1132, 2017.

[12] Z. Shang, Z.-G. Du, B. Guan et al., "Correlation analysis between characteristics under gastroscope and image information of tongue in patients with chronic gastriti," *Journal of Traditional Chinese Medicine*, vol. 42, no. 1, pp. 102–107, 2022.

[13] J. Xu, Y. Sun, Z. Zhang, Y. Bao, and W. Li, "Recognition of acantha and ecchymosis in tongue pattern," *Journal of Shanghai University of Traditional Chinese Medicine*, vol. 3, no. 4, pp. 38–40, 2004.

[14] X. Wang, R. Wang, D. Guo, X. Lu, and P. Zhou, "A research about tongue-prickled recognition method based on auxiliary light source," *Chinese Joural of Sensors and Actuators*, vol. 29, no. 10, pp. 1553–1559, 2016.

[15] X. Zhang, Y. Guo, Y. Cai, and M. Sun, "Tongue image segmentation algorithm based on deep convolutional neural network and fully conditional random fields," *Journal of Beijing University of Aeronautics and Astronautics*, vol. 45, no. 12, pp. 2364–2374, 2019.

[16] L. Wang, Y. Tang, P. Chen, X. He, and G. Yuan, "Segmentation, two-phase convolutional neural network," *Journal of Image and Graphics*, vol. 23, no. 10, pp. 1571–1581, 2018.

[17] J. Li, B. Xu, X. Ban, P. Tai, and B. Ma, "A tongue image segmentation method based on enhanced hsv convolutional neural network," *International Conference on Cooperative Design, Visualization and Engineering*, vol. 1, pp. 252–260, 2017.

[18] H. Zhang, R. Jiang, T. Yang, J. Gao, Y. Wang, and J. Zhang, "Study on TCM tongue image segmentation model based on convolutional neural network fused with superpixel," *Evidence-Based Complementary and Alternative Medicine*, vol. 2022, Article ID 3943920, 12 pages, 2022.

[19] L. Wu, X. Luo, and Y. Xu, "Using convolutional neural network for diabetes mellitus diagnosis based on tongue images," *Journal of Engineering*, vol. 13, pp. 635–638, 2020.

[20] G. Wyszecki and W. S. Stiles, *Color Science: Concepts and Methods Quantitative Data and Formulae*, Wiley, New York, NY, USA, 2000.

[21] Z. Liu, Y. Lin, Y. Cao et al., "Swin transformer: hierarchical vision transformer using shifted windows," in *Proceedings of the IEEE/CVF International Conference on Computer Vision*, pp. 10012–10022, IEEE, Seoul, Korea, 2021.

[22] B. Zhou, H. Zhao, X. Puig et al., "Semantic understanding of scenes through the ade20k dataset," *International Journal of Computer Vision*, vol. 127, no. 3, pp. 302–321, 2019.

[23] D. G. Bailey and M. J. Klaiber, "Zig-zag based single-pass connected components analysis," *Journal of imaging*, vol. 5, no. 4, p. 45, 2019.

[24] X. Wang, J. Liu, C. Wu et al., "Artificial intelligence in tongue diagnosis: using deep convolutional neural network for recognizing unhealthy tongue with tooth-mark," *Computational and Structural Biotechnology Journal*, vol. 18, pp. 973–980, 2020.

[25] Z. Qi, L. Tu, Z. Luo et al., "Tongue image database construction based on the expert opinions: assessment for individual agreement and methods for expert selection," *Evidence-Based Complementary and Alternative Medicine*, vol. 2018, Article ID 8491057, 9 pages, 2018.

[26] S. Ren, K. He, R. Girshick, and J. Sun, "Faster r-cnn: towards real-time object detection with region proposal networks," *Advances in Neural Information Processing Systems*, vol. 1, no. 28, pp. 91–99, 2015.

[27] S. Hosseinzadeh Kassani and P. Hosseinzadeh Kassani, "A comparative study of deep learning architectures on melanoma detection," *Tissue and Cell*, vol. 58, pp. 76–83, 2019.

[28] J. Redmon, S. Divvala, R. Girshick, and A. Farhadi, "You only look once: unified, real-time object detection," in *Proceedings of the IEEE Conference on Computer Vision and Pattern Recognition*, pp. 779–788, Las Vegas, NV, USA, 2016.

[29] X. Zhu, H. Hu, S. Lin, and J. Dai, "Deformable convnets v2: more deformable, better results," in *Proceedings of the 2019 IEEE/CVF Conference on Computer Vision and Pattern Recognition (CVPR)*, IEEE, Long Beach, CA, USA, 2019.

[30] W. Liu, D. Anguelov, D. Erhan et al., "SSD: single shot multibox detector," in *European Conference on Computer Vision*, pp. 21–37, Springer, Berlin, Germany, 2016.

[31] L.-C. Lo, T.-L. Cheng, J. Y. Chiang, and N. Damdinsuren, "Breast cancer index: a perspective on tongue diagnosis in traditional Chinese medicine," *Journal of Traditional and Complementary Medicine*, vol. 3, no. 3, pp. 194–203, 2013.

[32] P.-C. Hsu, H.-K. Wu, H.-H. Chang, J.-M. Chen, J. Y. Chiang, and L.-C. Lo, "A perspective on tongue diagnosis in patients with breast cancer," *Evidence-Based Complementary and Alternative Medicine*, vol. 2021, Article ID 4441192, 9 pages, 2021.

[33] C.-J. Chung, C.-H. Wu, W.-L. Hu, C. H. Shih, Y. N. Liao, and Y. C. Hung, "Tongue diagnosis index of chronic kidney disease," *Biomedical Journal*, 2022.

[34] W. Pang, D. Zhang, J. Zhang et al., "Tongue features of patients with coronavirus disease 2019: a retrospective cross-sectional study," *Integrative medicine research*, vol. 9, no. 3, Article ID 100493, 2020.

Hindawi
Evidence-Based Complementary and Alternative Medicine
Volume 2022, Article ID 9156186, 9 pages
https://doi.org/10.1155/2022/9156186

Research Article

Clinical Characteristics and Treatment Overview in Hand-Foot-and-Mouth Disease Using Real-World Evidence Based on Hospital Information System

Guoming Chen,[1,2] **Chuyao Huang**,[1] **Dongqiang Luo**,[1] **Jiawei Yang**,[1] **Yuzhen Shi**,[1] **Danyun Li**,[1] **Zhuoyao Li**,[1] **Tie Song**,[3] **Hua Xu**,[4] **and Fen Yang**[3]

[1]*Guangzhou University of Chinese Medicine, Guangzhou, China*
[2]*School of Chinese Medicine, Li Ka Shing Faculty of Medicine, The University of Hong Kong, Hong Kong SAR, China*
[3]*Guangdong Center for Disease Control and Prevention, Guangzhou, China*
[4]*First Affiliated Hospital of Guangzhou University of Chinese Medicine, Guangzhou, China*

Correspondence should be addressed to Hua Xu; ekxuhua@126.com and Fen Yang; 492242163@qq.com

Received 18 November 2021; Revised 6 July 2022; Accepted 10 August 2022; Published 20 September 2022

Academic Editor: Talha Bin Emran

Objectives. To describe the epidemiological characteristics and medication overview of HFMD in Guangzhou and analyze the factors of length of stay (LOS) based on TCM usage. *Method*. From January 1, 2014, to June 30, 2019, clinical data of HFMD (ICD-10 B08.401) as the initial diagnosis, based on HIS of five medical institutions for outpatient and inpatient cases, was collected. The inpatient cases of the five hospitals in Guangzhou were utilized for hospitalization analysis. Information extracted from the warehouse was standardized. Descriptive analysis was used for baseline characteristics, medication usage, and inpatient characteristics. Potential factors were analyzed by bivariate analysis. COX regression analysis and Kaplan–Meier analysis for calculating HRs and 95% CIs were adopted to determine the predictors of LOS. Stratified COX regression was applied to analyze the relationship between predictors and LOS and to calculate interaction. *Results*. A total of 14172 patients with HFMD were included. It showed that HFMD would occur in males, infants, and summer. Cause and symptoms are the two aspects of conventional Western medicine treatments, while TCM treatment of HFMD took clearing heat and detoxification as the basic principle. Inpatients with HFMD were divided into two groups by the use ratio of TCM. Age, season, and disease severity were possible correlated factors of LOS, extrapolating from their disparity in distribution. By stratified Cox regression, three factors following presented as possible contributions to shortening LOS, including TCM ≥ 0.1 (HR = 1.79, 95% CI (1.67–1.92), $P < 0.01$), winter (HR = 1.28, 95% CI (1.12–1.47)), $P < 0.01$), mild HFMD (HR = 1.93, 95% CI (1.69–2.22), $P < 0.01$). Additive interaction of TCM use and disease severity was significant (RERI = 1.014 (0.493–1.534), $P < 0.01$). *Conclusion*. Young children and high temperature were the risk factors of HFMD infection, which suggests that increasing surveillance for susceptible particular-age individuals and season is indispensable. Favorable factors to decrease LOS included a higher proportion of TCM use, mild HFMD, and onset in winter. The proportion of TCM use had additive interaction with disease severity, indicating that TCM may have antiviral and other biological effects on HFMD. Increasing the proportion of TCM use was probably beneficial to shortening LOS.

1. Introduction

Hand-foot-and-mouth disease (HFMD) is a common contagion caused by picornaviruses, especially human enteroviruses and coxsackieviruses [1]. Due to its features of self-limiting, few concentrations have been put on this disease. And its identical clinical manifestations, presenting as a low-grade fever with a maculopapular or papulovesicular rash on the hands and soles of the feet and painful oral ulcerations, make it easy to be overlooked [2]. While in recent years, some evidence has shown that HFMD can also cause neurologic or cardiopulmonary

complications, which can lead to poor prognosis or even death [3]. A 0.30% mortality was reported in China and it maintained a high recurrence rate from 2008 to 2014 [4]. Guangdong is a populous province in China, where rising morbidity of HFMD has been witnessed in recent years, making it a common infectious disease [5]. The timing of monitoring the susceptible population is of great significance for disease prevention.

Currently, a large sample of clinical data is still needed to support the optimal proposal of treatment. There has not been an approved antiviral treatment for HFMD, particularly for the causative virus [2]. While as suggested, mild HFMD should be managed according to the symptoms, whose primary therapeutic purpose is to relieve pain, abate fever, and stay hydrated [2]. And in severe cases, supportive treatment and symptomatic treatment are mainly applied to keep basic life signs. As for prevention, the vaccine seems to be the best measure to combat HFMD. In China, three kinds of vaccines have been identified to be safe and protective [6–8]. Within the system of terms of traditional Chinese medicine (TCM), HFMD is included in the category of plague, rashes related to contagion. TCM had been recommended by the China Ministry of Health in 2010 for the treatment of HFMD, for its safety and high curative effect [9]. TCM can be used alone for relieving HFMD, of which the plant extracts have been demonstrated to have anti-infection properties [10, 11]. Flavonoids can suppress viruses, including glycyrrhizin [12], chrysin [13], etc. However, the clinical efficacy of TCM is still limited and in most cases, we regard the improvement of clinical symptoms as a key indicator of discharge. Hence, the factor of the length of stay (LOS) is viewed as one of the primary categories to evaluate efficacy.

In this study, we collected cases whose first-listed diagnosis is HFMD from 5 hospitals in Guangzhou, Guangdong, China. Data were extracted from the Hospital Information System (HIS), which involves reservation registration, pharmacy management, hospitalization management system, and toll collection. Based on the statistical analysis results, we described the clinical characteristics and treatment of HFMD in Guangzhou and analyzed the factors of LOS based on TCM usage.

2. Methods

2.1. Data Set and Sample Selection. This cross-section study extracted clinical data of outpatient and inpatient cases with HFMD (ICD-10 B08.401) as the first diagnosis from HIS. The collecting time ranged from January 1, 2014, to June 30, 2019. Medical institutions included the First Affiliated Hospital of Guangzhou University of Chinese Medicine, Guangdong Second Provincial General Hospital, Guangdong Provincial Hospital of Traditional Chinese Medicine, Guangdong Provincial Maternal and Child Health Care Hospital, and Guangzhou Women and Children's Medical Center. Among these, Guangdong Provincial Hospital of Traditional Chinese Medicine and Guangdong Second Provincial General Hospital had only outpatients. The information collection of cases included personal details (gender, age, address, admission time, and medical ID), diagnosis, prescription, dosage, unit, usage, and frequency. Given that follow-up visits may affect total treatment, we retained the first-visit ID at the same hospital.

2.2. Data Standardization. As the exported case details varied in each hospital information system, the data was standardized for analysis. Year became a transformation unit for age. For diagnosis, HFMD identification and classification would refer to ICD-10 and guidelines for the diagnosis and treatment of HFMD (2018 version) [14]. The frequency of a single herb, drug, or Chinese patent medicine was denoted as one. According to the patient's prescription, the proportion of TCM use was recorded. Chinese patent medicine with the same composition but different dosage forms was defined as the same drug; Western medicine was standardized according to the chemical name; Traditional Chinese medicine pieces were referred to Chinese Pharmacopoeia (2020 version) for standardization. For seasonal onset analysis, the visit time was divided into spring (March, April, and May), summer (June, July, and August), autumn (September, October, and November), and winter (December, January, and February). To analyze the onset feature in different developmental stages, the age in the yearly unit was divided into neonate (0–1 month), infant (1 month-2 year), preschool (2–6 year), child (6–12 year), adolescent (12–18 year) and adult (>18 year) [15].

2.3. Statistical Analysis. All data analyses were performed by SPSS 23.0 and R software (version 4.0.5). Depending on whether the data followed a normal distribution, mean ± standard deviation (SD) or median (interquartile range (IQR)) were adopted to describe measurement data. Enumeration data were presented as frequency. Descriptive analysis was used for the overview description of baseline characteristics, drug use, and inpatient case characteristics. Potential factors were analyzed by bivariate analysis. Through the survminer and survival packages of R software, Cox regression analysis was used to calculate HRs and 95% CIs to determine the independent and significant predictors of inpatient of patients with HFMD. Kaplan–Meier analysis was used for evaluating the effect of predictors on the LOS of patients with HFMD. The interaction R package was used to calculate the additive and multiplicative interactions of the two factors, and the forest plot package was used to draw COX regression analysis. A P value <0.05 was considered statistically significant.

3. Results

3.1. Patient Demographics and Baseline Characteristics. A total of 14172 patients with HFMD as the first diagnosis were included. Male cases (62.14%) were more than female cases (37.86%). Infancy accounted for the largest proportion (53.71%), followed by preschool (41.14%). Summer was the season with a high incidence of HFMD. The majority of HFMD patients were treated as outpatients with no more than three visits (Table 1).

Table 1: Baseline characteristics.

Characteristic	Patients (n)
Gender	
Male	8807
Female	5365
Age, year	
Neonate	11
Infant	7612
Preschool	5830
Child	540
Adolescent	44
Adult	135
Visit time	
Spring (3–5)	3801
Summer (6–8)	4857
Autumn (9–11)	3680
Winter (12–2)	1834
Type of hospital	
Outpatient	10426
Inpatient	3746
Visit frequency	
1–3	14112
4–6	58
>6	2

3.2. Medication Use of HFMD. The most frequent Chinese herb was Glycyrrhizae radix et rhizoma, a tonifying medical, when it is not processed, it has the additional effect of heat-clearing, detoxicating, and dispelling phlegm. From the perspective of Chinese herb efficacy, the treatment of HFMD mainly focused on lowering the fever, clearing heat, removing dampness, and reducing phlegm (Table 2). The main application of Chinese patent medicine was an external application and oral administration, where, aerosol inhalation is a method to disperse the tiny droplet drug to the nose or throat, which is frequently used in respiratory disease. It can be seen from the above that TCM has flexible dosage form selection in the treatment of HFMD (Table 3). As for the use of Western drug, antimicrobial drugs had the highest frequency, aiming to control viral infections and other infectious complications. Adrenocortical hormones exerted anti-inflammatory and antiallergic synergy. *M* receptor blockers and adrenoceptor agonists can smooth wheezing (Table 4).

3.3. Factors of Hospitalization Day in HFMD. 3615 patients were enrolled in the COX regression and Kaplan–Meier analysis, including 2346 males and 1269 females, with an age ranging from 21 days to 25 years. The patients were divided into two groups according to the proportion of TCM use, and there were significant differences in the distribution of age, season, and disease between the two groups (Table 5). Univariate COX regression showed significant correlated factors with LOS, including the proportion of TCM use, disease distribution, specific age section (neonate, infant, preschool, and child), and specific season (summer and spring) (Table 6). Kaplan–Meier analysis showed that disease type and the proportion of TCM use correlated significantly with LOS (Figure 1). Due to the adults and adolescents involved with too less quantity, the data were excluded in stratified COX regression. Confounding factors were adjusted by using three models Model1 adjusted age and sex; Model2 adjusted age, sex, and season; Model3 adjusted age, sex, season, and disease. Stratified COX regression showed that three factors were statistically significant in shortening hospitalization stay, including TCM ≥ 0.1 (HR = 1.79, 95% CI (1.67–1.92), $P < 0.01$), winter (HR = 1.28, 95% CI (1.12–1.47)), $P < 0.01$), mild HFMD (HR = 1.93, 95% CI (1.69–2.22), $P < 0.01$) (Table 7). TCM ≥ 0.1, mild HFMD, and onset in winter were favorable factors in shortening LOS (Figure 2). It could be noted that HR of TCM ≥ 0.1 and winter decreased after the addition of disease severity in Model3, and the increased risk of LOS was 11% and 3%, respectively. Additive interaction of the proportion of TCM use and disease severity was significant (RERI = 1.014 (0.493–1.534), $P < 0.01$), while multiplicative interaction of them was not (RR = 1.13 (0.81–1.57), $P = 0.49$).

4. Discussion

HFMD is prevalent in China and is affected by living environment and meteorological factors. In 2008, the outbreak of HFMD in China led to a public health crisis, and consequently, it was classified as a *C*-class notifiable communicable disease by the Ministry of Health of China. The incidence of Guangdong was 4 times the national average [16], and a Bayesian spatiotemporal model showed a higher relative risk in Pearl River Delta [17]. To induce an overview of the characteristics and treatment of HFMD, this study collected real-world evidence of HFMD in Guangzhou, Guangdong.

For the epidemiological factors, HFMD seemed to be correlated with gender, age, and season. The ratio of men to

Table 2: Chinese herb use (Top 10).

Rank	Herbal drug	Efficacy	Frequency (n)
1	Glycyrrhizae radix et rhizoma	Tonifying and replenishing	1871
2	Forsythiae Fructus	Heat-clearing, detoxicating	1545
3	Pogostemonis Herba	Resolving dampness	1155
4	Belamcandae Rhizoma	Heat-clearing, detoxicating	1060
5	Phragmitis Rhizoma	Heat-clearing and fire-purging	988
6	Lophatheri Herba	Heat-clearing and fire-purging	984
7	Coicis semen	Dampness-draining diuretic	829
8	Platycodonis Radix	Clearing and resolving heat-phlegm	711
9	Scutellariae Radix	Clearing heat and drying dampness	697
10	Menthae Haplocalycis Herba	Releasing the exterior with pungent-cool	693

Table 3: Chinese patent medicine use (Top 10).

Rank	Chinese patent medicine	Usage	Frequency (n)
1	Kangfu Xinye	External application	3619
2	Chushi zhiyang xiye	External application	1944
3	Kaihoujian penwuji	Aerosol inhalation	1473
4	Kouqiangyan penwuji	Aerosol inhalation	1379
5	Jian'er qingjie ye	Oral administration	1306
6	Fuganlin koufuye	Oral administration	1080
7	Sihuangxiaoyan xiji	External application	1023
8	Qingrejieduqushi keli	Oral administration	908
9	Fufang yuxingcao keli	Oral administration	751
10	Jinlian qingre Paotengpian	Oral administration	606

Table 4: Systemic medication use (TOP 10).

Rank	Treatment	Frequency (n)
1	Antiviral drug	3269
2	Cephalosporin	1929
3	Adrenocortical hormones	1732
4	Penicillins	1374
5	M Receptor blocker	1158
6	H2 receptor blocker	933
7	Adrenoceptor agonists	757
8	Benzodiazepines	721
9	Mucolytic agents	571
10	Antituberculous drugs	390

Table 5: Characteristics of HFMD patient group based on the proportion of TCM use.

		Proportion of TCM use		P
		TCM < 0.1 ($n = 1698$)	TCM ≥ 0.1 ($n = 1917$)	
Age	Neonate	2	2	<0.01
	Infant	1032	1227	
	Preschool	644	649	
	Child	17	40	
	Adolescent	1	1	
	Adult	2	0	
Sex	Male	1093	1253	0.53
	Female	605	664	
Season	Spring	483	495	<0.01
	Summer	669	725	
	Autumn	396	571	
	Winter	150	126	
Disease severity	Mild	1512	1872	<0.01
	Severe	186	45	

Table 6: Univariate COX regression results.

		Coef	HR	*P*	95% CI
Age	Adolescent				
	Neonate	2.50	12.15	0.01	(1.70, 86.89)
	Infant	1.50	4.47	0.04	(1.11, 18.07)
	Preschool	1.47	4.34	0.04	(1.07, 17.53)
	Child	1.57	4.82	0.03	(1.17, 19.94)
	Adult	0.53	1.70	0.60	(0.24, 12.12)
Sex	Male				
	Female	0.03	1.03	0.40	(0.96, 1.10)
Season	Autumn				
	Spring	−0.15	0.86	0.00	(0.79, 0.94)
	Summer	−0.14	0.87	0.00	(0.80, 0.95)
	Winter	0.12	0.12	0.09	(0.98, 1.28)
Proportion of TCM use	<0.1				
	≥0.1	0.64	0.53	0.00	(0.49, 0.56)
Disease condition	Mild				
	Severe	−0.83	0.44	0.00	(0.38, 0.50)

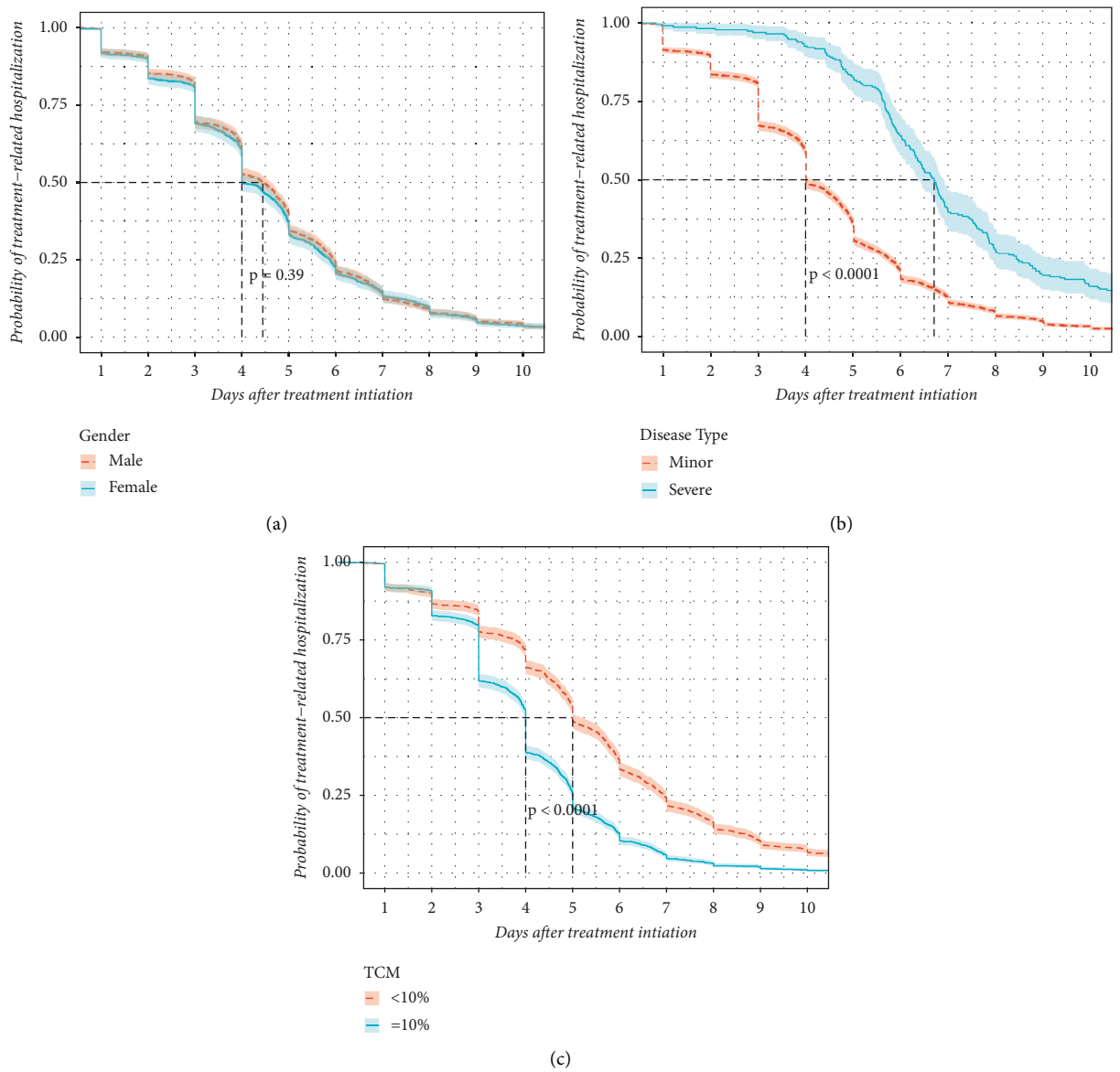

Figure 1: Kaplan–Meier for factors of hospitalization days of HFMD. (a) Comparison of gender. (b) Comparison of disease type. (c) Comparison of the proportion of TCM use).

Table 7: The relationship of LOS and factors in a patient with HFMD.

Factors	Model1	Model2	Model3
TCM ≥ 0.1	1.90 (1.77–2.03)	1.90 (1.78–2.04)	1.79 (1.67–1.92)
Age			
Neonate and infant			
Preschool	0.99 (0.92–1.06)	0.98 (0.92–1.05)	0.96 (0.89–1.03)
Child	0.97 (0.74–1.26)	0.96 (0.74–1.26)	0.99 (0.76–1.28)
Sex (female)	1.03 (0.96–1.10)	1.03 (0.96–1.10)	1.03 (0.96–1.10)
Season			
Spring			
Summer		1.00 (0.92–1.09)	1.02 (0.94–1.11)
Autumn		1.10 (1.00–1.20)	1.09 (1.00–1.20)
Winter		1.31 (1.15–1.50)	1.28 (1.12–1.47)
Disease (Nonserious)			1.93 (1.69–2.22)
Additive interaction: RERI = 1.014 (0.493–1.534), $P < 0.01$; Multiplicative interaction: Disease*TCM0.1 RR = 1.13 (0.81–1.57), $P = 0.49$			

Model1: adjust age, sex; Model2: adjust age, sex, season; Model3: adjust age, sex, season, disease.

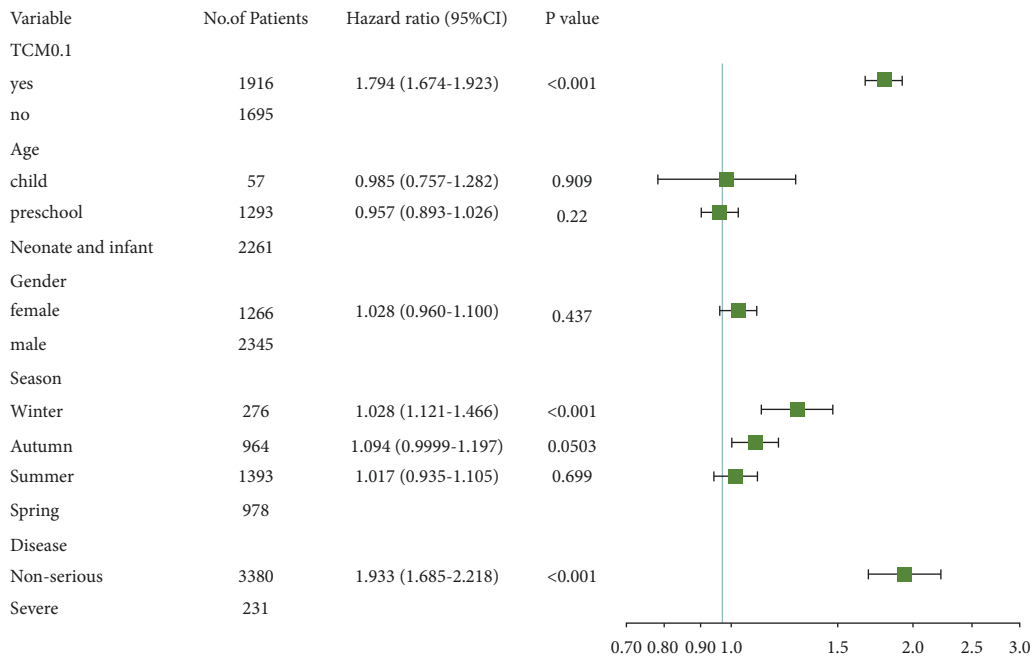

Figure 2: The analysis between LOS and factors is based on a forest plot of stratified COX regression.

women approximately was 1.64 : 1, which is in accordance with the result of a previous study [16, 18]. The etiology of HFMD was enterovirus infection, primarily caused by enterovirus 71 (EV71) and coxsackievirus A16 (Cox A16) [19]. It was reported that the latent infectious rate of enterovirus in healthy males in China was higher than in females [20]. Boys under high temperatures were at a higher risk of HFMD on lag 0 days in the distributed lag nonlinear model, while girls had an increasingly cumulative risk of HFMD with increased lag days [21]. Infants and preschools also had a higher incidence risk of HFMD in this study. The age-specific onset varied geographically: 3–5 years old in northern China and 0–2 years old in southern China [22], which was generally consistent with the results of this study. As infancy has not fully developed, the poor self-protection ability may be one of the factors for the high susceptibility. Of note, preschool children gathered in kindergarten, which could increase the risk of mutual infection [22]. However, the lack of stratification of vaccination history in this study may influence the results. Temperature (10–25°C), humidity (70–90%), wind speed (< 2.5 m/s), and sunshine time (> 9 h) are the risk factors for HFMD [23]. In Guangzhou, the temperature of summer maintains to be above 25°C, while high humidity can increase droplet transmission, and long-time sunshine generally raises the day/night temperature. This may be the reason for the highest prevalence in

summer. Except in winter, the temperature is kept above 10°C for a long time, providing favorable conditions for enterovirus survival.

For medication use, the treatment of HFMD included traditional Chinese medicine decoction, Chinese patent medication, and Western medicine. In TCM theory, HFMD belongs to the category of "plague warm and clip wet" and the TCM treatment of HFMD needs to follow the progression stages. At eruption, wind syndrome, and dyspnea collapse stages, the fundamental law of treatment is heat-clearing and detoxicating, flexibly coordinating resolving dampness, outthrusting the pathogen, and calming endogenous wind [14]. Our results showed that the use of Chinese herbs and oral Chinese patent medicine was corresponding with the TCM pathogenesis of HFMD. It has been verified that Forsythiae Fructus had a function of anti-inflammation, antivirus, antibacterial, and neuroprotection according to the literature so far [24]. The antiviral activities may originate from the phenolic acids of Forsythiae Fructus [25, 26]. The extraction of Pogostemonis Herba can inhibit influenza viral infection, contributing to the recovery of pneumonia [27, 28]. The efficacy of external application and aerosol inhalation of Chinese patent medication can basically relieve papulovesicular rash and oral ulcerations, but further clinical evidence is needed to support this. Antimicrobial drugs occupied the largest proportion of Western medicine. Due to the lack of specific medicine for the enterovirus, ribavirin was one of the common antiviral drugs in the treatment of HFMD in this study. Cephalosporin and penicillins were used to control bacterial infections. Adrenocortical hormone had an effect on anti-inflammation and controlling edema which was adopted in case of HFMD with high fever or encephalomyelitis, as appropriate. *M* receptor blockers and adrenoceptor agonis are effective in alleviating bronchospasm and dyspnea. It can be seen that clinical treatment was mainly divided into etiological treatment and symptomatic treatment. Fever for more than 3 days, lethargy, pathologic reflexes, and convulsions were risk factors for severe HFMD [29].

The proportion of TCM use, disease severity, and the particular season were the significant correlated factors with LOS based on univariate COX regression. Stratified COX regression showed that three factors were significantly beneficial to decrease LOS, including TCM ≥ 0.1 (HR = 1.79, 95% CI (1.67–1.92), $P < 0.01$), winter (HR = 1.28, 95% CI (1.12–1.47)), $P < 0.01$), mild HFMD (HR = 1.93, 95% CI (1.69–2.22), $P < 0.01$). This study collected the admission date of inpatients with HFMD. Given that HFMD was an acute febrile illness, the hospitalization date generally was close to the onset date. Consistent with the previous research, the relatively high temperature would be the potential risk of HFMD. Correspondingly, in the case of low temperatures in winter, the virus is not easy to survive, which was a favorable condition to promote recovery and shorten the LOS. A randomized controlled trial showed the defervescence time of rectal administration of TCM plus conventional therapy was significantly shorter than conventional therapy alone [10]. Compared to Western medicine, Reduning injection plus Western medicine could significantly lower the fever and shorten the time of rash disappearance in mild HFMD [30]. It was speculated that the increased proportion of TCM use could decrease LOS. In addition, stratified COX regression showed that the risk of increased LOS was 11% (TCM ≥ 0.1) and 3% (Winter) after disease severity was added to adjusted Model3. The mild HFMD could significantly shorten LOS. So additive interaction of the proportion of TCM use and disease severity was significant, while multiplicative interaction of them had no statistical significance. Addition is more reasonable than multiplication in analyzing biological interactions. There is biological synergy between the two factors with positive additive interaction [31]. This may suggest TCM affects the progression of HFMD through a biological mechanism. Glycyrrhizic acid (GA) is extracted from *Glycyrrhiza* uralensis Fisch and has an antivirus effect. GA dose-dependently blocked viral replication of EV71 and CVA16. However, the two antiviral mechanisms were distinct since GA inactivated CVA16 directly but its anti-EV71 effect was associated with events post virus cell entry [32].

In this study, the region, incidence factors, vaccination history, and clinical symptoms of HFMD were not subdivided, and the characteristics of HFMD depend on more demographic data supply. Due to the lack of symptoms comparison and biochemical indicators, it was not comprehensive to evaluate the efficacy of TCM on HFMD. Also, the hospital discharge was not totally equivalent to a cure, considering the possibility of being transferred to the hospital after discharge. And more indicator support is still in need to evidence the efficacy of TCM on HFMD.

5. Conclusion

Surveillance for young individuals and high-temperature periods may be beneficial to early prevention. TCM treatment is based on the law of clearing heat, detoxifying, and resolving dampness, with flexible dosage forms. However, its clinical efficacy needs support from more high-quality clinical studies. Western medication treatment was mainly antiviral treatment combined with symptomatic treatment. The increased proportion of TCM use, mild HFMD, and onset in winter were favorable factors in shortening LOS. The proportion of TCM use and disease severity had significant additive interaction, indicating that TCM use could affect the biological mechanism of HFMD and eventually influence the LOS.

Data Availability

The clinical data used to support the findings of this study were supplied by Fen Yang under license and so cannot be made freely available. Requests for access to these data should be made to Fen Yang, 160 Qunxian Road, Panyu District, Guangzhou, Guangdong (e-mails: 492242163@qq.com).

Conflicts of Interest

The authors declare that they have no conflicts of interest.

Authors' Contributions

Guoming Chen and Chuyao Huang are cofirst authors.

Acknowledgments

This study was supported by the Project of Administration of Traditional Chinese Medicine of Guangdong Province of China (20195005).

References

[1] G. L. Repass, W. C. Palmer, and F. F. Stancampiano, "Hand, foot, and mouth disease: identifying and managing an acute viral syndrome," *Cleveland Clinic Journal of Medicine*, vol. 81, no. 9, pp. 537–543, 2014.

[2] S. Esposito and N. Principi, "Hand, foot and mouth disease: current knowledge on clinical manifestations, epidemiology, aetiology and prevention," *European Journal of Clinical Microbiology & Infectious Diseases: Official Publication of the European Society of Clinical Microbiology*, vol. 37, pp. 391–398, 2018.

[3] L. Long, L. Xu, Z. Xiao et al., "Neurological complications and risk factors of cardiopulmonary failure of EV-A71-related hand, foot and mouth disease," *Scientific Reports*, vol. 6, no. 1, Article ID 23444, 2016.

[4] W. Xing, Q. Liao, C. Viboud et al., "Hand, foot, and mouth disease in China, 2008-12: an epidemiological study," *The Lancet Infectious Diseases*, vol. 14, no. 4, pp. 308–318, 2014.

[5] X. G.-z. Wang Si-jia and S.-fa Nie, "Advancement of epidemiology on hand-foot-mouth disease," *Chinese Journal of Public Health Management Medicine*, vol. 33, pp. 492–496, 2017.

[6] J. X. Li, Y. F. Song, L. Wang et al., "Two-year efficacy and immunogenicity of sinovac enterovirus 71 vaccine against hand, foot and mouth disease in children," *Expert Review of Vaccines*, vol. 15, no. 1, pp. 129–137, 2016.

[7] F. Zhu, W. Xu, J. Xia et al., "Efficacy, safety, and immunogenicity of an enterovirus 71 vaccine in China," *New England Journal of Medicine*, vol. 370, no. 9, pp. 818–828, 2014.

[8] F. C. Zhu, F. Y. Meng, J. X. Li et al., "Efficacy, safety, and immunology of an inactivated alum-adjuvant enterovirus 71 vaccine in children in China: a multicentre, randomised, double-blind, placebo-controlled, phase 3 trial," *The Lancet*, vol. 381, no. 9882, pp. 2024–2032, 2013.

[9] The Ministry of Health of the People's Republic of China, *Guideline for the Diagnosis and Treatment of Hand Foot and Mouth Disease*, 2010.

[10] X. Li, X. Zhang, J. Ding et al., "Comparison between Chinese herbal medicines and conventional therapy in the treatment of severe hand, foot, and mouth disease: a randomized controlled trial," *Evidence-Based Complementary and Alternative Medicine*, vol. 2014, Article ID 140764, 7 pages, 2014.

[11] M. M. Rahman, M. S. Rahaman, M. R. Islam et al., "Multifunctional therapeutic potential of phytocomplexes and natural extracts for antimicrobial properties," *Antibiotics*, vol. 10, 2021.

[12] J. Cinatl, B. Morgenstern, G. Bauer, P. Chandra, H. Rabenau, and H. Doerr, "Glycyrrhizin, an active component of liquorice roots, and replication of SARS-associated coronavirus," *The Lancet*, vol. 361, no. 9374, pp. 2045-2046, 2003.

[13] Y. Liu, X. Song, C. Li et al., "Chrysin ameliorates influenza virus infection in the upper airways by repressing virus-induced cell cycle arrest and mitochondria-dependent apoptosis," *Frontiers in Immunology*, vol. 13, Article ID 872958, 2022.

[14] X. W. Li, X. Ni, S. Y. Qian et al., "Chinese guidelines for the diagnosis and treatment of hand, foot and mouth disease," *World Journal of Pediatrics*, vol. 14, no. 5, pp. 437–447, 2018.

[15] A. Makri, M. Goveia, J. Balbus, and R. Parkin, "Children's susceptibility to chemicals: a review by developmental stage," *Journal of Toxicology and Environmental Health, Part A B*, vol. 7, no. 6, pp. 417–435, 2004.

[16] T. Deng, Y. Huang, S. Yu et al., "Spatial-temporal clusters and risk factors of hand, foot, and mouth disease at the district level in Guangdong Province, China," *PLoS One*, vol. 8, no. 2, Article ID e56943, 2013.

[17] Y. Wang, Y. Lai, Z. Du et al., "Spatiotemporal distribution of hand, foot, and mouth disease in Guangdong province, China and potential predictors, 2009–2012," *International Journal of Environmental Research and Public Health*, vol. 16, no. 7, p. 1191, 2019.

[18] B. Chen, Y. Yang, X. Xu et al., "Epidemiological characteristics of hand, foot, and mouth disease in China: a meta-analysis," *Medicine (Baltimore)*, vol. 100, no. 20, Article ID e25930, 2021.

[19] N. Goksugur and S. Goksugur, "Hand, foot, and mouth disease," *New England Journal of Medicine*, vol. 362, no. 14, p. e49, 2010.

[20] Y. J. Zhou, X. D. Niu, Y. Q. Ding, Z. Qian, and B. L. Zhao, "Prevalence of recessive infection of pathogens of hand, foot, and mouth disease in healthy people in China: a meta-analysis," *Medicine (Baltimore)*, vol. 100, no. 7, Article ID e24855, 2021.

[21] J. Wang and S. Li, "Nonlinear effect of temperature on hand, foot, and mouth disease in Lanzhou, China," *Medicine (Baltimore)*, vol. 99, no. 45, Article ID e23007, 2020.

[22] J. Zhao, F. Jiang, L. Zhong, J. Sun, and J. Ding, "Age patterns and transmission characteristics of hand, foot and mouth disease in China," *BMC Infectious Diseases*, vol. 16, no. 1, p. 691, 2016.

[23] W. Zhang, Z. Du, D. Zhang, S. Yu, and Y. Hao, "Boosted regression tree model-based assessment of the impacts of meteorological drivers of hand, foot and mouth disease in Guangdong, China," *The Science of the Total Environment*, vol. 553, pp. 366–371, 2016.

[24] L. Gong, C. Wang, H. Zhou et al., "A review of pharmacological and pharmacokinetic properties of Forsythiaside A," *Pharmacological Research*, vol. 169, Article ID 105690, 2021.

[25] L. Wei, Y. Mei, L. Zou et al., "Distribution patterns for bioactive constituents in pericarp, stalk and seed of forsythiae fructus," *Molecules*, vol. 25, no. 2, p. 340, 2020.

[26] M. M. Rahman, M. S. Rahaman, M. R. Islam et al., "Role of phenolic compounds in human disease: current knowledge and future prospects," *Molecules*, vol. 27, no. 1, p. 233, 2021.

[27] Y. Yu, Y. Zhang, S. Wang, W. Liu, C. Hao, and W. Wang, "Inhibition effects of patchouli alcohol against influenza a virus through targeting cellular PI3K/Akt and ERK/MAPK signaling pathways," *Virology Journal*, vol. 16, no. 1, p. 163, 2019.

[28] X. L. Wu, D. H. Ju, J. Chen et al., "Immunologic mechanism of Patchouli alcohol anti-H_1N_1 influenza virus may through regulation of the RLH signal pathway *in vitro*," *Current Microbiology*, vol. 67, no. 4, pp. 431–436, 2013.

[29] B. J. Sun, H. J. Chen, Y. Chen, X. D. An, and B. S. Zhou, "The risk factors of acquiring severe hand, foot, and mouth disease: a meta-analysis," *The Canadian Journal of Infectious Diseases & Medical Microbiology*, vol. 2018, Article ID 2751457, 12 pages, 2018.

[30] G. Zhang, J. Zhao, L. He et al., "Reduning injection for fever, rash, and ulcers in children with mild hand, foot, and mouth disease: a randomized controlled clinical study," *Journal of Traditional Chinese Medicine*, vol. 33, no. 6, pp. 733–742, 2013.

[31] S. Akhtar, "Areca nut chewing and esophageal squamous-cell carcinoma risk in Asians: a meta-analysis of case-control studies," *Cancer Causes & Control*, vol. 24, no. 2, pp. 257–265, 2013.

[32] J. Wang, X. Chen, W. Wang et al., "Glycyrrhizic acid as the antiviral component of Glycyrrhiza uralensis Fisch. Against coxsackievirus A16 and enterovirus 71 of hand foot and mouth disease," *Journal of Ethnopharmacology*, vol. 147, no. 1, pp. 114–121, 2013.

Hindawi
Evidence-Based Complementary and Alternative Medicine
Volume 2022, Article ID 9090697, 8 pages
https://doi.org/10.1155/2022/9090697

Review Article

The Origin and Development of Piji Pills: An Ancient Prescription of Traditional Chinese Medicine

Fudong Liu, Xiaochen Jiang, Chuanlong Zhang, Guibin Wang, Yi Li, and Bo Pang

Guang'anmen Hospital, China Academy of Chinese Medical Sciences, Beijing 100053, China

Correspondence should be addressed to Bo Pang; drpangbo@gmail.com

Received 19 April 2022; Revised 3 August 2022; Accepted 2 September 2022; Published 12 September 2022

Academic Editor: Talha Bin Emran

Objective. Ancient prescriptions of traditional Chinese medicine (TCM) are an important source for innovative drug research and development, which has garnered increasing attention in recent years. Piji Pills, an ancient TCM prescription, has a long history and remarkable clinical efficacy in the treatment of digestive disorders. Thus, the purpose of this study was to explore the origin and development of Piji Pills and to discuss the potential future direction of an ancient TCM prescription. *Method*. We analyzed the origin and development of the Piji Pills by reviewing literature records and their evolution in ancient books. We used a full-text database covering 2,090 TCM ancient books and implemented the full-text retrieval function based on Ulysses software. A full-text search was conducted using the keyword "Piji Pills" ("脾积丸" in Chinese). The results generated 128 pieces of literature from 35 ancient TCM books. In order to identify pertinent sections from the generated results, the results were proofread by two independent authors (Fudong Liu and Xiaochen Jiang) who had sufficient experience concerning ancient books. The developmental process of the Piji Pills was divided into early, late, and modern times. With the approach of statistical methods and chronological description, we manually searched, indexed, and transformed 2,090 ancient TCM books. *Result*. From the time Piji Pills were first proposed, the records in ancient books became increasingly detailed, providing an in-depth discussion of their composition, dosage, and action mechanisms. In modern times, the research on key drugs found in Piji Pills has made a great contribution to clinical practice. However, the compound research on Piji Pills is still relatively superficial and requires further in-depth study. *Conclusions*. In this study, statistical methods were used to chronologically clarify the developmental process of Piji Pills. We found that the Piji Pills were widely used and had a significant advantage in the treatment of digestive system diseases. In-depth knowledge mining of ancient books could potentially promote the theoretical innovation of TCM and the research of new drugs.

1. Introduction

The unique cognitive system and empirical methodology of traditional Chinese medicine (TCM) have evolved over millennia, and its theoretical system has consistently improved overtime. Ancient books are considered important wisdom carriers, depicting the achievements of TCM. They contain rich connotations that guide the continuous development and progress of TCM. One such example is the discovery of artemisinin by Tu Youyou, a Chinese pharmaceutical chemist and malariologist who was searching for a traditional malaria cure and was inspired by an ancient Chinese medical book (Zhou Hou Bei Ji Fang) and ultimately isolated and extracted artemisinin, an antimalaria drug. This was a breakthrough in twentieth-century medicine and later won the Nobel Prize [1]. Fan et al. confirmed that cepharanthine, an alkaloid from the TCM cephalothin, was a potential drug for treating 2019-nCoV infection [2]. Furthermore, a UK report addressed to the ministers on the statutory regulation of acupuncture practitioners, herbal medicine, TCM, and other traditional medicines indicated that the recorded history of traditional use should be assessed and incorporated into the existing evidence database to support the efficacy and safety of herbal/traditional medicines and acupuncture [3]. Directives by the European Parliament and the Council of the European Union on traditional herbal products have stated that long-term use of traditional medicinal products reduces the need for clinical

trials, as the efficacy of medicinal products is plausible based on their long-standing use and experience [4]. Furthermore, the Law of the People's Republic of China on TCM has stated that it is essential to provide information on clinical safety studies when applying for drug approval numbers for Chinese medicine compound preparations that are derived from ancient classical prescriptions that meet the state requirements [5].

Due to dietary changes, the incidence of digestive system diseases has gradually increased and imposes an enormous economic burden on both the patient and the healthcare system. Chinese and Western medicine combinations have significant advantages in the treatment of digestive system diseases; for example, some experiments have confirmed the efficacy of Chinese medicine in the treatment of elicobacter pylori infection [6], ulcerative colitis [7], and intestinal flora disorders [8].

Piji Pills have remarkable clinical effects in the treatment of digestive system diseases. Zhai et al. confirmed the potential value of β-elemene, isolated from the Curcuma Rhizoma (Ezhu), for its anticancer effects [9]. Zhang et al. using network pharmacology and molecular docking technology, found that Piji Pills played a role in the treatment of pancreatic cancer through multicomponent, multtarget, and multichannel approaches [10].

We are conducting a randomized controlled clinical trial in metastatic pancreatic cancer patients, using prescription medication containing the key compositional compounds found in the Piji Pills, to further validate its efficacy and safety (trial registration number: ClinicalTrials.gov Identifier ChiCTR2000032875). It is, therefore, imperative to systematically review the classical medical literature to analyze the origins and development of the Piji Pills and to further explore the sources of innovation and the development of TCM.

2. Materials and Methods

2.1. Literature Search and Data Collection. The author independently constructed a full-text database covering 2,090 TCM ancient books and implemented the full-text retrieval function based on Ulysses software. A full-text search was conducted using the keyword "Piji Pills" ("脾积丸" in Chinese). In order to identify pertinent sections, the results were proofread by two independent authors (Fudong Liu and Xiaochen Jiang) who had sufficient experience concerning ancient books. Thereafter, we manually indexed and classified the pertinent written sections. For data format compatibility (CSV, ARFF), required by the data mining system, we used Microsoft Excel for Mac 16.62 (22061100) for data entry purposes. CSV data included eight entries from A to H: A dynasty, B author, C books, D original text, E drugs, F disease, G dose, and H dosage form. Reference WHO international standard terminologies on traditional Chinese medicine regulated TCM standard terminology [11].

2.2. Search Result. We reviewed more than 128 pieces of literature from 35 books (Figure 1), generated from our database of 2,090 ancient TCM books. Our area of focus was full literature describing the history of Piji Pills. We used the following statistical methods in our literature search: frequency statistics, complex network analysis, and association rules, to sort through the development, main symptoms, prescription principle, and Piji Pills' dosage. The origin, development, and future direction were discussed, taking into consideration the knowledge of TCM theory and recent research related to Piji Pills, which were divided into early, middle, and modern times. We aimed to provide new ideas and methods for the study of famous ancient TCM prescriptions.

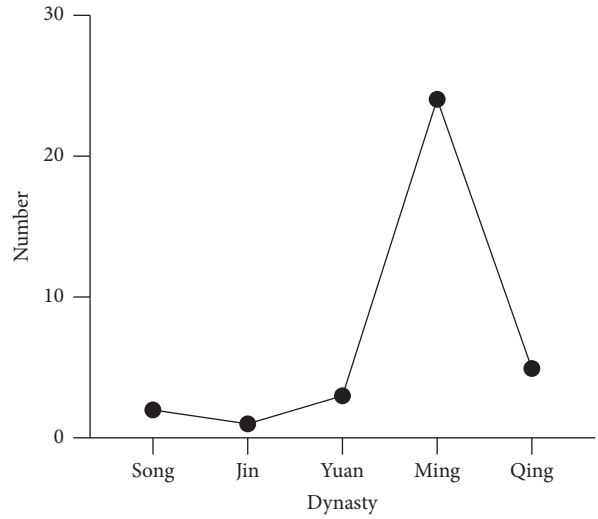

Figure 1: The number of ancient records of Piji Pills by dynasties from Song to Qing.

3. Result and Discussion

3.1. Early Stage. The early Piji Pills records in ancient TCM books stretched from the Song dynasty (960–1279 AD) to the Yuan dynasty (1271–1368 AD), during which period the ancient Chinese medical texts not only achieved a breakthrough starting from scratch but also made great progress in the composition of drugs and the treatment scope of diseases (Table 1).

During the Song dynasty (960-1279 AD), the government attached great importance to the development of medicine. The first record of Piji Pills appeared in Sheng Ji Zong Lu (1117 AD), which was compiled by the government. The book contained nearly 20,000 prescriptions, including prescriptions from ancient medical texts, folk experiences, and prescriptions provided by medical practitioners. Piji Pills recorded in this book were composed of Old Rice (Chen Cang Mi), Citri Reticulatae Pericarpium Viride (Qing Pi), Crotonis Fructus (Ba Dou), Sparganii Rhizoma (San Leng, including Shi San Leng, Jizhua San Leng, and Jing San Leng), Curcumae Rhizoma (E Zhu), and Arecae Semen (Bing Lang). It was mainly used to treat the disease "Masses in the spleen" (Pi Qi), manifested by abdominal swelling, epigastric distension, jaundice, dry mouth, weight loss, reduced diet, chest tightness and intermittent fever. The disease, in terms of symptoms, resembled the digestive systems of malignant

Table 1: Summary of the main contributions to the records of Piji Pills in the early stage.

Representative books	Author	Time	Contributions
Sheng Ji Zong Lu	Zhao ji	1117 AD	The first record of "Piji Pills," the main symptoms, composition, dosage, and production method.
Ren ZhaiZhiZhi Fang Lun	Yang Shi-ying	1264 AD	The meaning of "Piji" was expanded and the scope of treatment was enriched. The composition gradually matured and stabilized.
YiFang BianNuo	Li Gao	1266 AD	Based on the Treatise on spleen and stomach, Caryophylli Flos was added to the composition of Piji Pills. This prescription composition was widely used by doctors of later generations.

tumors and was treated by Piji Pills. However, the absence of a more detailed disease description in the book limited its further application. The Piji Pills were later described in Renzhai Zhizhi Fanglun, 1264 AD, where it was recorded that Piji Pills could potentially be used for the treatment of malaria, dyspepsia, indigestion, and constipation, among others. The prescription composition of Piji Pills had been "updated." Old Rice (Chen Cang Mi) and Arecae Semen (Bing Lang) were removed; Alpiniae Officinarum rhizoma (Gao Liang Jiang), Gleditsiae Sinensis Fructus (Da Zao Jiao), and Plant Soot (Bai Cao Shuang) were added. Thereafter, most of the ancient books described Piji pills based on this prescription composition.

During the Jin and Yuan dynasties, TCM developed rapidly. Four famous Jin and Yuan healers (Zhang Congzheng, Zhu Zhenheng, Liu Wansu, and Li Gao) made a great impact on the development of TCM. During this period, descriptions of Piji Pills were gradually enriched. Four ancient books recorded the composition, dosage, and main symptoms of this prescription. Convenient prescriptions for doctor's cowardice (Yi Fang BianNuo), written by Li Gao, the founder of the "Spleen-Stomach Theory," further expanded the therapeutic effect of Piji Pills. The book recorded that Piji pills were used to treat indigestion, acid reflux, vomiting, pediatric malnutrition, and abdominal pain in women caused by Qi-blood disharmony, covering internal medicine, pediatrics, and gynecological diseases. Li Gao added a Qi-regulating herb, CaryophylliFlos (Ding Xiang), to the pills, reflecting the academic view that "the spleen and stomach are the pivots of Qi movement." Influenced by Li Gao, this drug was later widely used by doctors.

3.2. Late Stage. The development of Chinese medical theory further matured from the Ming dynasty to the Qing dynasty (1368 AD-1644 AD). Especially toward the end of the Qing dynasty, the idea of combining Chinese and Western medicine began to seep into the minds of doctors as Western medicine was introduced into China. During this time, the development and application of Piji Pills became more widespread. Many monographs on pediatrics, internal medicine, and miscellaneous diseases elaborate on the indications for diseases and the medicine dosage.

Twenty-two pieces of literature recorded the drug composition of Piji Pills. Based on the analysis of this literature using the Gephi complex network (Figure 2), it was found that the core components of Piji Pills were eight herbs: Aucklandiae Radix (Mu Xiang), Crotonis Fructus (Ba Dou), Alpiniae Officinarum Rhizoma (Gao Liang Jiang), Sparganii Rhizoma (San Leng), Curcumae Rhizoma (E Zhu), Citri Reticulatae Pericarpium Viride (Qing Pi), Gleditsiae Sinensis Fructus (Da Zao Jiao), and Plant Soot (Bai Cao Shuang). Only a small number of books differ slightly in composition, including Pediatric parenting methods (YuYing JiaMi), cases of miscellaneous diseases (ZaBing ZhiLi), complete book on paediatrics (YouYou JiCheng), experience in treating pox and rash (DouZhen XinFa) and guidebook of pediatrics (YouKe YiXueZhiNan).

To fully discover the main diseases treated by Piji Pills and to more accurately guide clinical application, we cleaned, transformed, and summarized the data on the diseases (symptoms) recorded in the literature. We then used VBA programs to disaggregate the symptoms and perform descriptive statistics (Figure 3), which showed that most of the symptoms were closely related to the digestive system.

Wan Mizhai, a Yuan dynasty physician who was renowned in pediatrics and gynecology, often used the Piji Pills to treat pediatric pox and rash, dyspepsia, indigestion, and infantile convulsion. In You Ke Fa Hui, it was written that "the stomach is known as 'the sea of water and food', and the intestine is 'the way of water and food'. Diarrhea is a disease caused by damage to the stomach and intestines. If there is no pathogenic qi in the stomach and intestines, food and water will not become bad, and the person will have no disease. If food retention stays in the stomach and intestines, diarrhea will occur, just like more water in a container will flow out. If diarrhea is to be treated, the source of the disease must be found. The spleen jack pill is the medicine that can get rid of food retention at its source." This is one of the few discussions in ancient books of TCM on the mechanism of Piji Pills in treating digestive disorders, and it emphasizes the mechanism of Piji Pills with the spleen and stomach as its core. The famous pediatrician Zhou Zhen of the Qing dynasty was also inspired by this and used the Piji Pills to treat diarrhea, abdominal pain, night cries, and other pediatric diseases caused by food accumulation.

According to basic TCM theory, the spleen and stomach are the pivots of Qi movement. If Qi movement in the spleen and stomach is not properly regulated, abdominal distension and pain will occur. If there is an imbalance in the ascending and descending of Qi movement, Qi counterflow will lead to nausea, vomiting, acid reflux, and constipation. If the spleen-yang is trapped, diarrhea will follow. If Qi is blocked for a prolonged period of time, it will further develop into tangible

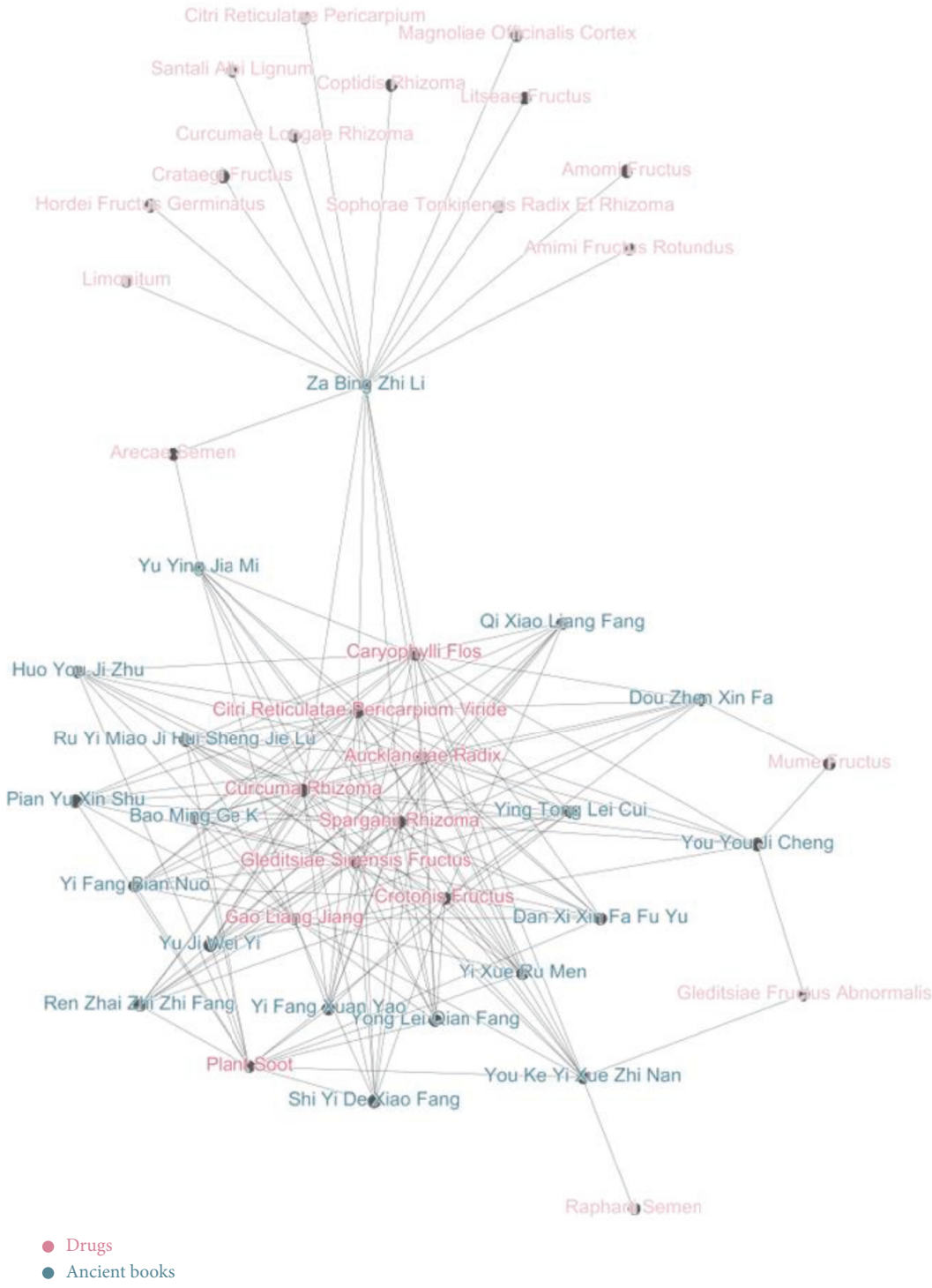

Figure 2: The complex network of core drug composition of Piji Pills and related ancient books.

accumulation. Therefore, with the use of a large number of herbs that promote the movement of Qi, the Piji Pills have become increasingly effective in the treatment of digestive disorders, especially after Li Gao added Caryophylli Flos (Ding Xiang) to the composition of the medicine.

Based on more complete records of Piji Pills in the Ming and Qing dynasties, combined with those from the Song, Jin, and Yuan dynasties, the dosages of Piji Pills' herbs were counted (Table 2). The analysis covered the maximum, minimum, and average amounts of each herb, the occurrence frequency of the maximum and minimum amounts, the highest occurrence frequency of the same dosage, and the specific dosage in ancient books. In our research, we found that over the last millennia since its development, there were significant differences in the drug's weights and measurements. To provide a standard for the modern

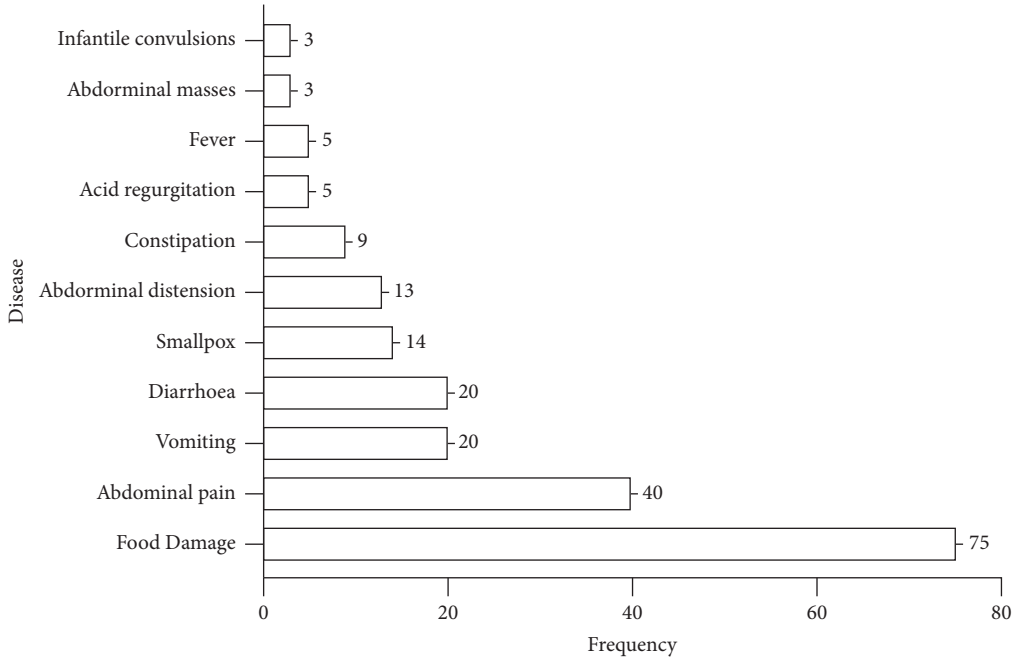

Figure 3: Frequency analysis of the main diseases (symptoms) treated with Piji Pills.

Table 2: Dosage and frequency of occurrence of Piji Pills.

Dugs	Minimum dosage and frequency		Maximum dosage and frequency		Average/g	Most common doses and frequencies	
	Minimum dosage/g	Frequency/no.	Maximum dosage/g	Frequency/no.		Dosage/g	Frequency/no.
Sparganii Rhizoma	1.87	1	82.6	1	45.59	74.6	9
Curcumae Rhizoma	1.87	1	123.9	1	58.21	111.9	6
Citri Reticulatae Pericarpium Viride	1.87	1	41.3	1	27.28	37.3	12
Aucklandiae Radix	2.98	1	20.65	1	15.60	18.65	14
Alpiniae Officinarum Rhizoma	1.87	1	55.95	1	18.46	18.65	14
Crotonis Fructus	1.87	1	20.65	1	16.94	18.65	10

clinical application of Piji Pills, we converted the units recorded in previous dynasties into "grams" (g). According to data provided in the History of Chinese Science and Technology—Weights and Measures Volume, one tael in the Song and Yuan dynasties was approximately 41.3 g in modern times, and one tael in the Ming and Qing dynasties was approximately 37.3 g in modern times.

In addition, there were some rare units of measure recorded in ancient books, making data conversion difficult. For example, the most frequent record of the amount of Gleditsiae Sinensis Fructus (Da Zao Jiao) was "3 ting," which was recorded in seven books. We also searched the relevant books and found that Pro. Shi Shenghan, in his commentary on QiMin Yao Shu, believed that the unit of "ting" was equivalent to the modern measurement of "ingot" (one piece). So "3 ingots" were three pieces. At the same time, the dosage of the large soapwort was recorded as "3 qian" (11.19 g) in Dou Zhen Xin Fa and You You Ji Cheng. In summary, we assumed that the dosage of Gleditsiae Sinensis Fructus (Da Zao Jiao) was indicative of approximately15 g. The dosage of Plant Soot (Bai Cao Shuang) was calculated in a similar manner as previously mentioned. Eight books contained a dosage of "3 spoons," and combined with the dosage of "3 qian" (11.19 g) in four books in the Ming and Qing dynasties, the dosage of Plant Soot (Bai Cao Shuang) was considered to be 12 g.

In terms of the maximum amount for each recipe, Sparganii Rhizoma (San Leng) and Curcumae Rhizoma (E Zhu) were the most commonly used. The minimum dosage of each herb was taken from You Ke Yi Xue Zhi Nan, written by Zhou Zhen in the Qing dynasty, which lacked statistical significance. In terms of average dosage, the dosage of Curcumae Rhizoma (E Zhu) was the largest, followed by Sparganii Rhizoma (San Leng), Citri Reticulatae Pericarpium Viride (Qing Pi), Alpiniae Officinarum Rhizom (Gao Liang Jiang), Crotonis Fructus (Ba Dou) and Aucklandiae Radix (Mu Xiang).

In regards to the dosage form, we screened 128 pieces of literature documenting Piji Pills and found that the dosage form used in 22 documents were all pills. We also searched

for information on pills in ancient texts. The most representative one was Li Gao's comment in his Yong Yao Fa Xiang that "pills are slow, soothing, and healing." Modern pharmacological studies have also confirmed the ability of solid oral agents to deliver live phages to the gastrointestinal tract [12], and the release of active ingredients from the pills was relatively slow in the intestinal fluid environment simulated by the bicarbonate buffered dissolution medium [13]. Therefore, the application of pills not only allowed the active ingredients to remain in the body for a longer period of time but also allowed for more precise targeting of herbal medicine. In the 2015 edition of the Chinese Pharmacopoeia, approximately 25.71% of the dosage forms were pills, indicating the wide usage of pills in TCM clinics.

3.3. Modern times. Modern times refer to the time period from the beginning of the Republic of China (1912 AD-1949 AD) to the present day. In the early stage of this period, TCM was challenged by western medicine. At the beginning of the twentieth century, the increasing attention to western medicine hindered the development of TCM [14]. Since 1949, under the guidance of scientific theory and technology, TCM has been able to gradually carry out in-depth research and perform experimental studies [15]. The study of various drugs found in Piji pills had also entered a new stage from macro to micro. For example, Chen et al. confirmed that Curcumae Rhizoma (E Zhu) had great potential for anti-inflammatory, anticancer, hepatoprotective, and immunomodulatory purposes [16]. In China, β-elemene isolated from Curcumae Rhizoma (E Zhu), had been developed into a drug for the treatment of solid tumors and malignant effusion by intravenous injection, intraperitoneal or peritoneal perfusion. The drug is currently being tested in clinical trials in the United States [17]. Simultaneously, Chang et al. had demonstrated that the new compounds resulting from the combination of Curcumae Rhizoma (E Zhu) and Sparganii Rhizoma (San Leng) had better antitumor activity than the single herbs [18]. Therefore, it was generally believed that strengthening the research of TCM compound prescriptions would be conducive to and promote the process of new drug research and development. However, at present, the modern scientific connotation of the compound theory for Piji Pills has not yet been elucidated, due to the complexity of the active ingredients and the mere fact that their safety and efficacy need to be further verified. Therefore, modern research on the Piji Pills is still at a blank stage.

3.4. Future Perspectives. Machine learning (ML) and artificial intelligence (AI) are developing rapidly in the medical field, which can be beneficial to both medical staff and patients. The IBM Corporation has developed an AI-assisted decision-making system, known as Watson for Oncology (WFO), that is based on cognitive computing and includes medical literature, patents, genomics information, and chemical and pharmacological data. Several studies have confirmed that WFO may be a helpful tool for cancer treatment decision-making [19–21]. Moreover, in the field of TCM, Fang et al. built a high-throughput experiment and reference-guided TCM database, named HERB, that could strongly support the modernization of TCM [22]. Furthermore, Xu et al. developed an Encyclopedia of TCM (ETCM), which contains comprehensive and standardized information on the commonly used herbs and formulas of TCM as well as their ingredients [23]. Huang et al. constructed the TCM Integrated Database (TCMID), which records TCM-related information collected from different resources and through a text-mining method [24, 25]. These databases are highly recognized by TCM researchers and would make a significant contribution to the modernization of TCM research.

However, most of these studies were conducted based on modern research and literature. The TCM classics and literature cannot be taken as the object of these studies because the ancient TCM books have accumulated a lot of data over the last millennia since its initial development. A lot of research achievements in prescriptions, herbs, ingredients, and other TCM-related information were dispersedly recorded in books and journals, which hindered the systematic research and application of TCM.

In 2018, the State Administration of TCM (SATCM) selected 100 ancient classical prescription records from more than 100,000 prescriptions recorded in 103 medical books. Currently, several documentary studies on classically famous prescriptions are being conducted. TCM has been garnering increasing attention, which has increased the need for TCM-related data resources. Our study had the following strengths. First, our database was extensive; we retrieved the information from a large number of ancient TCM books, including ancient books from the Song, Jin, Yuan, Ming, and Qing dynasties, which eliminated the deviation caused by historical factors and provided greater literature comprehension. Second, we designed an indexing manual and a manual classification strategy for ancient discourse and introduced statistical methods to provide a more objective picture of what was written in ancient texts about Piji Pills, eliminating the bias caused by limited researcher understanding.

Despite the aforementioned strengths, our study had some limitations. First, only 128 documents were included in the final review and analysis, and the maneuverability of the indexing manual and classification strategy designed in this study required more testing data. Second, this study used statistical methods to explore the mining of ancient TCM books, which needed to be further combined with ML and AI techniques. Third, this study has only clarified the information on the composition, dosage, and symptoms of Piji Pills; future research on the mechanism of Piji Pills needs to be conducted to promote the modernization of Chinese medicine.

4. Conclusions

Piji Pills, an ancient TCM prescription, has a long history and was inherited and developed in the Ming and Qing dynasties. This study applied statistical methods to extensively investigate and review ancient TCM books, using a

chronological approach to sort through the results of the analysis. Based on the study results, we found that the core components of Piji Pills were "Aucklandiae Radix (Mu Xiang), Crotonis Fructus (Ba Dou), Alpiniae Officinarum Rhizoma (Gao Liang Jiang), Sparganii Rhizoma (San Leng), Curcumae Rhizoma (E Zhu), CitriReticulatae Pericarpium Viride (Qing Pi), Gleditsiae Sinensis Fructus (Da Zao Jiao), and lPant Soot (Bai Cao Shuang)", with Sparganii Rhizoma (San Leng) and Curcumae Rhizoma (E Zhu) being the key drugs. Furthermore, we found it was used in clinical practice in the form of pills and had significant advantages in the treatment of digestive disorders. Modern scientific research supports the views expressed in ancient texts. This study concluded that promoting the deep integration of information technology with the content mining of ancient TCM books could facilitate theoretical innovation and the creation of new medicines.

Data Availability

All data were included in the manuscript and there was no restriction on availability.

Conflicts of Interest

The authors declare that they have no conflicts of interest.

Authors' Contributions

Fudong Liu contributed as the principal investigator and author and drafted the manuscript. Xiaochen Jiang and Chuanlong Zhang processed the literature data. Guibin Wang and Yi Li helped to correct the grammatical errors in the article. Bo Pang contributed to the overall design and summarized the feedback and comments. All the authors have read and approved the final version of the manuscript. These authors, Fudong Liu, Xiaochen Jiang, and Chuanlong Zhang,contributed equally as the co-first authors.

Acknowledgments

Funding was supported by the Scientific and Technological Innovation Project of the Chinese Academy of Chinese Medicine Sciences (No. CI2021A01805) and Capital's Funds for Health Improvement and Research (No. CFH 2022-2-4415).

References

[1] Y. Tu, "The discovery of artemisinin (qinghaosu) and gifts from Chinese medicine," *Nature Medicine*, vol. 17, no. 10, pp. 1217–1220, 2011.

[2] H. H. Fan, L. Q. Wang, W. L. Liu et al., "Repurposing of clinically approved drugs for treatment of coronavirus disease 2019 in a 2019-novel coronavirus-related coronavirus model," *Chinese Medical Journal*, vol. 133, no. 9, pp. 1051–1056, 2020.

[3] *Department of Health Steering Group on the Statutory Regulation of Practitioners of Acupuncture Report to Ministers from Herbal Medicine Traditional Chinese Medicine and Other Traditional Medicine Systems Practised in the UK*, Robert Gordon University, Aberdeen Scotland, 2008, https://hdlhandlenet/10059/176.

[4] The European Parliament and The Council Of The European Union, "Directive 2004/24/EC of the European Parliament and of the Council of 31 March 2004 on amending, as regards traditional herbal medicinal products, Directive 2001/83/ECon the Community code relating to medicinal products forhuman use," *Orkesterjournalen*, vol. 36, pp. 85–90, 2004.

[5] C. Gootscotnps, *Chinese medicine law of the People's Republic of China*, China Democratic Legal System Press, Beijing, China, 2016.

[6] Y. Li, X. Li, and Z. Tan, "An overview of traditional Chinese medicine therapy for Helicobacter pylori-related gastritis," *Helicobacter*, vol. 26, no. 3, Article ID e12799, 2021.

[7] S. Tang, W. Liu, Q. Zhao et al., "Combination of polysaccharides from Astragalus membranaceus and Codonopsis pilosula ameliorated mice colitis and underlying mechanisms," *Journal of Ethnopharmacology*, vol. 264, Article ID 113280, 2021.

[8] X. Li, D. Wu, J. Niu et al., "Intestinal flora: a pivotal role in investigation of traditional Chinese medicine," *The American Journal of Chinese Medicine*, vol. 49, no. 02, pp. 237–268, 2021.

[9] B. Zhai, N. Zhang, X. Han et al., "Molecular targets of beta-elemene, a herbal extract used in traditional Chinese medicine, and its potential role in cancer therapy: a review," *Biomedicine & Pharmacotherapy*, vol. 114, Article ID 108812, 2019.

[10] C. Zhang, X. Jiang, M. Gao, F. Liu, B. Pang, and B. Hua, "(Mechanism of Piji Pills in treatment of pancreatic cancer based on network pharmacology and molecular docking technology)," *XiandaiYaowu Yu Linchuang*, vol. 37, no. 05, pp. 961–969, 2022.

[11] WHO, *International Standard Terminologies on Traditional Chinese Medicine*, World Health Organization, Geneva, Switzerland, 2022.

[12] D. Khanal, R. Y. K. Chang, C. Hick, S. Morales, and H. K. Chan, "Enteric-coated bacteriophage tablets for oral administration against gastrointestinal infections," *International Journal of Pharmaceutics*, vol. 609, Article ID 121206, 2021.

[13] N. Scott, K. Patel, T. Sithole, K. Xenofontos, V. Mohylyuk, and F. Liu, "Regulating the pH of bicarbonate solutions without purging gases: application to dissolution testing of enteric coated tablets, pellets and microparticles," *International Journal of Pharmaceutics*, vol. 585, Article ID 119562, 2020.

[14] J. L. Tang, B. Y. Liu, and K. W. Ma, "Traditional Chinese medicine," *The Lancet*, vol. 372, no. 9654, pp. 1938–1940, 2008.

[15] C. Keji and X. U. Hao, "The integration of traditional Chinese medicine and Western medicine," *European Review*, vol. 11, no. 2, pp. 225–235, 2003.

[16] Y. Chen, Z. Zhu, J. Chen et al., "Terpenoids from Curcumae Rhizoma: their anticancer effects and clinical uses on combination and versus drug therapies," *Biomedicine & Pharmacotherapy*, vol. 138, Article ID 111350, 2021.

[17] G. Wang, X. Li, F. Huang et al., "Antitumor effect of beta-elemene in non-small-cell lung cancer cells is mediated via induction of cell cycle arrest and apoptotic cell death," *CMLS Cellular and Molecular Life Sciences*, vol. 62, no. 7-8, pp. 881–893, 2005.

[18] Y. L. Chang, G. L. Xu, X. P. Wang et al., "Anti-tumor activity and linear-diarylheptanoids of herbal couple Curcumae Rhizoma-Sparganii Rhizoma and the single herbs," *Journal of Ethnopharmacology*, vol. 250, Article ID 112465, 2020.

[19] S. P. Somashekhar, M. J. Sepúlveda, S. Puglielli et al., "Watson for Oncology and breast cancer treatment recommendations: agreement with an expert multidisciplinary tumor board," *Annals of Oncology*, vol. 29, no. 2, pp. 418–423, 2018.

[20] Z. Jie, Z. Zhiying, and L. Li, "A meta-analysis of Watson for Oncology in clinical application," *Scientific Reports*, vol. 11, no. 1, p. 5792, 2021.

[21] C. Liu, X. Liu, F. Wu, M. Xie, Y. Feng, and C. Hu, "Using artificial intelligence (Watson for Oncology) for treatment recommendations amongst Chinese patients with lung cancer: feasibility study," *Journal of Medical Internet Research*, vol. 20, no. 9, Article ID e11087, 2018.

[22] S. Fang, L. Dong, L. Liu et al., "HERB: a high-throughput experiment- and reference-guided database of traditional Chinese medicine," *Nucleic Acids Research*, vol. 49, 2021.

[23] H. Y. Xu, Y. Q. Zhang, Z. M. Liu et al., "ETCM: an encyclopaedia of traditional Chinese medicine," *Nucleic Acids Research*, vol. 47, 2019.

[24] R. Xue, Z. Fang, M. Zhang, Z. Yi, C. Wen, and T. Shi, "TCMID: traditional Chinese Medicine integrative database for herb molecular mechanism analysis," *Nucleic Acids Research*, vol. 41, 2012.

[25] L. Huang, D. Xie, Y. Yu et al., "Tcmid 2.0: a comprehensive resource for TCM," *Nucleic Acids Research*, vol. 46, 2018.

Hindawi
Evidence-Based Complementary and Alternative Medicine
Volume 2022, Article ID 9968171, 8 pages
https://doi.org/10.1155/2022/9968171

Research Article

Postmarketing Reevaluation of Chinese Traditional Therapy Kangbingdu Oral Liquid in the Treatment of the Common Cold

Hongjiao Li,[1] Yanke Ai,[1] Tianyi Zhao,[1] Di Zhang,[1] Xiaoying Lv,[1] Shaoyan Jia,[2] Zehuai Wen,[3] Guoxin Li,[4] Hongyu Wang,[5] Feng Gao,[6] Shaohong Li,[1] Zhishan Ge,[1] Yuning Qin,[1] Zhenbiao Wang,[7] and Liyun He[1]

[1]*Institute of Basic Research in Clinical Medicine, China Academy of Chinese Medical Sciences, Beijing, China*
[2]*Hospital of Beihang University, Beijing, China*
[3]*Guangdong Provincial Hospital of Chinese Medicine, Guangzhou, China*
[4]*Second Teaching Hospital of Liaoning University of Traditional Chinese Medicine, Shenyang, China*
[5]*Hospital of Renmin University of China, Beijing, China*
[6]*WangJing Hospital of China Academy of Chinese Medical Sciences, Beijing, China*
[7]*Beijing ShiJiTan Hospital, Capital Medical University, Beijing, China*

Correspondence should be addressed to Zhenbiao Wang; bjsjtyygck@126.com

Received 20 May 2022; Accepted 8 August 2022; Published 1 September 2022

Academic Editor: Vijaya Anand

Background. Observational studies from China suggest that Kangbingdu oral liquid (KBD) may be effective in treating the common cold. *Objective*. Reevaluation of efficacy and safety of Kangbingdu oral liquid after marketing and expanding population. *Design*. Prospective, Pragmatic randomized controlled trial (Chictr.org.cn registration number: chiCTR-TRC-12002399). *Setting*. Eleven hospitals from 3 provinces in China. Patients were recruited through 11 centers, including 7 teaching hospitals, 2 University health services, one military clinic, and one community hospital. *Patients*. 2647 persons aged 18 to 75 years with Common cold. *Intervention*. Patients were randomly allocated to 2 groups: the treatment group Kangbingdu oral liquid (composed of 9 Chinese herbal medicines and honey) and the placebo group were divided into a standard-dose group of 10 ml every time, a middle dose group of 20 ml every time, high dose group of 30 ml every time, 3 times daily. Interventions and control were given for 5 days. *Measurements*. The primary outcome is the mean amount of total scores measured by the 11-primary symptoms: to observe the change of main symptoms from severe to disappear and to calculate and compare the mean amount of total scores after the periods of observation. Secondary outcomes are the disappearance rate of each symptom and the median time of body temperature returned to normal. *Results*. On day 5, the Kangbingdu liquid group had significant reductions in the mean amount of total scores measured by the 11-primary symptoms (7.39 [95% CI 7.26 to 7.51] compared to the placebo group (6.43 [95%: CI 6.24 to 6.62]). The Kangbingdu liquid can improve the remission rate of accompanying symptoms on day 5 including aversion to wind, aversion to cold, fever, cough, stuffy, runny nose, sore throat, muscular aches, headache, fatigue, and sweat ($P < 0.0001$). Significant reductions in time of body temperature to return to normal in the Kangbingdu liquid group (P50, 48.33 [95% CI 46.00 to 52.50] compared with the control group (P50, 64.59 [95% CI 51.08 to 70.50] ($P = 0.0022$). 13 (0.7%) participants in the Kangbingdu liquid group and 1(0.2%) participants in the placebo group ($P > 0.05$) had treatment-related AEs, which mainly include diarrhea and dyspepsia in the Kangbingdu liquid group and constipation in the placebo group. *Conclusion*. The study's conclusion in this paper was based on the placebo, Kangbingdu oral liquid two groups which clinically diagnosed the common cold and flu. (1) Kangbingdu oral liquid can effectively improve the comprehensive clinical symptoms of common adult cold, also improved main symptoms, including sore throat, muscle aches, headache, and so on. (2) Kangbingdu oral liquid effectively shortens the time of body temperature to return to normal.

1. Introduction

A common cold is associated with significant morbidity and economic consequences. The common cold is the most common respiratory illness and medical condition [1]. Rhinoviruses mainly cause colds and other pathogens, such as respiratory syncytial virus, adenovirus, and coronavirus, are also common pathogens [2, 3]. In the United States, adults catch about 4–6 colds a year, and children catch about 6–8 colds a year. On average, 8.7 hours of working time will be wasted daily due to the cold, including 5.9 hours of on-the-job loss and 2.8 hours of absenteeism [4,5]. There are about 110 million general visits and 6 million emergency visits due to colds yearly, causing an economic burden of about 40 billion US dollars [6]. Colds with a longer duration, worsening, and frequency will prolong the presence of eosinophilic neutrophils in the nose, making asthma challenging to control and exacerbating COPD severity [7–9].

Kangbingdu (KBD) oral liquid, a classic traditional Chinese medicinal formula that is revised based on the traditional Chinese medicine (TCM) formulations of "BaiHuTang" and "QingWenBaiDuYin," is widely used for the clinical treatment of influenza and common cold [10,11].

2. Methods

2.1. Study Design. We conducted a prospective, randomized, double-blind, placebo-controlled trial at 11 medical sites in three provinces in China. The plan was included in the sample of 2647 cases in this test, using the stratified-block randomization method, with fever and no fever. Each subgroup met 100 samples, and the central randomization system was used to screen subjects, randomize subjects, and dispense drugs. The institutional review board of the Institute of Basic Research in Clinical Medicine (IBRCM) reviewed and approved the protocol and consent forms before the start of the study. All participants signed written informed consent forms before enrollment.

2.2. Patient Enrollment. A Consensus Recommendation from an Expert Panel for Primary Care Clinicians [12]. They usually aversion to wind, fever, cough, stuffy nose, runny nose, sore throat, muscle aches, headaches, tiredness, sweat, and so on. Patients who fulfilled all of the following criteria were included: patients in the studyaged 18 to 75 years and had a clinical diagnosis of influenza or common cold within 48 hours of the onset of symptoms of common cold or influenza; written informed consent was obtained; and without other prevention and control of cold drugs, including antibiotics, regularly in the 48 hours before inclusion.

Exclusion criteria were as follows:(1) Patients with pneumonia, bronchitis, otitis media, pharyngeal isthmus, viral myocarditis, acute nephritis, rheumatic joint disease, and other diseases.(2) Patients had hepatic and renal insufficiency; (3) Patients with allergies to clear antivirals in KBD components (plate blue root, gypsum, lugan, dihuang, turmeric, cicadas, rock calamus, patchouli, and forsythia). (4) Patients were pregnant or lactating women; had intellectual or behavioral dysfunction and were unable to cooperate with the completion of the clinical observer. (5) During a month, patients had taken part in other clinical studies. (6) Blood routine detection indicated a white blood cell count above $12^{*}10^{9}$/L; had antibiotics or other anticold medicines continuously for 48 hours; had other lesions or feelings that reduced the possibility of complicating.

2.3. Drug Administration. KBD and placebo that we used in our study were manufactured by Guangzhou Xiangxue Pharmaceutical Co., Ltd. KBD is composed of 9 herbs Radix isatidis (Banlangen; the radix of *Isatis indigotica* Fortune ex Lindl. of family Brassicaceae), Rhizoma phragmitis (Lugen; the rhizome of *Phragmites communis* Trin of family Poaceae), Radix Rehmanniae (Dihuang; the radix of *Rehmannia glutinosa* (Gaertn.) DC of family Scrophulariaceae), Radix Curcumae (Yujin; the radix of *Curcuma wenyujin* Y. H. Chen et al., C. Ling, a synonim of the accepted name *Curcuma aromatica* Salisb. According to theplantlist.org, of family Zingiberaceae), Rhizoma Anemarrhenae (Zhimu; the rhizome of *Anemarrhena asphodeloides*. Bunge of family Asparagaceae), Rhizoma acori tatarinowii (Shichangpu; the rhizome of *Acorus tatarinowii* Schott, a synonym of the accepted name Acorus calamus L, of family Acoraceae), Herba pogostemonis (Guanghuoxiang; the caulis of *Pogostemon cablin* (Blanco) Benth. of family Lamiaceae), Fructus Forsythiae (Lianqiao; the fructus of *Forsythia suspensa* (Thunb.) Vahl. of family Oleaceae), and Gypsum fibrosum (Shigao; one mineral with hydro calcium sulfate fibriform crystallized polymeric) in a dry weight of 129 g, 61 g, 32 g, 25 g, 25 g, 25 g, 29 g, 46 g and 57 g, respectively. The criteria for the quality of the herbs we used were by the 2005 Chinese pharmacopeia. And placebo keeps the color and taste the same as KBD.

Laboratory personnel was blinded to the identity of the groups. At each study site, a trained technician distributes drugs to subjects. After agreeing to participate, signing the informed consent form, and completing the baseline visit, all patients were randomly assigned to treatment groups or the control group by using random-number tables with a block size of 1 (SPSS software, version 13.0 [SPSS, Chicago, Illinois]. Randomization was stratified by the 11 study centers located in Beijing, Shenyang, and Guangzhou. The centers were selected to ensure the geographic spread and representation of common cold and influenza epidemic areas in mainland China. Participants were given placebos or KBD daily for 5 days, and participants were allowed to use ibuprofen if their body temperature was greater than 38°C. Each site had a coordinator who was assigned to follow-up on the participants' treatment and symptoms by telephoning.

2.4. Primary Outcomes. For the study's primary symptoms, we established an efficacy evaluation scale. At the study design stage, we convened an expert consultation session with clinical and methodological specialists on the efficacy assessment indexes of oral antiviral treatments to rationalize the selection of efficacy evaluation indexes. Considering the

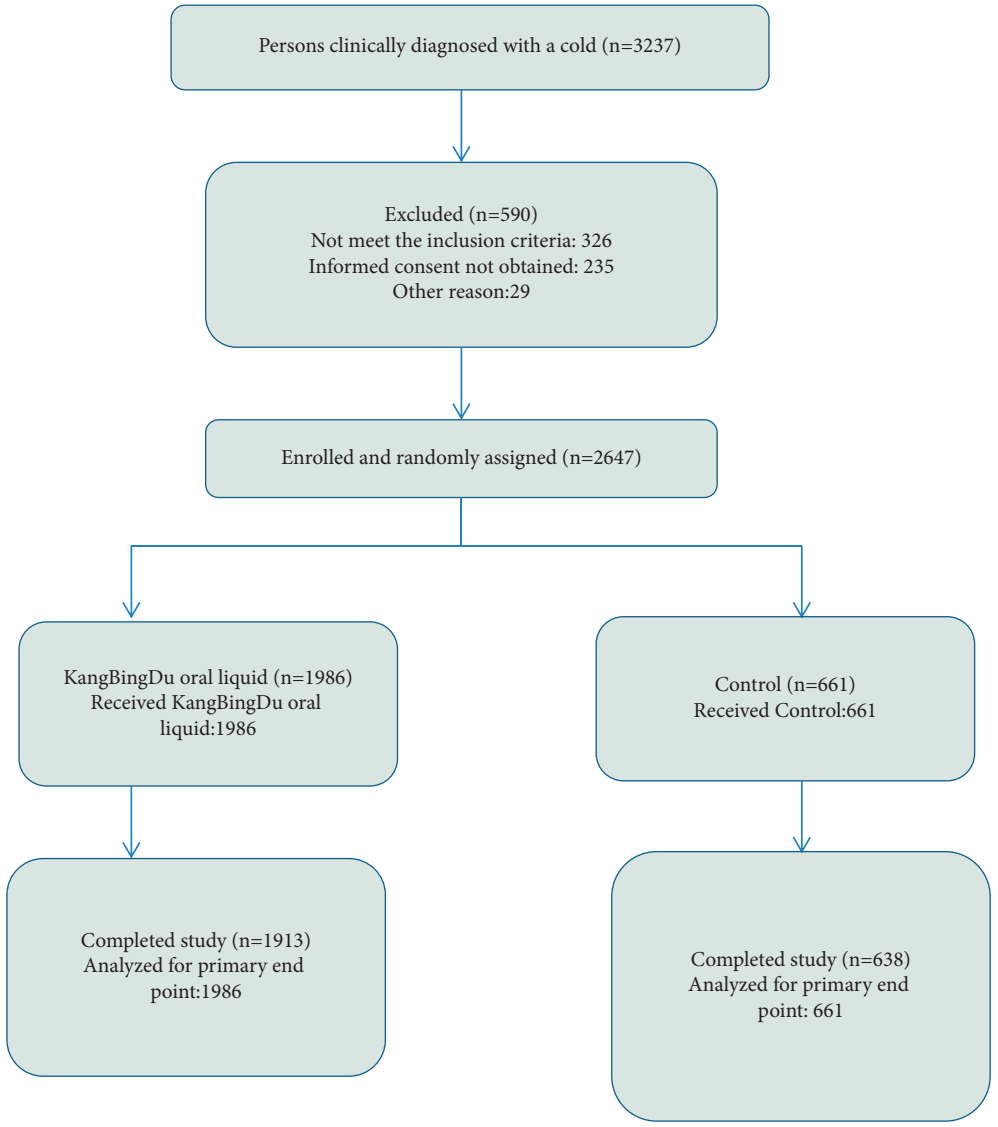

Figure 1: Study flow diagram.

contrasts between TCM and contemporary medicine's perspectives on the diagnosis and treatment of colds, symptoms such as aversion to wind, cold, and sweat are TCM diagnosis-specific symptoms. These symptoms are not included in the Western medicine consensus [12] or guidelines [13] on colds. As a result, we devised our own scale based on the most prevalent symptoms of common cold and complemented the primary symptoms in prior study reports from doctors and patients on the symptoms of the common cold. We finally formed the efficacy evaluation scale, which included 11 main symptoms of common cold patients in China, namely, aversion to wind, aversion to cold, fever, cough, stuffy nose, runny nose, sore throat, muscle aches, headache, fatigue, and sweat, when combined with the results of literature analysis.

Given that it is common for physicians and patients to describe the degree of disease as "mild, moderate, or severe" in clinical practice, we adopted a 4-point scale. We have adopted a 4-point scale to assess the severity of symptoms, described as follows: (1) None : no symptoms of the condition. (2)Slightly: the symptom is present but occurs infrequently or very mildly. (3) More clearly: the symptom is present but not severe, between mild and severe, and generally tolerable. (4) Severe: the frequency or/and intensity of the symptom is very severe and significantly affects work and life. None, slightly, more clearly, and severe were assigned according to 0, 1, 2, and 3 points, with a maximum total score of 44 points for the 11 major symptoms.

2.5. Assessment Process. Patients and researchers conducted the evaluations. Before the study begins, all 11 centers' researchers must complete standard operating procedures (SOP) training, and records must be kept in accordance with SOP. Patients in this study were given patient-administered diaries, and coordinators instructed them on how to fill the

Table 1: Demographic characteristics and baseline data.

Characteristics	Kangbingdu liquid ($n = 1986$)	Placebo ($n = 661$)	P value
Age, mean (SD)	36.1 (14.90)	36.1 (14.81)	0.7105
Sex			
Female	893 (45.12%)	303 (45.84%)	0.9106
Male	1086 (54.88%)	358 (54.16%)	
Race			0.2337
Han	1924 (96.88%)	631 (95.46%)	
Others	62 (3.12%)	30 (4.54%)	
Marriage			0.7909
Yes	1081 (54.43%)	361 (54.61%)	
No	905 (45.57%)	300 (45.39%)	
Clinic diagnosis			0.1080
Common cold	1857 (93.50%)	616 (93.19%)	
Flu	129 (6.50%)	45 (6.81%)	
Highest body temperature	37.1 ± 0.73	36.9 ± 0.70	0.5693
Fever			
No	1274 (64.15%)	418 (63.24%)	
Yes	712 (35.85%)	243 (36.76%)	
Time from cold to visit the doctor			0.9682
≤ 24h	1283 (64.60%)	393 (59.46%)	
> 24h且 ≤ 48h	703 (35.40%)	268 (40.54%)	
Influenza exposure in the week prior			0.0639
No	1808 (91.04%)	593 (89.71%)	
Yes	178 (8.96%)	68 (10.29%)	
Influenza vaccinations			0.5497
No	1698 (85.50%)	561 (84.87%)	
Yes	117 (5.89%)	42 (6.35%)	
Total score, mean (SD)	8.5 (4.59)	8.4 (4.21)	
Aversion to wind			0.9626
None	1156 (58.21%)	380 (57.49%)	
Slightly	574 (28.90%)	205 (31.01%)	
More clearly	213 (10.73%)	60 (9.08%)	
Severe	43 (2.17%)	16 (2.42%)	
Aversion to cold			0.9992
None	1074 (54.08%)	357 (54.01%)	
Slightly	602 (30.31%)	202 (30.56%)	
More clearly	261 (13.14%)	85 (12.86%)	
Severe	49 (2.47%)	17 (2.57%)	
Fever			0.9433
None	1181 (59.47%)	394 (59.61%)	
Slightly	380 (19.13%)	129 (19.52%)	
More clearly	394 (19.84%)	123 (18.61%)	
Severe	31 (1.56%)	15 (2.27%)	
Cough			0.1526
None	823 (41.44%)	251 (37.97%)	
Slightly	704 (35.45%)	246 (37.22%)	
More clearly	380 (19.13%)	141 (21.33%)	
Severe	79 (3.98%)	23 (3.48%)	
Stuffy nose			
None slightly	668 (33.64%)	246 (37.22%)	
More clearly	728 (36.66%)	232 (35.10%)	0.1044
Severe	520 (26.18%)	164 (24.81%)	
	70 (3.52%)	19 (2.87%)	
Runny nose			0.5931
None	594 (29.91%)	188 (28.44%)	
Slightly	718 (36.15%)	245 (37.07%)	
More clearly	571 (28.75%)	194 (29.35%)	
Severe	103 (5.19%)	34 (5.14%)	

Table 1: Continued.

Characteristics	Kangbingdu liquid ($n = 1986$)	Placebo ($n = 661$)	P value
Sore throat			0.5173
None	556 (28.00%)	186 (28.14%)	
Slightly	601 (30.26%)	215 (32.53%)	
More clearly	719 (36.20%)	222 (33.59%)	
Severe	110 (5.54%)	38 (5.75%)	
Muscle aches			0.4802
None	1076 (54.18%)	371 (56.13%)	
Slightly	570 (28.70%)	178 (26.93%)	
More clearly	303 (15.26%)	98 (14.83%)	
Severe	37 (1.86%)	14 (2.12%)	
Headache			0.4222
None	957 (48.19%)	323 (48.87%)	
Slightly	631 (31.77%)	221 (33.43%)	
More clearly	356 (17.93%)	110 (16.64%)	
Severe	42 (2.11%)	7 (1.06%)	
Fatigue			0.5125
None	826 (41.59%)	267 (40.39%)	
Slightly	787 (39.63%)	263 (39.79%)	
More clearly	333 (16.77%)	117 (17.70%)	
Severe	40 (2.01%)	14 (2.12%)	
Sweat			0.4521
None	1429 (71.95%)	485 (73.37%)	
Slightly	451 (22.71%)	145 (21.94%)	
More clearly	90 (4.53%)	26 (3.93%)	
Severe	16 (0.81%)	5 (0.76%)	
Total scores mean(95%CI)	8.50 (8.30 to 8.70)	8.42 (8.10 to 8.74)	0.6777

diaries according to the trial's protocols. A case report form(CRF) must be filled out by research.

The treatment period from the first day to the fifth day, as well as the interview, were conducted over the phone by the coordinator from the second to the fourth day, with the first and last days requiring face-to-face visits, with the last visit being automatically postponed to Monday in the event of a weekend. Patients were given test drugs on the first visit, and researchers should remind them to return all of the leftover test medications and packing boxes on the last visit. Clearly document the amount of distributing medicines that patients used during the experiment if drug recovery was challenging.

2.6. Statistical Analysis. The sample size is not based entirely on statistical considerations. The clinical trial included 2800 cases and ensured that 2600 cases were effective. The trial will be over once the situation is satisfying.

All analyses were based on the intention-to-treat (ITT) principle. For the primary outcome, we used a mixed-effect model with baseline value as a covariate, therapy, and site as fixed effects to examine the change in total symptom score from baseline on day 5. For missing data on the primary outcome, we employed the last observation carried forward (LOCF) approach.

We used the Chi-square test or Fisher exact test to compare the disappearance rate of single symptoms at baseline and the log-rank test to compare the time it took for body temperature to return to normal for fever cases at baseline. Secondary outcomes were performed in the observed cases without imputation of missing data.

All analyses were performed with SAS version 9.4 (SAS Institute, Cary, NC, USA), with a 2-sided P value of less than 0.05 considered significant. No adjustment was made for multiple comparisons and interim analysis.

3. Results

Between December 12th, 2012, and December 28th, 2015, we screened 3237 participants and randomly assigned 2647 participants to either the Kangbingdu liquid group ($n = 1986$) or the placebo ($n = 661$) group. Among the randomized participants, 1913 (96.3%) in the group and 638 (96.4%) in the placebo group completed the study (Figure 1). Baseline characteristics of the participants were similar between groups (Table 1).

(Figure 1) (Table 1)

For the primary outcome, the mean number of total scores measured by the 11-primary symptoms was 8.5 (95% CI, 8.3 to 8.7) at baseline and 1.1 (95%CI, 1.0 to 1.2) on day 5 in the Kangbingdu liquid group; the mean number of total scores measured by the 11-symptoms was 8.4 (95%CI, 8.1 to 8.7) at baseline and 2.0 (95%CI, 1.8 to 2.3) at day 5 in the placebo group. The reduction in total scores was greater in the Kangbingdu liquid group (7.39, 95% CI, 7.26 to 7.51) than in the placebo group (6.43, 95% CI, 6.24 to 6.62), with a mean difference of 0.96 (95% CI, 0.75 to 1.16; $P < 0.0001$) (Table 2). When compared to the placebo group, the Kangbingdu liquid group showed a higher rate of symptom

Table 2: Efficacy data.

Variable	Kangbingdu liquid	Placebo	Difference (95%CI)	*P* value
Primary outcome	*n* = 1986	*n* = 661		
Total- scores	8.5 (8.3 to 8.7)	8.4 (8.1 to 8.7)		
Total scores on day 5, mean(95%CI)	1.10 (1.00 to 1.20)	2.05 (1.82 to 2.28)		
Change on day 5, adjusted mean(95%CI)	7.39 (7.26 to 7.51)	6.43 (6.24 to 6.62)	0.96 (0.75 to 1.16)	<0.0001
Secondary outcomes				
Aversion to wind	n = 830 (%)	*n* = 281 (%)		
Symptom resolution rate on day 2	275 (33.13)	63 (22.42)	−10.71 (−16.55 to -−4.88)	0.0007
Symptom resolution rate on day 3	500 (60.24)	151 (53.74)	−6.5 (−13.22 to 0.21)	0.0557
Symptom resolution rate on day 4	672 (80.96)	204 (72.60)	−8.37 (-14.23 to −2.51)	0.0030
Symptom resolution rate on day 5	754 (90.84)	228 (81.14)	−9.7 (−14.68 to −4.73)	< 0.0001
Aversion to cold	*n* = 912 (%)	*n* = 304 (%)		
Symptom resolution rate on day 2	353 (38.71)	74 (24.34)	−14.36 (−20.13 to −8.6)	< 0.0001
Symptom resolution rate on day 3	606 (66.45)	156 (51.32)	−15.13 (−21.53 to −8.73)	< 0.0001
Symptom resolution rate on day 4	758 (83.11)	219 (72.04)	−11.07 (−16.67 to −5.47)	< 0.0001
Symptom resolution rate on day 5	843 (92.43)	258 (84.87)	−7.57 (−11.94 to −3.19)	< 0.0001
Fever	*n* = 805 (%)	*n* = 267 (%)		
Symptom resolution rate on day 2	321 (39.88)	63 (23.60)	−16.28 (−22.39 to −10.17)	< 0.0001
Symptom resolution rate on day 3	563 (69.94)	137 (51.31)	−18.63 (-25.41 to −11.85)	< 0.0001
Symptom resolution rate on day 4	700 (86.96)	205 (76.78)	−10.18 (−15.75 to −4.6)	< 0.0001
Symptom resolution rate on day 5	766 (95.16)	230 (86.14)	−9.01 (−13.41 to −4.61)	< 0.0001
Cough	*n* = 1163 (%)	*n* = 410 (%)		
Symptom resolution rate on day 2	225 (19.35)	49 (11.95)	−7.4 (−11.27 to −3.52)	0.0007
Symptom resolution rate on day 3	425 (36.54)	102 (24.88)	−11.67 (−16.68 to −6.65)	< 0.0001
Symptom resolution rate on day 4	614 (52.79)	168 (40.98)	−11.82 (−17.38 to −6.26)	< 0.0001
Symptom resolution rate on day 5	833 (71.63)	229 (55.85)	−15.77 (−21.23 to −10.31)	< 0.0001
Stuffy	*n* = 1318 (%)	*n* = 415 (%)		
Symptom resolution rate on day 2	288 (21.85)	47 (11.33)	−10.53 (−14.3 to −6.75)	< 0.0001
Symptom resolution rate on day 3	591 (44.84)	139 (33.49)	−11.35 (−16.62 to −6.07)	< 0.0001
Symptom resolution rate on day 4	876 (66.46)	228 (54.94)	−11.52 (−16.95 to −6.1)	< 0.0001
Symptom resolution rate on day 5	1133 (85.96)	295 (71.08)	−14.88 (−19.63 to −10.13)	< 0.0001
Runny nose	*n* = 1392 (%)	*n* = 473 (%)		
Symptom resolution rate on day 2	317 (22.77)	62 (13.11)	−9.67 (−13.42 to −5.91)	< 0.0001
Symptom resolution rate on day 3	639 (45.91)	161 (34.04)	−11.87 (−16.88 to −6.86)	< 0.0001
Symptom resolution rate on day 4	927 (66.59)	244 (51.59)	−15.01 (−20.15 to −9.87)	< 0.0001
Symptom resolution rate on day 5	1150 (82.61)	326 (68.92)	−13.69 (−18.31 to −9.07)	< 0.0001
Sore throat	*n* = 1430 (%)	*n* = 475 (%)		
Symptom resolution rate on day 2	301 (21.05)	64 (13.47)	−7.58 (−11.3 to −3.85)	0.0003
Symptom resolution rate on day 3	613 (42.87)	152 (32.00)	−10.87 (−15.78 to −5.95)	< 0.0001
Symptom resolution rate on day 4	928 (64.90)	252 (53.05)	−11.84 (−16.97 to −6.72)	< 0.0001
Symptom resolution rate on day 5	1183 (82.73)	330 (69.47)	−13.25 (−17.84 to −8.67)	< 0.0001
Muscular soreness	*n* = 910 (%)	*n* = 290 (%)		
Symptom resolution rate on day 2	356 (39.12)	66 (22.76)	−16.36 (−22.14 to −10.59)	< 0.0001
Symptom resolution rate on day 3	579 (63.63)	148 (51.03)	−12.59 (−19.14 to −6.04)	0.0001
Symptom resolution rate on day 4	757 (83.19)	211 (72.76)	−10.43 (−16.1 to −4.76)	< 0.0001
Symptom resolution rate on day 5	834 (91.65)	237 (81.72)	−9.92 (−14.72 to −5.13)	< 0.0001
Headache	*n* = 1029 (%)	*n* = 338 (%)		
Symptom resolution rate on day 2	427 (41.50)	94 (27.81)	−13.69 (−19.33 to −8.04)	< 0.0001
Symptom resolution rate on day 3	675 (65.60)	204 (60.36)	−5.24 (−11.21 to 0.73)	0.0809
Symptom resolution rate on day 4	847 (82.31)	252 (74.56)	−7.76 (−12.95 to −2.56)	0.0018
Symptom resolution rate on day 5	947 (92.03)	277 (81.95)	−10.08 (−14.5 to −5.66)	< 0.0001
Fatigue	*n* = 1160 (%)	*n* = 394 (%)		
Symptom resolution rate on day 2	395 (34.05)	79 (20.05)	−14 (−18.8 to −9.2)	< 0.0001
Symptom resolution rate on day 3	702 (60.52)	173 (43.91)	−16.61 (−22.26 to −10.96)	< 0.0001
Symptom resolution rate on day 4	874 (75.34)	259 (65.74)	−9.61 (−14.91 to −4.31)	0.0002
Symptom resolution rate on day 5	1019 (87.84)	301 (76.40)	−11.45 (−16.04 to −6.85)	< 0.0001
Sweat	*n* = 557 (%)	*n* = 176 (%)		
Symptom resolution rate on day 2	255 (45.78)	61 (34.66)	−11.12 (−19.28 to −2.96)	0.0094
Symptom resolution rate on day 3	404 (72.53)	102 (57.95)	−14.58 (−22.76 to −6.4)	0.0003

Table 2: Continued.

Variable	Kangbingdu liquid	Placebo	Difference (95%CI)	P value
Symptom resolution rate on day 4	482 (86.54)	128 (72.73)	−13.81 (−20.97 to −6.64)	< 0.0001
Symptom resolution rate on day 5	503 (90.31)	141 (80.11)	−10.19 (−16.58 to −3.8)	0.0003
Time for body temperature to return to normal	$n = 579$	$n = 196$		
P25 (95%CI)	28.00 (25.37 to 31.50)	35.34 (26.00 to 43.17)		0.0022
P50 (95%CI)	48.33 (46.00 to 52.50)	64.59 (51.08 to 70.50)		

Table 3: Adverse events (AE).

	Kangbingdu Liquid (n = 1986)		Placebo ($n = 661$)		Total ($n = 2647$)	
	Number (%)	Cases	Number (%)	Cases	Number (%)	Cases
Total AE	24 (1.2)	25	3 (0.5)	3	27 (1.0)	28
AE is associated with the study of drug	13 (0.7)	13	1 (0.2)	1	14 (0.5)	14
AE leading to withdrawal	2 (0.1)	2	0 (0)	0	2 (0.1)	2

disappearance (Table 2). The median time for body temperature returned to normal was 48.33 (46.00 to 52.50) hours in the Kangbingdu liquid group, compared with 64.59 (51.08 to 70.50) hours in the placebo group ($P = 0.0022$) (Table 2).

During the trial, 13 (0.7%) participants in the Kangbingdu liquid group and 1 (0.2%) participant in the placebo group ($P > 0.05$) had treatment-related AEs, which mainly included diarrhea and dyspepsia in the Kangbingdu liquid group and constipation in the placebo group. Two participants, all from the Kangbingdu liquid group, withdrew from the study because of adverse events (all for no-treatment-related stomachaches and dizziness) (Table 3).

4. Discussion

To our knowledge, this trial is one of the few prospective, randomized, double-blind, placebo-controlled trials investigating the efficacy and safety of TCM clinical treatment for influenza and the common cold in China. We found that the improvement in common cold-related symptoms [12]was significantly more rapid with KBD. Compared with placebo, KBD can decrease the mean total score of 11-main symptoms.

The common cold mainly affects the upper respiratory tract and is typically characterized by nasopharyngeal catarrhal symptoms. Sore throat, stuffy nose, runny nose, cough, and fatigue usually peak in 1–3 days and last 7–10 days but can last for several weeks [14,15]. Coughs might linger longer than other cold symptoms, and they can cause sleep deprivation, myalgia, urine incontinence (particularly in women), and anxiety [16,17]. According to the survey, 52 percent of cold patients say their symptoms have a substantial influence on their everyday lives, and 93 percent are unable to work properly owing to sleeping problems caused by a cough or stuffy nose [18].

Treatment focuses on symptom improvement. While nonsteroidal anti-inflammatory drugs do not reduce the total symptom score of cold patients, they also increase the score of some symptoms, such as sneezing [19]. The nasal constrictor can relieve congestion, but not cough [20]. It also increases the risk of rhinitis [21]. In the following two surveys on cold medicine choices, Chinese people were more likely to take proprietary traditional Chinese medicine or a combination of drugs to treat common colds.

Investigation and analysis of medication for common colds among students in school revealed that 97.12% of medical students and 85.96% of nonmedical students chose the self-purchase medicine types containing "proprietary Chinese medicine" or "traditional Chinese medicine decoction," indicating that the use of Traditional Chinese medicine in the treatment of colds is relatively popular among students in our school, and most students recognize the benefits. [22]. Students knew about medications mostly from pharmacists in drugstores, doctors, and commercials. Traditional Chinese Medicine decoctions and Chinese and Western medicine mixtures were their favored drug types [23].

In our trial, the Kangbingdu Liquid group(7.39, 95% CI, 7.26 to 7.51) significantly performed better than the placebo group (6.43, 95% CI, 6.24 to 6.62) in terms of total symptom score reduction on day five compared to baseline with a mean difference of 0.96 (95% CI, 0.75 to 1.16; P.0001).

The mechanism of TCM in the treatment of influenza is complex. A pharmacodynamic study of Kangbingdu oral liquid shows that Kangbingdu oral liquid has sound therapeutic and preventive effects on influenza A (H1N1) virus infection in vivo and in vitro [24]. Administration of Chinese herbs may have beneficial immunomodulatory effects for the rapid recovery of viral infections.

There were 14 adverse events in our trial (13 in the Kangbingdu liquid group and one in the placebo group). The adverse events observed in the KBD group were also reported in other KBD studies or reports [25,26], and none of the adverse events affected the progress of the study.

There are certain limitations to our research. Our study participants were mostly young and had been clinically diagnosed with the common cold. They went to the hospital to get relief from their symptoms and prevent aggravating their symptoms, which could lead to the development of other ailments. Following that, we intend to conduct real-world research to determine the appropriate population of KBD and, based on that, utilize positive control medications to evaluate the antiviral effect of KBD in clinical trials.

5. Conclusions

Through this trial, Kangbingdu oral liquid effectively improved the comprehensive clinical symptoms of an adult common cold, also improving the main symptoms including sore throat, muscle aches, headache, and so on. Kangbingdu oral liquid effectively shortens the time it takes for the body temperature to return to normal.

Data Availability

The data used are available from the corresponding author upon request.

Conflicts of Interest

The authors declare that they have no conflicts of interest.

Acknowledgments

This study was supported by the Scientific and Technological Innovation Project of China Academy of Chinese Medical Sciences (No.CI2021B003) and Guangzhou Science and Technology Plan (grants 201604016057).

References

[1] S. B. Mossad, "Fortnightly review: treatment of the common cold," *BMJ*, vol. 317, no. 7150, pp. 33–36, 1998.

[2] R. Eccles, "Pathophysiology of nasal symptoms," *American Journal of Rhinology*, vol. 14, no. 5, pp. 335–338, 2000.

[3] T. Heikkinen and A. Jarvinen, "The common cold," *The Lancet*, vol. 361, no. 9351, pp. 51–59, 2003.

[4] T. J. Bramley, D. Lerner, and M. Sarnes, "Productivity losses related to the common cold," *Journal of Occupational and Environmental Medicine*, vol. 44, no. 9, pp. 822–829, 2002.

[5] S. E. Jacobs, D. M. Lamson, K. George, and T. J. Walsh, "Human rhinoviruses," *Clinical Microbiology Reviews*, vol. 26, no. 1, pp. 135–162, 2013.

[6] A. M. Fendrick, A. S. Monto, B. Nightengale, and M. Sarnes, "The economic burden of non-influenza-related viral respiratory tract infection in the United States," *Archives of Internal Medicine*, vol. 163, no. 4, pp. 487–494, 2003.

[7] I. J. van Benten, A. KleinJan, H. J. Neijens, A. D. M. E. Osterhaus, and W. J. Fokkens, "Prolonged nasal eosinophilia in all_ergic patients after common cold," *Allergy*, vol. 56, no. 10, pp. 949–956, 2001.

[8] J. R. Hurst, G. C. Donaldson, T. M. Wilkinson, W. R. Perera, and J. A. Wedzicha, "Epidemiological relationships between the common cold and exacerbation frequency in COPD," *European Respiratory Journal*, vol. 26, no. 5, pp. 846–852, 2005.

[9] M. J. Walter, M. Castro, S. J. Kunselman et al., "Predicting worsening asthma control following the common cold," *European Respiratory Journal*, vol. 32, no. 6, pp. 1548–1554, 2008.

[10] X. Xue, "Treatment of upper respiratory tract infection with Antiviral oral liquid," *The light of traditional Chinese medicine*, vol. 27, no. 4, p. 725, 2012.

[11] H. Zhou, "Comparison of efficacy of oseltamivir and Antiviral oral liquid in the treatment of infantile influenza," *Modern diagnosis and treatment*, vol. 26, no. 22, pp. 5116-5117, 2015.

[12] T. R. Covington, R. Henkin, S. Miller, M. Sassetti, and W. Wright, "Treating the common cold: an expert panel consensus recommendation for primary care clinicians," *Am J Nurse Pract*, vol. 8, no. 11, pp. 77–88, 2004.

[13] Z. Wang, *Handbook for Diagnosis and Treatment of Respiratory Diseases*, People's Medical Publishing House, Beijing, China, 2000.

[14] G. M. Allan and B. Arroll, "Prevention and treatment of the common cold: making sense of the evidence," *Canadian Medical Association Journal*, vol. 186, no. 3, pp. 190–199, 2014.

[15] P. V. Dicpinigaitis, A. S. Tibb, D. L. Ramsey, A. N. Carr, and C. L. Poore, "Stability of cough reflex sensitivity during viral upper respiratory tract infection (common cold)," *Pulmonary Pharmacology & Therapeutics*, vol. 28, no. 2, pp. 154–157, 2014.

[16] P. V. Dicpinigaitis, G. L. Colice, M. J. Goolsby, G. I. Rogg, S. L. Spector, and B. Winther, "Acute cough: a diagnostic and therapeutic challenge," *Cough*, vol. 5, no. 1, p. 11, 2009.

[17] T. J. Witek, D. L. Ramsey, A. N. Carr, and D. K. Riker, "The natural history of community-acquired common colds symptoms assessed over 4-years," *Rhinology journal*, vol. 53, no. 1, pp. 81–88, 2015.

[18] P. V. Dicpinigaitis, R. Eccles, M. S. Blaiss, and M. A. Wingertzahn, "Impact of cough and common cold on productivity, absenteeism, and daily life in the United States: ACHOO Survey," *Current Medical Research and Opinion*, vol. 31, no. 8, pp. 1519–1525, 2015.

[19] S. Y. Kim, Y. J. Chang, H. M. Cho, Y. W. Hwang, and Y. S. Moon, "Non-steroidal anti-inflammatory drugs for the common cold," *Cochrane Database of Systematic Reviews*, vol. 9, Article ID D6362, 2015.

[20] L. Deckx, A. I. De Sutter, L. Guo, N. A. Mir, and M. L. van Driel, "Nasal decongestants in monotherapy for the common cold," *Cochrane Database of Systematic Reviews*, vol. 10, Article ID CD009612, 2016.

[21] M. S. Dykewicz, S. Fineman, D. P. Skoner et al., "Diagnosis and management of rhinitis: complete guidelines of the joint task force on practice parameters in allergy, asthma and immunology," *Annals of Allergy, Asthma, & Immunology*, vol. 81, no. 5, pp. 478–518, 1998.

[22] C. Tang, Y. Chen, H. Zhou, and Z. Zhang, "Investigation and Analysis of cold medication in college students," *Anhui Medicine*, vol. 24, no. 04, pp. 814–817, 2020.

[23] X. Tao, Z. Xu, J. Yang, Y. Yan, and H. Li, "Investigation on cognition of cold among College students majoring in pharmacy," *West China Medical Journal*, vol. 29, no. 10, pp. 1905–1907, 2014.

[24] M. Xin, R. Yao, and B. Lei, "Pharmacodynamics of antiviral oral liquid in the prevention and treatment of influenza A virus infection," *Western Traditional Chinese Medicine*, vol. 34, no. 12, pp. 12–15, 2021.

[25] X. Li, T. Yu, and Z. Wen, "Investigation on adverse reactions of Xiangxue Antiviral oral liquid in outpatient department of Guangzhou Hospital," *New Chinese medicine and clinical pharmacology*, vol. 30, no. 02, pp. 245–250, 2019.

[26] J. Fu and Q. Zou, "A case of dizziness and headache caused by antiviral oral liquid," *Journal of Modern Integrated Traditional Chinese and Western Medicine*, vol. 15, p. 2061, 2004.

Hindawi
Evidence-Based Complementary and Alternative Medicine
Volume 2022, Article ID 4138555, 15 pages
https://doi.org/10.1155/2022/4138555

Research Article

Comparative Efficacy of Chinese Patent Medicines for Clearing Heat and Dampness in the Treatment of NAFLD: A Network Meta-Analysis of Real-World Evidence

Yuan Xu,[1,2] Yan Wang,[3] Xiao-jun Gou,[2] and Man Wang[4]

[1]*School of Pharmacy, Shaanxi University of Traditional Chinese Medicine, Xianyang 712046, Shaanxi, China*
[2]*Central Laboratory, Baoshan District Hospital of Integrated Traditional Chinese and Western Medicine of Shanghai, Shanghai University of Traditional Chinese Medicine, Shanghai 201999, China*
[3]*Pharmacy Department, Shanghai Putuo District Liqun Hospital, Shanghai 200333, China*
[4]*Nutriology Department, Shanghai Fengxian District Central Hospital, Shanghai 201499, China*

Correspondence should be addressed to Xiao-jun Gou; gouxiaojun1975@163.com and Man Wang; 99378265@qq.com

Received 16 April 2022; Revised 26 May 2022; Accepted 27 June 2022; Published 31 July 2022

Academic Editor: Xuezhong Zhou

Background. Nonalcoholic fatty liver disease (NAFLD) has emerged as the most common chronic liver disease, as well as a worldwide medical problem with a substantial socioeconomic burden. In China, Chinese patent medicines (CPMs) have been widely utilized as promising and effective therapy options for NAFLD. Traditional Chinese medicine (TCM) is a particular kind of medical science reliant on real-world clinical practices and evidence. Therefore, using the real-world data extracted from pragmatic randomized controlled trials (PRCTs) have more reference value for the application of CPMs in NAFLD. *Method.* Six databases were searched from their inception up to March 18, 2022. The methodological quality of the included study was evaluated by the Cochrane risk-of-bias tool. Then, The STATA 13.0 program was then used to do a network meta-analysis (NMA) of real-world studies. The surface under the cumulative ranking curve (SUCRA) probability values were applied to rank the examined treatments. *Results.* Forty-three PRCTs (4997 cases in total) were identified. Da-Huang-Li-Dan capsule (DHLD), Dan-Ning tablet (DN), Dang-Fei-Li-Gan-Ning capsule (DFLGN), Qiang-Gan capsule (QG), and Hua-Zhi-Rou-Gan granule (HZRG) were among the five CPMs tested. As far as the clinical effective rate of the primary outcome index was concerned, the top three CPMs were DN + CDs: OR = 0.19, 95% CIs: 0.12, 0.31 (SUCRA: 81.8%); DFLGN + CDs: OR = 0.21, 95% CIs: 0.09, 0.46 (SUCRA: 74.9%), and DHLD + CDs: OR = 0.26, 95% CIs: 0.10, 0.67 (SUCRA: 61.1%). In terms of liver function index, DN + CDs ranked first in ALT index: MD = 15.81, 95% CIs: 10.05, 21.57 (SUCRA: 85.5%), DFLGN + CDs ranked first in AST index: MD = 14.94, 95% CIs: 4.77, 25.11 (SUCRA: 83.6%), HZRG + CDs ranked first in TC index: MD = 0.53, 95% CIs: 0.28, 1.03 (SUCRA: 87.1%) and TG index: MD = 1.8, 95% CIs: 1.41, 2.30 (SUCRA: 79.9%). *Conclusion.* Using CPMs as a coadjuvant treatment might be positive efficacious intervention from which patients with NAFLD will derive benefits. When it came to the clinical effective rate and other outcomes, DN + CDs demonstrated a significant improvement in individuals with NAFLD.

1. Introduction

Nonalcoholic fatty liver disease (NAFLD) has become the most prevalent liver metabolic disease, affecting approximately 1.7 billion individuals around the world [1–3]. NAFLD can be classified as simple steatosis and nonalcoholic steatohepatitis (NASH), cirrhosis, and hepatocellular carcinoma based on its pathological stages [4, 5]. In the United States, these increased trends in the prevalence and incidence of NAFLD may also be seen in children and adolescents. Similar increases have been observed in Europe, China, India, and other regions of the world. As a result, NAFLD has grown into a worldwide medical problem with severe socioeconomic implications [6].

Chinese patent medicines (CPMs) have been found in studies to have a greater therapeutic impact, less toxic and

side effects, and high safety when used in combination with CDs. CPMs have been widely used as adjuvant therapy for NAFLD in China in recent years [7–9]. We discovered that five CPMs, including Da-Huang-Li-Dan capsule (DHLD), Dan-Ning tablet (DN), Dang-Fei-Li-Gan-Ning capsule (DFLGN), Qiang-Gan capsule (QG), and Hua-Zhi-Rou-Gan granule (HZRG), have been widely used in NAFLD of the dampness and heat accumulation type due to their outstanding effects, based on clinical medication experience and previous searches in electronic databases. Systematic reviews have demonstrated their effectiveness [7, 10, 11]. Traditional Chinese medicine (TCM) has no term for "fatty liver," although it can be characterized as "hypochondriac pain," "accumulation," or "jaundice" based on clinical symptoms. Fatty liver is caused by overeating fat and spicy foods, endogenous damp evil, long-term stagnation or abnormal transportation and transformation of spleen and stomach functions, endogenous dampness, and turbidity. Therefore, clearing heat and dampness is an important treatment in the treatment of NAFLD.

When CPMs are used in conjunction with traditional CDs, clinical symptoms can be considerably improved. However, it is impossible to accurately and thoroughly examine the advantages and drawbacks of numerous therapies using pairwise meta-analysis. The network meta-analysis (NMA) is a new sort of evidence-based medical statistical approach which allows for simultaneous examination of the efficacy of many interventions by comparing direct and indirect evidence and ranking the efficacy of various therapies to make a conclusion [12, 13]. Another important characteristic of NMA is that it may rate each CPM based on its efficacy, assisting physicians in making the optimal treatment options. In recent years, the concept of real-world research has emerged, and real-world data and evidence have become more and more important in the field of medical and health decision-making. Randomized controlled trial is recognized as the "gold standard" for evaluating the effectiveness of intervention measures, which can be divided into exploratory randomized controlled trials and pragmatic randomized controlled trials (PRCTs). TCM is an empirical medicine that mainly relies on case reports and clinical experience summaries. Through the evidence in the real world, it can promote the personalized application of TCM diagnosis and treatment rules, so the reference significance based on PRCTs for TCM is more important. Therefore, the purpose of this study is to evaluate the clinical efficacy of various CPMs combined with CDs by combining big data with real-world data and provide further evidence for rational drug selection.

2. Materials and Methods

This study was registered on the PROSPERO (International Prospective Register of Systematic Reviews) and the registration ID is CRD42022323979. The present report follows the Preferred Reporting Items for Systematic Review and Meta-analysis (PRISMA) Protocols guidelines [14].

2.1. Data Sources and Search Strategy. From the establishment of each electronic database to March 18, 2022, PRCTs using methods of clearing heat and removing dampness to treat NAFLD were searched in the following 6 electronic databases: PubMed, Embase, Cochrane Library, the Chinese National Knowledge Infrastructure, Wanfang Database, and Weipu Database. No restriction on the publication year, language, or blinding methods were implemented.

Searching for the following terms: ("Complementary Therapies" OR "Complementary and alternative therapies" OR "Alternative Medicine" OR "Alternative Therapies" OR "Complementary Medicine" OR "Herbal therapy" OR "Therapy, Alternative" OR "Therapy, Complementary" OR "Therapies, Alternative") AND ("Non-alcoholic Fatty Liver Disease" OR "Steatohepatitis, Nonalcoholic" OR "Nonalcoholic Steatohepatitides" OR "NAFLD") AND ("clinical trial" OR "randomized controlled trial" OR "randomized controlled trial"). In our literature search, we did not define the language or status of the papers. Additional references were found by manually searching bibliographies of included trials and associated reviews.

2.2. Criteria for Literature Inclusion. Clinical studies using CPMs for clearing heat and dampness in the treatment of NAFLD were included in this network meta-analysis. Trials were excluded if

(1) there was no control group or there was a combination with other drugs;

(2) trials on effective analysis data could not be obtained;

(3) they were reviews, observational studies, cross-sectional, case reports, conference papers, meta-analyses, experience sharing, animal trials, etc.

Studies that matched the following criteria were considered eligible:

(1) PRCTs that evaluated the efficacy of CPMs combined with CDs were included.

(2) All of the patients were diagnosed with NAFLD using the Guidelines of prevention and therapy for NAFLD [15].

2.3. Outcomes. Clinical effectiveness was defined as the primary outcome. The improvement in clinical symptoms of patients before and after treatment was used to assess the clinical effect of medications, which might better reflect the therapeutic effect of pharmaceuticals. According to the degree of alleviation, symptoms were classed as effective or ineffective. Other outcomes included liver function: the Alanine aminotransferase (ALT) and aspartate aminotransferase (AST), and also blood lipid indexes such as triglyceride (TG) and total cholesterol (TC).

2.4. Study Selection and Data Extraction. Data extraction was performed independently by two reviewers who participated in training and calibration exercises using Endnote X9 to do the screening. If there was a disagreement, they worked it out

via conversation or had it evaluated by a third party. The third party also employed a standardized screening form and did calibration exercises prior to the screening procedure.

The researchers gathered information on the following features for all qualifying trials:

(1) Basic information (first author, title of study).

(2) Participant characteristics (sample size, gender, and age).

(3) Measures of prevention and control (dosage form, dose, and duration).

(4) Risks of bias investigation.

(5) Outcome Measures

2.5. Assessment of Literature Quality. Two reviewers independently assessed the risk of bias for PRCTs using the Cochrane Collaboration's "risk of bias" technique. The Cochrane handbook was used to develop the assessment criteria [16]. The two reviewers' disagreement was resolved through discussion. If there is a disagreement between two reviewers, the paper will be sent to a third person for review.

2.6. Statistical Analysis. The Cochrane Collaboration's RevMan 5.3 software was used to conduct statistical analyses of literature quality. Calculations and graphs were generated using STATA 13.0 software, the Bayesian random-effects NMA using Markov-chain Monte Carlo simulation. After an initial burn-in of 20,000 iterations and a thinning interval of 10, the random-effects model for outcomes was chosen in the NMA, which was run with four chains and 50,000 simulated iterations. We calculated mean differences (MD) with corresponding 95% credible intervals (CIs) for continuous outcomes and odds ratios (OR) with corresponding 95% CIs for dichotomous. We divided multiarm studies into two-arm trials, if there were any. The Chi-squared test was used to determine the degree of heterogeneity between studies [17]. If the inconsistency was not significant in direct and indirect comparisons, the consistency model was used for further analyses. The premise of consistency between direct and indirect evidence was not used in this NMA due to nonclosed loops.

3. Results

3.1. Selection and Identification of Studies. A total of 6119 possibly relevant trials were retrieved, with 1223 trials remaining after 4896 duplicates and irrelevant trials were removed. Following a review of the titles and abstracts, 1014 publications were eliminated because they did not fulfill the inclusion criteria, and 209 trials were found to meet the planned standards for further evaluation after reading the complete text. Finally, 43 studies [18–60] were included in the meta-analysis. Figure 1 depicts the PRISMA flow diagram of the literature retrieval process. All of the trials that were included in the study were published as complete publications.

3.2. Included Study Characteristics. Table 1 summarized the basic characteristics of the 43 trials, and a total of 4997 patients were included. In these 43 trials. 3 trials used DHLD + CDs vs. CDs [18–20], 16 trials used DN + CDs vs. CDs [21–36], 4 used DFLGN + CDs vs. CDs [37–40], 8 used QG + CDs vs. CDs [41–48], and 12 used HZRG + CDs vs. CDs [49–60]. Among these PRCTs, control groups have been treated with CDs like statin lipid-lowering agents, anti-inflammatory, hypoglycemic drugs, and nutritional support. The statin lipid-lowering agents mainly include atorvastatin, simvastatin, and rosuvastatin as a single treatment or a combination of treatments. The experimental group's intervention was one of the CPMs included in the control group's intervention. The therapy lasted from around 6 to 24 weeks. Table 1 shows the study's features in detail, and Figure 2 shows the comparative links between each intervention and each result.

3.3. Methodological Quality Assessment. Among the 43 PRCTs, 8 studies used the random number method or computer to create random number words, with low-risk bias, 16 studies used outpatient order or a period of hospitalization, so there was high-risk bias, and 4 studies used the method of distribution of low-risk bias. Because none of the 43 PRCTs indicated subject and researcher blinding or evaluator blinding to the result, they were all rated as "unclear". 4 of the studies did not explain the reasons for the missing data, the remaining 27 studies had no missing data, and 12 studies were unclear. We were unable to gather thorough information on the remaining two aspects, selective reporting outcomes, and other biases. Therefore, we rated them all as "unclear." Figures 3 and 4 provide the exact findings of the bias risk assessment for all PRCTs.

3.4. Results of the NMA

3.4.1. Clinical Effect. Clinical effect was reported in 43 trials, in which 3 used DHLD + CDs vs. CDs [18–20], 16 used DN + CDs vs. CDs [21–36], 4 used DFLGN + CDs vs. CDs [37–40], 8 used QG + CDs vs. CDs [41–48], and 12 used HZRG + CDs vs. CDs [49–60].

There were 43 comparisons in the network of comparisons in Table 2, and DHLD, DN, DFLGN, QG, HZRG combined with CDs improved the clinical effective rate more significantly than CDs alone (DHLD + CDs : OR = 0.26, 95% CIs: 0.10, 0.67; DN + CDs : OR = 0.19, 95% CIs: 0.12, 0.31; DFLGN + CDs : OR = 0.21, 95% CIs: 0.09, 0.46; QG + CDs : OR = 0.44, 95% CIs: 0.27, 0.74; HZRG + CDs : OR = 0.27, 95% CIs: 0.17, 0.43). Notably, there were significant differences between DN + CDs and QG + CDs.

The SUCRA values in Table 3 and Figure 5 indicated that DN + CDs was the best therapy, DFLGN + CDs was second, and DHLD + CDs was third.

3.4.2. The Level of ALT. 40 PRCTs (3 used DHLD + CDs vs. CDs [18–20], 15 used DN + CDs vs. CDs [21–29, 31, 32, 34, 35], 4 used DFLGN + CDs vs. CDs [37–40]

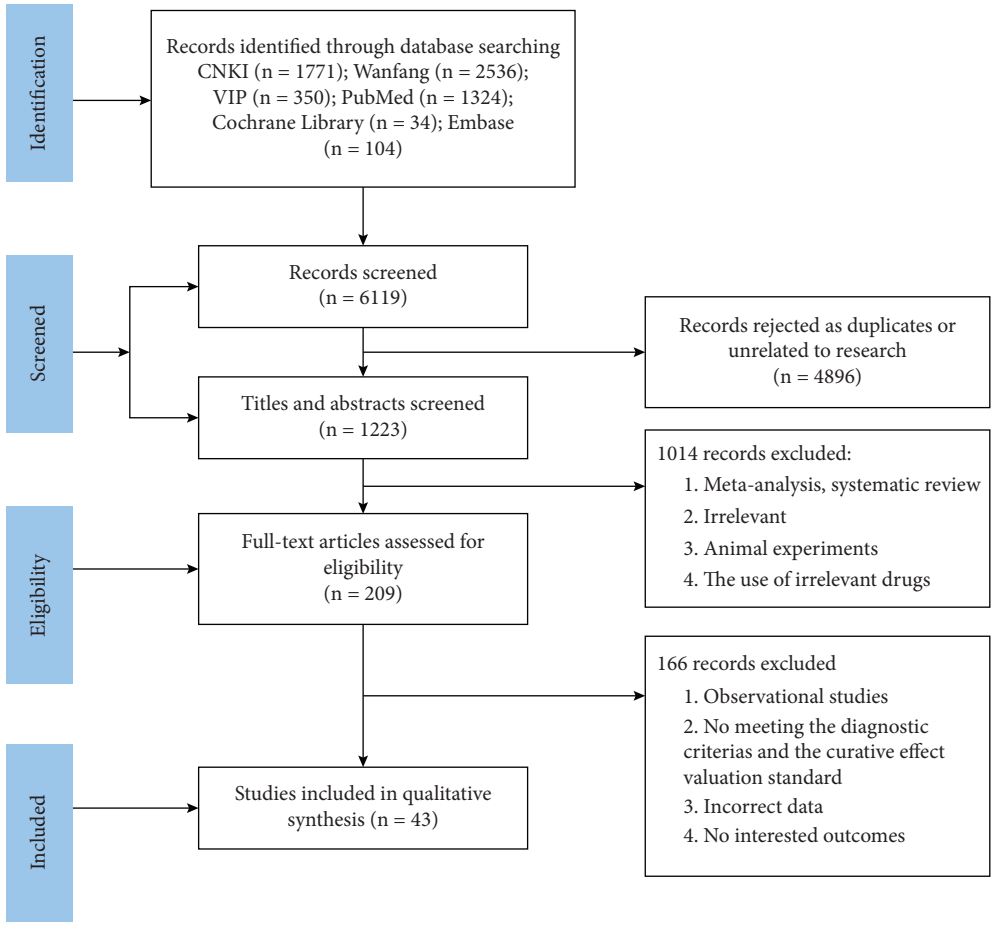

Figure 1: Flow diagram of study inclusion.

7 used QG + CDs vs. CDs [41–48], and 11 used HZRG + CDs vs. CDs [49–59]) with five treatments reported the TG. The results of the pairwise meta-analysis are shown in Table 4. According to Table 4, DN, QG, HZRG combined with CDs (DN + CDs : MD = 15.81, 95% CIs: 10.05, 21.57; QG + CDs : MD = 12.20, 95% CIs: 4.42, 19.99; HZRG + CDs : MD = 11.23, 95% CIs: 4.85, 17.62) were more effective than CDs alone; there were no significant differences between each comparison of different CPMs.

The SUCRA values in Table 3 and Figure 5 indicated that DN + CDs was the optimal treatment, QG + CDs was the second, and HZRG + CDs was the third.

3.4.3. The Level of AST. 35 PRCTs (3 used DHLD + CDs vs. CDs [18–20], 11 used DN + CDs vs. CDs [21, 23–25, 27, 29–33, 35], 3 used DFLGN + CDs vs. CDs [37–40] 7 used QG + CDs vs. CDs [41, 43–48], and 11 used HZRG + CDs vs. CDs [49–59]) with five treatments reported the AST. The results of the pairwise meta-analysis are shown in Table 5. According to Table 5, DHLD, DN, DFLGN, HZRG combined with CDs (DHLD + CDs : MD = 13.45, 95% CIs: 3.61, 23.28; DN + CDs : MD = 7.43, 95% CIs: 1.95, 12.91; DFLGN + CDs : MD = 14.94, 95% CIs: 4.77, 25.11; HZRG + CDs : MD = 11.63, 95% CIs: 6.25, 17.02) were more effective than CDs alone; QG + CDs did not perform more remarkable than CDs alone.

The SUCRA values in Table 3 and Figure 5 indicated that DFLGN + CDs was the optimal treatment, DHLD + CDs was the second, and HZRG + CDs was the third.

3.4.4. The Level of TC. TC was estimated in 37 PRCTs, in which 3 used DHLD + CDs vs. CDs [18–20], 14 used DN + CDs vs. CDs [21–32, 34, 35], 4 used DFLGN + CDs vs. CDs [37–40], 5 used QG + CDs vs. CDs [41, 43, 44, 47, 48], and 11 used HZRG + CDs vs. CDs [49–59]. The results of the pairwise meta-analysis are shown in Table 6. According to Table 6, DN, DFLGN, QG, HZRG combined with CDs (DFLGN + CDs : MD = 0.84, 95% CIs: 0.38, 1.83; QG + CDs : MD = 1.41, 95% CIs: 0.65, 3.08; HZRG + CDs : MD = 0.53, 95% CIs: 0.28, 1.03) had better treatment than CDs alone, and there were no significant differences among other groups.

The SUCRA values in Table 3 and Figure 5 indicated that HZRG + CDs was the optimal treatment, DFLGN + CDs was the second, and DHLD + CDs was the third.

3.4.5. The Level of TG. 37 PRCTs (3 used DHLD + CDs vs. CDs [18–20], 13 used DN + CDs vs. CDs [21–29, 31, 32, 34, 35], 4 used DFLGN + CDs vs. CDs [37–40] 6 used QG + CDs vs. CDs [41–44, 47, 48] and 11 used HZRG + CDs vs. CDs [49–59]) with five treatments reported

Table 1: Basic characteristics of the included studies.

No.	Literature source	Sample (treatment/control)	Gender			Age (years)		Course (week)	Contrast drugs		Outcome indicators
		T	*C*	*M*	*F*	*T*	*C*		*T*	*C*	
1	Li xiangyang (2021)	62	62	71	53	44.44 ± 9.67	44.87 ± 9.58	12	Da-huang-Li-Dancapsule + CDs	CDs	Clinical effective rate, ALT, AST, γ-GT, TC, TG
2	Li na (2021)	40	39	47	32	51.91 ± 7.52	51.49 ± 7.04	12	Da-huang-Li-Dancapsule + CDs	CDs	Clinical effective rate, ALT, AST, γ-GT, TC, TG, LDL, HDL
3	Wang zhengyan (2020)	43	43	53	33	—		12	Da-huang-Li-Dancapsule + CDs	CDs	Clinical effective rate, ALT, AST, γ-GT, TC, TG, LDL, HDL
4	Zhang yu (2018)	35	35	38	32	56.8 ± 6.5		12	Dan-ning tablet + CDs	CDs	Clinical effective rate, ALT, AST, TC, LDL
5	Tao yingjie (2018)	29	29	24	34	45.36 ± 11.54		12	Dan-ning tablet + CDs	CDs	Clinical effective rate, AST, TC, LDL, γ-GT
6	Lv junning (2017)	47	46	49	44	26 ~ 65	28 ~ 66	12	Dan-ning tablet + CDs	CDs	Clinical effective rate, ALT, TC, TG, TBIL
7	Yi ying (2018)	20	20	23	17	45.8 ± 2.9	45.2 ± 2.5	12	Dan-ning tablet + CDs	CDs	Clinical effective rate, ALT, TC, TG, TBIL
8	Xiang fangfei (2019)	39	39	47	31	40.76 ± 2.33	41.63 ± 2.16	12	Dan-ning tablet + CDs	CDs	Clinical effective rate, ALT, AST,
9	Gao ying (2017)	44	44	47	41	43.54 ± 6.43	43.57 ± 6.45	12	Dan-ning tablet + CDs	CDs	Clinical effective rate, ALT, AST, γ-GT, TC, TG, LDL, HDL, TBIL
10	Guo zhenying (2018)	66	66	72	60	44.36 ± 8.49	43.74 ± 7.89	12	Dan-ning tablet + CDs	CDs	Clinical effective rate, ALT, AST, γ-GT, TC, TG, LDL, HDL, TBIL
11	Peng lirui (2015)	25	25	36	14	51.7 ± 12.3	53.7 ± 13.3	12	Dan-ning tablet + CDs	CDs	Clinical effective rate, ALT, AST, TC, TG
12	Wang yujing (2019)	51	51	55	47	44.0 ± 3.3		12	Dan-ning tablet + CDs	CDs	Clinical effective rate, ALT, AST, TC, TG
13	Li xiaoqing (2019)	32	30	22	40	42.38 ± 10.85	43.37 ± 11.15	12	Dan-ning tablet + CDs	CDs	Clinical effective rate, ALT, AST, γ-GT, TC, TG, LDL, HDL, TBIL
14	Feng yan (2013)	48	47	50	45	41.5 ± 3.1	42.7 ± 4.2	12	Dan-ning tablet + CDs	CDs	Clinical effective rate, ALT, TC, TG, TBIL
15	Zhang xiyun (2020)	48	48	39	57	44.15 ± 7.52	43.25 ± 7.09	12	Dan-ning tablet + CDs	CDs	Clinical effective rate, ALT, AST, γ-GT, TC, TG
16	Wang zhiling (2014)	127	116	160	83	46.5 ± 7.5	47 ± 7.4	12	Dan-ning tablet + CDs	CDs	Clinical effective rate, ALT, AST, TC, TG
17	Li bing (2018)	52	52	45	59	41.82 ± 8.63	40.45 ± 8.35	12	Dan-ning tablet + CDs	CDs	Clinical effective rate, ALT, AST, γ-GT, TC, TG, LDL, HDL, TBIL
18	Fan qiaowen (2019)	50	50	72	28	55.5 ± 1.8	56 ± 1.8	12	Dan-ning tablet + CDs	CDs	Clinical effective rate, ALT, γ-GT, TC, TG
19	Ji guang (2008)	107	33	102	38	48.37 ± 9 .60	44.43 ± 10.40	12	Dan-ning tablet + CDs	CDs	Clinical effective rate, ALT, AST, γ-GT, TC, TG
20	Song shoulong (2018)	45	45	53	37	42.35 ± 4.26	42.31 ± 4.21	6	Dang-fei-Li-Gan-Ningcapsule + CDs	CDs	Clinical effective rate, ALT, AST, TBIL
21	Li chaomin (2012)	113	114	150	77	45.5 ± 11.8	46.7 ± 10.8	12	Dang-fei-Li-Gan-Ningcapsule + CDs	CDs	Clinical effective rate, ALT, AST, TC, TG, LDL, HDL

Table 1: Continued.

No.	Literature source	Sample (treatment/control)	Gender			Age (years)		Course (week)	Contrast drugs		Outcome indicators
		T	*C*	*M*	*F*	*T*	*C*		*T*	*C*	
22	LI guozheng (2009)	40	40	—		—		12	Dang-fei-Li-Gan-Ningcapsule + CDs	CDs	Clinical effective rate, ALT, AST, TC, TG, LDL, HDL
23	Zhang xue (2015)	30	30	29	31	20~55	18~60	24	Dang-fei-Li-Gan-Ningcapsule + CDs	CDs	Clinical effective rate, ALT, TC, TG
24	Li li (2010)	45	45	54	36	18~56	26~61	24	Qiang-Gancapsule + CDs	CDs	Clinical effective rate, ALT, AST, TC, TG, γ-GT
25	Tang liwei (2019)	58	58	—		—		24	Qiang-Gancapsule + CDs	CDs	Clinical effective rate, ALT, AST, TC, TG, γ-GT
26	Yao zhongcai (2011)	75	75	88	62	46.7 ± 11.8	45.3 ± 12.6	12	Qiang-Gancapsule + CDs	CDs	Clinical effective rate, ALT, AST, TC, TG, γ-GT
27	Bai lihua (2016)	45	45	55	35	23 ~ 67	21 ~ 64	24	Qiang-Gancapsule + CDs	CDs	Clinical effective rate, ALT, AST, γ-GT
28	Wang xiuqin (2019)	119	119	89	149	45.62 ± 10.21	44.53 ± 8.87	12	Qiang-Gancapsule + CDs	CDs	Clinical effective rate, ALT, AST, γ-GT
29	Liu hongfen (2016)	32	30	34	28	39.5 ± 10.2	39.1 ± 9.1	12	Qiang-Gancapsule + CDs	CDs	Clinical effective rate, ALT, γ-GT, TC
30	Chen zexiong (2006)	64	58	77	45	42.5	45.8	12	Qiang-Gancapsule + CDs	CDs	Clinical effective rate, ALT, AST, TC, TG, γ-GT
31	Wang yanping (2015)	150	150	128	172	35.8 ± 3.7	37.2 ± 3.3	24	Qiang-Gancapsule + CDs	CDs	Clinical effective rate, ALT, AST, TC, TG, γ-GT
32	Han qing (2019)	90	90	114	66	43.64 ± 5.82	41.28 ± 5.35	8	Hua-zhi-rou-Gangranule + CDs	CDs	Clinical effective rate, ALT, AST, TC, TG, LDL, HDL
33	Li haixia (2017)	57	58	62	53	41.3 ± 4.8	42.3 ± 5.4	12	Hua-zhi-rou-Gangranule + CDs	CDs	Clinical effective rate, ALT, AST, TC, TG, γ-GT
34	Zhang chunming (2019)	30	30	37	23	52.0 ± 10.8	52.3 ± 10.4	—	Hua-zhi-rou-Gangranule + CDs	CDs	Clinical effective rate
35	Wang xiling (2018)	57	57	74	40	48.5 ± 8.1	49.4 ± 6.1	12	Hua-zhi-rou-Gangranule + CDs	CDs	Clinical effective rate, ALT, AST, TC, TG
36	Guo suicheng (2013)	60	60	72	48	37 ± 4.21		8	Hua-zhi-rou-Gangranule + CDs	CDs	Clinical effective rate, ALT, AST, γ-GT
37	Luo qing (2019)	50	50	58	42	36.76 ± 1.58	36.54 ± 1.37	8	Hua-zhi-rou-Gangranule + CDs	CDs	Clinical effective rate, ALT, AST, γ-GT, TC, TG, LDL, HDL, TBIL
38	Fang junwei (2014)	132	131	178	85	42.84 ± 7.49	41.90 ± 8.32	12	Hua-zhi-rou-Gangranule + CDs	CDs	Clinical effective rate, ALT, AST, TC, TG, LDL, HDL
39	Lin yudong (2013)	60	60	90	30	43.3 ± 5.8	42.8 ± 6.3	12	Hua-zhi-rou-Gangranule + CDs	CDs	Clinical effective rate, ALT, AST, TC, TG
40	Yu yang (2014)	30	30	34	26	44.7 ± 9.3	43.7 ± 9.2	12	Hua-zhi-rou-Gangranule + CDs	CDs	Clinical effective rate, ALT, AST, TC, TG, γ-GT
41	Yang shushan (2015)	90	90	118	62	49.5 ± 7.5	50.4 ± 7.1	12	Hua-zhi-rou-Gangranule + CDs	CDs	Clinical effective rate, ALT, AST, TC, TG
42	Xu junlin (2018)	70	70	80	60	44.7 ± 7.5	43.5 ± 7.1	12	Hua-zhi-rou-Gangranule + CDs	CDs	Clinical effective rate, ALT, AST, TC, TG
43	Nan (2020)	40	40	31	49	37.2 ± 9.4		8	Hua-zhi-rou-Gangranule + CDs	CDs	Clinical effective rate, ALT, AST, TC, TG, γ-GT

Note. CDs: Chemical drugs, ALT: Alanine aminotransferase, AST: Aspartate aminotransferase, TC: Total cholesterol, TG: Triglycerides, γ-GT: γ-glutamyltranspeptidase, LDL: Low-density lipoprotein, HDL: High-density lipoprotein, TBIL: Total bilirubin.

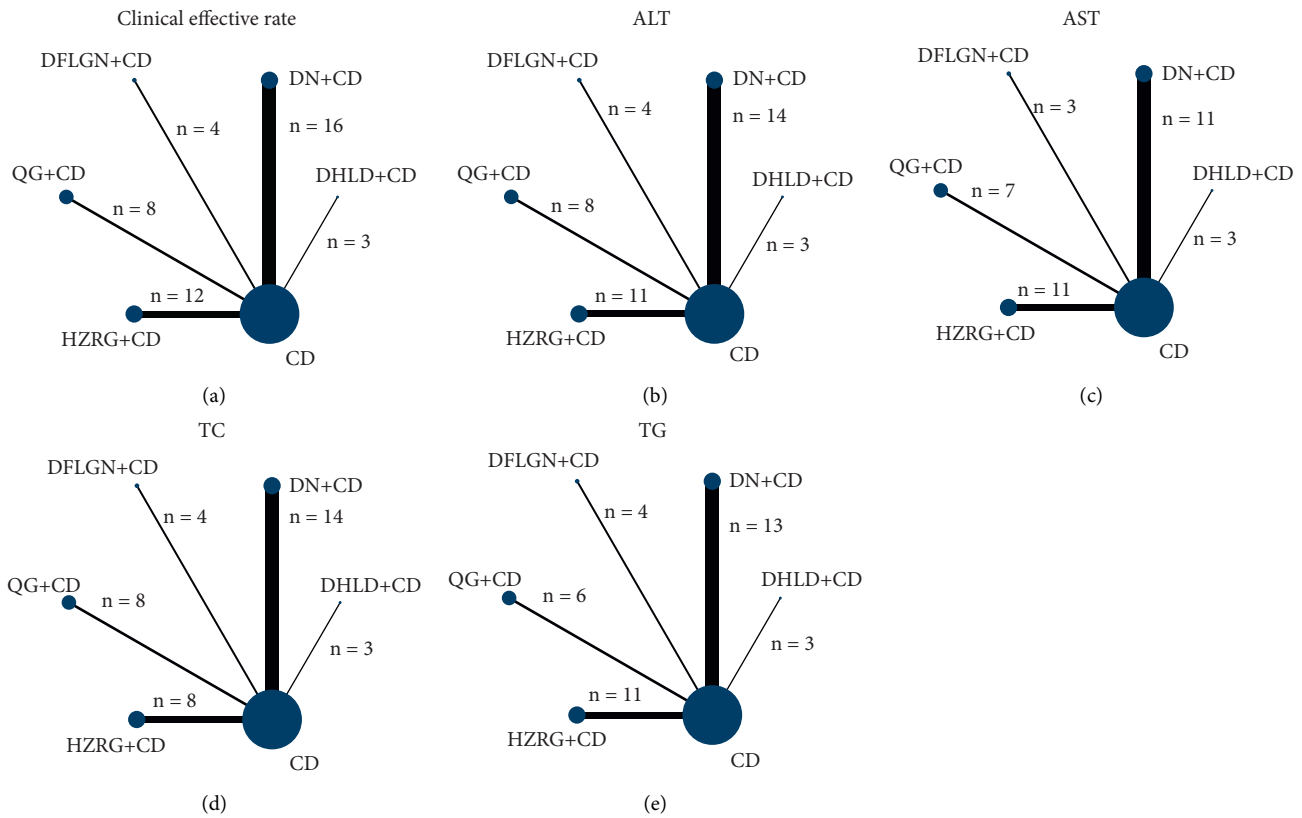

Figure 2: Network graph of the different outcomes. (a) Clinical effective rate, (b) Alanine aminotransferase (ALT), (c) Aspartate aminotransferase (AST), (d) Serum total cholesterol (TC), (e) Triglyceride (TG).

the TG. The heterogeneity results of the pairwise meta-analysis are shown in Table 7. According to Table 7, DHLD, DN, DFLGN, QG, HZRG combined with CDs (DHLD + CDs : MD = 1.52, 95% CIs: 1.04, 2.22; DN + CDs : MD = 1.63, 95% CIs: 1.34, 1.98; DFLGN + CDs : MD = 1.44, 95% CIs: 1.03, 2.01; QG + CDs : MD = 1.69, 95% CIs: 1.30, 2.21; and HZRG + CDs : MD = 1.8, 95% CIs: 1.41, 2.30) were more effective than CDs alone, and there were no significant differences among other groups.

In Table 3 and Figure 5, the SUCRA values suggested that HZRG + CDs was the optimal treatment, QG + CDs was the second, and DN + CDs was the third.

3.5. Funnel Plot Characteristics. Figure 6 shows comparison adjusted funnel plots for various outcomes. Results TG was the only funnel plot without bias. The majority of the dispersion points were positioned in the middle and top half of the inverted triangle. As a result, there was no bias due to publishing. The funnel plot was asymmetric, indicating a limited sample size and publication bias, among other outcomes.

4. Discussion

A total of 43 PRCTs involving 4997 individuals were included in the study. DHLD, DN, DFLGN, QG, and HZRG are five CPMs that have been found in the therapy of NAFLD. Because of the heterogeneity, the Mantel-Haenszel random-effects model was utilized for the meta-analysis. Due to the nonclosed loops in this NMA, the assumption of consistency between direct and indirect evidence was not used. This network meta-analysis found five interesting outcomes: clinical effective rate, ALT, AST, TC, and TG. In terms of clinical effective rate, the results showed that DHLD, DN, DFLGN, QG, and HZRG coupled with CDs had a better impact than CDs alone. We may infer that DN + CDs was the best in terms of clinical response rate and improvement based on SUCRA values. We can conclude that DN + CDs was the best in terms of clinical response rate and ALT improvement, DFLGN + CDs was the best in terms of AST improvement, and second in terms of clinical response rate and TC improvement, and HZRG + CDs was the best in terms of TC and TG outcomes improvement. However, it rated worse in other outcome indicators. As a consequence of the above analyses, we conclude that DN + CDs might be a potential therapy option. However, as can be observed from the funnel plot, the outcome indicator had a modest degree of bias in addition to TG, and other outcome indicators had a large degree of bias due to the existence of low-quality PRCTs. Thus the evidence strength of other outcomes may be reduced.

The pathogenesis of NAFLD cannot be clearly explained. The hypothesis widely accepted by scholars is the pathogenesis of "second hit;" the "first hit" induces fat accumulation in hepatocytes and increases hepatic uptake of free

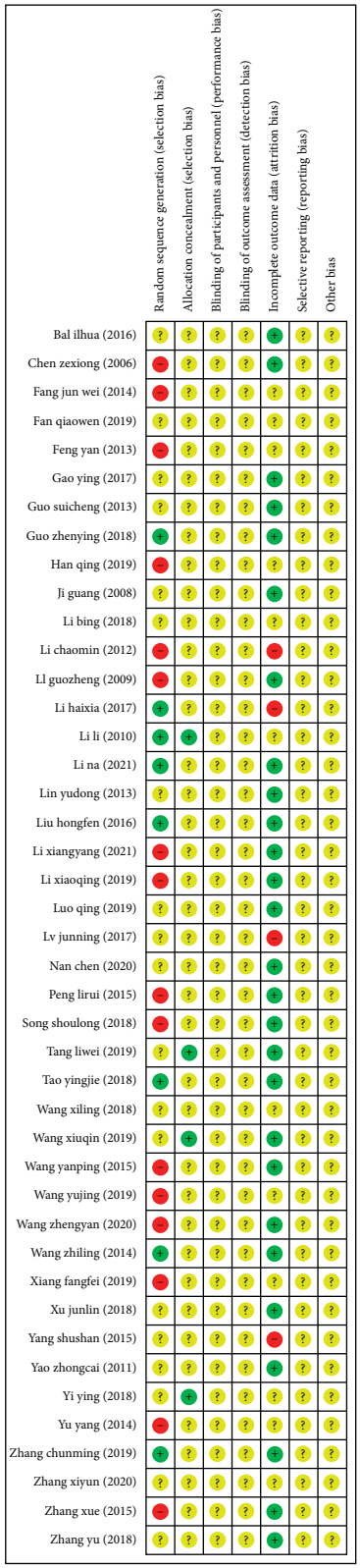

Figure 3: Risk-of-bias graph.

fatty acids. There are still many controversies about the "second hit." Jung et al. [61] believed that liver cell damage caused by oxidative stress and inflammation is a key factor in the pathological process from simple fat accumulation to severe liver disease. Another mechanism that leads to the pathogenesis of NAFLD emerging factor is the gut microbiota imbalance. Le et al. [62], with the same germ-free mice fed a high-fat diet, by inoculating fecal bacteria to isolate pathological and normal mice, found that in mice vaccinated with pathological bacterial isolates in adipose sex hepatitis, the normal mice fat only showed the low degree of degeneration. The reason for this phenomenon may be that the gut microbiota increased circulating bacterial endotoxins and triggers a cascade of proinflammatory cytokines in the liver. It is also possible that the gut microbiota leads to abnormal metabolism of endogenous metabolites, which increases fat production in the liver and leads to NAFLD. As clinical and basic research continues to deepen, the mechanisms of NAFLD are still being defined. NAFLD is an extremely complex and subtle disease, representing the convergence of various pathways, risk factors, and external influences, which are not uniform in all patients [63]. The only two treatment options currently available for the treatment of NAFLD are control of risk factors (diabetes, hypertension, and dyslipidemia) and weight loss [64]. Control energy intake of the surplus is a more effective way to lose weight. Excessive fat accumulation has resulted in a net in the form of triglycerides in the liver, too much energy over white fat storage limit at the same time, the excess energy accumulated in the liver and eventually promotes the emergence and development of NAFLD. Although excessive use of any food can lead to the occurrence of NAFLD, excessive intake of monosaccharides and disaccharides can activate the heparin regeneration process and further aggravate NAFLD metabolized as triglyceride [6].

Because there is no authorized medication specifically for NAFLD, the primary treatment for the disease is now lifestyle modification [65]. However, most individuals find it difficult to maintain a healthy lifestyle, whether it be via physical exercise or food limitations. As a result, researchers are working to develop novel treatments for NAFLD. So far, a variety of medications have been explored for the treatment of NAFLD. Although the following therapeutic classes may have demonstrated advantages in treating NAFLD, we are aware that finding a pharmacological treatment that targets a wide range of the previously reported complicated physiopathology of NAFLD is challenging. As a result of the multicomponent, multitarget, and multipathway nature of TCM, it has a lot of promise in treating NAFLD and avoiding disease development. Damp-heat accumulation syndrome is one of the main types of NAFLD. Because the etiology of NAFLD is not controlled by diet or exogenous damp-heat epidemic toxin, which leads to endogenous damp evil and phlegm turbidity, it is often used to treat NAFLD by clearing heat and dampness.

There is now a large body of data that CPMs can effectively improve NAFLD. Four weeks of QG therapy in rats with NAFLD caused by a high-fat diet reversed leptin resistance and reduced lipid accumulation and inflammation in the liver [66]. There was also evidence that CPMs were helpful in avoiding NASH, with the underlying probable

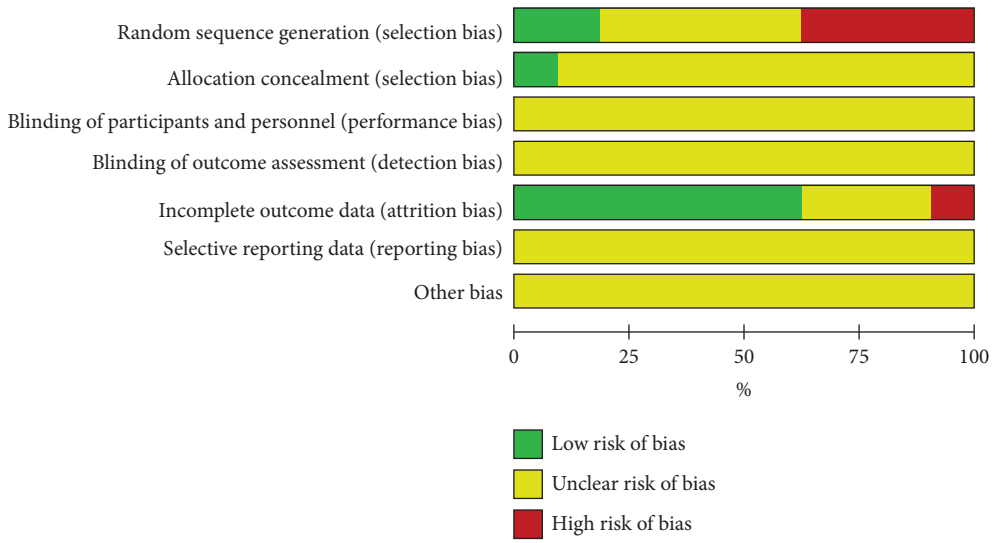

Figure 4: Risk-of-bias summary.

Table 2: Results of the network meta-analysis of the effective rate.

CDs					
0.26 (0.10, 0.67)	DHLD + CDs				
0.19 (0.12, 0.31)	0.76 (0.26, 2.21)	DN + CDs			
0.21 (0.09, 0.46)	0.81 (0.23, 2.83)	1.07 (0.42, 2.71)	DFLGN + CDs		
0.44 (0.27, 0.74)	1.74 (0.58, 5.17)	**2.30 (1.15, 4.59)**	2.15 (0.84, 5.51)	QG + CDs	
0.27 (0.17, 0.43)	1.06 (0.36, 3.09)	1.40 (0.73, 2.71)	1.31 (0.52, 3.29)	0.61 (0.31,1.21)	HZRG + CDs

Note. Significant effects are printed in bold.

Table 3: SUCRA for outcomes.

	Clinical effective rate (%)	ALT (%)	AST (%)	TC (%)	TG (%)
DHLD + CDs	61.1	55.4	77.5	55.8	49.9
DN + CDs	81.8	85.5	47.1	42.6	60.6
DFLGN + CDs	74.9	38.8	83.6	76.3	40.6
QG + CDs	25.9	62.3	10.0	37.4	68.4
HZRG + CDs	56.2	55.9	70.4	87.1	79.9
CDs	0.1	2.0	11.4	1.0	0.6

processes being linked to the interplay of gut microbiota and BA metabolism, as well as TGR5-mediated NF-κB suppression [67].

DN as a TCM formula has been broadly applied in treating hepatobiliary diseases, especially gallbladder stones, cholecystitis, and fatty liver syndromes in clinical trials [68, 69]. DN including Dahuang (*Rhei radix* et Rhizoma), *Hu zhang* (*Polygoni cuspidati* Rhizoma et Radix), Chenpi (Citri Reticulatae Pericarpium), Qingpi (Vatica mangachapoi Blauco), Baimaogen (*Rhizoma imperatae*), Yujin (Radix *Curcumae aromaticae*), Jianghuang (*Curcumae radix*), and Shanzha (*Crataegi fructus*). It has the function of clearing heat and soothing the liver and promoting gallbladder. Dahuang is the monarch medicine of DN, which has the effect of purging heat and clearing intestines, cooling blood, detoxification, and removing blood stasis; Huzhang clears away heat and toxic materials, Baimaogen clears heat and cools blood, both of which are ministerial medicines; Chenpi and Qingpi are the assistant medicines to reconcile the spleen and stomach; Yujin soothes the liver and promotes gallbladder; Shanzha can eliminate stagnation and blood stasis. One study showed that DN could attenuate the development of NAFLD and associated metabolic diseases in HFD-induced NAFLD mice. DN can inhibit the expression of SREBP-1 and SREBP-2 and their downstream genes might be the possible mechanisms of inhibiting liver fat production and cholesterol synthesis [70].

In this article, NMA is strictly complied with PRISMA guideline. Traditional clinical research, represented by RCT, investigates the therapeutic efficacy of intervention measures in an ideal environment of strict control and has high internal authenticity. However, because the subjects of RCT are highly homogeneous and the intervention measures are excessively uniform and standardized, the result is that RCT is divorced from the real clinical practice environment, and the extrapolation of research conclusions to clinical practice may face challenges. However, the medical practice of TCM treats patients as a whole, which is the earliest system of

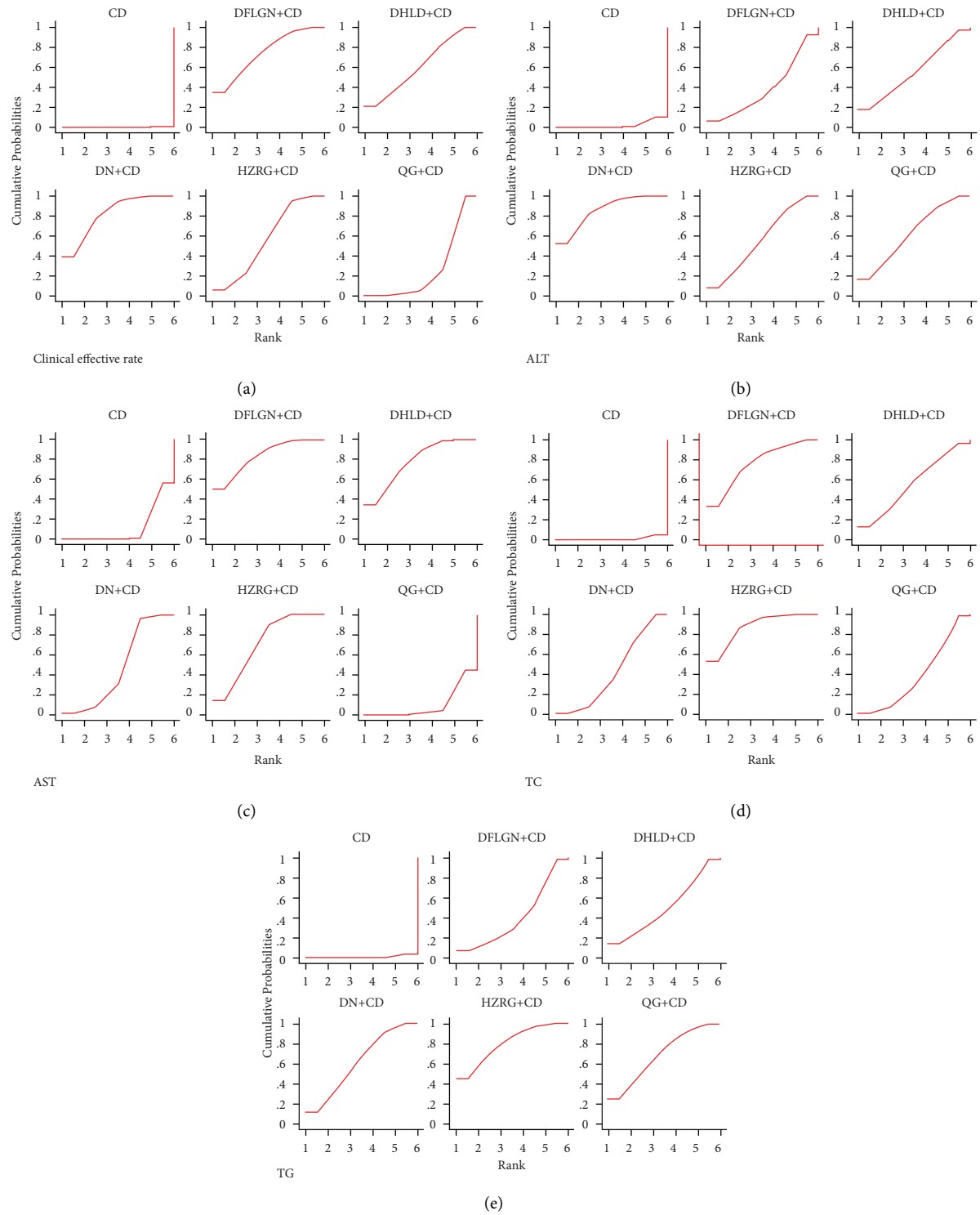

Figure 5: SUCRA plot for all different outcomes. (a) Clinical effective rate, (b) Alanine aminotransferase (ALT), (c) Aspartate aminotransferase (AST), (d) Serum total cholesterol (TC), (e) Triglyceride (TG).

Table 4: Results of the network meta-analysis of the ALT.

CDs					
11.05 (−0.37, 22.48)	DHLD + CDs				
15.81 (10.05, 21.57)	4.76 (−7.97, 17.48)	DN + CDs			
8.00 (−2.68, 18.67)	−3.06 (−18.64, 12.53)	−7.81 (−19.94, 4.32)	DFLGN + CDs		
12.20 (4.42, 19.99)	1.15 (−12.61, 14.90)	−3.61 (−13.29, 6.07)	4.21 (−9.01, 17.42)	QG + CDs	
11.23 (4.85, 17.62)	0.18 (−12.85, 13.20)	−4.58 (−13.18, 4.02)	3.23 (−9.20, 15.67)	−0.97 (−11.04, 9.10)	HZRG + CDs

Note. Significant effects are printed in bold.

Table 5: Results of the network meta-analysis of the AST.

CDs					
13.45 (3.61,23.28)	DHLD + CDs				
7.43 (1.95, 12.91)	−6.02 (−17.24, 5.21)	**DN + CDs**			
14.94 (4.77, 25.11)	1.50 (−12.62, 15.62)	7.51 (−4.04, 19.07)	**DFLGN + CDs**		
−0.62 (−7.48,6.25)	**−14.06 (−26.02, −2.10)**	−8.05 (−16.83, 0.74)	−15.56 (−27.83, −3.29)	**QG + CDs**	
11.63 (6.25, 17.02)	−1.81 (−12.99, 9.36)	4.20 (−3.48, 11.89)	−3.31 (−14.81, 8.20)	**12.25 (3.53, 20.98)**	**HZRG + CDs**

Note. Significant effects are printed in bold.

Table 6: Results of the network meta-analysis of the TC.

CDs					
0.63 (−0.03, 1.29)	**DHLD + CDs**				
0.50 (0.18, 0.82)	−0.13 (−0.86, 0.60)	**DN + CDs**			
0.87 (0.28, 1.45)	0.24 (−0.65, 1.12)	0.36 (−0.31, 1.03)	**DFLGN + CDs**		
0.45 (0.04, 0.87)	−0.18 (−0.96, 0.60)	−0.05 (−0.58, 0.48)	−0.41 (−1.13, 0.31)	**QG + CDs**	
0.97 (0.56, 1.39)	0.34 (−0.44, 1.12)	0.47 (−0.05, 1.00)	0.11 (−0.61, 0.83)	0.52 (−0.07, 1.11)	**HZRG + CDs**

Note. Significant effects are printed in bold.

Table 7: Results of the network meta-analysis of the TG.

CDs					
0.42 (0.04, 0.80)	DHLD + CDs				
0.49 (0.30, 0.68)	0.07 (−0.36, 0.49)	DN + CDs			
0.36 (0.03, 0.70)	−0.06 (−0.56, 0.45)	−0.12 (−0.51, 0.26)	DFLGN + CDs		
0.53 (0.26, 0.79)	0.11 (−0.36, 0.57)	0.04 (−0.29, 0.37)	0.16 (−0.26, 0.59)	QG + CDs	
0.59 (0.35, 0.83)	0.17 (−0.28, 0.62)	0.10 (−0.21, 0.41)	0.22 (−0.19, 0.64)	0.06 (−0.30, 0.42)	**HZRG + CDs**

Note. Significant effects are printed in bold.

individualized medical treatment. It is difficult to analyze TCM's therapeutic effect using a single study design type due to its uniqueness and complexity, which necessitates the flexibility to reflect objective reality while maintaining scientific rigor when evaluating the curative effect of TCM. Real-world research may properly reflect these qualities and give a novel way and methods for evaluating the clinical effect of TCM and collecting evidence. Our findings may provide evidence for the efficacy of CMPs in the treatment of NAFLD and further, indicate the possibility of obtaining clinical significance from CMPs in NAFLD patients.

Three advantages might help to boost the study's credibility. First, as far as we know, this is the first NMA to compare and rate the effectiveness of several CPMs for the treatment of NAFLD. Second, these findings may help physicians in making better treatment decisions for NAFLD. More critically, the ALT, AST, TC, and TG markers were examined in addition to the clinical effectiveness. The most significant transaminases are ALT and AST. ALT and AST levels in the blood are elevated when the liver is injured. The liver primarily produces TG, TC, and phospholipids, which are secreted and delivered into the bloodstream as very low-density lipoprotein for utilization by other tissues and organs [71]. When the quantity of TG produced by the liver exceeds the liver's ability to produce and release extremely low-density lipoprotein, TG is accumulated in liver cells, resulting in NAFLD [72].

However, there are various limitations to consider when understanding our findings. To begin with, the quality of the PRCTs included in this research is low. All PRCTs were conducted in China, and data from clinical research conducted in other languages was insufficient. None of the 43 papers included use the blind approach, and the majority of publications do not offer enough information, such as the randomization procedure, resulting in selection and reporting bias. Second, TCM dialectical diagnosis is a subjective process that might result in misdiagnosis or other biases. Third, the study lacks a planned follow-up, resulting in an erroneous assessment of critical outcome markers such as long-term therapeutic effectiveness. Furthermore, a substantial sample directly comparing the two CPMs was lacking. The fact that various CPMs have varying sample sizes reduces the strength of the evidence supporting the outcomes. A subgroup study based on background disorders, distinct forms of NAFLD, treatment duration, and CDs treatment measures are required. In addition, no subgroup analysis is challenging since the already included studies could not be accurately classified.

Meta-analyses give evidence-based treatment recommendations for clinics. Therefore, well-designed studies are critical. To increase methodological quality, higher-quality and larger-sample PRCTs should be registered in advance. Furthermore, it is recommended that researchers supply as much information on the baseline features as feasible. In the future, more rigorous clinical trials will be necessary to demonstrate the positive effects of CPMs paired with CDs for NAFLD patients.

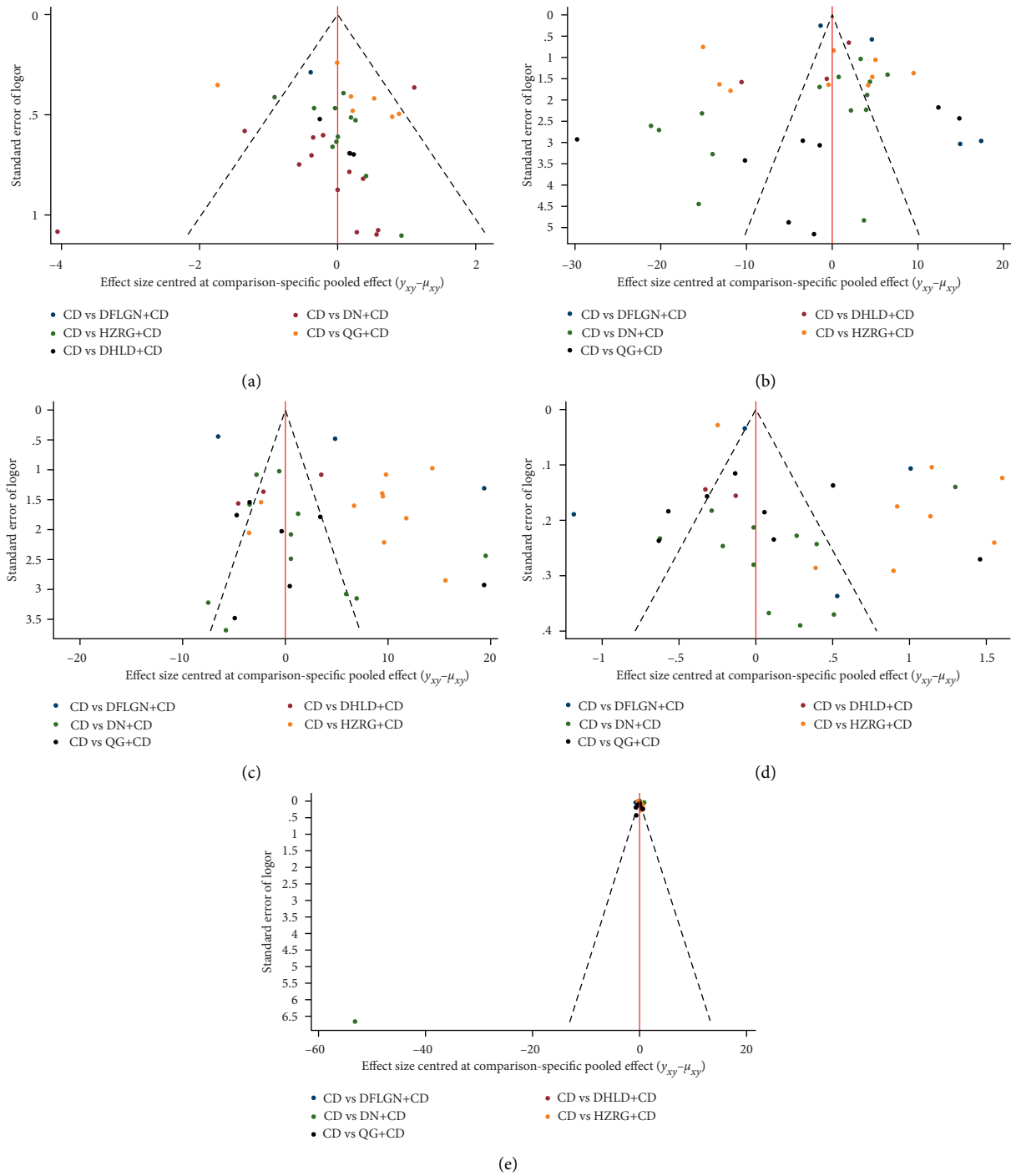

Figure 6: Funnel plot. (a) Clinical effective rate, (b) Alanine aminotransferase (ALT), (c) Aspartate aminotransferase (AST), (d) Serum total cholesterol (TC), (e) Triglyceride (TG).

5. Conclusion

In conclusion, the study discovered that CPMs might be effective as a coadjuvant treatment for patients with NAFLD of the dampness and heat accumulation type. In terms of enhancing the clinical effective rate of NAFLD, DN + CDs performed better. In terms of lowering TC and TG levels, HZRG + CDs proved to be more valid. In patients with NAFLD, DN + CDs demonstrated an outstanding improvement in terms of the clinical effective rate and other outcomes. However, owing to the study's limitations, the findings need to be confirmed by further high-quality, large-

sample multicenter PRCTs and stronger head-to-head comparative trials. Meanwhile, CPMs safety should be closely monitored and reported.

Abbreviations

CDs: Chemical drugs
NAFLD: Nonalcoholic fatty liver disease
CPMs: Chinese patent medicines
PRCTs: Pragmatic randomized controlled trials
DHLD: Da-huang-Li-dan capsule
DN: Dan-Ning tablet
DFLGN: Dang-fei-li-gan-ning capsule
QG: Qiang-gan capsule
HZRG: Hua-zhi-rou-gan granule
TCM: Traditional Chinese medicine.

Data Availability

The data used to support the findings of this study are available from the corresponding author upon request.

Conflicts of Interest

The authors declare that they have no conflicts of interest.

Authors' Contributions

YuanXu and Yan Wang participated in the study design. YuanXu analyzed the data. Man Wang and Xiao-jun Gou reviewed the manuscript. All authors read and approved the final manuscript. YuanXu and Yan Wang equally contributed to this work and should be considered co-first authors. Man Wang and Xiao-jun Gou contributed equally to this work and should be considered cocorresponding authors. Yuan Xu and Yan Wang contributed equally to this work and should be considered co-first authors.

Acknowledgments

This study was financially supported by the National Natural Science Foundation (no. 82074083), District level Medical and Health Key Project of Shanghai Baoshan District Science and Technology Commission Science and Technology Innovation Special Fund Project (21-E-63), and Shanghai Putuo District Clinical Specialties of Traditional Chinese Medicine (ptzyzk2109).

References

[1] J. H. Zhou, L. Bai, X. J. Zhang, H. L. Li, and J. J. Cai, "Nonalcoholic fatty liver disease and cardiac remodeling risk: pathophysiological mechanisms and clinical implications," *Hepatology*, vol. 74, no. 5, pp. 2839–2847, 2021.

[2] J. Cai, X. Zhang, Y. X. Ji, P. Zhang, Z. G. She, and H. Li, "Nonalcoholic fatty liver disease pandemic fuels the upsurge in cardiovascular diseases," *Circulation Research*, vol. 126, no. 5, pp. 679–704, 2020.

[3] J. Cai, X. Zhang, and H. Li, "Progress and challenges in the prevention and control of nonalcoholic fatty liver disease," *Medicinal Research Reviews*, vol. 39, no. 1, pp. 328–348, 2019.

[4] X. Zhang, Z. G. She, G. Li, and H. L. Li, "Time to step-up the fight against NAFLD," *Hepatology*, vol. 67, no. 6, pp. 2068–2071, 2018.

[5] Z. Chen, J. Y. Liu, F. Li et al., "Nonalcoholic fatty liver disease: an emerging driver of cardiac arrhythmia," *Circulation Research*, vol. 128, no. 11, pp. 1747–1765, 2021.

[6] R. Loomba, S. L. Friedman, and G. I. Shulman, "Mechanisms and disease consequences of nonalcoholic fatty liver disease," *Cell*, vol. 184, no. 10, pp. 2537–2564, 2021.

[7] Q. Feng, "Chinese patent medicine treatment of nonalcoholic fatty liver disease," *Gan*, vol. 4, pp. 20–24, 2017.

[8] W. X. Zhao and L. H. Zhang, "Rational application of Chinese patent medicine in the treatment of nonalcoholic fatty liver disease," *Journal of Practical Liver Diseases*, vol. 20, no. 2, pp. 132–134, 2017.

[9] L. Han and W. X. Zhao, "Clinical research progress of Chinese patent medicine on nonalcoholic fatty liver," *Electronic Journal of Clinical Medical Literature*, vol. 3, no. 16, pp. 3320–3322, 2016.

[10] L. Qin, "Clinical progress of traditional Chinese medicine in the treatment of nonalcoholic fatty liver," *China Urban and Rural Enterprise Health*, vol. 35, no. 07, pp. 90–92, 2020.

[11] C. X. Li, "Pathogenesis of nonalcoholic fatty liver and progress of traditional Chinese medicine treatment," *Guangming traditional Chinese medicine*, vol. 35, no. 12, pp. 1947–1950, 2020.

[12] J. P. T. Higgins and N. J. Welton, "Network meta-analysis: a norm for comparative effectiveness," *Lancet*, vol. 386, no. 9994, pp. 628–30, 2015.

[13] S. Shim, B. H. Yoon, I. S. Shin, and J. M. Bae, "Network meta-analysis: application and practice using stata," *Epidemiology and Health*, vol. 39, Article ID 2017047, 2017.

[14] M. J. Page, J. E. McKenzie, P. M. Bossuyt, I. Boutron, T. C. Hoffmann, and C. D. Mulrow, "The PRISMA 2022 statement: an updated guideline for reporting systematic reviews," *British Medical Journal*, vol. 372, 2021.

[15] J. P. Higgins and S. Green, *Cochrane Handbook for Systematic Reviews of Interventions*, John Wiley and Sons, Hoboken, NJ, USA, 2011.

[16] "Guidelines for the prevention and treatment of nonalcoholic fatty liver disease (2018 Revision)," *Infectious disease information*, vol. 31, no. 05, pp. 393–402, 2018.

[17] H. Zheng, Q. Chen, M. Chen, X. Wu, T. W. She, and J. Li, "Nonpharmacological conservative treatments for chronic functional constipation: a systematic review and network meta-analysis," *Neuro-Gastroenterology and Motility*, vol. 31, no. 1, Article ID 13441, 2019.

[18] X. Y. Li, C. Gao, and Q. Wang, "Clinical study of da-huang-li-dan capsule combined with silybin meglumine in the treatment of nonalcoholic fatty liver disease," *Modern Medicine and Clinical*, vol. 36, no. 2, pp. 340–344, 2021.

[19] N. Li, J. D. Li, Y. Li, H. L. Hua, Y. Z. Ji, and H. M. Zhou, "Effect of da-huang-li-dan capsule combined with silybin on intestinal microflora of nonalcoholic fatty liver disease," *Hepatology Journal of Integrated Traditional Chinese and Western Medicine*, vol. 2013, no. 1, pp. 37–39, 2021.

[20] Z. Y. Wang and Z. J. Li, "Effects of da-huang-li-dan tablets on serum IL-1RA, IL-1β, IL-18 and intestinal microflora in patients with damp-heat accumulation syndrome of non-alcoholic fatty liver disease," *Journal of Nanjing University of Chinese Medicine*, vol. 4, no. 5, pp. 762–766, 2020.

[21] Y. Zhang and X. X. Niu, "Effects of dan-ning tablets on liver function and blood lipid in patients with nonalcoholic fatty

liver disease and clinical efficacy analysis," *Chinese Community Physicians*, vol. 34, no. 34, pp. 124-125, 2018.

[22] Y. J. Tao, "Effect of dan-ning tablets on blood biochemical indexes and clinical efficacy in patients with nonalcoholic fatty liver disease," *Liver*, vol. 23, no. 1, pp. 65–68, 2018.

[23] J. N. Lu, "Clinical observation of dan-ning tablet combined with atorvastatin calcium tablet in treatment of nonalcoholic fatty liver disease," *Health Frontiers*, vol. 26, no. 2, pp. 165-166, 2017.

[24] Y. Yi, L. L. Wang, S. Y. Ren, and L. Wu, "Efficacy of dan-ning tablets combined with atorvastatin calcium tablets in treatment of nonalcoholic fatty liver disease," *Abstract the Latest Medical Information*, vol. 17, no. 25, pp. 135–145, 2018.

[25] F. F Xiang and B. B. Chen, "Effect of dan-ning tablets combined with polyene phosphatidylcholine on liver function in patients with nonalcoholic fatty liver disease," *Heilongjiang Medicine*, vol. 32, no. 3, pp. 598-599, 2019.

[26] Y. Gao and Y. Zhou, "Effect of dan-ning tablet combined with polyene phosphatidylcholine capsule in treatment of nonalcoholic fatty liver disease," *Modern Medicine and Clinical*, vol. 32, no. 3, pp. 464–467, 2017.

[27] Z. Y. Guo, "Effect of dan-ning tablet combined with polyene phosphatidylcholine in treatment of nonalcoholic fatty liver disease," *Practical Combine Traditional Chinese and Western Medicine Clinical*, vol. 17, no. 4, pp. 72–74, 2018.

[28] L. L. Peng and L. P. Ma, "Clinical observation of dan-ning tablet combined with rosuvastatin in the treatment of nonalcoholic fatty liver disease," *World Latest Medical Information Digest*, vol. 15, no. 16, p. 110, 2015.

[29] Y. J. Wang and H. Y. Qi, "Clinical study of dan-ning tablets combined with tononaphic acid in the treatment of nonalcoholic fatty liver disease," *Modern Drug and Clinical*, vol. 34, no. 1, pp. 88–92, 2019.

[30] X. Q. Li, X. R. Lan, and H. N. Lin, "Effect of dan-ning tablet combined with simvastatin on nonalcoholic fatty liver disease," *Taiwan Pharmacy*, vol. 31, no. 7, pp. 223–225, 2019.

[31] Y. Feng, "Clinical observation of dan-ning tablet combined with simvastatin in the treatment of nonalcoholic fatty liver disease," *Chinese Medicine Guidelines*, vol. 11, no. 9, pp. 640-641, 2013.

[32] X. Y. Zhang and Y. F. Song, "Clinical effect of dan-ning tablet combined with simvastatin in the treatment of nonalcoholic fatty liver disease," *Henan Medical Research*, vol. 29, no. 06, pp. 1092-1093, 2020.

[33] L. W. Zhi, "Bile better curative effect observation of treatment of nonalcoholic fatty liver disease," *China Medical Guide*, vol. 12, no. 23, pp. 158-159, 2014.

[34] B. Li, J. Y. Zhang, F. Y. Wang et al., "Clinical effect of dan-ning tablets on serum lipid, liver function and liver fibrosis in patients with nonalcoholic fatty liver disease," *Medical Journal of PLA*, vol. 30, no. 10, pp. 93–96, 2018.

[35] Q. W. Fan, "Clinical effect of dan-ning tablet in the treatment of nonalcoholic fatty liver and its effect on blood lipid, liver function and liver fibrosis," *Clinical Medicine Literature Electronic Journal*, vol. 6, no. 62, pp. 68-69, 2019.

[36] G. Ji, J. G. Fan, J. J. Chen et al., "Effectiveness of Danning Tablet in patients with non-alcoholic fatty liver of damp-heat syndrome type: a multicenter randomized controlled trial," *Journal of Chinese Integrative Medicine*, vol. 6, no. 2, pp. 128–133, 2008.

[37] S. L. Song, X. J. Xu, J. S. Zhang, and W. H. Liu, "Clinical observation on treatment of nonalcoholic fatty liver disease with Feiliganning capsule combined with atorvastatin calcium tablet," *Hebei traditional Chinese medicine*, vol. 40, no. 7, pp. 1051–1054, 2018.

[38] C. M. Li, M. Gong Mei, M. Q. Li, and Q. Xia, "Clinical study of dang-fei-li-gan-ning capsule in treatment of 113 patients with nonalcoholic simple fatty liver disease," *Chinese Journal of Traditional Chinese Medicine*, vol. 53, no. 1, pp. 38–41, 2012.

[39] G. Z. Li, *Clinical Study of Dang-Fei-Li-Gan-Ning Capsule in the Treatment of Non-alcoholic Simple Fatty Liver (Damp-heat Intrinsic Type)*, Guangxi University of Chinese Medicine, Guangxi, China, 2009.

[40] X. Zhang and G. J. Ma, "Clinical observation of Dang-Fei-Li-Gan-Ning capsule in the treatment of chronic hepatitis B complicated with nonalcoholic fatty liver disease," *New Traditional Chinese Medicine*, vol. 47, no. 9, pp. 91-92, 2015.

[41] L. Li, Y. Lan, L. Xu, X.-Z. Zhang, and H.-H. Wang, "Treatment of non-alcoholic fatty liver disease by Qianggan Capsule (强肝胶囊)," *Chinese Journal of Integrative Medicine*, vol. 16, no. 1, pp. 23–27, 2010.

[42] L. W. Tang, D. X. Tang, Z. M. Huang, and J. Q. Wu, "Clinical observation of entecavir combined with Qiang-Gan capsule in treatment of chronic hepatitis B complicated with nonalcoholic fatty liver disease," *Journal of Modern Integrated Chinese and Western Medicine*, vol. 28, no. 24, pp. 2648–2651, 2019.

[43] Z. C. Yao and H. S. Li, "Therapeutic effect and mechanism of Qiang-Gan capsule combined with polyene phosphatidylcholine capsule in treatment of NAFLD," *Chinese modern doctor*, vol. 49, no. 18, pp. 5–7, 2011.

[44] L. H. Bai, "Efficacy of qiang-gan capsule combined with metformin in the treatment of nonalcoholic fatty liver disease," *Journal of Modern Integrated Chinese and Western Medicine*, vol. 25, no. 15, pp. 1667-1668+1674, 2016.

[45] X. Q. Wang, "Effect of qiang-gan capsule combined with diammonium glycyrrhizinate enteric-soluble capsule in treatment of nonalcoholic fatty liver disease," *Journal of Hunan Medical Research*, vol. 28, no. 06, pp. 1089–1091, 2019.

[46] H. F. Liu, Y. K. Fan, S. M. Zhang, and L. L. Chang, "Clinical effect of qiang-gan capsule on leptin in patients with simple obesity and fatty liver," *Journal of Hebei Medical University*, vol. 37, no. 11, pp. 1257–1259, 2016.

[47] Z. X. Chen, S. J. Zhang, and L. R. Yin, "Clinical observation of Qiang-Gan capsule in the treatment of nonalcoholic fatty liver," *China Journal of traditional Chinese medicine*, vol. 31, no. 20, pp. 1739–1741, 2006.

[48] Y. P. Wang, T. L. Yao, Y. Zhang, and B. Bing, "Strong liver capsule in the treatment of nonalcoholic fatty liver disease combined hyperlipidemia study," *Journal of mudanjiang medical college*, vol. 4, no. 6, pp. 38–40, 2015, + 10.

[49] Q. Han, "Comparison of the clinical effect of Silibin capsule and Huazurogan granule in the treatment of non-alcoholic fatty liver disease," *The latest Medical Information Abstract*, vol. 12, no. 87, pp. 155-156, 2019.

[50] H. X. Li, Q. Zhou, L. Wang, and R. B. Liu, "Effect of Huazurogan granule on insulin resistance in patients with nonalcoholic steatohepatitis," *Proprietary Chinese Medicine*, vol. 33, no. 8, pp. 1586–1590, 2017.

[51] C. M. Zhang, "Huazuroogan granule in the treatment of damp-heat accumulation of nonalcoholic fatty liver disease and its effect on clinical symptoms," *Clinical Medicine Literature Electronic Journal*, vol. 6, no. 89, pp. 20-21, 2019.

[52] X. L. Wang, L. S. Zhao, and X. Y. Wang, "Effect of huazurogan granule on damp-heat accumulation of nonalcoholic fatty liver disease," *World Traditional Chinese medicine*, vol. 13, no. 07, pp. 1669–1672, 2018.

[53] S. C. Guo and J. Sun, "Effect of Huazuroogan granule combined with Duoxikang capsule and elastase enteric-coated tablet in treatment of nonalcoholic fatty liver disease," *Journal of Modern Integrated Chinese and Western Medicine*, vol. 22, no. 31, pp. 3472-3473, 2013.

[54] Q. Luo and R. D. Wei, "Clinical study of Huazhuroogan granule combined with tiopronin in the treatment of non-alcoholic fatty liver disease," *Modern Medicine and Clinical*, vol. 34, no. 05, pp. 1394–1397, 2019.

[55] J. W. Fang, X. M. Teng, J. H. Pan, and Z. Q. Zhang, "Comparison of huazurogan granule and silibin capsule in the treatment of nonalcoholic fatty liver disease," *The Chinese General Medicine*, vol. 12, no. 4, pp. 655-656, 2014.

[56] Y. D. Lin, F. G. Xu, D. Z. Wu, and B. B. Zhi, "Clinical study of huazurogan granule in treatment of nonalcoholic fatty liver disease," *Practical Clinical Medicine*, vol. 17, no. 03, pp. 75–77, 2013.

[57] Y. Yu, L. Q. Qian, P. Hou, and B. Wu, "Effect of huazurogan granule on treatment of nonalcoholic fatty liver disease," *Chinese Journal of Modern Integrated Traditional and Western Medicine*, vol. 23, no. 21, pp. 2302–2304, 2014.

[58] S. S. Yang, Y. Guo, T. Li, and Z. W. Su, "Turn stagnant liver granule in the treatment of damp and hot accumulate knot type nonalcoholic fatty liver disease," *Chinese Journal of Experimental Formulas of Chinese Medicine*, vol. 21, no. 24, pp. 157–160, 2015.

[59] J. L. Xu and Y. Tao, "Effect of Huazu Rogan granule on damp-heat accumulation of nonalcoholic fatty liver disease," *Clinical Medicine Literature Electronic Magazine*, vol. 5, no. 26, pp. 79–81, 2018.

[60] C. Nan, "Clinical observation of Huazhirougan granule in the treatment of damp-heat accumulation of nonalcoholic fatty liver disease," *Guangming Traditional Chinese Medicine*, vol. 35, no. 13, pp. 1998–2000, 2020.

[61] J. Jung, Y. H. Lee, S. Kim et al., "Hepatoprotective effect of licorice, the root of Glycyrrhiza uralensis Fischer, in alcohol-induced fatty liver disease," *BMC Complementary and Alternative Medicine*, vol. 16, no. 19, p. 19, 2016.

[62] R. T. Le, M. Llopis, P. Lepage et al., "Intestinal microbiota determines development of non-alcoholic fatty liver disease in mice," *Gut*, vol. 62, pp. 1787–1794, 2013.

[63] E. M. Brunt, V. W.-S. Wong, and V. Nobili, "Nonalcoholic fatty liver disease," *Nature Reviews Disease Primers*, vol. 48, Article ID 15080, 2015.

[64] L. Parlati, M. Régnier, and H. GuillouHervé, *New Targets for NAFLD*, Amsterdam, Netherlands, Article ID 100346, 2021.

[65] S. Marchisello, A. Di Pino, R. Urbano, S. Piro, F. Purrello, and A. M. Rabuazzo, "Pathophysiological, molecular and therapeutic issues of nonalcoholic fatty liver disease: an overview," *International Journal of Molecular Sciences*, vol. 20, no. 8, 2019.

[66] P. Zheng, L. Wang, L. Zhang, T. Liu, and L. Xing, "Therapeutic effect of Qiangganjiaonang on nonalcoholic rat fatty liver by increasing the expression of liver leptin receptor and P-JAK2/P-STAT3," *Chinese Journal of Integrated Traditional and Western Medicine on Digestion*, vol. 17, no. 3, pp. 141–145, 2009.

[67] Q. Li, M. Li, F. Li et al., "Qiang-Gan formula extract improves non-alcoholic steatohepatitis via regulating bile acid metabolism and gut microbiota in mice," *Journal of Ethnopharmacology*, vol. 258, Article ID 112896, 2020.

[68] J. G. Fan, "Evaluating the efficacy and safety of danning pian in the short-term treatment of patients with non-alcoholic fatty liver disease: a multicenter clinical trial," *Hepatobiliary and Pancreatic Diseases International: HBPD INT*vol. 3, pp. 375–380, 2004.

[69] K. W. Li, F. Ji, R. R. Wang, H. Jiang, and J. W. Shi, "Preventive effect and mechanism of dan-ning Tablet on the cholesterol gallstone," *J. Hepatopanereatobiliay*, vol. 16, pp. 44–46, 2004.

[70] Y. Ma, J. Li, Z. Ju et al., "Danning tablets alleviate high fat diet-induced obesity and fatty liver in mice via modulating SREBP pathway," *Journal of Ethnopharmacology*, vol. 279, Article ID 34116189, 2021.

[71] S. R. Kashyap, D. L. Diab, A. R. Baker et al., "Triglyceride levels and not adipokine concentrations are closely related to severity of nonalcoholic fatty liver disease in an obesity surgery cohort," *Obesity*, vol. 17, no. 9, pp. 1696–1701, 2009.

[72] M. Nakamuta, T. Fujino, R. Yada et al., "Impact of cholesterol metabolism and the LXRalpha-SREBP-1c pathway on non-alcoholic fatty liver disease," *International Journal of Molecular Medicine*, vol. 23, no. 5, pp. 603–8, 2009.

Hindawi
Evidence-Based Complementary and Alternative Medicine
Volume 2022, Article ID 4790910, 10 pages
https://doi.org/10.1155/2022/4790910

Research Article

A Real-World Study on Ge Gen Tang in Combination with Herbal Medicines for Relieving Common Cold-Associated Symptoms

Pei-Ying Chou,[1,2] Chen-Jei Tai,[1,3,4] You-Jen Tang,[5] Yu-Chuan Chen,[6] Kung-Yi Lin,[6] and Ching-Chiung Wang[1,4,7,8]

[1]*Ph.D. Program in Clinical Drug Development of Herbal Medicine, Taipei Medical University, Taipei, Taiwan*
[2]*Department of Pharmacy, Taipei Medical University Hospital, Taipei, Taiwan*
[3]*Department of Obstetrics and Gynecology, School of Medicine, College of Medicine, Taipei Medical University, Taipei, Taiwan*
[4]*Graduate Institute of Pharmacognosy, College of Pharmacy, Taipei Medical University, Taipei, Taiwan*
[5]*Department of Traditional Chinese Medicine, Chiayi Branch, Taichung Veterans General Hospital, Chiayi, Taiwan*
[6]*Consultant, Taipei, Taiwan*
[7]*School of Pharmacy, College of Pharmacy, Taipei Medical University, Taipei, Taiwan*
[8]*Traditional Herbal Medicine Research Center, Taipei Medical University Hospital, Taipei, Taiwan*

Correspondence should be addressed to Ching-Chiung Wang; crystal@tmu.edu.tw

Received 29 October 2021; Accepted 23 June 2022; Published 22 July 2022

Academic Editor: Talha Bin Emran

Purpose. Real-world evidence refers to patient data derived from the healthcare process. In this study, we used National Health Insurance Research Database (NHIRD) assessments and clinical studies of Ge Gen Tang (GGT, 葛根湯) in patients with common cold to establish a real-world study model of Traditional Chinese Medicine formulae. GGT is widely prescribed for the treatment of common cold in Taiwan, generally in combination with other medicines. The aim of this study was to determine whether a correlation exists between GGT combined with other medicines and an improvement in cold symptoms. We also established a GGT prescription compatibility system by analyzing Taiwan's NHIRD records for GGT prescription patterns in patients with different types of common cold. *Materials and Methods*. We extracted and analyzed records from the NHIRD for the period 2000–2015 to determine the most common clinical applications of GGT. GGT and GGT with Chuan Xiung Cha Tiao San were most commonly prescribed for common cold, as per NHIRD recommendations. Records for adults aged 20–65 years who were prescribed GGT for the treatment of common cold (Diagnosis Code ICD-9-460) were included in this study. We assessed the following indicators of the common cold, before and after treatment with GGT: nasal congestion, cough, runny nose, sneezing, sore throat, hoarseness, stiff shoulder, headache, and general physical condition. *Results*. The cold symptom scores before and after taking the GGT prescriptions significantly differed in the 29 volunteers. The 29 volunteers reported a significantly lower headache severity score after medication than before medication ($p < 0.004$). Furthermore, patient scores for general physical condition decreased significantly ($p < 0.01$) after medication.

1. Introduction

Real-world data (RWD) is the basis of real-world evidence (RWE) and can be collected from electronic health records, claims and billing activities, and patient-generated data, including in home-use settings [1, 2]. RWE is the conclusion of the proper statistical analysis of RWD that includes drafting an appropriate research design and statistical analysis methods, collecting appropriate RWD according to the research design, and performing data analysis so that analysis results that meet the research objectives can be generated. RWE can provide information about clinical settings and the health-system characteristics that influence treatment effects and outcomes [3]. This real-

world study design included an analysis of National Health Insurance Research Database (NHIRD) records and clinical studies of Ge Gen Tang (GGT) in the common cold.

GGT was recorded as an herbal formulation in the ancient text of Chinese medicine, Shang Han Lun (傷寒論). GGT formulations typically contain Puerariae radix, Cinnamomi Ramulus, Paeoniae Radix, Ephedrae Herba, Glycyrrhizae Radix, Zingiberis Rhizoma, and Jujubae Fructus. In traditional Chinese medicine (TCM) theory, wind (風邪), which is one of the six excesses (六邪), is the main cause of various types of common cold. Wind-cold (風寒) syndrome usually occurs in late autumn and winter, whereas wind-heat (風熱) syndrome usually occurs in summer. The incidence of the common cold is greater during spring and winter, with wind-cold and wind-heat syndromes being the most common. Wind-cold syndrome is characterized by an aversion to cold along with a fever without any sweating, a runny nose, scratchy throat, and cough. Wind-heat syndrome is characterized by fever, thick nasal discharge, cough, and yellowish purulent sputum [4]. According to TCM theory, indications for prescribing GGT include symptoms of wind-cold syndrome (i.e., headache, fever, aversion to cold and no sweating, and contracture of the nape and neck). A traditional Chinese medical physician follows eight principles (ba gang, 八綱) as a guideline for the diagnosis of these syndromes. These eight principles are: Yin (陰), Yang (陽), Exterior (表), Interior (裏), Cold (寒), Heat (熱), Deficiency (虛), and Excess (實). According to Ba Gang, GGT contains seven ingredients with different properties for different treatments. These ingredients include Puerariae radix for exterior-heat-deficiency, Ephedrae Herba for exterior-cold-excess, Cinnamomi Ramulus for exterior-cold-deficiency, Glycyrrhizae Radix for exterior-deficiency, Paeoniae Radix Alba for heat-deficiency, and Zingiberis Rhizoma and Jujubae Fructus for cold-deficiency. Therefore, via GGT, the combination of the above seven ingredients, can be used to treat exterior cold (heat) deficiency (excess) symptoms. The exterior-cold-excess syndrome arises when wind-cold invades the exterior and is characterized by a pronounced aversion to cold and mild fever, headache, generalized pain, absence of sweating, thin white tongue coating, and tight floating pulse, showing that the external part of the body is being attacked by cold, although the patient's defense qi is not damaged. However, Gui Zhi Tang can be used for exterior cold-deficiency syndrome (the patient's defense qi is damaged, manifested by intolerance of wind, persistent sweating, fever, headache). GGT is Gui Zhi Tang plus Puerariae radix and Ephedrae Herba and is used for "tonic convulsion." (exterior syndrome due to wind-cold marked by rigidity of the neck without sweating). Therefore, GGT is used to treat exterior-cold-deficiency syndrome to a greater extent than Gui Zhi Tang. Its state belongs to the exterior-cold-excess syndrome but is lower than the state of Ma Huang Tang [5]. In clinical practice, TCM physicians may comprehensively consider whether to prescribe GGT according to the symptoms of the common cold using the Ba Gang syndrome differentiation, in addition to other methods. In this study, we used clinical observations of GGT prescription patterns in patients to assess the GGT guidelines for treating the common cold.

Previous research has demonstrated that GGT is effective against human respiratory syncytial virus-induced plaque formation and stimulates mucosal cells to secrete interferon beta to counteract viral infection [6]. One experimental dog model revealed that body temperature and macrophage phagocytic activity increased 30 min after administering GGT [7]. Furthermore, a clinical trial proved that the beneficial effect of GGT on shoulder stiffness was due to an improvement in blood circulation, resulting in higher body surface temperature [8]. A study of the data obtained from the NHIRD between 2005 and 2007 revealed that GGT was the most commonly used formula for acute nasopharyngitis, chronic nasopharyngitis, and allergic rhinitis [9].

This study analyzed NHIRD records to determine GGT prescription patterns for patients with different types of common cold, as defined by TCM, and with cold symptoms, as described by Western medicine. The correlation between treatments using GGT combined with various other medicines and improved cold symptoms was used to establish a GGT prescription compatibility system for the common cold. Clinically, GGT is widely prescribed in Taiwan for the common cold, generally in combination with other medicines. However, the prescription patterns for GGT combined with other medicines have not previously been explored. Therefore, we used a real-world study design to investigate the clinical efficacy of GGT in patients with common cold and compared our findings with NHIRD to establish the clinical use guidelines of GGT for treatment of the common cold.

2. Materials and Methods

2.1. Prescription Patterns of GGT in NHIRD. The current study analyzed the records of one million individuals from the total population that were available on NHIRD between 2000 and 2015. We documented instances when GGT was prescribed, and the prescription patterns of GGT alone or in combination with other medicines were collated with reference to the diagnosis codes. We screened for diseases with the most frequently occurring prescription patterns, including GGT. Then, the contents of the prescriptions for common cold were analyzed to determine the most common prescription contents.

2.2. A Clinical Observation Study. A study was conducted with enrolled patients who visited the Department of Traditional Chinese Medicine at Taipei Medical University Hospital. The protocol was registered with the Taipei Medical University-Joint Institutional Review Board (Approval No. N201509008). In this study, GGT was prescribed in the form of concentrated medicine granules. The ratio between each herb of GGT is per 10 g contains Puerariae radix 6.0 g, Cinnamomi Ramulus 3.0 g, Paeoniae Radix 3.0 g, Ephedrae Herba 4.5 g, Glycyrrhizae Radix 3.0 g, Zingiberis Rhizoma 4.5 g, and Jujubae Fructus 4.0 g.

Individuals aged 20 to 65 years who had been prescribed GGT for the treatment of the common cold (Diagnosis Code ICD-9-460) were enrolled in the study. Patients who were pregnant, consumed other Western medicines or herbal

products along with GGT for the common cold, or did not maintain a healthy diet during the observation period were excluded.

After seven days of taking their prescribed medication, the participants revisited their physicians. The participants were asked to complete a daily questionnaire that assessed the nature of their cold symptoms, including the location and severity of any headache, their body temperature, and their general physical condition. Their headache location was described as follows: 1. top of the head, 2. back of the head, 3. rear neck, 4. sides of the head, 5. near the temples, and 6. front of the head (Figure 1). The patients were asked to assess their symptoms based on those determined in a previous randomized controlled trial [10]. The items included 13 specific complaints: runny nose, nasal congestion, frequent need to blow their nose, thick mucus discharge, sneezing, sore throat, scratchy throat, cough, chills, hoarseness, stiff shoulder, joint pain, and general malaise. The patients were asked to score their symptoms daily, based on five grades, where grade 0 was defined as no symptoms of the common cold; grade 1 as a few instances of the symptoms on that day; grade 2 as frequent occurrences of symptoms that did not cause difficulties in daily life; grade 3 as frequent occurrences of symptoms that caused difficulties in daily life; and grade 4 as the occurrence of severe symptoms of the common cold on that day. General physical conditions were classified using scores of 0 to 10, where a score of 10 indicated that the patient's general physical condition was seriously impacted. Participants kept a record of their headache severity score four times every day and reported their daily value for this symptom as the mean of their four headache severity readings. Any improvement in the severity of the cold symptoms was correlated with the patients' GGT prescription pattern. We also reviewed the patients' medical records for the following information: prescriptions, main symptoms of the participants, and their tongue, pulse, and TCM syndrome types, as confirmed by the TCM physician.

3. Study Analysis

Statistical analyses were performed using SPSS 18 software. Patient scores for cold symptoms, general physical condition, and headache severity between "before medication." and "on the fifth day after medication." were compared using a paired samples t-test. Body temperature readings between before medication and on the fifth day after medication were compared using a one sample t-test. The results of the t-tests were presented as the mean ± standard deviation, and $p < 0.05$ was considered statistically significant.

4. Results

4.1. Prescription Patterns of GGT for the Common Cold in NHIRD. We found the most common disease for which GGT was prescribed was acute nasopharyngitis (common cold, diagnosis code ICD-9-460), and approximately 20.18% of a total of 1,856,166 GGT prescriptions were for acute nasopharyngitis (common cold, ICD-9 460). The second most frequent indication was symptoms involving the head and neck (ICD-9 784) (Table 1). An analysis of the herbal components most commonly used in combination with GGT was performed among the 374,499 prescriptions. The most frequent herbal combination components for the common cold could be divided into five patterns: GGT alone; GGT combined with Chuan Xiung Cha Tiao San (CXCTS); GGT combined with Yin Qiao San (YQS); GGT combined with Xin Yi San (XYS); and GGT combined with Chiu Wei Chiang Huo Tang (CWCHT) (Table 2). GGT alone and GGT combined with CXCTS were the most common prescriptions for the common cold in the data obtained from the NHIRD.

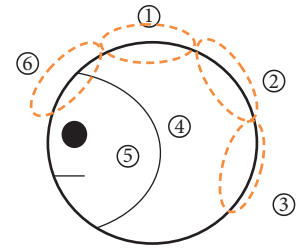

Figure 1: Headache locations.

4.2. A Retrospective Clinical Observation Study. Of the 30 patients enrolled in the study, 29 were included in the analysis, while one who consumed other medicine in this period was excluded. All body temperature readings in all participants during the study were below 37.5°C (Table 3). Most of the participants were women.

Table 4 presents data relating to the participants and their TCM-defined syndromes. Eight participants were diagnosed with wind-cold-exterior syndrome (excess-syndrome), and 14 were diagnosed with deficiency syndrome and reported muscle soreness, night cough, chills, runny nose, dizziness, white phlegm, and neck stiffness. Participants diagnosed with wind-cold-exterior dampness syndrome had symptoms of wind-cold-exterior syndrome, as well as an index finger with prurigo, heavy-headedness, headache, and painful stiff neck. Participants with wind-heat-exterior syndrome had throat suppuration.

The TCM common cold syndrome definitions as related to different symptoms are presented in Table 5. Differences in the patients' scores for their general physical condition before medication and on the fifth day after medication were significant (Table 6). This implies that the general physical condition of the patients improved after medication. A total of 16 participants reported headaches. Compared to their scores before medication, the headache frequencies reported for each location (refer to Figure 1) on the fifth day after medication were as follows: headache frequencies at locations 1, 3, 4, 5, and 6 decreased. The severity of headache at location 4 (sides of the head) decreased significantly, indicating quick recovery. At location 2 (back of the head), headache severity was higher on the fifth day after medication. However, a more detailed review of the headache

Table 1: Top 10 diseases for which treatment prescriptions contain GGT (according to the frequency distribution of ICD-9-CM code).

No.	Code	Disease	%
1	460	Acute nasopharyngitis (common cold)	20.18
2	784	Symptoms involving head and neck	11.95
3	477	Allergic rhinitis	8.3
4	729	Other disorders of soft tissues	4.91
5	472	Chronic pharyngitis and nasopharyngitis	4.55
6	786	Symptoms involving respiratory system and other chest symptoms	4.17
7	780	General symptoms	3.42
8	723	Other disorders of cervical region	3.26
9	724	Other and unspecified disorders of back	3.14
10	487	Influenza	2.11

Table 2: The frequency and indications for the application of GGT prescriptions[a] for the common cold.

Type	Formula	Frequency (%)	Applied syndrome	External pathogen	Indication
1	GGT	1.64	Exterior-cold-excess	Wind-cold	Headache, fever, aversion to cold, contracture of the nape and neck
2	GGT CXCTS	0.81	Exterior-cold-excess	Wind-cold	Headache, migraine, fever, aversion to cold, contracture of the nape and neck
3	GGT YQS	0.55	Exterior-cold-excess Exterior-heat-excess	Wind-cold	Headache, fever, thirst, sore throat
4	GGT XYS	0.55	Exterior-cold-excess	Wind-cold	Headache, fever, runny nose, nasal congestion
5	GGT CWCHT	0.51	Exterior-cold-excess	Wind-cold-dampness	Headache, fever, stiffness of the neck, postnasal drip

'a' represents total number of prescriptions, $n = 374{,}499$.

Table 3: Characteristics of the participants who received GGT prescriptions for common cold treatment (ICD-9-460).

Characteristic		No
Sex	Male	8
	Female	21
Age (years)	21–30	8
	31–40	6
	41–50	7
	51–65	8
Body temperature	<37.5°C	29
	>37.5°C	0
Taking other medication during the treatment period	Yes	1
	No	29

severity records revealed that the location of the headache before and after medication often differed. For example, the reporting of headaches at location 2 was less frequent before medication than on the fifth day after medication. By contrast, the frequency of reporting a headache at location 6 was higher before medication and lower on the fifth day after medication, indicating that the headache location changed during the course of the common cold (Table 7). A significant difference in headache severity was noted between before medication and on the fifth day after medication, according to the results of the paired t-test (Table 6).

Patient surveys for each cold symptom, including runny nose, nasal congestion, cough, sneezing, sore throat, hoarseness, stiff shoulder, chills, and general malaise, indicated significant differences between the scores given before medication and on the third day after medication (p value in column A of Table 8). Significant differences were also observed for scores before medication and those on the fifth day after medication (p value in column B of Table 8). However, no significant differences in nasal congestion and stiff shoulder conditions were observed between scores reported before medication and on the third day (p values in column A of Table 8). This indicates that except for nasal congestion and stiff shoulders, cold symptoms were alleviated on the third day after medication. This study included a review of chart reports for patients with common cold that documented patient age and prescriptions. We found that there were 20 different combinational prescriptions for GGT and 35 single-herb prescriptions. Based on their symptoms, patients were divided into wind-cold syndrome or wind-dampness syndrome groups, and GGT prescription patterns were compared. The GGT prescription that was used to treat the common cold comprised a single dose between 2.0 and 3.3 g, which was repeated three times a day, to total a daily GGT dose between 6.0 and 10.0 g.

Ma Huang Fu Zi Xi Xin Tang (MHFZXXT) was used to treat headaches in two patients. Qiang Huo Sheng Shi Tang (QHSST) was used to treat headaches in patients with wind-cold-dampness syndrome. Furthermore, MHFZXXT and QHSST synergized with GGT to treat headache and neck stiffness, respectively. Qing Bi Tang (QBT) alleviated the thick mucosal discharge symptoms for one patient, while Jin

Table 4: Objective and subjective symptoms of the common cold based on the classification of TCM syndrome.

TCM syndrome	Identified by TCM physician		No	Subjective symptom
	Numbers of excess syndrome	Numbers of deficiency syndrome		
Wind-cold-exterior	8	14	22	Muscle soreness, cough at night, chills, runny nose, dizzy, white phlegm, and neck stiffness
Wind-cold-dampness-exterior	2	4	6	Index finger with prurigo heavy-headedness and headache and painful stiff nape
Wind-heat-exterior	1	0	1	Throat suppuration

Table 5: TCM syndrome of the common cold based on different symptoms.

TCM syndrome	Symptom of common cold
Wind-cold syndrome	Scratchy throat Sore throat (no thirst) Cough (cold-phlegm)
Wind-heat syndrome	Sore throat (thirst)
Wind-heat syndrome Wind-dampness syndrome	Pussy discharge Cough and yellowish purulent sputum
Wind-cold syndrome Wind-heat syndrome Wind-dampness syndrome	Headache

Fey Tsao Saan (JFTS) alleviated the cough symptoms of two patients. Jie Geng (*Platycodon grandiflorum*), as a single herb prescription, improved sores and alleviated scratchy throat symptoms in four patients. Kan Chiang (*Zingiber officinale*) and Xin Gren (*Prunus armeniaca*) were used to treat coughs in five and two patients, respectively. Kan Chiang with Xin Gren ameliorated the cough symptoms of one patient. Table 9 displays the list of physician-prescribed single herbs and formulae that were reported to alleviate cold symptoms. The patients' scores for single herb and formulae prescriptions were compared before and after medication. Symptoms were deemed to have improved if the scores decreased by one or more points.

5. Discussion

The NHIRD contains RWD from physician clinical medication records. Table 2 shows that GGT alone and in combination with CXCTS were the most common prescriptions for the common cold. The effect of CXCTS is to dispel wind and relieve pain. In a study on TCM prescription patterns for patients with migraines in Taiwan, CXCTS was found to be the most frequently prescribed treatment [11]. GGT is mainly used for exterior cold-deficiency syndrome, which when combined with CXCTS, YQS, XYS, or CWCHT, is not limited to treating solely deficiency syndrome. Moreover, the compatibility of GGT and YQS will not be limited for only cold or heat syndromes of the common cold.

The research design of this study was based on a real-world study. The TCM physicians issued prescriptions based on the patient's cold symptoms, and we did not provide any limitations. When the patient took a prescription with GGT, we used a questionnaire to evaluate the improvement of his or her symptoms to analyze the prescription patterns for the common cold.

We discovered five types of GGT prescription patterns for the common cold that corresponded to TCM definitions of disease location (exterior-interior), strength (deficiency-excess), and symptoms (cold-heat). All the GGT prescription patterns that were documented in our dataset were for exterior-cold-excess, with the exception of YQS for exterior-heat-excess syndromes. According to TCM theories, we divided GGT prescriptions into five types for different common cold symptoms (Table 2).

We concluded that exterior (表) was the most common TCM diagnostic condition that led to GGT prescriptions for the common cold. Symptoms such as runny nose, nasal congestion, a need to frequently blow the nose, and thick mucosal discharge always occurred together in our dataset. A significant improvement was observed in patient scores for these nasal congestion symptoms by the fifth day after medication.

In Western medicine, antihistamine medication is often prescribed for a runny nose, and a bronchodilator, such as dextromethorphan, is used for a cough or asthma. We believe this is equivalent to TCM prescriptions for GGT combined with QBT for a thick mucosal discharge and GGT combined with Xin Gren for a cough. Notably, there was an advantage of no daytime sleepiness being reported when GGT was combined with herbal medicine for these symptoms.

During this study, the body temperature of all participants was consistently lower than 37.5°C. The most frequently reported symptoms were a cough, the need to frequently blow the nose, and a scratchy throat. The patients who received GGT alone experienced some relief from these reported cold symptoms, and those who received GGT combined with other formulae or herbs reported improvements in other symptoms. For example, GGT combined with MHFZXXT was reported to relieve headaches, and GGT combined with Jie Geng was reported to improve sore throats.

Overall, GGT was often used to treat common cold symptoms, both alone and in combination with other prescriptions, including MHFZXXT, QHSST, QBT, JFTS, Jie Geng, Kan Chiang, and Xin Gren. Based on TCM theory, the principle of medicine formulation follows a "sovereign, minister, assistant, and courier." theory. This clinical study

Table 6: Comparison of headache severity and general physical condition before and after medication.

Variable	No	Before medication	Fifth day after medication	p value
Headache severity	16	4.38 ± 3.519	1.63 ± 1.784	0.004^{**}
General physical condition	27	5.41 ± 2.308	3.19 ± 2.001	0.001^{***}

$^{*}p < 0.05, ^{**}p < 0.01, ^{***}p < 0.001$.

Table 7: Distribution of headache locations before and after medication.

Location	Before medication (%)	After medication				
		Day 1(%)	Day 2 (%)	Day 3 (%)	Day 4 (%)	Day 5 (%)
1	1.56	1.30	1.56	0.78	0.52	0.52
2	0.00	0.26	0.00	1.04	1.56	2.08
3	2.60	3.13	2.34	2.60	2.60	1.04
4	2.60	0.00	0.52	0.78	0.00	0.52
5	1.82	1.82	1.30	1.56	0.78	1.04
6	2.60	2.60	2.34	1.56	2.34	0.52

$N = 384$.

Table 8: Comparison of daily cold symptoms before and after medication.

Cold symptom	No	Before	Day 3	Day 5	p value 1	p value 2
Runny nose	14	2.07 (0.92)	0.85 (0.77)	0.64 (0.63)	0.001^{***}	0.001^{***}
Nasal congestion	15	1.60 (0.98)	1.13 (0.91)	0.67 (0.72)	0.131	0.002^{**}
Blow nose	17	1.65 (0.93)	0.88 (0.78)	0.70 (0.68)	0.005^{**}	0.0001^{***}
Pussy discharge	12	1.66 (0.98)	0.91 (0.67)	0.4 (0.51)	0.043^{*}	0.004^{**}
Sneezing	14	1.57 (0.94)	0.78 (0.57)	0.35 (0.49)	0.01^{**}	0.001^{***}
Sore throat	15	2.33 (1.17)	0.64 (0.84)	0.33 (0.61)	0.001^{***}	0.0001^{***}
Scratchy throat	16	2.31 (1.3)	1.12 (1.08)	0.56 (0.81)	0.005^{*}	0.0001^{***}
Cough	20	2.00 (1.07)	1.35 (1.08)	0.95 (0.94)	0.044^{*}	0.001^{***}
Chills	9	1.56 (0.72)	0.6 (0.69)	0.56 (0.72)	0.019^{*}	0.04^{*}
Hoarseness	14	2.00 (0.78)	1.00 (1.17)	0.50 (0.76)	0.020^{*}	0.0001^{***}
Stiff shoulder	13	1.92 (0.76)	1.54 (0.31)	1.38 (0.76)	0.096	0.003^{**}
Joint pain	5	1.8 (0.83)	0.6 (0.89)	0.6 (0.89)	0.033^{*}	0.033^{*}
General malaise	15	1.8 (1.10)	0.86 (1.18)	0.46 (0.63)	0.001^{***}	0.001^{***}

p value 1 is the value obtained using the paired t-test, comparing daily cold symptoms before and 3 days after medication. p value 2 is the value obtained using the paired t-test, comparing daily cold symptoms before and 5 days after medication.

Table 9: List of physician-prescribed reused single herbs and formula that improve cold symptoms.

Cold symptoms	Single herb			Formula			
	Xin Gren	Kan Chiang	Jie Geng	Qing Bi Tang	Ma Huang Fu Zi Xi Xin Tang	Qiang Huo Sheng Shi Tang	Jin Fey Tsao Saan
Dosage (TID)	0.3 g	0.3 g	0.3 g	1.0 g	0.9–1.0 g	1.2–2.0 g	1.0–2.0 g
Headache	●	●	●		●	●	
Stuffy nose	●	●	●	●	●		
Sore throat	●	●	●				
Scratchy throat	●	●	●			●	
Cough	●	●	●	●		●	●

revealed that prescription patterns for the common cold were based on "sovereign, minister, assistant, and courier." theory principles. GGT was mainly used under the sovereign theory with doses that ranged from 3.0 to 3.3 g (three times a day, TID).

In TCM theory, the head is the confluence of all yang meridians. The common cold attacks the greater yang meridian, causing a headache. Headache locations corresponded to yang meridians as follows: location 3, the greater yang meridian (太陽經); location 4, the gallbladder meridian (膽經); and location 6, the yang brightness meridian (陽明經). Patients commonly reported a headache in locations 3, 4, and 6 before medication. After medication, patient headache scores in these three locations decreased, whereas the headache score at location 2 was often higher after medication than before. This implies that GGT in

Table 10: List of reused single herbs and formula and their functions and pharmacological effects on cold symptoms in patients.

Main prescription	Combination prescription	Combination/origin	Function of combination prescription	Pharmacological effects of combination prescription
Ge Gen Tang	Ma Huang Fu Zi Xi Xin Tang	Ephedrae Herba, Aconiti Lateralis Radix Praeparata, and Asari Radix et Rhizoma	Exterior-effusing and dissipate cold or warm the meridian and dissipate cold	Antiallergy: Ma Huang Fu Zi Xi Xin Tang reduces blood histamine content and recovers the nasal mucosa [12]
	Qiang Huo sheng Shi Tang	Notopterygii Rhizoma et Radix, Angelicae Pubescentis Radix, Ligustici Rhizoma et Radix, Saposhnikoviae Radix, Glycyrrhizae Radix et Rhizoma Praeparata cum Melle, Viticis Fructus, and Chuanxiong Rhizoma	Promotes sweating, dispels wind, and dispels dampness	Gegen soup and Qianghuoshengshi soup combined with acupuncture treatment cured 44 patients, 8 patients, and 2 patients; the total efficiency was 96.30% [13]
	Qing Bi Tang	Puerariae Lobatae Radix, Ephedrae Herba, Platycodonis Radix, Magnoliae Flos, Chuanxiong Rhizoma, Scutellariae Radix, Cinnamomi Ramulus, Paeoniae Radix Alba, Glycyrrhizae Radix et Rhizoma, Zingiberis Rhizoma Recens, and Jujubae Fructus	Wind-cold-dispersing medicine; clears heat and relieves stuffy nose	After FESS surgery, Qingbi decoction (Qing Bi Tang) was used prescribed to patients with chronic sinusitis to ameliorate symptoms and signs, reduce agglutination time, and promote the regression of diseases [14]
	Jin Fey Tsao saan	Ephedrae Herba, Paeoniae Radix Rubra, Glycyrrhizae Radix et Rhizoma, Zingiberis Rhizoma Recens, Jujubae Fructus, Schizonepetae Herba, Peucedani Radix, Inulae Flos, and Pinelliae Rhizoma	Wind-cold-dispersing medicine; directs qi downward to resolve phlegm	The obvious effect of using Jinfeicao powder is cough alleviation after infection [21]Jinfeicao powder has significant effects on reliving cough and expelling phlegm [15]
	Jie Geng	The dried root of Platycodon grandiflorum (Jacq.) and A. DC. (Campanulaceae)	Diffuses in the lungs and resolves phlegm, soothes the throat, and expels pus	PLD effectively inhibits the expressions of nuclear factor-κB (NF-κB), caspase-3, and Bax in lung tissues, restores the expression of Bcl-2 in the lungs, and improves superoxide dismutase (SOD) activity in bronchoalveolar lavage fluid (BALF) [16]
	Kan Chiang	The dried rhizomes of Zingiber officinale (Wild.) Rosc. (Zingiberaceae)	Promotes sweating to release the exterior, warms the middle to check vomiting, and warms the lung to suppress cough	Ginger extract reduces the expression of IL-17 and IL-23 in experimental autoimmune encephalomyelitis (EAE) mice [17]
	Xin Gren	The dried mature seed of Prunus armeniaca L. var. ansu Masim., Prunus sibirica L., Prunus mandshurica (maxim.) koehne, or Prunus armeniaca L. (Rosaceae)	Downbear counterflow suppresses cough and calms panting, moistens the intestines to relax the bowels	Amygdalin is one of the active ingredients in Armeniacae Amarum semen with antirenal interstitial fibrosis as pharmacological effect [18]

combination with other formulae can alleviate headaches of the greater yang meridian, gallbladder meridian, and yang brightness meridian.

We found that headaches associated with the common cold were associated with external wind and cold. The 16 participants who reported a headache were prescribed a combination formula of MHFZXXT and QHSST based on the TCM diagnosis and treatment related to the wind-cold-dispersing medication. MHFZXXT has been documented in the Shang Han Lun as a substance that warms the meridian, dissipates cold, reduces blood histamine content, and promotes nasal mucosa recovery [12] (Table 10). In TCM, the common cold is described as having wind-cold and wind-heat syndromes, and TCM physicians prescribe medicines based on the differences between these syndromes. According to the questionnaires that the participants completed (Table 8), GGT combined with other formulae and herbs relieved common cold-associated symptoms (Table 9). A prior observational study that compared visual analog scales before and after the application of a GGT combined with MHFZXXT medication for 100 patients with migraines observed a significant improvement in symptoms [19]. Notably, MHFZXXT was used for exterior-effusing, warming the meridian, and dissipating cold (Table 10), whereas GGT was used to treat cold wind headache. According to Table 10, we speculate that MHFZXXT can

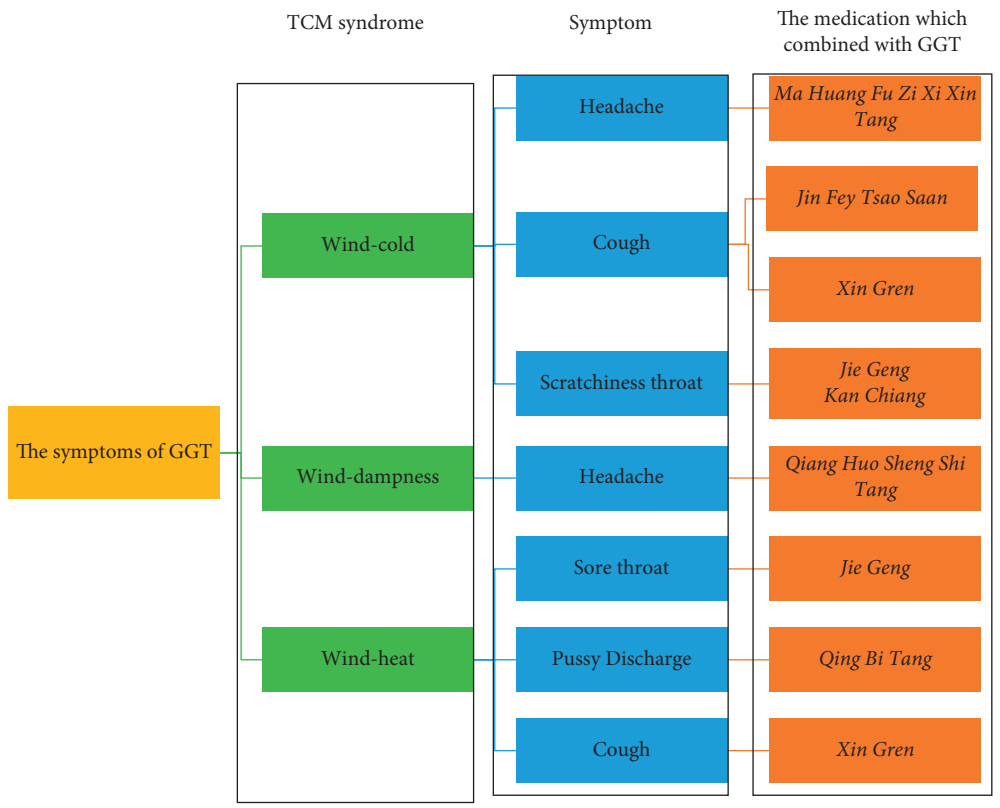

Figure 2: Applications of GGT and its prescription compatibility for the common cold. (a) TCM syndrome. (b) Symptom. (c) The medication which combined with GGT.

relieve a wind-cold headache. The combination dose of GGT with MHFZXXT ranged from 0.9 to 1.0 g (TID).

QHSST belongs to the TCM category of pungent and warm formulae and promotes sweating and dispelling of wind and dampness syndrome symptoms. In a randomized controlled study, the combination of GGT and QHSST was compared with acupuncture for the treatment of cervical spondylosis. The results revealed that 96.30% of 54 patients who received GGT combined with QHSST exhibited improvements [13]. In this study, QHSST was administered in combination with GGT for the wind-dampness headache, and the dose ranged from 1.2 to 2.0 g (TID).

QBT is a wind-cold-dispersing medicine that can clear heat and relieve a stuffy nose and chronic sinusitis [14]. In a clinical observation study, QBT treatment improved nasal congestion symptoms in 68 patients. The QBT ingredients include Platycodonis Radix, which promotes qi circulation and removes dampness, and Scutellariae Radix, which clears heat and expels pus [20]. The dosage of QBT that was administered was 1.0 g (TID). GGT was combined with QBT to relieve nasal congestion and stuffy noses.

JFTS also belongs to the TCM pungent and warm formulae category and can direct qi downward to resolve phlegm [15]. In an observational study, JFTS was compared with Western medicine for the treatment of cough symptoms in patients with wind-cold syndrome. After five days, cough symptoms improved in patients who received JFTS [21]. Additionally, Jie Geng contains Platycodonis Radix, which diffuses in the lungs and eliminates phlegm, promotes throat comfort, expels pus, and inhibits expression of nuclear factor-κB, caspase-3, and Bax [16]. Kan Chiang was found to warm the center, disperse cold, return yang, and reduce the expression of IL-17 and IL-23 in experimental mice with autoimmune encephalomyelitis [17]. To summarize, in prescriptions that improve symptoms of the common cold, GGT with QHSST was used for headaches; QHSST was used for wind-dampness headaches assailing the exterior; and MHFZXXT was used for headaches associated with cold wind syndrome with yang deficiency, exterior cold pattern, and long-term clinical effects for allergic rhinitis. QBT was used for treating nasal mucus in cold wind syndrome and interior heat patterns. JFTS was used for treating a cough and white sputum in cold wind syndrome. Xin Gren and Jie Geng were used for cough and throat pain, respectively, in cold wind and hot wind syndromes.

6. Conclusion

In NHIRD research, GGT alone and combined with CXCTS were the most common prescriptions for the common cold. We explored GGT and found the formula to be effective for treating runny nose, nasal congestion, sneezing, chills, stiff shoulder, joint pain, and general malaise of wind-cold syndrome. We also noted a statistically significant difference between cold symptoms before and after medication. Notably, the differences in patient headache and general physical condition scores before and after medication were statistically significant.

Figure 2 presents a summary of the TCM syndromes of wind, wind-cold, wind-heat, and wind dampness and the common prescriptions used to treat each condition. A combination of GGT and MHFZXXT was commonly used for headaches due to wind-cold syndrome with yang deficiency and exterior cold patterns. GGT with JFTS was often used for cough due to wind-cold syndrome with white sputum.

Abbreviations

GGT: Ge Gen Tang
CXCTS: Chuan Xiung Cha Tiao San
YQS: Yin Qiao San
XYS: Xin Yi San
CWCHT: Chiu Wei Chiang Huo Tang
XYQFT: Xin Yi Qing Fei Tang
MXGST: Ma Xsing Gan Shih Tang
JFBDS: Jing Fang Bai Du Sa
SJY: Sang Ju Yin
XSS: Xing Su San
JFTS: Jin Fey Tsao Saan
MHFZXXT: Ma Huang Fu Zi Xi Xin Tang
QBT: Qing Bi Tang
QHSST: Qiang Huo Sheng Shi Tang
TCM: Traditional Chinese Medicine
NHIRD: National health insurance research database.

Data Availability

Data used in this study are available within the article.

Conflicts of Interest

The authors declare that there are no conflicts of interest.

Acknowledgments

The research and publication of this article was funded by the Taipei Medical University. The authors received no significant financial support for this work that would have influenced its outcome. No significant financial support for this work that could have influenced its outcome. The research and publication of their article was funded by Taipei Medical University.

Supplementary Materials

Table S1: shows the combination and ratio of formula, which listed in the study. (*Supplementary Materials*)

References

[1] E. Baumfeld Andre, R. Reynolds, P. Caubel, L. Azoulay, and N. A. Dreyer, "Trial designs using real-world data: the changing landscape of the regulatory approval process," *Pharmacoepidemiology and Drug Safety*, vol. 29, no. 10, pp. 1201–1212, 2020.

[2] U. S. F Administration, "Real world evidence," 2019, https://www.fda.gov/ScienceResearch/SpecialTopics/RealWorldEvidence/default.htm.

[3] R. E. Sherman, S. A. Anderson, G. J. Dal Pan et al., "Real-world evidence-what is it and what can it tell us?" *New England Journal of Medicine*, vol. 375, no. 23, pp. 2293–2297, 2016.

[4] Y.-C. Su, "Study of the diagnosis of diseases result from environmental factor "Six-Yin." by Delphi methods," *Yearbook of Chinese Medicine and Pharmacy*, vol. 1, 2009.

[5] M. Guomin, "Research Thought of "four in one." on classic prescriptions based on Guizhi decoction (桂枝湯)," *Journal of Traditional Chinese Medicine*, vol. 61, no. 6, pp. 475–478, 2020.

[6] J. S. Chang, K. C. Wang, D. E. Shieh, F. F. Hsu, and L. C. Chiang, "Ge-Gen-Tang has anti-viral activity against human respiratory syncytial virus in human respiratory tract cell lines," *Journal of Ethnopharmacology*, vol. 139, no. 1, pp. 305–310, 2012.

[7] K. Muraoka, "Pharmacological study on the mechanism of action of the Kakkon-to preparation body temperature rise and phagocytic activation of macrophages in dogs," *Journal of Traditional Medicines*, vol. 20, pp. 30–37, 2003.

[8] S. Yakubo, K. Komaki, H. Yagi, and K. Kanmatsuse, "The effects of Kakkon-to on shoulder stiffness and neck body surface temperature by thermotracer," *Kampo Medicine*, vol. 47, no. 5, pp. 795–802, 1997.

[9] J. G. Lin, "Study of the clinical applications of Chinese medicinal prescription-in national health insurance," *Yearbook of Chinese Medicine and Pharmacy*, vol. 9, 2008.

[10] S. Okabayashi, M. Goto, T. Kawamura et al., "Non-superiority of Kakkon-to, a Japanese herbal medicine, to a representative multiple cold medicine with respect to anti-aggravation effects on the common cold: a randomized controlled trial," *Internal Medicine*, vol. 53, no. 9, pp. 949–956, 2014.

[11] Y. Y. Chang, Y. T. Tsai, J. N. Lai, C. H. Yeh, and S. K. Lin, "The traditional Chinese medicine prescription patterns for migraine patients in Taiwan: a population-based study," *Journal of Ethnopharmacology*, vol. 151, no. 3, pp. 1209–1217, 2014.

[12] W.-F. Wang, "Efficacy of Mahuang Fuzi Xixin decoction and Xiaoqinglong decoction on allergic rhinitis in Guinea pigs," *Chinese Journal of Experimental Traditional Medical Formulae*, vol. 17, pp. 176–178, 2011.

[13] Z. Chunyuan, "Gegen soup and Qianghuoshengshi soup combined with acupuncture treatment of cervical disease randomized controlled study," *Journal of Practical Traditional Chinese Internal Medicine*, vol. 11, pp. 148–150, 2015.

[14] Z. Hong-hai, "Qingbi decoction adjuvant treatment chronic sinusitis after endoscopic surgery with 96 cases," *Chinese Journal of Experimental Traditional Medical Formulae*, vol. 20, pp. 195–198, 2014.

[15] Q. Z. H. Xiaoqi, "Study on the antitussive and expelling phlegm effects of Jinfeicao powder," *Journal of Sichuan of Traditional Chinese Medicine*, vol. 31, pp. 33-34, 2013.

[16] W. Tao, Q. Su, H. Wang et al., "Platycodin D attenuates acute lung injury by suppressing apoptosis and inflammation in vivo and in vitro," *International Immunopharmacology*, vol. 27, no. 1, pp. 138–147, 2015.

[17] A. Jafarzadeh, S. V. Azizi, M. Nemati et al., "Ginger extract reduces the expression of IL-17 and IL-23 in the sera and central nervous system of EAE mice," *Iranian Journal of Immunology*, vol. 12, no. 4, pp. 288–301, 2015.

[18] D. J.-G. Lv Jian-zhen, "Research progress in pharmacological effects of amygdalin," *Drugs & Clinic*, vol. 27, pp. 530–535, 2012.

[19] H. Chunrong, "Analysis of the effect of Chuanxiong Gegen decoction and Mahuang Fuzi Xixin decoction on migraine," *Shenzhen Journal of Integrated Traditional Chinese and Western Medicine*, vol. 28, pp. 55-56, 2018.

[20] X. Zhang, "Therapeutic effect of Qingbi decoction on children with chronic sinusitis," *Liaoning Journal of Traditional Chinese Medicine*, vol. 32, no. 7, 2005.

[21] Q. Wnag, "Therapeutic effect of Jiawei Jin Fey Tsao Saan powder on cough after wind-cold-type cold," *Guangming Journal of Chinese Medicine*, vol. 7, pp. 1342-1343, 2012.

Hindawi
Evidence-Based Complementary and Alternative Medicine
Volume 2022, Article ID 9539944, 13 pages
https://doi.org/10.1155/2022/9539944

Research Article

Analysis of Medication Rule of Primary Epilepsy Based on *Xiaocheng Yan's* Clinical Experience Collection of Epilepsy

Yu Zhang,[1] **Lin Tong**,[1] **Guangkun Chen**,[1] **Jingpeng Deng**,[1] **Lei Zhang**,[1] **Hongtao Li**,[1] **and Pengfei Chang**[2]

[1]*Institute of Information on Traditional Chinese Medicine, China Academy of Chinese Medical Sciences, Beijing 100700, China*
[2]*Institute of Chinese Materia Medica, China Academy of Chinese Medical Sciences, Beijing 100700, China*

Correspondence should be addressed to Hongtao Li; newdream1013@163.com and Pengfei Chang; pfchang@icmm.ac.cn

Received 16 October 2021; Revised 15 January 2022; Accepted 22 April 2022; Published 25 June 2022

Academic Editor: Xuezhong Zhou

Objective. To explore and analyze the medication rule of Professor *Xiaocheng Yan* in the treatment of primary epilepsy, hoping to provide reference for the clinical treatment of primary epilepsy. *Methods.* Mining and analysis of Professor *Xiaocheng Yan* sorted out the medical cases of primary epilepsy in *Xiaocheng Yan's* clinical experience collection of epilepsy, extracted the traditional Chinese medicine (TCM) prescription data in the medical cases, standardized the obtained TCM prescription data, and used the data mining function integrated by the ancient and modern medical case cloud platform V2.3.5 to carry out frequency statistics, cluster analysis, association analysis, and complex network analysis on the TCM data, and the common herbs used by Professor *Xiaocheng Yan* in the treatment of primary epilepsy, properties and classifications of commonly used herbs, pairs of commonly used herbs, and core prescriptions were obtained. *Results.* A total of 39 cases, 228 medical records, and 230 prescriptions data of TCM were included. A total of 96 Chinese medicinal herbs were involved, and the total frequency of medication was 3,828. High-frequency herbs include Rhizoma Gastrodiae (Tianma) (222 times), Ramulus Uncariae cum Uncis (Gouteng) (220 times), Rhizoma Acori Tatarinowii (Shichangpu) (216 times), Rhizoma Pinelliae Praeparatum (Fabanxia) (207 times), Bombyx Batryticatus (Jiangcan) (206 times), and Periostracum Cicadae (Chantui) (181 times). The main properties and flavors of commonly used Chinese medicinal herbs were sweet, bitter, and pungent, which were mainly attributed to the four meridians of liver, lung, heart, and spleen. Commonly used couplet herbs were {Periostracum Cicadae (Chantui)} ≥ {Bombyx Batryticatus (Jiangcan)}, {Rhizoma Acori Tatarinowii (Shichangpu)} ≥{ Bombyx Batryticatus (Jiangcan)}, {Radix Bupleuri (Chaihu)} ≥ {Radix Scutellariae (Huangqin)}, {Rhizoma Gastrodiae (Tianma)} ≥ {Ramulus Uncariae cum Uncis (Gouteng)}, {Rhizoma Acori Tatarinowii (Shichangpu)} ≥ {Periostracum Cicadae (Chantui)}, {Ramulus Uncariae cum Uncis (Gouteng)} ≥ {Bombyx Batryticatus (Jiangcan)}, {Bombyx Batryticatus (Jiangcan)} ≥ {Rhizoma Gastrodiae (Tianma)}, {Rhizoma Acori Tatarinowii (Shichangpu)} ≥ {Ramulus Uncariae cum Uncis (Gouteng)}, etc. The core prescription composition was based on the addition and subtraction of Tianma Gouteng decoction and Erchen decoction. The main pharmacological mechanisms of core prescriptions are mainly reflected in antioxidation, enhancing GABA efficacy, and regulating NMDA channel and sodium channel, neuroprotection, and so on. *Conclusion.* Professor *Xiaocheng Yan*'s medication for the treatment of primary epilepsy was based on the principle of relieving wind and spasm, drying dampness and resolving phlegm, giving consideration to both Qi and blood, and harmonizing liver, lung, heart, and spleen.

1. Introduction

Epilepsy is a chronic brain disease caused by a variety of causes, which is characterized by recurrent, paroxysmal, and transient central nervous system dysfunction caused by excessive discharge of brain neurons [1]. The data of domestic epidemic survey show that there are more than 9 million epileptic patients in China, and about 400,000 new epileptic patients are added every year [2, 3]. Primary epilepsy refers to unknown etiology, and the brain cannot be found to cause seizures of abnormal function or structural damage, which may be related to genetic factors, generally in

a specific age stage of the disease [4]. At present, there is no ideal eradication method for the treatment of this disease at home and abroad. In the treatment of epilepsy, antiepileptic drugs are mainly used to control and reduce seizures, and try to dispel the etiology, in order to maintain the normal brain nerve function [5]. Repeated frequent seizures and the long-term use of a variety of antiepileptic drugs (AEDs) will not only bring physical damage to patients with epilepsy but also affect the living conditions of study, employment, marriage, and childbearing to varying degrees, and bring economic burden and mental pressure to patients, family members, and society.

A large number of clinical research practice and experience summary of famous TCM in China show definite advantages in the treatment of epilepsy, which can improve the curative effect of AEDs, reduce the dosage of AEDs, lighten the side effects and adverse reactions of drugs, and, meanwhile, improve the quality of life and social life function of patients significantly [6]. The TCM medical record is a clinical document that records the actual operation of diagnosis and treatment by doctors in the process of clinical practice under the guidance of the theory of TCM. It is the record of clinical diagnosis and treatment of TCM. It preserves a large number of first-hand data of disease diagnosis and treatment, which reflects the clinical experience and treatment characteristics of doctors, and is an important resource for the inheritance of TCM academic research and famous TCM experience and academic thought. The in-depth study of TCM medical records can not only explore and summarize the principle of the development of the disease, but also summarize the previous clinical experience and have an in-depth understanding of the formation and development of TCM academic schools [7]. This paper uses modern information technology to analyze the prescription information of TCM in *Xiaocheng Yan*'s medical cases of primary epilepsy, and excavates its medication rule, in order to provide reference for the clinical treatment of epilepsy.

2. Materials and Methods

2.1. Data Sources. Data sources were derived from the medical data of primary epilepsy collected in *Xiaocheng Yan's* clinical experience collection of epilepsy, which published by TCM Ancient Books Publishing House in 2017, and its cover is shown in Figure 1. The selected cases were diagnosed clearly, with objective examination basis (EEG or MRI), complete data records, and continuous treatment and observation for more than one year. There were 100 medical cases in the book, including 9 cases of benign epilepsy in children, 13 cases of epilepsy caused by febrile convulsion, 11 cases of epilepsy caused by craniocerebral trauma, 4 cases of absence epilepsy in children, 35 cases of idiopathic epilepsy, and 28 cases of secondary epilepsy [8].

2.2. Inclusion and Exclusion Criteria

2.2.1. Inclusion Criteria. ① The disease diagnosis belongs to hereditary generalized epilepsy (Note: *Xiaocheng Yan's* clinical experience collection of epilepsy was called "idiopathic epilepsy." In addition, it also includes the medical records diagnosed as "childhood absence epilepsy" in this book, which was "hereditary generalized epilepsy" according to the epilepsy classification standard of ILAE Classification of the Epilepsies Position Paper of the ILAE Commission for Classification and Terminology [9]). ② The disease diagnosis belongs to self-limiting focal epilepsy (Note: *Xiaocheng Yan's* clinical experience collection of epilepsy was called "children's benign epilepsy"); ③ the curative effect was cured, improved, and effective (Note: the curative effect referred to here was clearly stated in the book. In addition, according to the Diagnostic and Curative Effect Standard of TCM Disease and Syndrome [10], it was cured in the near future: compared with the intermittent time of attack before treatment, it was longer than that of the author for more than one year; Improvement: the symptoms of the attack were less than before, and the interval was obviously prolonged).

Figure 1: The cover of *Xiaocheng Yan's* clinical experience collection of epilepsy.

2.2.2. Exclusion Criteria. ① Epilepsy caused by central nervous system infection; ② epilepsy caused by hypoxia; ③ epilepsy caused by craniocerebral trauma; ④ epilepsy caused by central nervous system malformation; ⑤ epilepsy caused by shock; ⑥ epilepsy caused by brain tumor; ⑦ eclampsia (epilepsy caused by pregnancy induced hypertension); ⑧ invalid medical records (Note: for epilepsy caused by the

above causes, *Xiaocheng Yan's* clinical experience collection of epilepsy has indicated a clear diagnostic basis).

Select medical records according to the above inclusion and exclusion criteria, split diagnosis times, extract prescription data of TCM, and use the function in Microsoft Excel 2019 to check the consistency of the data, check the inconsistencies, input the original data according to the original data, and then import the split medical records and prescription data into the ancient and modern medical records cloud platform V2.3.5.

2.2.3. Data Normalization. The aliases and abbreviations of drugs are unified as the names of TCM written in the textbook "Chinese pharmacy" [11] (hereinafter referred to as "Chinese pharmacy") in the thirteenth five-year plan of higher education of TCM published in August 2016. For example, Yuanshen was unified as Xuanshen, and Shanzhi was unified as Fructus Gardeniae (Zhizi) and so on.

2.3. Data Analysis. This study mainly uses the ancient and modern medical record cloud platform V2.3.5 software to mine the prescription data of TCM in the medical case of primary epilepsy. First of all, we used the Apriori algorithm to analyze the association rules of the herbs. Additionally, hierarchical clustering was used to classify high-frequency herbs. Finally, complex network analysis was used to confirm the core herbs prescribed for primary epilepsy treatment.

2.3.1. Frequency Analysis. It carries on the frequency statistics to the herb, the meridian tropism, the medicinal property, and so on.

2.3.2. Apriori Algorithm. The Apriori algorithm is a frequent itemset algorithm for mining association rules. We used it to illustrate the specific rules of TCM in primary epilepsy treatment. In our data, each herb was treated as a variable. The association analysis algorithm (confidence ≥ 0.7, support ≥ 0.7, and promotion >0.99) was used to mine the commonly used medicine pairs in the treatment of epilepsy. The confidence is the probability of the occurrence of the associated postitem in the case of the occurrence of the associated antecedent; the degree of support is the percentage of the number of simultaneous occurrence of the associated antecedent and postassociated items to the total number of events, that is, the probability of the simultaneous occurrence of the antecedent and postassociated items. The degree of promotion is the ratio of confidence to the probability of the occurrence of the postcorrelation item. The higher the support and confidence, the stronger the relationship between the antecedent and the postcorrelation, and the promotion degree >1 indicates that the relationship between the former and the latter is effective and strong; otherwise, it is invalid.

2.3.3. Hierarchical Clustering Algorithm. In the hierarchical clustering algorithm, each herb was regarded as a cluster, and N clusters were combined to form a new class based on a similarity measure between objects. After testing, it is found that the absolute distance can get better classification effect than Euclidean distance and Chebyshev distance. The absolute distance was used to calculate the similarity between herbs. It can be described as calculating the polyline distance from one object to another, and sometimes, it can be further described as the average deviation of objects in each dimension of multidimensional space [12].

2.3.4. Complex Network Analysis. The complex network analysis method was used to find the core prescription composition of epilepsy treatment. Complex network analysis is used to analyze complex interaction laws in complex systems in the real world based on a network model of nodes and edges. The complexities of diseases and human life systems are gradually being recognized, such that medical research from a network perspective has become an important topic in current medical research. We regarded the constituent herbs for primary epilepsy treatment as nodes and connections between two herbs as edges. Thus, we could rationalize all medical record data into a network of medicine nodes and edges using ancient and modern medical record cloud platform V2.3.5 and the hierarchical network algorithm.

Hierarchical network is a display of the network after hierarchical division. The core network can be extracted from the sparse network. The algorithm needs to specify two parameters: layer number (which determines the number of network graphs generated from the center of the network to the periphery of the network) and degree coefficient (which determines the density of the generated graph, the smaller the value, the more nodes are left). The specific parameter settings are as follows: [layout: circle; layer number: 3; degree coefficient: 1] [13].

3. Results

According to the above-mentioned criteria, 39 medical cases of primary epilepsy were selected. After separation, 228 medical records (total number of medical cases) and a total of 230 prescriptions were obtained.

3.1. Statistics of Commonly Used Chinese Medicinal Herb. The prescription data of TCM included in the medical cases of primary epilepsy involved a total of 96 kinds of TCM, and the total frequency of herb use was 3,828. The top 30 commonly used Chinese medicinal herbs with frequency ≥ 30 are listed in Table 1 according to the frequency from high to low. Among them, Rhizoma Gastrodiae (Tianma) have the highest use frequency, up to 222 times, and the use frequency (frequency = frequency/total number of medical cases) was 96.52%.

3.2. Attribute Statistics of Chinese Medicinal Herb

3.2.1. Four Qi. Most of the prescriptions for primary epilepsy were mainly composed of mild, warm, and cold

Table 1: Related information of Chinese medicinal herb contained in medical records of primary epilepsy (frequency ≥30).

Genus	Family	Herb Chinese-Latin-English	Frequency	Percentage (%)	Average	Min	Max	Standard deviation
Gastrodia	Orchidaceae	[Tianma] Rhizoma Gastrodiae (tall gastrodia tuber)	222	96.52%	12.38	6	20	2.94
Uncaria	Rubiaceae	[Gouteng] Ramulus Uncariae cum Uncis (gambir plant)	220	95.65%	10.42	6	20	1.91
Acorus	Araceae	[Shichangpu] Rhizoma Acori Tatarinowii (grassleaf sweetflag Rhizome)	216	93.91%	20.9	5	30	9.25
Pinellia	Araceae	[Fabanxia] Rhizoma Pinelliae Praeparatum (prepared pinellia tuber)	207	90.00%	8.5	5	15	2.17
Bombyx	Bombycidae	[Jiangcan] Bombyx Batryticatus (Stiff Silkworm)	206	89.57%	9.8	6	15	1.08
Cicada	Cicadae	[Chantui] Periostracum Cicadae (Cicada Slough)	181	78.70%	5.59	3	6	1.04
Scutellaria	Labiatae	[Huangqin] Radix Scutellariae (Baical skullcap root)	172	74.78%	10.77	6	15	2.4
Bupleurum	Umbelliferae	[Chaihu] Radix Bupleuri (Chinese Thorowax root)	171	74.35%	11.44	6	15	2.77
Gardenia	Rubiaceae	[Zhizi] Fructus Gardeniae (cape jasmine fruit)	160	69.57%	10.44	6	15	1.84
Glycyrrhiza	leguminous	[Gancao] Radix Et Rhizoma Glycyrrhizae (Liquorice root)	151	65.65%	5.79	3	15	1.22
Citrus	Rutaceae	[Chenpi] Pericarpium Citri Reticulatae (Dried Tangerine peel)	127	55.22%	7.73	6	10	1.98
Phyllostachys	Gramineae	[Tianzhuhuang] Concretio Silicea Bambusae (Tabasheer)	114	49.57%	9.12	6	15	2.17
Poria	Polyporaceae	[Fushen] Poria cum Ligno Hospite (Poria with hostwood)	112	48.70%	11.57	6	15	2.39
Polygala	Polygalaceae	[Yuanzhi] Radix Polygalae (thinleaf milkwort root)	99	43.04%	11.02	6	20	3.22
Cynanchum	Asclepiadaceae	[Baishao] Radix Paeoniae Alba (white peony root)	92	40.00%	11.71	6	15	2.89
Curcuma	Zingiberaceae	[Yujin] Radix Curcumae (turmeric root tuber)	88	38.26%	9.69	6	15	1.92
Paeonia	Ranunculaceae	[Mudanpi] Cortex moutan (tree peony bark)	73	31.74%	11.82	6	15	2.7
Angelica	Umbelliferae	[Danggui] Radix Angelicae Sinensis (Chinese Angelica)	70	30.43%	9.8	6	15	2.68
Arisaema	Araceae	[Dannanxing] Arisaema cum Bile (bile Arisaema)	61	26.52%	8.38	5	10	2.03
Paeonia	Ranunculaceae	[Chishao] Radix Paeoniae Rubra (red peony root)	59	25.65%	11.69	6	15	2.94
—	—	[Shenglonggu] Raw Fossil Fragments (raw keel)	57	24.78%	27.11	10	30	5.99
Ostrea	Ostreae	[Shenguli] Raw Concha Ostreae (Raw Oyster Shell)	57	24.78%	27.11	10	30	5.99
Ligusticum	Umbelliferae	[Chuanxiong] Rhizoma Chuanxiong (Szechwan Lovage Rhizome)	52	22.61%	18.08	6	30	8.92
Platycladus	Cupressaceae	[Baiziren] Semen Platycladi (Chinese Arborvitae Kernel)	49	21.30%	13.78	10	30	5.76
Citrus	Rutaceae	[Zhishi] Fructus Aurantii Immaturus (immature orange fruit)	47	20.43%	7.96	6	10	2
Zizyphus	Rhamnaceae	[Suanzaoren] Semen Ziziphi Spinosae (spine date seed)	46	20.00%	14.02	10	30	5.58
Poria	Polyporaceae	[Fuling] Poria (Indian bread)	45	19.57%	11.36	6	20	2.62
Salvia	Labiatae	[Dangshen] Radix Codonopsis (Tangshen)	39	16.96%	12.56	10	30	4.22
Hawksbill	Carapace	[Daimao] Hawksbill Carapace (hawksbill turtle shell)	37	16.09%	2.84	1.5	3	0.47
Chrysanthemum	Compositae	[Juhua] Flos Chrysanthemi (Chrysanthemum Flower)	35	15.22%	10	6	15	2.27

* *Note*. "—" means no.

Chinese medicinal herb. Among them, the frequency of mild herb use was the highest (1012 times). The details are shown in Figure 2.

3.2.2. Five Flavors. Most of the prescriptions for primary epilepsy were sweet, bitter, and pungent. Among them, pungent herbs were used most frequently (1569 times), as shown in Figure 3.

3.2.3. Meridian Tropism. The main prescriptions for primary epilepsy were liver meridian and lung meridian. Among them, the herb use frequency of liver meridian was the highest (2064 times), as shown in Figure 4.

3.2.4. Efficacy. The main prescriptions of primary epilepsy were relieved wind and spasm, removed dampness, and phlegm. Among them, the frequency of the use of antispasmodic herbs was the highest (428 times), as shown in Figure 5.

3.3. Clustering of Commonly Used Herbs. Cluster analysis of Chinese medicinal herb commonly used in medical cases of primary epilepsy was carried out. The cluster analysis of 30 Chinese medicinal herbs with frequency ≥30 times was carried out by using absolute distance and the longest distance method, as shown in Figure 6. The results showed that the above herbs could be divided into three categories according to the absolute distance of 140. The first category was Concretio Silicea Bambusae (Tianzhuhuang), Poria cum Ligno Hospite (Fushen), Radix Polygalae (Yuanzhi), Radix Et Rhizoma Glycyrrhizae (Gancao), and Pericarpium Citri Reticulatae (Chenpi). The second category was Fructus Gardeniae (Zhizi), Radix Scutellariae (Huangqin), Radix Bupleuri (Chaihu), Periostracum Cicadae (Chantui), Rhizoma Pinelliae Praeparatum (Fabanxia), Bombyx Batryticatus (Jiangcan), Rhizoma Acori Tatarinowii (Shichangpu), Rhizoma Gastrodiae (Tianma), and Ramulus Uncariae cum Uncis (Gouteng). The third category was subdivided with the absolute value distance of 100 and could be divided into three groups (group a: Radix Curcumae (Yujin), Radix Angelicae Sinensis<Danggui>, Radix Paeoniae Alba (Baishao), Radix Paeoniae Rubra<Chishao>), group b: Cortex moutan<Mudanpi>, Radix Codonopsis<Dangshen>, Raw Fossil Fragments<Shenglonggu>, Raw Concha Ostreae<Shenguli>, group c: Arisaema cum Bile<Dannanxing>, Fructus Aurantii Immaturus<Zhishi>, Poria<Fuling>, Rhizoma Chuanxiong<Chuanxiong>, Flos Chrysanthemi<Juhua>, Hawksbill Carapace<Daimao>, Semen Platycladi<Baiziren>, and Semen Ziziphi Spinosae<Suanzaoren>.

3.4. Commonly Used Medicine Pair. The relationship between Chinese medicinal herb and Chinese medicinal herb in the prescription data of primary epilepsy was analyzed by the method of association rules, and arranged in descending order according to the degree of support, as shown in Table 2. The results showed that the effective and strongly related herbs used frequently in the treatment of primary epilepsy were {Periostracum Cicadae (Chantui)} ≥ {Bombyx Batryticatus (Jiangcan)}, {Rhizoma Acori Tatarinowii (Shichangpu)} ≥ {Bombyx Batryticatus (Jiangcan)}, {Radix

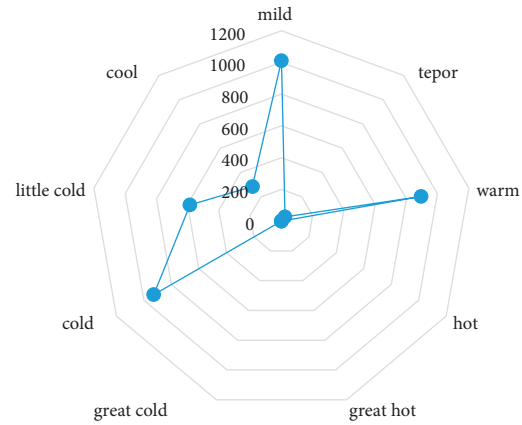

Figure 2: Radar chart of four properties of TCM in medical cases of primary epilepsy.

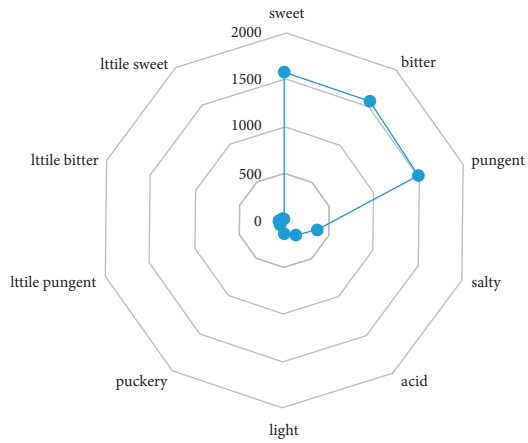

Figure 3: Radar chart of five flavors of TCM in medical cases of primary epilepsy.

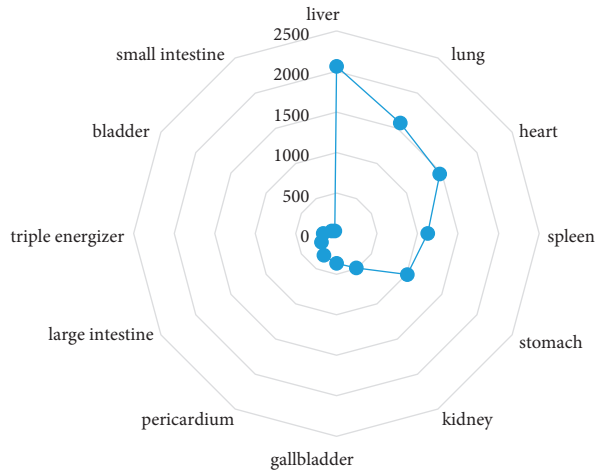

Figure 4: Radar chart of channel tropism of TCM in medical cases of primary epilepsy.

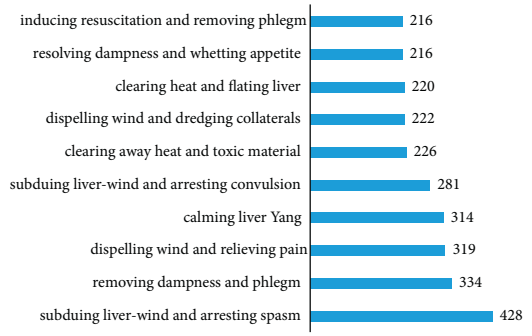

Figure 5: Bar chart of efficacy distribution of TCM in medical cases of primary epilepsy.

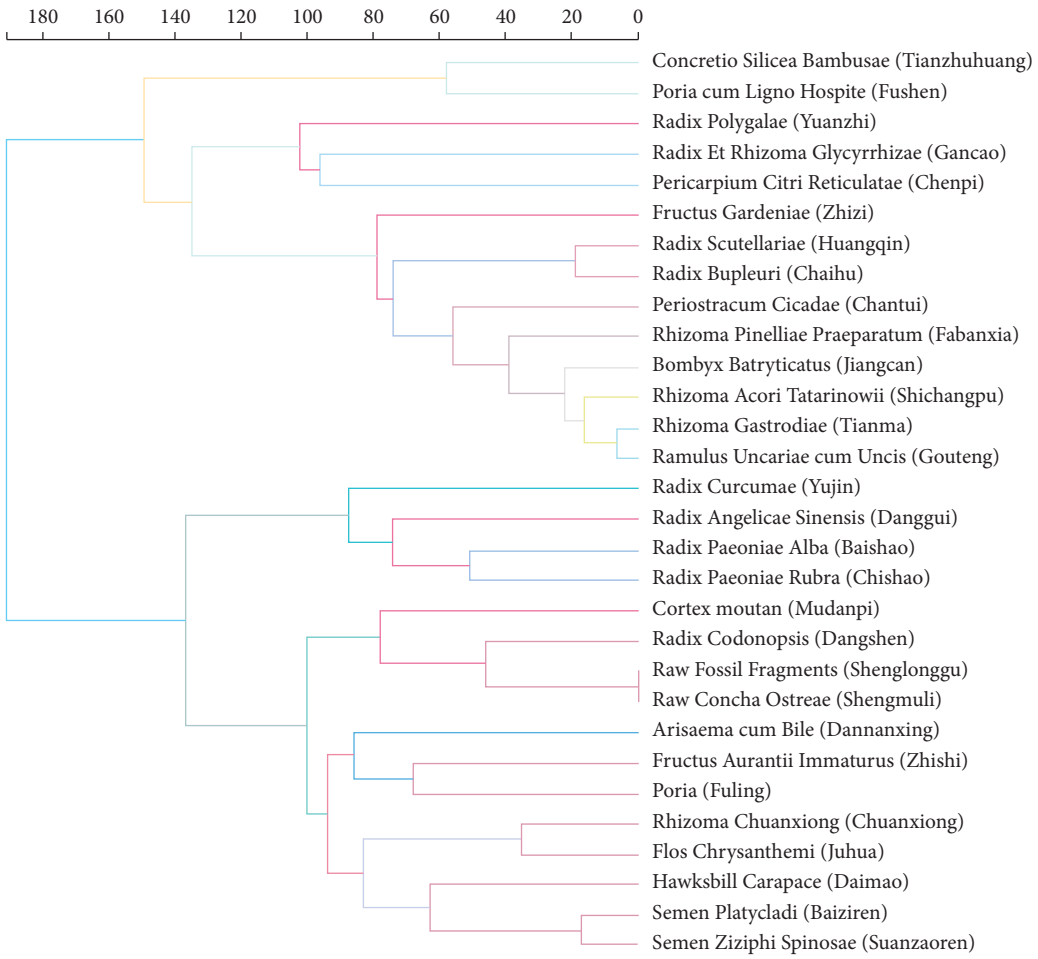

Figure 6: Cluster analysis of Chinese medicine in medical cases of primary epilepsy.

Bupleuri (Chaihu)} ≥ {Radix Scutellariae (Huangqin)}, {Rhizoma Gastrodiae (Tianma)} ≥ {Ramulus Uncariae cum Uncis (Gouteng)}, {Rhizoma Acori Tatarinowii (Shichangpu)} ≥ {Periostracum Cicadae (Chantui)}, {Ramulus Uncariae cum Uncis (Gouteng)} ≥ {Bombyx Batryticatus (Jiangcan)}, {Bombyx Batryticatus (Jiangcan)} ≥ {Rhizoma Gastrodiae (Tianma)}, {Rhizoma Acori Tatarinowii (Shichangpu)} ≥ {Ramulus Uncariae cum Uncis (Gouteng)}, and so on.

3.5. Core Prescription Composition. The composition of the core prescription used in the treatment of primary epilepsy was obtained through complex network analysis, as shown in Figure 7. The results showed that the herb components were Rhizoma Gastrodiae (Tianma), Ramulus Uncariae cum Uncis (Gouteng), Fructus Gardeniae (Zhizi), Radix Scutellariae (Huangqin), Poria cum Ligno Hospite (Fushen), Rhizoma Acori Tatarinowii (Shichangpu), Radix Polygalae (Yuanzhi), Bombyx Batryticatus (Jiangcan), Periostracum Cicadae (Chantui), Rhizoma Pinelliae Praeparatum (Fabanxia), Pericarpium Citri Reticulatae (Chenpi), Radix Bupleuri (Chaihu), Radix Paeoniae Alba (Baishao), Concretio Silicea Bambusae (Tianzhuhuang), Radix

Table 2: Commonly used herbs in the prescription of primary epilepsy.

No.	Items (LHS ≥ RHS)	Support degree	Confidence degree	Lifting degree
1	{Ramulus Uncariae cum Uncis (Gouteng)} ≥ {Rhizoma Gastrodiae (Tianma)}	0.95	0.99	1.03
2	{Rhizoma Gastrodiae (Tianma)} ≥ {Ramulus Uncariae cum Uncis (Gouteng)}	0.95	0.98	1.02
3	{Rhizoma Acori Tatarinowii (Shichangpu)} ≥ {Rhizoma Gastrodiae (Tianma)}	0.92	0.98	1.02
4	{Rhizoma Gastrodiae (Tianma)} ≥ {Rhizoma Acori Tatarinowii (Shichangpu)}	0.92	0.95	1.01
5	{Rhizoma Acori Tatarinowii (Shichangpu)} ≥ {Ramulus Uncariae cum Uncis (Gouteng)}	0.91	0.97	1.01
6	{Ramulus Uncariae cum Uncis (Gouteng)} ≥ {Rhizoma Acori Tatarinowii (Shichangpu)}	0.91	0.95	1.01
7	{Bombyx Batryticatus (Jiangcan)} ≥ {Rhizoma Gastrodiae (Tianma)}	0.89	0.99	1.03
8	{Rhizoma Gastrodiae (Tianma)} ≥ {Bombyx Batryticatus (Jiangcan)}	0.89	0.92	1.03
9	{Ramulus Uncariae cum Uncis (Gouteng)} ≥ {Bombyx Batryticatus (Jiangcan)}	0.88	0.92	1.03
10	{Bombyx Batryticatus (Jiangcan)} ≥ {Ramulus Uncariae cum Uncis (Gouteng)}	0.88	0.99	1.04
11	{Rhizoma Acori Tatarinowii (Shichangpu)} ≥ {Bombyx Batryticatus (Jiangcan)}	0.87	0.93	1.04
12	{Rhizoma Pinelliae Praeparatum (Fabanxia)} ≥ {Rhizoma Gastrodiae (Tianma)}	0.87	0.97	1.0
13	{Bombyx Batryticatus (Jiangcan)} ≥ {Rhizoma Acori Tatarinowii (Shichangpu)}	0.87	0.97	1.03
14	{Rhizoma Gastrodiae (Tianma)} ≥ {Rhizoma Pinelliae Praeparatum (Fabanxia)}	0.87	0.9	1.0
15	{Rhizoma Pinelliae Praeparatum (Fabanxia)} ≥ {Ramulus Uncariae cum Uncis (Gouteng)}	0.86	0.95	0.99
16	{Ramulus Uncariae cum Uncis (Gouteng)} ≥ {Rhizoma Pinelliae Praeparatum (Fabanxia)}	0.86	0.9	1.0
17	{Rhizoma Acori Tatarinowii (Shichangpu)} ≥ {Rhizoma Pinelliae Praeparatum (Fabanxia)}	0.84	0.9	1.0
18	{Rhizoma Pinelliae Praeparatum (Fabanxia)} ≥ {Rhizoma Acori Tatarinowii (Shichangpu)}	0.84	0.94	1.0
19	{Rhizoma Pinelliae Praeparatum (Fabanxia)} ≥ {Bombyx Batryticatus (Jiangcan)}	0.81	0.9	1.0
20	{Bombyx Batryticatus (Jiangcan)} ≥ {Rhizoma Pinelliae Praeparatum (Fabanxia)}	0.81	0.91	1.01
21	{Ramulus Uncariae cum Uncis (Gouteng)} ≥ {Periostracum Cicadae (Chantui)}	0.79	0.82	1.04
22	{Bombyx Batryticatus (Jiangcan)} ≥ {Periostracum Cicadae (Chantui)}	0.79	0.88	1.12
23	{Periostracum Cicadae (Chantui)} ≥ {Ramulus Uncariae cum Uncis (Gouteng)}	0.79	1.0	1.05
24	{Periostracum Cicadae (Chantui)} ≥ {Bombyx Batryticatus (Jiangcan)}	0.79	1.0	1.12
25	{Rhizoma Gastrodiae (Tianma)} ≥ {Periostracum Cicadae (Chantui)}	0.78	0.81	1.03
26	{Periostracum Cicadae (Chantui)} ≥ {Rhizoma Gastrodiae (Tianma)}	0.78	0.99	1.03
27	{Rhizoma Acori Tatarinowii (Shichangpu)} ≥ {Periostracum Cicadae (Chantui)}	0.77	0.81	1.03
28	{Periostracum Cicadae (Chantui)} ≥ {Rhizoma Acori Tatarinowii (Shichangpu)}	0.77	0.97	1.03
29	{Ramulus Uncariae cum Uncis (Gouteng)} ≥ {Radix Scutellariae (Huangqin)}	0.73	0.76	1.02
30	{Radix Scutellariae (Huangqin)} ≥ {Rhizoma Gastrodiae (Tianma)}	0.73	0.97	1.0
31	{Radix Scutellariae (Huangqin)} ≥ {Ramulus Uncariae cum Uncis (Gouteng)}	0.73	0.97	1.01
32	{Rhizoma Gastrodiae (Tianma)} ≥ {Radix Scutellariae (Huangqin)}	0.73	0.75	1.0
33	{Rhizoma Pinelliae Praeparatum (Fabanxia)} ≥ {Periostracum Cicadae (Chantui)}	0.72	0.8	1.02
34	{Ramulus Uncariae cum Uncis (Gouteng)} ≥ {Radix Bupleuri (Chaihu)}	0.72	0.75	1.01
35	{Radix Bupleuri (Chaihu)} ≥ {Rhizoma Gastrodiae (Tianma)}	0.72	0.97	1.0
36	{Radix Bupleuri (Chaihu)} ≥ {Ramulus Uncariae cum Uncis (Gouteng)}	0.72	0.97	1.01
37	{Rhizoma Gastrodiae (Tianma)} ≥ {Radix Bupleuri (Chaihu)}	0.72	0.75	1.01
38	{Periostracum Cicadae (Chantui)} ≥ {Rhizoma Pinelliae Praeparatum (Fabanxia)}	0.72	0.92	1.02
39	{Radix Bupleuri (Chaihu)} ≥ {Radix Scutellariae (Huangqin)}	0.7	0.95	1.27
40	{Radix Scutellariae (Huangqin)} ≥ {Radix Bupleuri (Chaihu)}	0.7	0.94	1.26

Note. Confidence ≥ 0.7, support ≥ 0.7, improvement ≥ 0.99.

Curcumae (Yujin), Cortex moutan(Mudanpi), Cortex moutan (Mudanpi) and Radix Et Rhizoma Glycyrrhizae (Gancao). From the composition of the prescription, the core prescription used in the treatment of primary epilepsy was Tianma Gouteng decoction and Erchen decoction.

3.6. Allopathic Drugs Used in Primary Epilepsy. Many patients take one or more antiepileptic drugs for a long time before using Chinese medicine herbs. Although antiepileptic drugs (AEDs) can control seizures, it also induces a variety of adverse reactions such as mental, psychological, behavioral, cognitive function, and fatigue [14]. In addition, the adverse reactions of AEDs may have a cumulative effect, and the risk of adverse reactions in patients with epilepsy caused by multidrug combination was significantly increased [15]. This paper summarizes the mechanism and common adverse reactions of antiepileptic Western drugs involved in Professor *Xiaocheng Yan*'s treatment of primary epilepsy. The types, specific drugs, mechanism of action, adverse reactions, and literature sources of antiepileptic drugs are listed in Table 3. A total of 6 drugs were included such as

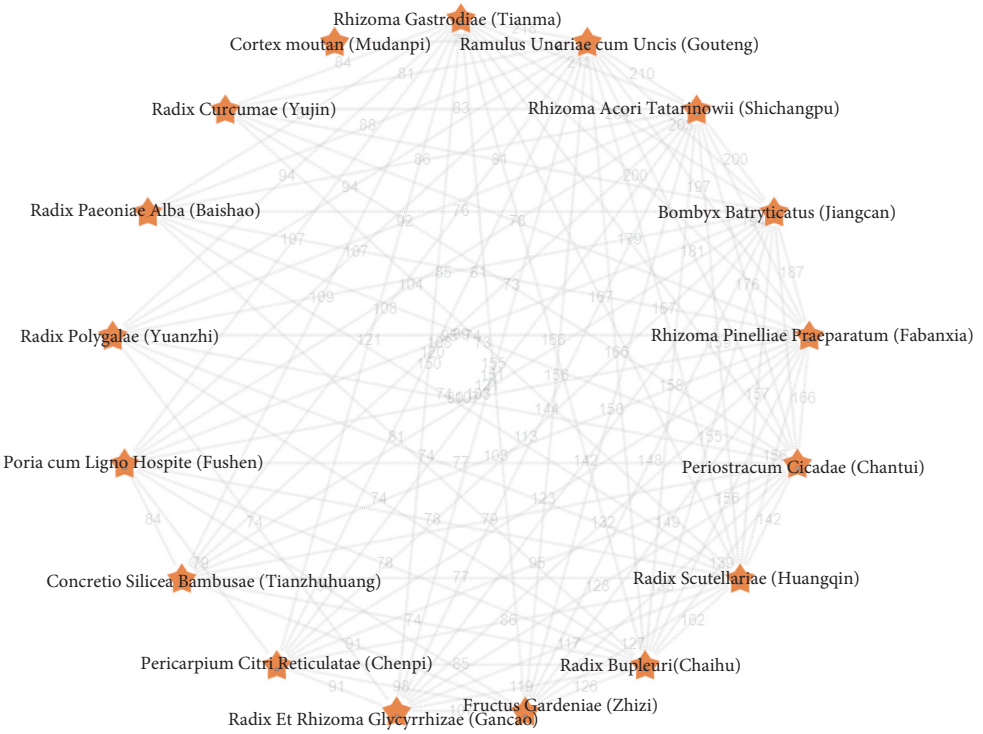

Figure 7: Complex network analysis of the core prescription of primary epilepsy. Note. The boundary value represents the frequency of co-occurrence of the two nodes.

Table 3: Mechanism of action of antiepileptic allopathic drugs.

No.	Category	Drugs	Mechanism of action	Side effects	References
1	Iminostilbene	Carbamazepine and oxcarbazepine	Inhibition of neuronal Na + currents	Bone marrow suppression, skin rash, and visual disturbances	(Ambrósio et al.) [16]
2	Benzodiazepine	Clonazepam	Agonist action at the GABAA receptor	Drowsiness, cognitive impairment, and euphoria	(Campo-Soria et al.) [17]
3	Aliphatic carboxylic acid	Valproic acid	Increases the synthesis of GABA	Blurred vision, hair loss, change in appetite, and constipation	(Rosenberg) [18]
4		Levetiracetam	It modulates synaptic neurotransmitter release through binding to the synaptic vesicle protein SV2A in the brain	Vomiting, tiredness, throat irritation, headache, diarrhea, and cough	(Noachtar et al.) [19]
5		Topiramate	It inhibits the AMPA subtype glutamate receptor and blocks Na + channels. It also increases GABA activity at GABA receptors	Dizziness, somnolence, diarrhea, depression, and nystagmus	(Kenna et al.) [20]

carbamazepine, oxcarbazepine, clonazepam, valproic acid, levetiracetam, and topiramate.

In general, when serious adverse reactions occur in patients with epilepsy or seizures were effectively controlled, drug reduction or withdrawal was helpful to improve the quality of life of patients with epilepsy. Among patients without serious adverse reactions, seizure-free period (SFP) was the main reference to determine the stopping time of AED. The empirical treatment of SFP has been gradually reduced recent 2~3 years in clinic. The speed of drug withdrawal should be considered after determining the stopping time, which refers to how much the drug gradient reduces and how long it takes to stop using drug completely. Withdrawal of AED too quickly may lead to withdrawal, and the frequency and severity of withdrawal were higher than those before treatment [21]. Professor *Xiaocheng Yan* usually adopts the scheme of reducing the dosage of Western medicine slowly in the treatment of primary epilepsy.

3.7. Analysis of the Main Pharmacological Mechanisms of Core Prescriptions. Through the analysis of the main pharmacological mechanisms of the core prescriptions used by Professor *Xiaocheng Yan* in the treatment of primary epilepsy, it can be found that different traditional Chinese medicines can enhance the antiepileptic effects through anti-inflammation,

Table 4: Related active ingredients, functions, and possible mechanisms of Chinese herbs.

Chinese herbs	Active ingredients	Functions	Possible mechanism
[Tianma] Rhizoma Gastrodiae	Vanillyl alcohol Gastrodin Parishin Gastrodia elata extract 4-Hydroxybenzyl alcohol 4-Hydroxybenzaldehyde and analogs	Antioxidation Anticonvulsion Anti-inflammation Neuroprotection	(1) Adjust AP-1 expression through the JNK signaling pathway [22] (2) Preclude NMDA excitotoxicity [23] (3) Equalize the activity of GABA and glutamate [24] (4) Modulate the MAPK-associated inflammatory responses [25, 26] (5) Restrain $Na_v1.6$ sodium currents [25, 26]
[Gouteng] Ramulus Uncariae cum Uncis	Rhynchophylline	Anticonvulsion Antioxidation Neuroprotection	(1) Regulate the expressions of MIF and cyclophilin A [27] (2) Reduce the expression of JNKp of MAPK signal pathways [28] (3) Restrain $Na_v1.6$ I_{NaP} and NMDA receptor currents [23] (4) Reduce GFAP, S100 B proteins, and RAGE [29, 30] (5) Attenuate mossy fiber sprouting and astrocyte proliferation [29, 30] (6) Prevent neuron death [29, 30] (7) Modulate TLR and neurotrophin signaling pathways [31] (8) Restrain the expression of IL-1 and BDNF genes [31]
[Shichangpu] Rhizoma Acori Tatarinowii	Volatile oil a-asarone β-asarone Eudesmin a-asarone	Anticonvulsion Anti-apoptosis Neuroprotection	(1) Protect GABA-immunoreactive neurons [32] (2) Modulate $GABA_A$ receptors then enhance tonic GABAergic inhibition [33] (3) Increase GABA, and reduce glutamate [32] (4) Increase neurotrophic factors by triggering the PKA signaling pathway [34] (5) Regulate Caspase-3 and Bcl-2 [34]
[Jiangcan] Bombyx Batryticatus	Beauvericin Ammonium oxalate Protein-rich extracts Other ethanol extracts	Anticonvulsion Anti-apoptosis Antioxidation Neuroprotection	(1) Modulate the PI3K/Akt signaling pathways [35] (2) Reduce IL-1β, IL-4, and TNF-a, and increase 5-HT and GABA [36] (3) Reduce intracellular Ca2+ levels to prevent neuronal signaling [36]
[Fabanxia] Rhizoma Pinelliae Praeparatum	Pinellia total alkaloids	Anticonvulsion	(1) Modulate GABAergic system [37] (2) Upregulate $GABA_A$ receptors [37]
[Chantui] Periostracum Cicadae	Amino acid Trace element (Al/P/Ca/Mg) [38]	Anticonvulsion	Not clear
[Chaihu] Radix Bupleuri	Saikosaponin A	Anticonvulsion Neuroprotection	(1) Suppress NMDA receptor current, I_{Nap} [39–41] (2) Inhibit mTOR signaling pathway [39–41] (3) Increase Kv4.2-mediated IA [39–41]
[Huangqin] Radix Scutellariae	Wogonin	Spasmolysis	Enhancing expression of GABAA receptors [42]
[Zhizi] Fructus Gardeniae	Geniposide	Antioxidation	Decreasing TNF-a, IL-1β levels, and plasma expression of vascular pseudohemophilia factor [43]
[Chenpi] Pericarpium Citri Reticulatae	Tangeretin Nobiletin	Antiepileptic Antioxidation Neuroprotection	Decreasing TNF, IL-17, NF-κB, and MAPK levels [44]
[Gancao] Radix Et Rhizoma Glycyrrhizae	Carbenoxolone	Antiepileptic	Reduce cortical glial fibrillary acidic protein and connexin 43 expression [45]
[Tianzhuhuang] Concretio Silicea Bambusae	Amino acid	Antiepileptic Anticonvulsion Neuroprotection	Reduce IL-1β, ICAM-1, IL-8, NF-κB, GFAP, and TNF-a [46]
[Fushen] Poria cum Ligno Hospite	Triterpene	Tranquilization	Not clear

Table 4: Continued.

Chinese herbs	Active ingredients	Functions	Possible mechanism
[Yuanzhi] Radix Polygalae	(3-sinapoyl) fructofu-ranosyl-(6-sinapoyl) glucopyranoside 3,4,5-trimethoxy-cinnamic acid (TMCA)	Neuroprotection Antiepileptic	(1) Reduce Bax and increase Bcl-2 [47] (2) Enhancing expression of GABAA receptors [48]
[Baishao] Radix Paeoniae Alba	Paeoniflorin	Anticonvulsion Neuroprotection	(1) Suppress the elevation of c-Fos protein and increase transthyretin and phosphoglycerate mutase 1 [49] (2) Suppress the elevation of glutamate-induced intracellular Ca2 + [50]
[Yujin] Radix Curcumae	Curcumin	Antidepressant Improving-memory	Increase the expression of VEGF and its receptor FLK-1 [51]

antioxidation, enhancing GABA efficacy, regulating NMDA channels and sodium channels, and neuroprotection (Table 4).

4. Discussion

Through the analysis, we can know that the high-frequency Chinese medicinal herbs commonly used in the treatment of primary epilepsy were Ramulus Uncariae cum Uncis (Gouteng), Rhizoma Gastrodiae (Tianma), Rhizoma Acori Tatarinowii (Shichangpu), Bombyx Batryticatus (Jiangcan), Radix Paeoniae Alba (Baishao), and cicada, which can calm the liver, relieve shock, and calm the mind. They are effective, safe, and can be taken for a long time without significant side effects.

The main symptoms of epilepsy were convulsions, "all the wind was dizzy, all belong to the liver," "all the violent rigidity, all belong to the wind," so the treatment must start from the liver and the wind. The liver qi was smooth, and the accumulation of depression was avoided, the first thing of treating the liver was to soothe the liver and regulate qi; therefore, Radix Bupleuri (Chaihu), Radix Curcumae (Yujin), and Fructus Aurantii Immaturus were frequently used; in addition, the liver stores blood, if blood deficiency or blood stasis, the liver wind was easy to move and twitch, so the liver must nourish blood and activate blood, medicinal Radix Paeoniae Rubra, Radix Angelicae Sinensis, Rhizoma Chuanxiong, promoting blood circulation can calming liver wind; Rhizoma Pinelliae Praeparatum (Fabanxia), Pericarpium Citri Reticulatae, Poria, Dannanxing dryness, and phlegm; and Suanzaoren, Fushen, Radix Polygalae awakening and enlightening. Cortex moutan, Gardenia jasminoides, and Radix Scutellariae (Huangqin) Georgi clear away heat, relieve the fire caused by qi depression, and dispel phlegm and heat with expectorant herbs. The herb properties with the functions of calming the liver and relieving wind, clearing heat, promoting blood circulation, dryness, dampness, and resolving phlegm were mainly mild, warm, and cold. Epilepsy was difficult to be treated, which may easily suffer from chronic disease, qi depression, fire injury, bitter cold medicine clearing away heat, purging fire, and strengthening Yin. The herb of pungent and warm can help yang to activate qi, relieve qi depression, and help spleen transport at the same time.

Another major symptom of epilepsy was unconsciousness, which was located in the heart, "the heart dominates the mind," and the spirits were disturbed, resulting in loss of consciousness (coma). Phlegm heat and blood stasis were the most common causes of disturbance of the spirits, so resolving phlegm and promoting blood circulation, awakening, and opening the mind were the main points in the treatment of epilepsy. The liver wood transverses the spleen soil, the spleen loses healthy movement, the biochemical source of qi and blood was deficient, and the heart loses nourishment; the qi was abnormal, which affects the main qi function of the lung, and the pungent herb mainly enters the lung meridian; the herbs used mainly belong to the four meridians of liver, lung, heart, and spleen, which shows that Professor *Xiaocheng Yan*'s medication for epilepsy takes into account the characteristics of the liver, lung, heart, and spleen.

After cluster analysis of herbs, it was found that the treatment of epilepsy can be divided into three categories: dryness and dampness, relieve wind and relieve spasm, calm the heart, and tranquilize the mind. The first kind of herb has the main effect of dryness, dampness and phlegm, calm the heart, and calm the mind; the second kind of herb has the main effect of calm the liver and relieve wind, relieve spasm, and convulsions; the third kind of herb can regulate qi and calm nerves, calm shock, and resolve phlegm. The combination of Chinese medicinal herb commonly used by Professor *Xiaocheng Yan* in the treatment of primary epilepsy was found through association rules, included Ramulus Uncariae cum Uncis (Gouteng), Rhizoma Gastrodiae (Tianma), Rhizoma Acori Tatarinowii (Shichangpu), Polygala, Bombyx Batryticatus (Jiangcan), slough of cicada, Radix Bupleuri (Chaihu), Radix Scutellariae (Huangqin), and Radix Paeoniae Alba (Baishao). Yuan et al. [52] used the frequency analysis method in the ancient and modern medical case cloud platform (v2.2.2) to conduct data mining on the syndrome differentiation and medication rules of modern Chinese medicine in

the treatment of epilepsy. They concluded that Rhizoma Acori Tatarinowii(Shichangpu) ranked first in the high-frequency herbs, which was also Xiaocheng Yan's clinical high-frequency medication. Wang et al. [53] used Apriori algorithm to mine the medication rule of TCM in the database for the treatment of epilepsy and found that the medicine pair with the highest reliability and strong correlation was {Pericarpium Citri Reticulatae (Chenpi)} ≥ {Rhizoma Pinelliae Praeparatum (Fabanxia)}, which reflected the importance of drying dampness and resolving phlegm in the treatment of epilepsy by TCM. However, it only carried out data mining from the perspective of the literature, and the results have limitations. In comparison, the innovation of this study was that taking primary epilepsy as the research object, starting from the clinical effective cases, and using the absolute distance algorithm, we have achieved a better classification, and the results also confirm that it was in line with the clinical characteristics of Professor *Xiaocheng Yan*.

Zhang et al. [54] used the complex network algorithm to mine and analyze the diagnosis and treatment data of YingaoYu's treatment of epilepsy, found the relationship between medicine symptom and medicine treatment, and compared the dose range of core herbs used by adults and children, respectively. However, she did not analyze the pharmacological mechanism of the core prescription. In our study, the core prescriptions used in the treatment of primary epilepsy were obtained by complex network analysis, which were based on Tianma Gouteng decoction and Erchen decoction, including Uncinaria, Rhizoma Gastrodiae (Tianma), Bombyx Batryticatus (Jiangcan), Periostracum Cicadae (Chantui), Gardenia jasminoides, and Radix Scutellariae (Huangqin), which can suppressing hyperactive liver, calming endogenous wind, and relieving spasm; Radix Bupleuri (Chaihu), Rhizoma Pinelliae Praeparatum (Fabanxia), Pericarpium Citri Reticulatae, Tianzhu Huang, Yuanjin phlegm and qi; Rhizoma Acori Tatarinowii (Shichangpu), Radix Polygalae, and Poria can calming the heart and tranquilizing the mind. On this basis, we analyzed the main pharmacological mechanism of the core prescription furtherly, which were mainly reflected in anti-inflammatory, antioxidation, enhancing GABA efficacy, regulating NMDA channel and sodium channel, neuroprotection, and so on.

5. Conclusions

In this study, by collecting and sorting out Professor *Xiaocheng Yan*'s medical records in the treatment of primary epilepsy, standardizing the data of Chinese medicinal herb, and using the method of data mining to analyze the prescription data obtained, we obtained Professor *Xiaocheng Yan*'s commonly used herbs, herb attribute characteristics, compatibility rule, and core prescription composition in the treatment of primary epilepsy. It was found that Professor *Xiaocheng Yan*'s treatment of primary epilepsy was based on the principle of relieving wind and relieving spasm, dryness and dampness, and resolving phlegm. In addition, the mechanism and common adverse reactions of anti-epileptic Western herbs involved in Professor *Xiaocheng Yan*'s medical cases of treating primary epilepsy were summarized, and the main pharmacological mechanisms of core prescriptions were summarized and analyzed. It was hoped that this conclusion can provide a useful reference for the clinical treatment of primary epilepsy.

Data Availability

The data used to support the findings of this study are included within the article.

Disclosure

Some contents of this article were published in the form of conference papers in "IEEE CPS Press" (2021 IEEE International Conference on Bioinformatics and Biomedicine <BIBM>) [55].

Conflicts of Interest

The authors declared that there are no conflicts of interest regarding the publication of this article.

Authors' Contributions

Yu Zhang, Hongtao Li, and Pengfei Chang designed the research. Yu Zhang collected and processed the data. Yu Zhang and Hongtao Li analyzed the data. Lin Tong, Guangkun Chen, and Jingpeng Deng participated in intellectual discussions. Yu Zhang wrote the paper. All authors approved the final edited version of the manuscript.

Acknowledgments

This research was supported by Special Fund for Basic Scientific Research Business Expenses of Central Public Welfare Scientific Research Institutes (ZZ13-028 and ZC20202); Project of State Administration of Traditional Chinese Medicine (K0312); and National Key Research and Development Project (no. 2019YFC1709802).

References

[1] Chinese Medical Association, *Clinical Guidelines For Diagnosis and Treatment of Epilepsy*, People's Health Publishing House, Beijing, China, 2018.

[2] M. J. Brodie, "Road to refractory epilepsy: the glasgow story," *Epilepsia*, vol. 54, pp. 5–8, 2013.

[3] A. L. Miao and X. S. Wang, "Diagnosis and treatment of epilepsy," *Journal of Clinical Medicine*, vol. 13, no. 12, pp. 797–799, 2013.

[4] J. P. Jia and S. D. Chen, *Neurology*, People's Health Publishing House, Beijing, China, 2013.

[5] Y. F. Yang and L. B. Xia, *Diagnosis and Treatment of Epilepsy*, Shanxi Science and Technology Press, Taiyuan, China, 1997.

[6] X. Wu and D. L. Shen, "Refractory epilepsy," *Chinese Journal of Neurology*, vol. 311998, in Chinese.

[7] L. G. Wang, Q. H. He, and D. X. Jia, "Professor Sun Guangrong's ideas and methods of studying typical medical cases of contemporary famous traditional Chinese medicine," *Chinese Journal of traditional Chinese Medicine*, vol. 25, no. 6, pp. 885–887, 2010.

[8] X. C. Yan, *Xiaocheng Yan's Clinical Experience of Epilepsy*, Traditional Chinese Medicine Ancient Books Publishing House, Beijing, China, 2017.

[9] I. E. Scheffer, S. Berkovic, G. Capovilla et al., "ILAE classification of the epilepsies: position paper of the ILAE commission for classification and terminology," *Epilepsia*, vol. 58, no. 4, pp. 512–521, 2017.

[10] Compiled by the State Administration, *Traditional Chinese Medicine Diagnostic Efficacy Criteria of TCM Diseases and Syndromes*, Nanjing University Press, Nanjing, China, 1994.

[11] S. Zhong, *Traditional Chinese Medicine*, China Traditional Chinese Medicine Press, Beijing, China, 2016.

[12] Y. Cen, X. Pan, X. J. Gao, and X. Liu, "Palmprint recognition using MB-LBP algorithm and HOG algorithm," *Computer Application Research*, vol. 34, 2017, in Chinese.

[13] X. Z. Zhou, B. Y. Liu, Y. H. Wang, R. S. Zhang, N. L. Yao, and M. Cui, "Study on complex network method for compatibility of compound herbs," *Journal of Chinese Medicine*, vol. 15, 2008, in Chinese.

[14] R. A. Sarkis, Y. Goksen, Y. Mu, B. Rosner, and J. W. Lee, "Cognitive and fatigue side effects of anti-epileptic drugs: an analysis of phase III add-on trials," *Journal of Neurology*, vol. 265, no. 9, pp. 2137–2142, 2018.

[15] A. Verrotti, S. Lattanzi, F. Brigo, and G. Zaccara, "Pharmacodynamic interactions of antiepileptic drugs: from bench to clinical practice," *Epilepsy & Behavior*, vol. 104, Article ID 106939, 2020.

[16] A. F. Ambrósio, P. Soares-da-Silva, C. M. Carvalho, and A. P. Carvalho, "Mechanisms of action of carbamazepine and its derivatives, oxcarbazepine, BIA 2-093, and BIA 2-024," *Neurochemical Research*, vol. 27, pp. 121–130, 2002.

[17] C. Campo-Soria, Y. Chang, and D. S. Weiss, "Mechanism of action of benzodiazepines on GABAAreceptors," *British Journal of Pharmacology*, vol. 148, no. 7, pp. 984–990, 2006.

[18] G. Rosenberg, "The mechanisms of action of valproate in neuropsychiatric disorders: can we see the forest for the trees?" *Cellular and Molecular Life Sciences*, vol. 64, pp. 2090–2103, 2007.

[19] S. Noachtar, E. Andermann, P. Meyvisch, F. Andermann, W. B. Gough, and J. Schiemann-Delgado, "Levetiracetam for the treatment of idiopathic generalized epilepsy with myoclonic seizures," *Neurology*, vol. 70, pp. 607–616, 2008.

[20] G. Kenna, T. Lomastro, A. Schiesl, L. Leggio, and R. Swift, "Review of topiramate: an antiepileptic for the treatment of alcohol dependence," *Current Drug Abuse Reviewse*, vol. 2, no. 2, pp. 135–142, 2009.

[21] E. Hartl, M. Seethaler, M. Lauseker, J. Rémi, C. Vollmar, and S. Noachtar, "Impact of withdrawal of antiepileptic medication on the duration of focal onset seizures," *Seizure*, vol. 67, pp. 40–44, 2019.

[22] C.-L. Hsieh, J.-J. Lin, S.-Y. Chiang et al., "Gastrodia elata modulated activator protein 1 via c-Jun N-terminal kinase signaling pathway in kainic acid-induced epilepsy in rats," *Journal of Ethnopharmacology*, vol. 109, no. 2, pp. 241–247, 2007.

[23] H. Shao, Y. Yang, Z. Mi et al., "Anticonvulsant effect of rhynchophylline involved in the inhibition of persistent sodium current and NMDA receptor current in the pilocarpine rat model of temporal lobe epilepsy," *Neuroscience*, vol. 337, no. 337, pp. 355–369, 2016.

[24] Y. Liu, J. Gao, M. Peng et al., "A review on central nervous system effects of gastrodin," *Frontiers in Pharmacology*, vol. 9, pp. 1–18, 2018.

[25] L. Chen, X. Liu, H. Wang, and M. Qu, "Gastrodin attenuates pentylenetetrazole-induced seizures by modulating the mitogen-activated protein kinase-associated inflammatory responses in mice," *Neuroscience Bulletin*, vol. 33, pp. 264–272, 2017.

[26] H. Shao, Y. Yang, A.-p. Qi et al., "Gastrodin reduces the severity of status epilepticus in the rat pilocarpine model of temporal lobe epilepsy by inhibiting Nav1.6 sodium currents," *Neurochemical Research*, vol. 42, no. 2, pp. 360–374, 2017.

[27] W.-Y. Lo, F.-J. Tsai, C.-H. Liu et al., "Uncaria rhynchophylla up regulates the expression of MIF and cyclophilin A in kainic acid-induced epilepsy rats: a proteomic analysis," *The American Journal of Chinese Medicine*, vol. 38, pp. 745–759, 2010.

[28] H.-C. Hsu, N.-Y. Tang, C.-H. Liu, and C.-L. Hsieh, "Antiepileptic effect of uncaria rhynchophylla and rhynchophyl line involved in the initiation of c-Jun n-terminal kinase phosphorylation of MAPK signal pathways in acute seizures of kainic acid-treated rats," *Evidence-Based Complementary and Alternative Medicine*, vol. 2013, Article ID 961289, 9 pages, 2013.

[29] Y.-W. Lin and C.-L. Hsieh, "Oral uncaria rhynchophylla (UR) reduces kainic acid-induced epileptic seizures and neuronal death accompanied by attenuating glial cell proliferation and S100B proteins in rats," *Journal of Ethnopharmacology*, vol. 135, pp. 313–320, 2011.

[30] C.-H. Liu, Y.-W. Lin, N.-Y. Tang, H.-J. Liu, and C.-L. Hsieh, "Neuroprotective effect of uncaria rhynchophyllain kainic acid-induced epileptic seizures by modulating hippocampal mossy fiber sprouting, neuron survival, astrocyte proliferation, and S100B expression," *Evidence-Based Complementary and Alternative Medicine*, vol. 2012, Article ID 194790, 11 pages, 2012.

[31] T.-Y. Ho, N.-Y. Tang, C.-Y. Hsiang, and C.-L. Hsieh, "Uncaria rhynchophylla and rhynchophylline improved kainic acid-induced epileptic seizures via IL-1β and brain-derived neurotrophic factor," *Phytomedicine*, vol. 21, pp. 893–900, 2014.

[32] H. Liu, Z. Song, D.-G. Liao et al., "Anticonvulsant and sedative effects of eudesmin isolated from acorus tatarinowii on mice and rats," *Phytotherapy Research*, vol. 29, pp. 996–1003, 2015.

[33] C. Huang, W.-G. Li, X.-B. Zhang et al., "Alpha-asarone from Acorus gramineus alleviates epilepsy by modulating A-type GABA receptors," *Neuropharmacology*, vol. 65, pp. 1–11, 2013.

[34] K. Y. C. Lam, Q.-Y. Wu, W.-H. Hu et al., "Asarones from acori tatarinowii rhizoma stimulate expression and secretion of neurotrophic factors in cultured astrocytes," *Neuroscience Letters*, vol. 707, Article ID 134308, 2019.

[35] M. Hu, Y. Liu, L. He, X. Yuan, W. Peng, and C. Wu, "Antiepileptic effects of protein-rich extract from bombyx batryticatus on mice and its protective effects against H_2O_2-induced oxidative damage in PC12 cells via regulating PI3K/Akt signaling pathways," *Oxidative Medicine and Cellular Longevity*, vol. 2019, Article ID 7897584, 13 pages, 2019.

[36] L.-Y. He, M.-B. Hu, R.-L. Li et al., "The effect of protein-rich extract from bombyx batryticatus against glutamate-damaged PC12 cells via regulating γ-aminobutyric acid signaling pathway," *Molecules*, vol. 25, p. 553, 2020.

[37] C.-X. Deng, Z.-B. Wu, Y. Chen, and Z.-M. Yu, "Pinellia total alkaloids modulate the GABAergic system in hippocampal formation on pilocarpine-induced epileptic rats," *Chinese Journal of Integrative Medicine*, vol. 26, pp. 138–145, 2020.

[38] L. An, "Anticonvulsant effect of cicada decidua," *China Medical Herald*, vol. 5, no. 15, pp. 35-36, 2008.

[39] Y.-H. Yu, W. Xie, Y. Bao, H.-M. Li, S.-J. Hu, and J.-L. Xing, "Saikosaponin a mediates the anticonvulsant properties in the HNC models of AE and SE by inhibiting NMDA receptor current and persistent sodium current," *PLoS One*, vol. 7, 2012.

[40] M. Ye, Y.-F. Bi, L. Ding, W.-W. Zhu, and W. Gao, "Saikosaponin a functions as anti-epileptic effect in pentylenetetrazol induced rats through inhibiting mTOR signaling pathway," *Biomedicine & Pharmacotherapy*, vol. 81, pp. 281–287, 2016.

[41] Y. Hong, N. Deng, H.-N. Jin et al., "Saikosaponin a modulates remodeling of Kv4.2-mediated A-type voltage-gated potassium currents in rat chronic temporal lobe epilepsy," *Drug Design, Development and Therapy*, vol. 12, pp. 2945–2958, 2018.

[42] T. C. Diniz, J. C. Silva, S. R. G. D. Lima-Saraiva et al., "The role of flavonoids on oxidative stress in epilepsy," *Oxidative Medicine and Cellular Longevity*, vol. 2015, Article ID 171756, 9 pages, 2015.

[43] H. Wei, G. Duan, J. He et al., "Geniposide attenuates epilepsy symptoms in a mouse model through the PI3K/Akt/GSK-3β signaling pathway," *Experimental and Therapeutic Medicine*, vol. 15, pp. 1136–1142, 2018.

[44] X. F. Huang, G. Z. Yu, and J. J. Tong, "Analysis of pharmacological mechanism of tangerine peel based on network pharmacology," *Chinese Traditional Patent Medicine*, vol. 12, pp. 3038–3045, 2019.

[45] W. Chen, Z. Gao, Y. Ni, and Z. Dai, "Carbenoxolone pretreatment and treatment of posttraumatic epilepsy," *Neural Regeneration Research*, vol. 8, pp. 169–76, 2013.

[46] J. D. Han, *Neuroprotective Effect And Mechanism of Tongluo Huatan Capsule and its Active Components on Cerebral Ischemia-Reperfusion Injury*, Beijing University of Traditional Chinese Medicine, Beijing, China, 2012.

[47] Y. Hu, J. Li, P. Liu et al., "Protection of SH-SY5Y neuronal cells from glutamate-induced apoptosis by 3,6'-disinapoyl sucrose, a bioactive compound isolated from radix polygala," *Journal of Biomedicine and Biotechnology*, vol. 2012, Article ID 728342, 5 pages, 2012.

[48] C.-Y. Chen, X.-D. Wei, C.-R. Chen, and C. R. Chen, "3,4,5-Trimethoxycinnamic acid, one of the constituents of Polygalae Radix exerts anti-seizure effects by modulating GABAAergic systems in mice," *Journal of Pharmacological Sciences*, vol. 131, pp. 1–5, 2016.

[49] K. Kajiwara, K. Sunaga, T. Tsuda, A. Sugaya, E. Sugaya, and M. Kimura, "Peony root extract upregulates transthyretin and phosphoglycerate mutase in mouse cobalt focus seizure," *Biochemical and Biophysical Research Communications*, vol. 371, pp. 375–379, 2008.

[50] H. Hino, H. Takahashi, Y. Suzuki, J. Tanaka, E. Ishii, and M. Fukuda, "Anticonvulsive effect of paeoniflorin on experimental febrile seizures in immature rats: possible application for febrile seizures in children," *PLoS One*, vol. 7, no. 8, 2012.

[51] H. B. Qian, Y. Wang, and G. J. Huang, "Effects of wenyujin aqueous extract on behavior and angiogenesis in rats with post-stroke depression," *Shi Zhen, Guo Yi Guo Yao*, vol. 23, 2012, in Chinese.

[52] S. Y. Yuan and J. M. Liu, "The prescription rule of traditional chinese medicine for epilepsy by data mining," *Chinese Journal of Integrative Medicine on Cardio-Cerebrovascular Disease*, vol. 19, no. 23, pp. 4044–4049, 2021, in Chinese.

[53] J. H. Wang, H. L. Zhao, X. Jin, and L. Hou, "Data mining Chinese herbal medicine for epilepsy drugs analysis of "Chenpi-Banxia" and its network pharmacological mechanism," *Research and Development of Natural Products*, vol. 322020, in Chinese.

[54] N. N. Zhang, H. W. Zhou, R. F. Lin et al., "Analysis of Mr. YingaoYu's general treatment formula for epilepsy based on clinical diagnosis and treatment data," *Chinese Journal of Experimental Prescriptions*, vol. 26, 2020, in Chinese.

[55] Y. Zhang, L. Tong, G. K. Chen, J. P. Deng, and H. T. Li, "Analysis of medication rule of Professor Yan Xiaocheng on the treatment of primary epilepsy," in *Proceedings of the 2021 IEEE International Conference on Bioinformatics and Biomedicine (BIBM)*, pp. 3927–3933, Beijing, China, 2021.

Hindawi
Evidence-Based Complementary and Alternative Medicine
Volume 2022, Article ID 2056039, 9 pages
https://doi.org/10.1155/2022/2056039

Research Article

Chinese Clinical Named Entity Recognition with ALBERT and MHA Mechanism

Dongmei Li,[1,2] **Jiao Long**,[1,2] **Jintao Qu**,[1,2] **and Xiaoping Zhang**[3]

[1]*School of Information Science and Technology, Beijing Forestry University, Beijing 100083, China*
[2]*Engineering Research Center for Forestry-oriented Intelligent Information Processing, National Forestry and Grassland Administration, Beijing 100083, China*
[3]*Institute of Information on Traditional Chinese Medicine, China Academy of Chinese Medical Sciences, Beijing 100053, China*

Correspondence should be addressed to Xiaoping Zhang; xiao_ping_zhang@139.com

Received 17 March 2022; Accepted 29 April 2022; Published 23 May 2022

Academic Editor: Xuezhong Zhou

Traditional clinical named entity recognition methods fail to balance the effectiveness of feature extraction of unstructured text and the complexity of neural network models. We propose a model based on ALBERT and a multihead attention (MHA) mechanism to solve this problem. Structurally, the model first obtains character-level word embeddings through the ALBERT pretraining language model, then inputs the word embeddings into the iterated dilated convolutional neural network model to quickly extract global semantic information, and decodes the predicted labels through conditional random fields to obtain the optimal label sequence. Also, we apply the MHA mechanism to capture intercharacter dependencies from multiple aspects. Furthermore, we use the RAdam optimizer to boost the convergence speed and improve the generalization ability of our model. Experimental results show that our model achieves an F1 score of 85.63% on the CCKS-2019 dataset—an increase of 4.36% compared to the baseline model.

1. Introduction

Clinical named entity recognition (CNER) is a fundamental and crucial task in medical natural language processing problems. Researchers aim to identify and extract the clinical entity mentioned in electronic medical records (EMRs) and classify them into predefined categories (e.g., disease, symptom, and treatment). Additionally, extracting named entities from semistructured or unstructured EMRs is helpful for further research, such as building clinical decision support systems and medical knowledge graphs.

Recent developments of deep learning (DL) have led to their overwhelming performances in the field of natural language processing. At the same time, researchers have adopted DL methods on biomedical tasks [1–4]. Compared with traditional rules and dictionary-based methods or machine learning (ML) methods [5–7], DL methods have the advantage of stronger generalization ability and less reliance on rule design or feature engineering. In particular, the bidirectional long short-term memory with conditional random field (BiLSTM-CRF) method [8, 9] has achieved significant results in CNER [10–12]. However, the word-level BiLSTM model cannot solve the problem of error propagation caused by the wrong entity boundary recognition, nor can it make full use of the parallelism of the graphics processing unit (GPU). Also, the entities in Chinese EMRs have a unique and rigorous language structure [13], which makes Chinese CNER more challenging.

To solve the above problems, Strubell et al. [14] proposed an iterated dilated convolutional neural network (IDCNN) model for named entity recognition, which simultaneously improved training speed and accuracy. Gao et al. [15] used an attention-based IDCNN-CRF model for the CNER task and demonstrated the effectiveness of combining word order features and local context. However, this approach does not effectively integrate the contextual semantic information of a sentence, nor does it accurately represent polysemous words. Li et al. [16] proposed the BERT-BiLSTM-CRF model, which

incorporated dictionary features and radical features of Chinese characters to improve model performance. However, the model's stringent requirements for the quality of dictionary and storage space limit its performance in actual scenarios. Fang et al. [17] developed an end-to-end neural network based on a multi-head attention (MHA) mechanism and two hint mechanisms for the joint extraction model of entities and relations. The model outperformed the state-of-the-art methods of joint entity and relation extraction.

For the Chinese CNER task, we propose the ALBERT-IDCNN-MHA-CRF model. This paper's main contributions are as following:

(1) We fine-tune the ALBERT pretraining model to enhance the semantic representation.

(2) We use the IDCNN model to encode the global information of the entity and speed up the training process.

(3) We use a multi-head attention mechanism to capture the context information.

(4) We use the RAdam optimizer to boost the convergence speed and improve the model's generalization ability.

(5) The evaluation results show that our model achieves good performance on the CCKS-2019 datasets.

2. Related Work

At present, the methods for the CNER task are divided into three categories: rule-based and dictionary-based methods, ML-based methods, and DL-based methods [18].

Rule-based and dictionary-based methods have been mainly used in the early CNER system and related applications. They rely only on existing dictionaries and manually constructed rules, which cause problems of long system development cycles and poor portability for complex and diverse entities in EMRs. In contrast to the above methods, the ML-based method has good versatility, which regards the CNER task as a sequence labeling problem and uses a large-scale corpus to label each position of the sentence. Classical ML methods such as the hidden Markov model, maximum entropy Markov model, support vector machine, and CRF are widely used in the CNER task. Nevertheless, constructing a large-scale labeled corpus in the early stage is costly, and the high dependence on manual feature engineering is time-consuming.

Recently, methods based on DL have been successfully applied to the CNER task. The BiLSTM-CRF method achieved the most advanced performance on many CNER datasets. However, the time series-based calculation in the LSTM model could not achieve efficient parallelism, and it is challenging to capture the long-term dependence between characters in the face of long sentences. For large-scale electronic medical record corpora, there have been problems with high model complexity and slow training speed. Therefore, researchers have attempted to use the CNN method to effectively capture contextual semantic information while taking full advantage of GPU parallelism to improve the model efficiency.

Unfortunately, the above DL-based methods failed to distinguish ambiguous characters or words. For example, the character "清" (clean) has completely different meanings in the two sentences of "患者神志清、精神可" (the patient is conscious and in good spirits) and "于我院行淋巴结清扫术" (lymph node dissection in our hospital), but they would be mapped to the same vector in static word embedding representation methods (such as Word2Vec). So, it could not consider the contextual semantic information of the sentence.

In recent years, many pretrained contextual word embedding models have been proposed, such as EMLo and OpenAI-GPT. However, the above two pretraining models cannot simultaneously obtain the semantic information of the EMRs in the front and back directions. Bidirectional encoder representations from transformers (BERTs) solve the above problems well. For the CNER task, we only need to set the downstream task interface and use the relevant data to fine-tune the model to obtain a more accurate embedded representation of each word in the EMRs. Cai [19] first enhanced the semantic representation of characters through BERT, further inputting the word embedding into BiGRU-CRF for training, and finally achieved better performance. Zhang et al. [20] pretrained BERT on the corpus of Chinese clinical text and used the embedding as input features of BiLSTM-CRF to solve the breast cancer CNER problem, and achieved an F1 score of 93.53%.

BERT had excellent performance in CNER, which mainly benefited from its "overparameterized" nature. Owing to its millions or even billions of parameters, its computational efficiency is low, which greatly hinders its application in actual CNER systems. Therefore, researchers have begun to study on compressing BERT's size with an acceptable tradeoff on performance to speed up the training progress. Sun et al. [21] outlined a "patient knowledge distillation" method by compressing the model into a lightweight shallow network. Fan et al. [22] proposed LayerDrop, a structured dropout method, to train the transformer model. Without fine-tuning, they sampled subnetwork from the original model through a pruning strategy to generate a high-quality small BERT model. Shen et al. [23] proposed a new group-by-group quantization scheme and compressed the model with Hessian-based mixed-precision quantization. The ALBERT model proposed by Lan et al. [24] applied two parameter-reduction techniques to reduce memory consumption and improve the training speed of BERT while using a self-supervised loss to improve the training effect.

3. Materials and Methods

Figure 1 illustrates the overall ALBERT-IDCNN-MHA-CRF network architecture of our model. First, for each Chinese character of EMRs, the character, sentence, and position features are computed by ALBERT. Second, we concatenate the three embeddings and feed them into the IDCNN network to extract the global features, and then input the embeddings to the MHA layer to capture the long-distance dependencies between characters by calculating the attention probability of sentences from multiple aspects. Finally, we concatenate the output vector of the MHA layer into a

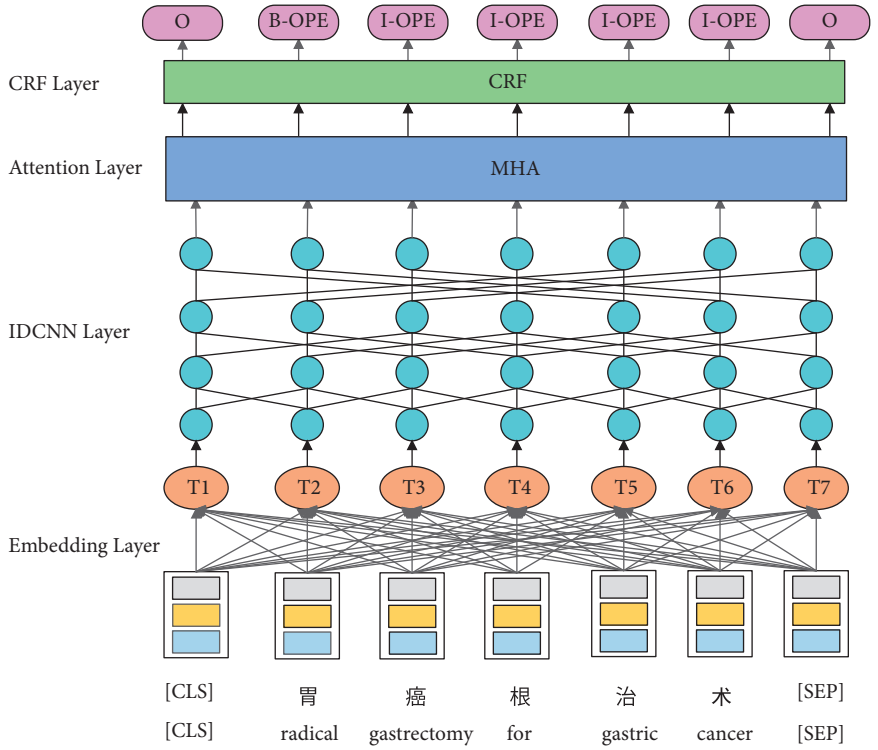

Figure 1: Main architecture of our ALBERT-IDCNN-MHA-CRF model.

CRF layer, which constrains the dependency relationship between the prediction labels and obtains the best label sequence. To improve the generalization ability of the model, we add a dropout layer between the embedding layer and the IDCNN layer.

3.1. Embedding. Language modeling is a key concept in natural-language processing tasks. While BERT enjoys an outstanding performance in CNER, its overparameterization leads to a large memory footprint and time consuming.

Compared with BERT, ALBERT has mainly made improvements in three aspects: factorized embedding parameterization, cross-layer parameter sharing, and intersentence coherence loss, which remarkably reduces the total number of parameters and reduces the model's complexity.

For each word in the EMRs, the input representation of ALBERT consists of three parts: token embedding, segment embedding, and position embedding. Token embedding represents a word vector that can be either a word vector or a character vector in the Chinese language. Owing to the unique sublanguage characteristics and complex language structure of EMRs, we use character embedding for representation. Segment embedding is used to distinguish pairs of sentences. Position embedding is the position information obtained from the model learning. The calculation equation is:

$$PE_{(pos,2i)} = \sin\left(\frac{pos}{10000^{2i/d_{\text{model}}}}\right),$$
$$PE_{(pos,2i+1)} = \cos\left(\frac{pos}{10000^{2i/d_{\text{model}}}}\right), \quad (1)$$

where pos is the position in EMR, i is the dimension, and d_{model} is the vector dimension after encoding. Figure 2 shows an example of this input.

3.2. IDCNN. To effectively extract the text features of EMRs, while speeding up the training process and improving prediction efficiency, this study uses the IDCNN model for feature extraction. Dilated convolution was originally applied in the field of image processing. Unlike traditional CNNs, it uses the dilation width between the convolution kernels without the pooling operation to reduce information loss and increase the receptive field. The receptive field of dilated convolution is calculated as

$$F_{i+1} = \left(2^{i+2} - 1\right) \times \left(2^{i+2} - 1\right). \quad (2)$$

Here, we use four identical blocks of dilated convolution. Each block has three dilated convolution layers with dilation widths of 1, 1, and 2. Thus, there are four iterations, where each iteration takes the previous result as the input. This parameter-sharing mechanism effectively prevents overfitting. As the number of layers increases, the receptive field increases exponentially, while the parameters increase linearly so that the receptive field quickly covers all input sequences. In the IDCNN model, the parameters of each layer are independent and of the same scale, which effectively reduces the parameters during training, and thereby speed up the training.

The IDCNN model encodes each character in EMRs and extracts the features in the text to generate corresponding feature vector. Although the encoded vector contains long-

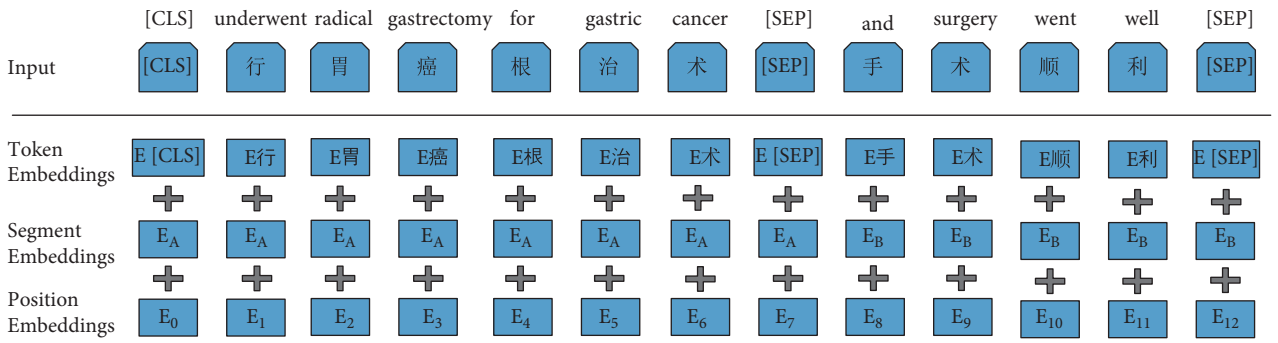

Figure 2: Input example.

distance semantic features, these features share the same weight and cannot solve the problem of different correlations between characters. Hence, further feature extraction is required through the multi-head attention layer.

3.3. MHA. Since the entities in EMRs do not exist in isolation, there are specific dependencies between each other, accompanying a long interval between the characters of the entity. For example, in the sentence "患者因胃癌于2015-5-19于我院行胃癌根治术, 术后恢复良好" (the patient underwent radical gastrectomy for gastric cancer in our hospital on May 19, 2015, and recovered well after the operation.), "胃癌"(gastric cancer) belongs to the disease entity, and "胃癌根治术" (radical gastrectomy for gastric cancer) represents the operation entity. These two entities often appear in the same EMR, suggesting a certain dependence between them.

To capture this dependency, the model has to pay more attention to the characters dependent on the current character and assigns higher weights to these dependent characters and smaller weights to other irrelevant characters so as to recognize the entity type of the character better.

Here, we pick the MHA model for multiple self-attention calculations in order to learn relevant information in different representation subspaces. The MHA model also ensures parallel computing performance superior to recurrent neural networks. Scaled dot-product attention in the model is defined as

$$\text{Attention}(Q, K, V) = \text{soft max}\left(\frac{QK^T}{\sqrt{d_k}}\right)V, \tag{3}$$

where the query Q, key K, and value V are all in vector form, $1/\sqrt{d_k}$ is the k-dimension adjustment smoothing term, and the softmax function value is the normalization factor. We set $Q = K = V$ when calculating self-attention, which represents the characters in the sentence.

In the CNER task, for an input sentence $X = (x_1, x_2, \ldots, x_n)$, the output after IDCNN layer is $Y = (Y_1, Y_2, \ldots, Y_n)$. For the output state Y_t of the t-th character in the sentence, the single-head self-attention calculation is performed using formula (4). A total of h calculations are performed, and the result of the i-th calculation is head_i.

$$\text{head}_i = \text{Attention}\left(Y_t W_i^Q, Y_t W_i^K, Y_t W_i^V\right), \tag{4}$$

where $W_i^Q \in \mathbb{R}^{d_{\text{model}} \times d_k}$, $W_i^K \in \mathbb{R}^{d_{\text{model}} \times d_k}$, and $W_i^V \in \mathbb{R}^{d_{\text{model}} \times d_k}$ are weight matrices of the i-th calculation.

After concatenating the calculation results of these h times and performing a linear transformation, the result of the t-th character in the sentence is obtained, which is given by

$$MHA_t = \text{concat}(\text{head}_1, \text{head}_2, \ldots, \text{head}_h)W^O, \tag{5}$$

where concat is the splicing function and $W^O \in \mathbb{R}^{hd_v \times d_{\text{model}}}$ is the weight parameter.

3.4. CRF. The output of the MHA layer is the probability or score of each label corresponding to each character in the sentence. Denote the scoring matrix by P. If the label is modeled and output independently, the dependency between labels is ignored (for example, the "I-CHE" label cannot be immediately followed by the "B-DIS" label), which is essential information for the decoding module. Therefore, we introduce the CRF layer for label decoding, which constrains the dependency relationship between predicted labels to decode the global optimal label sequence.

For a given input sequence $X = (x_1, x_2, \ldots, x_n)$, and the corresponding label sequence $y = (y_1, y_2, \ldots, y_n)$, let W be the transition matrix, the evaluation score is defined as

$$S(X, y) = \sum_{i=1}^{n} P_{i,y_i} + \sum_{i=0}^{n} W_{y_i, y_{i+1}}, \tag{6}$$

where $P_{i,j}$ is the score of the i-th character labeled as label j, and $W_{i,j}$ is the state transition score from label i to label j.

Given X, the conditional probability of the sequence label y is calculated through the softmax function:

$$P(y|X) = \frac{e^{S(X,y)}}{\sum_{\widetilde{y} \in Y_x} e^{S(X,\widetilde{y})}}, \tag{7}$$

where Y_x is all possible label sequences of sentence X.

During training, we maximize the log likelihood of the correct label sequence:

$$\log P(y|X) = S(X, y) - \log\left(\sum_{\widetilde{y} \in Y_x} e^{S(X,\widetilde{y})}\right). \tag{8}$$

Table 1: Statistics of different types of entities for the CCKS-2019.

	Disease	Exam	Test	Operation	Drug	Anatomy	Sum
Train	2116	222	318	765	456	1486	5363
Test	682	91	193	140	263	447	1816

While decoding, we predict the sequence of labels with the highest conditional probability and use the Viterbi algorithm to decode the optimal label sequence.

$$y^* = \underset{\widetilde{y} \in Y_x}{\operatorname{argmax}} S(X, \widetilde{y}). \tag{9}$$

4. Results and Discussion

4.1. Dataset and Annotation Strategy. We run the experiments on the CCKS-2019 Task 1 benchmark dataset released by the 2019 China Conference on Knowledge Graph and Semantic Computing for a task about Chinese CNER. There are 1,000 records as the training dataset and 379 as the test dataset with six types of entities, i.e., disease, exam, test, operation, drug, and anatomy. Table 1 lists the statistics of the entities of different types.

Here, we represent the entities with "BIO" (B-begin, I-inside, O-outside) tags in the following formats: B-X, I-X and O. B represents the starting position of the medical entity, I represents the remaining part of the medical entity, and O represents the nonmedical entity. X is the type of medical entity, which could be DIS, EXA, TES, OPE, DRU, and ANA.

4.2. Experimental Settings. Each clinical record may contain several sentences, leading to a too-long sample if we treat a record as a whole. Hence, we separate each record by a period to restrict the sentence length. After cutting the records, we set the maximum sequence length to 128. The IDCNN consists of 128 filters and the number of heads in MHA is 4. During training, we use the back-propagation algorithm and Adam optimizer with an initial learning rate of 3×10^{-5}. The word embedding size is 128, and the activation function is ReLU. Also, the batch size is 20 and the dropout rate is 0.5.

4.3. Results and Analysis

4.3.1. Comparison with Basic Models. To verify the effectiveness of the ALBERT-IDCNN-MHA-CRF, we compare the model with the following models:

(a) BiLSTM-CRF: a model based on BiLSTM and CRF. In this model, the dimension of the Word2Vec static word vector is 128.

(b) IDCNN-CRF: a model based on IDCNN and CRF. In this model, the dimension of the Word2Vec static word vector is 128.

(c) IDCNN–MHA-CRF: a model adding the MHA layer based on (b).

Table 2: Results of different models.

Method	P (%)	R (%)	F1 (%)
BiLSTM-CRF(Baseline)	79.79	82.81	81.27
IDCNN-CRF	80.37	82.65	81.49
IDCNN-MHA-CRF	82.16	82.81	82.48
ALBERT-IDCNN-CRF	82.70	84.03	83.36
ALBERT-IDCNN-MHA-CRF	**83.46**	**85.96**	**84.69**

The best result on each metric is shown in bold face.

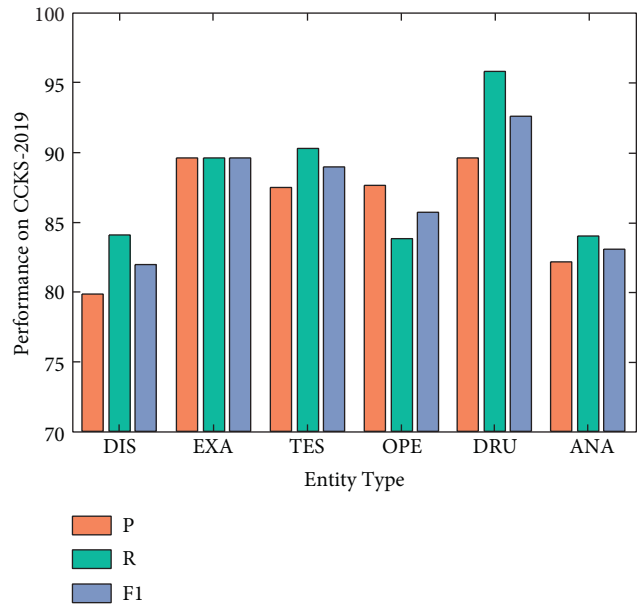

Figure 3: Results on different types of entities.

(d) ALBERT-IDCNN-CRF: a model adding the ALBERT pretraining model and fine-tuning based on (b).

Table 2 lists the experimental results of the different models. The experimental results show that our model's precision, recall and F1 score reach the highest values among the counterparts, with an increase of 3.67%, 3.15%, and 3.42%, respectively, from the baseline model, verifying the effectiveness of our model. The F1 scores of BiLSTM-CRF and IDCNN-CRF models are 81.27% and 81.49%, respectively, indicating that the recognition effects of the two models are equivalent. However, the 21-seconds-shorter per epoch running time demonstrates a better parallel computing power of IDCNN than BiLSTM. After adding the MHA layer, the F1 score increases by 0.99% (compared to 81.49%) and 1.33% (compared to 83.36%), respectively, which outlines the MHA's ability on extracting the contextual features. Also, replacing the traditional word vector model with fine-tuned ALBERT improves the F1 score by 1.87% (compared to 81.49%) and 2.21% (compared to 82.48%), respectively. This result has further strengthened our confidence that ALBERT has better semantic representation ability and has a more significant impact on the performance of the CNER task.

In addition to observing the evaluation metrics of the test dataset, we take a closer look at the predicted results. Figure 3 reports the performance of the proposed model on different types of clinical entities. The plot reveals that the

Table 3: Error samples.

Prediction	True entity
肝细胞性肝癌 (hepatocellular carcinoma)	(左肝)肝细胞性肝癌(中度分化) ((left liver) hepatocellular carcinoma (moderately differentiated))
胃癌 (gastric cancer)	胃癌根治术 (radical gastrectomy for gastric cancer)
肾上腺 (adrenal gland)	左肾上腺 (left adrenal gland)
淋巴结 (lymph nodes)	腹主动脉旁淋巴结 (abdominal para-aortic lymph nodes)

Table 4: Summary of different optimizers.

Optimizer	Year	Learning rate	Gradient
AdaGrad	2011	√	×
RMSprop	2012	√	×
Adam	2014	√	√
Lookahead + Adam	2019	√	√
RAdam	2019	√	√

"√" means dynamic adjustment, "×" means not.

Table 5: Results on different optimizers.

Optimizer	P (%)	R (%)	F1 (%)
AdaGrad	78.12	80.99	79.53
RMSprop	80.62	83.71	82.13
Adam	83.46	85.96	84.69
Lookahead + Adam	83.69	85.8	84.74
RAdam	**84.82**	**86.46**	**85.63**

The best result on each metric is shown in bold face.

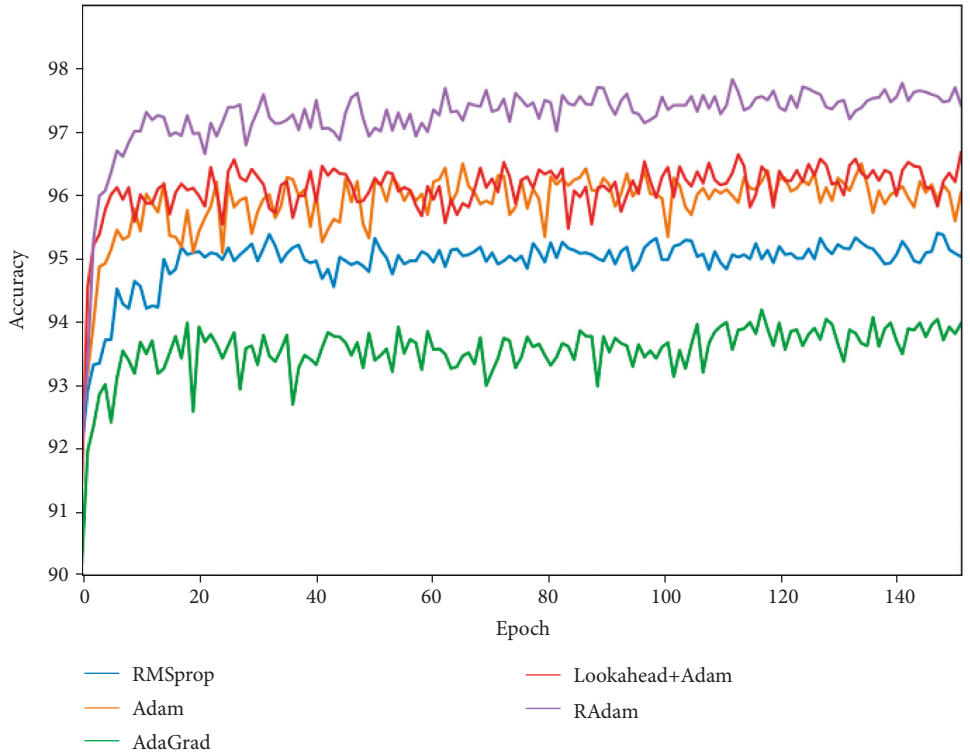

Figure 4: Comparison of the performance of different optimizers.

model performed well on drug and exam, reaching F1 scores of 92.62% and 89.66%, respectively, but fails to identify disease and anatomy effectively. After observing the errors, Table 3 lists the representative errors. First, these two types of entities are generally long, and supplementary information is in parentheses. For example, "(左肝)肝细胞性肝癌(中度分化)" ((left liver) hepatocellular carcinoma (moderately differentiated)), "腹主动脉旁淋巴结" (abdominal para-aortic

Table 6: Comparison with state-of-the-art models.

Team name	Method	F1 (%)
Alihealth	BBC + BBT + FBBC + rule	85.62
THU_MSIIP	Ensemble	85.59
DUTIR	ELMO + BiLSTM-CRF	85.16
Jfhealthcare	—	84.85
Suda-hlt	—	84.12
ZJUCST	—	83.80
Ours	ALBERT-IDCNN-MHA-CRF	**85.63**

The best result is shown in bold face.

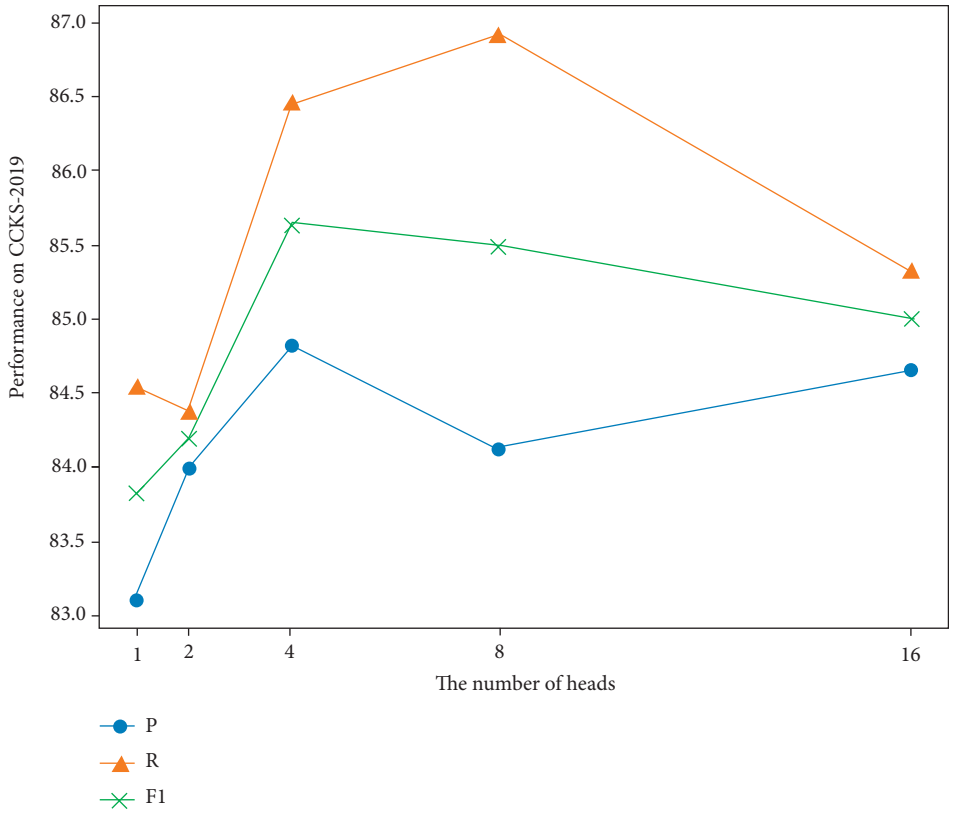

Figure 5: Influence of the number of heads.

lymph nodes). Therefore, when predicting this type of entity, there is a problem with boundary prediction errors, which leads to entity recognition errors. Second, some disease entities and operation entities are similar in text structure or nesting phenomena, resulting in the misclassification of this type of entity. As an illustration, among "胃癌" (gastric cancer) and "胃癌根治术" (radical gastrectomy for gastric cancer), the former belongs to the disease entity, while the latter is an operation entity. Third, the complex features of the two types of entities complicate the recognition.

4.3.2. Comparison of Different Optimizers. We run the above experiment with Adam optimizer. Furthermore, we explore the influences of the Adagrad [25], RMSprop [26], Lookahead [27]+Adam, and RAdam [28] optimizers on entity recognition. Table 4 presents how each optimizer improves the learning rate and gradient.

Applying the above optimizers to our model, Table 5 shows the experimental results, and Figure 4 shows the accuracy rate changes. The results identify that combining the dynamic adjustment of the gradient components is better than the one of dynamically adjusting the learning rate. Compared with the Adam baseline method, the performance is slightly improved after adding Lookahead, and its convergence speed is faster, which verifies the effectiveness of its exploration and integration strategy. We obtain the best model with the RAdam optimizer, whose F1 score reaches 85.63% and has an increase of 0.94% compared to Adam. The dynamic rectifier in RAdam adjusts Adam's adaptive momentum according to the variance and provides an automatic warm-up mechanism with regard to the dataset.

4.3.3. Comparison with State-of-the-Art Models. Table 6 lists the test results of the other methods on the CCKS-2019 dataset [29]. The DUTIR team used the ELMO model to learn the contextual embedding representation of characters; then, it identified medical entities through the BiLSTM-CRF network; furthermore, it improved the model performance through transfer learning. The THU_MSIIP team used multiple different types of deep neural network models to complementarily introduce multiaspect information and used a postprocessing model based on dictionaries and context models to supplement. The Alihealth team proposed a method based on BERT and model fusion and constructed a series of rules through frequent pattern mining. However, the weak generality of those rules limited the scope of application. With RAdam optimizer, we achieve the best performance with an F1 score of 85.63%, and outperform other teams.

4.3.4. Influence of the Number of Heads in MHA. The MHA layer can extract features from multiple aspects as different head can extract different features. To explore the influence of the most important hyperparameter on our model, recall that h is the number of heads, we set its value to 1, 2, 4, 8, and 16, respectively. We illustrate the results in Figure 5.

Figure 5 highlights the impact of h, where the performance improves as h increases from 1, since the text features are not fully extracted when h is small. On the other hand, the model learns too much redundant information when h is too large, harming the entity recognition. Therefore, by exploiting the value of h, we obtain the optimal performance when h is equal to 4.

5. Conclusions

This paper proposes a named entity recognition method, ALBERT-IDCNN-MHA-CRF, for the Chinese CNER task. The ALBERT pretraining language model more accurately represents contextual semantics in EMRs. Encoding entities through IDCNN achieves better recognition results, and the training speed has been improved. MHA captures rich semantic information in sentences. Furthermore, the RAdam optimizer benefits the performance. The proposed model achieves an F1 score of 85.63% on the CCKS-2019 dataset, superior to the state-of-the-art models. In future work, we will enrich the semantic representation of the embedding layer and introduce other features into the model. We will also consider the impact of nested entities to predict the boundaries of entities more accurately, thereby improving the overall entity recognition effect.

Data Availability

The data used to support the findings of this study are available from the corresponding author upon request.

Conflicts of Interest

The authors declare that there are no conflicts of interest regarding the publication of this paper.

Acknowledgments

This work was supported by the Fundamental Research Funds for the Central Public Welfare Research Institutes under grant ZZ140319-W and the National Nature Science Foundation of China under grant no. 61772078.

References

[1] N. Greenberg, T. Bansal, P. Verga, and A. McCallum, "Marginal likelihood training of BiLSTM-CRF for biomedical named entity recognition from disjoint label sets," in *Proceedings of the 2018 Conference on Empirical Methods in Natural Language Processing*, Brussels, Belgium, October 2018.

[2] Q. Zhu, X. Li, A. Conesa, and C. Pereira, "GRAM-CNN: a deep learning approach with local context for named entity recognition in biomedical text," *Bioinformatics*, vol. 34, no. 9, pp. 1547–1554, 2018.

[3] S. K. Hong and J. G. Lee, "DTranNER: biomedical named entity recognition with deep learning-based label-label transition model," *BMC Bioinformatics*, vol. 21, no. 1, pp. 53–11, 2020.

[4] Y. Zhang, Z. Liu, and W. Zhou, "Biomedical named entity recognition based on self-supervised deep belief network," *Chinese Journal of Electronics*, vol. 29, no. 3, pp. 455–462, 2020.

[5] D. Li, G. Savova, and K. Kipper, "Conditional random fields and support vector machines for disorder named entity recognition in clinical texts," in *Proceedings of the Workshop on Current Trends in Biomedical Natural Language Processing*, Stroudsburg, PA, USA, June 2008.

[6] A. L. Minard, A. L. Ligozat, A. Ben Abacha et al., "Hybrid methods for improving information access in clinical documents: concept, assertion, and relation identification," *Journal of the American Medical Informatics Association: JAMIA*, vol. 18, no. 5, pp. 588–593, 2011.

[7] Y. Xu, J. Hua, Z. Ni et al., "Anatomical entity recognition with a hierarchical framework augmented by external resources," *PLoS One*, vol. 9, no. 10, Article ID e108396, 2014.

[8] Z. Huang, W. Xu, and K. Yu, "Bidirectional LSTM-CRF models for sequence tagging," 2015, https://arxiv.org/abs/1508.01991.

[9] C. S. Gao, J. F. Zhang, W. P. Li, W. Zhao, and S. K. Zhang, "A joint model of named entity recognition and coreference resolution based on hybrid neural network," *Acta Electronica Sinica*, vol. 48, no. 3, pp. 28–34, 2020.

[10] N. Lu, J. Zheng, W. Wu, Y. Yang, K. Chen, and W. Hu, "Chinese clinical named entity recognition with word-level information incorporating dictionaries," in *Proceedings of the 2019 International Joint Conference on Neural Networks (IJCNN)*, Budapest, Hungary, July 2019.

[11] Q. Wang, Y. Zhou, T. Ruan, D. Gao, Y. Xia, and P. He, "Incorporating dictionaries into deep neural networks for the Chinese clinical named entity recognition," *Journal of Biomedical Informatics*, vol. 92, Article ID 103133, 2019.

[12] J. Wu, D. R. Shao, J. H. Guo, Y. Cheng, and G. Huang, "Character-based deep learning approaches for clinical named entity recognition: a comparative study using Chinese EHR texts," in *Proceedings of the International Conference on Smart Health*, Shenzhen, China, July 2019.

[13] J. Yang, Q. Yu, Y. Guan, and Z. Jiang, "An overview of research on electronic medical record oriented named entity

recognition and entity relation extraction," *Acta Automatica Sinica*, vol. 40, no. 8, pp. 1537–1562, 2014.

[14] E. Strubell, P. Verga, D. Belanger, and A. McCallum, "Bidirectional LSTM-CRF models for sequence tagging," 2017, https://arxiv.org/abs/1702.02098.

[15] M. Gao, Q. Xiao, S. Wu, and K. Deng, "An attention-based ID-CNNs-CRF model for named entity recognition on clinical electronic medical records," in *Proceedings of the International Conference on Artificial Neural Networks*, Munich, Germany, September 2019.

[16] X. Li, H. Zhang, and X. H. Zhou, "Chinese clinical named entity recognition with variant neural structures based on BERT methods," *Journal of Biomedical Informatics*, vol. 107, Article ID 103422, 2020.

[17] C. H. Fang, Y. L. Chen, M. Y. Yeh, and Y. S. Lin, "Multi-head attention with hint mechanisms for joint extraction of entity and relation," in *Proceedings of the International Conference on Database Systems for Advanced Applications*, Taipei, Taiwan, April 2021.

[18] Z. Wu, K. Bai, L. Yang, Y. Wang, and Y. Tian, "Review on text mining of electronic medical record," *Journal of Computer Research and Development*, vol. 58, no. 3, pp. 513–527, 2021.

[19] Q. Cai, "Research on Chinese naming recognition model based on BERT embedding," in *Proceedings of the IEEE 10th International Conference on Software Engineering and Service Science (ICSESS)*, Beijing, China, October 2019.

[20] X. Zhang, Y. Zhang, Q. Zhang et al., "Extracting comprehensive clinical information for breast cancer using deep learning methods," *International Journal of Medical Informatics*, vol. 132, Article ID 103985, 2019.

[21] S. Sun, Y. Cheng, Z. Gan, and J. Liu, "Patient knowledge distillation for bert model compression," 2019, https://arxiv.org/abs/1908.09355.

[22] A. Fan, E. Grave, and A. Joulin, "Reducing transformer depth on demand with structured dropout," 2019, https://arxiv.org/abs/1909.11556.

[23] S. Shen, Z. Dong, J. Ye et al., "Q-bert: Hessian based ultra low precision quantization of bert," *Proceedings of the AAAI Conference on Artificial Intelligence*, vol. 34, no. 5, pp. 8815–8821, 2020.

[24] Z. Lan, M. Chen, S. Goodman, K. Gimpel, P. Sharma, and R. Soricut, "Albert: A Lite bert for self-supervised learning of language representations," 2019, https://arxiv.org/abs/1909.11942.

[25] J. Duchi, E. Hazan, and Y. Singer, "Adaptive subgradient methods for online learning and stochastic optimization," *Journal of Machine Learning Research*, vol. 12, no. 7, pp. 257–269, 2011.

[26] G. Hinton, N. Srivastava, and K. Swersky, "Neural networks for machine learning lecture 6a overview of mini-batch gradient descent," 2012, https://www.cs.toronto.edu/~tijmen/csc321/slides/lecture_slides_lec6.pdf.

[27] M. Zhang, J. Lucas, J. Ba, and G. E. Hinton, "Lookahead optimizer: k steps forward, 1 step back," *Advances in Neural Information Processing Systems*, vol. 32, 2019.

[28] L. Liu, H. Jiang, P. He et al., "On the variance of the adaptive learning rate and beyond," 2019, https://arxiv.org/abs/1908.03265.

[29] X. Han, Z. Wang, J. Zhang et al., "Overview of the CCKS 2019 knowledge graph evaluation track: Entity, relation, event and QA," 2020, https://arxiv.org/abs/2003.03875.

Hindawi
Evidence-Based Complementary and Alternative Medicine
Volume 2022, Article ID 6408073, 16 pages
https://doi.org/10.1155/2022/6408073

Research Article

Network Meta-Analysis of Acupoint Catgut Embedding in Treatment of Simple Obesity

Zhuo-yuan Wang,[1,2] Xiao-yan Li,[1,2] Xiao-jun Gou,[1,2] Chun-lan Chen,[1,2] Zun-yuan Li,[1,2] Chuang Zhao,[1,2] Wen-ge Huo,[1,2] Yu-hong Guo,[1,2] Yan Yang,[1,2] and Zhi-dan Liu[1,2]

[1]*Baoshan Hospital affiliated to Shanghai University of Traditional Chinese Medicine, Shanghai 201999, China*
[2]*Baoshan District Hospital of Integrated Traditional Chinese and Western Medicine of Shanghai, Shanghai 201999, China*

Correspondence should be addressed to Xiao-yan Li; lxy_0220@163.com and Xiao-jun Gou; gouxiaojun1975@163.com

Received 24 February 2022; Accepted 10 May 2022; Published 23 May 2022

Academic Editor: Jianan Xia

Objective. To evaluate the clinical efficacy of acupoint catgut embedding in the treatment of simple obesity through network meta-analysis. *Methods*. PubMed, Cochrane, Embase, China National Knowledge Infrastructure (CNKI), Wanfang, and VIP database (VIP) were searched by using computer from 2011 to August 2021, and 35 RCT studies were retrieved. The quality of the literature was evaluated using the modified Jadad scoring table, and Stata 15.0 software was used for traditional meta-analysis and network meta-analysis. *Results*. Thirty-five RCTs (3040 cases in total) were included. Acupoint embedding, acupuncture, electroacupuncture, TCM, acupoint embedding + acupuncture, acupoint embedding + exercise diet therapy, acupoint embedding + TCM, exercise diet therapy, acupoint embedding + moxibustion, and acupoint embedding + cupping were investigated in the studies. The results of network meta-analysis were as follows: in terms of total effective rate, acupoint catgut embedding was superior to acupuncture, electroacupuncture, and exercise diet therapy ($P < 0.05$); electroacupuncture, acupoint catgut embedding + acupuncture, acupoint catgut embedding + exercise diet therapy, acupoint catgut + TCM, acupoint catgut + moxibustion, and acupoint catgut + cupping were superior to acupuncture ($P < 0.05$); acupoint catgut + moxibustion was superior to electroacupuncture ($P < 0.05$); acupoint catgut + TCM, acupoint catgut + moxibustion, and acupoint catgut + cupping were superior to TCM treatment ($P < 0.05$); and electroacupuncture, acupoint catgut, acupoint catgut + acupuncture, acupoint catgut + exercise diet therapy, acupoint catgut + TCM, acupoint catgut embedding + moxibustion, and acupoint catgut embedding + cupping were superior to sports diet therapy ($P < 0.05$). Regarding weight loss, acupuncture treatment was superior to acupoint catgut embedding therapy ($P < 0.05$); acupoint catgut embedding + exercise diet therapy, acupoint catgut embedding + TCM, acupoint catgut embedding + moxibustion, and acupoint catgut embedding + cupping were superior to acupuncture and electroacupuncture treatment ($P < 0.05$); acupoint catgut embedding + exercise diet therapy, acupoint catgut embedding + TCM, and acupoint catgut embedding + moxibustion were superior to TCM treatment ($P < 0.05$); and acupoint catgut embedding, acupoint catgut embedding + acupuncture, catgut embedding + exercise diet therapy, acupoint catgut embedding + TCM, acupoint catgut embedding + moxibustion, and acupoint catgut embedding + cupping were superior to exercise diet therapy ($P < 0.05$). In terms of BMI reduction, acupoint catgut embedding + moxibustion and acupoint catgut embedding + cupping were more evident than acupuncture treatment ($P < 0.05$); and acupoint catgut embedding + moxibustion was more evident than electroacupuncture treatment ($P < 0.05$). *Conclusion*. Acupoint catgut embedding and its combination with other therapies are the first choice for the treatment of simple obesity.

1. Introduction

Obesity is a chronic disease due to excessive accumulation or abnormal distribution of fat in the body [1]. Simple obesity is a kind of obesity caused by excessively more intake than consumption, excluding other diseases or medical factors [2]. Simple obesity is now an epidemic health problem, leading to higher incidence of other diseases. Excessive fat accumulation in the body is an important manifestation of obese people, resulting in a higher body mass index (BMI)

than normal [3]. Over the past few decades, obesity has been considered to be the result of unbalanced intake and consumption of high-calorie diet. The survey shows that from 1993 to 2015, the prevalence of overweight and obesity, especially abdominal obesity, increased significantly among Chinese adults [4]. Obesity is the main risk factor of dyslipidemia and cardiovascular disease (CVD) [5]. At present, there are many treatment methods for obesity. Some literature studies show that acupoint catgut embedding and joint use with other therapies can improve the effective rate of treatment for simple obesity and reduce the BMI of patients [6]. This study used network meta-analysis to compare the efficacy of acupoint catgut embedding and its combination with other methods in the treatment of simple obesity, so as to provide some evidence support for clinical adjuvant therapy.

2. Data and Methods

2.1. Methods. PubMed, Cochrane, Embase, China National Knowledge Infrastructure (CNKI), Wanfang, and VIP Database (VIP) were selected as databases. "Catgut embedding at acupoints", "simple obesity", and "obesity" were Chinese and English search terms. The combination of subject headings and free words was the retrieval method. Title, abstract and keywords or Title, Abstract and Keywords were used as search entries. From the establishment of the database to August 2021 was the time for publication of the literature.

2.2. Inclusion and Exclusion Criteria. The inclusion criteria of the literature were as follows: (1) patients who met the diagnostic criteria established by the Fifth National Obesity Academic Research Conference [7]; (2) type of study: RCTs were included according to the criteria in the Cochrane Collaborative Workbook; (3) intervention measures: the baseline data were complete, and at least two groups were included. Catgut embedding therapy was used in the test group, and the main indicators were drug response rate, body weight change, and BMI; and (4) languages were limited to Chinese and English.

The exclusion criteria were as follows: (1) nonrandomized control; (2) literature with a sample size of less than 10 or repeated publications; (3) studies with incomplete data and lack of rigorous study design; and (4) studies with unclear efficacy outcome evaluation and analysis.

2.3. Literature Evaluation. The quality of the literature was assessed using the risk of bias assessment tool provided by the Cochrane Collaboration. The following items were considered: (1) the generation of the random assignment plan, (2) whether the patients and doctors were blinded, (3) whether the outcome evaluation was blinded or not, (4) whether it was a hidden allocation scheme, (5) whether it was a selectively reported study result, (6) whether the result data were complete or not, and (7) whether there was other bias.

The quality of the included literature was evaluated on a scale of 1 to 7 using the modified Jadad scale from the aspects of random sequence generation, randomization concealment, blinding, and complete follow-up. Scores 1–3 were considered low quality and 4–7 high quality.

2.4. Data Extraction. According to the above principles, two researchers independently searched and screened the literature and evaluated the quality of the final included results using EndNote software. In case of any disagreement, the third researcher would join and make a decision.

2.5. Statistical Processing. Body weight and BMI were numerical variables. The difference between the variables before and after treatment was used to calculate the standard deviation of the variable difference with the help of the correlation coefficient ($R = 0.5$), and 95% confidence intervals (CI) of the median and percentile of the difference were estimated. Effectiveness was count data, for which the odds ratio (OR) was used for statistical analysis, and with 95% CI were calculated. The heterogeneity analysis was performed using the I^2 value. If $I^2<50\%$, the heterogeneity was small and could be ignored, and the fixed effect model was used. If $I^2>50\%$, the heterogeneity was large, and the random effect model was used.

STATA15.0 software was used to draw the network evidence relationship diagram, forest plot, rank probability diagram, and funnel plot with corresponding statistics, and the consistency test was used to compare the ring consistency. In this study, the surface under the cumulative ranking curve (SUCRA) was used to calculate the cumulative ranking probability of each treatment regimen. A higher SUCRA value indicates more effective intervention.

3. Literature Search Results

3.1. Literature Search. Using the above retrieval strategies, 2385 studies were retrieved from the databases, 864 duplicate studies were deleted, 1470 studies that obviously did not meet the inclusion criteria were excluded according to the title and abstract, and 51 were initially included. After intensive reading of the full text, 16 substandard studies were excluded, and finally 35 RCTs were included. The document screening process is shown in Figure 1.

3.2. Basic Information of Included Literature. The included 35 RCTs were all from China, with a total of eligible 3040 patients. Acupoint catgut embedding, acupuncture, electroacupuncture, TCM, acupoint catgut embedding + acupuncture, acupoint catgut embedding + exercise diet therapy, acupoint catgut embedding + TCM, exercise diet therapy, acupoint catgut embedding + moxibustion, and acupoint catgut embedding + cupping were used mainly for treatment. The basic characteristics of the included literature studies are shown in Table 1.

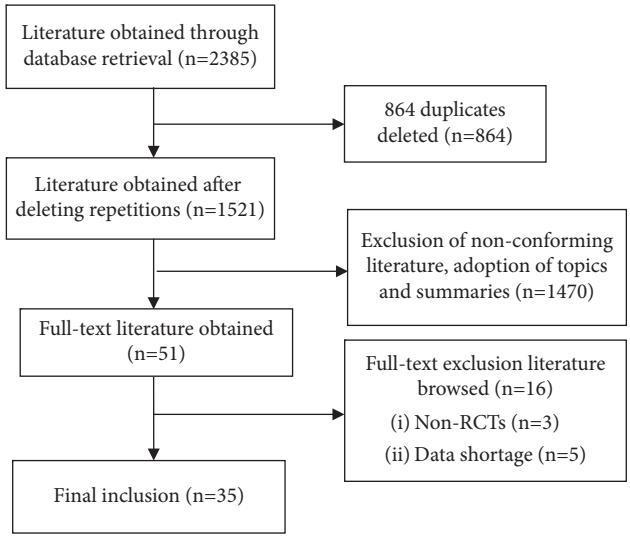

Figure 1: Flowchart of literature screening.

3.3. Literature Quality Research. In the included literature, there were 15 studies [12, 16, 18, 19, 21, 22, 24, 26, 28, 34, 36, 38, 39, 41, 42] using the random number table method, 16 studies [10, 11, 13–15, 17, 20, 23, 25, 27, 29–32, 37, 40] only presented random, 1 study [33] used the treatment method, 1 study [8] adopted the odd-even numbering method, 1 study [9] used the envelope assignment method, 1 study [35] used the odd and even admission numbers, 1 study [24] mentioned single-blindness, no study mentioned allocation concealment, and all study results data were complete. See Table 2 for details.

3.4. Traditional Meta-Analysis Results. Meta-analysis showed that the total effective rate of acupoint catgut embedding + TCM treatment, acupoint catgut embedding + moxibustion treatment, and acupoint catgut embedding + cupping treatment was higher than that of acupoint catgut embedding treatment alone with statistically significant differences. Acupoint catgut embedding and acupoint catgut embedding + acupuncture were superior to acupuncture treatment, and the differences were statistically significant. Acupoint catgut embedding + TCM treatment was more effective than TCM treatment with statistically significant differences. Acupoint catgut embedding was superior to electroacupuncture, and the difference was statistically significant; other direct comparisons showed no significant difference.

Meta-analysis results of weight loss showed that acupoint catgut embedding + TCM treatment, acupoint catgut embedding + moxibustion treatment, and acupoint catgut embedding + cupping treatment were superior to acupoint catgut embedding, and the difference was statistically significant. Acupoint catgut embedding was superior to acupuncture, and the difference was statistically significant. Acupoint catgut embedding + TCM treatment was superior to TCM treatment, and the difference was statistically significant. Other direct comparisons showed no statistically significant differences.

Meta-analysis results showed that BMI reduction by acupoint catgut embedding + TCM treatment, acupoint catgut embedding + moxibustion treatment, and acupoint catgut embedding + cupping treatment were more evident than that by acupoint catgut embedding treatment alone, acupoint embedding + TCM treatment was superior to TCM treatment, acupoint embedding treatment was superior to acupuncture, acupoint catgut embedding was superior to electroacupuncture, acupoint catgut embedding + exercise diet therapy was superior to exercise diet therapy, and there was no significant difference in other direct comparison results. The meta-analysis results are shown in Table 3.

3.5. Results of Network Meta-Analysis

3.5.1. Evidence Network. The results of the total effective rate were as follows: the acupoint embedding was the center point, and the star-shaped structure of 10 intervention nodes formed 6 triangular closed loops, which were acupoint embedding-acupuncture-acupoint embedding + acupuncture, acupoint embedding-electrical acupuncture-exercise diet therapy, acupoint embedding-acupuncture-acupoint embedding + TCM, acupoint embedding-acupuncture-acupoint embedding + cupping, acupoint embedding-TCM-acupoint embedding + TCM, and acupoint embedding-acupoint embedding + exercise diet therapy-exercise diet therapy.

The reduction of body mass was as follows: the star-shaped structure of 9 intervention nodes centered on acupoint embedding, forming a total of 5 triangular closed loops, namely, acupoint embedding-acupuncture-acupoint embedding + TCM, acupoint embedding-acupuncture needling-acupoint catgut embedding + cupping, acupoint catgut embedding-electroacupuncture-exercise diet therapy, acupoint catgut embedding-TCM-acupoint catgut embedding + TCM, and acupoint catgut embedding-acupoint catgut embedding + exercise diet therapy-exercise diet therapy.

The reduction of BMI was as follows: the star-shaped structure with 9 intervention nodes centered on acupoint embedding, forming a total of 5 triangular closed loops, namely, acupoint embedding-acupuncture-acupoint embedding + TCM, acupoint embedding-acupuncture-catgut embedding + cupping, catgut embedding-electroacupuncture-sports diet therapy, acupoint catgut-TCM-acupoint catgut embedding + TCM, and acupoint catgut-acupoint catgut embedding + exercise diet therapy-exercise diet therapy. The network evidence graph results are shown in Figures 2–4.

3.5.2. Consistency Test. The variable of the total effective rate of treatment contained 6 closed loops, the lower limit of the 95% CI of the 5 loop inconsistency factors (IFs) after the consistency test was 0, there was no obvious inconsistency, and the 95% lower limit of 1 closed loop IF was 0.16, failing to reach 0. Inconsistency was statistically significant, indicating inconsistency.

The decrease in body mass involved 5 closed loops, the lower limit of the 95% CI of the discordance factor IF contained 0, and there was no significant discordance.

Table 1: Basic characteristics of included studies.

Author and year	Trial 1			Trial 2			Trial 3			Period of treatment (week)	Evaluation standard course of disease
	Interventions	Number (male/female)	Age (years)	Interventions	Number (male/female)	Age (years)	Interventions	Number (male/female)	Age (years)		
Luo Liangqi 2016 [8]	Acupoint catgut embedding	30 (11/19)	32.8 ± 3.6	Acupuncture	30 (10/20)	31.6 ± 4.3				4/4	(1)
Zhou Wei 2020 [9]	Acupoint catgut embedding	45	21–45	Electroacupuncture	45	21–45	Exercise diet therapy	45	21–45	8/8/8	(1) (2) (3) (4) (5)
Li Miaomiao 2017 [10]	Acupoint catgut embedding	30 (4/26)	18–58	Electroacupuncture	30 (4/26)	25–53				4/4	(1) (2) (3)
Zheng Xi 2020 [11]	Acupoint catgut embedding + moxibustion	48 (24/24)	41.97 ± 15.22	Acupoint catgut embedding	48 (25/23)	42.15 ± 15.69				8/8	(1) (2) (3) (6) (7) (8)
Duan Xiaorong 2017 [12]	Acupoint catgut embedding + cupping	50 (11/39)	35.48 ± 8.269	Acupuncture	50 (10/40)	35.14 ± 7.743				12/12	(1) (2) (3)
Wang Zheng 2020 [13]	Acupoint catgut embedding	56 (32/24)	43.3 ± 2.6	Acupuncture	56 (30/26)	43.5 ± 2.7				4/4	(1) (2) (3) (9)
Zhou Lijie 2017 [14]	Acupoint catgut embedding	33 (4/29)		Acupuncture	33 (2/31)					4/4	(1) (2) (3) (9)
Wu Xiaomei 2015 [15]	Acupoint catgut embedding	32 (7/25)	33 ± 11	Acupuncture	30 (6/24)	35 ± 10				4/4	(1) (2) (3) (5)
Huang Qiong 2020 [16]	Acupoint catgut embedding	39 (21/18)	38.27 ± 2.52	Acupuncture	39 (20/19)	37.34 ± 2.57				12/12	(2) (3) (7) (8)
Lin Guanghua 2015 [17]	Acupoint catgut embedding + cupping	30 (4/26)	32.56 ± 16.62	Acupoint catgut embedding	30 (3/27)	31.98 ± 17.05				8/8	(1) (2) (3)
Deng Ru 2021 [18]	Acupoint catgut embedding	30 (15/15)	58.5 ± 2.4	Acupuncture	30 (14/16)	47.7 ± 3.6				8/8	(1) (2) (3) (5)
Huang Wei 2015 [19]	Acupoint catgut embedding + exercise diet therapy	80 (0/80)	20–45	Acupoint catgut embedding	80 (0/80)	20–45				12/12	(1) (2) (3) (4)
Lin Chenjuan 2020 [20]	Acupoint catgut embedding + TCM	30 (17/13)	33.81 ± 6.32	Acupoint catgut embedding	30 (14/16)	33.12 ± 6.45	TCM	30 (16/14)	33.49 ± 6.70	12/12/12	(1) (2) (3) (5) (7) (8) (10) (11) (13)
Wen Qingfen 2021 [21]	Acupoint catgut embedding + TCM	41 (17/24)	33.48 ± 10.39	Acupoint catgut embedding	30 (18/23)	33.56 ± 10.52				8/8	(2) (3) (5) (6) (12) (14) (15)
Su Junxian 2017 [22]	Acupoint catgut embedding + TCM	38 (11/27)	38.05 ± 5.91	Acupoint catgut embedding	39 (14/15)	38.70 ± 6.16	TCM	38 (12/16)	38.45 ± 6.19	4/4/4	(1) (3) (5)
Wang Rui 2017 [23]	Acupoint catgut embedding + exercise diet therapy	30 (5/25)	32.45 ± 10.40	Exercise diet therapy	30 (7/23)	29.62 ± 7.25				8/12	(3) (6)

Table 1: Continued.

Author and year	Trial 1			Trial 2			Trial 3			Period of treatment (week)	Evaluation standard course of disease
	Interventions	Number (male/female)	Age (years)	Interventions	Number (male/female)	Age (years)	Interventions	Number (male/female)	Age (years)		
Wang Lingshu 2019 [24]	Acupoint catgut embedding + TCM	60 (28/32)	34.1 ± 7.42	Acupoint catgut embedding	60 (29/31)	34.0 ± 7.40				6/6	(1) (2) (3) (5) (6)
Chen Rongzhong 2016 [25]	Acupoint catgut embedding	47	42.8 ± 2.9	Acupuncture	47	42.8 ± 2.9				8/8	(1) (2) (5) (12) (16)
Zhou Hualing 2018 [26]	Acupoint catgut embedding + TCM	28 (4/24)	30.67 ± 2.48	Acupuncture	28 (3/25)	31.25 ± 2.07				16/4	(1) (2) (3) (5) (12)
Zheng Xiao 2015 [27]	Acupoint catgut embedding	40 (4/36)	15–56	Electroacupuncture	40 (3/37)	14–60				12/12	(1) (3) (5)
Guo Wenjiang 2014 [28]	Acupoint catgut embedding	36 (14/22)	33.6 ± 1.5	Acupuncture	35 (11/24)	34.2 ± 1.5				6/6	(1)
Zhang Hong 2017 [29]	Acupoint catgut embedding	40 (22/18)	61.35 ± 3.11	Acupuncture	40 (23/17)	61.26 ± 3.07				12/12	(1) (2) (3) (5) (7) (8) (10) (11) (12)
Zhao Huayi 2015 [30]	Acupoint catgut embedding	50 (2/48)	25–60	Electroacupuncture	50 (2/48)	23–60				4/6	(1) (2) (3) (5) (12)
Yao Rujie 2014 [31]	Acupoint catgut embedding	25 (10/15)	38.3 ± 9.83	Acupuncture	25 (9/16)	37.78 ± 9.27				12/12	(1) (4) (5) (6) (12) (17)
Chen Zeli 2013 [32]	Acupoint catgut embedding	40 (5/35)	39.65 ± 4.82	Acupuncture	40 (6/34)	38.95 ± 4.54				6/6	(1) (2) (3)
Huang Weixuan 2019 [33]	Acupoint catgut embedding + exercise diet therapy	100 (29/71)	48.9 ± 12.1	Exercise Diet therapy	100 (26/74)	49.3 ± 11.8				12/12	(1) (2) (3) (5) (7) (8) (10)
Yan Bing 2021 [34]	Acupoint catgut embedding	29 (11/18)	33.5 ± 9.4	Acupuncture	30 (10/20)	33.7 ± 10.2				8/8	(3) (5) (7) (8) (10) (11) (12) (14) (18)
Li Lujuan 2016 [35]	Acupoint catgut embedding	50 (20/30)	35.2 ± 12.6	Electroacupuncture	50 (19/31)	36.7 ± 11.8				8/8	(1) (2) (3)
Wang Quan 2018 [36]	Acupoint catgut embedding + TCM	50 (26/24)	31.32 ± 2.72	TCM	50 (26/24)	31.31 ± 2.72				12/12	(2) (3) (5) (7) (8) (10)
Zhao Binbin 2015 [37]	Acupoint catgut embedding + cupping	30 (4/26)	32.56 ± 16.62	Acupoint catgut embedding	30 (3/27)	31.98 ± 17.05				8/8	(1) (2) (3) (5)
Liang Bingjun 2019 [38]	Acupoint catgut embedding + TCM	40 (24/16)	41.23 ± 7.41	TCM	40 (25/15)	41.25 ± 7.59				4/4	(1) (2) (3)

Table 1: Continued.

Author and year	Trial 1			Trial 2			Trial 3			Period of treatment (week)	Evaluation standard course of disease
	Interventions	Number (male/female)	Age (years)	Interventions	Number (male/female)	Age (years)	Interventions	Number (male/female)	Age (years)		
Lv Mingfang 2020 [39]	Acupoint catgut embedding + moxibustion	40 (25/15)	30.7 ± 4.1	Acupoint catgut embedding	40 (23/17)	31.5 ± 3.7				8/8	(1) (2) (3) (5) (6) (12) (17) (19)
Chen Yuanyuan 2015 [40]	Acupoint catgut embedding + acupuncture	40	18–46	Acupoint catgut embedding	40	18–46	Acupuncture	40	18–46	4/4/4	(1)
Hou Sujuan 2016 [41]	Acupoint catgut embedding + acupuncture	68 (44/24)	27.1 ± 1.5	Acupuncture	68 (45/13)	26.8 ± 1.2				5/5	(1) (4) (6) (8)
Tian Feng 2014 [42]	Acupoint catgut embedding	22	26–49	Acupuncture	22	26–49				8/8	(1)

Note. TCM: traditional Chinese medicine; (1): effective rate; (2): body weight (kg); (3): BMI (kg/m2); (4): body fat percentage (%); (5): waistline (cm); (6): WHR (waist-hip ratio); (7): TC; (8): TG; (9): appetite score; (10): LDL-C; (11): HDL-C; (12): hip circumference; (13): adverse reaction; (14): fat thickness; (15): Chinese medicine syndrome scores; (16): chest circumference; (17): plumpness; (18): IWQOL-Lite score; (19): body fat percentage.

Table 2: Literature quality research.

Study	Stochastic method	Randomized hiding	Blinding	Results data integrity	Jadad score
Luo Liangqi 2016 [8]	Parity number	Unclear	Unclear	Integrity	5
Zhou Wei 2020 [9]	Envelope drawing method	Unclear	Unclear	Integrity	5
Li Miaomiao2017 [10]	Random	Unclear	Unclear	Integrity	4
Zheng Xi 2020 [11]	Random	Unclear	Unclear	Integrity	4
Duan Xiaorong 2017 [12]	Random number list	Unclear	Unclear	Integrity	5
Wang Zheng 2020 [13]	Random	Unclear	Unclear	Integrity	4
Zhou Lijie 2017 [14]	Random	Unclear	Unclear	Integrity	4
Wu Xiaomei 2015 [15]	Random	Unclear	Unclear	Integrity	4
Huang Qiong 2020 [16]	Random number list	Unclear	Unclear	Integrity	5
Lin Guanghua 2015 [17]	Random	Unclear	Unclear	Integrity	4
Deng Ru 2021 [18]	Random number list	Unclear	Unclear	Integrity	4
Huang Wei 2015 [19]	Random number list	Unclear	Unclear	Integrity	5
Lin Chenjuan 2020 [20]	Random	Unclear	Unclear	Integrity	4
Wen Qingfen 2021 [21]	Random number list	Unclear	Unclear	Integrity	5
Su Junxian 2017 [22]	Random number list	Unclear	Unclear	Integrity	5
Wang Rui 2017 [23]	Random	Unclear	Unclear	Integrity	4
Wang Lingshu 2019 [24]	Random number list	Unclear	Unclear	Integrity	6
Chen Rongzhong 2016 [25]	Random	Unclear	Unclear	Integrity	4
Zhou Hualing 2018 [26]	Random number list	Unclear	Unclear	Integrity	5
Zheng Xiao 2015 [27]	Random	Unclear	Unclear	Integrity	4
Guo Wenjiang 2014 [28]	Random number list	Unclear	Unclear	Integrity	5
Zhang Hong 2017 [29]	Random	Unclear	Unclear	Integrity	4
Zhao Huayi 2015 [30]	Random	Unclear	Unclear	Integrity	4
Yao Rujie 2014 [31]	Random	Unclear	Unclear	Integrity	4
Chen Zeli 2013 [32]	Random	Unclear	Unclear	Integrity	4
Huang Weixuan 2019 [33]	Therapies	Unclear	Unclear	Integrity	3
Yan Bing 2021 [34]	Random number list	Unclear	Unclear	Integrity	5
Li Lujuan 2016 [35]	Single and double numbers	Unclear	Unclear	Integrity	5
Wang Quan 2018 [36]	Random number list	Unclear	Unclear	Integrity	5
Zhao Binbin 2015 [37]	Random	Unclear	Unclear	Integrity	4
Liang Bingjun 2019 [38]	Random number list	Unclear	Unclear	Integrity	5
Lv Mingfang 2020 [39]	Random number list	Unclear	Unclear	Integrity	5
Chen Yuanyuan 2015 [40]	Random	Unclear	Unclear	Integrity	4
Hou Sujuan 2016 [41]	Random number list	Unclear	Unclear	Integrity	5
Tian Feng 2014 [42]	Random number list	Unclear	Unclear	Integrity	5

BMI reduction involved 5 closed loops, the lower limit of the 95% CI of the discordance factor IF contained 0, and there was no significant discordance. The results of the consistency check are shown in Figures 5–7.

3.5.3. Results of Network Meta-Analysis. The results of the total effective rate were as follows: the healing of acupoint catgut embedding was better than that of acupuncture, electroacupuncture, and exercise diet therapy ($P < 0.05$). The total effective rate of acupoint catgut embedding + moxibustion was higher than that of acupoint catgut embedding ($P < 0.05$); electroacupuncture, catgut embedding + acupuncture, acupoint catgut + exercise diet therapy, acupoint catgut + TCM, acupoint catgut + moxibustion, and acupoint catgut + cupping were superior to acupuncture ($P < 0.05$); the total effective rate of acupoint catgut embedding + moxibustion was higher than that of electroacupuncture ($P < 0.05$); the total effective rate of acupoint catgut embedding + Chinese medicine, acupoint catgut embedding + moxibustion, and acupoint catgut embedding + cupping was higher than that of TCM treatment ($P < 0.05$); and electroacupuncture, acupoint catgut embedding, acupoint catgut embedding + acupuncture, acupoint catgut embedding + sports diet therapy, acupoint catgut embedding + TCM, acupoint catgut embedding + moxibustion, and acupoint catgut embedding + cupping were superior to sports diet therapy ($P < 0.05$). The results are shown in Figure 8.

The results of weight loss were as follows: acupuncture treatment was superior to acupoint catgut embedding therapy ($P < 0.05$); acupoint catgut embedding + exercise diet therapy, acupoint catgut embedding + TCM, acupoint catgut embedding + moxibustion, and acupoint catgut embedding + cupping were superior to acupuncture and electroacupuncture treatment ($P < 0.05$); acupoint catgut embedding + exercise diet therapy, acupoint catgut embedding + TCM, and acupoint catgut embedding + moxibustion were superior to TCM treatment ($P < 0.05$); and acupoint catgut embedding, acupoint catgut embedding + acupuncture, acupoint catgut embedding + exercise diet therapy, catgut embedding + TCM, acupoint catgut embedding + moxibustion, and acupoint

Table 3: Traditional meta-analysis results.

Interventions	Number of studies included	OR/MD (95% CI)	P	χ^2	P	I^2
Total effective rate						
Acupoint catgut embedding vs. acupuncture	12	3.77 (2.49, 5.71)	≤0.001	7.56	0.75	0%
Acupoint catgut embedding vs. electroacupuncture	5	1.99 (1.10, 3.61)	0.02	4.82	0.31	17%
Acupoint catgut embedding + TCM vs. acupoint catgut embedding	3	2.32 (1.14, 4.72)	0.02	2.70	0.26	26%
Acupoint catgut embedding + TCM vs. TCM	3	5.99 (2.63, 13.66)	≤0.001	0.46	0.80	0%
Acupoint catgut embedding + moxibustion vs. acupoint catgut embedding	2	4.57 (1.75, 11.92)	0.002	0.00	0.96	0%
Acupoint catgut embedding + cupping vs. acupoint catgut embedding	2	4.46 (0.91, 21.97)	0.07	0.00	1.00	0%
Acupoint catgut embedding + acupuncture vs. acupuncture	2	3.49 (1.42, 8.61)	0.007	0.00	0.96	0%
Acupoint catgut embedding + exercise diet therapy vs. exercise diet therapy	1	3.33 (1.51, 7.32)	0.003			
Acupoint catgut embedding + exercise diet therapy vs. acupoint catgut embedding	1	3.35 (1.03, 10.89)	0.04			
Acupoint catgut embedding + TCM vs. acupuncture	1	3.27 (0.63, 17.07)	0.16			
Acupoint catgut embedding + cupping vs. acupuncture	1	3.55 (0.65, 19.37)	0.14			
Body weight						
Acupoint catgut embedding vs. acupuncture	9	−3.86 (−5.56, −2.61)	≤0.001	19.16	0.01	58%
Acupoint catgut embedding vs. electroacupuncture	4	−0.34 (−3.11, 2.43)	0.81	0.99	0.80	0%
Acupoint catgut embedding + TCM vs. acupoint catgut embedding	3	−2.04 (−3.24, −0.84)	≤0.001	1.24	0.54	0%
Acupoint catgut embedding + TCM vs. TCM	3	−5.61 (−7.21, −4.01)	≤0.001	0.35	0.84	0%
Acupoint catgut embedding + moxibustion vs. acupoint catgut embedding	2	−4.96 (−6.26, −3.67)	≤0.001	1.24	0.27	19%
Acupoint catgut embedding + cupping vs. acupoint catgut embedding	2	−4.14 (−8.18, −0.10)	0.04	0.00	1.00	0%
Acupoint catgut embedding + exercise diet therapy vs. exercise diet therapy	1	−4.20 (−6.45, −1.95)	≤0.001			
Acupoint catgut embedding + exercise diet therapy vs. acupoint catgut embedding	1	−2.78 (−4.47, −1.09)	0.001			
Acupoint catgut embedding + TCM vs. acupuncture	1	−5.44 (−7.85, −3.03)	≤0.001			
Acupoint catgut embedding + cupping vs. acupuncture	1	−2.85 (−9.33, 3.63)	0.39			
BMI						
Acupoint catgut embedding vs. acupuncture	8	−1.84 (−2.23, −1.44)	≤0.001	134.27	0.000	95%
Acupoint catgut embedding vs. electroacupuncture	5	−0.47 (−1.11, 0.17)	0.15	7.56	0.11	47%
Acupoint catgut embedding + TCM vs. acupoint catgut embedding	4	−1.30 (−2.33, −0.27)	0.01	50.67	0.000	94%
Acupoint catgut embedding + TCM vs. TCM	4	−1.56 (−2.30, −0.82)	≤0.001	18.60	0.000	84%
Acupoint catgut embedding + moxibustion vs. acupoint catgut embedding	2	−2.69 (−3.22, −2.16)	≤0.001	0.04	0.84	0%
Acupoint catgut embedding + cupping vs. acupoint catgut embedding	2	−1.92 (−2.90, −0.94)	≤0.001	0.00	1.00	0%
Acupoint catgut embedding + exercise diet therapy vs. exercise diet therapy	2	−1.66 (−2.16, −1.15)	≤0.001	0.36	0.55	0%
Acupoint catgut embedding + exercise diet therapy vs. acupoint catgut embedding	1	−2.18 (−5.25, 0.89)	0.16			
Acupoint catgut embedding + TCM vs. acupuncture	1	−4.82 (−5.75, −3.89)	≤0.001			
Acupoint catgut embedding + cupping vs. acupuncture	1	−0.98 (−1.87, −0.09)	0.03			

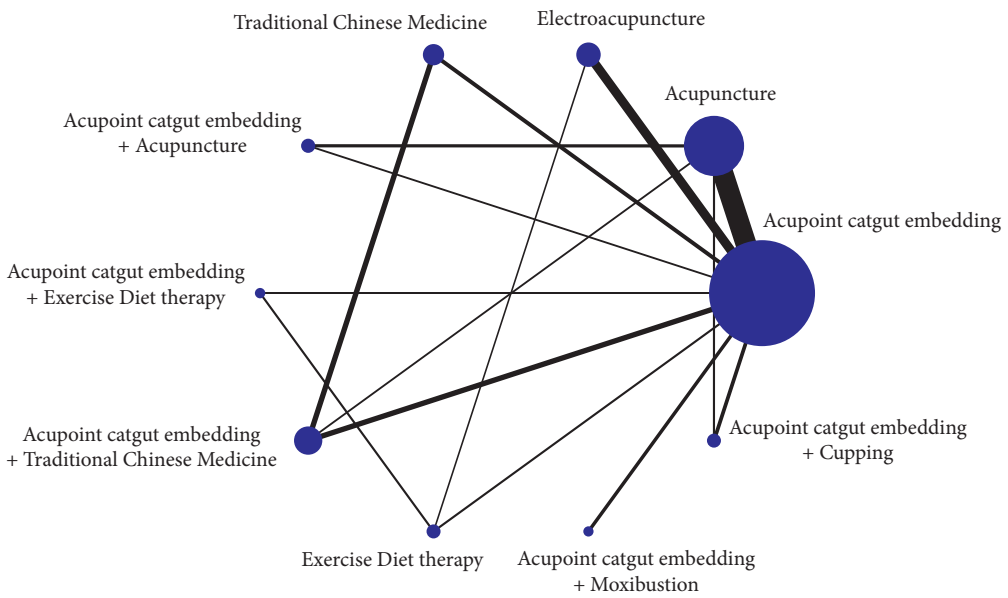

Figure 2: Evidence graph of total effective rate by network meta-analysis of different therapies and catgut embedding at acupoints in the treatment of simple obesity.

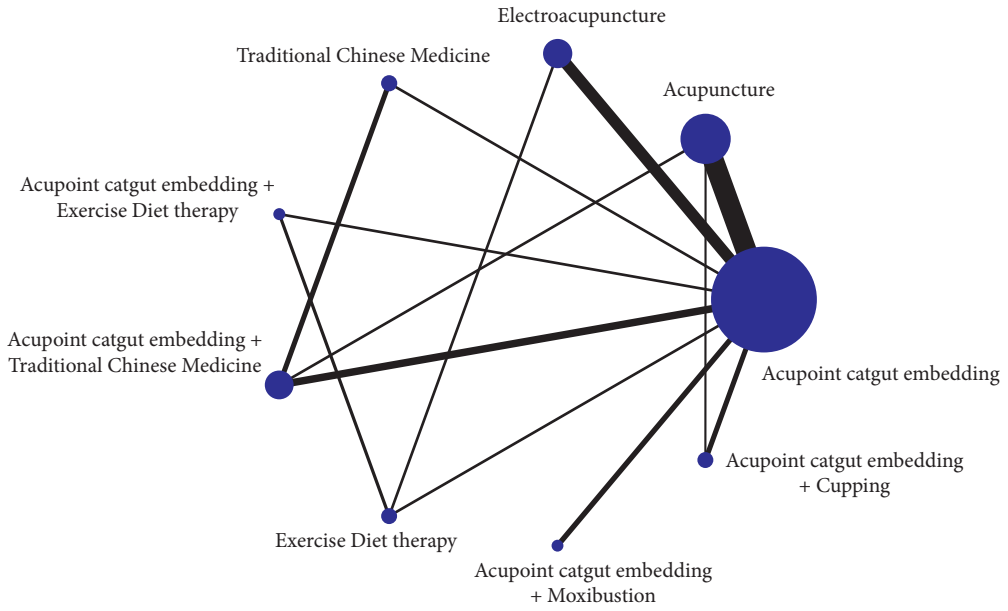

Figure 3: Evidence chart of weight loss by network meta-analysis of different therapies and catgut embedding at acupoints for simple obesity.

catgut embedding + cupping were superior to exercise diet therapy ($P < 0.05$). The results are shown in Figure 9.

The results of BMI reduction were as follows: acupoint catgut embedding + moxibustion and acupoint catgut embedding + cupping were superior to acupuncture treatment ($P < 0.05$); and acupoint catgut embedding + moxibustion was superior to electroacupuncture treatment ($P < 0.05$). The results are shown in Figure 10.

3.5.4. Sorting of Mesh Meta-Analysis Results. Three different outcome indicators were ranked, and there were some differences in the ranking results. Lower average rank indicates better outcome indicators. Finally, it was revealed the intervention measures of acupoint catgut embedding combined with moxibustion showed a better effect in the treatment of simple obesity. The ranking of network meta-analysis results is shown in Table 4.

3.6. Publication Bias. The funnel plot was drawn according to the total effective rate, and the scatter points were mostly located in the upper half, symmetrically distributed on both sides of the red indicator line, indicating small publication bias. However, there was a scatter at the bottom of the funnel plot, indicating a small sample effect, as shown in Figure 11.

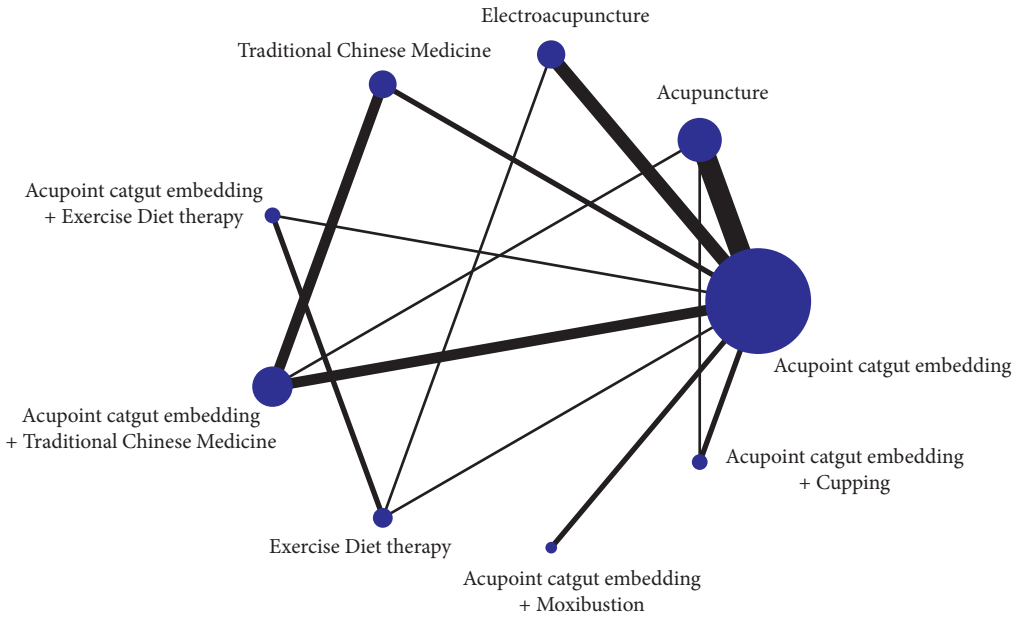

Figure 4: Evidence graph of BMI reduction by network meta-analysis of different therapies and catgut embedding at acupoints for simple obesity.

Loop	IF	95%CI (truncated)	Loop-specific Heterogeneity (T^2)
A-F-H	1.95	(0.16,3.75)	0.000
A-B-J	1.55	(0.00,3.89)	0.000
A-B-E	1.11	(0.00,2.87)	0.000
A-B-G	0.77	(0.00,2.67)	0.000
A-C-H	0.41	(0.00,2.80)	0.234
A-D-G	0.40	(0.00,1.94)	0.22

0 1 2 3 4

Figure 5: Inconsistency test results of total effective rate. A: acupoint catgut embedding; B: acupuncture; C: electroacupuncture; D: TCM; E: acupoint catgut embedding + acupuncture; F: acupoint catgut embedding + exercise diet therapy; G: acupoint catgut embedding + TCM; H: exercise diet therapy; J: acupoint catgut embedding + cupping.

Loop	IF	95%CI (truncated)	Loop-specific Heterogeneity (T^2)
A-E-G	3.58	(0.00,8.42)	0.000
A-B-F	2.52	(0.00,8.95)	0.000
A-C-G	2.23	(0.00,8.14)	0.000
A-D-F	2.05	(0.00,6.22)	0.000
A-B-I	1.95	(0.00,7.27)	0.000

0 3 5 7 9

Figure 6: Inconsistency test results of body weight reduction. A: acupoint catgut embedding; B: acupuncture; C: electroacupuncture; D: TCM; E: acupoint catgut embedding + acupuncture; F: acupoint catgut embedding + exercise diet therapy; G: acupoint catgut embedding + TCM; I: acupoint catgut embedding + moxibustion.

4. Discussion

Simple obesity is defined as malnutrition without obvious causes. When the accumulation of body fat exceeds the consumption level of the body, the patient's weight exceeds the standard weight due to excessive body fat [43]. Nowadays, many factors are considered to be the etiology of obesity, such as neuroregulation, free radicals, and heredity [44, 45]. In traditional Chinese medicine, it is believed that dysfunction of the spleen and stomach is the root cause of obesity. Increasing intake of sweet and greasy food and declining function of the spleen and stomach leads to accumulation of fat in the body. Obesity affects the quality of life of patients and damages their physical and mental health. In clinical reports, acupoint catgut embedding is a safe and effective intervention for obesity.

Adipocytes, adipose tissue, endocrine regulation, and inflammatory factors are the focus of study on the mechanism of action of acupoint catgut embedding in the treatment of simple obesity [46]. In the process of acupoint catgut embedding, needle insertion can cause tissue damage, fat cell death, or a small range of fat liquefaction and, to a certain extent, can reduce the number of cells in adipose tissue [47]. Under an optical microscope, less adipocytes, less

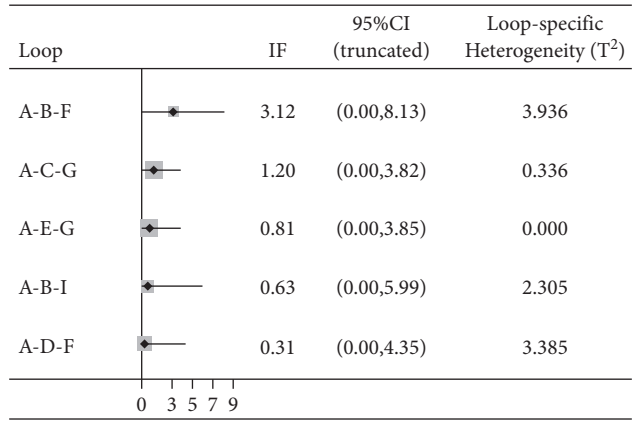

Figure 7: Results of inconsistency test of BMI reduction. A: acupoint catgut embedding; B: acupuncture; C: electroacupuncture; D: TCM; E: acupoint catgut embedding + acupuncture; F: acupoint catgut embedding + exercise diet therapy; G: acupoint catgut embedding + TCM; I: acupoint catgut embedding + moxibustion.

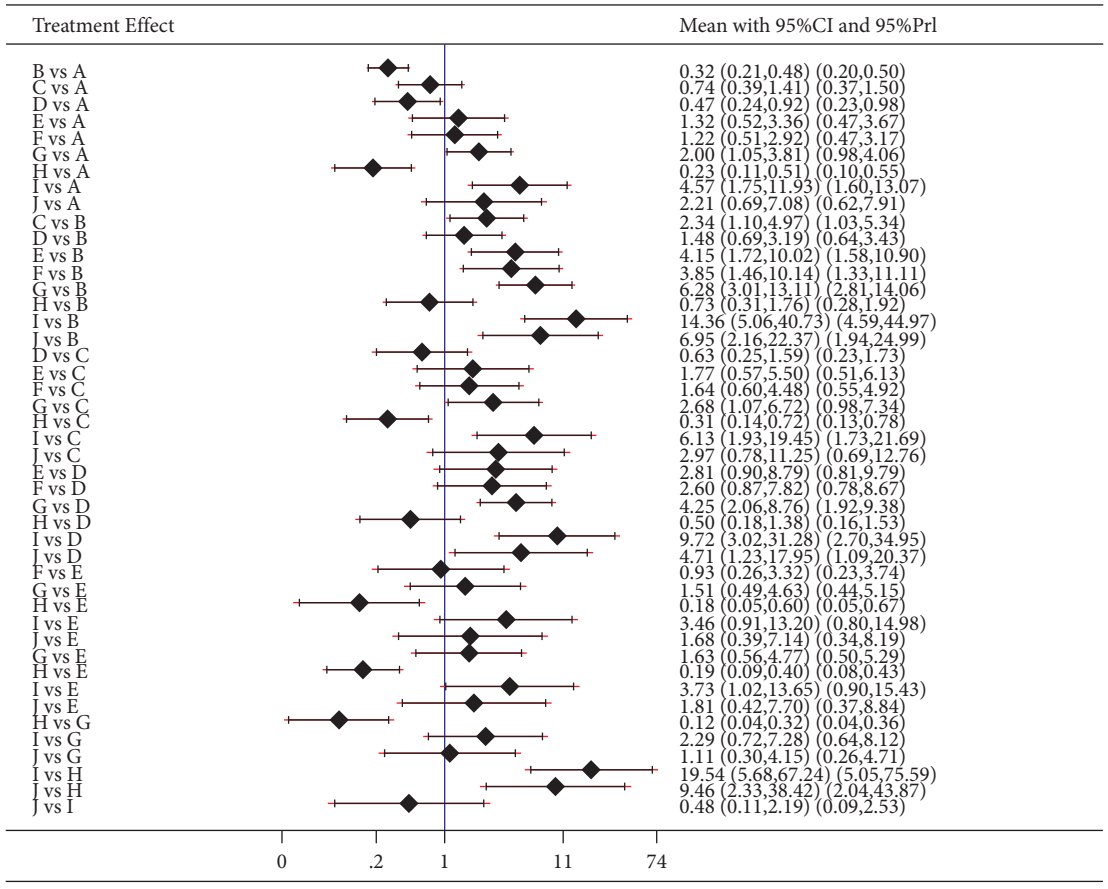

Figure 8: The total effective rate in treatment of simple obesity with different methods and catgut embedding at acupoints in meta-analysis forest plot. A: acupoint catgut embedding; B: acupuncture, C: electroacupuncture; D: TCM; E: acupoint catgut embedding + acupuncture; F: acupoint catgut embedding + exercise diet therapy; G: acupoint catgut embedding + TCM; H: exercise diet therapy; I: acupoint catgut embedding + moxibustion; J: acupoint catgut embedding + cupping.

lipid droplets in the cytoplasm, uniform cells, and more compact adipocytes were observed in obese mice [48]. Leptin (LP), as a product of adipocyte secretion, is a peptide hormone that acts on multiple tissues and organs through its receptor and has multiple effects on regulation of the body. Yan Runhu [49] treated rats fed with high-fat diet for 12 weeks with catgut implantation at acupoints. The results showed that catgut implantation at acupoints could upregulate the expression of OB-Rb mRNA in the hypothalamus of obese rats and reduce the expression of SOCS-3 mRNA in

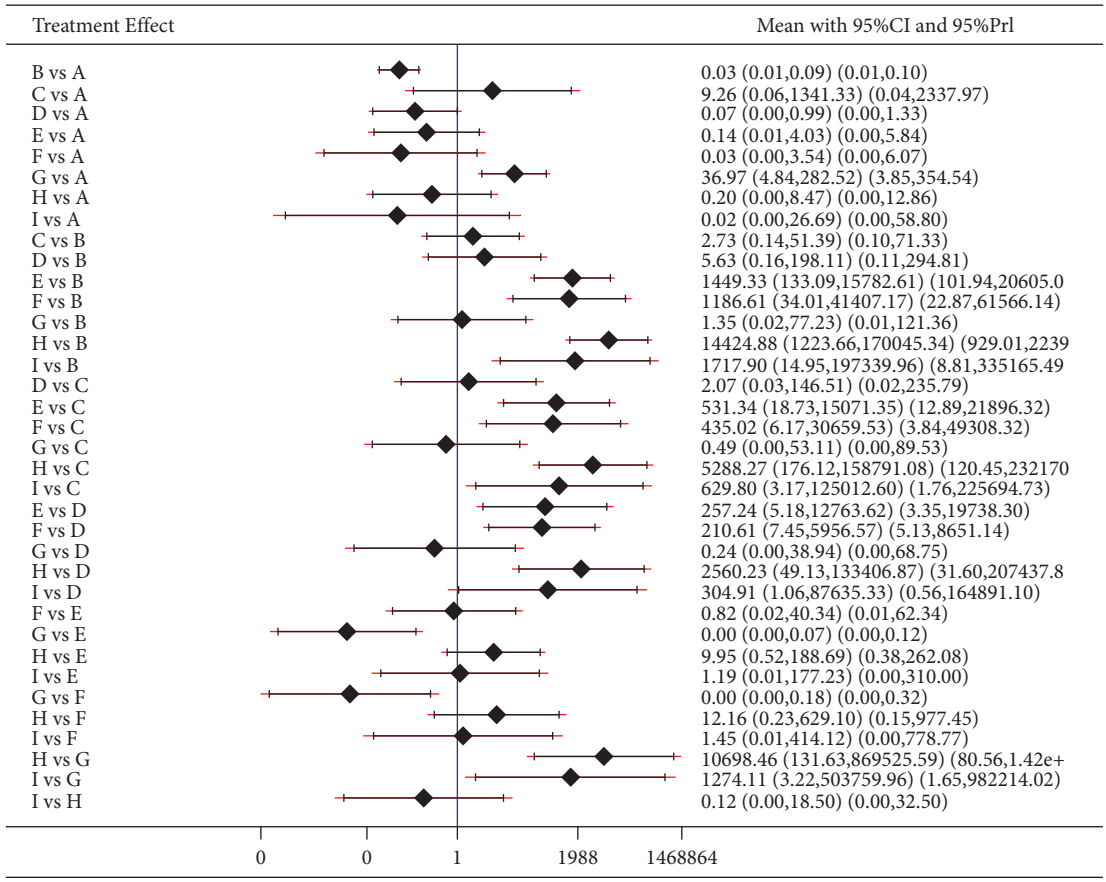

Figure 9: Weight loss in treatment of simple obesity with different methods and catgut embedding at acupoints in meta-analysis forest plot. A: acupoint catgut embedding; B: acupuncture; C: electroacupuncture; D: TCM; E: acupoint catgut embedding + exercise diet therapy; F: acupoint catgut embedding + TCM; G: exercise diet therapy; H: acupoint catgut embedding + moxibustion; I: acupoint catgut embedding + cupping.

hypothalamus cells and the content of SOCS-3 in peripheral blood serum, which suggested that catgut implantation at acupoints promoted signal transduction after LP and fasting insulin receptors, improved leptin resistance (LR) and insulin resistance (IR), and promoted LP and fasting insulin to exert biological effects. Therefore, it can be used as an important mechanism of acupoint catgut embedding for weight loss. Deng Min [50] observed the effect of catgut implantation at acupoints on inflammatory factors in mice and found that catgut implantation at acupoints could inhibit the expression of interleukin-mRNA, tumor necrosis factor-α-mRNA, and monocyte chemoattractant protein-1 mRNA in adipose tissue and could reduce the occurrence and development of inflammatory reactions. Therefore, it is further predicted that the possible mechanism of weight loss by catgut implantation at acupoints is to increase the expression of inflammatory factors in adipose tissue. The meta-analysis of acupoint catgut embedding and related therapies for obesity revealed that acupoint catgut embedding and other therapies showed a high healing rate in the treatment of simple obesity and could reduce the BMI of the patients [6]. Acupoint catgut embedding has become one of the effective measures for the treatment of obesity and has shown good clinical results with a variety of combined therapies, which are widely used [51].

To investigate the curative effect of catgut implantation at each acupoint and related therapies, a network meta-analysis was conducted. A total of 35 studies were included in this study, including 3040 patients. There was a significant difference between the two groups before and after treatment. In network meta-analysis, the effect of various treatment methods was compared. Compared with traditional meta-analysis, it contains more original data. The statistical accuracy of different groups is not enough, but it has no impact on the final results of network meta-analysis [47]. This study ranked the improvement of treatment effect, body mass, and BMI of patients with simple obesity by comparing the treatments including acupoint catgut embedding, acupuncture, TCM, electroacupuncture, and exercise diet therapy alone, as well as the combination of acupoint catgut embedding with different therapies. The results of network meta-analysis showed that, in terms of total effective rate, the top three were acupoint catgut embedding + moxibustion, acupoint catgut embedding + TCM, and acupoint catgut embedding + cupping; in terms of reduced body mass of patients, the top three were acupoint catgut embedding + moxibustion, acupoint catgut embedding + exercise and diet therapy, and acupoint catgut embedding + cupping; and in terms of reduced BMI of patients, the top three were acupoint catgut

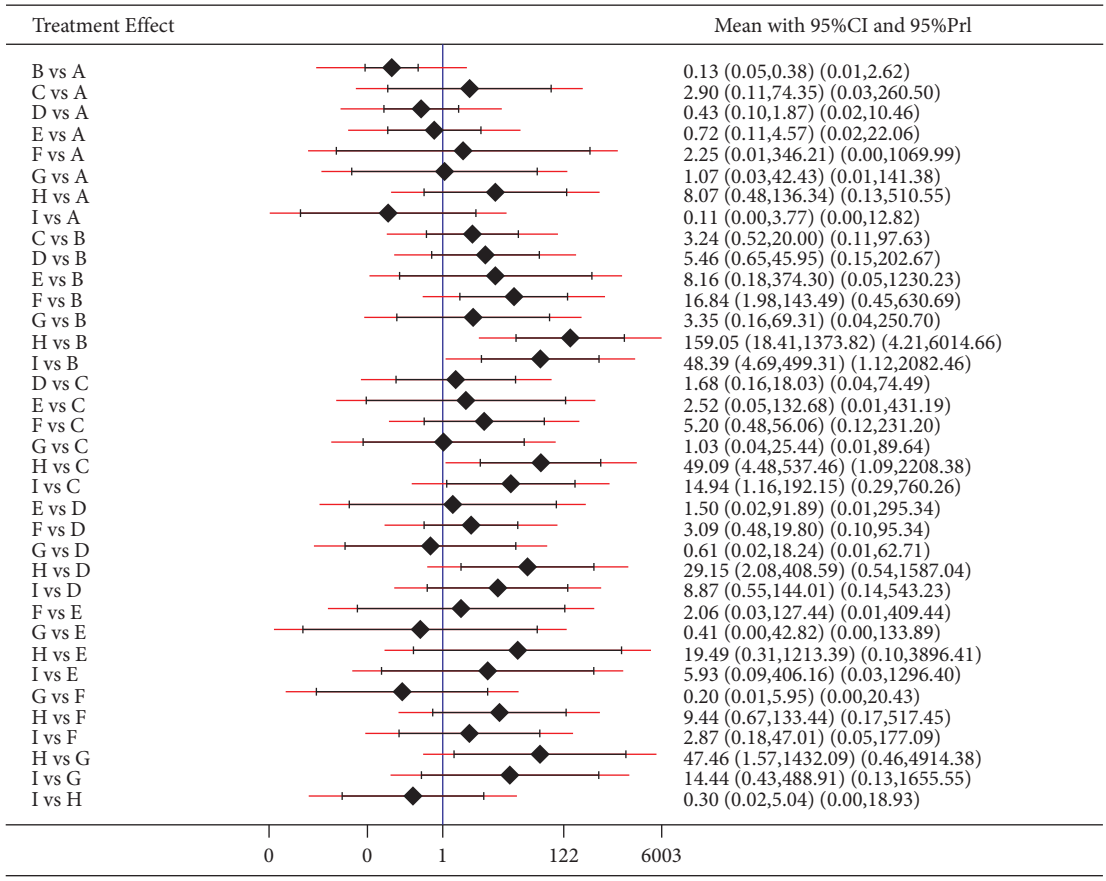

Figure 10: BMI reduction in treatment of simple obesity with different methods and catgut embedding at acupoints in meta-analysis forest plot. A: acupoint catgut embedding; B: acupuncture; C: electroacupuncture; D: TCM; E: acupoint catgut embedding + exercise diet therapy; F: acupoint catgut embedding + TCM; G: exercise diet therapy; H: acupoint catgut embedding + moxibustion; I: acupoint catgut embedding + cupping.

Table 4: The sorting table of network meta-analysis results of different treatment methods and catgut embedding at acupoints for simple obesity.

Interventions	Total efficacy ranking		Weight loss ranking		BMI reduction ranking	
	SUCRA	Rank	SUCRA	Rank	SUCRA	Rank
Acupoint catgut embedding	50.7	6	48.4	5	47.9	4
Acupuncture	10.3	9	8.4	9	7.4	8
Electroacupuncture	37.7	7	32.0	6	31.3	7
TCM	22.2	8	10.8	8	36.3	6
Acupoint catgut embedding + acupuncture	61.6	4				
Acupoint catgut embedding + exercise diet therapy	59.9	5	77.1	2	53.9	5
Acupoint catgut embedding + TCM	79.3	2	72.4	4	73.5	3
Exercise diet therapy	4.1	10	26.4	7	17.2	9
Acupoint catgut embedding + moxibustion	96.5	1	99.5	1	95.5	1
Acupoint catgut embedding + cupping	77.8	3	75.0	3	87.1	2

embedding + moxibustion, acupoint catgut embedding + TCM, and acupoint catgut embedding + cupping. Based on the results of network meta-analysis of the three indexes, acupoint catgut embedding and its combination with other therapies were the best treatments for simple obesity. There was no obvious asymmetry in the comparison correction funnel chart, indicating no publication bias, but there was a scatter at the bottom, indicating the influence of small samples. The inconsistency test indicated good consistency of each closed loop. However, the use of different acupoints, treatment courses, and drugs in the studies leads to clinical heterogeneity, which needs more high-quality RCT studies to verify.

There are some limitations in this study. Firstly, there are adverse reactions in the included literature, so it may cause bias. Secondly, some studies do not mention the random

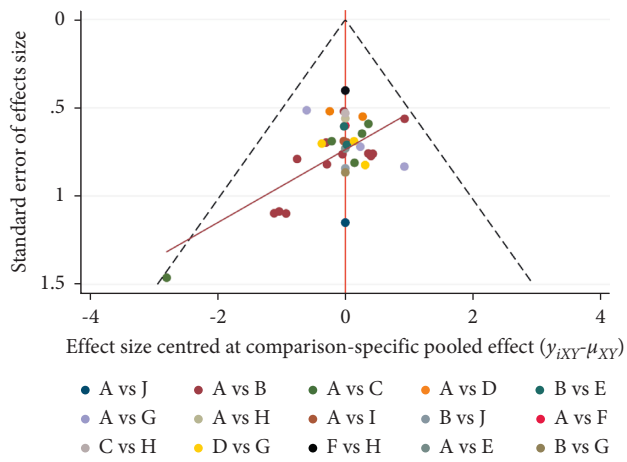

FIGURE 11: Comparison of total effective rate of treatment of simple obesity-corrected funnel plot. A: acupoint catgut embedding; B: acupuncture; C: electroacupuncture; D: TCM; E: acupoint catgut embedding + acupuncture; F: acupoint catgut embedding + exercise diet therapy; G: acupoint catgut embedding + TCM; H: exercise diet therapy; I: acupoint catgut embedding + moxibustion; J: acupoint catgut embedding + cupping.

sequence method and do not blind the subjects and doctors, which may have an impact on the efficacy results. Thirdly, most of the observation indexes were body mass, effective rate, BMI, WC, HC, waist-hip ratio, and so on, lacking objective laboratory indexes. Finally, the short-term effect is good, but there are few follow-up records. The long-term effect needs to be further discussed. This systematic review aims to update and improve.

5. Conclusion

Acupoint catgut embedding and its combination with different therapies significantly increase the effective rate in treatment of simple obesity, resulting in improved body mass and BMI of the patients. The use of acupoint catgut embedding therapy is a better choice and provides a more reliable clinical reference. In clinical treatment, acupoint catgut embedding can be selected based on the conclusion of this study and considering syndrome differentiation. However, the conclusion is affected by the quality of the included studies, and this study needs more high-quality, large-sample RCT studies to verify.

Data Availability

The data used to support the findings of this study are available from the corresponding author upon request.

Conflicts of Interest

The authors declare that they have no conflicts of interest.

Authors' Contributions

Chun-lan Chen, Zun-yuan Li, Chuang Zhao, Wen-ge Huo, Yu-hong Guo, Yan Yang, and Zhi-dan Liu participated in the study design and wrote the article. Zhuo-yuan Wang analyzed the data. Xiao-yan Li and Xiao-jun Gou reviewed the manuscript. All the authors read and approved the final manuscript. Xiao-yan Li and Xiao-jun Gou contributed equally to this work and should be considered corresponding authors.

Acknowledgments

This study was financially supported by the "Medical and Health Project of Special Fund for Scientific and Technological Innovation of Shanghai Baoshan District Commission of Science and Technology" (20-E-13), "Shanghai Talent Development Fund Support Plan" (2020086), and "Hospital-Level Key Specialty Cultivation Project of Shanghai Baoshan Hospital of Integrated Chinese and Western Medicine "(bsyyzdzk-2019-03, bsyyzdzk-2019-04).

References

[1] L. He, X. A. Gao, and L. Yu, "Forty cases of simple obesity treated by acupuncture," *Journal of traditional Chinese medicine = Chung i tsa chih ying wen pan*, vol. 26, no. 1, pp. 24-25, 2006.

[2] X. Chen, W. Huang, D. Wei et al., "Clinical effect of catgut implantation at acupoints for the treatment of simple obesity," *Medicine*, vol. 99, no. 48, Article ID e23390, 2020.

[3] Y. M. Zhong, X. C. Luo, Y. Chen et al., "Acupuncture versus sham acupuncture for simple obesity: a systematic review and meta-analysis," *Postgraduate Medical Journal*, vol. 96, no. 1134, pp. 221–227, 2020.

[4] S. Ma, B. Xi, L. Yang, J. Sun, M. Zhao, and P. Bovet, "Trends in the prevalence of overweight, obesity, and abdominal obesity among Chinese adults between 1993 and 2015," *International Journal of Obesity*, vol. 45, no. 2, pp. 427–437, 2020.

[5] X. Chen, W. Huang, and J. Deng, "Recent clinical research of traditional Chinese medicine for simple obesity," *Chinese Archives of Traditional Chinese*, vol. 35, no. 6, pp. 1454–1458, 2017.

[6] X. Y. Hu, Y. L. Gao, and Y. Wang, "A meta analysis of acupoint catgut-embedding therapy for simple obesity," *Henan Traditional Chinese Medicine*, vol. 41, no. 6, pp. 923–931, 2021.

[7] H. L. Li, Q. Y. Sun, and W. Gao, ""Shenque bazhenpoint"-ginger-separated moxibustion combined with acupoint catgut embedding," *Guiding Journal of Traditional Chinese Medicine and Pharmacology*, vol. 25, no. 14, pp. 86–91, 2019.

[8] L. Q. Luo, "Effect of acupoint catgut embedding therapy on simple obesity," *The Medical Forum*, vol. 20, no. 2, pp. 212-213, 2016.

[9] W. Zhou, Z. Y. Zhou, and F. Hu, "Clinical comparative study on electroacupuncture and acupoint catgut embedding therapy for treatment of obesity," *Liaoning Journal of Traditional Chinese Medicine*, vol. 47, no. 9, pp. 156–159, 2020.

[10] M. M. Li, J. X. Ni, J. Wang, X. Fang, B. Su, and X. Wu, "Clinical observation of catgut-embedding therapy based on respiration induced reinforcing and reducing for treatment of simple obesity with spleen deficiency and dampness retention," *Journal of Guangzhou University of Traditional Chinese Medicine*, vol. 34, no. 4, pp. 534–538, 2017.

[11] X. Zheng and X. N. Wang, "Clinical effect of thunder fire moxibustion combined with acupoint catgut embeddingin the treatment of simple obesity," *Clinical Research and Practice*, vol. 5, no. 6, pp. 150-151, 2020.

[12] X. R. Duan, X. Liao, and C. L. Li, "Clinical observation on 50 cases of simple obesity treated by flash can of Shenque Bazhen point combined with acupoint catgut embedding," *Yunnan Journal of Traditional Chinese Medicine and Materia Medica*, vol. 38, no. 9, pp. 51–53, 2017.

[13] Z. Wang, X. H. Pang, and M. Ma, "Effect of painless acupoint catgut embedding therapy on simple obesity," *Contemporary Medical Symposium*, vol. 18, no. 7, pp. 196-197, 2020.

[14] L. J. Zhou, J. Li, and W. Ma, "Clinical study on painless acupoint embedding therapy in simple obesity," *World Chinese Medicine*, vol. 12, no. 7, pp. 1645–1651, 2017.

[15] X. M. Wu, Y. S. Zheng, and H. N. Zhou, "Effects of acupoint catgut embedding and electroacupuncture on the treatment of simple obesity," *Modern Nursing*, no. 4, pp. 77-78, 2015.

[16] Q. Huang, "Effect of acupoints catgut embedding on weight and blood lipid of simple obesity patients," *Journal of External Therapy of Traditional Chinese Medicine*, vol. 29, no. 1, pp. 52-53, 2020.

[17] G. H. Lin, S. Q. Yang, and X. T. Xiao, "Clinical study on acupoint catgut embedding combined with cupping in the treatment of simple obesity," *New Chinese Medicine*, vol. 47, no. 7, pp. 229-230, 2015.

[18] R. Deng, Z. Q. Lei, D. Wang et al., "Clinical observation of acupoint embedding combined with umbilical moxibustion for simple abdominal obesity," *Jilin Journal of Chinese Medicine*, vol. 41, no. 3, pp. 391–395, 2021.

[19] W. Huang, D. Wei, and T. Y. Yang, "Clinical observation on the therapeutic effect of acupoint catgut-embedding integrated with diet and exercise for simple obesity," *Journal of Clinical Acupuncture and Moxibustion*, vol. 31, no. 10, pp. 1–3, 2015.

[20] C. J. Lin, X. M. Wang, and Q. Q. Ye, "Acupoint catgut embedding combined with Shenling Baizhu Powder in the treatment of 30 cases of simple obesity with spleen deficiency and dampness syndrome," *Zhejiang Journal of Traditional Chinese Medicine*, vol. 55, no. 3, pp. 217-218, 2020.

[21] Q. F. Wen, H. J. Qi, and L. H. Chen, "Clinical study on acupoint catgut embedding combined with Jiawei Wendan Decoction in the treatment of simple obesity," *Shenzhen Journal of Integrated Traditional Chinese and Western Medicine*, vol. 31, no. 8, pp. 80–82, 2021.

[22] J. X. Su, Y. Zhang, and Z. Z. Wang, "Clinical observation of 115 patients with simple obesity treated by catgut-embedding therapy combined with Chinese herbal compound Xiaozhi decoction," *Clinical Journal of Traditional Chinese Medicine*, vol. 29, no. 9, pp. 1497–1500, 2017.

[23] R. Wang, H. S. Luo, and Y. X. Xu, "Clinical observation of acupoint catgut embedding combined with exercise management in the treatment of simple obesity," *Zhejiang Journal of Traditional Chinese Medicine*, vol. 52, no. 6, p. 452, 2017.

[24] L. S. Wang, X. Luo, and G. Yang, "Clinical study of acupoint thread embedding plus fat sweep method for simple obesity," *Shaanxi Journal of Traditional Chinese Medicine*, vol. 40, no. 3, pp. 390–393, 2019.

[25] R. Z. Chen, "Clinical study on acupoint catgut embedding therapy for simple obesity," *Electronic Journal of Clinical Medical Literature*, vol. 3, no. 43, pp. 8506-8507, 2016.

[26] H. L. Zhou, Q. Xu, Q. L. Liu, J. Xie, T. Wang, and Y. Deng, "Clinical effect observation of acupoint catgut embedding combined with TCM granule Qingzhi decoction in treating simple obesity," *Clinical Journal of Chinese Medicine*, vol. 10, no. 18, pp. 89–91, 2018.

[27] X. Zheng and H. C. Ji, "Acupoint catgut embedding therapy for 40 cases of simple obesity," *Journal of External Therapy of Traditional Chinese Medicine*, vol. 24, no. 6, pp. 28-29, 2015.

[28] W. J. Guo and S. W. Zhao, "71 cases of simple obesity were treated of simple obesity," *China Medical Cosmetology*, vol. 4, no. 6, p. 175, 2014.

[29] H. Zhang and T. H. Ding, "Therapeutic effect of acupoint catgut embedding on simple obesity and its influence on blood lipids," *Modern Journal of Integrated Traditional Chinese and Western Medicine*, vol. 26, no. 12, pp. 1334–1336, 2017.

[30] H. Y. Zhao and B. W. Ai, "Clinical observation on treating simple obesity by acupoint catgut embedding," *Clinical Journal of Chinese Medicine*, vol. 7, no. 4, pp. 41–43, 2015.

[31] R. J. Yao, "Clinical study on acupoint catgut embedding in the treatment of simple obesity," *Modern Diagnosis and Treatment*, vol. 25, no. 13, pp. 2918-2919, 2014.

[32] Z. L. Chen, Z. G. Feng, and L. J. Xu, "Acupoints buried line treatment to simple obesity," *Journal of Zhejiang Chinese Medical University*, vol. 37, no. 11, pp. 1341-1342, 2013.

[33] W. X. Huang, S. R. Liao, and X. F. Chen, "Observation on treating simple obesity of the Pishen Liangxu type by the acupoint catgut embedding therapy," *Clinical Journal of Chinese Medicine*, vol. 11, no. 35, pp. 49–51, 2019.

[34] B. Yan, S. X. Li, and Y. P. Hu, "Clinical study on catgut embedment in point for simple obesity of spleen deficiency with dampness obstruction type concomitant with dyslipidemia," *New Chinese Medicine*, vol. 53, no. 9, pp. 134–138, 2021.

[35] L. J. Li, Y. J. Li, and D. F. Lin, "Therapeutic effect of acupoint catgut embedding on simple obesity with spleen deficiency and dampness resistance," *Journal of Baotou Medical College*, vol. 32, no. 3, pp. 105-106, 2016.

[36] Q. Wang and R. S. Na, "Clinical mechanism of acupoint catgut embedding and TCM prescription of Peilian Mahuang for patients with spleen deficiency and dampness stagnation of simple obesity," *Guiding Journal of Traditional Chinese Medicine and Pharmacy*, vol. 24, no. 1, pp. 75–83, 2018.

[37] B. B. Zhao and Z. H. Ma, "Clinical study on simple obesity by moving cupping combined with acupoint catgut embedding therapy," *Journal of Clinical Acupuncture and Moxibustion*, vol. 31, no. 3, pp. 47–49, 2015.

[38] B. J. Liang, W. Z. Shen, and S. R. Liao, "Clinical study on acupoint catgut embedding combined with modified linguizhugan decoction in treating simple obesity of spleen deficiency and phlegm turbidity type," *Chinese Journal of Modern Drug Application*, vol. 13, no. 13, pp. 145-146, 2019.

[39] M. F. Lv, X. Y. Zhu, and X. J. Yu, "Observation of the therapeutic effect of long-snake moxibustion combined with acupoint catgut implantation," *Modern Hospital*, vol. 20, no. 1, pp. 140–142, 2020.

[40] Y. Y. Chen, N. F. Li, C. Cui, and X. F. Chen, "Clinical observation of acupuncture combined with acupoint catgut embedding in the treatment of simple obesity," *Guangming Journal of Chinese Medicine*, vol. 30, no. 6, pp. 1266–1268, 2015.

[41] S. J. Hou, "Simple obesity treated by acupuncture combined with catgut embedding: 68 cases," *Chinese Journal of Ethnomedicine and Ethnopharmacy*, vol. 25, no. 17, pp. 74–76, 2016.

[42] F. Tian and Q. He, "Acupuncture point embedding therapy for simple obesity: 44 cases," *Chinese Medicine Modern Distance Education of China*, vol. 12, no. 10, pp. 63-64, 2014.

[43] W. Huang, X. Chen, Y. Zhang et al., "Acupoint catgut embedding for obesity," *Medicine*, vol. 99, no. 51, Article ID e23728, 2020.

[44] J. Yamamoto, J. Imai, T. Izumi et al., "Neuronal signals regulate obesity induced β-cell proliferation by FoxM1 dependent mechanism," *Nature Communications*, vol. 8, no. 1, p. 1930, 2017.

[45] K. E. Bouter, D. H. van Raalte, A. K. Groen, and M. Nieuwdorp, "Role of the gut microbiome in the pathogenesis of obesity and obesity-related metabolic dysfunction," *Gastroenterology*, vol. 152, no. 7, pp. 1671–1678, 2017.

[46] Q. F. Zeng, Y. Q. Li, X. L. Wu, Z. Chen, and B. Luo, "Research progress of acupoint catgut embedding in treating simple obesity in recent five years," *Journal of Clinical Acupuncture and Moxibustion*, vol. 37, no. 10, pp. 96–100, 2021.

[47] R. Neira, J. Arroyave, H. Ramirez et al., "Fat liquefaction: effect of low-level laser energy on adipose tissue," *Plastic and Reconstructive Surgery*, vol. 110, no. 3, pp. 912–922, 2002.

[48] M. Deng, Y. N. Sun, and M. R. Gong, "Effect of acupoint catgut embedding on lipid-lowering effect of simple obese mice," *Liaoning Journal of Traditional Chinese Medicine*, vol. 43, no. 7, pp. 1479–1481, 2016.

[49] R. H. Yan, J. Bai, J. S. Gu, J. Yu, X. Li, and J. Sui, "Effect of SOCS-3 gene expression on obese rats with catgut implantation at acupoints," *Chinese Archives of Traditional Chinese Medicine*, vol. 34, no. 1, pp. 121–125, 2016.

[50] M. Deng, S. S. Xu, and Y. N. Sun, "Effects of acupoint catgut-embedding therapy on fat reduction and the inflammatory factor in adipose tissues of the obese mice," *Lishizhen Medicine and Materia Medica Research*, vol. 27, no. 5, pp. 1277–1279, 2016.

[51] J. Tang, H. X. Xie, and C. T. Mo, "Research overview of acupoint catgut embedding and its combined therapy for simple obesity," *Acta Chinese Medicine and Pharmacology*, vol. 49, no. 4, pp. 117–120, 2021.

Hindawi
Evidence-Based Complementary and Alternative Medicine
Volume 2022, Article ID 1679589, 19 pages
https://doi.org/10.1155/2022/1679589

Review Article

Information Extraction from the Text Data on Traditional Chinese Medicine: A Review on Tasks, Challenges, and Methods from 2010 to 2021

Tingting Zhang,[1] **Zonghai Huang**,[1] **Yaqiang Wang**,[2] **Chuanbiao Wen**,[1] **Yangzhi Peng**,[1] **and Ying Ye**[1]

[1]*Chengdu University of Traditional Chinese Medicine, Chengdu, China*
[2]*Chengdu University of Information Technology, Chengdu, China*

Correspondence should be addressed to Yaqiang Wang; yaqwang@cuit.edu.cn and Ying Ye; yeyingtcm@163.com

Received 11 February 2022; Revised 31 March 2022; Accepted 6 April 2022; Published 13 May 2022

Academic Editor: Xuezhong Zhou

Background. The practice of traditional Chinese medicine (TCM) began several thousand years ago, and the knowledge of practitioners is recorded in paper and electronic versions of case notes, manuscripts, and books in multiple languages. Developing a method of information extraction (IE) from these sources to generate a cohesive data set would be a great contribution to the medical field. The goal of this study was to perform a systematic review of the status of IE from TCM sources over the last 10 years. *Methods*. We conducted a search of four literature databases for articles published from 2010 to 2021 that focused on the use of natural language processing (NLP) methods to extract information from unstructured TCM text data. Two reviewers and one adjudicator contributed to article search, article selection, data extraction, and synthesis processes. *Results*. We retrieved 1234 records, 49 of which met our inclusion criteria. We used the articles to (i) assess the key tasks of IE in the TCM domain, (ii) summarize the challenges to extracting information from TCM text data, and (iii) identify effective frameworks, models, and key findings of TCM IE through classification. *Conclusions*. Our analysis showed that IE from TCM text data has improved over the past decade. However, the extraction of TCM text still faces some challenges involving the lack of gold standard corpora, nonstandardized expressions, and multiple types of relations. In the future, IE work should be promoted by extracting more existing entities and relations, constructing gold standard data sets, and exploring IE methods based on a small amount of labeled data. Furthermore, fine-grained and interpretable IE technologies are necessary for further exploration.

1. Introduction

Traditional Chinese medicine (TCM), a unique theoretical and practical approach to the treatment of diseases, has played an indispensable role in the health care of the Chinese population for several thousand years [1]. According to the latest global medical outline (Ver.2019) of the World Health Organization (WHO), TCM is a popular and effective complementary and alternative medicine in preventing and treating many diseases [2]. An example is the integrated use of TCM in the treatment of COVID-19, which was shown to be more effective than the use of modern therapies alone [3, 4].

Textual data is the most common data type in TCM. Throughout history, the rich data source of TCM that dates back thousands of years is scattered in different text formats in paper versions such as case notes, manuscripts, printed books, and publications [5]. All these text data contain valuable medical information such as manifestations of disease, diagnostic rules, therapeutic methods, and effective prescriptions. Hence, it is a crucial carrier of TCM knowledge and contributes to the inheritance and dissemination of TCM. However, human labor is insufficient to deal with the increasing accumulation of text data, and hence

automated TCM knowledge discovery is necessary and urgently needed.

With the continuous development of information technology and artificial intelligence (AI), data mining is an approach that can be used to obtain information from many sources and is increasingly applied in mining of medical texts, including the TCM literature [6]. More fortunately, informatization of TCM text sources has brought opportunities for the deep utilization of diverse TCM texts in recent decades [7]. However, the majority of electronic TCM texts are stored as unstructured data, including a tremendous amount of case notes, with chief complaint and history of present illness, abstracts of publications, Web data, etc., that cannot be directly used for text mining. Therefore, the imperative task before data mining can be conducted is to transform TCM narratives into structured data.

Information extraction (IE) techniques, an important part of natural language processing (NLP), have assisted automatic information acquisition from TCM texts and have been increasingly used in text mining in recent years [8, 9]. By building large-scale and comprehensive structured data sets, TCM texts can be widely used in clinical applications such as information retrieval [10], computer-aided syndrome differentiation and diagnosis [11, 12], and analysis of prognosis [13]. An example of extracting information from a clinical record of TCM is shown in Figure 1.

To our knowledge, there are many IE tools that can extract information from English language unstructured data, such as MedLEE [14], MetaMap [15], and MedTagger [16]. However, owing to the differences between the Chinese and Western languages, such as different word segmentation methods, different syntactic structures, and word and sentence ambiguity, these tools or systems of IE in English cannot be transplanted directly to Chinese IE tasks, and TCM texts are even more challenging. With this background, more approaches were explored to extract information from different types of TCM text data, and IE from TCM texts has shown encouraging improvements accordingly [17, 18]. Although previous research has summarized some IE work in TCM [19–21], the new advanced technologies and emerging methods need to be further summarized and synthesized, for example, improved deep learning approaches and more types of extracted information [22, 23]. In this study, we searched four literature databases for articles published from 2010 to 2021 that focused on the use of NLP methods to extract information from unstructured TCM text data. Based on what we found in the articles, we assessed the status of IE from TCM sources as related to (1) data sources and extracted information, (2) challenges, (3) NLP frameworks and models, and (4) key findings. We conclude with some recommendations for future studies.

2. Methods

Review procedures were carried out under the guidance of Preferred Reporting Items for Systematic Reviews and Meta-Analyses (PRISMA) [24], which lists priority report items for systematic reviews and meta-analyses. Under the instructions in PRISMA, we undertook our review in three steps: (1) article search, (2) article selection, and (3) data extraction and synthesis. The PRISMA checklist is attached as Supplementary 1.

2.1. Article Search. We searched PubMed, Web of Science, EMBASE, and Engineering Village on 31 December 2021 to identify all potentially relevant publications related to extracting information from TCM text data. The search strategy and the reasons for each search string category are shown in Figure 2. The selected keywords and the associations between these keywords were identical in the searches for each database. Queries were limited to English language. The time period ranged from 2010 to 2021. The searches returned 564 articles from PubMed, 435 from Web of Science, 427 from Embase, and 779 from Engineering Village. Subsequently, the titles, abstracts, keywords, and other information from all retrieved papers were imported into EndNote X7 reference management software for data selection. We made use of the "find duplicates" function to find the 970 duplicated papers. A total of 1,234 publications were retrieved in this step.

2.2. Selection of Articles. We used EndNote X7 reference management software to manage many of the screening and coding processes of our systematic review procedures. Attention was paid to the methodology and content in the selection process. The filtering criteria and eligibility criteria are listed in Figure 3. In the data selection step, the articles were labeled with "include", "exclude", and "undetermined" according to the criterion applied. Two reviewers (Zhang, Ye) independently reviewed the titles, abstracts, and full texts of the retrieved publications and an adjudicator (Wang) reviewed the articles with disagreement. One of the two reviewers has background knowledge of TCM, and the other reviewer and the adjudicator are mainly engaged in NLP research. The cooperation of three reviewers with TCM and computer knowledge background ensured the reliability of the paper screening results. For articles on which the adjudicator could not make a decision, the three reviewers discussed together to decide whether to include or exclude the article. After the first screening, 131 articles that were probably related to IE for TCM were included. Afterward, we downloaded the full-text PDF file to conduct the next round of screening. During this step, the methodology and data source for each publication were reviewed to make a final decision. The same selection procedure was used as before: two reviewers screened the full text for all records, and the third adjudicator reviewed the disagreements between them. Finally, a total of 49 eligible papers were determined to meet the review criteria.

2.3. Data Extraction and Synthesis. Data extraction from the 49 articles included in the paper selection step was performed manually by two reviews and one adjudicator. First, two reviewers (Zhang and Ye) independently reviewed the articles and extracted information to form an Excel table.

TCM clinical record

Basic information	*Wang, male, 31 years old, visited on November 14, 2020*
Chief complaints	*Chief complaints:* facial paralysis for 2 days
History of present illness	*Current history:* 2 days ago, the patient has deviated mouth to the left side with no inducement, air leakage of the mouth, incomplete closure of the right eyelid, disappearance of the right frontal stria, no postauricular pain, no external auditory canal herpes, sloppy stool for a long time, normal urination and diet, pale tongue with white and thin tongue coating, thready and weak pulse with rapid beating.
Disease diagnosis	*TCM diagnosis:* stroke (apoplexy involving both collaterals and meridians)
Sydrome differentiation	*Syndrome differentiation:* wind evil hurts meridians and collaterals, qi deficiency of lung and spleen, with blood stasis and dampness
Treatment	*Treatment:* removing blood stasis, dispelling the wind, dredging collaterals, tonifying lung, strengthening spleen and dehumidification. *Prescription:* Sijunzi Decoction Combined with Yupingfeng Powder *Medicine:* astragalus mongholicus 30 g, saposhnikovia divaricata 12 g, stir-fried bighead atractylodes rhizome 15 g, codonopsis pilosula 20 g, poria cocos 30 g, prepared radix glycyrrhizae 6 g, peach kernel 10 g, safflower 10 g, pberetima 12 g, fructus liquidambaris 15 g, agastache rugosus 10 g. 3 doses, decocting with water. A dose a day, take the warm medicine after meals three times per day.
Doctor's advice	Avoid cold food, avoid catching cold.

Section name	Extracted concepts	Examples
Basic information	Name	Wang
	Gender	Male
	Age	31 years old
	Visit time	November 14, 2020
	…	…
Chief complaints	Symptom	Facial paralysis
	Duration	2 days
	…	…
History of present illness	Symptom	Deviated mouth to the left side; air leakage of the mouth; disappearance of the right frontal stria…
	Tongue manifestation	Pale tongue with white and thin tongue coating
	Pulse condition	Thready and weak pulse with rapid beating
	…	…
Disease diagnosis	Disease name	Stroke; apoplexy involving both collaterals and meridians
Syndrome differentiation	Syndrome	Wind evil hurts meridians and collaterals; qi deficiency of lung and spleen; with blood stasis; with dampness
Treatment	Prescription	Sijunzi Decoction; Yupingfeng Powder
	Treatment principle	Removing blood stasis; dispelling the wind; dredging collaterals; tonifying lung; strengthening spleen; dehumidification
	Traditional chinese medicine	Astragalus mongholicus; Saposhnikovia divaricate; stir-fried bighead atractylodes rhizome; codonopsis pilosula…
	Decoction method	Decocting with water
	Methods of taking medicine	Three times per day; take the warm medicine after meals
	…	…
Doctor's advice	Attention points	Avoid cold food; avoid catching cold
	…	…

Figure 1: Example of extracting information from a TCM clinical record.

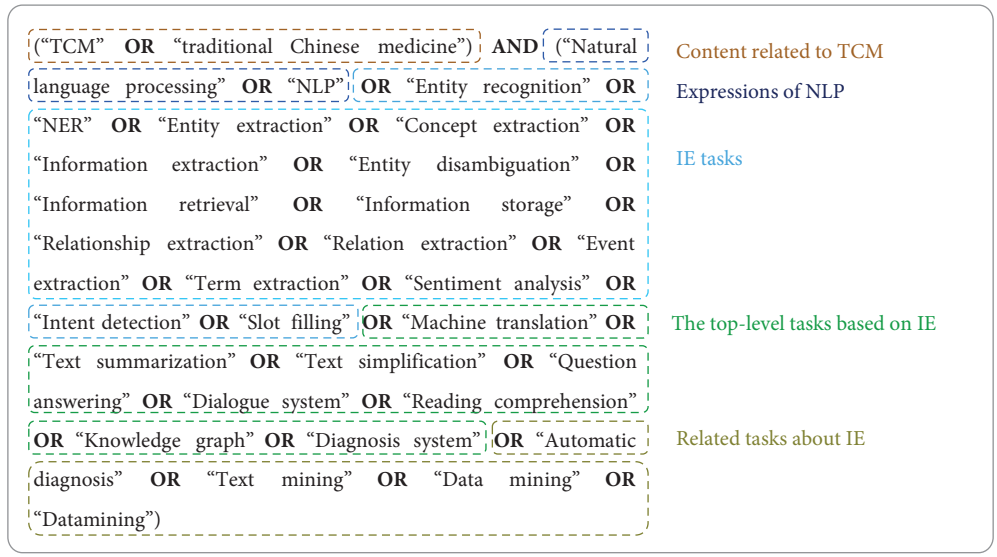

Figure 2: The search strategy and reasons for each search string category.

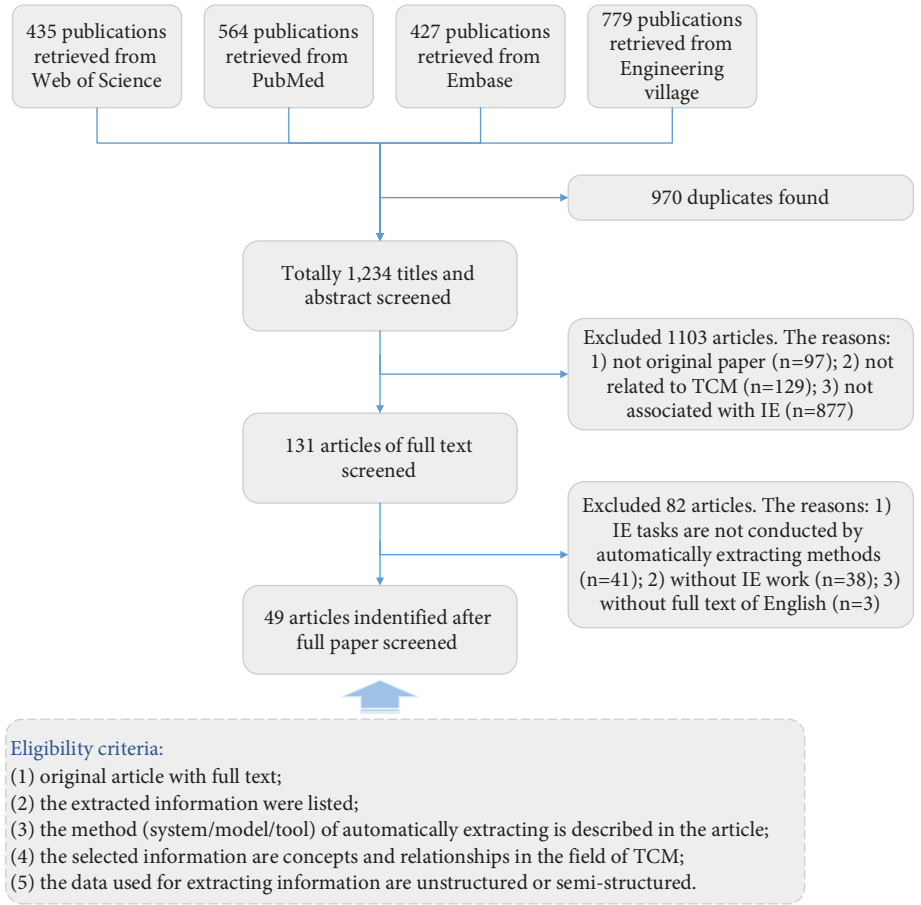

Figure 3: Flow diagram of included articles and eligibility criteria.

The information or items extracted included author, title, year published, data type, data number and source, disease, approach (system/model/tool, method type), extracted information, evaluation measures and performance, comparative evaluations, challenges, objective, and relevant outcomes. After that, an adjudicator (Wang) reviewed the table of papers with disagreements and made a final data sheet. The final table of the extracted data is attached as Supplementary 2. In this paper, our aim is to describe and assess the following aspects of the studies: (1) data sources

Figure 4: Timeline of data sources, models (or algorithms), and extracted targets of TCM.

and extracted information, (2) challenges, (3) NLP frameworks and models, and (4) key findings. On the basis of these results, we conclude with some recommendations for future studies.

3. Results of TCM Information Extraction in the Last Ten Years

We synthesized the data sources, models (or algorithms), and extracted targets of TCM into a timeline, as shown in Figure 4. In Figure 4, the number of colored shapes on the left side represents the number of articles published in the corresponding time interval. Obviously, the number of published papers on IE from TCM is increasing. In particular, from 2020 we counted a total of 25 published papers. The trend of growth in IE work indicates that IE from TCM texts has attracted much attention and is developing rapidly.

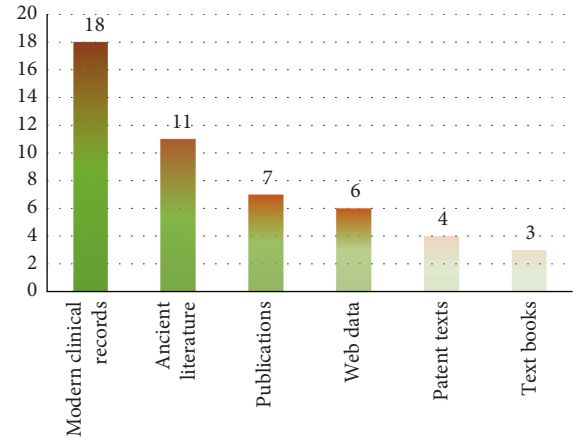

Figure 5: The number of papers enrolled for each type of data source.

In terms of IE methods, researchers have explored many deep learning methods in the last two years.

3.1. The Tasks of Extracting Information from TCM Texts

3.1.1. Data Sources. The data used and structured in the 49 studies in this review came from six types of TCM free text. The distribution of the number of papers for six types of data source is shown in Figure 5. As shown in Figure 5, clinical records were the most commonly used data source for IE in the TCM domain, followed by the ancient literature and four other types of data source. Given that TCM data varied widely in different data sources, we organized the basic data composition of each data source below, hoping that this would be helpful for future IE research.

Modern Clinical Records. Modern clinical records can be divided into resident admission notes (RANs) and outpatient records. RANs, also called inpatient clinical records, are an important source of data for IE tasks and clinical applications. The RANs contain comprehensive information on the patient's hospitalization period, such as basic information, chief complaints, personal history, current history, past history, physical examinations, biochemical examinations, diagnoses, and treatments. In the above sections, the types of TCM data were name, gender, temporal words, symptoms, pulse conditions, tongue manifestations, disease names, syndromes, prescriptions, acupoints, differential symptoms, viscera, etc. Unlike RANs, outpatient records are simple records of the patient's condition at the time of their visit, often in electronic or handwritten (or a transcript of a manuscript) form. Outpatient records are always concise, and only the key information is recorded, such as important symptoms and signs, differential symptoms, diagnoses, and treatments (mainly prescriptions and Chinese medicine). In particular, most of the case records of famous past TCM experts were recorded in the form of outpatient medical records. For example, the record "dizziness for three days" is extracted as chief complaints. In this record, "dizziness" is symptom, and "three days" is duration.

Ancient Literature. The ancient literature (also called ancient clinical record) documented by ancient TCM practitioners was always written in an obscure and concise style, without a standard format. Consequently, ancient literature is more unintelligible than modern records. In this review, all ancient literature came from ancient Chinese medicine books, including case records books (case records books record the typical examples of doctors' clinical diagnosis and treatment), comprehensive prescription books (comprehensive prescription books, with diseases and prescriptions as the core, are a summary description of ancient Chinese medicine experts in the process of diagnosis and treatment, not just for a patient), classic books of TCM (the classic books of TCM refer to the four classic works of TCM, including "黄帝内经" (Inner Canon of Yellow Emperor), "难经" (Classic of Questioning), "伤寒杂病论" (Treatise on Cold Pathogenic and Miscellaneous Diseases), and "神农本草经" (Sheng Nong's Herbal Classic)), etc. There were a number of significant data types in the ancient literature, including disease names, symptoms, syndromes, zang-fu organs, yin and yang, the five elements, meridians and collaterals, acupuncture points, prescriptions, medicine, explanations for the mechanism of TCM, etc. For example, in an ancient record "妇人怀孕, 腹中疼痛, 当归芍药散主之" (pregnant women has abdominal pain, angelica paeonia powder can treat it), "pregnant women has abdominal pain" is symptom, and "angelica paeonia powder" is prescription name.

Journal Publications. There was much useful data in countless published papers, such as titles, abstract, keywords, text sections, and references. Taking the "abstract" as an example, the abstract is easily accessible and contains a wealth of information, such as objectives, methods, results, and conclusions.

Text Books. Text books used as the IE sources include text books compiled by modern experts and books based on the original text of ancient books, such as *TCM diagnostics* and *TCM basic theory*. The data composition of the text books was similar to that of ancient literature and clinical records. Additionally, there were many explanations and descriptions of TCM theories in text books that would be helpful for understanding TCM concepts and decision-making.

Web Data. The web data came from Web page data and Web data sets. Large masses of Web pages contained almost all types of TCM data. The online data sets were part of the standard data sources for IE, including data sets from various data integration and search platforms such as PubMed and the National Center for Biotechnology Information (NCBI) and Chinese health websites.

Patent Data. TCM patents often contain descriptions of drug efficacy, composition, processing methods, etc. More specifically, the extracted information included disease, syndromes, symptoms, herbal medicine, prescriptions, drug regimens, etc. The patent data always come from patent searching system or intellectual property websites.

3.1.2. Extracted Information. Based on Figure 4, we further reorganized the IE tasks of TCM. It should be observed that three studies performed both entity (or term) recognition and relation extraction tasks. We were surprised that only nine studies featured relation extraction as an objective, suggesting that research on relation extraction in the field of TCM is insufficient. Remarkably, all the articles reported the data sources, and 44 reported a specific number (total words or the number of records/books). Most of the IE tasks did not focus on a particular disease or disease category ($N = 45$) but used comprehensive text as the data source. Some studies ($N = 4$) carried out extraction work from text data for a type or category of disease.

In this systematic review, we classified the information extracted from the selected studies into extracted entities and extracted relations.

Extracted Entities. We identified 43 studies on entity recognition (or term extraction) ($N = 38$), attribute extraction ($N = 3$), and section (or unit) extraction ($N = (2)$ tasks for TCM free-text data. Recognition tasks were divided into word-level recognition work and section-level recognition work. (1) The extracted concepts of word-level recognition involved "symptom" ($N = 24$), "drug" (or medicine) ($N = 19$), "disease" ($N = 12$), "syndrome" ($N = 7$), "formula" (or prescription) ($N = 10$), "body structure" ($N = 3$), "tongue-like" ($N = 4$), "pulse" ($N = 4$), "pathogenesis" ($N = 2$), "department" ($N = 2$), "dose" ($N = 3$), "names of people" ($N = 2$), "place" ($N = 2$), "sign" ($N = 2$), "meridian" ($N = 1$), "temporal fact" ($N = 1$), "color" ($N = 1$), "quantity" ($N = 1$), "disease location" ($N = 1$), "frequency" ($N = 1$), etc. The attributes extracted ($N = 3$) contained patented drug attributes [25], disease attributes [26], and attributes of herbal medicine entities and prescriptions [27]. Among these word-level extracted entities, Zhang et al. [28] and Xu H. et al. [29] made more fine-grained division of the entities when annotating electronic health notes, which provided good demonstrations of fine-grained entity recognition. (2) Section-level entities included the clinical record unit and the sections on subjects, methods, and results [30, 31]. As the unit or section extraction is carried out on unstructured narratives, it is also classified as IE work.

Extraction Relations. The extracted relations involved in nine reports were the "herb-disease" relation ($N = 4$), "herb-syndrome" relation ($N = 3$), "formula-syndrome" relation ($N = 3$), "formula-disease" relation ($N = 3$), "syndrome-disease" relation ($N = 3$), "effect" relation ($N = 1$), "good for" relation ($N = 1$), "bad for" relation ($N = 1$), "same" relation ($N = 1$), "different" relation ($N = 1$), "related" relation ($N = 1$), "disease-treatment" relation ($N = 1$), "healthcare" relation ($N = 1$), "herbal-chemical" relation ($N = 1$), "therapeutic" relation ($N = 1$), and "causal" relation ($N = 1$).

3.2. Challenges in Extracting Information from TCM Text Data. The challenges or difficulties discussed in most papers were related to the content of TCM data and IE methods. Taking into account the domain particularity of the TCM text data, we synthesized the challenges of IE in the field of TCM into the following four points:

(1) TCM texts are always unstructured and lack gold standard corpora. Chinese expressions are formed by continuous Chinese characters without spaces, and the boundary of entities is not clear. Besides, owing to the domain-specific presentation form, TCM narratives are more difficult to process than public Chinese free text [32]. Therefore, the participation of TCM experts is often indispensable to the labeling work, which increases the difficulty and cost of constructing the corpora. At present, the published corpora have a coverage rate of current semantic lexicons and the ambiguities of the lexicon words. In fact, there is still a lack of gold standard annotated data sets in the TCM field, which hinders the development of IE technologies.

(2) Most of the unstructured text data in the TCM domain are nonstandardized. The contents of TCM records are always in old Chinese language and have various writing styles, as they were accomplished by different writers. Different doctors have their own social and knowledge backgrounds and different experiences, resulting in abundant nonstandard descriptions of ancient and modern TCM free-text data. For instance, "气虚", "气弱", and "气不足" all express the pathogenesis of Qi deficiency. "头痛", "头疼", and "巅顶痛" all refer to headache symptoms. Consequently, TCM always contains a hundred contending schools (TCM academic schools refer to the different divisions within the TCM clinical practice; different schools have some differences in the diagnosis and treatment methods) of thought. Clinical practitioners with historical backgrounds have different knowledge reserves and academic perspectives. This leads to the diversity of written expressions and academic views of TCM. For example, "同义词" (one meaning with different descriptions) and "一词多义" (one expression with different meanings according to the context) are very common nonstandardized phenomena in ancient and modern TCM records. Therefore, there are many differences in TCM records, including writing styles, habitual vocabularies, forms of thinking logic, and treatment habits, which bring difficulties and challenges to IE tasks.

(3) There are multiple types of intricate relations in TCM data. In TCM records, there are many complicated theoretical connections in implicit form with few hints in the original text, which can only be comprehended by TCM experts. This phenomenon causes complicated relationship networks among these heterogeneous medical entities. Taking an example, the traditional Chinese Medicine Language System (TCMLS) has listed and defined 96 basic semantics types and 58 semantic relationships on the ontology top level [33]. In fact, the numbers of types of concepts and the relationships among them are far greater. Currently, more than 120,000 concepts, 300,000 terms, and 1.27 million semantic relational links have been included in the TCMLS [33]. The TCM entity relationship network is huge and complex, increasing the workload and difficulty of IE work.

(4) Automatically and effectively extracting information from raw TCM text is a technical challenge. With the rapid accumulation of text data, it is impossible to construct structured data sets manually. Although more and more IE systems have been developed, the development of IE technology still needs to be explored in the face of the above three challenges. For example, how to extract information without manually annotating a large number of text data, how to extract many-to-many relations from complex TCM semantic information, and how to collect features from short texts of TCM.

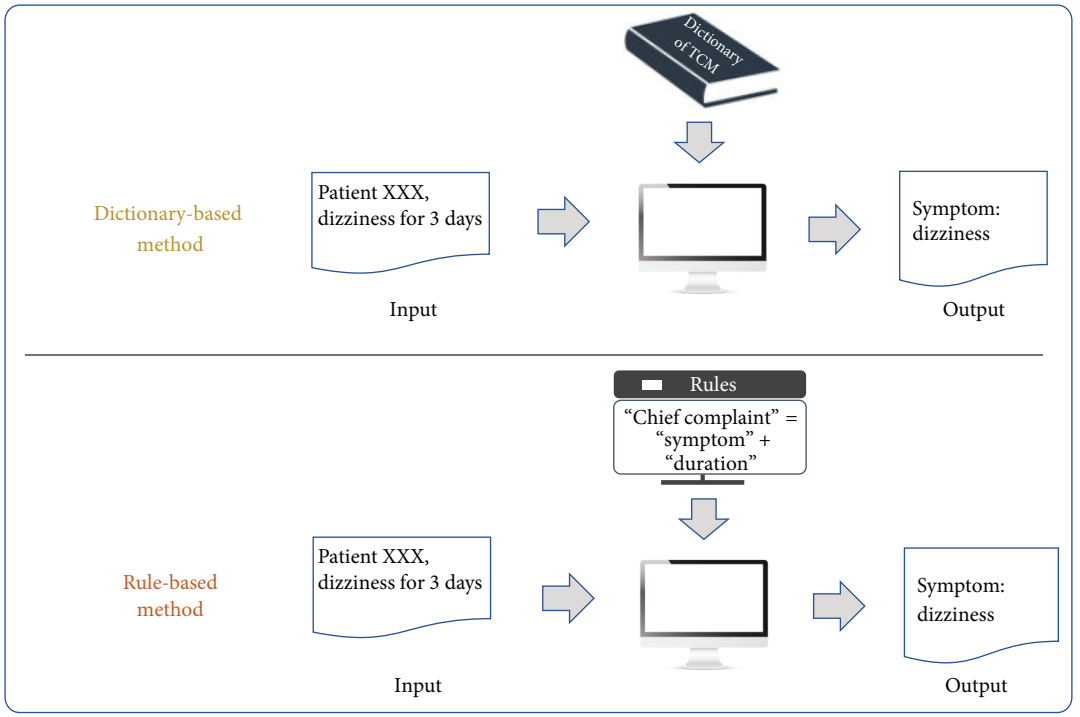

Figure 6: Frameworks of dictionary-based methods and rule-based methods in IE tasks.

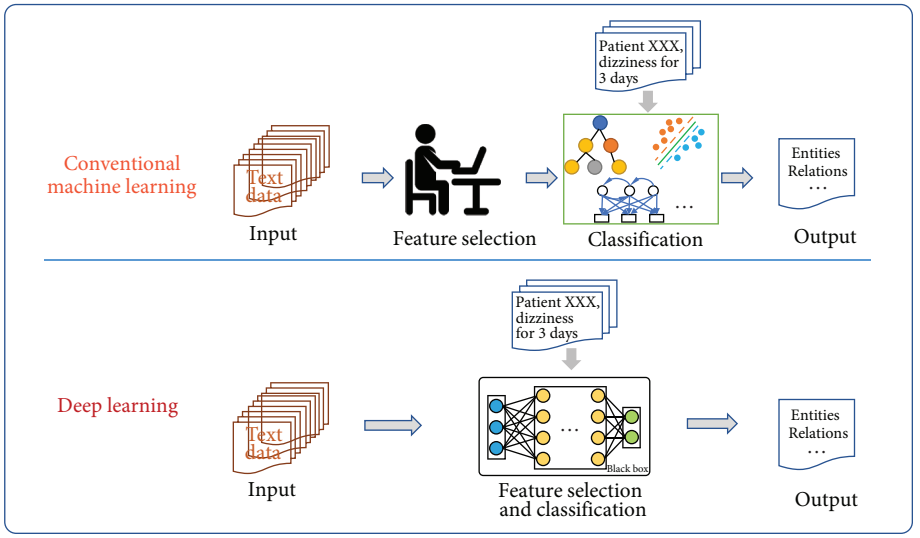

Figure 7: Frameworks of shallow machine learning and deep learning methods in IE tasks.

3.3. Frameworks of Text Data Information Extraction for TCM. IE research methods can be divided into four categories, namely, dictionary-based methods ($N = 7$), rule-based methods ($N = 5$), shallow machine learning methods ($N = 19$), and deep learning methods ($N = 20$). The frameworks of the four types of methods are shown in Figures 6 and 7.

Dictionary-based approaches were commonly used in IE tasks in early years; they utilize existing data resources to locate entities appearing in text. Rule-based methods were frequently used in IE tasks as well. The constructed rules should fully reflect domain knowledge and language knowledge of the IE corpus. Thus, the more complete the rule set, the better the result of IE. However, rule-based methods usually require considerable manual work in constructing complicated and structured rule templates [34].

In the past decade, machine learning (ML) has become the popular method of IE with acceptable performance in the TCM domain. The breakthrough of the ML algorithm in some aspects, especially the deep learning method based on the neural network framework, has provided strong support for the progress of IE technologies. In this review, the shallow machine learning methods used to extract TCM information included supervised ML methods ($N = 13$) and

the semisupervised method ($N = 5$). Supervised ML methods generally performed well in IE tasks for TCM; however, limited by the amount of training data, the semisupervised learning approach is increasingly favored by researchers.

Since 2018, deep learning methods have played an important role in IE from TCM text. A total of 18 IE tasks had used deep learning methods in this review. Among them, most of the tasks ($N = 16$) chose supervised methods to conduct extraction work. However, deep learning methods need large-scale training to prevent overfitting of the training model, and the valuable TCM clinical electronic medical records used in training are precious and few. Hence, some researchers were committed to studying how to use small amounts of labeled data to complete high-quality IE using, for example, semisupervised methods ($N = 2$) and distantly supervised methods ($N = 2$).

3.4. Models of Text Data Information Extraction of TCM. The algorithms of dictionary-based methods and rule-based methods were frequently used in early IE tasks. The dictionary-based IE methods relied on the artificial word library (dictionary) and mainly used string similarity algorithms, such as the matching maximum match algorithm and instance matching algorithm [35–38]. For example, Wang et al. [35] extracted symptom names exactly from segmented subsentences based on a maximum match algorithm. Zhou et al. [39] presented a domain ontology-driven semantic graph autoextraction system to discover knowledge from TCM text publications. In this work, TCMLS was used as a dictionary to extract valid domain-specific words. In the past ten years, the dictionaries used for IE have included TCM dictionaries, the TCMLS, published books of terminology of TCM, the MeSH dictionary, etc. Regarding the rule-based methods, they rely on linguistic experts to manually construct rule templates and use features including statistics, punctuation marks, keywords, indicators and direction words, location words (such as tail words), central words, etc. A common and simple form of the rule is a regular expression that uses a sequence of characters to define a search pattern [40, 41]. For instance, Yang et al. [41] extracted the temporal facts from TCM clinical records by using the regular expression method. The rule-based methods show good performance in a document where language expression has a certain pattern, such as instructions for Chinese patent medicine [25]. In addition, Cao et al. [42] combined the rules and likelihood ratio to find new terms in an iterative manner. On data from only 42 annotated health records, this method achieved a precision rate of 88.18% and a recall rate of 94.21%. Moreover, in small data sets, the rule-based approach might be superior to the feature-based approach in relation extraction tasks [43].

In the following section, we will focus on statistical-based methods, including shallow machine learning models and deep learning models. We have listed the details of model, core content, and evaluation and best performance in Table 1.

3.4.1. Machine Learning Models. Shallow machine learning approaches consider IE as a classification problem and generally use supervised learning and feature engineering to obtain acceptable performance. The IE workflow of TCM using unstructured data usually consists of two main processes (as shown in Figure 7): (1) feature selection—the quality of feature selection often determines the performance of IE. In this review, the extracted features included the position feature, weight feature, counting feature, part-of-speech feature, literal feature, category feature, frequency of keywords, etc.; and (2) training or construction of a classifier based on the selected features followed by classification of new inputted unstructured data by the trained classifier. Among the 19 studies using shallow ML methods, the classifiers included decision tree (DT) [30, 43], naive Bayes (NB) [53], support vector machine (SVM) [27, 40, 51, 53], hidden Markov model (HMM) [19, 47], maximum entropy Markov model (MEMM) [19, 47], conditional random fields (CRF) [19, 30, 45–50, 53], heterogeneous factor graph [20], other NLP tools [67], etc. The unique tree structure of DT enables it to deal with continuous sequence data in IE tasks, but it ignores the correlation between attributes and easily causes overfitting results. The NB algorithm is not sensitive to missing data due to its classification stability, which is very critical in text tasks. However, its assumption of attribute conditional independence is also insensitive to the correlation between attributes. SVM is one of the most popular models for shallow machine learning classification tasks with strong advantages, and its unique kernel functions solve a wide range of classification problems. However, due to the application of kernel function, SVM is very slow in large-scale data processing, and the selection of different kernel function is sensitive to missing data. HMM contains observation sequences and hidden state sequences, which can be used for word segmentation according to different contexts by capturing potential real-time state relationships between words. However, since HMM focuses less on the context contributed, it needs to raise a certain order, which leads to the huge consumption of time and space resources in the word segmentation task of a large number of training data. The MEMM integrates the advantages of HMM and the maximum entropy model (MEM) into a production model. The model allows the state transition probability to depend on the nonindependent features in the observation sequence, which is similar to the introduction of context information by HMM. However, because it is based on the improvement of the Markov chain, it is easy to fall into the same local optimal solution as the Markov chain in the convergence process. In the process of convergence, it is easy to fall into local optimal solution. CRF is further optimized on this basis to obtain the global optimal solution by finding the joint probability for the whole sequence. To obtain more information about the sequence, various feature templates are defined to fully utilize the contextual information provided in the text. CRF-based recognizers achieved outstanding performance in different sequence annotation tasks of entity extraction [19, 47].

In order to reduce the cost and demand of manual labeling, Cai et al. [44] used semisupervised learning combined with the rule extraction method to select the window

Table 1: Details of the statistical-based methods, core content, evaluation and best performance of IE systems.

Author, year	Method	Method type	Supervised type	Core content of extracted TCM information	Evaluation and best performance
Zhu W et al. [27], 2010	SVM	Machine learning	Supervised	Attributes of herbal medicine entities and prescriptions, including medicine application, medicine class, medicine dosage, medicine property, prescription usage, prescription attend illness, and prescription function	Medicine application: $P = 99.6\%$, $R = 98.3\%$; medicine class: $P = 98.1\%$, $R = 99.3\%$; medicine dosage: $P = 91.4\%$, $R = 93.9\%$; medicine property: $P = 84.8\%$, $R = 89.5\%$; prescription usage: $P = 97.9\%$, $R = 92.7\%$; prescription attend illness: $P = 85.1\%$, $R = 88.7\%$; prescription function: $P = 83.6\%$, $R = 92.5\%$
Zhu W et al. [40], 2011	SVM and regular expression	Combine the machine learning and rule-based method	Supervised	Symptom, diagnosis	Not mentioned
Cai D et al. [44], 2012	Bootstrapping approach	Machine learning	Semisupervised	Prescriptions, drugs	F value of prescription and drugs are 74.9% and 90.6%, respectively
Zhu W et al. [30], 2013	Decision tree and CRF	Machine learning	Supervised	Irrelevant information, basic information, multiclass information, symptom information, prescription information, and result information	Paragraph (unit) identification: $P > 84\%$; information extraction: $P > 80\%$ (except for a book)
Feng L et al. [45], 2014	CRF and bootstrapping	Machine learning	Supervised	Clinical phenotype	Not mentioned
Wang Y et al. [19], 2014	HMM/MEMM/CRF	Machine learning	Supervised	Symptom	The best F-measure achieved by CRF reaches 95.12% ($P = 94.77\%$ and $R = 95.48\%$)
Liu H et al. [46], 2015	CRF	Machine learning	Supervised	Symptoms and pathogenesis	Symptoms: $P = 84.02\%$, $R = 81.10\%$, $F1 = 82.53\%$; pathogenesis: $P = 86.40\%$, $R = 84.65\%$, $F1 = 85.52\%$
Jiang Q et al. [47], 2016	CRF/HMM/MEMM	Machine learning	Supervised	Symptoms, signs, TCM diagnosis, Chinese medicines (drug), prescriptions, TCM syndrome type, etc.	CRF : $P = 90.57\%$, $R = 85.85\%$, $F = 88.15\%$; HMM = 86.29%, $R = 79.92\%$, $F = 82.98\%$
Jiang Q et al. [48], 2016	CRF	Machine learning	Supervised	Symptoms or signs, TCM diagnosis, TCM syndrome type, Chinese medicines (drug), and names of TCM prescriptions	With all features: $P = 89.74\%$, $R = 82.9\%$, $F = 86.18\%$
Wang J et al. [43], 2016	Decision tree/rules	Machine learning and rule-based method	Supervised	Effect relation and conditional effect relation	Rule-based approach: $F = 46\%$; feature-based approach: $F = 41\%$
Wan H et al. [20], 2016	Heterogeneous factor graph model (HFGM)	Machine learning	Semisupervised	Herb-syndrome relations, herb-disease relations, formula-syndrome relations, formula-disease relations, and syndrome-disease relations	$P = 90.39\%$, $R = 86.98\%$, $F1 = 88.56\%$
Liang J et al. [49], 2017	CRF	Machine learning	Supervised	TCM drug name	Recognition of traditional Chinese medicine drug names: $P = 94.2\%$, $R = 92.8\%$, $F = 93.5\%$

Table 1: Continued.

Author, year	Method	Method type	Supervised type	Core content of extracted TCM information	Evaluation and best performance
Ruan T et al. [50], 2017	CRF	Machine learning	Supervised	Symptoms, departments, disease, medicines, and examinations	Precision of TCM symptom is 93.26%
Sun S. et al. [51], 2017	SVM	Machine learning	Supervised	Disease-treatment relation, healthcare relation, meridian points treatment and healthcare method relation, and medication treatment and healthcare method relation	The *F*-measure of entity relation classification model of disease-treatment, healthcare, meridian points treatment and healthcare method, and medication treatment and healthcare method reached 93.25%, 87.19%, 86.57%, and 84.57%, respectively
Zhang H. et al. [52], 2018	Short-text LSTM classifier (STLC)	Deep learning	Supervised	Person name	$F1 = 92.75\%$
Chi Y. et al. [53], 2018	CRF for entity extraction; SVM, naive Bayes (NB), LSTM, and KNN for relation extraction	Machine learning and deep learning	Supervised	Entities: food material, dish, nutritional element, symptom, and crowd; relations: "good for" or "bad for" relationships between "food material" and "symptom", and "same", "related", or "different" relationships between two "food material" entities	Concept extraction and relationship recognition were all above 85%
Chen T et al. [18], 2019	Combine BERT with a one-dimensional CNN to fine-tune the pretrained model	Deep learning	Supervised	Herb-syndrome relation, herb-disease relation, formula-syndrome relation, formula-disease relation, and syndrome-disease relation	The "1d-CNN fine-tuning" approach: $P = 95.18\%$, $R = 90.61\%$, $F1 = 92.82\%$
Jin Z et al. [54], 2019	TCMKG-LSTM-CRF	Deep learning	Supervised	Medicine, alias, prescription, pieces, disease, symptom, syndrome, meridian, property, flavor, and function	$F = 85.41\%$
Song B et al. [55], 2020	BiLSTM-CRF	Deep learning	Supervised	Symptom	$P = 76.80\%$, $R = 72.11\%$, $F1 = 74.38\%$
Deng N et al. [56, 57], 2020	Co-training-based method	Machine learning	Semisupervised	Four-character medicine effect phrases	In each iteration, the extraction accuracy is all above 97%
Deng N et al. [57], 2020	Serialized co-training method	Machine learning	Semisupervised	Medicine names	Precision is 98.6% when the number of patent texts reaches 3000
Feng L et al. [58], 2020	BiLSTM-CRF, lattice LSTM-CRF, BERT	Deep learning	Supervised	Symptom	The BERT model: $P = 89.94\%$, $R = 88.27\%$, $F1 = 89.10\%$
Liu L et al. [22], 2020	BiLSTM-CRF	Deep learning	Semisupervised	Traditional Chinese medicine, symptoms, patterns, disease, and formulas	$F1 = 78.70\%$, $P = 77.56\%$, $R = 79.87\%$
Zhang M et al. [59], 2020	BERT-BiLSTM-CRF	Deep learning	Semisupervised	Symptoms, syndromes, treatment, Chinese medicine, prescriptions, pulse, tongue, and efficacy	Accuracy = 81.24%, $R = 80.84\%$, $F1 = 81.04\%$.

Table 1: Continued.

Author, year	Method	Method type	Supervised type	Core content of extracted TCM information	Evaluation and best performance
Deng N et al. [60], 2020	Serialized co-training method	Machine learning	Semisupervised	Disease name	Not mentioned
Qu Q et al. [61], 2020	BERT-BiLSTM-CRF	Deep learning	Supervised	Symptoms, disease names, time, prescription names, and drug names	The best recognition effect on drugs, with an F value as high as 88.79%
Ruan C et al. [21], 2020	Multiview graph model to extract relation (MVG2RE)	Deep learning	Supervised	Herb-syndrome, herb-disease, formula-disease, formula-syndrome, and syndrome-disease	$P = 86.38\%$, $R = 81.42\%$, $F1 = 84.07\%$
Zhang D et al. [17], 2020	BiLSTM	Deep learning	Distantly supervised	Chinese medicine, symptom, medicine prescription, dose, tongue-like, and pulse	$P = 73.06\%$, $R = 66.75\%$, $F = 69.76\%$
Zhang H et al. [28], 2020	BiLSTM-CRF	Deep learning	Supervised	Chief complaints (symptom name, symptom duration, accompanying symptom, etc.); pathological history (symptom name, symptom cause, etc.); personal history (place of birth, smoking history, drinking history, etc.); and TCM diagnosis (tongue quality, furred tongue, tongue body, pulse, etc.)	Not mentioned
Zheng Z et al. [62], 2020	BiLSTM-CRF	Deep learning	Supervised	Syndrome, disease, symptom, prescription, therapy, herb	$F1 > 97\%$
Zhou S et al. [31], 2020	Structural bidirectional long short-term memory (SLSTM) model	Deep learning	Supervised	Subjects, methods, and results	SLSTM model achieves close to 90% performance in precision, recall, and $F1$-measures
Bai T et al. [63], 2021	SEGATT-CNN combined with different classifiers	Deep learning	Supervised	Entity: disease, herb names; relation: herbal-disease relation, herbal-chemical relation	Herbal-disease relation: SVM combined SEGATT-CNN: $P = 95.43\%$, $R = 92.92\%$, $F = 94.15\%$, AUC = 95.13%, accuracy = 95.69%
Deng N et al. [64], 2021	BiLSTM-CRF	Deep learning	Supervised	Herb name, disease name, symptom, therapeutic effect, and nonentity	$P = 94.63\%$, $R = 94.47\%$, $F1 = 94.48\%$
Jia Q et al. [23], 2021	Span-level distantly supervised NER approach	Deep learning	Distantly supervised	Symptom, medicine, prescriptions, dose, tongue-like, and pulse	$P = 78.28\%$, $R = 76.52\%$, $F1 = 77.34\%$
Zhang T et al. [65], 2021	Multihop self-attention mechanism + BiLSTM	Deep learning	Supervised	Therapeutic relation and causal relation	Therapeutic relation: $P = 88.65\%$, $R = 98.23\%$, F1-score = 93.19% and causal relation: $P = 69.23\%$, $R = 78.26\%$, $F1 = 73.47\%$
Xu H et al. [29], 2021	Nested NER model based on LSTM-CRF	Deep learning	Supervised	Medicine, symptom, pulse, tongue, medicine prescription, dose, disease location, onset time and duration, severity, color, quantity, and frequency	$P = 85.64\%$, $R = 86.18\%$, $F1 = 85.91\%$
Guan Y et al. [66], 2021	BERT-BiLSTM-CRF	Deep learning	Supervised	Disease, pattern, and symptom	$P = 86.54\%$, $R = 88.59\%$, $F1 = 87.55\%$, when the size of training set is 10,000

Table 2: Details of evaluation metrics.

Evaluation index	Formula	Role
Precision	Precision = $TP/TP + FP$	Determine the ratio of correctly predicted positive samples
Accuracy	Accuracy = $TP + TN/TP + TN + FP + FN$	Determine the correct rate of all classifications
Recall	Recall = $TP/TP + FN$	Ratio of correctly predicted positive samples to the total number of real positive samples
F-measure	F − measure = $(1 + \beta^2)$precision* recall/β^2precision + recall	Examine precision and recall
AUC	Area under curve	Intuitively express the real classification ability of the model

patterns of size 3 to capture the candidate words and divide them into incorrect word, correct word, and modified word, and the human-computer interaction information is added in the cycle process. In the bootstrapping process, artificially optimized selection can change the vocabulary to the drug vocabulary set. Due to the semantic ambiguity of the initial correct word seed set, artificial word judgment was added at the beginning of the semisupervised learning cycle to control the correct words seed set to prevent semantic drift. It reduces the demand for labeling data and improves the accuracy of drug vocabulary extraction from 0.682 to 0.734. Zhang et al. [17] used the method of distant supervision, in which an optimized reverse annotation method based on "Tie or Break" and the existing Chinese medicine vocabulary dictionary set are used to solve the problem of nonentity interference existing in the original annotation. The recall rate and $F1$-score index of this model in the annotation of "Complete Library of Chinese Named Motions in Past Dynasties" are ahead of other models, and the algorithm may have better room for improvement. Deng et al. [56, 57, 60] proposed a semisupervised learning method, using a small amount of data as an annotation for training, constructing a data set of first-hand Chinese herbal medicine names as the initial data set of the semisupervised learning loop, a serialized initial word segmentation, word length, pause words, valid words, and word structure as species different classifiers. The co-training method to extract disease names, medicine names, and four-character medication effect phrases from TCM patent text data.

3.4.2. Deep Learning Models. With strong representations of data, better performance, and less feature engineering, deep learning methods have become the most popular method of IE and achievements have been reported. A key factor in introducing deep learning algorithms to NLP is the pretrained language model used [68], such as Word2vec or bidirectional encoder representations from transformers (BERT). Note that the BERT model is a classic and state-of-the-art language representation model of NLP technique [69], which is able to predict masked information from the context. In this review, some studies reported that the application or combination of BERT could significantly improve the result of entity recognition or relation extraction [18, 58, 59, 61]. In the last decade, the proposed deep learning models for IE tasks include BERT-convolutional neural network (CNN) [18], convolutional neural network with segment attention mechanism (SEGATT-CNN) [63], K-nearest neighbor (KNN) [53], long short-term memory (LSTM) [52, 53], bidirectional long short-term memory (BiLSTM) [17], structural BiLSTM [31], LSTM-CRF [54, 58], BiLSTM-CRF [22, 28, 55, 58, 62, 64], BERT-BiLSTM-CRF [59, 61, 66], graph neural networks [21], and a nested NER model based on LSTM-CRF [29]. Among the above-mentioned models, the "BiLSTM-CRF" and "BERT-BiLSTM-CRF" have become popular deep learning models because of their good extraction performance: the BiLSTM model can capture more context information than the LSTM model.

3.5. Evaluations of Information Extraction from TCM Text Data. With the exception of 10 papers that did not mention evaluation, the remaining 39 papers reported one or more evaluation metrics such as precision (or positive predictive value), recall (or sensitivity), F-measure (harmonic mean of recall and precision), accuracy, or AUC (area under curve). The details of evaluation metrics are shown in Table 2. Of the 39 studies that reported evaluation metrics, 28 featured true comparative evaluations. Comparisons were made between the proposed model and other models developed as part of the study or brought forward previously. Furthermore, no trend in evaluation methods was found over time.

3.6. Key Findings of Text Data Information Extraction for TCM. From 2010, the IE tasks used on TCM text data had achieved some results. On the one hand, there were already plenty of types of entity and several relations extracted from six data types that have been illustrated in Figure 4. On the other hand, IE technologies in the TCM domain have also yielded some results in more recent years, especially with machine learning methods.

3.6.1. Key Findings on Feature Selection and Classifiers. With regard to feature selection, Zhang et al. [51] discussed the fact that the effective feature set of entity relationship classification, the contributions of verb features, all word features of entities, word distance features, and clause features are different for different types of entity relation classification and defined five types of TCM acupuncture entities, namely disease, healthcare, treatment and healthcare methods, meridians, and medication, and four entity relationship types disease-treatment, healthcare, meridian points treatment and healthcare method, and medication

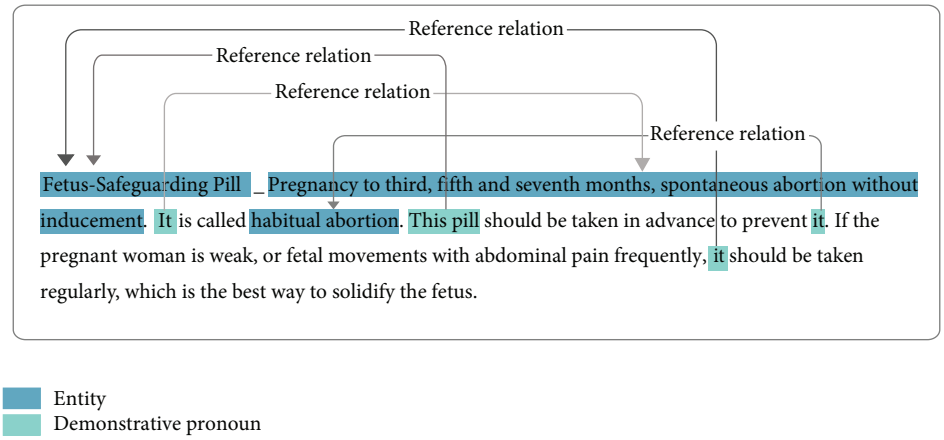

Figure 8: Example of the reference relations in the ancient TCM literature.

treatment and healthcare method. Dictionary learning is used to obtain the types of TCM entities in the text, and SVM is used to classify the different entity relationships. Jiang et al. [48] divided each case history into five attributes—words in sentences, grammatical properties of words, words in clinical dictionaries, set words acting on adjacent contexts, and set words acting at a distance—and finally found that the "grammatical property of words" is the best labeling feature among all individual labeling features and the multi-combination of labeling features can improve term recognition with the CRF model constructed by local state features and local marker features for text mining in medical cases of TCM.

Regarding the classifier, Wang et al. [19] considered the signal-to-noise problem of the chief complaint as a sequence labeling problem and proposed an improved sequence labeling strategy applied to different classifiers based on certain empirical reasons. And they found that the discriminative models (MEMM and CRF) are more suitable for the symptom name recognition task than the generative model (HMM), as MEMM and CRF with useful features can achieve higher labeling performance than HMM. Liang et al. [49] proposed a novel cascade-type Chinese medication entity recognition approach, which integrated the sentence category classifier from an SVM and the CRF-based medication entity recognition. Although CRF shows good potential in IE tasks, its over-reliance on context leads to difficulties in vocabulary extraction in different contexts. In addition, an SVM is added before CRF to classify the medical records into sentences containing drug names and other sentences, and then the sentences containing target extracted drugs are introduced into CRF to reduce the confusion of word meaning in context. This approach could avoid the side effects of abundant negative samples and improve the performance of the NER from Chinese admission notes. Moreover, Wan et al. [20] used co-occurring frequency, lexical context, semantic distance as prior knowledge and the transitivity of ternary closure to explore the correlation between prior knowledge. They presented a heterogeneous factor graph model that used the correlations between all types of relations to overcome difficulties by employing collective inference in the context of heterogeneous entity networks, thus greatly improving the model's ability to extract TCM relations.

3.6.2. Deep Learning Methods Improve the Performance of the Model of IE. In recent years, some findings have also been obtained by using deep learning methods. In the pretraining process, the pretraining BERT model was more accurate in learning contextual features [61]. Taking into account that there were many types of complex relation existing between many heterogeneous medical entities, Ruan et al. [21] proposed a multiview graph representation learning method that adopted the heterogeneous graph convolutional network (GCN) and attention mechanism for the extraction of complex relationships among multitype entities. They first constructed a heterogeneous entity graph from the co-occurring relations and used domain knowledge to enhance the semantic information of the above graph to infer the labels of all the candidate relations simultaneously by employing node representation learning and classification. In addition, Bai et al. [63] designed a new segment attention mechanism based on CNN, adding an attention mechanism to each segment to obtain an attention vector, which is helpful to focus on the sensitive words in the segment domain for relational classification. This study demonstrates that combining the new context representation with the word-level attention mechanism can improve the ability to extract local features of convolutional neural networks. Moreover, to address the common problem of low recognition rate of rare words in the field of TCM, Jin et al. [54] proposed an effective TCMKG-LSTM-CRF model that uses the bidirectional LSTM network chain to output features into knowledge attention vector model and finally transfer the knowledge attention vector into the conditional random field to strengthen the learning ability and recognize rare words. They also used the knowledge attention vector model to retrieve candidate entities and calculate the embedded attention vector of entities to improve the performance of existing models.

3.6.3. Efforts Have Been Made to Reduce the Dependence on the Annotated Corpus. Supervision-based methods always

obtain acceptable performance with enough annotated training data. However, the construction of a high-quality corpus requires laborious and time-consuming labeling work. Consequently, constructing large, high-quality corpora is difficult and costly. Currently, there are few large-scale open corpora in the field of TCM, although some corpora have already been published [19, 50, 70]. In order to reduce the cost of manual labeling under supervised learning and improve the clinical extraction ability for TCM based on feature words, Liu et al. [22] put forward a semisupervised approach for extracting TCM clinical terms based on the BiLSTM-CRF model, which combined the character vector trained by the encyclopedia corpus with that trained by the TCM-related corpus. In this study, the best $F1$ value reached 78.70% on the test data set. Zhang et al. [59] presented a semi-BERT-BiLSTM-CRF model to identify TCM entities. By adding semisupervised pseudolabel learning for model training, the recognition accuracy of the BERT-BiLSTM-CRF model was effectively improved, and the manual labeling work was reduced to a certain extent. Moreover, Zhang et al. [17] proposed a method for entity recognition based on distant-BiLSTM and completed the entity recognition task under the premise of only using the entity vocabulary related to the TCM field. This method performed better than the distant-LSTM-CRF and dictionary matching method on TCM texts. In another study, Jia et al. [23] introduced an effective distantly supervised approach at the span level to extract TCM medical entities. Unlike general sequence tagging, this method utilized the pretrained language model as a text feature extractor and constructed the span representation containing inner, boundary, and context features. In addition, they designed a negative sampling strategy for the span-level model. The strategy randomly selected negative samples in every epoch, periodically filtering possible false-negative samples and finally reducing the bad influence from false-negative samples.

4. Discussion and Future Work

We reviewed and narrowed down over 1,234 papers to a final set of 49 reports. Our review indicated that IE for TCM has developed rapidly and has achieved some progress. At the same time, there remain many problems to be addressed in the future. The early IE tasks relied mainly on the dictionary-based method and rule-based methods. However, domain entity dictionaries were always incomplete and could not cover all entity names in practice. In addition, the rule-based methods were heavily dependent on a good grammatical knowledge base in the TCM domain, and accordingly, the completeness and reasonability of rules were hard to guarantee [71]. In recent years, IE techniques have been dominated by statistical ML methods, including shallow ML approaches and deep learning approaches. The statistical methods of IE are widely considered advanced, with good performance. Nevertheless, the portability and generalizability of clinical IE systems remain limited and challenging. Based on these challenges, tasks, and methods presented in this review, we put forward some suggestions for future research.

First, we point out that the present methods still have strong dependence on large-scale labeled training data. Obviously, the amount of case data used for training should be enriched. At present, hospitals are becoming more and more intelligent, and it is necessary to unify the standardization of various terms in the HIS system, improve the ICD standard of traditional Chinese medicine, and obtain more and more standardized electronic medical record data. Even if the model is pretrained, the machine learning algorithms used in IE tasks are mostly conditional random fields, variants of BERT and LSTM. The few-shot learning or meta-learning technology will bring hope for the solution of this problem [72–74]. In the TCM domain, there are few publicly available corpora of TCM at present, which hinders the development of IE technology in the field of TCM. As a result, new IE tasks often require reconstruction of corpora and training of new models, resulting in lack of portability and generalizability of the models. One potential solution to this problem is to construct gold standard data sets with consensus in the field of TCM. On the basis of this, it will be helpful if more evaluation conferences of TCM IE tasks are organized. Another promising solution is developing new methods that use very small amounts of labeled data or perform without labeled data to achieve higher performance, such as meta-learning and few-shot learning technologies. Meta-learning, also known as "learning to learn", aims to address the problem of data limitation when learning new tasks. Few-shot learning brings AI technology closer to human intelligence. Currently, meta-learning and few-shot learning have been applied in classification and target detection [75]. In the field of TCM text processing, they also have positive prospects and opportunities.

Second, there are still many concepts and relations that have not been enrolled in previous research. Therefore, the extraction of more concepts and complex relationships of TCM is an important research direction in the future, especially the implicit relations, such as the relationships among five elements (including generation, restriction, subjugation, and reverse restriction) and the compatibility relationships of Chinese herbal medicine [76]. It remains an important task to extract implicit relations directly from unstructured TCM text, which are implicitly represented in the low-dimensional and semantic space [77], as there is no relational word to prompt the type of the relation. For instance, in the record "the kidney is injured by wind evil, manifested as fast and unclear enunciation", "is injured by" suggests a pathogenic relationship between the kidney and wind evil, while there is no cue word in the sentence to express the relationship between wind evil and the symptom "fast and unclear enunciation". For this reason, we appeal to future research to focus on extraction of implicit relations through the cooperation of TCM experts and computer technicians.

Among the six types of TCM text data, the ancient literature is a special one. It always consists of many short sentences with concise and obscure semantics, which contain enriching experience in the diagnosis and treatment of TCM [78]. For example, complex anaphora relations exist commonly in TCM ancient literature (as shown in Figure 8),

and the analysis of the demonstrative pronouns and the intended referent will facilitate a deeper understanding of the meaning of the literature. However, taking the sentence in Figure 8 as an example, the demonstrative pronouns "it" and "this pill" with different syntactic positions all correspond to different contents. At the same time, the first "it" refers to the symptom "abortion without cause or reason at three, five, seven months of pregnancy", and another "it" refers to the disease "abortion". Obviously, the annotation of reference relations requires a sound understanding of the words, the sentences, and the context. Hence, it is challenging and meaningful to extract entities and relations from ancient literature. In future research, we expect more exploratory work on ancient literature, such as part-of-speech tagging, semantic analysis, and relation extraction.

Third, we found that most of the extracted information was coarse-grained; however, in TCM narratives, nested phenomena (entities inside an entity) are ubiquitous. For example, the syndrome "liver depression and spleen deficiency" also contains the location "liver", "spleen", and the nature "depression", "deficiency". Therefore, we hope that future studies extract entities and relationships at the fine-grained level. In this review, only one report [28] had adopted a nearly fine-grained labeling approach, in which most of the symptom entities had been disassembled into a finer one. For example, the symptom "pale complexion" was annotated as "complexion" and its attribute "pale". In a fine-grained annotation, the coarse-grained entities will be divided into finer subcategories until no further divisions can be made. Thus, more information will be captured if fine-grained extraction is performed.

Last but not least, although deep learning methods have obtained excellent performance, the training processes are usually difficult to explain. Interpretable research on IE from TCM is still in the initial stage and will be the trend of future research. In the real-world process of clinical diagnosis and treatment, wrong decisions can have very serious consequences and will not be widely accepted. As fundamental work, the quality of extracted information will affect the performance of high-level tasks such as automatic syndrome differentiation and diagnosis and automatic prescription. Therefore, it is essential to explain the results of IE from a more detailed and representational perspective. Regarding the explicability, in August 2016, DARPA (the US Defense Advanced Research Projects Agency) proposed an explainable AI program [79]. Following this, in 2017, the NIPS (Neural Information Processing Systems) working group launched a heated discussion on the issue of whether interpretability is necessary in machine learning [80]. This discussion emphasized the importance and necessity of interpretability in the healthcare industry. For the TCM clinical domain, explanations are essential in allowing users to understand, trust, and effectively manage these AI experts [81]. With this background, explainable IE technology has attracted some attention and been explored. Taking an example, Zhang et al. [65] proposed an attention-based model to extract the semantic information on multiple aspects for the extraction of Chinese medical relations by a multihop attention mechanism. In this study, the weighting mechanism assigned weight to each word in the sentence to increase the interpretability of neural networks. Interpretability will provide more possibilities for clinical research and application of IE in the field of TCM.

There are some limitations to this review. The search strings and databases selected in this review might not be comprehensive and may have introduced bias into the review. Additionally, the review was limited to articles written in English. Articles written in other languages, such as Chinese, would also provide valuable information. Furthermore, this study focused on the tasks, challenges, and methods of IE in TCM domain; consequently some other information was not summarized in this review, such as the system development language, demographic characteristics of clinical records, and citation counts.

5. Conclusions

Our analyses showed that IE from TCM text data has improved over the past decade. However, the extraction of TCM text still faces some challenges involving the lack of gold standard corpora, nonstandardized expressions, and multiple types of relation. In the future, IE work should be promoted by extracting more existing entities and relations, especially the implicit relations in modern clinical records and ancient literature, constructing gold standard data sets with consensus in the field of TCM, and exploring the IE methods based on a small amount of labeled data, such as few-shot learning and meta-learning. Furthermore, fine-grained and interpretable IE technologies are necessary for further exploration. In addition, owing to the particularity of the TCM text content, more cooperation is needed between experts in the field of TCM and computer experts. Experts in ancient Chinese linguistics will be extraordinarily helpful in annotation work if the IE work is conducted on ancient literature.

Abbreviations

IE: Information extraction
TCM: Traditional Chinese medicine
AI: Artificial intelligence
NLP: Natural language processing
PRISMA: Preferred Reporting Items for Systematic Reviews and Meta-Analyses
RANs: Resident admit notes
NCBI: National Center for Biotechnology Information
TCMLS: Traditional Chinese Medicine Language System
CRF: Conditional random fields
SVM: Support vector machine
HMM: Hidden Markov model
MEMM: Maximum entropy Markov model
DT: Decision tree
NB: Naive Bayes
BERT: Bidirectional encoder representations from transformers
CNN: Convolutional neural network
SEGATT: Segment attention mechanism
KNN: K-nearest neighbor

LSTM: Long short-time memory
BiLSTM: Bidirectional long short-term memory
AUC: Area under curve
GCN: Graph convolutional network
DARPA: Defense Advanced Research Projects Agency
NIPS: Neural Information Processing Systems.

Data Availability

The data extracted from the included papers used to support the findings of this study are included within the supplementary information files.

Ethical Approval

Ethical approval is not applicable.

Consent

Consent is not applicable.

Conflicts of Interest

The authors declare that they have no conflicts of interest.

Authors' Contributions

WYQ and ZTT guided the whole research work; ZTT, HZH, YY, and WYQ performed the article search and selection; and ZTT, HZH, and PYZ completed data extraction and synthesis. ZTT drafted the manuscript. WYQ and WCB did the critical revision of the manuscript for important intellectual content. All the authors read and approved the final manuscript. Tingting Zhang and Zonghai Huang contributed equally to this article.

Acknowledgments

The authors thank International Science Editing (http://www.internationalscienceediting.com) for editing this manuscript. This work was supported by the National Natural Science Foundation of China (Grant no. 61801058) and Talent Fund of Chengdu University of Traditional Chinese Medicine (Grant no. BSH2020031).

Supplementary Materials

Supplementary 1. PRISMA checklist. Supplementary 2. The basic information and extracted data of included papers. (*Supplementary Materials*)

References

[1] J. Qiu, "A culture in the balance," *Nature*, vol. 448, no. 7150, pp. 126–128, 2007.
[2] D. Cyranoski, "Why Chinese medicine is heading for clinics around the world," *Nature*, vol. 561, no. 7724, pp. 448–450, 2018.
[3] M. Liu, Y. Gao, Y. Yuan et al., "Efficacy and safety of herbal medicine (Lianhuaqingwen) for treating COVID-19: a systematic review and meta-analysis," *Integrative Medicine Research*, vol. 10, no. 1, Article ID 100644, 2021.
[4] Y. C. Fang, H. C. Huang, H. H. Chen, and H. F. Juan, "TCMGeneDIT: a database for associated traditional Chinese medicine, gene and disease information using text mining," *BMC Complementary and Alternative Medicine*, vol. 8, no. 1, p. 58, 2008.
[5] X. Zhou, Y. Peng, and B. Liu, "Text mining for traditional Chinese medical knowledge discovery: a survey," *Journal of Biomedical Informatics*, vol. 43, no. 4, pp. 650–660, 2010.
[6] B. Liu, X. Zhou, Y. Wang et al., "Data processing and analysis in real-world traditional Chinese medicine clinical data: challenges and approaches," *Statistics in Medicine*, vol. 31, no. 7, pp. 653–660, 2012.
[7] W. Y. Wang, H. Zhou, Y. F. Wang, B. S. Sang, and L. Liu, "Current policies and measures on the development of traditional Chinese medicine in China," *Pharmacological Research*, vol. 163, Article ID 105187, 2021.
[8] H. Chai, L. Haiming, and Q. Liu, "Overview of research methods for natural language processing in traditional Chinese medicine," *Journal of Medical Informatics*, vol. 10, pp. 58–63, 2015.
[9] X. Chu, B. Sun, Q. Huang, S. Peng, Y. Zhou, and Y. Zhang, "Quantitative knowledge presentation models of traditional Chinese medicine (TCM): a review," *Artificial Intelligence in Medicine*, vol. 103, Article ID 101810, 2020.
[10] Z. Qin, J. Yu, Y. Cong, and T. Wan, "Topic correlation model for cross-modal multimedia information retrieval," *Pattern Analysis & Applications*, vol. 19, no. 4, pp. 1007–1022, 2016.
[11] D. Lin, A. V. Vasilakos, Y. Tang, and Y. Yao, "Neural networks for computer-aided diagnosis in medicine: a review," *Neurocomputing*, vol. 216, pp. 700–708, 2016.
[12] M. Jiang, C. Lu, C. Zhang et al., "Syndrome differentiation in modern research of traditional Chinese medicine," *Journal of Ethnopharmacology*, vol. 140, no. 3, pp. 634–642, 2012.
[13] Z. Wu, C. Wei, L. Wang, and L. He, "Determining the traditional Chinese medicine (TCM) syndrome with the best prognosis of HBV-related HCC and exploring the related mechanism using network pharmacology," *Evidence-based Complementary and Alternative Medicine*, vol. 2021, pp. 1–13, 2021.
[14] C. Friedman, P. O. Alderson, J. H. M. Austin, J. J. Cimino, and S. B. Johnson, "A general natural-language text processor for clinical radiology," *Journal of the American Medical Informatics Association*, vol. 1, no. 2, pp. 161–174, 1994.
[15] A. R. Aronson and F. M. Lang, "An overview of MetaMap: historical perspective and recent advances," *Journal of the American Medical Informatics Association*, vol. 17, no. 3, pp. 229–236, 2010.
[16] H. Liu, S. J. Bielinski, S. Sohn et al., "An information extraction framework for cohort identification using electronic health records," *AMIA Joint Summits on Translational Science proceedings*, vol. 2013, pp. 149–153, 2013.
[17] D. Zhang, C. Xia, C. Xu et al., "Improving distantly-supervised named entity recognition for traditional Chinese medicine text via a novel back-labeling approach," *IEEE Access*, vol. 8, pp. 145413–145421, 2020.
[18] T. Chen, M. Wu, and H. Li, "A general approach for improving deep learning-based medical relation extraction using a pre-trained model and fine-tuning," *Database*, vol. 2019, pp. 1–15, 2019.
[19] Y. Wang, Z. Yu, L. Chen et al., "Supervised methods for symptom name recognition in free-text clinical records of

traditional Chinese medicine: an empirical study," *Journal of Biomedical Informatics*, vol. 47, pp. 91–104, 2014.

[20] H. Wan, M. F. Moens, W. Luyten et al., "Extracting relations from traditional Chinese medicine literature via heterogeneous entity networks," *Journal of the American Medical Informatics Association*, vol. 23, no. 2, pp. 356–365, 2016.

[21] C. Ruan, Y. Wu, G. Sheng Luo, Y. Yang, and P. Ma, "Relation extraction for Chinese clinical records using multi-view graph learning," *IEEE Access*, vol. 8, pp. 215613–215622, 2020.

[22] L. Liu, X. Wu, H. Liu et al., "A semi-supervised approach for extracting TCM clinical terms based on feature words," *BMC Medical Informatics and Decision Making*, vol. 20, no. S3, Article ID 118, 2020.

[23] Q. Jia, D. Zhang, and H. Y. Xu, "Extraction of traditional Chinese medicine entity: design of a novel span-level named entity recognition method with distant supervision," *JMIR Medical Informatics*, vol. 9, no. 6, Article ID e28219, 2021.

[24] D. Moher, A. Liberati, J. Tetzlaff, and D. G. Altman, "Preferred reporting items for systematic reviews and meta-analyses: the PRISMA statement," *International Journal of Surgery*, vol. 8, no. 5, pp. 336–341, 2010.

[25] L. Wang, Y. Zhang, M. Jiang et al., "Toward a normalized clinical drug knowledge base in China-applying the RxNorm model to Chinese clinical drugs," *Journal of the American Medical Informatics Association*, vol. 25, no. 7, pp. 809–818, 2018.

[26] Y. Zhou, X. Qi, Y. Huang, and F. Ju, *Research on Construction and Application of TCM Knowledge Graph Based on Ancient Chinese Texts*, pp. 144–147, Assoc Computing Machinery, New York, USA, 2019.

[27] W. Zhu, S. Bai, B. Zhang, W. Xu, and D. Wei, "An information extraction method for digitized textbooks of traditional Chinese medicine," in *Proceedings of the 2010 10th IEEE International Conference on Computer and Information Technology*, pp. 1645–1648, Bradford, UK, July 2010.

[28] H. Zhang, W. Ni, and J. J. Li, "Artificial intelligence-based traditional Chinese medicine assistive diagnostic system: validation study," *JMIR Medical Informatics*, vol. 8, no. 6, pp. e17608–12, 2020.

[29] H. Xu, H. Liu, Q. Jia, Y. Zhan, Y. Zhang, and Y. Xie, "A nested named entity recognition method for traditional Chinese medicine records," *Advances in Artificial Intelligence and Security*, vol. 1422, pp. 488–497, 2021, Springer Science and Business Media Deutschland GmbH.

[30] W. Zhu, C. Ju, W. Xu, J. Xia, and L. Fu, "Extracting medical records with hierarchical information extraction method," *Information Technology Journal*, vol. 12, no. 18, pp. 4441–4446, 2013.

[31] S. Zhou and X. Li, "Feature engineering vs. deep learning for paper section identification: toward applications in Chinese medical literature," *Information Processing & Management*, vol. 57, no. 3, Article ID 102206, 2020.

[32] D. Xu, M. Zhang, T. Zhao et al., "Data-driven information extraction from Chinese electronic medical records," *PLoS One*, vol. 10, no. 8, Article ID e0136270, 2015.

[33] H. Long, Y. Zhu, L. Jia et al., "An ontological framework for the formalization, organization and usage of TCM-Knowledge," *BMC Medical Informatics and Decision Making*, vol. 19, no. S2, p. 53, 2019.

[34] A. Mykowiecka, M. Marciniak, and A. Kupść, "Rule-based information extraction from patients' clinical data," *Journal of Biomedical Informatics*, vol. 42, no. 5, pp. 923–936, 2009.

[35] Y. Wang, Z. Yu, Y. Jiang, Y. Liu, L. Chen, and Y. Liu, "A framework and its empirical study of automatic diagnosis of traditional Chinese medicine utilizing raw free-text clinical records," *Journal of Biomedical Informatics*, vol. 45, no. 2, pp. 210–223, 2012.

[36] X. Chen, H. Chen, X. Bi, P. Gu, J. Chen, and Z. Wu, "BioTCM-SE: a semantic search engine for the information retrieval of modern biology and Traditional Chinese Medicine," *Computational and Mathematical Methods in Medicine*, vol. 2014, pp. 1–13, 2014.

[37] F. Gong, Y. Chen, H. Wang, and H. Lu, "On building a diabetes centric knowledge base via mining the web," *BMC Medical Informatics and Decision Making*, vol. 19, no. S2, pp. 49–197, 2019.

[38] J. Xie, J. He, W. He, C. Hu, K. Hu, and R. Jiang, *Research on Structured Information Extraction Method of Electronic Medical Records of Traditional Chinese Medicine*, pp. 1613–1616, IEEE, Piscataway, NJ, USA, 2020.

[39] C. Zhou, H. Chen, and J. Tao, "GRAPH: a domain ontology-driven semantic graph auto extraction system," *Applied Mathematics & Information Sciences*, vol. 5, no. 2, pp. 9–16, 2011.

[40] W. Zhu, L. Fu, L. Xu, and B. Zhang, *A TCM diagnosis system based on textbook information extraction*, pp. 483–487, IEEE Computer Society, Los Alamitos, CA, USA, 2011.

[41] C. Yang, W. Li, X. Zhang, R. Zhang, and G. Qi, *A Temporal Semantic Search System for Traditional Chinese Medicine Based on Temporal Knowledge Graphs*Springer Science and Business Media Deutschland GmbH, Hangzhou, China, 2020.

[42] C. Cao, M. Sun, and S. Wang, "Extracting terms from clinical records of traditional Chinese medicine," *Frontiers of Medicine*, vol. 8, no. 3, pp. 347–351, 2014.

[43] J. Wang and J. Poon, *Relation Extraction from Traditional Chinese Medicine Journal Publication*, pp. 1394–1398, IEEE, Piscataway, NJ, USA, 2016.

[44] D. Cai, C. Ding, J. Zuo, and Y. Bai, *A Semi-supervised Learning Method for Names of Traditional Chinese Prescriptions and Drugs Recognition*, pp. 394–397, IEEE, Piscataway, NJ, USA, 2012.

[45] L. Feng, X. Zhou, H. Qi, R. Zhang, Y. Wang, and B. Liu, "Development of large-scale TCM corpus using hybrid named entity recognition methods for clinical phenotype detection: an initial study," in *Proceedings of the 2014 IEEE Symposium on Computational Intelligence in Big Data (CIBD)*, pp. 1–7, Orlando, USA, 2014.

[46] H. Liu, X. Qin, and B. Fu, *The Symptoms and Pathogenesis Entity Recognition of TCM Medical Records Based on CRF*, pp. 1479–1484, Institute of Electrical and Electronics Engineers Inc, Beijing, China, 2015.

[47] Q. Jiang, H. Li, and J. Liang, *Free Text Mining of TCM Medical Records Based on Conditional Random Fields*, pp. 242–247, Institute of Electrical and Electronics Engineers Inc, Shanghai, China, 2016.

[48] Q. Jiang, H. Li, J. Liang, Q. Wang, X. Luo, and H. Liu, "Multi-combined features text mining of TCM medical cases with CRF," in *Proceedings of the 2016 8th International Conference on Information Technology in Medicine and Education (ITME)*, pp. 621–626, Fuzhou, China, December 2016.

[49] J. Liang, X. Xian, X. He et al., "A novel approach towards medical entity recognition in Chinese clinical text," *Journal of Healthcare Engineering*, vol. 2017, pp. 1–16, 2017.

[50] T. Ruan, M. Wang, J. Sun et al., "An automatic approach for constructing a knowledge base of symptoms in Chinese," *Journal of Biomedical Semantics*, vol. 8, no. S1, pp. 33–79, 2017.

[51] S. Sun, D. Huang, and J. Zhang, "Research on entity relation extraction in TCM acupuncture and moxibustion field," *Journal of Information Hiding and Multimedia Signal Processing*, vol. 8, no. 2, pp. 358–367, 2017.

[52] H. Zhang, S. Cheng, L. Liu, and W. Shi, "TCMEF: a TCM entity filter using less text," in *Proceedings of the 11th International Conference, KSEM 2018*, pp. 125–133, Changchun, China, August 2018.

[53] Y. Chi, C. Yu, X. Qi, and H. Xu, "Knowledge management in healthcare sustainability: a smart healthy diet assistant in traditional Chinese medicine culture," *Sustainability*, vol. 10, no. 11, pp. 1–21, 2018.

[54] Z. Jin, Y. Zhang, H. Kuang, L. Yao, W. Zhang, and Y. Pan, "Named entity recognition in traditional Chinese medicine clinical cases combining BiLSTM-CRF with knowledge graph," *Knowledge Science, Engineering and Management*, vol. 11775, pp. 537–548, 2019.

[55] B. Song, Z. Bao, Y. Wang, W. Zhang, and C. Sun, "Incorporating lexicon for named entity recognition of traditional Chinese medicine books," in *Proceedings of the 9th CCF International Conference, NLPCC 2020*, pp. 481–489, Zhengzhou, China, October 2020.

[56] N. Deng, X. Chen, C. Xiong et al., *A Method of Collecting Four Character Medicine Effect Phrases in TCM Patents Based on Semi-supervised Learning*, pp. 462–473, Springer International Publishing, Cham, 2020.

[57] N. Deng and C. Xiong, "Serialized Co-Training-Based recognition of medicine names for patent mining and retrieval," *International Journal of Data Warehousing and Mining*, vol. 16, no. 3, pp. 87–107, 2020.

[58] L. Feng and D. Xie, *Research on Named Entity Recognition of Traditional Chinese Medicine Electronic Medical Records*, pp. 61–67, Springer International Publishing, Cham, 2020.

[59] M. Zhang, Z. Yang, C. Liu, and L. Fang, "Traditional Chinese medicine knowledge service based on semi-supervised BERT-BiLSTM-CRF model," in *Proceedings of the 2020 International Conference on Service Science (ICSS)*, pp. 64–69, Xining, China, August 2020.

[60] N. Deng, X. Chen, and C. Xiong, *A Method of Annotating Disease Names in TCM Patents Based on Co-training*, pp. 389–398, , Springer International Publishing, Cham, 2020, Advances on P2P, Parallel, Grid, Cloud and Internet Computing.

[61] Q. Qu, H. Kan, Y. Wu, and Y. Gao, "Named entity recognition of TCM text based on bert model," in *Proceedings of the 2020 7th International Forum on Electrical Engineering and Automation (IFEEA)*, pp. 652–655, Hefei, China, September 2020.

[62] Z. Zheng, Y. Liu, Y. Zhang, and C. Wen, *TCMKG: A Deep Learning Based Traditional Chinese Medicine Knowledge Graph Platform*, pp. 560–564, Institute of Electrical and Electronics Engineers Inc, Nanjing, China, 2020.

[63] T. Bai, H. Guan, S. Wang, Y. Wang, and L. Huang, "Traditional Chinese medicine entity relation extraction based on CNN with segment attention," *Neural Computing & Applications*, vol. 34, no. 4, pp. 2739–2748, 2021.

[64] N. Deng, H. Fu, and X. Chen, "Named entity recognition of traditional Chinese medicine patents based on BiLSTM-CRF," *Wireless Communications and Mobile Computing*, vol. 2021, pp. 1–12, 2021.

[65] T. Zhang, H. Lin, M. M. Tadesse, Y. Ren, X. Duan, and B. Xu, "Chinese medical relation extraction based on multi-hop self-attention mechanism," *International Journal of Machine Learning and Cybernetics*, vol. 12, no. 2, pp. 355–363, 2021.

[66] Y. Guan, H. Li, and W. Xu, "A traditional Chinese medicine terminology recognition model based on deep learning: a TCM terminology recognition model," in *Proceedings of the ICBDC 2021: 2021 6th International Conference on Big Data and Computing*, pp. 15–20, Shenzhen China, May 2021.

[67] X. Y. Xu, K. Zhao, N. Shi et al., "Text mining and analysis of treatise on febrile diseases based on natural language processing," *World Journal of Traditional Chinese Medicine*, vol. 6, no. 1, pp. 67–73, 2020.

[68] Y. Lecun, Y. Bengio, and G. Hinton, "Deep learning," *Nature*, vol. 521, no. 7553, pp. 436–444, 2015.

[69] J. Devlin, M. Chang, K. Lee, and K. Toutanova, BERT: Pre-training of Deep Bidirectional Transformers for Language Understanding, 2018, https://arxiv.org/abs/1810.04805.

[70] T. Zhang, Y. Wang, X. Wang, Y. Yang, and Y. Ye, "Constructing fine-grained entity recognition corpora based on clinical records of traditional Chinese medicine," *BMC Medical Informatics and Decision Making*, vol. 20, no. 1, pp. 64–20, 2020.

[71] Y. Wang, L. Wang, M. Rastegar-Mojarad et al., "Clinical information extraction applications: a literature review," *Journal of Biomedical Informatics*, vol. 77, pp. 34–49, 2018.

[72] Y. Wang, Q. Yao, J. T. Kwok, and L. M. Ni, "Generalizing from a few examples," *ACM Computing Surveys*, vol. 53, no. 3, pp. 1–34, 2021.

[73] L. Li Fei-Fei, R. Fergus, and P. Perona, "One-shot learning of object categories," *IEEE Transactions on Pattern Analysis and Machine Intelligence*, vol. 28, no. 4, pp. 594–611, 2006.

[74] J. Vanschoren, Meta-learning: A Survey arXiv preprint arXiv: 1810.03548, 2018.

[75] P. Ma, Z. Zhang, J. Wang et al., "Review on the application of metalearning in artificial intelligence," *Computational Intelligence and Neuroscience*, vol. 2021, pp. 1–12, 2021.

[76] H. Y. Chen, Y. H. Lin, J. C. Wu et al., "Prescription patterns of Chinese herbal products for menopausal syndrome: analysis of a nationwide prescription database," *Journal of Ethnopharmacology*, vol. 137, no. 3, pp. 1261–1266, 2011.

[77] J. Kuang, Y. Cao, J. Zheng, X. He, M. Gao, and A. Zhou, "Improving neural relation extraction with implicit mutual relations," in *Proceedings of the 2020 IEEE 36th International Conference on Data Engineering (ICDE)*, pp. 1021–1032, Dallas, TX, USA, April 2020.

[78] L. Gao, C. H. Jia, and W. Wang, "Recent advances in the study of ancient books on traditional Chinese medicine," *World Journal of Traditional Chinese Medicine*, vol. 6, no. 1, p. 61, 2020.

[79] D. Gunning and D. Aha, "DARPA's explainable artificial intelligence (XAI) program," *AI Magazine*, vol. 40, no. 2, pp. 44–58, 2019.

[80] W. Samek, G. Montavon, A. Vedaldi, L. Hansen, and K. Muller, *Explainable AI: interpreting, explaining and visualizing deep learning*, Kindle Edition, Seattle, Washington, USA, 2019.

[81] S. Kundu, "AI in medicine must be explainable," *Nature Medicine*, vol. 27, no. 8, Article ID 1328, 2021.

Hindawi
Evidence-Based Complementary and Alternative Medicine
Volume 2022, Article ID 3943920, 12 pages
https://doi.org/10.1155/2022/3943920

Research Article

Study on TCM Tongue Image Segmentation Model Based on Convolutional Neural Network Fused with Superpixel

Han Zhang[1], **Rongrong Jiang**[2], **Tao Yang**[1,3], **Jiayi Gao**[1], **Yi Wang**[1] and **Junfeng Zhang**[4]

[1]*School of Artificial Intelligence and Information Technology, Nanjing University of Chinese Medicine, Nanjing, China*
[2]*School of Nursing, Nanjing University of Chinese Medicine, Nanjing, China*
[3]*School of Information Management, Nanjing University, Nanjing, China*
[4]*School of Medicine & Holistic Integrative Medicine, Nanjing University of Chinese Medicine, Nanjing, China*

Correspondence should be addressed to Tao Yang; yangtao@njucm.edu.cn and Junfeng Zhang; zhangjunfeng419@njucm.edu.cn

Received 5 November 2021; Accepted 25 January 2022; Published 8 March 2022

Academic Editor: Talha Bin Emran

Tongue image segmentation is a base work of TCM tongue processing. Nowadays, deep learning methods are widely used on tongue segmentation, which has better performance than conventional methods. However, when the tongue color is close to the color of the adjoining area, the contour of tongue segmentation by deep learning may be coarse which could influence the subsequent analysis. Here a novel tongue image segmentation model based on a convolutional neural network fused with superpixel was proposed to solve the problem. *Methods*. On the basis of a convolutional neural network fused with superpixel, the novel tongue image segmentation model SpurNet was proposed in this study. The residual structure of ResNet18 was introduced as the feature extraction layer on the encoding path, to construct the first stage processing module UrNet of SpurNet. The superpixel segmentation was fused with UrNet to form the second stage process of SpurNet. To verify the effect of SpurNet. The models before and after fusion with superpixel, classical image segmentation models FCN and DeepLab were compared with SpurNet on the dataset of 367 manually labeled tongue images. *Results*. The SpurNet model performance test with 10-fold cross-validation showed PA of 0.9145 ± 0.0043, MPA of 0.9168 ± 0.0048, MIoU of 0.8417 ± 0.0072 and FWIoU of 0.8454 ± 0.0072. Relative to FCN, DeepLab and their superpixel fused models, the SpurNet model was superior in tongue image segmentation and could increase PA by 1.91%–3.17%, MPA by 1.38%–2.61%, MIoU by 3.09%–5.07%, and FWIoU by 3.11%–5.08%. Compared to UrNet, the first stage processing module, the SpurNet model also increased the PA, MPA, MIoU and FWIoU by 0.15%, 0.09%, 0.24% and 0.24%, respectively. *Conclusion*. The SpurNet model, after fusing with superpixel image segmentation, can better accomplish the task of tongue image segmentation, more accurately process the margins of tongue and resolve the over-segmentation and under-segmentation. The thought of this study is a new exploration in the field of tongue image segmentation, which could provide a reference for the modern research on TCM tongue images.

1. Introduction

Traditional Chinese medicine (TCM) is a treasure of ancient science and the intelligence of Chinese culture that has been celebrated in China for thousands of years. Its effective practical methods have made noble contributions to the prosperity and healthy development of the Chinese nation. There are four basic diagnostic methods in TCM, including inspection, auscultation and olfaction, inquisition and pulse diagnosis, in which inspection is the most effective and visual one. As an old saying goes, "there may be a false pulse but no false tongue feature." The internal organs in human body are connected with the tongue through meridians and collaterals, and the patients' body constitutions can be preliminarily diagnosed, and the medical conditions can be analyzed by the clinical physicians via observation of the tongue features, including tongue color, tongue shape and tongue state. This noninvasive diagnostic method enables tongue diagnosis as a necessary step in the TCM diagnosis [1]. However, since the results of tongue diagnosis only depend on the accumulated experience of the clinical physicians, cannot be easily replicated, and may be affected

by the exogenous factors, objectification and standardization of tongue feature diagnosis has become a hot topic in the studies of TCM informatics. Tongue image segmentation [2–4], as the first step of intellectualization of tongue features, has provided a basis for the subsequent tongue processing and analysis, and has become an inseparable part in the process of intellectualizing tongue diagnosis [5,6].

Traditional tongue image processing mainly depends on conventional image processing techniques [7–9]. The tongue segmentation, also known as the pixel-level classification task, is to remove the regions (including lips, tooth and the space between lips and teeth) unrelated to the tongue based on the unprocessed tongue image, similar to the foreground and background classification for each pixel in the tongue image. The common traditional segmentation algorithms include threshold segmentation [10–12], gradient segmentation [4, 13] and GrabCut [14–16]. For example, Ren JJ [17] proposed a color tongue image auto-thresholding segmentation algorithm based on RGB spatial histogram and used this threshold for the tongue image segmentation in the gray space. Zhang *L* and others. [18] proposed a segmentation method based on gray projection and threshold-adaptive method. Fu ZC and others. [19] adopted radial edge detection to obtain the approximate contour of tongue, and then used paired color removal method to remove the lips, and applied snake model to obtain the precise contour of tongue finally. Shi MJ and others. [20] combined geometric snake model and the parameterized GVFSnake model and proposed a novel tongue auto-segmentation method. Nonetheless, above methods have certain limitations: As to auto-adaptive threshold segmentation method, the color of the regions (such as lips) outside of tongue are similar to the color of tongue, and single threshold cannot accurately distinguish the foreground and background; Snake algorithm easily runs into local extremum and neglect some fine characteristics during the process of contour energization; Grabcut is related to the prior knowledge and maximally depends on the range of interest (ROI) given by the user with a degree of automation when segmentation the tongue features.

With the development of deep learning, some scholars have attempted to use deep learning algorithms into tongue feature segmentation [21–23]. Wang *L* and others. [24] proposed a segmentation method of tongue based on the two-phase convolutional neural network. Zhang *X* [25] used atrous spatial pyramid pooling (ASPP) module to perceive the multiresolution characteristics of the tongue features, and then combined the deep convolutional neural network with the full connection conditional random field to refine the margins of tongue image. Jiang *L* and others. [26] adopted convolutional neural network of the enhanced HSV (hue, saturation, value) color model into tongue segmentation. Lin B and others. [27] proposed DeepLingue, an end-to-end depth convolutional neural network model based on ResNet and discovered that this model was not affected by light or the size of tongue image, and was superior to conventional segmentation algorithms in the segmentation velocity ratio and accuracy. Li et al. [28] designed an iterative cross-domain tongue segmentation framework based on UNet and transfer learning. Gholami et al. [29] used to separate the tongue region from the face image using R–CNN to provide images for subsequent tongue classification.

It has been known from above studies that deep learning methods are widely used on tongue segmentation. However, when the tongue color is close to the color of the adjoining area, the contour of tongue segmentation may be coarse which could lead negative influence on the subsequent quantitative analysis. Therefore this study designed a TCM tongue segmentation algorithm by fusing the convolutional neural network with the superpixels to achieve more accurate processing of the margins of tongue and resolve the over-segmentation and under-segmentation issues. To perform stable segmentation and refine the margins of tongue in different photography environment, this study mainly completed following tasks:

(1) Designed a novel tongue segmentation model which introduced ResNet18 residual structure as the characteristics abstraction layer of coding path based on UNet.

(2) Proposed to use superpixel image segmentation to optimize and increase the segmentation accuracy in view of the noisiness of the tongue image background and certain errors between the convolutional neural network in processing the margins of tongue.

(3) Compared the segmentation effectiveness of the model before and after fusion with superpixels, and compared the novel model with the classic convolutional networks (FCN and Deeplab).

The remainder of the paper was organized as follows: The materials and methods were specified in section 2, the results of the established model was introduced, analyzed and discussed in section 3 and section 4, and the study was summarized in section 5.

2. Materials and Methods

2.1. Sampling and Labeling of the Tongue Images. The experimental data were acquired by the tongue diagnosis study group from the Nanjing University of Chinese Medicine. The study group collected the tongue images of 257 patients with gastric carcinoma using smartphones during the treatment in hospital, and finally selected 367 tongue images after excluding the images that did not contain the tongue regions (multiple tongue images were collected from the same patients at different visit date) to establish the tongue image dataset. Compared with traditional tongue image acquisition equipment, it is more convenient and efficient to use smartphones to collect tongue images. Moreover, models built on common tongue images collected by smartphones have more applicability and operability, which can be embedded in apps and provide AI services of tongue processing.

The tongue contour was labeled using the graphic interface provided by the Python Labelme package. The tongue contour was drawn after the name of the region category was

set (Figure 1). The labeled tongue feature data were used to establish the sample set for tongue feature segmentation.

2.2. Framework of Tongue Segmentation Model Based on Convolutional Neural Network Fused with Superpixel. As to tongue images, most of them had ill-defined margins and needed to refer to more low-resolution information and use context fusion to achieve precise segmentation. Moreover, since the tongue structure was relatively fixed and the semantics of segmentation target was definite and straightforward, and high-resolution characteristics could provide more location information. Therefore, SpurNet, a TCM tongue feature segmentation model, was proposed, with structure specified in Figure 2.

To extract the underlying semantic characteristics and high-level semantic characteristics of tongue images, UNet [30] was used as the model skeleton, and ResNet18 [31] residual network was introduced as the feature extraction layer of UNet coding path to improve the sensitivity of feature mapping to output changes and improve tongue segmentation accuracy, A tongue image segmentation model UrNet (UNet-Resnet18) containing encoding and decoding is constructed to realize rough segmentation of tongue. On this basis, superpixel characteristics were added for the optimizing process of the coarse segmentation results. It was verified by subsequent experiments that SpurNet (UrNet + superpixel) could effectively resolve the issues including unsmoothness of margin segmentation as well as the over-segmentation and under-segmentation of the background.

The UNet is the base of SpurNet. In the classic UNet network structure, an end-to-end "U"-shaped encoder-decoder framework was used, as shown in Figure 3. It contained 3 parts: Extraction of the features of backbone, a fusion of characteristics and tongue segmentation. In the extraction of the features of backbone, skip connection was performed for high-level semantic features and underlying semantic features to ensure that the downstream feature maps could fuse more low-dimension features (most of which were marginal information), so that multi-scale features could be efficiently fused.

Since the backbone feature extraction of UNet was composed of common CBR modules (Conv + BN + ReLU), this study learned the stronger Resnet as the BackBone of UNet. Residual links were introduced into the original UNet, and the encoder was connected to the decoder, so as to retain the lost information in different layers in the encoding part, enhance the perception of feature mapping to the changes of output, and promote the accuracy of tongue segmentation. The structure of one Unit in UrNet is shown in Figure 4.

On the basis of UrNet, the SpurNet proposed in this study further considered the over-segmentation and under-segmentation at the margins of tongue, so that fusion with superpixels was put forward to achieve the refine tongue segmentation. SpurNet fused superpixel image segmentation after the coarse segmentation of tongue features, which was used as the TCM tongue segmentation model for optimizing process of the coarse segmentation. Superpixel is defined as a

Figure 1: Labeling result of a tongue image.

set of multiple pixels with adjacent locations and similar characteristics (such as gray level and markings), which groups the pixels based on the similarity of the characteristics of different pixels. Given that SLIC [32] method is simple in thought, convenient in implementation and compact and orderly in superpixel blocks, SLIC algorithm was used by SpurNet to generate superpixels.

The SLIC algorithm procedures are as follows:

Step 1. Initialize the seed points, set the width of a image as (N, N), segmentate the image into K superpixels, and set the size of each superpixel as N/K. The step size of adjacent two seed points is:

$$S = \sqrt{\frac{N * N}{K}}. \tag{1}$$

Step 2. Calculate the gradient values of all pixel points in the adjacent region $n * n$ $(n = 3)$ of a seed point, and transfer the seed point to the region with the minimum gradient value to reselect a seed point.

Step 3. Calculate the distance of each pixel point and the seed point (color distance d_c and space distance d_s), and allocate class tags to each pixel point in the region $(2S * 2S)$ of each seed point. The search range is shown in Figure 5.

The distance measurement equation is as follow:

$$D\prime = \sqrt{\left(\frac{d_c}{m}\right)^2 + \left(\frac{d_s}{S}\right)^2}. \tag{2}$$

Step 4. Iterative optimization.

Step 5. Output superpixel.

When different number of seed points is selected, the superpixel image segmentation effectiveness is shown in Figure 6.

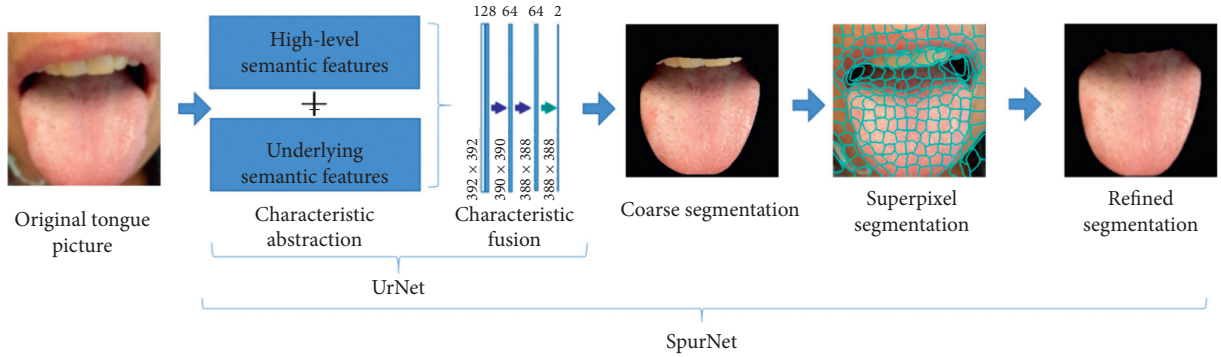

Figure 2: SpurNet framework.

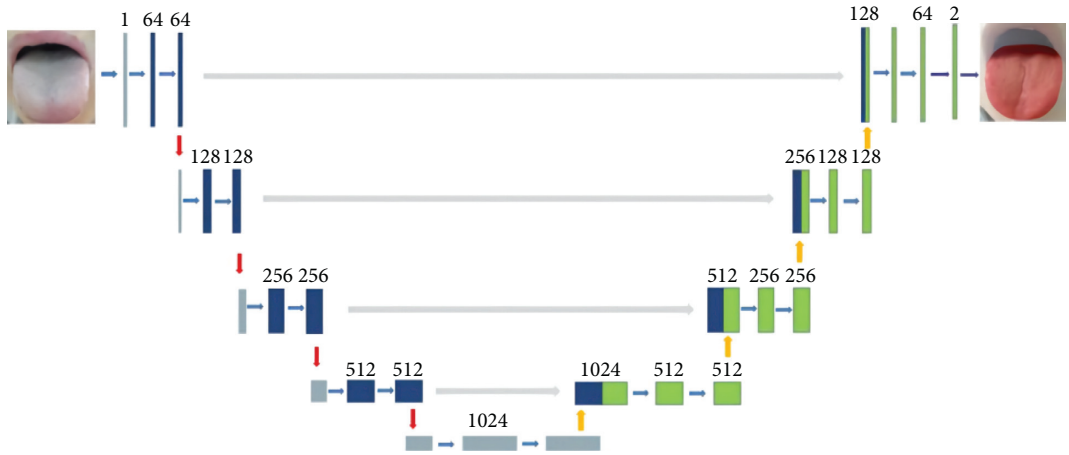

Figure 3: UNet structure.

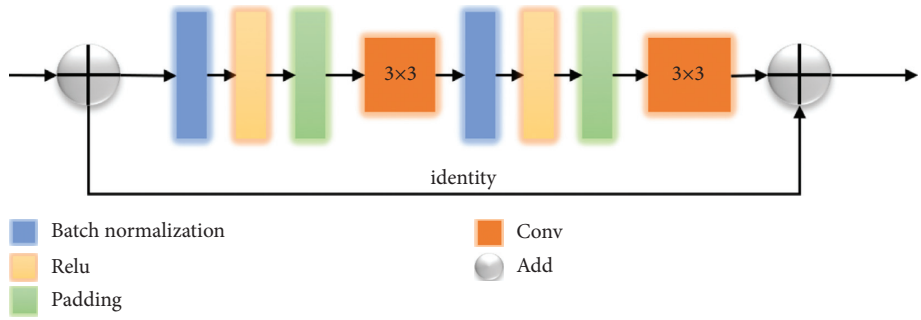

Figure 4: One unit in UrNet.

The calculation procedures of SpurNet are specified in Figure 7. Firstly, the TCM tongue images were uploaded into UrNet network, and the coarse segmentation results of tongue were obtained through procedures including convolution, downsampling, feature fusion and upsampling. Secondly, superpixel image segmentation was performed specific to the coarsely segmented images, with the number of initially selected seed points. The categories of the pixels in the same superpixel block were counted to calculate the coverage of the pixel categories in the superpixel block (relative to the segmented tongue image). For example, if the tongue pixel label was 1, the coverage of label 1 in the superpixel block was calculated. Finally, the pixel categories in each superpixel block were selectively updated, and when the coverage of tongue pixel categories was more than θ, the pixels in this pixel block were retained, otherwise, the image was updated as the background (label 0), so as to refine the margins of the coarsely segmented image and achieve the refined segmentation of the image.

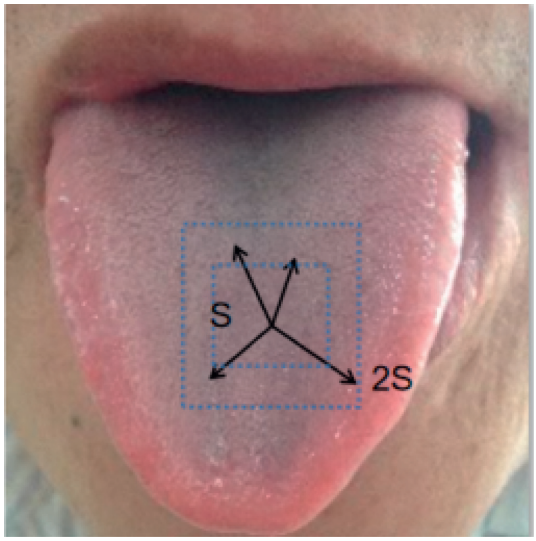

Figure 5: Search range of the seed points.

3. Results

3.1. Dataset and Pre Processing

(1) Preprocessing: In view of the different sizes of original images and the full connection layer needed to predefine the size of weight matrix, the sizes of the images were uniformly adjusted to $256 * 256 * 3$ in advance.

To unitize the data distribution of the sample set and promote the network generalization ability, the entered images were normalized in advance and the pixel values of all samples were adjusted to [−1, +1] interval:

$$\text{pixel}_{xy} = 2 * \left(\frac{\text{pixel}_{xy}}{255}\right) - 1. \quad (3)$$

(2) Data augmentation: Since the tongue images dataset obtained in this study was limited, data augmentation was performed before the tongue images were entered into the network, and rotatory, horizontally/vertically flipped, and translatory data augmentation was applied, with parameter settings specified in Table 1. In addition, the samples were randomly scattered before the tongue features were entered into the network in order to avoid category imbalance in the training set.

3.2. Experimental Settings. The model in this study was established based on Tensorflow framework. Specific training process: Initialize weight of network; upload the experimental data; extract tongue features; predict the tongue labels; update network parameters via loss calculation and back gradient propagation; use 10-fold cross-validation to assess the performance of the model.

In this study, Adam was selected as optimizer while cross-entropy as loss function, and learning rate (lr) was set as 1e-3. The learning rate attenuation strategy shown below was applied in the training process, with decay of 1e-4:

$$\text{lr} = \text{lr} * \frac{1}{1 + \text{decay} * \text{iteration}}. \quad (4)$$

To prevent over-fitting, the dropout was set as 0.6, and early stopping strategy was adopted in the training process. The training was stopped if the loss did not decrease on continuous 10 epochs. GPU was introduced for acceleration in the training process, with a display card of Tesla K80.

3.3. Contrast Test. To further verify the effectiveness of the model in the tongue segmentation, FCN and Deeplab models were used for comparison.

(1) FCN. Fully convolutional network (FCN) is a semantic segmentation network proposed by Jonathan Long et al. [33] at the Institute of Electrical and Electronics Engineers (IEEE) conference in 2015. This network establishes an end-to-end and pixel-to-pixel convolutional semantic segmentation model, and is the basis of a series of semantic segmentation networks subsequently. Since FCN only contains convolutional layers without full connection layer, it can accept the input of any size, with simple structure and high efficacy.It also uses the thought of skip connection and fuses the predictive results of different depths.

(2) Deeplab. Deeplab is a semantic segmentation network proposed by Chen LC and others. [34] in European Conference on Computer Vision (ECCV) in 2018 (Deeplab v3). This network applies empty convolutions with different dilation rates to capture the context information of multiscales. It establishes a simple encoder-decoder structure in which the encoder is used to capture the features of the images while the decoder to recover the specific features and spatial dimension of an image, so as to achieve the classification of pixel levels.

3.4. Model Assessment. Pixel accuracy (PA) [17], mean pixel accuracy (MPA) [17], mean intersection over union (MIoU) [17], and frequency weighted intersection over union (FWIoU) [17] were applied to assess the performance of the tongue feature segmentation model.

As to the same tongue image, if the label of the predicted tongue is the same as that of the artificially labeled tongue, true positive (TP) is considered, and if the predicted result is tongue while the artificially labeled result is the background, false positive (FP) is determined. Suppose the predicted result is background while the artificially labeled result is tongue, FP is considered, and if both the predicted result and the artificially labeled result are backgrounds, false negative (FN) is considered.

Calculation equations of assessment indicators:

PA : The proportion of the number of pixels with correctly predicted categories in the total number of pixels.

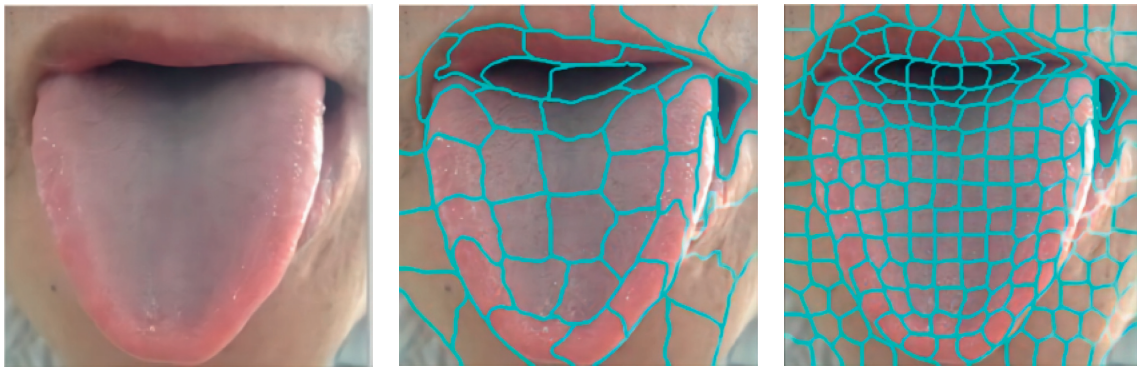

(a) (b) (c)

Figure 6: Superpixel image segmentation (a) Original image (b) Number of seed points: 50 (c) Number of seed points: 200.

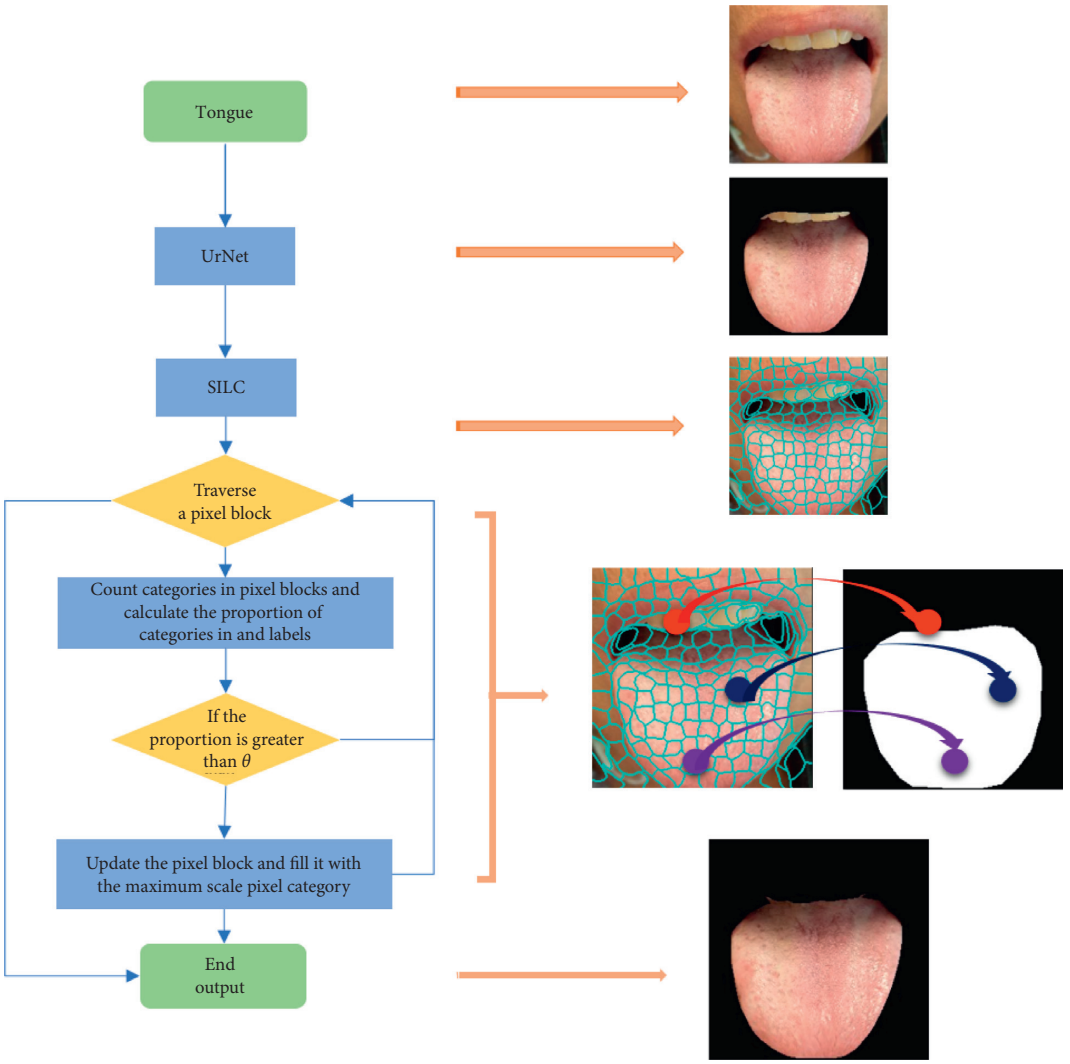

Figure 7: SpurNet processing procedures.

Table 1: Data augmentation parameters.

Data augmentation mode	Parameters
Rotation_range	10
Width_shift_range	0.2
Height_shift_range	0.2
Channel_shift_range	0.2
Horizontal_flip	True
Vertical_flip	True

$$\mathrm{PA} = \frac{\mathrm{TP} + \mathrm{TN}}{\mathrm{TP} + \mathrm{TN} + \mathrm{FP} + \mathrm{TN}}. \quad (5)$$

MPA : Calculate the proportion of the number of correctly categorized pixels in each category, and then accumulate the proportions to compute the mean PA (MPA).

$$\mathrm{MPA} = \frac{\sum_{i=1}^{n} \mathrm{TP}_i/\mathrm{TP}_i + \mathrm{FP}_i}{n}, \quad (6)$$

where i is the label i.

MIoU : The mean intersection over union between the predicted result by the model and the real value in each category. Since binary variables (tongue and background) were discussed in this study, the equation was:

$$\mathrm{MIoU} = \frac{1}{2}\left(\frac{\mathrm{TP}}{\mathrm{TP} + \mathrm{FP} + \mathrm{FN}} + \frac{\mathrm{TN}}{\mathrm{TN} + \mathrm{FN} + \mathrm{FP}}\right). \quad (7)$$

FWIoU : A algorithm slightly promoted on basis of MIoU, in which the weight was set based on the frequency in each category.

$$\mathrm{FWIoU} = \frac{\mathrm{TP} + \mathrm{FN}}{\mathrm{TP} + \mathrm{FP} + \mathrm{FN} + \mathrm{TN}} * \frac{\mathrm{TP}}{\mathrm{TP} + \mathrm{FP} + \mathrm{FN}}. \quad (8)$$

3.5. Experimental Results. The 10-fold cross-validation was used to train the model, and results was shown in Table 2. Comparing with FCN and DeepLab, the UrNet has a better performance on all the indicators with *PA* 0.9130 ± 0.0039, *MPA* 0.9159 ± 0.0046, *MIoU* 0.8393 ± 0.0065 and *FWIoU* 0.8430 ± 0.0065.

In order to observe the performance of the algorithm on the tongue images, the visualized segmentation results are shown in Figure 8 where the segmented tongue regions are marked red.

Based on the analysis of visualized results, the algorithms based on deep learning could approximately localize the tongue and were insensitive to the environment around the tongue, and showed intensive adaptability to the TCM tongue images. As visually shown in Figure 8, the tongue edge segmented by UrNet is smoother and the segmented area is more complete. However, after FCN and Deeplab segmentation, the margins of tongue were relatively coarse, which might cause the presence of false teeth marks at the margins of tongue, thus leading negative influence on the subsequent quantitative analysis. Therefore, UrNet adopted in this study was more advisable for tongue segmentation.

The UrNet has a better performance than FCN and DeepLab, however, when the color of lips is similar to the tongue, there are still some biases during the segmentation. To improve the performance of the UrNet in further, the SpurNet, UrNet fused with superpixel, was proposed.

In order to find the appropriate superpixel segmentation parameters, we test the number of superpixel seeds and the pixel proportion θ (proportion of tongue label pixels in super pixel block) in SpurNet, and the results are shown in Figure 9.

In Figure 9, the mIoU tends to be stable with the increase of the number of seeds. In the subsequent experiments, we searches for the best superpixel parameters in the parameter space and fuses them with FCN, deeplab and Urnet respectively. The segmentation results of FCN, DeepLab, UrNet fused with superpixel (SpurNet) separately were compared in Table 3:

The visualized segmentation results after fusion with superpixel characteristics are shown in Figure 10.

As shown in Table 3, after superpixel characteristics were fused for post-processing, the segmentation results were promoted to certain extent than before. FCN with superpixels was superior to FCN by 0.98%, 0.71%, 1.51%, and 1.55% on indicators PA, MPA, MIoU, and FWIoU, respectively. Deeplab with superpixels was superior to Deeplab by 0.93%, 0.83%, 1.46%, and 1.47%, and SpurNet was superior to UrNet by 0.15%, 0.09%, 0.24%, and 0.24%, respectively. Relative to FCN, DeepLab and their superpixel fused models, the SpurNet model was superior in tongue image segmentation and could increase PA by 1.91%–3.17%, MPA by 1.38%–2.61%, MIoU by 3.09%–5.07%, and FWIoU by 3.11%–5.08%. Compared to UrNet, the first stage processing module, the SpurNet model also increased the PA, MPA, MIoU and FWIoU by 0.15%, 0.09%, 0.24% and 0.24%, respectively. Moreover, it was visually shown in Figure 10 that after refined segmentation by the model combined with superpixels, the contour margins were more approximate to the margins of tongue.

4. Discussion

Tongue diagnosis is one of the cores in TCM syndrome differentiation and has exerted a dominant function in the TCM clinical diagnosis. The waxing and waning of the healthy state can be judged and the depth of the disease location can be distinguished through tongue diagnosis to further identify the nature of the pathogenic factors and predict the medical conditions. However, the traditional TCM diagnosis of tongue features mainly depend on the experience of the clinical physicians, which may be affected by the objective or subjective environment. With the development of information technology, the objectification of TCM tongue diagnosis has become one of the hot topics in the study in TCM field. Tongue segmentation, as the basis of intellectualization of tongue diagnosis, is an indispensable step in the subsequent characteristic analysis and quantitative of TCM tongue diagnosis. However, although the traditional segmentation algorithm has a good effect, it is easily affected by light, environment, and so on, resulting in an incomplete segmentation tongue. The segmentation robustness needs to be improved. In this study, the intact and

Table 2: Convolutional neural network segmentation results (mean ± standard deviation).

Algorithm	*PA*	MPA	MIoU	FWIoU
FCN	0.8856 ± 0.0099	0.8959 ± 0.0079	0.7957 ± 0.0153	0.7988 ± 0.0153
DeepLab	0.8828 ± 0.0070	0.8907 ± 0.0064	0.7910 ± 0.0115	0.7946 ± 0.0110
UrNet	**0.9130 ± 0.0039**	**0.9159 ± 0.0046**	**0.8393 ± 0.0065**	**0.8430 ± 0.0065**

The best result on each metric is shown in bold face.

Figure 8: Comparison of tongue segmentation results among different models (a) Tongue (b) FCN (c) Deeplab (d) UrNet.

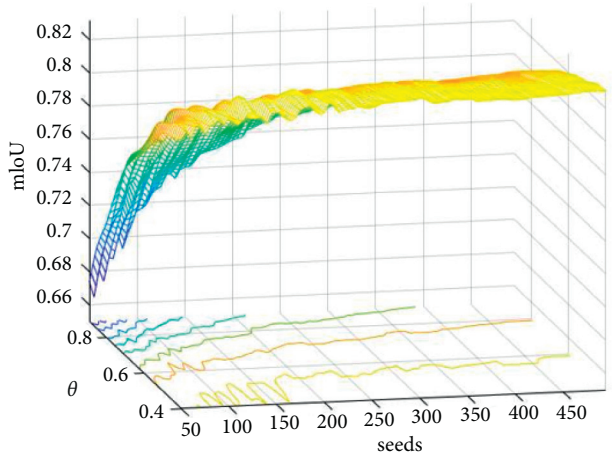

Figure 9: Superpixel segmentation parameter results (X-axis is the seeds, Y-axis is the θ, and Z-axis is mIoU).

Table 3: Segmentation results after fusion with superpixel (mean ± standard deviation).

Algorithm	*PA*	MPA	MIoU	FWIoU
FCN	0.8856 ± 0.0099	0.8959 ± 0.0079	0.7957 ± 0.0153	0.7988 ± 0.0153
FCN + superpixel	0.8954 ± 0.0079	0.9030 ± 0.0070	0.8108 ± 0.0128	0.8143 ± 0.0126
DeepLab	0.8828 ± 0.0070	0.8907 ± 0.0064	0.7910 ± 0.0115	0.7946 ± 0.0110
DeepLab + superpixel	0.8921 ± 0.0049	0.8990 ± 0.0050	0.8056 ± 0.0082	0.8093 ± 0.0078
UrNet	0.9130 ± 0.0039	0.9159 ± 0.0046	0.8393 ± 0.0065	0.8430 ± 0.0065
SpurNet (UrNet + superpixel)	**0.9145 ± 0.0043**	**0.9168 ± 0.0048**	**0.8417 ± 0.0072**	**0.8454 ± 0.0072**

The best result on each metric is shown in bold face.

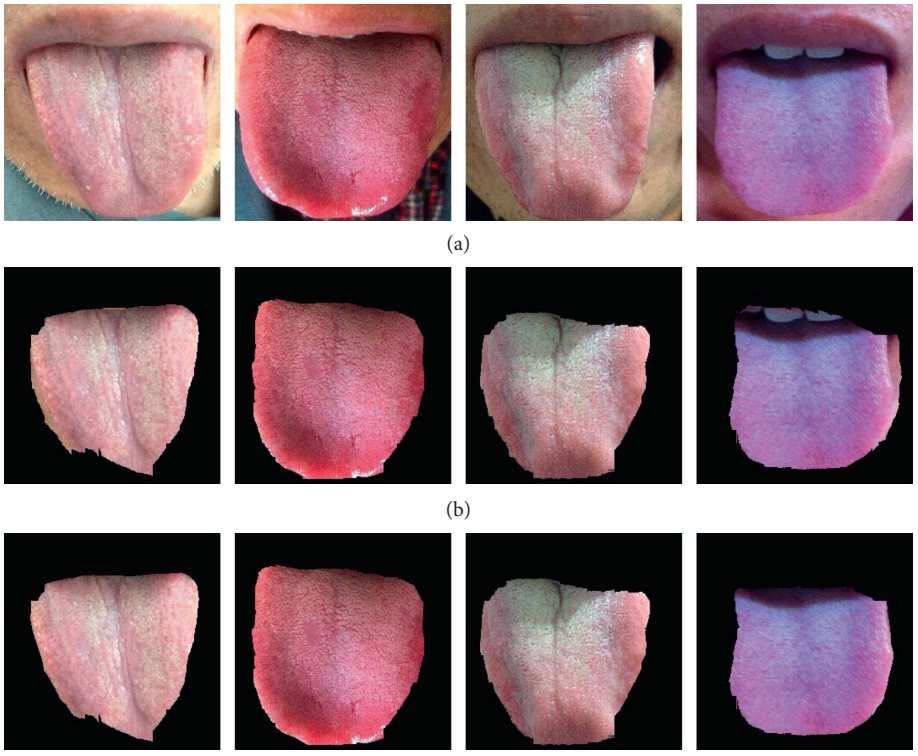

(a)

(b)

(c)

Figure 10: Continued.

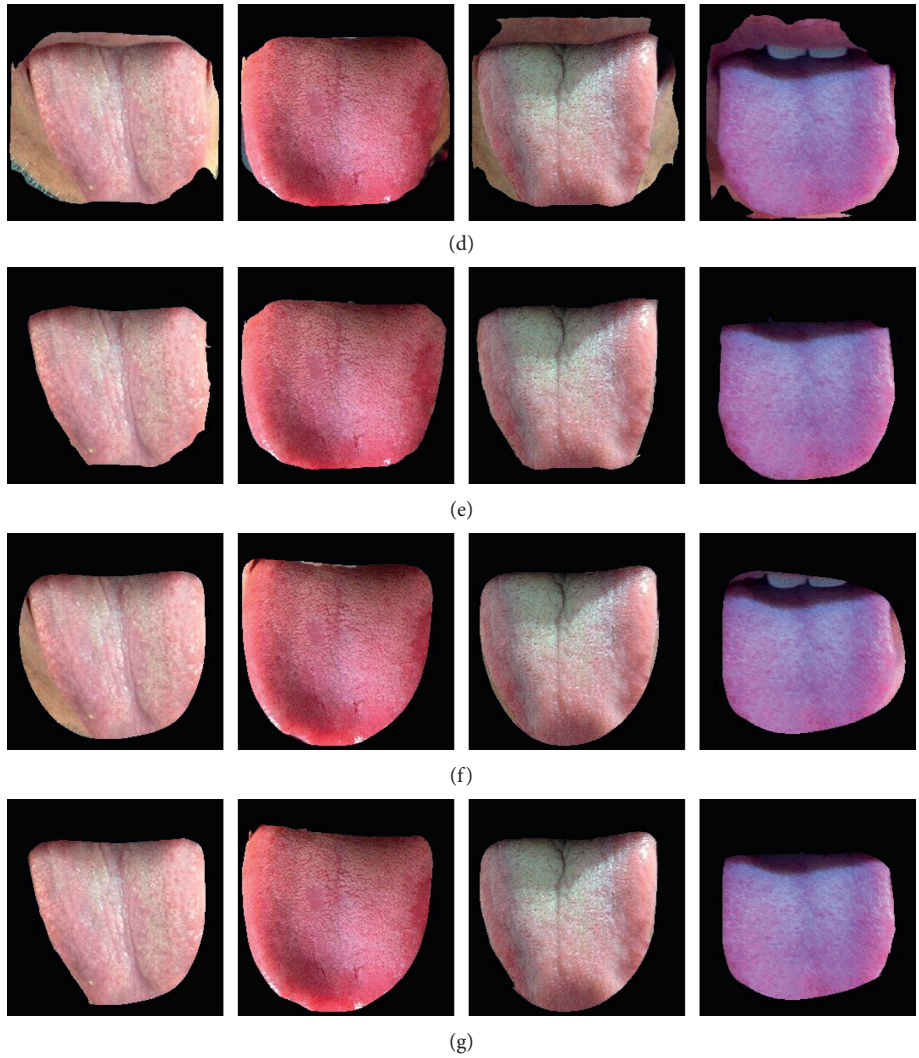

Figure 10: Comparison of segmentation results among different models (a) Tongue (b) FCN (c) FCN + superpixel (d) Deeplab (e) Deeplab + superpixel (f) UrNet (g) SpurNet.

refined segmentation of the tongue was achieved using convolutional neural network concomitant with superpixel, and data augmentation technique was used, which resolved the issue of less data of tongue and ensured the robustness and generalization ability of the model.

It was known from the quantitative results in Table 2 that UrNet established in this study could exclude the influence of the locations and colors of the tongue to better refine and segmentate the tongue and background. Relative to other convolutional neural network models, UrNet convolutional network was superior to FCN and Deeplab models in segmentation effectiveness because it was more sensitive to the segmentation of the margins of tongue. Given that the UNet showed U-shaped structure and fused the high-resolution information (providing the gradient information including margins and markings, for precise localization) and low-resolution information (providing the context semantic information of each image to identify the pixel category) of the same scale in each layer, so that it could provide more accurate segmentation results. Meanwhile, it could better reserve the surface information because Resnet was selected as the Backbone. Nonetheless, FCN (which only fused the multi-layer predicted results) and Deeplab (which is only the fusion of multi-scale features) does not realize the fusion of shallow and deep information, resulting in a poor segmentation effect for details.

According to the visualized results in Figure 10, when a convolutional neural network alone was used for tongue segmentation, it led to some issues such as incomplete tongue segmentation, unsmooth margins, and the presence of additional background pixels. However, when superpixels were added for post-processing, the above issues could be effectively resolved. The superpixel blocks were obtained based on current pixel points and the features of the adjacent regions. The current pixel category has a certain association with the pixel categories in the adjacent regions. If the current pixel category is predicted wrong, it can be corrected through the pixel categories in the adjacent regions.

Combining the superpixel with coarse segmentation (based on convolutional neural network) could resolve the over-segmentation and under-segmentation of a pixel at margins. It was known from the quantitative results in Table 3, after fusion with superpixel image segmentation, the four assessment indicators were all significantly promoted, and the model showed intensive adaptability to the surrounding environments, indicating that the SpurNet proposed in this study could better complete the TCM tongue feature segmentation.

Although convolutional neural network fused with superpixel image segmentation promoted the accuracy of segmentation in this study, there are still some defects urgently to be resolved: (1) The dataset labels mainly come from artificial labels, which may cause some inevitable errors. Therefore, it needs to design a procedure or depend on a clinical physician to assess whether the error range is reasonable objectively. (2) The clustering operation of super pixels is non differentiable, which makes it impossible to use back propagation for deep learning. In the follow-up work, we intend to integrate super pixels into the network to optimize the segmentation effect through network calculation. (3) This study focused on the segmentation of 2D static images and did not achieve real-time segmentation of the dynamic tongue images. Therefore, how to accurately segmentate the tongue from dynamic images and abstract and analyze the characteristics of the dynamic tongue features urgently needs to be resolved in future study. In the future, we will collect more tongue images, aiming to verify and promote the performance of tongue segmentation model in a larger and broader dataset, and try to study the subsequent models such as tongue feature extraction, classification, and so on, aiming to achieve the intellectualization of tongue diagnosis.

5. Conclusion

This study mainly explored the design and application of a tongue segmentation model (SpurNet) fusing convolutional neural network and superpixel characteristics, in which a tongue segmentation model containing an encoder-decoder structure was formed via introducing the residual backbone into the classic UNet model, and the segmentation results were optimized using superpixels. The experimental results have concluded that the SpurNet model, after fusing with superpixel image segmentation, is superior to classic deep learning segmentation model in segmentation effectiveness and can more accurately process the margins of tongue and resolve the over-segmentation and under-segmentation. The thought of this study is a new exploration of the deep learning in the tongue feature segmentation field, which can provide a reference for the intelligent study on tongue images.

Data Availability

The experimental data used to support the findings of this study are available from the corresponding author upon reasonable request (yangtao@njucm edu cn).

Conflicts of Interest

The authors declare that they have no conflicts of interest.

Authors' Contributions

Han Zhang and Rongrong Jiang contributed equally to this work.

Acknowledgments

The research in the paper is supported by the National Key Research and Development Program of China No. 2017YFC1703506; National Science Foundation of China under Grant No. 82174276; China Postdoctoral Foundation No. 2021M701674; Postdoctoral Research Program of Jiangsu Province No. 2021K457C; Jiangsu University philosophy and Social Science research No. 2021SJA0333 and 2020SJA0320; Qinglan Project of Jiangsu Universities; Natural Science Research Project of Higher Education Institutions in Jiangsu Province Nos. 21KJB360024; Graduate Student Cultivation Innovative Engineering Graduate Research and Practice Innovation Program of Jiangsu Province No. KYCX20_1517; 2021 College Student Innovation Training Project Nos. 223, 225, and 227.

References

[1] G. Maciocia, *Tongue Diagnosis in Chinese Medicine*, Eastland press, Seattle, 1995.

[2] B. Bo Pang, D. Zhang, and K. Kuanquan Wang, "The bi-elliptical deformable contour and its application to automated tongue segmentation in Chinese medicine," *IEEE Transactions on Medical Imaging*, vol. 24, no. 8, pp. 946–956, 2005.

[3] Z. Liu, J.-q. Yan, D. Zhang, and Q.-L. Li, "Automated tongue segmentation in hyperspectral images for medicine," *Applied Optics*, vol. 46, no. 34, pp. 8328–8334, 2007.

[4] J. Ning, D. Zhang, C. Wu, and F. Yue, "Automatic tongue image segmentation based on gradient vector flow and region merging," *Neural Computing & Applications*, vol. 21, no. 8, pp. 1819–1826, 2012.

[5] Q. Gao, J. Gang, and H. Wang, *Research and Application of Tongue Image Segmentation and Feature Extraction Method in Traditional Chinese Medicine*, p. 13, Chinese Medicine Modern Distance Education of China, China, 2017.

[6] L. Zhang, J. T. Xu, and T. W. He, "Progress in research and application of tongue image segmentation method," *China Journal of Traditional Chinese Medicine and Pharmacy*, vol. 25, no. 4, pp. 565–567, 2010.

[7] Y. Wang, B. Wei, and Y. Cai, "A knowledge-based arithmetic for automatic tongue segmentation," *Acta Electronica Sinica*, vol. 32, no. 3, pp. 489–491, 2004.

[8] Q. Xing, B. Z. Yuan, and X. F. Tang, "Unsupervised multiresolution image segmentation integrating color and texture," *IEEE Transactions on Pattern Analysis and Machine Intelligence*, vol. 13, no. 001, pp. 49–53, 2004.

[9] Y. B. Sheng, W. Y. Ke, and L. J. Ping, "Research and application of image segmentation algorithm based on the shortest path in medical tongue processing[C]//2009 WRI World Congress on Software Engineering," *IEEE*, vol. 1, pp. 239–243, 2009.

[10] N. Otsu, "A threshold selection method from gray-level histograms," *IEEE Transactions on Systems Man & Cybernetics*, vol. 9, no. 1, pp. 62–66, 2007.

[11] Y. Tan and Z. Wang, "Study on applied technology arithmetic of image threshold segmentation," *Microcomputer Information*, vol. 23, no. 24, pp. 298–300, 2007.

[12] M. Hanping, H. Bo, and Z. Yancheng, "Optimization of color index and threshold segmentation in weed recognition," *Transactions of the Chinese Society of Agricultural Engineering*, vol. 9, no. 23, pp. 154–158, 2007.

[13] T. F. Chan and L. A. Vese, "Active contours without edges," *IEEE Transactions on Image Processing*, vol. 10, no. 2, pp. 266–277, 2001.

[14] C. Rother, V. Kolmogorov, and A. Blake, "GrabCut," *ACM Transactions on Graphics*, vol. 23, no. 3, pp. 309–314, 2004.

[15] M. Tang, L. Gorelick, and O. Veksler, "Grabcut in one cut," in *Proceedings of the IEEE International Conference on Computer Vision*, pp. 1769–1776, IEEE, NJ, USA, December 2013.

[16] M. Tang, I. Ben Ayed, and D. Marin, "Secrets of grabcut and kernel k-means," in *Proceedings of the IEEE International Conference on Computer Vision*, pp. 1555–1563, IEEE, DC, USA, December 2015.

[17] R. E. N. Ji-jun, "Color tongue image segmentation algorithm based on grey space auto-thresholding selection," *Journal of Shaanxi University of Science & Technology*, vol. 2, 2005.

[18] L. Zhang and J. Qin, "Tongue-image segmentation based on gray projection and threshold-adaptive method," *Journal of Clinical Rehabilitative Tissue Engineering Research*, vol. 14, no. 9, pp. 1638–1641, 2010.

[19] Z. C. Fu, X. Q. Li, and F. F. Li, "Tongue image segmentation based on snake model and radial edge detection," *Journal of Image and Graphics*, vol. 14, no. 4, pp. 688–693, 2009.

[20] M. J. Shi, L. I. Guozheng, and L. I. Fufeng, "C2G2FSnake: automatic tongue image segmentation utilizing prior knowledge," *Science China Information Sciences*, no. 09, pp. 1–14, 2013.

[21] Y. Cai, T. Wang, and W. Liu, "A robust interclass and intraclass loss function for deep learning based tongue segmentation," *Concurrency and Computation: Practice and Experience*, vol. 32, no. 22, Article ID e5849, 2020.

[22] Q. Xu, Y. Zeng, W. Tang et al., "Multi-task joint learning model for segmenting and classifying tongue images using a deep neural network," *IEEE journal of biomedical and health informatics*, vol. 24, no. 9, pp. 2481–2489, 2020.

[23] A. Sage, Z. Miodońska, M. Kręcichwost, J. Trzaskalik, E. Kwaśniok, and P. Badura, *Deep Learning Approach to Automated Segmentation of Tongue in Camera Images for Computer-Aided Speech Diagnosis*, pp. 41–51, Springer, Cham, 2021, Information Technology in Biomedicine.

[24] L. Wang, Y. Tang, and P. Chen, "Two-phase convolutional neural network design for tongue segmentation," *Journal of Image and Graphics*, vol. 23, no. 10, pp. 1571–1581, 2018.

[25] X. Zhang, Y. Guo, and Y. Cai, "Tongue image segmentation algorithm based on deep convolutional neural network and fully conditional random fields[J]," *Journal of Beijing University of Aeronautics and Astronautics*, vol. 45, no. 12, 2364 pages, 2019.

[26] J. Li, B. Xu, X. Ban, P. Tai, and B. Ma, "A tongue image segmentation method based on enhanced HSV convolutional neural network," in *Lecture Notes in Computer Science*, pp. 252–260, Springer, Cham, 2017.

[27] B. Lin, J. Xie, and C. Li, "Deeptongue: tongue segmentation via resnet," in *Proceedings of the 2018 IEEE International Conference on Acoustics, Speech and Signal Processing (ICASSP)*, pp. 1035–1039, IEEE, Calgary, Canada, April 2018.

[28] L. Li, Z. Luo, and M. Zhang, "An iterative transfer learning framework for cross-domain tongue segmentation," *Concurrency and Computation: Practice and Experience*, vol. 32, no. 14, Article ID e5714, 2020.

[29] E. Gholami, S. R. K. Tabbakh, and M. Kheirabadi, "Proposing method to Increase the detection accuracy of stomach cancer based on color and lint features of tongue using CNN and SVM," arXiv:2011.09962, 2020.

[30] O. Ronneberger, P. Fischer, and T. Brox, "U-net: convolutional networks for biomedical image segmentation," in *Medical Image Computing and Computer-Assisted Intervention – MICCAI 2015, Lecture Notes in Computer Science*, pp. 234–241, Springer, Munich, Germany, 2015.

[31] K. He, X. Zhang, and S. Ren, "Deep residual learning for image recognition," in *Proceedings of the IEEE conference on computer vision and pattern recognition. IEEE*, pp. 770–778, NV, USA, June 2016.

[32] R. Achanta, A. Shaji, K. Smith, A. Lucchi, P. Fua, and S. Süsstrunk, "SLIC superpixels compared to state-of-the-art superpixel methods," *IEEE Transactions on Pattern Analysis and Machine Intelligence*, vol. 34, no. 11, pp. 2274–2282, 2012.

[33] J. Long, E. Shelhamer, and T. Darrell, "Fully convolutional networks for semantic segmentation," *IEEE Transactions on Pattern Analysis and Machine Intelligence*, vol. 39, no. 4, pp. 640–651, 2015.

[34] L. C. Chen, G. Papandreou, and I. Kokkinos, "Semantic image segmentation with deep convolutional nets and fully connected crfs," arXiv preprint arXiv:1412.7062, 2014.

Hindawi
Evidence-Based Complementary and Alternative Medicine
Volume 2022, Article ID 1381683, 10 pages
https://doi.org/10.1155/2022/1381683

Research Article

Predicting Prognostic Effects of Acupuncture for Depression Using the Electroencephalogram

Xiaomao Fan,[1] **Xingxian Huang**,[2] **Yang Zhao**,[3] **Lin Wang**,[4] **Haibo Yu**,[2] **and Gansen Zhao**[1]

[1]*School of Computer Science, South China Normal University, Guangzhou, China*
[2]*Department of Acupuncture and Moxibustion, Shenzhen Traditional Chinese Medicine Hospital, Shenzhen, China*
[3]*School of Data Science, City University of Hong Kong, Hong Kong SAR, China*
[4]*Shenzhen Institutes of Advanced Technology, Chinese Academy of Sciences, Beijing, China*

Correspondence should be addressed to Haibo Yu; 13603066098@163.com

Received 19 October 2021; Accepted 7 February 2022; Published 2 March 2022

Academic Editor: Xuezhong Zhou

Depression is considered to be a major public health problem with significant implications for individuals and society. Patients with depression can be with complementary therapies such as acupuncture. Predicting the prognostic effects of acupuncture has a big significance in helping physicians make early interventions for patients with depression and avoid malignant events. In this work, a novel framework of predicting prognostic effects of acupuncture for depression based on electroencephalogram (EEG) recordings is presented. Specifically, EEG, as a widely used measurement to evaluate the therapeutic effects of acupuncture, is utilized for predicting prognostic effects of acupuncture. Max-relevance and min-redundancy (mRMR), with merits of removing redundant information among selected features and remaining high relevance between selected features and response variable, is employed to select important lead-rhythm features extracted from EEG recordings. Then, according to the subject Hamilton Depression Rating Scale (HAMD) scores before and after acupuncture for eight weeks, the reduction rate of HAMD score is calculated as a measure of the prognostic effects of acupuncture. Finally, five widely used machine learning methods are utilized for building the predicting models of prognostic effects of acupuncture for depression. Experimental results show that nonlinear machine learning methods have better performance than linear ones on predicting prognostic effects of acupuncture using EEG recordings. Especially, the support vector machine with Gaussian kernel (SVM-RBF) can achieve the best and most stable performance using the mRMR with both evaluating criteria of FCD and FCQ for feature selection. Both mRMR-FCD and mRMR-FCQ obtain the same best performance, where the accuracy and F_1 score are 84.61% and 86.67%, respectively. Moreover, lead-rhythm features selected by mRMR-FCD and mRMR-FCQ are analyzed. The top seven selected lead-rhythm features have much higher mRMR evaluating scores, which guarantee the good predicting performance for machine learning methods to some degree. The presented framework in this work is effective in predicting the prognostic effects of acupuncture for depression. It can be integrated into an intelligent medical system and provide information on the prognostic effects of acupuncture for physicians. Informed prognostic effects of acupuncture for depression in advance and taking interventions can greatly reduce the risk of malignant events for patients with mental disorders.

1. Introduction

Depression is one of the most common mental disorders, characterized by a persistent low mood, loss of interest, or reduced energy. According to the World Health Organization's (WHO) report, over 264 million persons at all ages suffer from depression [1, 2]. Depression has a serious impact on the person's study, work, and social life. In the worst case, depression can cause the affected person to self-harm or even commit suicide when she/he is under long-lasting moderate or severe intensity [3]. Acupuncture has good clinical efficacy in the treatment of depression, with no side effects or adverse reactions. However, the mechanism of acupuncture treatment is still controversial and there is still no objective evidence for evaluating its therapeutic effects [4, 5]. The Hamilton Depression Rating Scale (HAMD) [6] is a widely used tool to assess

the efficacy of depression treatment. Its assessment is quite subjective and requires a trained physician; therefore, designing an objective method to assess the efficacy of depression treatment has great significance.

Electroencephalogram (EEG) is a common tool to capture the electrical activity changes caused by acupuncture [7]. Specifically, in the central nervous system of the human brain, there are many neurons. Moreover, those neurons will continuously produce potential changes. Through EEG equipment, EEG signals can be acquired by recording the electrical activity of the aforementioned neurons from the scalp [8]. Many researchers attempted to utilize EEG recordings to identify depression [9–12]. Cai et al. [10] presented a case-based reasoning model for identifying depression with three-electrode EEG signals. Steiger et al. [12] analyzed EEG characteristics from an individual during the wake and sleep phase and provided a series of biomarkers to screen depression. Hosseinifard et al. [11] investigated a nonlinear analysis method for EEG signals to identify depression patients and normal individuals. Acharya et al. [9] employed a state-of-the-art convolutional neural network (CNN) to screen patients with depression based on EEG signals. Meanwhile, researchers also utilized EEG signals to evaluate the therapeutic effects of depression [13, 14]. Noemi et al. [13] investigated the brain oscillations in the gamma frequency band of EEG signals and evaluated the therapeutic effects with selective serotonin reuptake inhibitors (SSRIs) for depression. Shadli et al. [14] studied the effects of ketamine on the EEG of patients with treatment-resistant generalized anxiety and social anxiety disorders. Since EEG has different signal morphological patterns on patients with depression or not [15, 16], it is shown from experiment and analysis results that all of the aforementioned studies achieved a good performance using EEG recordings on screening patients with depression and evaluating the therapeutic effectiveness of antidepressants. Therefore, EEG can also be utilized to evaluate the prognostic effects of acupuncture, which enables physicians to understand the prognosis and health conditions of patients in advance.

In this article, we proposed a framework based on EEG recordings with machine learning methods for predicting the prognostic effectiveness of acupuncture for depression. Specifically, lead-rhythm features extracted from EEG recordings are selected by max-relevance and min-redundancy (mRMR) with both evaluating criteria of FCD and FCQ. Then, according to the subjects' HAMD scores before and after acupuncture for eight weeks, the reduction rate of HAMD scores is calculated as a measure of the prognostic effects of acupuncture. Finally, popular machine learning methods of logistic regression (LR), random forest (RF), and support vector machine with the linear kernel (SVM-Linear), poly kernel (SVM-Poly), and Gaussian kernel (SVM-RBF) are employed to build 8-week predicting models of prognostic effectiveness of acupuncture for depression. With the help of the predicting model of prognostic effects of acupuncture, physicians can learn about their patients' mental conditions in advance and take necessary interventions to reduce the risk of malignant events.

2. Materials and Methods

Figure 1 shows the proposed predicting framework of prognostic effects of acupuncture for depression. It mainly consists of EEG recording acquisition, feature selection with the mRMR [17, 18], and predicting models built by widely used machine learning methods. The details are described as follows.

2.1. Participants. Subjects with depression who were admitted to Shenzhen Traditional Chinese Medicine Hospital for inclusion criteria were collected. This study was approved by the Ethics Committee of the Shenzhen Traditional Chinese Medicine Hospital with the IRB Number of 2017-8. All the patients signed informed consent and voluntarily participated in this clinical study. Subjects inclusion criteria include the following: (1) meeting the western medical diagnostic criteria for digression; (2) conscious; (3) over 18 years old or under 65 years old. Meanwhile, subjects are excluded under the following conditions: (1) schizophrenia, organic diseases, and physical diseases; (2) pregnant women; (3) those with severe liver and kidney function, cardiovascular and cerebrovascular diseases, and hematopoietic system diseases; (4) not cooperating with acupuncture treatment and poor drug compliance. Regarding treatment intervention, physicians employ acupuncture for depression treatment with the technique of transferring and regulating acupuncture [19], which is proposed by our research team: five times a week, a four-week course of treatment, and a total of 2 courses of acupuncture treatment.

2.1.1. Depression Assessment. The 17-item HAMD [6] is the most widely used scale for depression assessment at present. It has good reliability and validity and can reflect the changes of depression symptoms in a relatively sensitive manner. It is one of the best assessment tools in therapeutic research and can better reflect the severity of depression. Therefore, we utilize the HAMD-17 score to assess the prognostic effects of acupuncture for depression.

2.2. EEG Recording Acquisition. A Neuron-Spectrum-5 EEG device manufactured by Neursoft Ltd., Russia, is used to collect EEG recordings from patients with depression syndrome. The room temperature is controlled at 18–25°C. Scalp electrodes are placed in accordance with the international 10/20 system electrode placement method (Figure 2), and bilateral ear lobes are used as the reference electrodes to record 19 conductive EEG signals. EEG was collected under the condition of quiet eye closure and relaxation. Steady EEG signals are collected before acupuncture (https://www.medicalexpo.com/prod/neurosoft/product-69506-454186.html).

2.3. Features

2.3.1. Feature Description. Figure 2 shows the distribution of scalp electrodes of EEG signals. In this study, EEG recordings we collected consist of 19-lead signals, which are

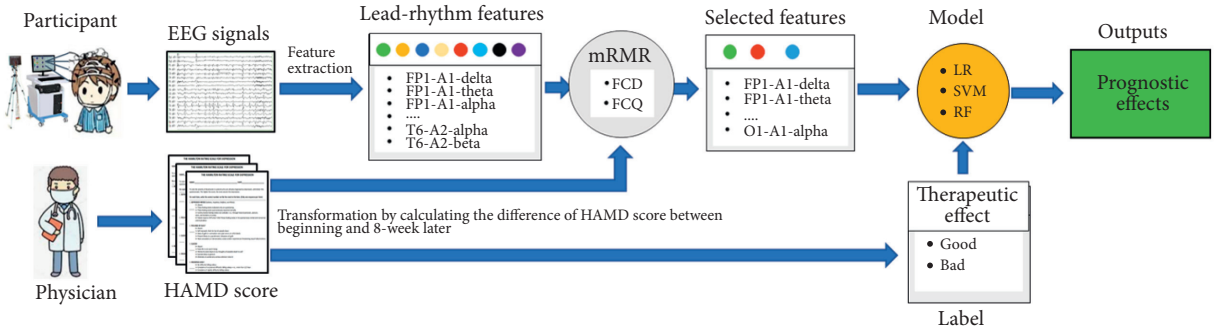

Figure 1: Overview of the predicting framework of prognostic effects of acupuncture for depression with EEG recordings.

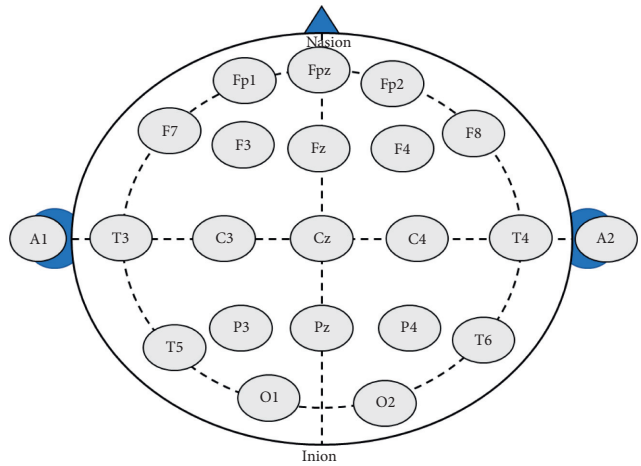

Figure 2: International "10-20" system, which describes the location of scalp electrodes of EEG signals.

presented as FP1-A1, FP2-A2, F3-A1, F4-A2, FZ-A2, C3-A1, C4-A2, CZ-A1, P3-A1, P4-A2, PZ-A2, O1-A1, O2-A2, F7-A1, F8-A2, T3-A1, T4-A2, T5-A1, and T6-A2. FP1-A1, for example, means that the lead signal is acquired from scalp electrodes of FP1 and A1. Four rhythm features (signal amplitude) of delta (δ), theta (θ), alpha (α), and beta (β) are extracted by the embedded digital EEG system in Neuron-Spectrum-5 EEG device. In this case, there are a total of 76 lead-rhythm features for subsequent processing. The lead-rhythm features can be presented in the form of "(lead)-(rhythm)." For example, the four rhythm indexes of lead FP1-A1 can be described as FP1-A1-delta, FP1-A1-theta, FP1-A1-alpha, and FP1-A1-beta, respectively.

2.3.2. Prognostic Effect Evaluation. In this study, the 17-item HAMD rating scale (HRS) is utilized to assess depression conditions for each subject before acupuncture and after acupuncture for eight weeks. To assess the prognostic effects of acupuncture for depression, the reduction rate R_{HRS} of HAMD scores with the difference of HAMD scores of two times on each subject is used to evaluate the prognostic therapeutic effects [20], which is defined as follows:

$$R_{HRS} = \frac{DScore_{pre} - DScore_{pos}}{DScore_{pre}}, \quad (1)$$

where $DScore_{pre}$ refers to the HAMD score before acupuncture and $DScore_{pos}$ refers to the HAMD score of acupuncture for eight weeks. Here, to simplify the problem of predicting prognostic effects, the reduction rate of HAMD scores is mapped into binary values 0 and 1. If R_{HRS} is greater than 0.5, the class label y of the prognostic effect is defined as 1, which means good prognostic effects. Otherwise, y is defined as 0, which means bad prognostic effects.

2.3.3. Feature Selection and Normalization. Feature selection is a very important procedure before building a predicting model of prognostic effects of acupuncture for depression when the sample size is not more than the number of features. The mRMR [17], as one of the popular feature selection methods, is with the advantages of removing redundancy information among selected features and keeping high relevance between selected features and response variables. The relevance and redundancy information of mRMR can be measured by mutual information for category data features and class labels. For continuous data features and category labels, the relevant information is measured by F-statistic and Pearson's correlation coefficients. In this study, the lead-rhythm features are continuous variables and class labels of prognostic effects are binary category variables. Therefore, the mRMR in this study employs F-statistic and Pearson's coefficients to measure the

relevance and redundancy information among selected lead-rhythm features and class labels.

Generally, given two random vectors x and y with continuous values, the Pearson correlation coefficients $P(f_i, f_j)$ can be defined as follows:

$$P(f_i, f_j) = \frac{E(f_i f_j) - E(f_i)E(f_j)}{\sqrt{E(f_i^2 - E^2(f_i))}\sqrt{E(f_j^2) - E^2(f_j)}}, \quad (2)$$

where f_i and f_j are two features in the selected lead-rhythm feature set. Therefore, minimum-redundancy information (M Red) of selected lead-rhythm features S can be defined as follows:

$$M\,\mathrm{Red}(S) = \min \frac{1}{\|S\|^2} \sum_{f_i, f_j \in S} \left|P(f_i, f_j)\right|. \quad (3)$$

To obtain maximum-relevance information M Rel between selected features S and class label vector y, it can be defined as follows:

$$M\,\mathrm{Rel}(S, y) = \max \frac{1}{\|S\|} \sum_{f_i \in S} F(f_i, y), \quad (4)$$

where F is the F-statics, which can be defined as follows:

$$F(f_i, y) = \frac{(n-K)\sum_k n_k (\overline{m_{ik}} - \overline{m_i})^2}{(K-1)\sum_k \sigma_k^2}, \quad (5)$$

where m_{ik} is the mean value of the i-th selected feature within the k-th class ($k = 1, \ldots K$); m_i is the mean value across all entries in the i-th selected feature; σ_k is the variance of the k-th selected features across all data entries.; n is the size of the whole data entries and n_k is the size of the data entries in the k-th class; K is the number of class labels. There are two ways to obtain maximum-relevance minimum-redundancy information, namely, mRMR evaluating score, with F-test correlation difference (FCD) and the F-test correlation quotient (FCQ), which can be defined as follows, respectively:

$$FC\ D = M\,\mathrm{Rel}(S, y) - M\,\mathrm{Red}(S), \quad (6)$$

$$FCQ = M\,\mathrm{Rel}(S, y) \backslash M\,\mathrm{Red}(S). \quad (7)$$

Due to a large variation in terms of amplitudes among lead-rhythm selected features, it is necessary to utilize a normalization technique to map the selected features into a uniform range. In this study, the Min–Max normalization technique with the range from 0 to 1 is employed, which is defined as follows:

$$\mathrm{Norm}(f_i) = \frac{f_i - f_{\min}}{f_{\max} - f_{\min}}, \quad (8)$$

where f_i is the i-th selected lead-rhythm feature, $f_{\max}$ refers to the maximum value of the f_i, and $f_{\min}$ refers to the minimum value of the f_i.

2.4. Machine Learning Methods. In this study, popular machine learning methods of logistic regression, random forest, and support vector machine are utilized to build predicting model of prognostic effects of acupuncture for depression based on EEG recordings. The details are described as follows.

2.4.1. Logistic Regression. Logistic regression (LR) is a classification method that utilizes the Sigmoid function as a posterior probability distribution to classify the input data [21]. The LR can be used for both binary and multiple classification problems. On the other hand, the LR is easy to be implemented and can be applied to both distributed and real-time application scenarios. In this study, we utilize the default threshold value of 0.5 to classify the good and bad prognostic effects of acupuncture. Specifically, if the probability of the LR output is more than the threshold, the prognostic effect should be predicted to be good prognostic effect; otherwise, it is a bad prognostic effect.

2.4.2. Random Forest. Random forest (RF) is an ensemble classifier that contains multiple decision trees [22]. It is widely used for variant classification tasks and achieves quite well performance. Specifically, given a training dataset D with sample size N, the RF employs the bootstrap resampling technique to repeatedly extract k ($k < N$) samples from the original training dataset. The extracted datasets are the new training datasets for decision trees. If the dimension of each sample is M, specify a constant m ($m \leq M$) and randomly select m feature subsets from M features. In this study, we employ the model of CART as the base decision tree model [23], which uses the minimum criterion of the Gini index for optimal feature selection. Train the base decision trees based on the newly generated training data subsets, and the major voting method is utilized for all the base decision tree models to make the final prediction.

2.4.3. Support Vector Machine. Support vector machine (SVM) is a binary classification model, which searches a hyperplane with the largest support vector margin in affine high-dimensional feature space with kernel techniques [24]. Given a training dataset D, the SVM aims to search a separate hyperplane in terms of the training dataset to classify samples into their class groups as many as possible. Furthermore, to map original data features to higher feature dimensions, a total of three kinds of different kernels of linear, poly, and Gaussian are utilized for predicting prognostic effects in this article, which are called SVM-Linear, SVM-Poly, and SVM-RBF in short, respectively.

2.5. Performance Metrics. In this article, four classification performance metrics of precision (Pre), recall (Rec), accuracy (Acc), and $F1$ score are employed to evaluate the predicting models of prognostic effects of acupuncture. As shown in Table 1, TP means the number of subjects with good prognostic effects predicted to be ones with good prognostic effects. FP means the number of subjects with bad prognostic effects predicted to be ones with good prognostic effects. FN means the number of subjects with

Table 1: Confusion matrix of four metrics for classification performance.

Confusion matrix		Truth	
		Positive	Negative
Prediction	Positive	TP	FP
	Negative	FN	TN

good prognostic effects predicted to be ones with bad prognostic effects. TN means the number of subjects with bad prognostic effects predicted to be ones with bad prognostic effects. Therefore, the aforementioned performance metrics can be defined as follows:

$$\begin{aligned} \text{Pre} &= \frac{TP}{TP + FP}, \\ \text{Rec} &= \frac{TP}{TP + FN}, \\ \text{Acc} &= \frac{TP + TN}{TP + TN + FP + FN}, \\ F1 &= \frac{2 \cdot \text{Pre} \cdot \text{Rec}}{\text{Pre} + \text{Rec}}. \end{aligned} \tag{9}$$

3. Results

3.1. Computing Environment. All experiments are conducted on a computing server equipped with a 20-core Intel Xeon E2660 v2 processor and 252 GByte memory. Regarding the three machine learning methods, they run on the machine learning platform of SKlearn V0.23.1, which is deployed in the CentOS 6.5 operation system.

3.2. Data Source. In this article, 92 subjects (age: 37.58 ± 10.99 years; gender: 31 male and 61 female) satisfied inclusion criteria are recruited from Shenzhen Traditional Chinese Medicine Hospital to collect EEG data and HAMD scores. A physician of Shenzhen Traditional Chinese Medicine Hospital takes charge of this data collection lasting almost one year from October 2018 to May 2019. Especially for HAMD scores collected, each subject has to be inquired with the HRS form two times. The first HAMD score is obtained before the acupuncture; the second one is obtained by a follow-up way after acupuncture for eight weeks. However, most of the recruited subjects are lost contacts or did not want to go to the hospital to complete the test and only 26 subjects with completed EEG recordings and two times HAMD scores remained. In other words, there are 26 observations we use to build the predicting model of prognostic effects of acupuncture in this article.

3.3. Classification Performance. In this section, leave-one-out cross-validation is utilized to evaluate the classification performance of the predicting models of the prognostic effect of acupuncture for depression. Specifically, only one observation is left at a time as the test dataset, and the remaining observations as the training dataset are used for the training predicting model of prognostic effect. Given that the size of the dataset is N, the predicting model of prognostic effect is needed to train N times and test N times. However, the classification performance of prognostic effects of acupuncture is calculated according to the accumulated test results from each validation test.

To train the predicting models of prognostic effects of acupuncture, five popular machine learning methods of LR, RF, SVM-Linear, SVM-Poly, and SVM-RBF are implemented with important hyperparameters listed in Table 2. Specifically, for the LR model, there are three hyperparameters of tolerance, solver, and iterated epochs. In order to obtain the best classification performance of the LR model, tolerance is set to be $1e^{-4}$ and the iterated epochs are to be 100. To overcome the small size problem, we utilize "newton-cg" as the solver of the LR model. For the RF model, hyperparameters of a number of estimators, split criterion, and a number of features to train are important for its classification performance. In this study, they are set to be 100, "gini," and "sqrt," respectively. Regarding the SVM model, three respective kernels are employed to train a predicting model of prognostic effects of acupuncture. These three kernels are the linear kernel, poly kernel, and Gaussian kernel. Excluding different kernels of the SVM-Linear, SVM-Poly, and SVM-RBF model, there are also some specified hyperparameters for each predicting model. For example, the SVM-Poly has the hyperparameter of the degree to be set, which determines the order of the poly kernel. Here, we set the degree to be 3. For the SVM-RBF, it has a hyperparameter of gamma to be set. The gamma is mainly used to map the height of low-dimensional samples. The higher the gamma is, the higher the mapped dimension is. In this study, the gamma is set to be "scale," which is defined as follows:

$$\text{gamma} = \frac{1}{N_{\text{fea}}\sigma}, \tag{10}$$

where N_{fea} is the number of features and σ is the variance of the training data.

It is noted that the number of features to select is critical to the predicting models of prognostic effects of acupuncture. However, there are no criteria to determine the number of selected features in the mRMR itself. Therefore, the number of selected features is determined by a wrapper technique with the predicting models. First of all, concerning the sample size of the training dataset, the number of selected features of the mRMR ranges from 3 to 30 in this work. Then, the selected lead-rhythm features are ranked in descending order according to the scores of mRMR. Finally, prognostic effect models of acupuncture are built with the machine learning methods of LR, RF, SVM-Linear, SVM-Poly, and SVM-RBF. As shown in Figures 3 and 4, the classification performance of precision, recall, accuracy, and F1 score varies a lot with the number of features to select using the mRMR of FCD and FCQ. Obviously, nonlinear

Table 2: Hyperparameter configuration of machine learning methods.

Methods	Optimized hyperparameter settings
LR	Tolerance: $1e^{-4}$; solver:"Newton-cg"; Iterated epochs:100.
RF	No. of estimators:100; criterion = "gini"; Max features: "Sqrt".
SVM-linear	kernel:"linear"; tolerance: $1e^{-3}$.
SVM-poly	kernel:"poly"; tolerance: $1e^{-3}$; degree: 3.
SVM-RBF	kernel:"rbf"; tolerance: $1e^{-3}$; Gamma: "Scale".

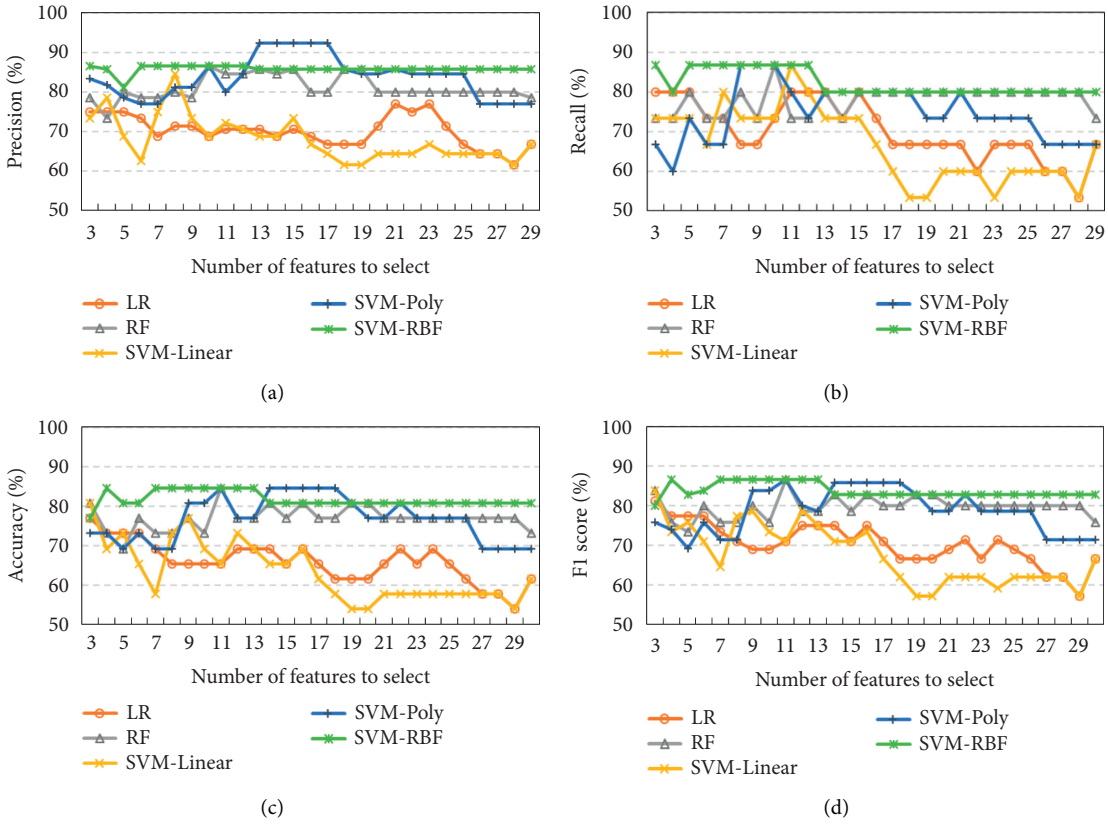

Figure 3: Classification performance of machine learning methods with the number of features to select using mRMR of FCD. (a) Precision. (b) Recall. (c) Accuracy. (d) F1 score.

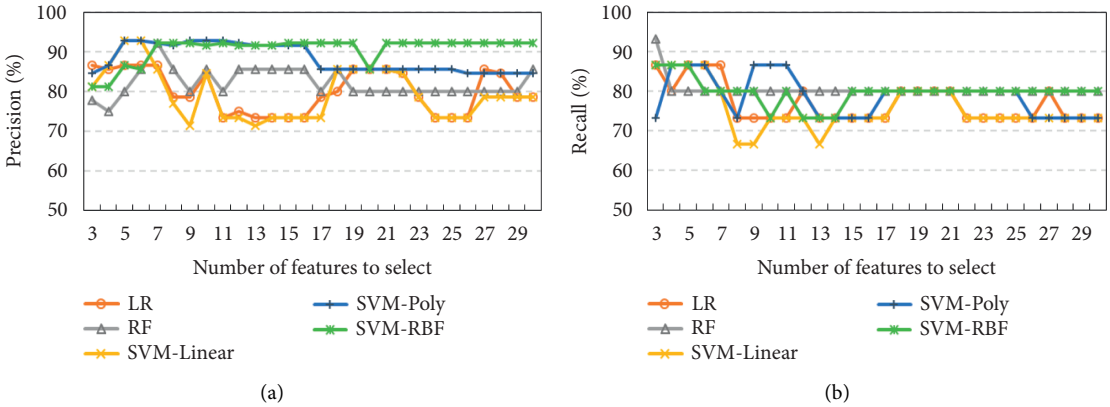

Figure 4: Continued.

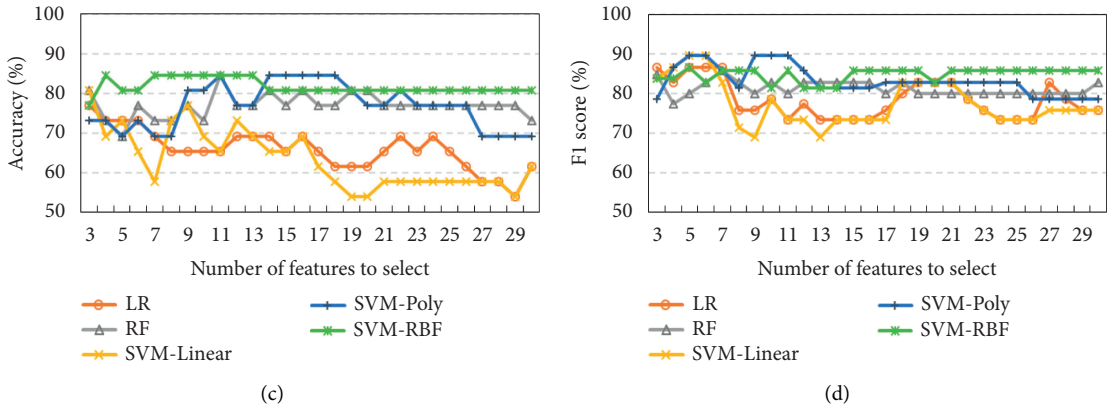

Figure 4: Classification performance of machine learning methods with the number of features to select using mRMR of FCQ. (a) Precision. (b) Recall. (c) Accuracy. (d) F1 score.

models of RF, SVM-Poly, and SVM-RBF are better than linear models of LR and SVM-Linear in predicting prognostic effects of acupuncture regardless of whether mRMR-FCD or mRMR-FCQ is used. Additionally, among those nonlinear models, the SVM-RBF can achieve better and more stable classification performance. Specifically, the SVM-RBF can obtain its best performance with mRMR-FCD and mRMR-FCQ. For the mRMR-FCD, precision is 86.66%, recall is 86.66%, accuracy is 84.61%, and F1 score is 86.67%. Regarding the mRMR-FCQ, precision is 92.30%, recall is 86.66%, accuracy is 84.61%, and F1 score is 86.67%. There is no obvious difference of classification performance of the SVM-RBF with mRMR-FCD and mRMR-FCQ.

4. Discussion

Figures 3 and 4 show that the SVM-RBF can achieve quite well classification performance when the number of features to select is 7 in both mRMR-FCD and mRMR-FCQ. As shown in Figure 5, most of lead-rhythm features with high mRMR scores, which are calculated by equations (6) and (7), are in the top 7. In terms of the mRMR-FCD, the top 7 features to select are "CZ-A1-theta," "F4-A2-theta," "F3-A1-theta," "C4-A2-theta," "F3-A1-delta," "FP2-A2-theta," and "CZ-A1-delta." For the mRMR-FCQ, the top seven features to select are "F7-A1-beta," "CZ-A1-theta," "T3-A1-alpha," "FZ-A2-beta," "F4-A2-theta," "O1-A1-delta," and "O1-A1-theta." Among the top seven features to select, the lead-rhythm features of "CZ-A1-theta" and "F4-A2-theta" are selected by both mRMR-FCD and mRMR-FCQ. As for the remaining ten different selected features, mRMR-FCD and mRMR-FCQ have five respective features. In addition, to learn about the causes of why mRMR-FCD and mRMR-FCQ select different lead-rhythm features, we investigate the relationship among the selected features from mRMR-FCD and mRMR-FCQ. According to the theory of the mRMR, it minimizes the redundancy among selected features. In other words, a selected feature can be substituted by another one if they have a high correlation between them. Therefore, correlation coefficients of selected features between mRMR-FCD and mRMR-FCQ are calculated, which is shown in Figure 6. It is noted that the selected features from mRMR-FCD have at least one feature selected by mRMR-FCQ with a high correlation coefficient. For instance, the selected feature "O1-A1-delta" from mRMR-FCD has a high relationship with the selected feature "F3-A1-delta" from mRMR-FCQ; the correlation coefficient is 0.72. For the selected feature "F7-A1-beta" from mRMR-FCD, there are two selected features of "FP2-A2-theta" and "F3-A1-delta" from mRMR-FCQ with a high relationship. The correlation coefficients are 0.53 and 0.55, respectively. It means that the selected lead-rhythm features with a high relationship can be replaced with each other to some degree. Namely, there is no big difference between mRMR-FCD and mRMR-FCQ to select crucial lead-rhythm features even if they have respective mRMR score mechanisms.

Meanwhile, it is noted that most of the selected top lead-rhythm features using mRMR-FCD and mRMR-FCQ are with theta and delta rhythm, both of which belong to the slow wave. The theta rhythm is related to the amygdaloid nucleus, hippocampus, and thalamus from the limbic system [25]. The occurrence of theta wave is a manifestation of central nervous system depression, which is closely related to mental state, cognition and emotion. On the other hand, most of the selected important lead-rhythm features are from the leads of "F3," "F4," "FP2," "F7," and "FZ," which are located at the frontal and central region of a human brain. The prefrontal cortex plays a key role in determining psychopathological susceptibility [26]. For example, selected lead-rhythm features of "F3-A1-theta" and "F4-A2-theta" are located on the dorsolateral prefrontal cortex, which are verified to be significant to the occurrence of depression [27, 28].

To sum up, the main contributions of this article are concluded as follows. (1) We present a novel framework of predicting prognostic effectiveness of acupuncture for depression with EEG recordings. (2) The mRMR with the advantages of removing redundant features and keeping maximum relevance with the response variable is utilized to select important lead-rhythm features. Meanwhile, the reduction rate of HAMD score as a measure of prognostic effects of acupuncture is employed to produce the class labels with a threshold value of 0.5. (3) Widely used

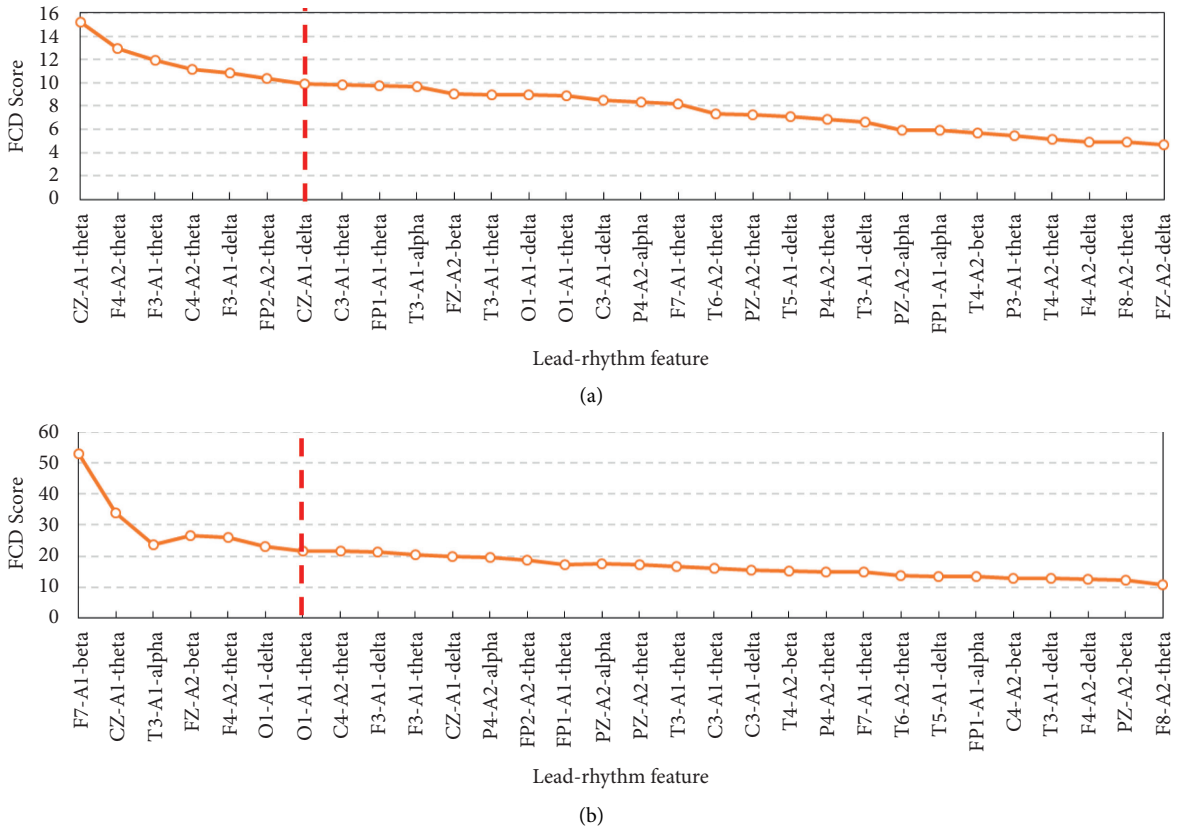

Figure 5: Score trend chart of lead-rhythm features to select. (a) FCD. (b) FCQ.

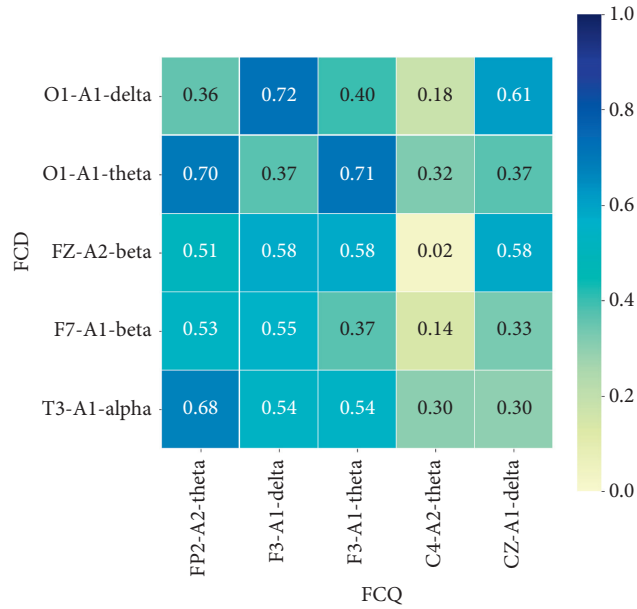

Figure 6: Heatmap of correlation coefficients between selected lead-rhythm features with FCD and FCQ.

machine learning methods of LR, RF, SVM-Linear, SVM-Poly, and SVM-RBF are employed to build the 8-week predicting model of prognostic effects of acupuncture for depression. (4) Experiment results show that the proposed framework with nonlinear machine methods of RF, SVM-Poly, and SVM-RBF outperforms that with linear machine learning methods of LR and SVM-Linear. Furthermore, selected lead-rhythm features from mRMR-FCD and mRMR-FCQ are analyzed for clinical functions related to depression.

5. Conclusions

In this article, a novel framework for predicting prognostic effects of acupuncture for depression with EEG recordings is presented. More specifically, the mRMR, with merits of minimum redundancy among lead-rhythm features and maximum relevance between lead-rhythm features and prognostic effects, is utilized to select important lead-rhythm features. Meanwhile, the reduction rate of HAMD score is calculated and binarized to the prognostic effect label. Widely used machine learning methods of LR, RF and SVM are employed to build the predicting models of prognostic effects of acupuncture. Extensive experiments show that the presented framework of prognostic effects of acupuncture for depression can achieve well performance, where the best accuracy and $F1$ score are 84.61% and 86.67%, respectively. Furthermore, the selected important lead-rhythm features from mRMR-FCD and mRMR-FCQ are analyzed with correlationship technique, and we find that there is a strong relationship between lead-rhythm features selected by mRMR-FCD and mRMR-FCQ. Therefore, the presented framework can help physicians and health providers learn about patients' mental conditions in advance and make essential interventions to reduce the risk of malignant events.

Data Availability

According to the requirement from the IRB of Shenzhen Traditional Chinese Medicine Hospital, all the data cannot be public due to the concerns of patients' privacy.

Disclosure

This manuscript has been submitted as a preprint which can be available at https://www.researchsquare.com/article/rs-41076/v1 [29]. All authors declare that this work has not been submitted elsewhere for publication or under consideration by any other publisher, in whole or in part.

Conflicts of Interest

All authors declare that they have no conflicts of interest for this article.

Authors' Contributions

Xiaomao Fan took charge of writing this manuscript and conducting corresponding data analysis. Xingxian Huang took charge of recruiting participants and acquiring EEG recordings from Shenzhen Traditional Chinese Medicine Hospital. Yang Zhao and Lin Wang helped improve the quality of this article. Haibo Yu, as a senior physician, designed this study and discussed experimental results associated with medical clinical domain knowledge. Gansen Zhao guided the whole study and revised the manuscript.

Acknowledgments

The authors would like to thank Dr. Haoyu Luo, who worked at South China Normal University, and Dr. Liyan Yin, who worked at the Shenzhen Institutes of Advanced Technology, Chinese Academy of Sciences, for their precious suggestions on improving the quality of this article. This work was supported in part by the National Key Research and Development Project (nos. 2017YFC1703604 and 2018YFB1404402) and Sanming Project of Medicine in Shenzhen (no. SZSM201612001).

References

[1] K. Kroenke, R. L. Spitzer, and J. B. W. Williams, "The PHQ-9: validity of a brief depression severity measure," *Journal of General Internal Medicine*, vol. 16, no. 9, pp. 606–613, 2001.

[2] World Health Organization, "Depression and other common mental disorders: global health estimates," Technical Report, World Health Organization, Geneva, Switzerland, 2017.

[3] K. Y. Oh, N. T. Van Dam, J. T. Doucette, and J. W. Murrough, "Effects of chronic physical disease and systemic inflammation on suicide risk in patients with depression: a hospital-based case-control study," *Psychological Medicine*, vol. 50, no. 1, pp. 29–37, 2020.

[4] M. T. Cabýoglu, N. Ergene, and U. Tan, "The mechanism of acupuncture and clinical applications," *International Journal of Neuroscience*, vol. 116, no. 2, pp. 115–125, 2006.

[5] J. Capodice, *Healing in Urology: Clinical Guidebook to Herbal and Alternative Therapies*, pp. 109–127, World Scientific, Singapore, 2017.

[6] A. Almi, H. Mihardja, A. Srilestari, and N. Amir, "Therapeutic effect of acupuncture combined with antidepressants on changes in the HAMD-17 score in major depressive disorder," *Journal of Physics: Conference Series*, vol. 1073, Article ID 062037, 2018.

[7] H. Yu, J. Liu, L. Cai, J. Wang, Y. Cao, and C. Hao, "Functional brain networks in healthy subjects under acupuncture stimulation: an eeg study based on nonlinear synchronization likelihood analysis," *Physica A: Statistical Mechanics and its Applications*, vol. 468, pp. 566–577, 2017.

[8] W. Qin, L. Bai, L. Jin, and J. Tian, "Findings of acupuncture mechanisms using eeg and meg," *Multi-Modality Neuroimaging Study on Neurobiological Mechanisms of Acupuncture*, Springer, Singapore, 2018.

[9] U. R. Acharya, S. L. Oh, Y. Hagiwara, J. H. Tan, H. Adeli, and D. P. Subha, "Automated eeg-based screening of depression using deep convolutional neural network," *Computer Methods and Programs in Biomedicine*, vol. 161, pp. 103–113, 2018.

[10] H. Cai, X. Zhang, Y. Zhang, Z. Wang, and B. Hu, "A case-based reasoning model for depression based on three-electrode eeg data," *IEEE Transactions on Affective Computing*, vol. 11, 2018.

[11] B. Hosseinifard, M. H. Moradi, and R. Rostami, "Classifying depression patients and normal subjects using machine learning techniques and nonlinear features from eeg signal," *Computer Methods and Programs in Biomedicine*, vol. 109, no. 3, pp. 339–345, 2013.

[12] A. Steiger and M. Kimura, "Wake and sleep eeg provide biomarkers in depression," *Journal of Psychiatric Research*, vol. 44, no. 4, pp. 242–252, 2010.

[13] P. Noemi, V. Szilvia, B. Emese, K. Zita, K. Diana, and B. Gyorgy, "Acute and chronic escitalopram alter eeg gamma oscillations differently: relevance to therapeutic effects," *European Journal of Pharmaceutical Sciences*, vol. 121, pp. 347–355, 2018.

[14] S. M. Shadli, T. Kawe, D. Martin, N. Mcnaughton, S. Neehoff, and P. Glue, "Ketamine effects on eeg during therapy of treatment-resistant generalized anxiety and social anxiety,"

International Journal of Neuropsychopharmacology, vol. 21, pp. 717–724, 2018.

[15] J. J. Allen and S. J. Reznik, "Frontal eeg asymmetry as a promising marker of depression vulnerability: summary and methodological considerations," *Current Opinion in Psychology*, vol. 4, pp. 93–97, 2015.

[16] M. Sharifa, R. Goecke, M. Wagner, J. Epps, M. Breakspear, and G. Parker, "From joyous to clinically depressed: mood detection using spontaneous speech," 2012, https://www.aaai.org/ocs/index.php/FLAIRS/FLAIRS12/paper/viewPaper/4478.

[17] H. Hanchuan Peng, F. Fuhui Long, and C. Ding, "Feature selection based on mutual information criteria of max-dependency, max-relevance, and min-redundancy," *IEEE Transactions on Pattern Analysis and Machine Intelligence*, vol. 27, no. 8, pp. 1226–1238, 2005.

[18] S. Shen, T. Gui, and C. Ma, "Identification of molecular biomarkers for pancreatic cancer with mrmr shortest path method," *Oncotarget*, vol. 8, no. 25, pp. 41432–41439, 2017.

[19] M. Pi, Y. Hou, F. Qiu, B. Yan, and Z. Yang, "Clinical study on the optimization of acupuncture treatment for insomnia with technique of transferring and regulating," *Shanghai Journal of Acupuncture and Moxibustion*, vol. 8, no. 3, pp. 270–272.

[20] N. Bedi, C. Chilvers, R. Churchill et al., "Assessing effectiveness of treatment of depression in primary care: partially randomised preference trial," *British Journal of Psychiatry*, vol. 177, no. 4, pp. 312–318, 2000.

[21] C.-Y. J. Peng, K. L. Lee, and G. M. Ingersoll, "An introduction to logistic regression analysis and reporting," *The Journal of Educational Research*, vol. 96, no. 1, pp. 3–14, 2002.

[22] A. Liaw and M. Wiener, "Classification and regression by randomforest," *R News*, vol. 2, pp. 18–22, 2002.

[23] W. Y. Loh, "Classification and regression trees," *Wiley Interdisciplinary Reviews: Data Mining and Knowledge Discovery*, vol. 1, no. 1, pp. 14–23, 2011.

[24] X. Fan, Y. Zhao, H. Wang, and K. L. Tsui, "Forecasting one-day-forward wellness conditions for community-dwelling elderly with single lead short electrocardiogram signals," *BMC Medical Informatics and Decision Making*, vol. 19, no. 1, 2019.

[25] F. Stella and A. Treves, "Associative memory storage and retrieval: involvement of theta oscillations in hippocampal information processing," *Neural Plasticity*, vol. 2011, Article ID 683961, 15 pages, 2011.

[26] E. Harmon-Jones, P. A. Gable, and C. K. Peterson, "The role of asymmetric frontal cortical activity in emotion-related phenomena: a review and update," *Biological Psychology*, vol. 84, no. 3, pp. 451–462, 2010.

[27] J. P. Hamilton, M. Siemer, and I. H. Gotlib, "Amygdala volume in major depressive disorder: a meta-analysis of magnetic resonance imaging studies," *Molecular Psychiatry*, vol. 13, no. 11, pp. 993–1000, 2008.

[28] M. J. Kempton, Z. Salvador, M. R. Munafò et al., "Structural neuroimaging studies in major depressive disorder meta-analysis and comparison with bipolar disorder," *Archives of General Psychiatry*, vol. 68, no. 7, pp. 675–690, 2011.

[29] X. Fan, X. Huang, Y. Zhao, L. Wang, and G. Zhao, "Predicting prognostic effects of acupuncture for depression using electroencephalogram," 2020, https://www.researchgate.net/publication/343003841_Predicting_Prognostic_Effects_of_Acupuncture_for_Depression_Using_Electroencephalogram.

Hindawi
Evidence-Based Complementary and Alternative Medicine
Volume 2022, Article ID 8693937, 9 pages
https://doi.org/10.1155/2022/8693937

Research Article

Decision-Making System for the Diagnosis of Syndrome Based on Traditional Chinese Medicine Knowledge Graph

Rui Yang, Qing Ye, Chunlei Cheng, Suhua Zhang, Yong Lan, and Jing Zou

School of Computer, Jiangxi University of Chinese Medicine, Nanchang 330004, Jiangxi, China

Correspondence should be addressed to Qing Ye; 78466490@qq.com and Chunlei Cheng; chunlei_cheng@163.com

Received 9 October 2021; Accepted 15 January 2022; Published 10 February 2022

Academic Editor: Xuezhong Zhou

The clinical informatization of traditional Chinese medicine (TCM) focuses on serving users and assisting in diagnosis. The rules of clinical knowledge play an important role in improving the TCM informatization service. However, many rules are difficult to find because of the complexity of the data in the current TCM syndrome prediction. Therefore, we proposed an end-to-end model, called Decision-making System for the Diagnosis of Syndrome (DSDS), which is based on the knowledge graph (KG) of TCM. This paper introduces the link prediction for the diagnosis of syndrome by dismantling medical records into multiple symptoms. In addition, based on the symptoms and predicted syndromes, the most relevant syndrome could be determined by the scoring and voting method in this paper. The results show that the accuracy of DSDS is 80.6%.

1. Introduction

Knowledge graph (KG) is a multirelational graph composing of entities and relationships [1]. Recently, KG has attracted great attention from academia and industry. Many examples of large KGs include Freebase [2], DBPedia [3], Yago [4], and NELL [5]. Furthermore, decision-making systems on KG have become an important research area in the past few years. In medicine recommendation systems, the recommended syndrome is based on the analysis of KG, which contains a lot of Chinese medicine information. It is challenging to build the ontology of Chinese medicine and use data to build a KG to realize the application of downstream tasks. In the previous study, Yu et al. [6] constructed a KG of traditional Chinese medicine (TCM) health care based on the "TCM health care ontology" and formed a KG based on the semantic network and further developed retrieval, browsing, and visualization methods. Zhou et al. [7] used clinical data to build a warehouse, which combined structured electronic medical record (EMR) data for medical knowledge discovery and TCM clinical decision support. These studies have promoted the development of Chinese medicine informatization. Unfortunately, most previous studies have focused on the theoretical aspects of Chinese medicine, and there are not many studies in the field of syndrome recommendation.

In the TCM decision-making system, it is necessary to reason about four diagnosis methods and related information in the EMR and analyze the recommended syndromes [8]. This system based on the KG of TCM mainly relies on the intrinsic relationship between symptoms and syndromes. Many studies have proposed auxiliary diagnosis and treatment methods based on machine learning and deep learning [9]. These methods can discover rules in clinical prescriptions of TCM, including the potential connection between symptoms and syndromes [10, 11]. However, these methods lack the TCM dialectical thinking, and the problem of symptom overlap is difficult to solve.

We used the example in Figure 1 to illustrate this problem. For example, "two-inch floating pulse (两寸浮)" and "second-degree swollen tonsil (扁桃体二度肿)" were symptoms in EMRs, but both were included in "Syndrome1" and "Syndrome2." Thus, it is not easy to identify syndrome through repeated signs. Therefore, we constructed a KG that retains the diagnostic information of a single medical record. The KG can maintain the relationship between the symptom information in syndromes. We generated the triples of the predicted medical records that lack the tail entity and

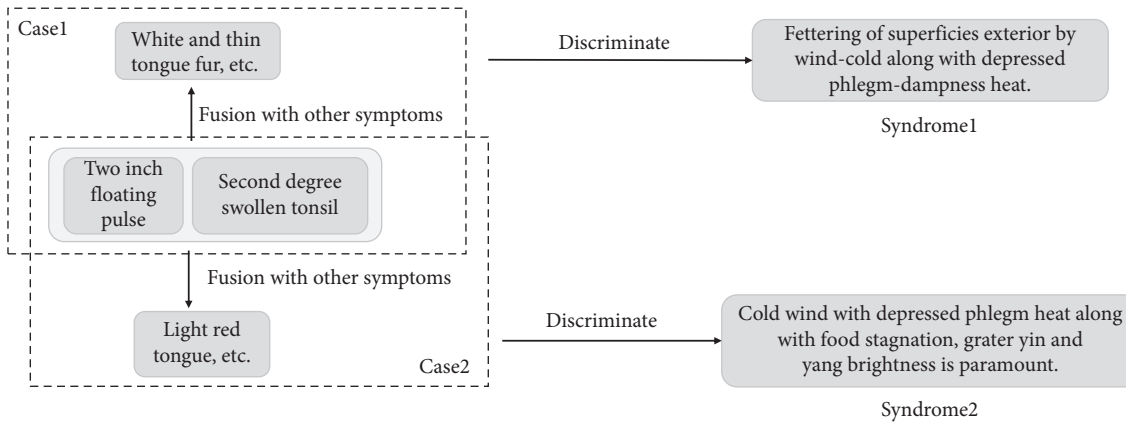

Figure 1: An indication of the overlapping of symptoms between syndromes.

completed triples to obtain the recommended syndromes from the medical records through the scoring and voting method.

We made the following contributions: (1) This paper constructed a KG based on EMR of TCM (KG-EMR-TCM). It contained a single EMR information of TCM. (2) Decision-making System for the Diagnosis of Syndrome (DSDS) can flexibly combine symptom information and reduce symptom overlap between syndromes. In addition, the accuracy of diagnosis reached 80.6% for five similar syndromes. (3) Even if the predicted result of DSDS is different from the label, there is a certain similarity in the symptoms with the expected symptom, expanding the diagnostic thinking.

2. Related Work

2.1. Knowledge Graph Completion Methods. In recent years, link prediction in the KG embedded by KG has become a hot field. The general framework defines a scoring function for triples $(h, l, ?)$ in KG and constrains them so that the score of the correct triple is greater than that of the wrong triples [12].

TransE [13] embedded entities into a high-dimensional real space and relation as translation between the head and the tail entities. RESCAL [14] and DistMult [15] consist of a score function containing a bilinear product between the head entity and tail entity vectors and a relation matrix. ComplEx [16] represented entity vectors and relation matrix in the complex space. ConvE [17] used convolutional neural network to learn the scoring function among head entity, tail entity, and relationships. RotatE [18] projected entities in the complex space, and relations are represented as rotations in the complex plane. InteractE [19] added feature interaction based on ConvE. Conv-TransE [20] kept the global learning metric for entities and relation entities embedded in triples unchanged.

2.2. TCM Knowledge Graph and Its Applications. Li et al. [21] constructed a graph containing 16,217,270 deidentified clinical visit data. They proposed a novel quadruplet structure instead of the classical triplet in KG. TCMRel [22] constructed a candidate relation graph composed of four types of node: herbs, formula, syndrome, and disease, connected by five types of links: formula-disease, formula -syndrome, herbs-disease, herbs-syndrome, and disease-syndrome. CMD [23] used TCM information to create a four-node type graph and proposed a diagnosis model based only on symptoms according to the network. CLLT [24] contained three types of nodes to construct clinical maps: herb, symptom, and diseases and their correlations from 7,000 clinical prescriptions for lung tumors. Furthermore, the system can use the patient's current symptoms as input to obtain medical advice, possible diseases, and treatment options. Xie et al. [8] used ancient TCM books to construct a KG and inferred from symptoms to syndromes. This can assist in diagnosis and treatment. Balažević et al. [25] embedded node2vec into the existing KG and recommended prescription based on the similarity between the vectors. Trouillon et al. [26] proposed an improved algorithm to learn representation vectors from probabilistic medicine KG and applied embedding to link prediction.

Compared with the previous works on the application of TCM, there are several novelties in our work. The basic principle of TCM understanding and treatment of diseases is syndrome differentiation based on the holistic concept of TCM. We converted a complex dialectical problem into a simple completion problem of multiple symptoms in the KG. This is in line with the diagnosis of syndrome based on the four-diagnosis information. In addition, we evaluated the results of simple questions and obtained relevant syndromes.

3. Methods

3.1. Framework Overview. The DSDS in this paper was divided into three steps: KG-EMR-TCM construction module, KG-EMR-TCM representation module, and the syndrome prediction module. The framework of DSDS is shown in Figure 2.

Step 1. We processed the data and formulated logical structure of the symptom information and syndromes (Figure 3).

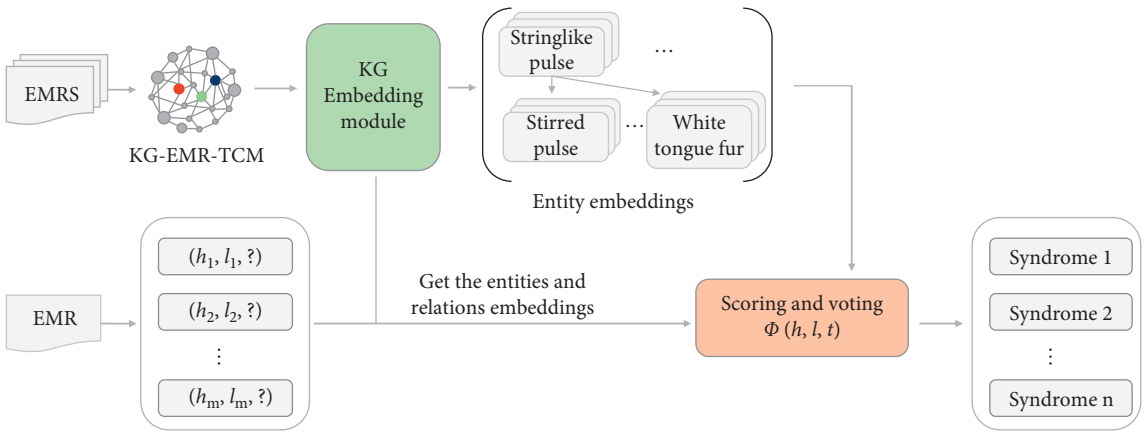

Figure 2: DSDS model architecture based on KG-EMR-TCM.

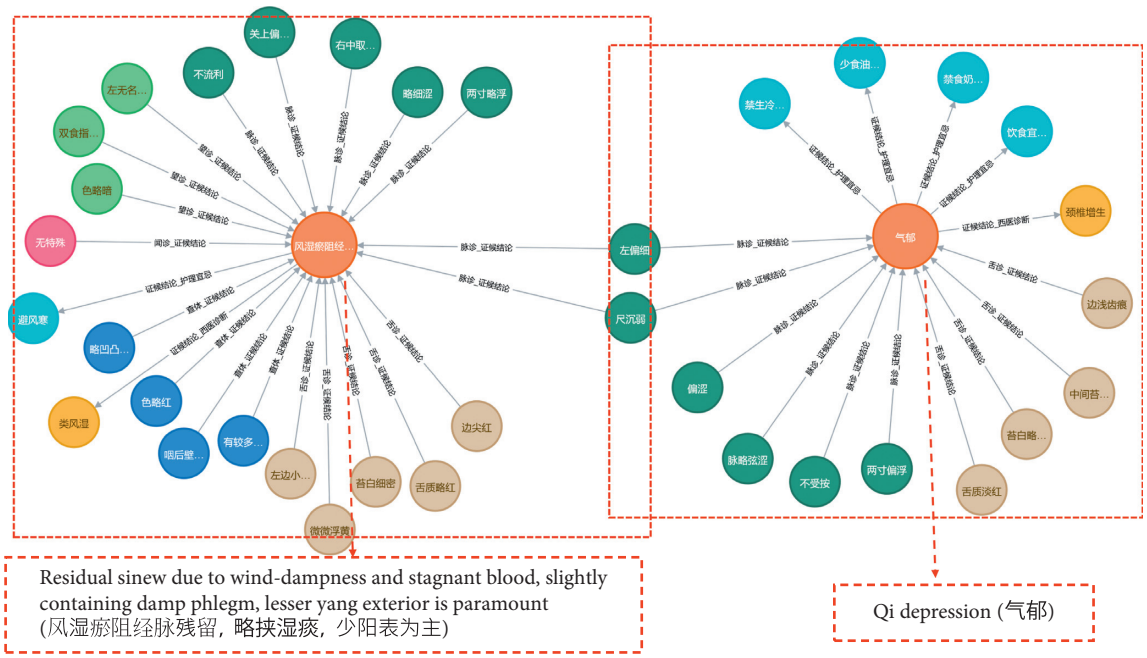

Figure 3: Display of two medical records structures in KG-EMR-TCM.

Step 2. Then, we used the processed data to build KG-EMR-TCM and created embeddings for all entities and relationships in KG.

Step 3. We completed missing triples by KG and then obtained top-N recommended syndromes through the scoring and voting module.

The detailed information about each module is in the following subsections.

3.2. KG-EMR-TCM Construction Module. There is a wealth of knowledge in Chinese medicine records, including symptoms, physical examination, diagnosis, treatment principles, and so on. After desensitizing the existing 131650 TCM medical records, 108746 medical records remain. We used the method of aggregating the information of a single EMR to construct a KG. In this way, the symptoms of a medical record can be effectively associated with the syndrome, which can be used to dig out the complex relationship between symptom and syndrome. The experiment of syndrome recommendation proved the validity of the KG construction. Figure 3 is an example of two medical records in KG. In this example, there are two symptoms of the two syndromes that are repeated, namely "the left side thin (左偏细)" and "the weak foot(尺沉弱)." Through the KG, we can find the associated symptoms between different syndromes.

According to the logical identifying symptom of TCM diagnosis, this paper constructed a KG and aggregated the entities in the KG. Figure 3 shows the two syndromes in KG-EMR-TCM with related entities. We used the EMRs to build KG-EMR-TCM and stored it in Neo4j.

3.3. KG-EMR-TCM Embedding. The KG embedding model embeds all entities and relationships into low-dimensional

vectors and captures their semantics [27]. For each $e \in \mathscr{E}$ and $l \in \mathscr{L}$, KG embeddings models generate $e_e \in \mathbb{R}^{d_e}$ and $e_r \in \mathbb{R}^{d_r}$, where e_e and e_r are d_e and d_r dimensional vectors, respectively. Each embedding method also has a scoring function $\phi(\cdot)$: $\mathscr{E} \times \mathscr{L} \times \mathscr{E} \longrightarrow \mathbb{R}$ to assign score $\phi(h,l,t)$ to a possible triple (h,l,t) $h,l \in \mathscr{E}$, $l \in \mathscr{L}$. We trained in a certain way that for each correct triple $(h,l,t) \in KG$ and wrong triple $(h,l,t') \notin KG$, the model assigns scores such that $\phi(h,l,t) > 0$ and $\phi(h,l,t') < 0$. The scoring function is usually a function of (e_h, e_l, e_t).

ComplEx model represented entities and relations in a complex space instead of using a real-valued space. We captured both symmetric and antisymmetric relations in this model and used the hermitian dot product to do composition for relation, head, and the conjugate of the tail. Given $h,t \in \mathscr{E}$ and $l \in \mathscr{L}$, ComplEx generated $e_h, e_l, e_t \in \mathbb{R}^d$a and defined the scoring function:

$$\phi(h,l,t) = \mathrm{Re}\left(\langle e_h, e_l, \overline{e}_t \rangle\right) = \mathrm{Re}\left(\sum_{k=1}^{d} e_h^{(k)} e_l^{(k)} \overline{e}_t^{(k)}\right), \quad (1)$$

where $\phi(h,l,t) > 0$ is for correct triples and $\phi(h,l,t) < 0$ is for wrong triples. *Re* represents the genuine part of a complex number.

3.4. Syndrome Prediction. In the DSDS model, we used a series of complete triples for training, such as (pulse taking, performance of pulse taking, two-inch floating pulse) and (two-inch floating pulse, pulse taking-syndrome, fettering of superficies exterior by wind-cold along with depressed phlegm-dampness heat). However, when we tested an EMR, the syndrome was the predicted answer. Thus, we classified the test EMR according to the word segmentation rules and obtained a series of missing triples $(h,l,?)$, such as (two-inch floating pulse, pulse taking-syndrome, ?) and (white and thin tongue fur, tongue inspection-syndrome, ?). We used KG-EMR-TCM to predict these triples with missing tail entities. The tail entities of the missing triples are complemented by the score function of the ComplEx model. There was a corresponding score for each completed triple [25, 27].

The value obtained from the scoring function was meaningless. To interpret the score [16], we generated the corruptions and compared the triple score against the scores of corruptions. This shows how the model ranks the test triple against them. We chose the top-N of the rank as the correct option. Therefore, we were learning to rank task instead of classification task. If there are m symptoms, we defined (h,l,t') obtained by negative sampling as $T_1, T_2, \ldots, T_m$, and for each $T_1, T_2, \ldots, T_m$ candidate n entities, we used an $m \times n$ matrix to represent all candidate prediction syndromes.

After obtaining $T_1, T_2, \ldots, T_m$, their scores were calculated, as shown in Figure 4. The higher the score, the more suitable the combination of triples. However, due to the problem of symptom overlap between syndromes in TCM, the highest score did not mean that the current EMR was correct. Therefore, we proposed a scoring and voting method to solve this problem.

We counted all the candidate syndromes by using $f(\cdot)$ and then used $G(\cdot)$ to rank the syndromes with the highest number of occurrences. $f(\cdot)$ is the calculation method of the score function of complex, and $G(\cdot)$ is the method of frequency statistics. Finally, we obtained S_n, which was the recommended syndromes.

$$S_n = G\left(\sum_{i=1}^{m}\sum_{j=1}^{n} f\left(T_{ij}\right)\right). \quad (2)$$

The comprehensive judgment of all symptoms can solve the problems caused by multiple symptoms and comprehensively consider the impact of all symptoms.

4. Results

4.1. Dataset. The clinical medical records were mainly from QIHUANG TCM. After desensitization, each case in the medical record data provided the symptoms and related syndromes of the fourth diagnosis of TCM, body surface examination, diagnosis of TCM, and nursing precautions. After cleaning and formatting the database, 108,746 cases were finally obtained as functional syndromes, including many symptoms and syndromes of TCM. In order to discover more information between symptoms and syndromes, we performed statistics on entities in KG. Table 1 shows that the average percentage of repeated symptoms in eight types of entities reached 91.2%. This indicates that the percentage of repeating symptoms between different syndromes was high, and the relationship was complicated.

Based on 202,619 entities, we constructed 1,499,457 triples in KG-EMR-TCM. Tongue inspection and pulse-taking entities were the most significant among the syndrome-related entities, and listening and smelling were the least significant. The repetition of nursing precautions, listening, and smelling in all medical records were the highest, ranging from 96.7% to 97.5%. The recurrences of these two types of entities in different syndromes were very high.

Most of the information in the medical records is relatively standardized, so this paper used punctuation to segment the four-diagnosis information, body surface examination, and nursing precautions and added the data after the segmentation to the database. In addition, the expression of Chinese medicine is complicated, and the establishment of the synonym table is much work, so this paper does not establish a synonym table. Table 1 shows the statistics after entity processing. The columns in the list: the name of the entity type, the number of entities in the original data, the number of entities after word segmentation, the number of entities remaining after deduplication, and finally, the repetition rate of the entities. In order to maintain the richness of KG-EMR-TCM, we added nursing precautions when constructing the KG, but they were not used as the basis for diagnosis and decision-making when the actual symptoms were recommended.

4.2. Experimental Setup. There are few studies on predicting specific TCM syndromes, and most of them used expert

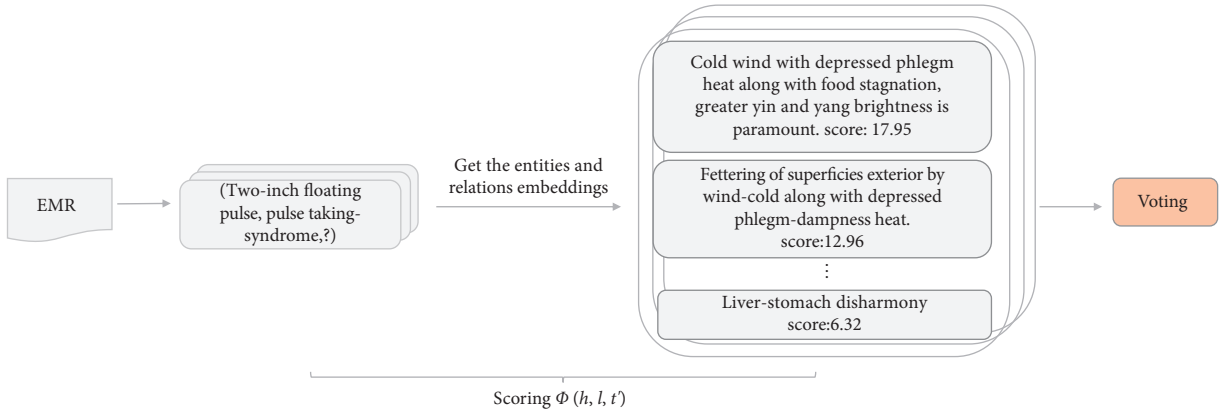

Figure 4: The scores for predicting syndromes.

Table 1: Statistics of each entity category in KG-EMR-TCM.

Entity type	Original	Participle	Deduplication	Percentage of repeating (%)
Tongue inspection	121709	371760	34144	90.8
Pulse taking	121545	462192	39633	91.5
Listening and smelling	7972	116435	2899	**97.5**
Inspection	33758	152316	12911	91.5
Body surface examination	63248	248111	28752	88.4
Nursing precautions	57288	315496	10262	**96.7**
Diagnosis of TCM	100038	95543	12102	87.3
Syndrome	108746	—	61916	85.8
Total	614304	1870599	**202619**	**91.2**

Bold shows the target predicted by this article, the total number of entities, categories with the highest repetition rate, and overall repetition rate.

systems. We adopted the methods of multiclassification and multilabel classification to measure the effectiveness of our model for the TCM clinical medical record in this paper.

In order to verify the performance of DSDS, we compared it with the following methods: GBC [28] is a one-vs-rest multiclassification strategy that fits a classifier to each category. XML-CNN [29], an algorithm for large-scale multilabeled data, is a classic method of convolutional neural networks for multilabel text classification. We used the maximum pooling layer to add as much feature information as possible. KG-XML-CNN added the KG-EMR-TCM vector in this paper based on XML-CNN for more input information to improve the accuracy.

The dataset used in the comparison experiment is KG-EMR-TCM. The difference is that GBC, KG-XML-CNN, and the DSDS all use KG-EMR-TCM embedding vectors as input, whereas XML-CNN uses KG-EMR-TCM randomly generated vectors as input.

4.3. Experimental Results. We conducted a series of comparative experiments on syndrome prediction to simulate dialectical clinical analysis. To obtain node embeddings, we selected a set of symptom and syndrome nodes and used their representations as feature to learn and test the application of syndrome prediction based on EMRs. Considering the uneven distribution of various categories of Chinese medicine data, we used accuracy, weight-recall, weight-f1 as metrics for evaluation. Different classes are given different weights through the weighted average method. The proper distribution ratio of the category determined the weights. Each type was multiplied by the weight and then added.

For the convenience, we have defined the following symbols. The samples in the studied class are positive samples, and the elements in other classes are negative samples. TP_i indicates that there is a correct positive sample classification in a certain category. FP_i indicates that a negative sample is misclassified as a positive sample in a certain class. FN_i indicates sample misclassified as a negative sample in a certain class.

Precision and recall calculation under each category are as follows:

$$Precision_i = \frac{TP_i}{TP_i + FP_i}, \tag{3}$$

$$Recall_i = \frac{TP_i}{TP_i + FN_i}. \tag{4}$$

W_{si} represents the weight of each category in the calculation, and N_{si} represents the true number of samples in that category.

$$W_{s1} : W_{s2} \ldots W_{si} = N_{s1} : N_{s2} \ldots N_{si}. \tag{5}$$

After calculating $Precision_i$ and $Recall_i$, the following indicators are calculated:

$$Precison_{Weighted} = \frac{\sum_{i=1}^{L} Precision_i \times W_i}{|L|}, \quad (6)$$

$$Recall_{Weighted} = \frac{\sum_{i=1}^{L} Recall_i \times W_i}{|L|}, \quad (7)$$

$$F1_{Weighted} = \frac{2 \times Precison_{Weighted} \times Recall_{Weighted}}{Precison_{Weighted} + Recall_{Weighted}}. \quad (8)$$

After we have calculated the above indicators, we need to measure the accuracy of the DSDS model for the prediction of syndrome results. In equation (9), *pre* is the number of correct cases for the predicted syndrome, and *Total* is the total number of tested medical records.

$$Accuracy = \frac{pre}{Total}. \quad (9)$$

We design an end-to-end model; so, the following method is used to evaluate the accuracy of the model calculation: when the syndrome predicted by the model is the same as the label, it is correct; when the accuracy under the candidate top-N is correct, the label of the test case appears in the *n* results predicted by the model.

The results obtained by equations (3)–(9) are shown in Table 2.

We used the syndrome groups (Figure 5) as candidate sets for the clinical syndrome prediction to reduce the number of syndromes predicted. The performance of all the methods on TCM dataset are listed in Table 2. DSDS showed better performance than GBC and XML-CNN in all metrics. The overall performance of the traditional machine learning model based on GBC was worse than that of the method based on deep learning.

In Table 2, there are no results for the GBC model. The first reason is that the GBC model obtained the symptom vectors in KG-EMR-TCM as a feature for training. However, the repetition among the facts in Table 1 reached 91.2%. This means that the vectors trained in the GBC model had a certain similarity. The second reason is that the experiment can obtain valid metrics to evaluate when the number of samples and categories was reduced. However, the metrics values were too small to compare.

When the vector representation of symptoms and syndromes were added to the model XML-CNN, accuracy, weight-recall, and weight-f1 of KG-XML-CNN were 5.2%, 5.9%, and 5.3% greater than XML-CNN, respectively. This proves that the vectors of syndrome-related entities and relationships obtained after embedding KG-EMR-TCM through the representation learning model for KG were better than directly randomly generating the vector of input syndrome-related entities and relationships.

Finally, DSDS was compared to KG-XML-CNN, although KG-XML-CNN was slightly better on accuracy, DSDS was 3.4% and 3.6% higher than KG-XML-CNN on weight-recall and weight-f1, respectively. The results show that the improved multiclass DSDS model based on the ranking has particular effectiveness. The central part of the DSDS superior to KG-XML-CNN is that the DSDS disassembles the input triples, successfully distinguishes the symptom-related symptoms, and casts a vote on the symptom prediction to give the predicted syndrome.

Table 2: Performance comparison of different models.

Method	Weight-recall	Weight-*F*1	Accuracy
GBC	—	—	—
XML-CNN	0.525	0.527	0.574
KG-XML-CNN	0.584	0.580	**0.626**
DSDS	**0.618**	**0.612**	0.621

Bold values represent the best results in the comparative experiment.

4.4. Decision-Making Performance. Chinese medicine auxiliary decision-making aims to provide doctors with top-N recommended syndromes to facilitate follow-up treatment. The recommended syndromes ranked 1, 3, and 5 of this experiment are listed in Table 3. When only one recommended syndrome was given, the accuracy reached 62.1%. When three recommended syndromes were given, the accuracy was increased by 8.9%. When five recommended syndromes were given, the accuracy was 9.6% greater than that of top-3.

This paper aims to rank node pairs in terms of their relevancy, leading to potential linkages between syndromes. This potential linkage indicates that even if the predictive syndrome is incorrect, there are some symptoms overlap between the predicted syndrome and the right syndrome. This is conducive to expanding diagnostic thinking.

When the number of the recommended syndrome is one, we have given an analysis for the wrong predicted syndrome. In Table 4, the right syndrome is "fettering of superficies exterior by wind-cold along with depressed phlegm-dampness heat (风寒闭表,兼有痰湿郁热)," and the prediction is "cold wind with depressed phlegm heat along with food stagnation, greater yin, and yang brightness is paramount (寒风挟痰郁热, 兼有食滞, 太阴阳明为主)."

There was an inevitable overlap in the related entities between the correct syndrome and the predicted syndrome, such as "two-inch floating pulse" and "second-degree swelling of tonsils." However, the scores of "stringlike pulse" and "cough" were lower than other entities. This indicates that they were more closely related to other syndromes.

Furthermore, we compared the following two scores: (1) the score was calculated to predict the syndrome and its symptoms and (2) the score between the predicted symptoms and the correct syndrome was calculated. From the data in Table 4, the latter's scores were lower than those of the former, and the symptoms with higher scores of the latter are related entities that overlap with the correct syndrome. This indicates that there is a certain similarity between the predicted syndrome and the correct syndrome. Therefore, even if the predicted syndrome is different from the correct syndrome, doctors can get help from DSDS.

4.5. Representation of KG-EMR-TCM. After constructing the KG, we embedded the complex vector space through the

Figure 5: Analysis of KG-EMR-TCM embedded clustering.

Table 3: Syndrome recommendation results.

Results of top-N	Accuracy
Top-1	0.621
Top-3	0.71
Top-5	0.806

Table 4: Comparison of symptom entity scores of syndromes.

Syndrome	Symptom		Score	Compare to true syndrome
	English	Chinese		
Fettering of superficies exterior by wind-cold along with depressed phlegm-dampness heat (true) 风寒闭表,兼有痰湿郁热	Stringlike pulse	脉偏弦	4.40	—
	Two-inch floating pulse	两寸浮	**12.96**	—
	Reddish tongue texture	舌质偏红	9.65	—
	White and thin tongue fur	苔薄白	9.00	—
	The middle and back part of the tongue is thicker	中后部略厚	8.95	—
	Second-degree swollen tonsil	扁桃体2度肿	**9.34**	—
	Cough	咳嗽	4.40	—
	Little stringlike pulse	脉略弦	10.98	9.56
	Stirred pulse	不静	16.53	9.30
	Two-inch floating pulse	两寸浮	17.95	**12.96**
	Light red tongue	舌质淡红	9.62	6.02
	White tongue fur	舌苔白	13.55	3.05
	Reddish pharynx Larynx	咽喉略红	14.70	8.37
	Second-degree Swollen tonsil	扁桃体2度肿	14.19	**9.34**
	Phlegm rale in the lung	两肺闻及痰鸣音	7.53	2.10
	Common cold	感冒	3.95	0.03

Bold values show the values mentioned in the article.

ComplEx model. The comparison between XML-CNN and KG-XML-CNN proved the effectiveness of the embedding.

In order to further study the embedding effect of KG-EMR-TCM, we analyzed the embeddings through TensorBoard. In Figure 5, all entities had successfully been gathered into eight categories. These corresponded to the conclusions of pulse taking, tongue inspection, listening and smelling, inspection, body surface examination, diagnosis of TCM, nursing precautions, and syndrome. In addition, the distances between the nodes of the syndrome type are the nearest points in the original space, listed in the right column of Figure 5.

5. Conclusion

In this paper, we constructed a KG based on clinical TCM data and proposed a syndrome prediction model. DSDS can realize the recommendation of syndromes through KG representation learning method. Experimental results show that the performance of DSDS in syndrome prediction was significantly better. This proved the effectiveness of DSDS. When the number of recommended syndromes was five, the accuracy of predicting syndromes reached 80.6%. This proved the effectiveness of DSDS. The model can perform auxiliary diagnosis, and the recommended syndromes are similar to a certain degree.

Abbreviations

EMR:	electronic medical record
TCM:	traditional Chinese medicine
DSDS:	Decision-making System for the Diagnosis of Syndrome
KG:	knowledge graph
KG-EMR-TCM:	KG based on EMR of TCM.

Data Availability

The data used to support the findings of this study are available from the corresponding author upon request.

Disclosure

The funding agreements ensured the authors' independence in the design of the study, collection, analysis, and interpretation of the data, and in writing the manuscript.

Conflicts of Interest

The authors declare that they have no conflicts of interest.

Acknowledgments

This research was funded by the National Key Research and Development Plan of China (2019YFC1712301), Jiangxi Provincial Department of Education Science and Technology Research Key Project (GJJ201204), and Jiangxi Provincial Department of Education Science and Technology Research Project (GJJ170727).

References

[1] S. X. Ji, P. Shirui, C. Erik, M. Pekka, and P. S. Yu, "A survey on knowledge graphs: representation, acquisition, and applications," *IEEE Transactions on Neural Networks and Learning Systems*, 2021.

[2] T. P. Tanon, D. Vrandečić, S. Schaffert, T. Steiner, and L. Pintscher, "From Freebase to wikidata," in *Proceedings of the 25th International Conference on World Wide Web*, pp. 1419–1428, Montreal, Canada, April 2016.

[3] L. Jens, I. Robert, J. Max, Jentzsch, and J. Anja, "Dbpedia—a large-scale, multilingual knowledge base extracted from wikipedia," *Semantic Web*, vol. 6, pp. 167–195, 2015.

[4] F. M. Suchanek, G. Kasneci, and G. Weikum, "Yago: a core of semantic knowledge," in *Proceedings of the 16th international conference on World Wide Web*, pp. 697–706, Banff, Canada, May 2007.

[5] T. Mitchell, W. Cohen, E. Hruschka et al., "Never-ending learning," *Communications of the ACM*, vol. 61, no. 5, pp. 103–115, 2018.

[6] T. Yu, J. Li, Q. Yu et al., "Knowledge graph for tcm health preservation: design, construction, and applications," *Artificial Intelligence in Medicine*, vol. 77, pp. 48–52, 2017.

[7] X. Z. Zhou, S. B. Chen, B. Y. Liu, and R. S. Zhang, "Development of traditional Chinese medicine clinical data warehouse for medical knowledge discovery and decision support," *Artificial Intelligence in Medicine*, vol. 48, pp. 139–152, 2009.

[8] Y. Xie, L. Hu, X. Chen, J. Feng, and D. Zhang, "Auxiliary diagnosis based on the knowledge graph of tcm syndrome," *Computers, Materials & Continua*, vol. 65, no. 1, pp. 481–494, 2020.

[9] Y. Duan, J. S. Edwards, and Y. K. Dwivedi, "Artificial intelligence for decision making in the era of big data - evolution, challenges and research agenda," *International Journal of Information Management*, vol. 48, pp. 63–71, 2019.

[10] Y. H. Wang, "A novel Chinese traditional medicine prescription recommendation system based on knowledge graph," *Journal of Physics: Conference Series*, vol. 1487, 2020.

[11] G. Kong, D.-L. Xu, and J.-B. Yang, "Clinical decision support systems: a review on knowledge representation and inference under uncertainties," *International Journal of Computational Intelligence Systems*, vol. 1, no. 2, pp. 159–167, 2008.

[12] A. Saxena, A. Tripathi, and P. Talukdar, "Improving multi-hop question answering over knowledge graphs using knowledge base embeddings," in *Proceedings of the 58th Annual Meeting of the Association for Computational Linguistics*, pp. 4498–4507, Seattle, WA, USA, July 2020.

[13] A. Bordes, N. Usunier, and J. Weston, "Translating embeddings for modeling multi-relational data," *Advances in Neural Information Processing Systems*, vol. 4, pp. 2799–2807, 2013.

[14] M. Nickel, V. Tresp, and H. P. Kriegel, "A three-way model for collective learning on multi-relational data," in *Proceedings of the Twenty-Eighth International Conference on Machine Learning*, pp. 809–816, Bellevue, WA, USA, June 2011.

[15] B. S. Yang, W. T. Yih, X. D. He, J. F. Gao, and L. Deng, "Embedding entities and relations for learning and inference in knowledge bases," 2014, https://arxiv.org/pdf/1412.6575.

[16] T. Trouillon, J. Welbl, and S. Riedel, "Complex embeddings for simple link prediction," in *Proceedings of the 33rd International Conference on Machine Learning*, vol. 48, pp. 2071–2080, New York, NY, USA, June 2016.

[17] T. Dettmers, P. Minervini, P. Stenetorp, and S. Riedel, "Convolutional 2d knowledge graph embeddings," in

Proceedings of the AAAI Conference on Artificial Intelligence, vol. 32, New Orleans, LO, USA, February 2018.

[18] Z. Q. Sun, Z. H. Deng, J. Y. Nie, and J. Tang, "Rotate: knowledge graph embedding by relational rotation in complex space," 2019, https://arxiv.org/pdf/1902.10197.

[19] S. Vashishth, S. Sanyal, V. Nitin, N. Agrawal, and P. Talukdar, "Interacte: improving convolution-based knowledge graph embeddings by increasing feature interactions," *Proceedings of the AAAI Conference on Artificial Intelligence*, vol. 34, 2020.

[20] C. Shang, Y. Tang, J. Huang, J. Bi, X. He, and B. Zhou, "End-to-End structure-aware convolutional networks for knowledge base completion," *Proceedings of the AAAI Conference on Artificial Intelligence*, vol. 33, pp. 3060–3067, 2019.

[21] L. F. Li, P. Wang, and J. Yan, "Real-world data medical knowledge graph: construction and applications," *Artificial Intelligence in Medicine*, vol. 103, 2020.

[22] H. Wan, M. F. Moens, W. Luyten et al., "Extracting relations from traditional Chinese medicine literature via heterogeneous entity networks," *Journal of the American Medical Informatics Association: JAMIA*, vol. 23, pp. 356–65, 2016.

[23] O. Byambasuren, Y. F. Yang, Z. F. Sui, and D. Dai, "Preliminary study on the construction of Chinese medical knowledge graph," *Journal of Chinese Information Processing*, vol. 33, pp. 1–9, 2019.

[24] C. Ruan, Y. Wu, Y. Yang, and G. Luo, "Semantic-aware graph convolutional networks for clinical auxiliary diagnosis and treatment of traditional Chinese medicine," *IEEE Access*, vol. 9, pp. 8797–8807, 2021.

[25] I. Balažević, C. Allen, and T. M. Hospedales, "Tucker: tensor factorization for knowledge graph completion," 2019, https://arxiv.org/pdf/1901.09590.

[26] T. Trouillon, C. R. Dance, E. Gaussier, and J. Welbl, "Knowledge graph completion via complex tensor factorization," *Journal of Machine Learning Research*, vol. 18, 2017.

[27] S. Z. Dai, Y. C. Liang, S. Y. Liu, and Y. Wang, "Learning entity and relation embeddings with entity description for knowledge graph completion," in *Proceedings of the 2018 2nd International Conference on Artificial Intelligence: Technologies and Applications (ICAITA 2018)*, pp. 202–205, Chengdu, China, March 2018.

[28] J. H. Friedman, "Greedy function approximation: a gradient boosting machine," *Annals of Statistics*, vol. 29, no. 5, pp. 1189–1232, 2001.

[29] J. Z. Liu, W. C. Chang, Y. X. Wu, and Y. M. Yang, "Deep learning for extreme multi-label text classification," in *Proceedings of the 40th International ACM SIGIR Conference on Research and Development in Information Retrieval*, pp. 115–124, Tokyo, Japan, August 2017.

Hindawi
Evidence-Based Complementary and Alternative Medicine
Volume 2022, Article ID 7285312, 13 pages
https://doi.org/10.1155/2022/7285312

Research Article

Refined Multiscale Entropy Analysis of Wrist Pulse for Gender Difference in Traditional Chinese Medicine among Young Individuals

Huaxing Xu,[1] **Qia Wang**,[2] **Xiaobo Mao**,[1] **Zhigang Shang**,[1] **Yuping Zhao**,[3] **and Luqi Huang**[3]

[1]*School of Electrical Engineering, Zhengzhou University, Zhengzhou 450001, Henan, China*
[2]*Institute of Quantitative and Technological Economics, Chinese Academy of Social Sciences, Beijing 100732, China*
[3]*China Academy of Chinese Medical Sciences, Beijing 100020, China*

Correspondence should be addressed to Qia Wang; wangqia@cass.org.cn

Received 17 October 2021; Accepted 22 December 2021; Published 8 February 2022

Academic Editor: Xuezhong Zhou

Pulse signal analysis plays an important role in promoting the objectification of traditional Chinese medicine (TCM). Like electrocardiogram (ECG) signals, wrist pulse signals are mainly caused by cardiac activities and are valuable in analyzing cardiac diseases. A large number of studies have reported ECG signals can distinguish gender characteristics of normal healthy subjects using entropy complexity measures, consistently showing more complexity in females than males. No research up to date, however, has been found on examining gender differences with wrist pulse signals of healthy subjects on entropy complexity measures. This paper is aimed to fill in the research gap, which could, in turn, provide a deeper insight into the pulse signal and might identify potential differences between ECG signals and pulse signals. In particular, several complementary entropy measures with corresponding refined composite multiscale versions are established to perform the analysis for the filtered TCM pulse signals. Experimental results reveal that regardless of entropy measures used, there is no statistically significant gender difference in terms of entropy complexity, indicating that the pulse signal holds less gender characteristics than the ECG signal. In view of these findings, wrist pulse signals could be likely to provide different pieces of information to ECG signals. The present study is the first to quantitatively evaluate gender differences in healthy pulse signals with measures of entropy complexity and more importantly; we expect this study could make contribution to the ongoing pulse intelligent diagnosis and objective analysis, further facilitating the modernization of TCM pulse diagnosis.

1. Introduction

In general, there are four major diagnostic methods of traditional Chinese medicine (TCM), i.e., looking, listening, asking, and feeling the pulse. Among them, pulse diagnosis refers to placing the doctor's three fingers on the wrist radial artery to analyze the health condition [1–4]. For thousands of years, pulse diagnosis has played an indispensable role in TCM as well as in traditional Indian/Korean medicine. Even in today's disease diagnosis, pulse diagnosis is still very competitive due to its convenient, inexpensive, and non-invasive advantages. Furthermore, TCM has also been increasingly adopted in the West by medical practitioners as a supplementary and alternative medical treatment [5].

The basic principle behind wrist pulse-based diagnosis relies on the fact that when blood flows through the organs of the whole body, the disease of which will be eventually reflected in the pulse fluctuation pattern [6]. It is held in TCM theory that pulse conditions are closely tied to the heart beating, blood patency and adequacy, and deficiency of Qi and blood [2, 7]. However, the practice of TCM pulse diagnosis is highly subjective, extremely depending on the experience of the practitioners which usually require years of training. In this case, diagnosis results may be not so objective and reliable. To overcome these limitations, objective analysis and interpretation of the wrist pulse signal, known as computational pulse signal analysis, has been developed in the last few decades [8–13].

Being a physiological signal, the wrist pulse signal is the same as the electrocardiogram (ECG) signal, mainly driven by cardiac contraction and relaxation [14, 15]. Analysis approaches derived from the nonlinear dynamic system have been extensively explored in the study of the characteristics of cardiovascular dynamics [16]. For healthy individuals, a large number of studies have reported that there is a significant gender difference in ECG signals in terms of various complexity measures, such as [17–21]. Since pulse signals can also reflect the heart condition and the vascular system, it is a natural and reasonable assumption for the pulse signal obtained from the subject's superficial artery also to be an indicator of gender differences. On the other hand, gender differences are also considered as an important intrinsic factor in wrist pulse assessment in TCM.

For physiological signal processing, analysis methods can be linear or nonlinear. Several previous works have already applied linear methods in time-domain [22, 23] and frequency-domain [23] to investigate the gender difference in the pulse signal from healthy people. Based on their findings, it has been confirmed that gender differences can be characterized by some features in the pulse signal. Nevertheless, linear analysis techniques may provide less information about the integrated dynamic characteristics of pulse signals. For this reason, it is imperative to examine the gender dependency of the pulse signal with widely used nonlinear dynamics indices.

As one of the nonlinear dynamics indices, some nonlinear complexity entropies, such as approximate entropy [24] or sample entropy [11, 25, 26], have been proposed for computational pulse diagnosis. As expected, signal entropy is distinct between normal people and patients with respect to complexity measures. In view of this, the available studies are primarily focusing on extracting the entropy feature to perform classification on different patients or healthy people and patients. To our best knowledge, there is no report on distinguishing the gender of healthy subjects based on entropy complexity measures. This paper makes an attempt to fill this gap. Specifically, we utilize four kinds of complementary entropy statistics to seek gender difference characteristics embedded in the pulse signal of normal people, which will probably provide additional valuable information related to dynamical changes of the pulse signal. Furthermore, the study presented in the paper might identify potential differences between ECG signals and pulse signals in terms of entropy complexity.

Entropy, as a complexity measure, has been widely applied for different time series analyses, such as industrial fault diagnostic systems [27] and biological signal analyses [28]. Over the years, many different entropy algorithms have been introduced in the literature. For a more comprehensive analysis, our research covers two large families: one is based on Shannon's entropy and the other is based on embedding [29]. As far as entropy measures are concerned in the paper, sample entropy (SaEn) and its improved variant-fuzzy entropy (FuEn) belong to the former group, while permutation entropy (PeEn) [30] and dispersion entropy (DiEn) [31] are the representatives of the latter family [29]. For detailed comparative analysis, both single and multiscale entropy algorithms are implemented.

Approximate entropy (ApEn) is the first widely used entropy measure developed for nonlinear time series analysis [32]. It is however biased resulting from self-matching included when calculating the occurrences of similarity. To address this issue, SaEn is proposed as an extension of ApEn [33] and has been verified to be superior to it [34, 35]. Therefore, in this paper, we first choose the SaEn measure instead of the ApEn measure to analyze the pulse signal. Unfortunately, the SaEn performance is very sensitive to the tolerance since the hard threshold is used. FuEn with the smooth threshold function is then introduced to improve the robustness of SaEn [36, 37]. Irrespective of healthy people or patients, FuEn has not been applied to computational pulse signal analysis yet. This paper also tries to evaluate the performance of the FuEn measure for healthy people.

Despite the popularity of SaEn or FuEn, there are still some problems. First, both ApEn and FuEn ignore the temporal order of the values in a time series. In addition, SaEn, including FuEn, is sensitive to signal amplitude changes. Instead of calculating the entropy with respect to the amplitude, PeEn takes into count the analysis of ordinal patterns by estimating the relative frequencies in time series [30]. Since only ordinal patterns are considered, the amplitude of the signal is practically irrelevant, resulting in structural robustness to the noise. Furthermore, it has the quality of simplicity, robustness, and very high calculation efficiency. Therefore, permutation entropy is also used as an analysis index. On the other hand, PE solely considers the order of the amplitude values, and hence, some crucial information may be missed. To tackle these problems, recently Rostaghi and Azami [31] proposed a new method, termed dispersion entropy (DiEn), which also considers the mean value of amplitudes and differences between amplitude values. They show that the DiEn method considerably outperforms PeEn to discriminate different groups of each dataset. In addition, the computation time of DiEn is significantly less than that of PeEn. For a comprehensive comparison, we also include the DiEn measure to characterize ordinal patterns of the pulse signal.

In practice, time series derived from physiological and complex nonlinear dynamic systems contain multiple temporal scale structures [38]. It is found that traditional entropy measures, like SaEn, may lead to misleading results due to their single-scale-based measures. To prevent this, Costa et al. [38] propose a new entropy complexity measure, known as multiscale entropy measure (MSE), which takes different scales of a time series into account. To be specific, the multiple scales of input data are first derived and the associated entropy measures are subsequently calculated for each scale separately. Based on this novel idea, a large number of corresponding MSEs have been successfully applied in the biomedical research field [39–42]. It is worth noting that, compared to other physiological signals, pulse data recording is shorter (several thousand in general). As a result, for traditional MSE algorithms, the coarse-grained procedures can reduce the length of a time series, which may induce an inaccurate estimation of entropy or undefined entropy. Wu et al. [43] have demonstrated that the refined

composite MSE (RCMSE) algorithm, which is independent of the data length, is more reliable and better than traditional MSE algorithms. This paper, therefore, incorporates the refined composite multiscale architecture [44–46] into the used four entropy measures.

The primary objective of this work is to comprehensively and systematically examine gender differences of wrist pulse signals from healthy people in terms of various entropy measures with a refined composite multiscale framework. To do this, the remainder of the paper is organized as follows. Section 2 describes the acquisition of wrist pulse data and the necessary preprocessing process for pulse signals, followed by the brief review of four kinds of entropy measures and the refined composite multiscale framework in Section 3. Experimental results and analysis with different entropies and scales are presented in Section 4. Section 5 compares the difference between the pulse and ECG signals in distinguishing the healthy people's gender, investigates other existing related pulse work, and at last states limitations of our work. The conclusion is finally drawn in Section 6. We believe that in terms of entropy measures, new findings regarding gender differences in our work may advance guidelines for improved pulse diagnosis or analysis and further provide some insights into the modernization of traditional pulse diagnosis.

2. Materials and Preliminaries

2.1. Research Subjects. The volunteers are all adult college students of Zhengzhou University. All participants have good health without clinical evidence of any disease. Anyone taking any medicine or unable to complete pulse measurement is excluded, especially women who are in menstruation. In order to measure the wrist pulse signal as accurately as possible and prevent interference from other factors, participants are informed not to consume caffeine or alcohol and vigorous exercise the day before the pulse-taking. The same activities as well as eating and smoking are not allowed within 2 hours before the test.

In order to ensure data quality and balance, from the collected data, a total of 200 right-handers are equally divided into two groups of 100 males and 100 females to study gender differences. Table 1 lists their physical conditions including height, age, and weight expressed as mean ± standard deviation (SD). From the table, we can figure out that the female group is lower in weight and height than the male group, but almost the same in age.

2.2. Wrist Pulse Signal Acquisition. By far, a number of sensors, such as pressure, photoelectric, and ultrasonic sensors, have been developed for acquiring pressure pulse signals. Compared with photoelectricity and Doppler ultrasonic sensors, the operating principle of the pressure sensor is more consistent with the TCM theory [47]. In this study, the ZM-300 intelligent TCM pulse pressure detector (made by Shanghai University of Traditional Chinese Medicine, Shanghai, China) is used to collect the wrist ulna pulse signal (at the chi position) in both the left arm and right arm, respectively. The pulse signal acquisition system used in this work is illustrated in Figure 1.

Table 1: Physical conditions of the subjects examined in this study.

Variable	Men	Women	p value
Age (year)	20.45 ± 0.63	20.39 ± 1.03	0.38
Height (cm)	177.36 ± 4.63	162.86 ± 4.25	<0.001
Weight (kg)	65.46 ± 8.28	55.14 ± 5.62	<0.001

2.3. Experimental Setup. This study is conducted in a very quiet room and follows relevant guidelines and regulations. All subjects rested for 10 minutes to stabilize the resting heart rate prior to taking the pulse. During the signal acquisition process, subjects sit in a relaxed and comfortable way and keep their back straight. Pulse collectors have been trained by professional doctors and wrap the pressure sensor in the radial arteries of the wrist in order of right arm to the left arm.

For each volunteer, pulses are monitored for 10 seconds at a sampling rate of 200 Hz; therefore, 2000 samples in total are captured. Pulse manifestation signals under different pressures are obtained by imposing 6 different pressures on each hand and the optimal pulse signal is picked for processing and analysis.

2.4. Pulse Signal Preprocessing. The sampling frequency we used is high enough to prevent pulse waveform distortion. However, the pulse signal is inevitably corrupted by background noise and baseline drift. Before subsequent signal processing, these interferences need to be eliminated to obtain a clean pulse signal. For the preprocessing, we adopt the robust signal preprocessing framework proposed in [48], which first denoises the pulse and then removes baseline drift with a wavelet-based cascaded adaptive filter [49].

Generally, the frequency range of the pulse signal is between 0 Hz and 10 Hz, not exceeding 40 Hz [50]. The background noise is mainly caused by high-frequency interference such as environment disturbance and electricity interruption. Therefore, the noise can be filtered out by a low-pass filter with a cut-off frequency of 40 Hz. As for the baseline drift, various solutions have been proposed to correct it in physiological signals, among which the wavelet-based cascaded adaptive filter method stands out [49]. In the filter, the pulse signal is decomposed and its baseline drift level is detected by computing its energy ratio. According to the given threshold, the pulse is then filtered with a discrete Meyer wavelet filter followed by cubic spline estimation.

Figure 2 shows a snapshot of pulse waveform preprocessing. As we can see, the raw pulse waveform is greatly enhanced so that the accurate extraction of pulse interval can be assured in the following step.

After preprocessing, some pulse signals are excluded by visual inspection due to technical artifacts. Furthermore, we remove incomplete cycles and normalize the pulse further for ensuring precise and validated entropy computing [24].

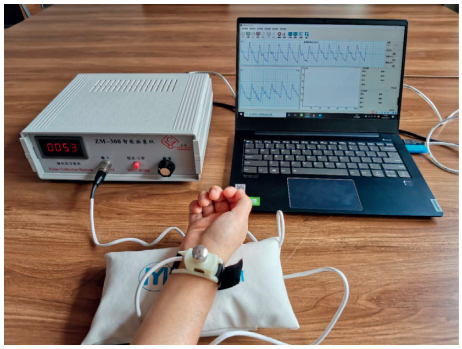

Figure 1: Wrist pulse signal acquisition.

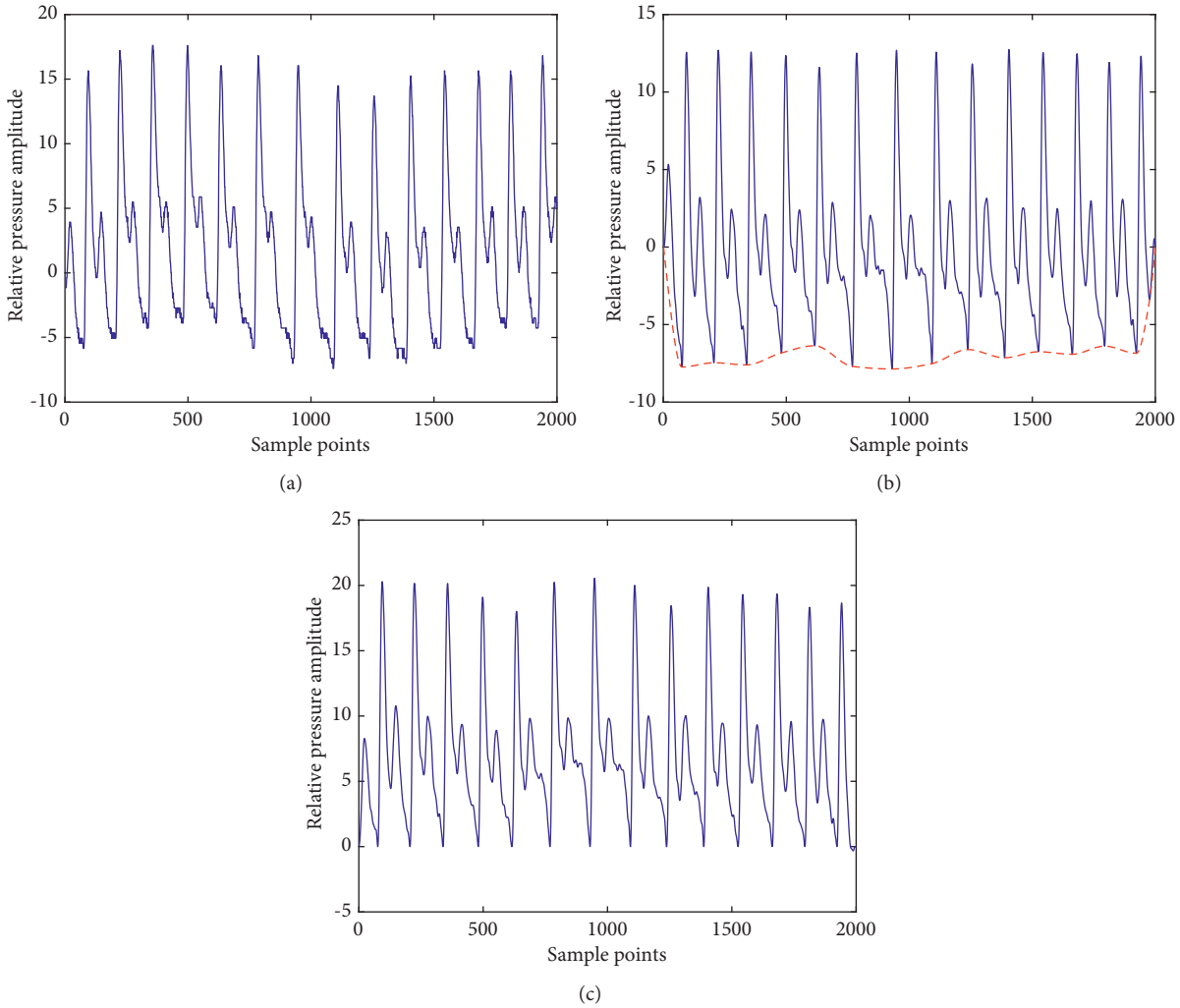

Figure 2: Pulse waveform preprocessing. (a) Original pulse signal. (b) Denoised pulse signal after a low-pass filter; the baseline of the signal is shown in black. (c) Baseline-removed pulse signal.

3. Methods

Entropy measure is widely used to evaluate the complexity of physiological signals in many research fields. In this section, the basic ideas underlying the definition of these selected entropy measures are briefly reviewed; the reader is recommended to refer to [30, 37, 44, 45] and references therein for more details.

3.1. Sample Entropy Measure. For the wrist pulse signal $x(i)(1 \le i \le N)$, given the embedding dimension m and tolerance r, the SaEn of time series can be computed as follows:

(1) First, construct the template vectors $X_i^m(1 \le i \le N - m + 1)$ as follows:

$$X_i^m = \{x(i), x(i+1), \ldots, x(i+m-1)\}. \quad (1)$$

Vector sequences X_i^m represent m consecutive $x(i)$.

(2) Second, for each X_i^m, the distance between X_i^m and X_j^m is calculated by using the infinite norm, defined as

$$d_{ij}^m = \max_{k=0,\ldots,m-1} (|x(i+k) - x(j+k)|). \quad (2)$$

(3) Third, with the Heaviside function $\Theta(x)$, the number of vector matches is counted as a tolerance r in the following way:

$$C_i^m(r) = \frac{1}{N-m-1} \sum_{j=1, j\neq i}^{N-m} \Theta\left(r - d_{ij}^m\right), \quad (3)$$

where $j \neq i$ excludes self-matches. Based on this, the probability that two vectors of length m match with tolerance r is then

$$\phi^m(r) = \frac{1}{N-m} \sum_{i=1}^{N-m} \ln C_i^m(r). \quad (4)$$

Similarly, repeat the above process for vectors of length $m + 1$:

$$C_i^{m+1}(r) = \frac{1}{N-m-1} \sum_{j=1, j\neq i}^{N-m} \Theta\left(r - d_{ij}^{m+1}\right),$$
$$\phi^{m+1}(r) = \frac{1}{N-m} \sum_{i=1}^{N-m} C_i^{m+1}(r). \quad (5)$$

(4) Finally, the SaEn is calculated with the following equation:

$$\mathrm{SaEn}(m, r, N) = \ln\left(\phi^m(r)\right) - \ln\left(\phi^{m+1}(r)\right). \quad (6)$$

The calculation of SaEn requires two parameters to be determined in advance: (i) the embedding dimension m, describing the length of vectors to compare; and (ii) the tolerance threshold r, the distance threshold for two template vectors. The data length is preferred in the range between 10^m and 20^m [51]. The tolerance is usually recommended between 10% and 20% of the standard deviation σ of the signal's amplitudes [38]. In what follows the values of $m = 3$ and $r = 0.15\,\sigma$ have been used.

3.2. Fuzzy Entropy Measure. In SaEn, the pattern similarity is determined by the Heaviside function $\Theta(d_{ij}^m - r)$ given in equation (3). To counter this discontinuity, FuEn employs a fuzzy membership function to compute the similarity degree between two patterns. Essentially, the computation of FuEn is only modified with a new distance measure.

Typically, the similarity degree is determined using a family of an exponentially decaying function:

$$D_{ij}^m(n, r) = \exp\left(-\left(\frac{d_{ij}^m}{r}\right)^n\right), \quad (7)$$

where n defines the membership function shape. In this paper, we use $n = 2$ as proposed in [36, 37]. Then, the equations for the match counts are

$$C_i^m(r) = \frac{1}{N-m-1} \sum_{j=1, j\neq i}^{N-m} D_{ij}^m(n, r),$$
$$C_i^{m+1}(r) = \frac{1}{N-m-1} \sum_{j=1, j\neq i}^{N-m} D_{ij}^{m+1}(n, r). \quad (8)$$

Under given tolerance r, the matching probabilities of vectors of lengths m and $m + 1$ are calculated the same as SaEn, and finally, FuEn is estimated as

$$\mathrm{FuEn}(m, 2, r, N) = \ln\left(\phi^m(r)\right) - \ln\left(\phi^{m+1}(r)\right). \quad (9)$$

3.3. Permutation Entropy Measure. The concept of PeEn is to map a continuous time series onto a symbolic sequence, where the statistics of the symbolic sequences are called permutation entropy. The specific calculation process is as follows:

(1) First, for given embedding dimension m, the phase space $X_i^m(1 \le i \le N - m + 1)$ of a time series wrist pulse signal $x(i)(1 \le i \le N)$ can be constructed as

$$X_i^m = \{x(i), x(i+1), \ldots, x(i+m-1)\}. \quad (10)$$

Furthermore, each sequence X_j^m is sorted in ascending order with a permutation pattern π_i^m and there will be $m!$ possible permutations π for an m–tuple vector.

(2) Based on the probabilities of all permutations, the PeEn is defined as follows:

$$H_p(m) = -\sum_{i=1}^{m!} p(\pi_i^m) \ln\, p(\pi_i^m), \quad (11)$$

where $p(\pi_i^m)$ is calculated as

$$p(\pi_i^m) = \frac{\#\{j | j = 1, \ldots, N - m + 1; X_j^m \text{ has type } \pi_i^m\}}{N - m + 1}. \tag{12}$$

(3) It is clear that PeEn values are between in the range $[0, \log m!]$. For convenience, the normalized permutation entropy is computed as

$$0 \le \text{PeEn} = \frac{H_p(m)}{\log(m!)} \le 1. \tag{13}$$

The maximum (minimum) value of PeEn is 1 (0), indicating that each ordinal pattern has the same probability or the time series is very regular. In brief, the smaller the value of PeEn, the more regular the time series.

The evaluation of the appropriate permutation distribution relies on the embedding dimension m. To achieve reliable statistics, PeEn requires that the length N of the time series satisfies $N \gg m!$ [52]. In practice, it is suggested to work with $3 \le m \le 7$ [30]. In our study, we set $m = 3$ in order to maintain consistency with the aforementioned two entropy measures.

3.4. Dispersion Entropy Measure. Dispersion entropy originates from permutation entropy and is also related to the embedding dimension m and the time delay. In practice, it is recommended $d = 1$ [31]; thus, for clarity, the specific calculation process of DiEn is as follows:

(1) First, for the given pulse signal, employ the normal cumulative distribution function (NCDF) to map $x(i)$ into $y = \{y_1, y_2, \ldots, y_N\}$ from 0 to 1. The new time series y_j is assigned each to an integer from 1 to c with the following linear algorithm:

$$z_j^c = \text{round}\left(c^* y_j + 0.5\right), \tag{14}$$

where z_j^c shows the jth member of the classified time series and *roun d* is the integer function.

(2) Next, for given embedding dimension m, compute the phase space reconstruction $z_i^{m,c}$ $(1 \le i \le N - m + 1)$ for the time series z_j^c,

$$z_i^{m,c} = \left\{z_i^c, z_{i+1}^c, \ldots, z_{i+(m-1)}^c\right\}. \tag{15}$$

Each time series $z_i^{m,c}$ is mapped to a dispersion pattern $\pi_{v_0, v_1, \ldots, v_{m-1}}$, where $z_i^c = v_0, z_{i+1}^c = v_1, \ldots, z_{i+(m-1)}^c = v_{m-1}$ and the number of all possible dispersion patterns is c^m.

(3) For each of c^m potential dispersion patterns, the relative frequency is obtained as follows:

$$p\left(\pi_{v_0 \ldots v_{m-1}}\right) = \frac{\#\left\{i | i \le N - (m-1)d, z_i^{m,c} \text{ has type } \pi_{v_0 \ldots v_{m-1}}\right\}}{N - (m-1)d}. \tag{16}$$

(4) Finally, based on Shannon's definition of entropy, the dispersion entropy is computed as

$$H_d(m) = -\sum_{\pi=1}^{c^m} p\left(\pi_{v_0 v_1 \ldots v_{m-1}}\right) \ln\left(p\left(\pi_{v_0 v_1 \ldots v_{m-1}}\right)\right). \tag{17}$$

Clearly, DiEn values range in $[0, \log(c^m)]$. For convenience, the normalized dispersion entropy is computed as

$$0 \le \text{DiEn} = \frac{H_d(m)}{\log(c^m)} \le 1. \tag{18}$$

For the practical purpose of DiEn, we choose $c = 6$, just as recommended in [31]. Again, the embedding dimension m is set 3 as in the PeEn.

3.5. RCMSE Framework. Traditional MSE may produce incorrect entropy estimates and lead to uncertain entropy because coarse-grained processes will greatly reduce data length on a large scale. To address these drawbacks, the RCMSE algorithm is employed in this paper, with specific procedures summarized as follows:

(1) First, construct multiple coarse-graining series. For time scale τ, there are k coarse-grained time series $y_k^{(\tau)} = \left\{y_{k,1}^{(\tau)}, y_{k,2}^{(\tau)}, \ldots, y_{k,p}^{(\tau)}\right\}$, which is defined as follows:

$$y_k^{(\tau)} = \frac{1}{\tau} \sum_{i=(j-1)\tau+k}^{j\tau+k-1} x_i, \quad 1 \le j \le \frac{N}{\tau}, 1 \le k \le \tau. \tag{19}$$

(2) For SaEn or FuEn, the number of matched vector Paris $n_{k,\tau}^{m+1}$ and $n_{k,\tau}^m$ is computed for all τ coarse-grained series. RCMSE is then defined as the logarithm of ration mean number of matched vector Paris [43, 44].

$$\text{RCMSE}(\mathbf{x}, \tau, m, r) = -\ln\left(\frac{\overline{n}_{k,\tau}^{m+1}}{\overline{n}_{k,\tau}^m}\right) = -\ln\left(\frac{\sum_{k=1}^{\tau} n_{k,\tau}^{m+1}}{\sum_{k=1}^{\tau} n_{k,\tau}^m}\right). \tag{20}$$

For calculating the matching template, using different distance metrics will produce corresponding refined composite multiscale entropy. In this paper, we refer to the refined composite multiscale version of SaEn and FuEn as RC_{MSE} and RC_{MFE} in respective order.

(3) For refined composite multiscale permutation entropy (abbreviated as RC_{MPE}) [45] and refined composite multiscale permutation entropy (abbreviated as RC_{MDE}) [46], the calculation is slightly different, which is computed as

$$\text{RC}_{MP(D)E}(\mathbf{x}, \tau, m, L) = -\sum_{\pi_i=1}^{m!} \overline{p^{(\tau)}}(\pi_i) \ln\left(\overline{p^{(\tau)}}(\pi_i)\right), \tag{21}$$

where $\overline{p^{(\tau)}}(\pi_i) = 1/\tau \sum_{k=1}^{\tau} p_k^{(\tau)}(\pi_i)$ with $p_k^{(\tau)}(\pi_i)$ representing the relative frequency of the permutation pattern or dispersion pattern π_i in the time series $y_k^{(\tau)}$.

4. Experimental Results

In this section, we conduct a series of comparative experiments. Comprehensive analyses of multiscale entropy values between male and female groups in the left and right hands are presented, respectively, and then the statistical difference analysis is adopted to evaluate the statistical significance of gender difference.

For each entropy measure, the mean ± SD of the MSE results is presented across all male and female subjects. The normality of the entropy results distributions is determined by the Shapiro–Wilk test. It is shown in subsequent analysis that for each entropy measure, the values in each group comply with normal distribution. On this basis, an independent two-sample t-test is conducted to determine the significance of differences among male and female groups. All statistical analyses are conducted using the MATLAB software, and without loss of generality, statistical significance is set to be $p < 0.05$.

4.1. RC_{MSE} Results. Figure 3 shows the results of $\mathrm{RC_{MSE}}$ measured in the left and right hands. Roughly speaking, as the scale increases, a general trend of increase regardless of the gender is revealed in the entropy values and thus the complexity of the wrist pulse signal for both hands. Moreover, the higher the scale is, the higher the complexity and variability are. A closer look at Figure 3 indicates that in the left hand, the interquartile range of entropy values for males is larger than that of females, whereas the opposite is true for the right hand. Although the actual entropy value is numerically small and the gap is very little, the median of the right hand in each group is still slightly larger than that of the left hand across all scales. Therefore, it can be concluded that compared to the left hand, the gender is more distinguishable using the right hand. However, there are some outliers found in the measurements, probably due to the hard threshold function in the computation of the SaEn.

Statistical indicators are evaluated in Table 2 for further quantitative comparison, where data are expressed as mean ± SD. We can see that there is no significant difference between genders across all scales1, although the right hand is demonstrated to be more effective than the left hand.

4.2. RC_{MFE} Results. Similarly, the results of $\mathrm{RC_{MFE}}$ in the left and right hands are illustrated in Figure 4, showing the same trend as $\mathrm{RC_{MFE}}$ in both complexity and variability. Fortunately, the FuEn is more stable than the SaEn because of the more smooth growth on the scale without any outliers. The reason is that the soft and continuous boundaries used in FuEn computation enable stronger relative consistency. This confirms the FuEn measure is a better choice in follow-up pulse analysis and diagnosis research. Table 3 tabulates the statistical indicators as well. These observations are consistent with the SaEn's.

4.3. RC_{MPE} Results. Figure 5 shows the results of $\mathrm{RC_{MPE}}$ in the left and right hands. In contrast, the PeEn is more robust than the two above entropy measures with a smaller fluctuation range and thereby can be provided as an alternative in subsequent diagnosis and analysis. The results of statistical analysis are shown in Table 4. Consistent with those obtained in previous studies, there is no observation of significant gender differences.

4.4. RC_{MDE} Results. Figure 6 shows the results of $\mathrm{RC_{MDE}}$ in the left and right hands. As seen from the bars, the entropy fluctuation range is smaller, especially the left hand, and thus, the DiEn is most robust among the four entropy measures. This also confirms that the dispersion entropy is more robust in the study. Thereby, dispersion entropy should be the first choice in subsequent diagnosis and analysis, among TCM practitioners. The results of statistical analysis are shown in Table 5. Again, consistent with those obtained in previous studies, there is no observation of significant gender differences.

As can be seen, the results obtained with these four entropy measures are in good correspondence. In summary, two important facts can be determined. (a) For both genders, the values of the right hand exhibit slightly higher than that of the left hand, but the gap is very small with no statistical difference between left and right hands. (b) No matter which entropy measure is used, there are no overall significant gender differences over all scales. Further comparison with normal ECG signals and previous researches related to gender differences of pulse signals will be discussed in depth in the next section.

5. Discussion

In the present study, we assess gender differences in healthy Chinese male and female groups with four complementary entropy measures. For detailed comparative analysis, both single and multiscale sample entropy algorithms are implemented. In contrast to the previous conclusion drawn in ECG, the primary findings are that the observed difference in terms of entropy measure between males and females is not significant overall.

As stated in the Introduction, the entropy measure has also been used to distinguish between normal and control groups (different patients). Due to the different groups involved, this study cannot be directly compared. Instead, the following analysis and comparison of the research results will be discussed from three aspects: (1) the gender difference of ECG signals in normal people with respect to entropy measure, (2) the gender difference of pulse signals in existing studies, and (3) the limitations of this study. Unless otherwise specified, men and women mentioned below refer to healthy adults.

5.1. Comparison with Gender Difference in ECG Signals. For long-term ECG analysis, it is generally accepted that gender differences are statistically found in healthy people with respect to entropy measures. With ApEn measures,

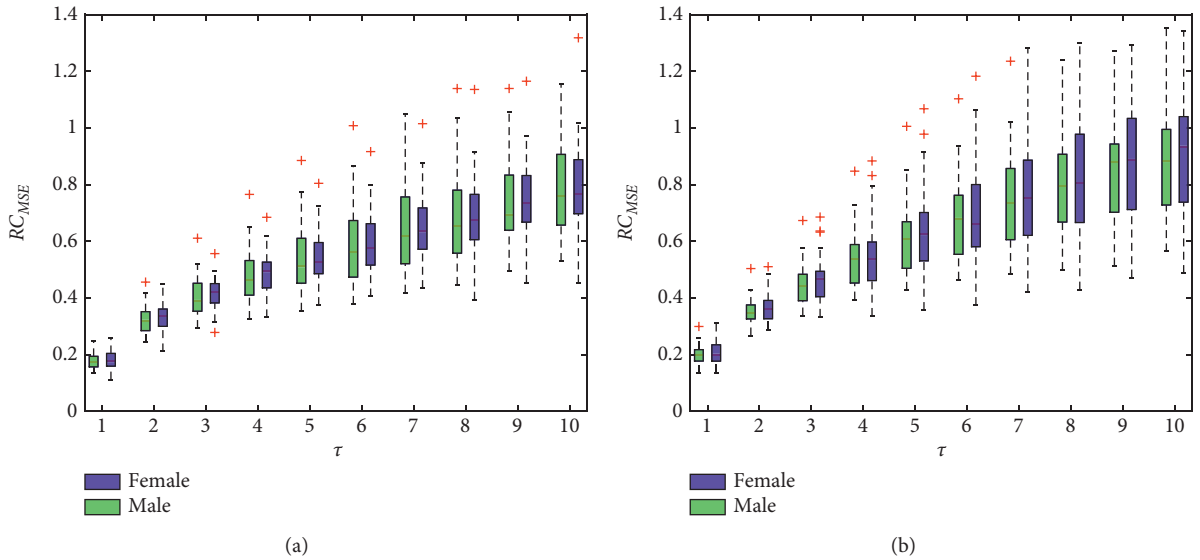

Figure 3: RC_{MSE} under different scales for the left hand (a) and right hand (b). The boxes show the data between the 25th and 75th percentiles, and the middle line inside each box is the median MSE value at a specified scale.

Table 2: Statistical indicators of RC_{MSE}.

τ	Left hand			Right hand		
	Male	Female	P value	Male	Female	P value
1	0.1802 ± 0.0325	0.1801 ± 0.0342	0.9911	0.2000 ± 0.0362	0.2087 ± 0.0461	0.4446
2	0.3233 ± 0.0491	0.3306 ± 0.0485	0.5859	0.3513 ± 0.0483	0.3673 ± 0.0563	0.2685
3	0.4065 ± 0.0744	0.4159 ± 0.0588	0.6102	0.4473 ± 0.0727	0.4688 ± 0.0855	0.3258
4	0.4773 ± 0.1016	0.4827 ± 0.0783	0.8825	0.5338 ± 0.1036	0.5605 ± 0.1302	0.4087
5	0.5404 ± 0.1286	0.5431 ± 0.0960	0.9293	0.6156 ± 0.1325	0.6464 ± 0.1664	0.4544
6	0.5969 ± 0.1509	0.5943 ± 0.1134	0.9435	0.6827 ± 0.1513	0.7140 ± 0.1933	0.5109
7	0.6508 ± 0.1631	0.6486 ± 0.1256	0.9566	0.7527 ± 0.1778	0.7689 ± 0.2012	0.7556
8	0.6882 ± 0.1732	0.6866 ± 0.1491	0.9703	0.7995 ± 0.1797	0.8248 ± 0.2042	0.6305
9	0.7342 ± 0.1712	0.7443 ± 0.1469	0.8169	0.8492 ± 0.1920	0.8687 ± 0.2077	0.7218
10	0.7820 ± 0.1807	0.7895 ± 0.1704	0.8761	0.8906 ± 0.1988	0.9055 ± 0.2058	0.7882

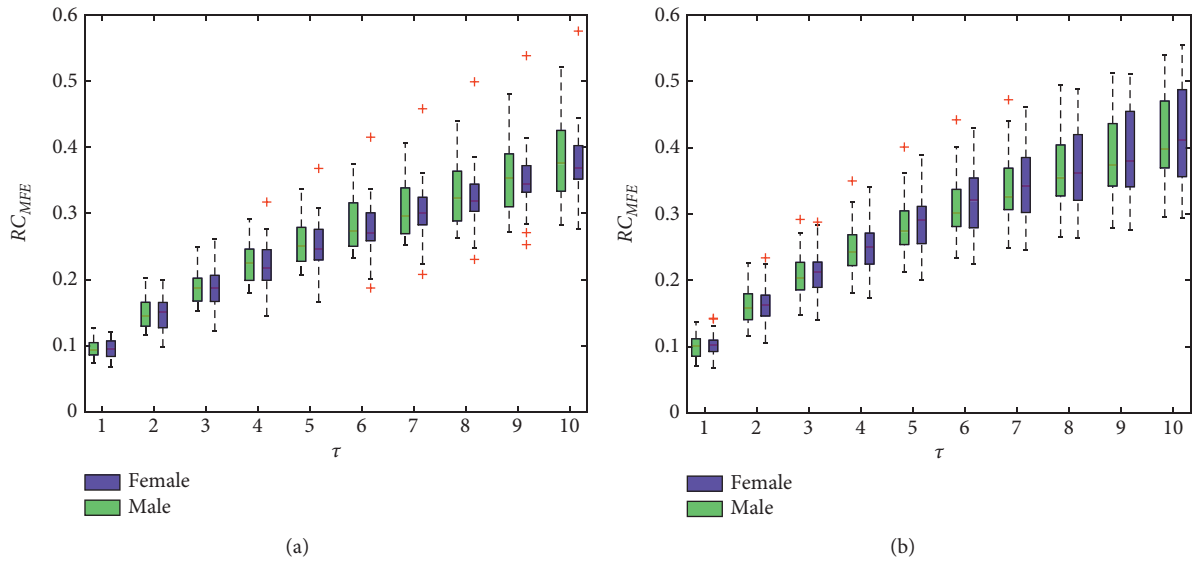

Figure 4: RC_{MFE} under different scales for the left hand (a) and right hand (b). The boxes show the data between the 25th and 75th percentiles, and the middle line inside each box is the median MFE value at a specified scale.

Table 3: Statistical indicators of RC_{MFE}.

τ	Left hand			Right hand		
	Male	Female	P value	Male	Female	P value
1	0.0956 ± 0.0134	0.0954 ± 0.0155	0.9608	0.1008 ± 0.0176	0.1034 ± 0.0182	0.5926
2	0.1499 ± 0.0233	0.1485 ± 0.0268	0.8387	0.1624 ± 0.0296	0.1644 ± 0.0306	0.8080
3	0.1899 ± 0.0288	0.1875 ± 0.0328	0.7800	0.2086 ± 0.0361	0.2113 ± 0.0374	0.7813
4	0.2255 ± 0.0330	0.2219 ± 0.0373	0.7144	0.2488 ± 0.0410	0.2514 ± 0.0416	0.8197
5	0.2570 ± 0.0373	0.2520 ± 0.0409	0.6414	0.2837 ± 0.0460	0.2856 ± 0.0455	0.8773
6	0.2846 ± 0.0417	0.2777 ± 0.0439	0.5526	0.3135 ± 0.0507	0.3145 ± 0.0499	0.9404
7	0.3092 ± 0.0465	0.3015 ± 0.0467	0.5492	0.3403 ± 0.0554	0.3406 ± 0.0542	0.9845
8	0.3335 ± 0.0517	0.3247 ± 0.0498	0.5262	0.3657 ± 0.0595	0.3657 ± 0.0597	0.9972
9	0.3579 ± 0.0568	0.3508 ± 0.0539	0.6389	0.3895 ± 0.0629	0.3909 ± 0.0663	0.9398
10	0.3829 ± 0.0621	0.3769 ± 0.0579	0.7120	0.4155 ± 0.0664	0.4171 ± 0.0731	0.9325

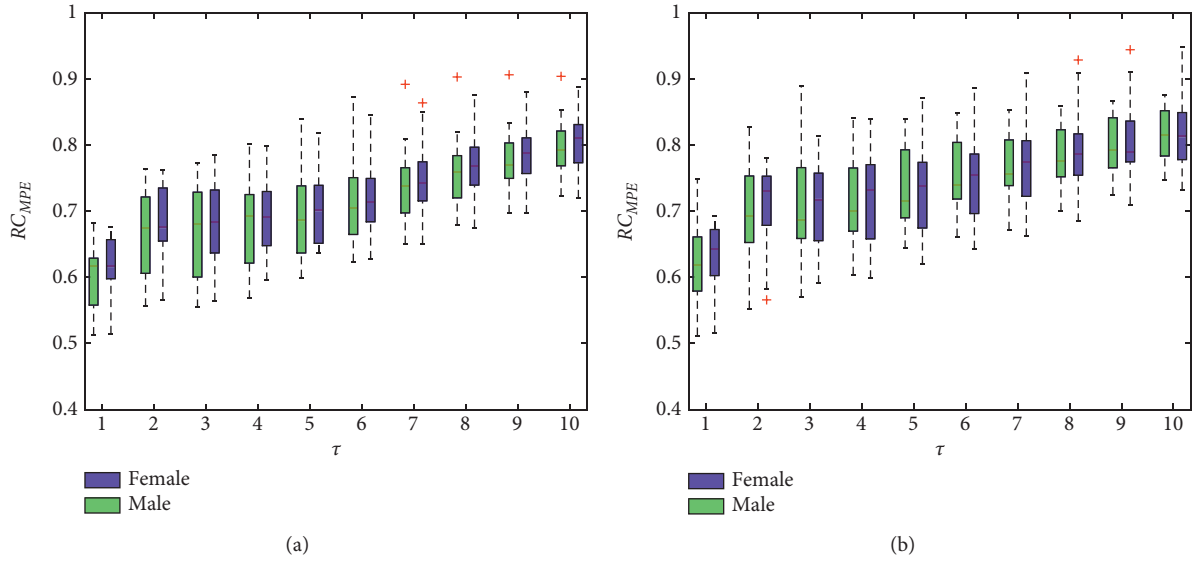

Figure 5: RC_{MPE} under different scales for the left hand (a) and right hand (b). The boxes show the data between the 25th and 75th percentiles, and the middle line inside each box is the median MPE value at a specified scale.

Table 4: Statistical indicators of RC_{MPE}.

τ	Left hand			Right hand		
	Male	Female	P value	Male	Female	P value
1	0.6022 ± 0.0480	0.6221 ± 0.0431	0.1153	0.6184 ± 0.0594	0.6325 ± 0.0486	0.3430
2	0.6648 ± 0.0632	0.6843 ± 0.0581	0.2427	0.6944 ± 0.0700	0.7077 ± 0.0594	0.4524
3	0.6675 ± 0.0679	0.6806 ± 0.0623	0.4644	0.7062 ± 0.0728	0.7107 ± 0.0640	0.8103
4	0.6770 ± 0.0639	0.6872 ± 0.0559	0.5330	0.7148 ± 0.0648	0.7174 ± 0.0676	0.8857
5	0.6926 ± 0.0588	0.7031 ± 0.0528	0.4937	0.7331 ± 0.0594	0.7342 ± 0.0671	0.9524
6	0.7119 ± 0.0549	0.7222 ± 0.0506	0.4784	0.7522 ± 0.0530	0.7531 ± 0.0656	0.9585
7	0.7351 ± 0.0521	0.7467 ± 0.0471	0.3953	0.7700 ± 0.0495	0.7709 ± 0.0636	0.9503
8	0.7561 ± 0.0489	0.7691 ± 0.0443	0.3102	0.7873 ± 0.0444	0.7874 ± 0.0612	0.9950
9	0.7760 ± 0.0451	0.7893 ± 0.0410	0.2629	0.8014 ± 0.0409	0.8028 ± 0.0586	0.9180
10	0.7955 ± 0.0417	0.8081 ± 0.0407	0.2662	0.8166 ± 0.0378	0.8173 ± 0.0540	0.9544

several previous works of literature [17–19] have presented similar results of higher ApEn values for women than men. It is reasonably hypothesized that these differences are due to the fact that women generally live longer and suffer from cardiovascular disease later than men [17]. On the other hand, the short-term ECG signal does not clearly show the gender difference. With multiscale sample entropy measures (only two scales of 1 and 2), it is demonstrated that there are no meaningful gender differences in short-term (5-minute) HRV for any indices [53]. Subsequently, using more multiple complexity measures [20], such as compression entropy, and by means of the detrended fluctuation analysis,

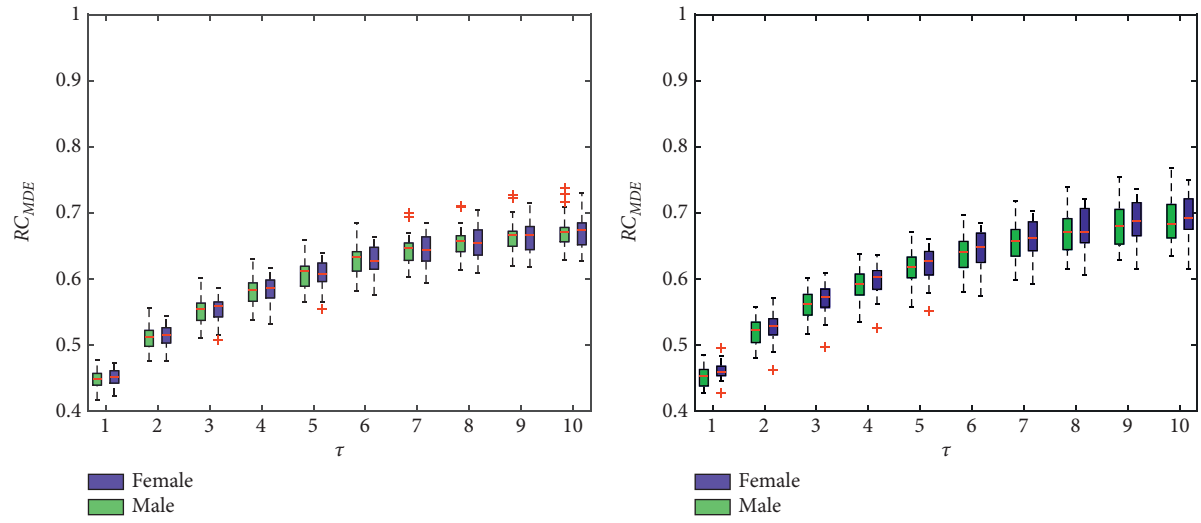

Figure 6: RC_{MDE} under different scales for the left hand (a) and right hands (b). The boxes show the data between the 25th and 75th percentiles, and the middle line inside each box is the median MDE value at a specified scale.

Table 5: Statistical indicators of RC_{MDE}.

τ	Left hand			Right hand		
	Male	Female	P value	Male	Female	P value
1	0.4488 ± 0.0143	0.4510 ± 0.0133	0.5468	0.4505 ± 0.0218	0.4600 ± 0.0169	0.2773
2	0.5116 ± 0.0187	0.5136 ± 0.0167	0.6868	0.5164 ± 0.0278	0.5268 ± 0.0218	0.3324
3	0.5529 ± 0.0219	0.5539 ± 0.0193	0.8568	0.5580 ± 0.0324	0.5692 ± 0.0245	0.3585
4	0.5818 ± 0.0229	0.5837 ± 0.0210	0.7544	0.5880 ± 0.0350	0.5984 ± 0.0254	0.3162
5	0.6072 ± 0.0238	0.6068 ± 0.0221	0.9477	0.6133 ± 0.0382	0.6223 ± 0.0271	0.3243
6	0.6276 ± 0.0251	0.6264 ± 0.0236	0.8633	0.6333 ± 0.0412	0.6430 ± 0.0289	0.3204
7	0.6429 ± 0.0248	0.6424 ± 0.0247	0.9473	0.6498 ± 0.0431	0.6600 ± 0.0299	0.3193
8	0.6553 ± 0.0255	0.6557 ± 0.0259	0.9511	0.6640 ± 0.0456	0.6740 ± 0.0323	0.3572
9	0.6648 ± 0.0267	0.6659 ± 0.0260	0.8781	0.6741 ± 0.0476	0.6847 ± 0.0341	0.3488
10	0.6724 ± 0.0279	0.6743 ± 0.0275	0.8065	0.6812 ± 0.0530	0.6928 ± 0.0368	0.3536

the dependence on gender for some indices is proven in young subjects (25 – 34 years). However, the gender influences are considerably weaker than the age influences.

Therefore, from the above ECG signal analysis, we can see that the ECG signal is able to identify the gender on some complexity measures. Although similar to it, the results in this paper show that the pulse signal has no ability to distinguish between genders. The reason for this inconsistency may be explained as follows:

The pulse is measured at the wrist instead of the vicinity of the heart. During the blood transfer from the heart to the wrist, many factors, such as the thickness and elasticity of vessel walls, the blood composition, and the skin conditions, will ultimately influence the fluctuations. Consequently, Kaplan [54] conjectures that the interaction of many cardiovascular feedback loops, as well as random environmental influences, may eliminate detectable traces of nonlinearity, even though the time series is caused by nonlinear mechanisms.

On the other hand, it is inconclusive whether the normal pulse signal is nonlinear in terms of signal characteristics. With the Delay Vector Variance method [55], Yan et al. [56] examine the nonlinearity of the wrist pulse signals between the healthy group and the coronary heart disease group. Their findings report that in the coronary heart disease group, most of the wrist pulse signals (80% of 59) are nonlinear, while the wrist pulse signals of the healthy group (76% of 29) are commonly linear. But the mechanism of difference of wrist pulse's nonlinearity between two groups remains unclear.

As mentioned in a previous study [20], the gender differences are not strong for the short-term ECG signal. In our study, the recording sample is about 2000, which may reinforce our primary findings. Due to the short data length, the nonlinear difference may be ambiguous.

It should be noted that the entropy is only one measure of complexity; no significant gender difference in entropy measure does not mean that there is no difference in complexity. As pointed out in [54], there is the possibility of gender differences in terms of complexity between healthy

male and female subjects in some other nonlinear dynamics, which is just not directly supported by the used data and employed statistics. Therefore, to fully determine gender differences for pulse signals, a more thorough complexity analysis is required in the future.

5.2. Comparison with Gender Difference in Existing Pulse Signals Analysis. Compared with ECG signals, there are relatively few studies on gender differences of wrist pulse signals in healthy individuals. The research focus of existing work is the optimization of time-domain waveform parameters or frequency-domain spectrum parameters, not involved with complexity statistics.

Some findings have suggested the gender difference in healthy people is present in arterial pulses. For example, King et al. [57] examine the radial pulse characteristics for a sample of healthy subjects. The characteristics used include presence at the three TCM locations (Cun, Guan, Chi), depth (superficial, middle, deep), relative force, and width, most of which are qualitative measures. Although in terms of the overall pulse force, male pulses are more forceful than female pulses, the study provides limited support for TCM assumptions concerning gender-based differences in these pulse metrics. Yim et al. [22] investigate pulse differences according to gender and measuring positions in healthy individuals in a more objective manner. In this work, several time-domain parameters of the pulse signal are compared to confirm that the radial pulse differs significantly with respect to gender and measuring positions. Subsequently, Lee et al. [23] demonstrate highly significant differences in gender by performing the analysis of wrist pulse waves of healthy Korean adults at the three positions in time and frequency domains. They infer that the reason may be that men tend to have larger vascular diameters and higher blood velocities, which increase blood flow and blood pressure in the wrist artery.

TCM practitioners claim that there exist gender differences between men and women, and these previous studies have somewhat confirmed that. Yet in our study, there are no significant gender differences in nonlinear entropy measures. As stated before, no difference between the entropy does not mean that there is no difference between genders. Moreover, early studies have also shown different and special changes for specific diseases in the pulse spectrum analysis [14, 15]. Instead of entropy computation in time-domain, entropy analysis of frequency spectrum may reveal some new different results, which is worthwhile to study further.

5.3. Limitations and Future Studies. Undoubtedly, this paper is just a preliminary exploration to use wrist pulse signals to identify the gender of healthy people, and there are several limitations. First, the participants in this study are aged in their 20s, requiring more middle-aged healthy subjects. Also, the sample size of participants is relatively small (about 200). Second, the pulse signal itself exhibits intersubject variability. According to TCM theory, such variability has something to do with the collection time and seasonal changes [2]. In other words, it varies every day even for the same person according to his (or her) physical condition. In addition, we do not perform the pulse acquisition at multiple different locations, while existing studies have shown that the gender difference of different measures is related to collection location [58]. Third, the present study mainly assesses the entropy measure. As stated in [59], one single parameter cannot sufficiently describe complex physiological systems. Perhaps other complexity measures such as correlation dimension and detrended fluctuation analysis can provide more complementary information. Finally, some unmeasured variables, such as individual levels of fitness, may also have an impact on the gender differences we observed in wrist pulse signals. Additionally, the associated embedding dimension or tolerance parameters in entropy computation may be relevant.

In short, a further prospective study with a larger sample size, more multiple collection positions, and more broad healthy adults and complexity measures is needed to reinforce our conclusions described above, which is also our further study.

6. Conclusions

Pulse signal analysis is crucial to the objectification of TCM pulse diagnosis. The pulse signal and the ECG signal are similar and very important physiological signals. Regarding entropy measures, ECG signals have been confirmed to have gender differences for normal people, while corresponding characteristics of the pulse signal have not been studied. In this paper, a nonlinear analysis to investigate the gender difference within wrist pulse signals of healthy people for the first time is presented. We employ four kinds of entropy measures in the framework of refined composite multiscale to evaluate the wrist pulse signal. Extensive experiments and analyses are conducted to study the potential gender difference.

The results show that the wrist pulse signal is not as effective as the ECG signal to exhibit statistically significant gender differences for healthy people. It is however better to use the dispersion entropy measure for subsequent intelligent diagnosis since we experimentally demonstrate that it is the most robust and reliable entropy measure for the wrist pulse signal. Moreover, we believe that our findings will contribute to the modernization of pulse diagnosis and facilitate the development of pulse diagnosis systems.

Future research will investigate more influence factors of entropy measures that may be related to the gender difference. In addition, more extensive and comprehensive experiments are further required for a thorough evaluation of the wrist pulse signals.

Data Availability

The data used to support the findings of this study are available from the corresponding author upon request.

Conflicts of Interest

The authors declare that there are no conflicts of interest regarding the publication of this paper.

Acknowledgments

This work was supported by the National Key R&D Program of China (2020YFC2006100), the National Natural Science Foundation of China (Grant no. 11804309) and Natural Science Foundation (Grant no. L192005), and the Key Project at the Central Government Level: The Ability Establishment of Sustainable Use for Valuable Chinese Medicine Resources (Grant no. 2060302). The authors also would like to appreciate all volunteers for providing invaluable pulse waveform data and doctors providing help in pulse signal collection.

References

[1] S. Li, *Pulse Diagnosis*, Paradigm Publications, Boulder, Colorado, 1985.

[2] Z. Fei, *Contemporary Sphygmology in Traditional Chinese Medicine*, pp. 205–227, People's Medical Publishing House, Beijing, China, 2003.

[3] L. Xu, K. Wang, D. Zhang, Y. Li, Z. Wan, and J. Wang, "Objectifying researches on traditional Chinese pulse diagnosis," *Informatica Medica Slovenica*, vol. 8, no. 1, pp. 56–63, 2003.

[4] D. Zhang, W. Zuo, and P. Wang, *Computational Pulse Signal Analysis*, Springer, Beijing, China, 2018.

[5] C. Zhao, G.-Z. Li, C. Wang, and J. Niu, "Advances in patient classification for traditional Chinese medicine: a machine learning perspective," *Evidence-Based Complementary and Alternative Medicine*, vol. 2015, Article ID 376716, 18 pages, 2015.

[6] S. Lukman, Y. He, and S.-C. Hui, "Computational methods for traditional Chinese medicine: a survey," *Computer Methods and Programs in Biomedicine*, vol. 88, no. 3, pp. 283–294, 2007.

[7] H. X. Yan, Y. Q. Wang, R. Guo et al., "Feature extraction and recognition for pulse waveform in traditional Chinese medicine based on hemodynamics principle," in *Proceedings of the IEEE ICCA 2010*, pp. 972–976, Xiamen, China, Jun 2010.

[8] L. Xu, K. Wang, and D. Zhang, "Modern researches on pulse waveform of tcpd," in *Proceedings of the IEEE 2002 International Conference on Communications, Circuits and Systems and West Sino Expositions*, pp. 1073–1077, Chengdu, China, June 2002.

[9] L. Xu, M. Q.-H. Meng, K. Wang, W. Lu, and N. Li, "Pulse images recognition using fuzzy neural network," *Expert Systems with Applications*, vol. 36, no. 2, pp. 3805–3811, 2009.

[10] L. Lei Liu, W. Wangmeng Zuo, D. Zhang, N. Naimin Li, and H. Hongzhi Zhang, "Combination of heterogeneous features for wrist pulse blood flow signal diagnosis via multiple kernel learning," *IEEE Transactions on Information Technology in Biomedicine*, vol. 16, no. 4, pp. 598–606, 2012.

[11] R. Guo, Y. Wang, H. Yan et al., "Analysis and recognition of traditional Chinese medicine pulse based on the hilbert-huang transform and random forest in patients with coronary heart disease," *Evidence-based Complementary and Alternative Medicine*, vol. 2015, Article ID 895749, 8 pages, 2015.

[12] D. Wang, D. Zhang, and G. Lu, "Generalized feature extraction for wrist pulse analysis: from 1-d time series to 2-d matrix," *IEEE Journal of Biomedical and Health Informatics*, vol. 21, no. 4, pp. 978–985, 2017.

[13] Z. Jiang, C. Guo, J. Zang, G. Lu, and D. Zhang, "Features fusion of multichannel wrist pulse signal based on kl-mgdcca and decision level combination," *Biomedical Signal Processing and Control*, vol. 57, p. 101751, 2020.

[14] C. T. Lee and L. Y. Wei, "Spectrum analysis of human pulse," *IEEE Transactions on Biomedical Engineering*, vol. BME-30, no. 6, pp. 348–352, 1983.

[15] L. Y. Wei and P. Chow, "Frequency distribution of human pulse spectra," *IEEE Transactions on Biomedical Engineering*, vol. BME-32, no. 3, pp. 245-246, 1985.

[16] Y. Shiogai, A. Stefanovska, and P. V. McClintock, "Nonlinear dynamics of cardiovascular ageing," *Physics Reports*, vol. 488, no. 2-3, pp. 51–110, 2010.

[17] S. M. Ryan, A. L. Goldberger, S. M. Pincus, J. Mietus, and L. A. Lipsitz, "Gender- and age-related differences in heart rate dynamics: are women more complex than men?" *Journal of the American College of Cardiology*, vol. 24, no. 7, pp. 1700–1707, 1994.

[18] F. Beckers, B. Verheyden, and A. E. Aubert, "Aging and nonlinear heart rate control in a healthy population," *American Journal of Physiology-Heart and Circulatory Physiology*, vol. 290, no. 6, pp. H2560–H2570, 2006.

[19] S. Vandeput, B. Verheyden, A. E. Aubert, and S. Van Huffel, "Nonlinear heart rate dynamics: circadian profile and influence of age and gender," *Medical Engineering & Physics*, vol. 34, no. 1, pp. 108–117, 2012.

[20] A. Voss, R. Schroeder, A. Heitmann, A. Peters, and S. Perz, "Short-term heart rate variability-influence of gender and age in healthy subjects," *PLoS One*, vol. 10, no. 3, p. e0118308, 2015.

[21] R. Barbieri, E. P. Scilingo, and G. Valenza, *Complexity and Nonlinearity in Cardiovascular Signals*, Springer, Berlin, Germany, 2017.

[22] Y.-K. Yim, C. Lee, H.-J. Lee, and K.-S. Park, "Gender and measuring-position differences in the radial pulse of healthy individuals," *Journal of acupuncture and meridian studies*, vol. 7, no. 6, pp. 324–330, 2014.

[23] B. J. Lee, Y. J. Jeon, J.-H. Bae, M. H. Yim, and J. Y. Kim, "Gender differences in arterial pulse wave and anatomical properties in healthy Korean adults," *European Journal of Integrative Medicine*, vol. 25, pp. 41–48, 2019.

[24] K. Wang, L. Xu, Z. Li, D. Zhang, N. Li, and S. Wang, "Approximate entropy based pulse variability analysis," in *Proceedings of the 16th IEEE Symposium Computer-Based Medical Systems*, pp. 236–241, New York, NY, USA, June 2003.

[25] L. Xu, M. Q.-H. Meng, X. Qi, and K. Wang, "Morphology variability analysis of wrist pulse waveform for assessment of arteriosclerosis status," *Journal of Medical Systems*, vol. 34, no. 3, pp. 331–339, 2010.

[26] L. Liu, N. Li, W. Zuo, D. Zhang, and H. Zhang, "Multiscale sample entropy analysis of wrist pulse blood flow signal for disease diagnosis," in *Proceedings of the International Conference on Intelligent Science and Intelligent Data Engineering*, pp. 475–482, Beijing, China, August 2013.

[27] Z. Huo, M. Martínez-García, Y. Zhang, R. Yan, and L. Shu, "Entropy measures in machine fault diagnosis: insights and applications," *IEEE Transactions on Instrumentation and Measurement*, vol. 69, no. 6, pp. 2607–2620, 2020.

[28] J. Gao, J. Hu, and W.-W. Tung, "Entropy measures for biological signal analyses," *Nonlinear Dynamics*, vol. 68, no. 3, pp. 431–444, 2012.

[29] L. C. Amarantidis and D. Abásolo, "Interpretation of entropy algorithms in the context of biomedical signal analysis and their application to eeg analysis in epilepsy," *Entropy*, vol. 21, no. 9, p. 840, 2019.

[30] C. Bandt and B. Pompe, "Permutation entropy: a natural complexity measure for time series," *Physical Review Letters*, vol. 88, no. 17, p. 174102, 2002.

[31] M. Rostaghi and H. Azami, "Dispersion entropy: a measure for time-series analysis," *IEEE Signal Processing Letters*, vol. 23, no. 5, pp. 610–614, 2016.

[32] S. M. Pincus, "Approximate entropy as a measure of system complexity," *Proceedings of the National Academy of Sciences*, vol. 88, no. 6, pp. 2297–2301, 1991.

[33] J. S. Richman and J. R. Moorman, "Physiological time-series analysis using approximate entropy and sample entropy," *American Journal of Physiology - Heart and Circulatory Physiology*, vol. 278, no. 6, pp. H2039–H2049, 2000.

[34] H. M. Al-Angari and A. V. Sahakian, "Use of sample entropy approach to study heart rate variability in obstructive sleep apnea syndrome," *IEEE Transactions on Biomedical Engineering*, vol. 54, no. 10, pp. 1900–1904, 2007.

[35] R. Alcaraz and J. J. Rieta, "A review on sample entropy applications for the non-invasive analysis of atrial fibrillation electrocardiograms," *Biomedical Signal Processing and Control*, vol. 5, no. 1, pp. 1–14, 2010.

[36] W. Chen, Z. Wang, H. Xie, and W. Yu, "Characterization of surface emg signal based on fuzzy entropy," *IEEE Transactions on Neural Systems and Rehabilitation Engineering*, vol. 15, no. 2, pp. 266–272, 2007.

[37] W. Chen, J. Zhuang, W. Yu, and Z. Wang, "Measuring complexity using fuzzyen, apen, and sampen," *Medical Engineering & Physics*, vol. 31, no. 1, pp. 61–68, 2009.

[38] M. Costa, A. L. Goldberger, and C. K. Peng, "Multiscale entropy analysis of complex physiologic time series," *Physical Review Letters*, vol. 89, no. 6, p. 068102, 2002.

[39] L. E. V. Silva, B. C. T. Cabella, U. P. D. C. Neves, and L. O. Murta Junior, "Multiscale entropy-based methods for heart rate variability complexity analysis," *Physica A: Statistical Mechanics and its Applications*, vol. 422, pp. 143–152, 2015.

[40] T. Liu, W. Yao, M. Wu, Z. Shi, J. Wang, and X. Ning, "Multiscale permutation entropy analysis of electrocardiogram," *Physica A: Statistical Mechanics and its Applications*, vol. 471, pp. 492–498, 2017.

[41] Y. Liu, Y. Lin, J. Wang, and P. Shang, "Refined generalized multiscale entropy analysis for physiological signals," *Physica A: Statistical Mechanics and its Applications*, vol. 490, pp. 975–985, 2018.

[42] H. Hadoush, M. Alafeef, and E. Abdulhay, "Brain complexity in children with mild and severe autism spectrum disorders: analysis of multiscale entropy in eeg," *Brain Topography*, vol. 32, no. 5, pp. 914–921, 2019.

[43] S.-D. Wu, C.-W. Wu, S.-G. Lin, K.-Y. Lee, and C.-K. Peng, "Analysis of complex time series using refined composite multiscale entropy," *Physics Letters A*, vol. 378, no. 20, pp. 1369–1374, 2014.

[44] A. Humeau-Heurtier, "Multivariate refined composite multiscale entropy analysis," *Physics Letters A*, vol. 380, no. 16, pp. 1426–1431, 2016.

[45] A. Humeau-Heurtier, C.-W. Wu, and S.-D. Wu, "Refined composite multiscale permutation entropy to overcome multiscale permutation entropy length dependence," *IEEE Signal Processing Letters*, vol. 22, no. 12, pp. 2364–2367, 2015.

[46] H. Azami, M. Rostaghi, D. Abásolo, and J. Escudero, "Refined composite multiscale dispersion entropy and its application to biomedical signals," *IEEE Transactions on Biomedical Engineering*, vol. 64, no. 12, pp. 2872–2879, 2017.

[47] P. Peng Wang, W. Wangmeng Zuo, and D. Zhang, "A compound pressure signal acquisition system for multichannel wrist pulse signal analysis," *IEEE Transactions on Instrumentation and Measurement*, vol. 63, no. 6, pp. 1556–1565, 2014.

[48] D. Wang, D. Zhang, and G. Lu, "A robust signal preprocessing framework for wrist pulse analysis," *Biomedical Signal Processing and Control*, vol. 23, pp. 62–75, 2016.

[49] L. Xu, D. Zhang, and K. Wang, "Wavelet-based cascaded adaptive filter for removing baseline drift in pulse waveforms," *IEEE*, vol. 52, no. 11, pp. 1973–1975, 2005.

[50] B. Thakker and A. L. Vyas, "Suppressed dicrotic notch pulse classifier design," *International Journal of Machine Learning and Computing*, vol. 1, no. 2, pp. 148–153, 2011.

[51] S. M. Pincus and A. L. Goldberger, "Physiological time-series analysis: what does regularity quantify?" *American Journal of Physiology-Heart and Circulatory Physiology*, vol. 266, no. 4, pp. H1643–H1656, 1994.

[52] O. A. Rosso, H. A. Larrondo, M. T. Martin, A. Plastino, and M. A. Fuentes, "Distinguishing noise from chaos," *Physical Review Letters*, vol. 99, no. 15, p. 154102, 2007.

[53] A. Voss, R. Schroeder, C. Fischer, A. Heitmann, A. Peters, and S. Perz, "Influence of age and gender on complexity measures for short term heart rate variability analysis in healthy subjects," in *Proceedings of the 2013 35th Annual International Conference of the IEEE Engineering in Medicine and Biology Society (EMBC)*, pp. 5574–5577, Osaka, Japan, June 2013.

[54] D. T. Kaplan, "Nonlinearity and nonstationarity: the use of surrogate data in interpreting fluctuations in heart rate," in *Proceedings of the Third Annual Workshop on Computer Applications of Blood Pressure and Heart Rate Signals*, pp. 15–28, Florence, Italy, 1995.

[55] T. Gautama, D. P. Mandic, and M. M. Van Hulle, "The delay vector variance method for detecting determinism and nonlinearity in time series," *Physica D: Nonlinear Phenomena*, vol. 190, no. 3-4, pp. 167–176, 2004.

[56] J. Yan, Y. Wang, C. Xia, F. Li, and R. Guo, "Detecting nonlinearity in wrist pulse using delay vector variance method," in *Advances in Cognitive Neurodynamics ICCN 2007*Springer, Berlin, Germany, 2008.

[57] E. King, D. Cobbin, and D. Ryan, "The reliable measurement of radial pulse: gender differences in pulse profiles," *Acupuncture in Medicine*, vol. 20, no. 4, pp. 160–167, 2002.

[58] Y.-N. Tsai, Y.-H. Chang, Y.-C. Huang et al., "The use of time-domain analysis on the choice of measurement location for pulse diagnosis research," *Journal of the Chinese Medical Association*, vol. 82, no. 1, pp. 78–85, 2019.

[59] A. Voss, S. Schulz, R. Schroeder, M. Baumert, and P. Caminal, "Methods derived from nonlinear dynamics for analysing heart rate variability," *Philosophical Transactions of the Royal Society A: Mathematical, Physical & Engineering Sciences*, vol. 367, no. 1887, pp. 277–296, 2009.

Hindawi
Evidence-Based Complementary and Alternative Medicine
Volume 2022, Article ID 5103768, 8 pages
https://doi.org/10.1155/2022/5103768

Research Article

Effects of Chinese Medicine on the Survival of AIDS Patients Administered Second-Line ART in Rural Areas of China: A Retrospective Cohort Study Based on Real-World Data

Yantao Jin,[1,2] **Miao Zhang**,[3] **Yanmin Ma**,[4] **Feng Sang**,[2] **Pengyu Li**,[1] **Chunling Yang**,[3] **Dongli Wang**,[2] **Huijun Guo**,[1] **Zhibin Liu**,[1,3] **and Qianlei Xu**[2,3]

[1]*Department of Acquired Immune Deficiency Syndrome Treatment and Research Center, First Affiliated Hospital of Henan University of Chinese Medicine, Zhengzhou, China*
[2]*Henan Key Laboratory of Viral Diseases Prevention and Treatment of Chinese Medicine, Henan University of Chinese Medicine, Zhengzhou, China*
[3]*The First Clinical Medical School, Henan University of Chinese Medicine, Zhengzhou, China*
[4]*Center for AIDS/STD Control and Prevention, Center for Disease Control and Prevention of Henan Province, Zhengzhou, China*

Correspondence should be addressed to Zhibin Liu; drlzbcn@163.com and Qianlei Xu; xuqianlei666@126.com

Received 28 October 2021; Accepted 5 January 2022; Published 27 January 2022

Academic Editor: Xuezhong Zhou

Objectives. Chinese medicine (CM) improves the symptoms of patients with acquired immune deficiency syndrome (AIDS) and prolongs their survival. This real-world study aimed to evaluate the effects of CM on the survival of AIDS patients administered second-line antiretroviral therapy (ART). *Methods*. We conducted a retrospective cohort study of the medical records of patients with AIDS who switched to second-line ART between January 2009 and December 2014. Patients were divided into ART and CM + ART groups. Propensity score matching (PSM) was performed to correct for biases between groups. Kaplan–Meier analysis and the log-rank test were used to compare survival rates, and Cox regression models were employed to identify factors significantly associated with survival. *Results*. The study population ($n = 4180$) was comprised of the CM + ART group ($n = 855$) and the ART group ($n = 3325$). After 1 : 2 PSM, 855 patients in the CM + ART group and 1699 in the ART group were selected for analysis. Patients in the CM + ART group were followed for 4246.8 person-years, and the mortality rate was 2.12/100 person-years. Patients in the ART group were followed for 8381.2 person-years, and the mortality rate was 2.91/100 person-years. Cox regression model analysis revealed that patients in the CM + ART group survived significantly longer than those in the ART group (hazard ratio: 0.73 and 95% confidence interval: 0.57–0.93). Gender, age, symptoms, CD4 cell counts, and viral loads were independently associated with the survival of AIDS patients treated with second-line ART. *Conclusions*. CM significantly improved the survival rate of AIDS patients treated with second-line ART.

1. Introduction

The survival of patients with acquired immune deficiency syndrome (AIDS) improved after the introduction of antiretroviral therapy (ART) over 30 years ago. However, the global prevalence of AIDS (37.7 million cases in 2020) remains a serious threat to public health [1]. Although ART is a well-established and effective therapy for AIDS, the increasingly common problems of duration of ART, nonadherence, drug resistance, and treatment failure represent challenges to achieving better responses to treatment [2, 3]. In 1997, a second-line ART regimen, including one protease inhibitor (PI) and two nucleoside reverse transcriptase inhibitors, was recommended as the preferred treatment strategy for patients with AIDS [4].

An increasing number of patients with AIDS have been administered this second-line regimen with the expectation of a significant benefit. For example, a study on patients with AIDS in Asia found that 19% of patients were administered second-line ART [5]. However, some patients failed to

respond to second-line ART [6–9]. The WHO recently recommended third-line ART for patients with AIDS. Unfortunately, access to this treatment is restricted by its high cost and barriers to its implementation [3]. Thus, maximizing the efficacy and access to first- or second-line regimens is an emerging global priority. We believe that Chinese medicine (CM) may serve this purpose for the reasons outlined below.

CM has been used for thousands of years as an effective treatment for acute viral infections; recent examples are COVID-19, caused by SARS-CoV-2 [10], influenza caused by influenza A virus subtype H1N1 [11], as well as severe acute respiratory syndrome [12]. Moreover, CM plays an important role in the treatment of AIDS, particularly in China. Previous studies found that CM based on first-line ART could ameliorate symptoms and signs of AIDS [13], improve quality of life [14], increase CD4+ T cell counts [15], promote adaptive immunity, and prolong survival [16]. Increasing numbers of patients with AIDS in China are taking CM along with second-line ART, but its effects are unclear. Therefore, we conducted a retrospective cohort study using standard medical records to evaluate the effects of CM on the survival of AIDS patients administered second-line ART.

2. Methods

2.1. Study Setting. During the 1990s in Henan Province, which is located in the center of China, patients with AIDS were infected with commercially available blood as well as with illegally collected blood plasma [17]. From 2003, ART was administered to these patients in accordance with the guidelines of the National Free Antiretroviral Treatment Program (NFATP), and second-line ART, which comprises lamivudine (3TC) + tenofovir (TDF) + lopinavir/ritonavir (Lpv/r), was introduced in 2009 in Henan Province [18]. Since 2004, the State Administration of Traditional Chinese Medicine has sponsored a national CM–AIDS Treatment Trial Program (NCMATP) for patients with AIDS. All of the study patients voluntarily chose to participate in the NCMATP and provided signed informed consent. The patients in the NCMATP of Henan were given the patented Chinese drug yi ai kang (containing substances such as ginseng, Huangqi, Chaobaishu, Tuckahoe, Chinese angelica, Chuanxiong, Baishao, and Scutellariae) free of charge (five capsules three times a day) and were required to record medical information related to their AIDS condition on a monthly basis [19].

2.2. Study Design and Patient Population. We conducted a retrospective cohort study of the standard medical records of patients with AIDS who were administered second-line ART in rural areas of Henan Province, where such patients were enrolled in NCMATP before 2009. Patients who switched to second-line ART from January 2009 to December 2014, who were older than 18 years or younger than 65 years, were included. Individuals with incomplete baseline data were excluded from the study. The start of the analysis period was defined as the time patients switched to second-line ART. Survival was defined as time to death on December 30, 2019, or 6 years after treatment commenced. Patients' data were censored if their dates of death were not recorded, if they were lost to follow-up, if they withdrew from treatment with CM plus or ART, or if they were alive when the study was completed.

2.3. Data Collection and Patients' Characteristics. Patients' clinical and demographic information was acquired from the standard medical records of the NCMATP or NFATP, Henan. This information included age; gender; marital status; ethnicity; education; occupation; route of infection; year of confirmed human immunodeficiency virus (HIV) infection; dates when ART and second-line ART commenced; administration of CM; symptoms of AIDS such as skin lesion, thrush, oral hairy leukoplakia, persistent diarrhea (>1 month), constant fever (>38°C, >1 month), severe bacterial infections, pulmonary tuberculosis, chronic herpes simplex infection, herpes zoster; CD4 cell count; viral load (VL); date of death; and date censored. If patients had one type of symptom, this variable was recorded as "yes." CD4 cell counts and VLs were those recorded within 6 months from the commencement of second-line ART, and if no value was entered during this interval, the variable was defined as missing. Patients were divided into ART and CM + ART groups according to their enrollment in the NCMATP.

2.4. Ethics Approval. This study was approved by the institutional review board of the first hospital affiliated to Henan University of Traditional Chinese Medicine (2019HL-068). Individual informed consent was not obtained because this analysis used currently existing data collected during the course of routine treatment and the data were reported in aggregate without the use of individual identifying information.

2.5. Data Analysis. Demographic and clinical data before and after matching were compared between patients in the CM + ART and ART groups. Categorical variables are expressed as numbers with percentages and were compared using the Fisher exact or chi-square tests. The study of data resources from real-world data (RWD) is defined as a real-world study (RWS) [20]. Propensity score matching (PSM) is widely used to more effectively control for baseline imbalances among groups in RWS [21]. Propensity scores were generated using a multivariable logistic regression model with the group as the dependent variable. Baseline variables such as age, gender, marital status, education, route of infection, time on HIV positive, time on ART before second-line, symptoms, CD4 cell counts, and VL were independent variables. Matching of the CM + ART and ART groups in 1 : 2 ratios was performed using the nearest neighbor method with a fixed caliper width = 0.1. After matching, the standardized difference (SD) was used to assess the degree of balance among baseline variables. SD ≤ 0.1 indicates a high degree of balance [22].

The survival rates of patients in the CM + ART and ART groups were calculated using the Kaplan–Meier method and compared using the log-rank test. Univariate and multivariable Cox proportional hazards regression models of the matched data were performed to identify factors that influenced the survival of patients with AIDS. The results of the Cox proportional hazards regression model are presented as the hazard ratio (HR) and 95% confidence interval (CI).

The PSM method was performed using the "MatchIt" package, SD was calculated using the "stddiff" package, and the Cox proportional hazards regression model is included in the "Survival" package in R 3.6.2 software. Significant differences are defined as $P < 0.05$.

3. Results

3.1. Subjects. We included 4180 patients with AIDS treated with second-line ART in rural China from 2009 to 2014. Patients were allocated into the CM + ART ($n = 855$) and ART ($n = 3325$) groups. The results before and after performing 1 : 2 PSM of 855 patients in the CM + ART group and 1699 patients in the ART group are summarized in Table 1. There were significant differences ($P < 0.05$) in age, route of infection, time on ART before second-line, CD4 cell counts between the CM + ART and ART groups before matching, and there were no significant differences after PSM.

To further assess balance, we analyzed the histograms of the propensity score distribution and SD of variables in the two groups before and after PSM. Figure 1(a) presents a histogram showing the balanced distribution of propensity scores in the two groups according to PSM. Figure 1(b) presents a scatter diagram showing that the SD of all variables after PSM was <0.1.

3.2. Survival Analysis of Patients with AIDS Administered Second-Line ART. Among the 2544 patients with AIDS after PSM who were followed for 12,628 person-years, 334 died, and the mortality rate was 2.64/100 person-years. Among the 855 patients with AIDS in the CM + ART group who were followed for 4246.8 person-years, 90 (6.5%) died, and the mortality rate was 2.12/100 person-years. Among the 1699 AIDS patients in the ART group who were followed for 8381.2 person-years, 244 (6.5%) died, and the mortality rate was 2.91/100 person-years. The survival curves of the CM + ART and ART groups are shown in Figure 2. The HR for mortality of patients in the CM + ART group compared with those in the ART group was 0.73 (95% CI: 0.57–0.93).

3.3. Factors Associated with the Survival of Patients with AIDS Treated with Second-Line ART. CM, gender, age, symptoms, CD4 cell count, and VL were independently associated with mortality of patients with AIDS administered second-line ART. The results of the multivariable model showed that the HRs of patients aged 40 years to 50 years and 18 years to 40 years were 0.49 (95% CI: 0.39–0.61) and 0.28 (95% CI: 0.18–0.44), respectively, compared with patients aged 50 to 65 years. The HR of patients with <200 CD4 cells/μl was 2.06 (95% CI: 1.44–2.95). The details of the results of the analyses using the univariate and multivariable Cox proportional hazards models are presented in Figure 3.

4. Discussion

Here we evaluated the efficacy of CM administered to AIDS patients treated with second-line ART. For this purpose, we retrospectively analyzed standard medical records of the NCMATP or NFATP for Henan Province based on RWS. There are many advantages of a RWS, such as the validity of the data. However, intrinsic selection biases are associated with the data resource, which influenced the design of the present study. PSM was used to control for baseline imbalances among groups in the study. After we conducted PSM here, the selection biases were well controlled as indicated by SDs <0.1 for all variables.

We show here that the overall mortality rate of patients with AIDS administered second-line ART was 2.64/100 person-years, which is lower than that reported by most studies on the mortality rates of patients with AIDS after initial or no second-line administration of ART [17, 23, 24]. The data are as follows: 8.53 person-years in Guizhou [17], 5.1/100 person-years in Sichuan [23], and 3.9/100 person-years in Henan [24]. These data suggest that second-line ART is more effective for reducing mortality rates. Another study conducted in Africa and Asia in 2010 reported a mortality rate equal to 4.42/100 person-years after patients switched to second-line ART [25]. According to the Global HIV Statistics Fact Sheet published by the WHO, the mortality rate of AIDS patients sharply declined [1]. The differences among the results of these studies may be explained by differences in patients' characteristics, the numbers of patients, treatment strategies, length of study, and study date.

In the present study, the mortality rate of patients with AIDS in the CM + ART group was 2.12/100 person-years and the HR was 0.73, which is comparable with mortality data for the ART group (2.91/100 person-years). These results suggest that CM combined with second-line ART significantly lengthened the survival of patients with AIDS. The theory of CM states that the body is recognized and treated as an entire entity, and diseases are identified as evil spirits that enter the body and cause internal imbalances. The yi ai kang, which was used in the CM + ART group, was taken to invigorate the spleen and supplement qi, nourishing Yin and blood, dispelling wind and clearing heat as the treatment principle, and to achieve the effect of strengthening the root, that is, to increase the body's *positive qi* to improve immune function [26], enhance immune function, and reduce AIDS-associated symptoms [27].

Except for CM, we show here that gender, age, symptoms, CD4 cell count, and VL were significantly associated with the survival of patients with AIDS administered second-line ART. Male patients had a higher risk of death compared with female patients, which is consistent with many studies [17, 28, 29]. Older patients

Table 1: Comparisons of baseline data of the CM + ART and ART groups before and after PSM.

Variables	Before PSM			After PSM		
	ART ($n = 3,325$)	CM + ART ($n = 855$)	P value	ART ($n = 1,699$)	CM + ART ($n = 855$)	P value
Gender			0.476			0.945
Female	1545 (46.5%)	385 (45.0%)		930 (54.7%)	470 (55.0%)	
Male	1780 (53.5%)	470 (55.0%)		769 (45.3%)	385 (45.0%)	
Age (years)			0.002			0.936
18–40	591 (17.8%)	110 (12.9%)		210 (12.4%)	110 (12.9%)	
40–50	1547 (46.5%)	412 (48.2%)		823 (48.4%)	412 (48.2%)	
50–65	1187 (35.7%)	333 (38.9%)		666 (39.2%)	333 (38.9%)	
Marital status			0.430			0.930
Married	2728 (82.0%)	712 (83.3%)		1411 (83.0%)	712 (83.3%)	
Single/widow	597 (18.0%)	143 (16.7%)		288 (17.0%)	143 (16.7%)	
Ethnicity			0.774			0.740
Han	3311 (99.6%)	851 (99.5%)		1693 (99.6%)	851 (99.5%)	
Others	14 (0.42%)	4 (0.47%)		6 (0.35%)	4 (0.47%)	
Occupation			0.712			0.144
Farmer	3209 (96.5%)	828 (96.8%)		1663 (97.9%)	828 (96.8%)	
Others	116 (3.49%)	27 (3.16%)		36 (2.12%)	27 (3.16%)	
Educational status			0.112			0.539
≤6 years	1021 (30.7%)	238 (27.8%)		452 (26.6%)	238 (27.8%)	
>6 years	2304 (69.3%)	617 (72.2%)		1247 (73.4%)	617 (72.2%)	
Route of infection			<0.001			0.577
Others	719 (21.6%)	120 (14.0%)		1445 (85.1%)	735 (86.0%)	
Plasma	2606 (78.4%)	735 (86.0%)		254 (14.9%)	120 (14.0%)	
Time on HIV positive (years)			0.066			0.735
<3	683 (20.5%)	159 (18.6%)		82 (4.83%)	36 (4.21%)	
3–8	1013 (30.5%)	295 (34.5%)		888 (52.3%)	456 (53.3%)	
>8	1629 (49.0%)	401 (46.9%)		729 (42.9%)	363 (42.5%)	
Time on ART before second-line (years)			<0.001			0.974
<3	323 (9.71%)	36 (4.21%)		322 (19.0%)	159 (18.6%)	
3–6	1756 (52.8%)	456 (53.3%)		586 (34.5%)	295 (34.5%)	
>6	1246 (37.5%)	363 (42.5%)		791 (46.6%)	401 (46.9%)	
Symptoms			0.069			0.924
No	2083 (62.6%)	565 (66.1%)		1118 (65.8%)	565 (66.1%)	
Yes	1242 (37.4%)	290 (33.9%)		581 (34.2%)	290 (33.9%)	
CD4 cell count (cells/μl)			0.002			0.902
>500	719 (21.6%)	149 (17.4%)		315 (18.5%)	149 (17.4%)	
350–500	686 (20.6%)	162 (18.9%)		311 (18.3%)	162 (18.9%)	
200–350	973 (29.3%)	301 (35.2%)		588 (34.6%)	301 (35.2%)	
<200	947 (28.5%)	243 (28.4%)		485 (28.5%)	243 (28.4%)	
Viral load			0.833			0.678
<500	2069 (62.2%)	536 (62.7%)		1075 (63.3%)	536 (62.7%)	
500–10000	636 (19.1%)	156 (18.2%)		323 (19.0%)	156 (18.2%)	
>10000	620 (18.6%)	163 (19.1%)		301 (17.7%)	163 (19.1%)	

PSM, propensity score matching; HIV, human immunodeficiency virus; ART, antiretroviral therapy.

are at higher risk of death because of more comorbidity and may be significantly associated with the failure of second-line ART [30]. Lower CD4 cell counts or higher VLs upon the switch to second-line ART were independent risk factors for time to death, which is consistent with many studies. Patients with a lower CD4 cell count were found to be significantly associated with the failure of second-line ART and have a higher probability of developing different opportunistic infections [8], all of which are more apt to cause death.

The aims of this study were to evaluate the effects of CM and the role of the NCMAPT, specifically, on the survival of AIDS patients taking second-line ART. The curative effects of participation in the project reflect not only the effects of the ART or CM drugs, but likely include humanistic factors as well, such as the provision of more health care, which may have enhanced the positive results of the study. Although we used PSM to control for selection bias, a retrospective cohort study is intrinsically biased. Furthermore, specific important variables associated with mortality, such as adherence to ART, body mass index, anemia, hyperlipemia, and liver injury [31–33], were not recorded when patients switched to second-line ART.

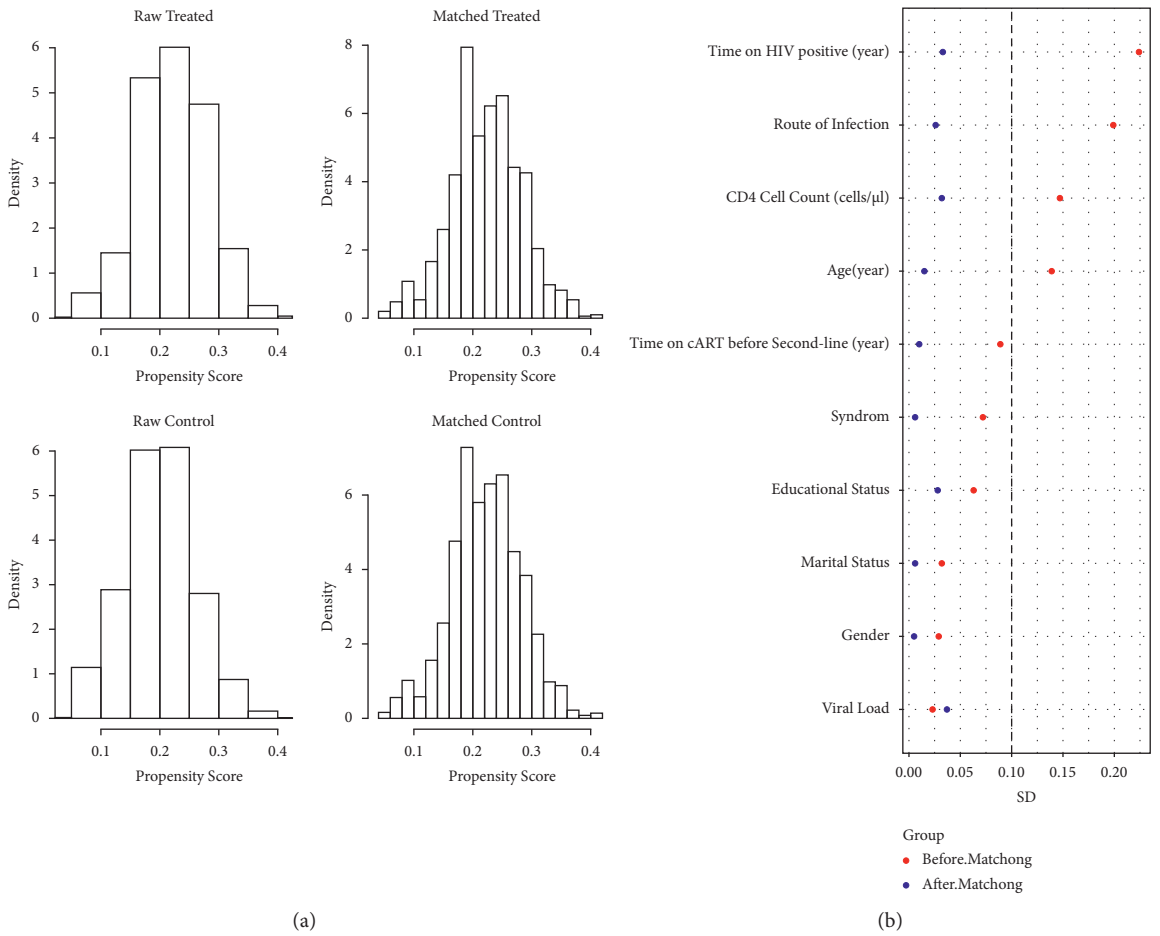

Figure 1: The balance between the CM + ART and ART groups after PSM. (a) Histograms of the propensity scores of the two groups before and after matching; (b) standardized difference (SD) of baseline characteristics of the two groups before and after matching.

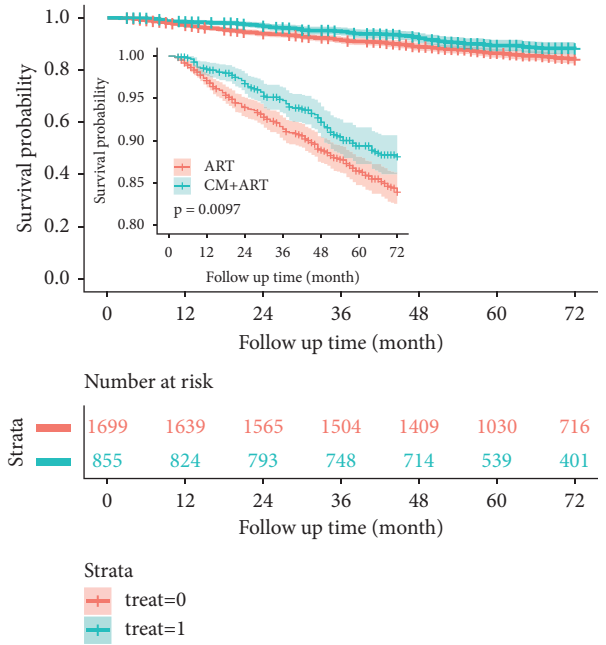

Figure 2: Kaplan–Meier survival analysis of patients with AIDS treated with second-line ART after PSM.

Variables	Mortality (/100 person-years)	Univariate Cox Analysis HR(95%CI)	Univariate Cox Analysis P Value	Multivariable Cox Analysis HR(95%CI)	Multivariable Cox Analysis P Value
Group					
ART	2.91	1		1	
CM+ART	2.12	0.73 [0.57-0.93]	0.01	0.73 [0.57-0.93]	0.01
Gender					
Female	2.11	1		1	
Male	3.31	1.57 [1.26-1.95]	<0.001	1.61 [1.29-2.01]	<0.001
Age (year)					
50-65	4.00	1		1	
40-50	1.99	0.50 [0.40-0.62]	<0.001	0.49 [0.39-0.61]	<0.001
18-40	1.24	0.31 [0.20-0.49]	<0.001	0.28 [0.18-0.44]	<0.001
Marital Status					
Married	2.51	1		1	
Sig/window	3.33	1.33 [1.02-1.73]	0.037	1.20 [0.92-1.56]	0.185
Educational Status					
≤6years	2.74	1		1	
>6years	2.61	0.95 [0.75-1.21]	0.687	1.01 [0.79-1.28]	0.965
Route of Infection					
Others	1.86	1		1	
Plasma	2.78	1.50 [1.05-2.13]	0.026	1.36 [0.92-2.00]	0.119
Time on HIV positive (year)					
<3	3.22	1		1	
3-8	2.70	0.84 [0.52-1.36]	0.476	0.86 [0.49-1.51]	0.602
>8	2.51	0.78 [0.47-1.27]	0.312	0.78 [0.43-1.41]	0.405
Time on cART before Second-line (year)					
<3	2.99	1		1	
3-8	2.40	0.80 [0.60-1.09]	0.154	0.88 [0.63-1.22]	0.436
>8	2.69	0.90 [0.68-1.19]	0.444	1.04 [0.75-1.45]	0.806
Symptoms					
No	2.30	1		1	
Yes	3.30	1.44 [1.16-1.79]	0.001	1.33 [1.07-1.67]	0.011
CD4 Cell Count (cell/μl)					
500+	1.83	1		1	
350-500	1.78	0.98 [0.64-1.50]	0.909	0.91 [0.59-1.4]	0.681
200-350	2.34	1.28 [0.90-1.83]	0.173	1.20 [0.84-1.73]	0.312
200-	4.15	2.28 [1.62-3.22]	<0.001	2.06 [1.44-2.95]	<0.001
Viral Load (copies/ml)					
<500	2.21	1		1	
500-10000	2.83	1.28 [0.97-1.70]	0.081	1.23 [0.92-1.63]	0.158
>10000	3.99	1.81 [1.40-2.33]	<0.001	1.45 [1.11-1.90]	0.006

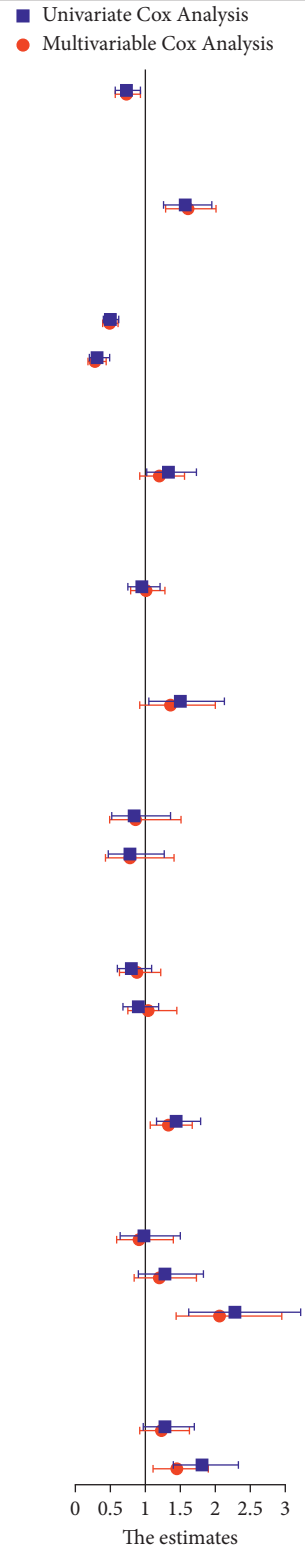

Figure 3: The Cox proportional hazards model analysis showing the significance of the associations of variables with mortality of patients with AIDS.

5. Conclusions

Our study indicates that patients who were with AIDS administered CM therapy and second-line ART experienced lower mortality compared with patients administered second-line ART alone. CM may therefore enhance the benefit of second-line ART. Prospective studies on the use of pure CM must be performed to confirm our results.

Data Availability

The data used to support the findings of this study are available from the corresponding author upon request.

Disclosure

The findings and conclusions of this article are only those of the authors and do not represent the views of the founders.

Conflicts of Interest

The authors declare that there are no conflicts of interest regarding the publication of this study.

Acknowledgments

The authors are grateful to the founders of our work. This work was supported by the National Natural Science Foundation (grant nos. 81803953, 81873289, and 81873187), China Postdoctoral Foundation (grant no. 2018T110729), Henan Province TCM Research Project (grant nos. 2016ZY2036 and 20-21ZYZD03), and National Special Science and Technology Program on Major Infectious Diseases (grant nos. 2017ZX10205502002 and 2017ZX10205502003).

References

[1] UNAIDS, "Global HIV statistics fact sheet 2021," 2021, https://www.unaids.org/sites/default/files/media_asset/UNAIDS_FactSheet_en.pdf.

[2] M. Alene, T. Awoke, M. K. Yenit, A. T. Tsegaye, L. Yismaw, and R. Yeshambel, "Second-line antiretroviral therapy regimen change among adults living with HIV in Amhara region: a multi-centered retrospective follow-up study," *BMC Research Notes*, vol. 12, no. 1, p. 407, 2019.

[3] S. K. Barik, A. K. Bansal, P. S. Mohanty et al., "Detection of drug resistance mutations in the reverse transcriptase gene of HIV-1-Infected north Indian population failing first-line antiretroviral therapy "A follow-up cohort study"," *AIDS Research and Human Retroviruses*, vol. 37, no. 10, pp. 796–805, 2021.

[4] WHO, *Consolidated Guidelines on the Use of Antiretroviral Drugs for Treating and Preventing HIV Infection: Recommendations for a Public Health Approach*, World Health Organization, Geneva, Switzerland, 2013.

[5] R. Martinez-Vega, N. L. De La Mata, N. Kumarasamy, P. S. Ly, K. Van Nguyen, and T. P. Merati, "Durability of antiretroviral therapy regimens and determinants for change in HIV-1-infected patients in the TREAT Asia HIV Observational Database (TAHOD-LITE)," *Antiviral Therapy*, vol. 23, no. 2, pp. 167–178, 2018.

[6] H. Musana, J. T. Ssensamba, M. Nakafeero, H. Mugerwa, F. M. Kiweewa, and D. Serwadda, "Predictors of failure on second-line antiretroviral therapy with protease inhibitor mutations in Uganda," *AIDS Research and Therapy*, vol. 18, no. 1, p. 17, 2021.

[7] D. Edessa, M. Sisay, and F. Asefa, "Second-line HIV treatment failure in sub-Saharan Africa: a systematic review and meta-analysis," *PLoS One*, vol. 14, no. 7, Article ID e0220159, 2019.

[8] J. Ross, A. Jiamsakul, N. Kumarasamy et al., "Virological failure and HIV drug resistance among adults living with HIV on second-line antiretroviral therapy in the Asia-Pacific," *HIV Medicine*, vol. 22, no. 3, pp. 201–211, 2020.

[9] A. Zenebe Haftu, A. A. Desta, N. M. Bezabih, A. Bayray Kahsay, K. M. Kidane, and Y. Zewdie, "Incidence and factors associated with treatment failure among HIV infected adolescent and adult patients on second-line antiretroviral therapy in public hospitals of Northern Ethiopia: multicenter retrospective study," *PLoS One*, vol. 15, no. 9, Article ID e0239191, 2020.

[10] D. Xing and Z. Liu, "Effectiveness and safety of traditional Chinese medicine in treating COVID-19:clinical evidence from China," *Aging and Disease*, vol. 12, no. 8, pp. 1850–1856, 2021.

[11] J.-H. Li, R.-Q. Wang, W.-J. Guo, and J.-S. Li, "Efficacy and safety of traditional Chinese medicine for the treatment of influenza A (H1N1): a meta-analysis," *Journal of the Chinese Medical Association*, vol. 79, no. 5, pp. 281–291, 2016.

[12] M.-M. Zhang, X. M. Liu, and L. He, "Effect of integrated traditional Chinese and Western medicine on SARS: a review of clinical evidence," *World Journal of Gastroenterology*, vol. 10, no. 23, pp. 3500–3505, 2004.

[13] J. Yuan, H. J. Guo, Y. T. Jin, Z. Q. Jiang, and Z. Li, ""Retrospective analysis of the effects of TCM on skin lesions of AIDS patients," *Zhong Guo pi fu Xing Bing Xue za zhi*, vol. 30, no. 2, pp. 193–195, 2016.

[14] Z. Liu, "Treating older patients with AIDS using traditional Chinese medicine combined with conventional western medicine in China," *Aging and Disease*, vol. 12, no. 8, pp. 1872–1878, 2021.

[15] D. L. Wang, S. N. Ma, Y. M. Ma et al., "Effect of traditional chinese medicine therapy on the trend in CD4+T-cell counts among patients with HIV/AIDS treated with antiretroviral therapy: a retrospective cohort study," *Evidence-Based Complementary and Alternative Medicine*, vol. 2021, Article ID 5576612, 8 pages, 2021.

[16] Y. Jin, H. Guo, X. Wang et al., "Traditional Chinese medicine could increase the survival of people living with HIV in rural Central China: a retrospective cohort study, 2004–2012," *The American Journal of Chinese Medicine*, vol. 42, no. 6, pp. 1333–1344, 2014.

[17] Z. H. Dou, R. Y. Chen, Z. Wang, G. P. Ji, G. P. Peng, and X. L. Qiao, "HIV-infected former plasma donors in rural Central China: from infection to survival outcomes, 1985–2008," *PLoS One*, vol. 5, no. 10, Article ID e13737, 2010.

[18] J. Chen, M. Zhang, M. Shang, W. Yang, Z. Wang, and H. Shang, "Research on the treatment effects and drug resistances of long-term second-line antiretroviral therapy among HIV-infected patients from Henan Province in China," *BMC Infectious Diseases*, vol. 18, no. 1, p. 571, 2018.

[19] L.-r. Xu, H.-j. Guo, Z.-b. Liu, Q. Li, J.-p. Yang, and Y. He, "Unified-planning, graded-administration, and centralized-controlling: a management modality for treating acquired immune deficiency syndrome with Chinese medicine in Henan Province of China," *Chinese Journal of Integrative Medicine*, vol. 21, no. 4, pp. 243–248, 2015.

[20] T. Stürmer, T. Wang, Y. M. Golightly, A. Keil, J. L. Lund, and M. Jonsson Funk, "Methodological considerations when analysing and interpreting real-world data," *Rheumatology*, vol. 59, no. 1, pp. 14–25, 2020.

[21] Y. K. Loke and K. Mattishent, "Propensity score methods in real-world epidemiology: a practical guide for first-time users," *Diabetes, Obesity and Metabolism*, vol. 22, no. S3, pp. 13–20, 2020.

[22] E. Buratto, W. Y. Shi, R. Wynne et al., "Improved survival after the ross procedure compared with mechanical aortic valve replacement," *Journal of the American College of Cardiology*, vol. 71, no. 12, pp. 1337–1344, 2018.

[23] L. Deng, Z. F. Liu, S. Z. Zhang, Z. H. Dou, Q. X. Wang, and Y. Ma, "Survival time and related influencing factors of AIDS patients in Liangshan prefecture, Sichuan province, during 2008–2013," *Zhonghua Liu Xing Bing Xue Za Zhi*, vol. 36, no. 6, pp. 569–575, 2015.

[24] Y. Liang, W. J. Yang, D. Y. Sun, N. Li, and Z. Wang, "Survival analysis on former plasma donors living with HIV/AIDS after initiation of antiretroviral therapy in Henan province, 2002–2017," *Zhonghua Liu Xing Bing Xue Za Zhi*, vol. 40, no. 6, pp. 638–642, 2019.

[25] M. Pujades-Rodríguez, S. Balkan, L. Arnould, M. A. Brinkhof, and A. Calmy, "Treatment failure and mortality factors in patients receiving second-line HIV therapy in resource-limited countries," *JAMA*, vol. 304, no. 3, pp. 303–312, 2010.

[26] L. R. Xu, F. Z. Li, Y. He, J. Z. Guo, and D. Wang, "Sixty-month clinical observation of HIV carriers/AIDS patients treated with Yiaikang capsule in terms of theirs CD+4T cell counts and viral load," *Zhong Guo Ai Zi Bing Xing Bing*, vol. 16, no. 3, pp. 231–233, 2010.

[27] W. Zou, J. Wang, and Y. Liu, "Effect of traditional Chinese medicine for treating human immunodeficiency virus infections and acquired immune deficiency syndrome: boosting immune and alleviating symptoms," *Chinese Journal of Integrative Medicine*, vol. 22, no. 1, pp. 3–8, 2016.

[28] M. Li, W. Tang, K. Bu et al., "Mortality among people living with HIV and AIDS in China: implications for enhancing linkage," *Scientific Reports*, vol. 6, no. 1, Article ID 28005, 2016.

[29] T. D. Mangal, M. V. Meireles, A. R. P. Pascom, R. de Almeida Coelho, A. S. Benzaken, and T. B. Hallett, "Determinants of survival of people living with HIV/AIDS on antiretroviral therapy in Brazil 2006–2015," *BMC Infectious Diseases*, vol. 19, no. 1, p. 206, 2019.

[30] M. Y. Ahn, A. Jiamsakul, S. Khusuwan, V. Khol, T. T. Pham, and R. Chaiwarith, "The influence of age-associated comorbidities on responses to combination antiretroviral therapy in older people living with HIV," *Journal of the International AIDS Society*, vol. 22, no. 2, Article ID e25228, 2019.

[31] W. Abuto, A. Abera, T. Gobena, T. Dingeta, and M. Markos, "Survival and predictors of mortality among HIV positive adult patients on highly active antiretroviral therapy in public hospitals of kambata tambaro zone, southern Ethiopia: a retrospective cohort study," *HIV*, vol. 13, pp. 271–281, 2021.

[32] F. Nigussie, A. Alamer, Z. Mengistu, and E. Tachbele, "Survival and predictors of mortality among adult HIV/AIDS patients initiating highly active antiretroviral therapy in debre-berhan referral hospital, amhara, Ethiopia: a retrospective study," *HIV*, vol. 12, pp. 757–768, 2020.

[33] M. Taborelli, B. Suligoi, F. Toffolutti, L. Frova, E. Grande, and F. Grippo, "Excess liver-related mortality among people with AIDS compared to the general population: an Italian nationwide cohort study using multiple causes of death," *HIV Medicine*, vol. 21, no. 10, pp. 642–649, 2020.

Hindawi
Evidence-Based Complementary and Alternative Medicine
Volume 2022, Article ID 8285111, 12 pages
https://doi.org/10.1155/2022/8285111

Research Article

Predicting Coupled Herbs for the Treatment of Hypertension Complicated with Coronary Heart Disease in Real-World Data Based on a Complex Network and Machine Learning

Jia-Ming Huan,[1] **Yun-Lun Li**,[2] **Xin Zhang**,[3] **Jian-Liang Wei**,[3] **Wei Peng**,[3] **Yi-Min Wang**,[2] **Xiao-Yi Su**,[2] **Yi-Fei Wang**,[3] **and Wen-Ge Su**[3]

[1]*School of Traditional Chinese Medicine, Shandong University of Traditional Chinese Medicine, Jinan 250014, China*
[2]*First School of Clinical Medicine, Shandong University of Traditional Chinese Medicine, Jinan 250014, China*
[3]*The Affiliated Hospital of Shandong University of Traditional Chinese Medicine, Jinan 250014, China*

Correspondence should be addressed to Yi-Fei Wang; 15853150460@163.com and Wen-Ge Su; 71000768@sdutcm.edu.cn

Received 16 October 2021; Revised 20 November 2021; Accepted 5 January 2022; Published 22 January 2022

Academic Editor: Xuezhong Zhou

Hypertension and coronary heart disease are the most common cardiovascular diseases, and traditional Chinese medicine is applied as an auxiliary treatment for common cardiovascular diseases. This study is based on 3 years of electronic medical record data from the Affiliated Hospital of Shandong University of Traditional Chinese Medicine. A complex network and machine learning algorithm were used to establish a screening model of coupled herbs for the treatment of hypertension complicated with coronary heart disease. A total of 5688 electronic medical records were collected to establish the prescription network and symptom database. The hierarchical network extraction algorithm was used to obtain core herbs. Biological features of herbs were collected from public databases. At the same time, five supervised machine learning models were established based on the biological features of the coupled herbs. Finally, the K-nearest neighbor model was established as a screening model with an AUROC of 91.0%. Seventy coupled herbs for adjuvant treatment of hypertension complicated with coronary heart disease were obtained. It was found that the coupled herbs achieved the purpose of adjuvant therapy mainly by interfering with cytokines and regulating inflammatory and metabolic pathways. These results show that this model can integrate the molecular biological characteristics of herbs, preliminarily screen combinations of herbs, and provide ideas for explaining the value in clinical applications.

1. Introduction

Every year, 10.4 million people die of complications of hypertension worldwide [1]. Organ damage caused by hypertension and cardiovascular disease (CVD) are currently the main causes of death [2]. Due to the abnormal increase in arterial pressure, the coronary artery is more likely to experience increased local tensile stress, causing endothelial injury, the accumulation of lipid particles, induction of inflammatory reactions, and acceleration of the growth of plaques [3]. More than 50% of hypertension sufferers have multiple cardiovascular risk factors, and 25%–30% of coronary heart disease (CHD) patients have hypertension [4–6].

Traditional Chinese medicine (TCM) is recommended as a complementary and alternative therapy in the treatment of hypertension and CHD in China. An existing systematic review shows that TCM herbs can improve the vascular endothelial function of patients with hypertension, inhibit inflammatory reactions, regulate blood lipids, and improve mood. Adjuvant TCM therapy more easily achieves the targeted blood pressure and improves the comfort of patients, protecting target organs and reducing cardiovascular events [7–9].

In the theory of TCM, herbs are combined to form a prescription according to the principle of "Jun-Chen-Zuo-Shi." Among them, the herbs of "Jun" that play a core role

are often applied as drug combinations, usually no more than three herbs for the core disease. On the other hand, there are obvious individual differences in concurrent diseases. TCM theory emphasizes that medication for individual patients should have suitable herb pairing rules. But it is difficult to reflect its curative effect by relying on traditional randomized controlled trials (RCTs). To fully reflect the disease characteristics of the individual and groups of patients, it is necessary to analyze them on the basis of real-world data (RWD) [10]. The traditional summary of drug compatibility is often based on the physician's long-term diagnosis and treatment experience, and the screening period takes too long to apply to rapidly changing disease spectrum. Through the algorithm analysis of RWD, we can quickly find the drug compatibility information hidden in the effective prescriptions, carry out bioinformatics analysis to achieve preliminary screening, and provide ideas for further experimental verification and clinical applications to accelerate and summarize the application rules of herbs.

Therefore, we developed a mining method based on RWD to explore effective coupled herbs for the treatment of hypertension complicated with CHD by combining their symptom information and target information. Existing network pharmacology and bioinformatics techniques have been widely used to discover the core targets of herbs, and the understanding of multiple targets with TCM therapy has become increasingly profound [11, 12]. However, most of the existing studies are based on the relationship between herbs, compounds, targets, and diseases. Previous studies [13] used the Dijkstra algorithm to integrate the symptom information emphasized by TCM into the herb information network. However, it is still unable to fully evaluate the closeness of herb combinations and complicated diseases, including the target similarity of different herbs and their contribution to the curative effect.

Supervised machine learning can aggregate a variety of herb feature information to generate a model, matching the input features of the herbs with the expected output to form a learning function and to complete the classifier after adjusting the parameters by cross-validation. Commonly used models include K-nearest neighbor (KNN), support vector machine (SVM), gradient boosting decision tree (GBDT), Bayesian network (BN), and logistic regression (LR). KNN is more sensitive to the local information in the feature space of the input herbs, while SVM and others reflect its global characteristics.

In this study, we established a prescription database and symptom database of patients with hypertension complicated with CHD. First, we used the hierarchical network extraction algorithm to extract the main herbs and symptoms from the database, collected biological information, established a biological network, including herbal compounds, targets, and related disease symptom information, and then used supervised machine learning models compared with the classical Apriori algorithm. The best model was used to evaluate the pertinence of each coupled herb in the treatment of hypertension complicated with CHD.

2. Materials and Methods

2.1. Data Preparation. In this study, 5688 electronic medical records (EMRs) of hypertension complicated with CHD collected from the Affiliated Hospital of Shandong University of Traditional Chinese Medicine (between July 1, 2014, and May 31, 2017) were used to extract and standardize the symptoms in the prescription and medical history of TCM [14], and the prescription database and symptom database were established. After that, we took the herbs in the prescription database as the node and the frequency of the two herbs as the weight. The hierarchical network extraction algorithm uses Liquorice software [15] to obtain the core herbs of the prescription network based on the degree coefficient prescription = 1.9.

2.1.1. Identifying Compounds and Targets of Core Herbs. We identified compounds and targets of core herbs from online public databases: Traditional Chinese Medicine Systems Pharmacology Database and Analysis Platform (TCMSP) [16], SymMap [17], and The Encyclopedia of Traditional Chinese Medicine (ETCM) [18], and published biomedical literature in the PubMed and CNKI databases. The names of the compounds were merged after being unified by PubChem and UniProt. The target of the core herbs was imported into the STRING database [19], and a protein–protein interaction network (PPIN) with a confidence ≥0.9 of *Homo sapiens* was established.

2.1.2. Identifying the TCM Symptoms of Core Herbs. The SymMap database contains TCM symptoms corresponding to herbs and their compounds, and the TCM symptoms of the core herbs can be obtained from the SymMap database and compared with the symptom database in EMRs to screen and determine the symptoms of hypertension complicated with CHD that can be effectively treated by each herb.

2.1.3. Collecting the Related Genes of Hypertension and CHD. The expression data of hypertension and CHD were retrieved from MalaCards [20] and the NCBI GEO database. The GSE76845 dataset contains 5 hypertension patient samples and 5 healthy control samples. The GSE71226 dataset contains 3 coronary heart disease patient samples and 3 healthy control samples. Then, the differentially expressed genes with $Q < 0.05$ and adj. $P < 0.05$ were analyzed by the GEO2R tool.

2.2. Evaluating the Features of the Coupled Herbs. The coupling of herbs can increase the pertinence of disease treatment. In this study, the core herbs coupled with each other. The main clinical and biological features of the herbs were quantified to evaluate the action characteristics of the coupled herbs.

2.2.1. Frequency Assessment of the Coupled Herbs. To evaluate the correlation of the two matched herbs in the prescription database, we established the frequency matrix of the herbs in the prescriptions. The Manhattan distance [21] between two herbs was calculated to evaluate their coupling characteristics in the prescription.

2.2.2. Symptom Similarity Assessment. The Jaccard similarity coefficient is used to compare the similarity between the sample sets. We obtained the symptom set of hypertension complicated with CHD and the herbal regulation symptom sets by screening the information of the RWD symptom database and the SymMap database. The Jaccard similarity coefficient was used to compare the similarity between the sample sets. We obtained the TCM symptom information of compound-regulated hypertension complicated with CHD by screening the information of the EMRs symptom database and the SymMap database, which was used to calculate the Jaccard similarity coefficient to evaluate the closeness of the herb-related symptoms to the disease-related symptoms.

2.2.3. Bioavailability Assessment. Oral bioavailability (OB) represents the percentage of oral doses reaching the systemic circulation, and high OB is usually a key indicator for identifying bioactive molecules as having therapeutic properties. In this study, the OB values of the herbal compounds obtained from the SymMap database were added to evaluate the bioavailability of the coupled herb.

2.2.4. Herb Target Identification and Functional Enrichment Analysis. A full understanding of human biological function cannot be realized by individual genes, only by the ubiquitous interaction between different genes. Therefore, the random walk with restart (RWR) algorithm was used in PPIN to evaluate the connection degree of herbal targets to disease-related genes. The disease-related genes in PPIN were used as seed node sets, and the restart probability was 0.75 [22]. The stable probability of diffusion to each herbal target was obtained by the RWR operation, which was realized in the *PyRWR* package (version 1.0.0) in Python 3.7.5. The summation was used to evaluate the regulation of disease-related proteins of herbs.

The semantic comparison of gene ontology (GO) annotations provides a method to calculate the similarity between genes and genomes. To measure the similarity between herbal targets and disease-related genes, GO biological process semantic similarity (GoSim) was used to evaluate its effectiveness. We relied on the annotated data provided by *Bioconductor* and used the algorithm designed by Wang et al. [23], implemented in the *GOSemSim* package [24] (version 2.12.1) in R 3.6.3.

2.3. Machine Learning Model Training. We took the lift value of the coupled herbs calculated by the Apriori algorithm as the classification criterion and the evaluation value of the effectiveness of the coupled herbs as the input information for the machine learning tasks (Figure 1) and used the *kknn* (version 1.3.1), *e*1071 (version 1.7-8), *gbm* (version 2.1.8), and *klaR* (version 0.6-15) packages in R 3.6.3 to complete the model training of KNN, SVM, GBDT, BN, and LR. Ten cross-validations were used to evaluate the performance of the models. We, in particular, randomly divide the performance data of the coupled herbs into 10 subsets, selected one as the test set in turn, and repeated the other 9 training sets 10 times. According to the verification of a large amount of data [25], 10% can obtain the best error estimate, which can be used to prevent overfitting of the model, and all drug pair data can be used as training sets and test sets to effectively avoid data waste.

2.4. Analysis of the Mechanism of Coupled Herbs. We used the *clusterProfiler* package [26] (version 3.14.3) in R 3.6.3 to annotate genes with *org.Hs.eg.db* (version 3.10.0) and analyzed the related genes of the effective coupled herbs by KEGG enrichment analysis. Based on the hypergeometric distribution, $Q < 0.05$ was considered a significant enrichment pathway, and the same method was used for GO enrichment analysis, $Q < 0.05$ and adj. $P < 0.05$ as significant enrichment. Hierarchical clustering (HCT) was used to classify the herbs and pathways to distinguish the biological processes of intervention. At the same time, we introduced genes into *Metascape* [27] for multigene list meta-analysis, including functional proteomics and gene screening.

3. Results

3.1. The Core Herbs. A total of 5,689 electronic medical records data of Chinese medicines for the treatment of hypertension and CHD were collected to establish a database. Among them, the TCM prescription database contains 3697 prescriptions, which included 442 herbs used 85662 times, and each prescription contained, on average, 23.17 ± 10.38 herbs. A total of 234 disease-related symptoms were found in the symptoms database. Through the hierarchical extraction algorithm, we obtained 18 core herbs, including Atractylodis Macrocephalae Rhizoma, Citri Reticulatae Pericarpium, Glycyrrhizae Radix Et Rhizoma, Rhizoma Pinelliae, Poria, Radix Salviae Liguliobae, Codonopsis Radix, Rhizoma Coptidis, Radix Angelicae Sinensis, Astragali Radix, Radix Paeoniae Alba, Puerariae Lobatae Radix, Chuanxiong Rhizoma, Radix Notoginseng, Ophiopogonis Radix, Rehmanniae Radix, Schisandrae Chinensis Fructus, Ziziphi Spinosae Semen.

After 18 herbs were coupled with each other, 77 coupled herbs (Figure 2) were selected as the main herb pairs through the Apriori algorithm, of which Schisandrae Chinensis Fructus, Codonopsis Radix, Astragali Radix, Radix Notoginseng, Chuanxiong Rhizoma, Ziziphi Spinosae Semen, Radix Angelicae Sinensis, Atractylodis Macrocephalae Rhizoma, Radix Paeoniae Alba, and Rhizoma Coptidis accounted for a high proportion (Table 1).

3.2. Genes Related to Hypertension Complicated with CHD. As shown in Figure 3, 211 hypertension-related genes were obtained from GSE76845. The main upregulated genes

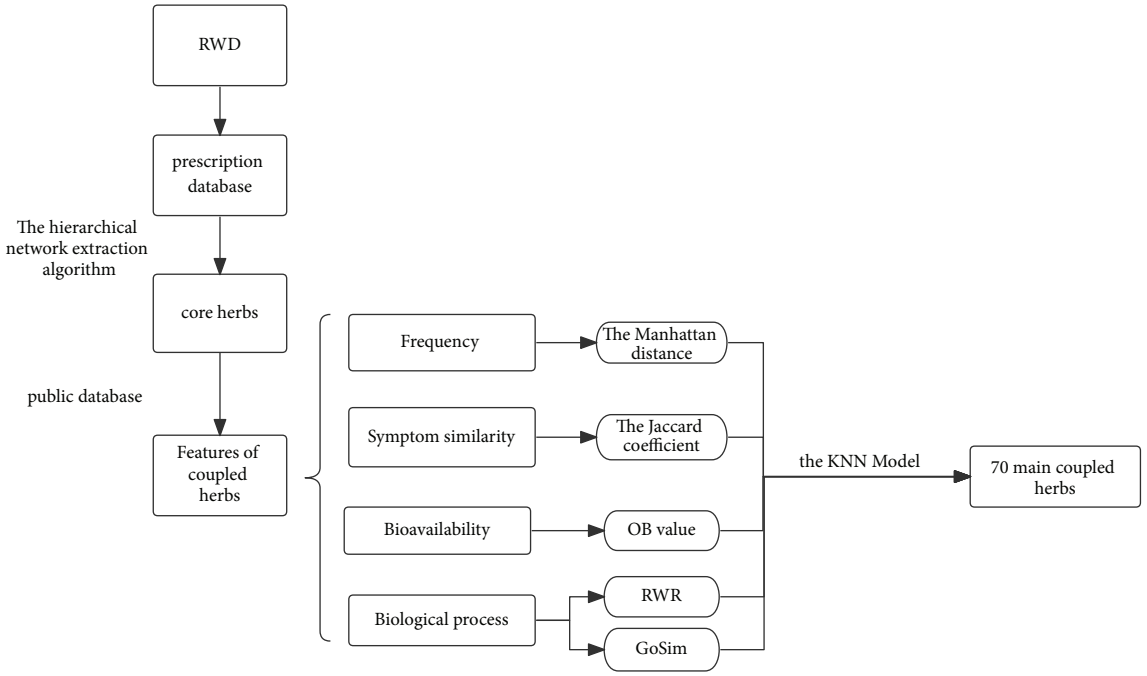

Figure 1: Overview of herb screening: first, we used the hierarchical extraction algorithm to analyze the core herbs from the prescription database. Second, we obtained the features of the coupled herbs from a public database. Finally, we input the features into the machine learning model to obtain 70 main coupled herbs.

included RNF6, UBE2L5, MTX1, FTL, SLITRK2, OGG1, HMGA1, RHAG, and TRIM8. The main downregulated genes included SPAG17, ALPG, ENO1, ESYT2, DNAJB1, HFE, RAPSN, DLGAP5, and OST4. Then, 246 CHD-related genes were obtained from GSE71226. The main upregulated genes included TM2D1, SRSF11, SLC33A1, NFATC2IP, GPRIN3, FRG1JP, DROSHA, and CHD2. The main downregulated genes included YBX3, TMCC3, OAZ2, MME, KRTTN1, IL1R2, GYPA, and HYPA. MalaCards obtained 33 hypertension-related genes and 20 CHD-related genes.

3.3. Performance of the Models. In this study, 5 machine learning models, KNN, SVM, GBDT, BN, and LR, were used to analyze the effectiveness feature data of the coupled herbs and establish the coupled herbs classification. As shown in Figure 4, the area under the receiver operating characteristic (ROC) curve (AUROC) was used to evaluate the performance of the models. We found that the 5 models had good classification performance. Among them, the KNN effect was the best, with an AUROC of 91.0%. BN, GBDT, and SVM were all over 80%, 87.3%, 82.9%, and 80.4%, respectively. The GBDT was 76.6%.

3.4. Prediction of the Coupled Herbs. The performance of the KNN model was the best when the parameter k was 9. According to its best cutoff point value, we obtained a herb combination relationship network between the paired drugs containing 18 herbs. There were 70 main coupled herbs. The top 15 effective coupled herbs screened by the KNN model are shown in Table 2. Combining the information of Tables 1 and 2, we found that Schisandrae Chinensis Fructus, Codonopsis Radix, Radix Notoginseng, Atractylodis Macrocephalae Rhizoma, Ziziphi Spinosae Semen, and Radix Paeoniae Alba were the 6 herbs most related to the other drugs. The percentages of Radix Notoginseng, Atractylodis Macrocephalae Rhizoma, Ziziphi Spinosae Semen, and Radix Paeoniae Alba increased compared to the result of Apriori, while the percentages of Astragali Radix, Chuanxiong Rhizoma, and Radix Angelicae Sinensis decreased. At the same time, there were Citri Reticulatae Pericarpium-Rhizoma Pinelliae, Citri Reticulatae Pericarpium-Poria, Schisandrae Chinensis Fructus-Ophiopogonis Radix, and Radix Notoginseng-Rhizoma Coptidis which are individually strongly associated drugs.

3.5. Validation of the Models' Effect. To verify the effect of the KNN model, we used the data diagnosed as hypertensive nephropathy (HN) in the standardized electronic medical record data from the Affiliated Hospital of Shandong University of Traditional Chinese Medicine. GEO2R was used to analyze GSE99325 to obtain HN-related genes. The final AUROC obtained using the KNN model was 94.2% with parameter k being 4. The effective therapeutic coupled herbs obtained include Radix Salviae Liguliobae-Astragali Radix, Radix Achyranthis Bidentatae-Radix Angelicae Sinensis, Astragali Radix-Radix Angelicae Sinensis, and Ophiopogonis Radix-Poria. According to recent HN-related studies [28–32], all of the coupled herbs screened in the KNN model have therapeutic effects on HN.

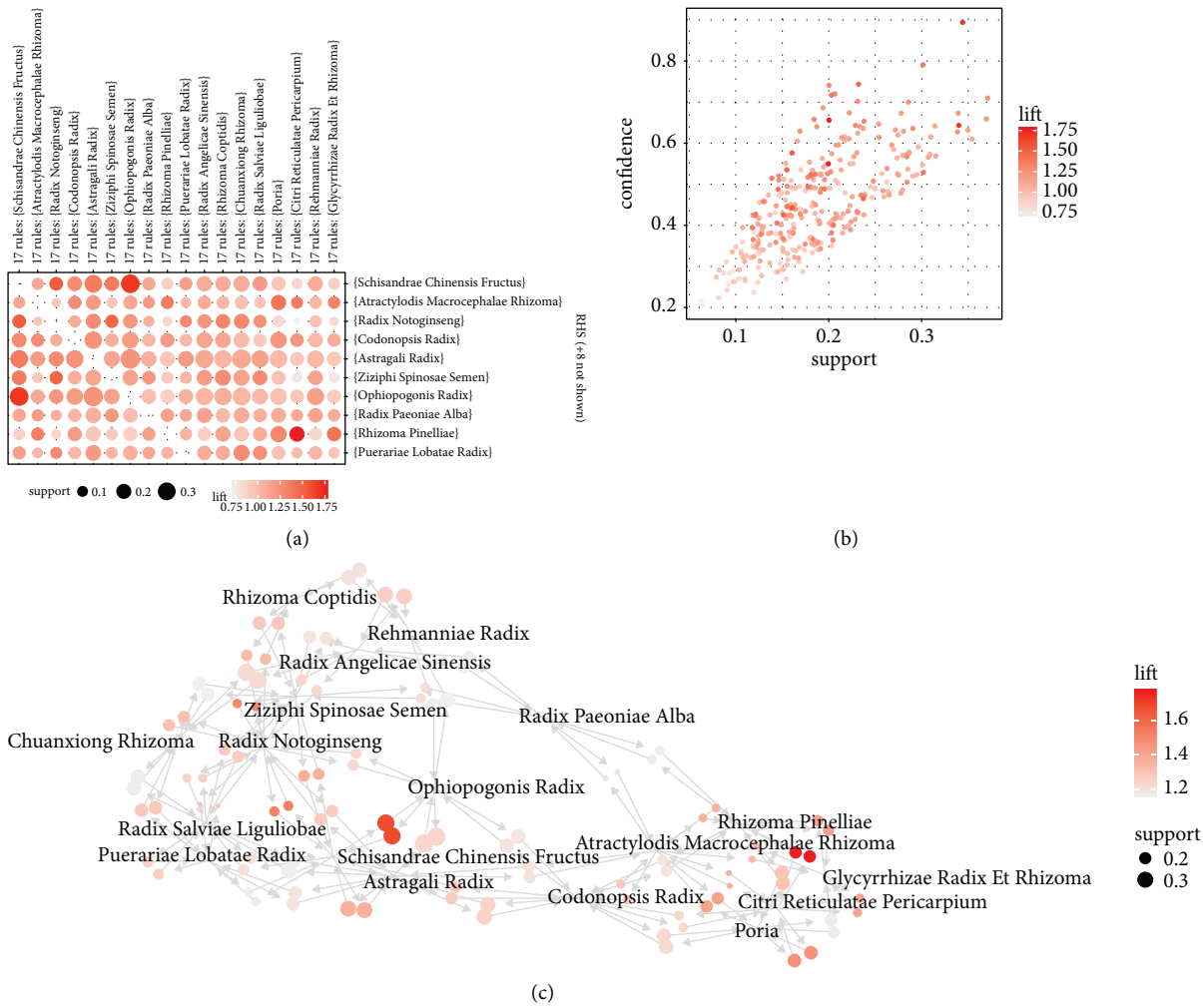

Figure 2: Results of apriori: (a) and (c) are the paired relationships between the core herbs obtained by the apriori algorithm. The size of the dot indicates the support between two herbs, and the darker the color of the dot, the larger the lift. (b) shows the coupling feature of all herbs obtained by the apriori algorithm.

Table 1: Regional division of the core herbs.

Core herbs	Proportion in the main coupled herbs		Regional division
	According to apriori (%)	According to the KNN model (%)	
Radix paeoniae alba	5.84	6.52	K1
Atractylodis macrocephalae rhizoma	5.84	7.97	K1
Chuanxiong rhizoma	6.49	5.80	K1
Rehmanniae radix	4.55	1.45	K1
Ophiopogonis radix	4.55	5.07	K1
Astragali radix	6.49	5.80	K2
Puerariae lobatae radix	5.19	5.07	K3
Ziziphi spinosae semen	6.49	7.25	K3
Codonopsis radix	7.14	7.97	K4
Schisandrae chinensis fructus	8.44	7.97	K4
Rhizoma pinelliae	5.19	5.07	K5
Citri reticulatae pericarpium	3.90	4.35	K5
Radix angelicae sinensis	6.49	5.80	K5
Radix salviae liguliobae	4.55	4.35	K5
Poria	3.25	2.90	K5
Glycyrrhizae radix et rhizoma	3.25	2.90	K5
Rhizoma coptidis	5.84	5.80	K5
Radix notoginseng	6.49	7.97	K5

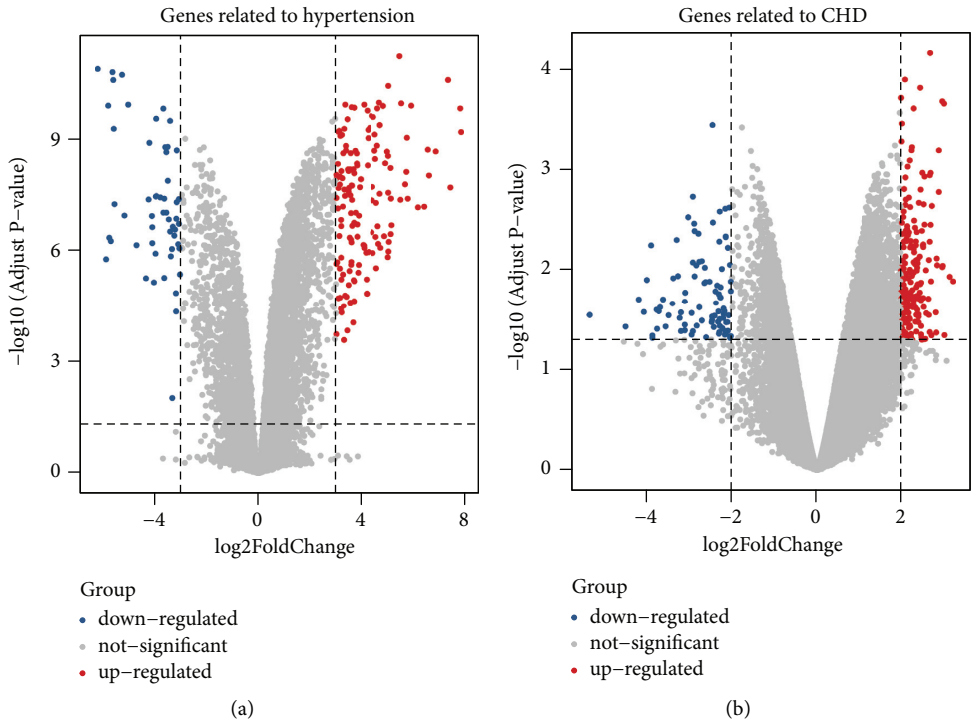

Figure 3: Genes related to hypertension (a) and CHD (b): a blue dot indicates a downregulated gene, and a red dot indicates an upregulated gene.

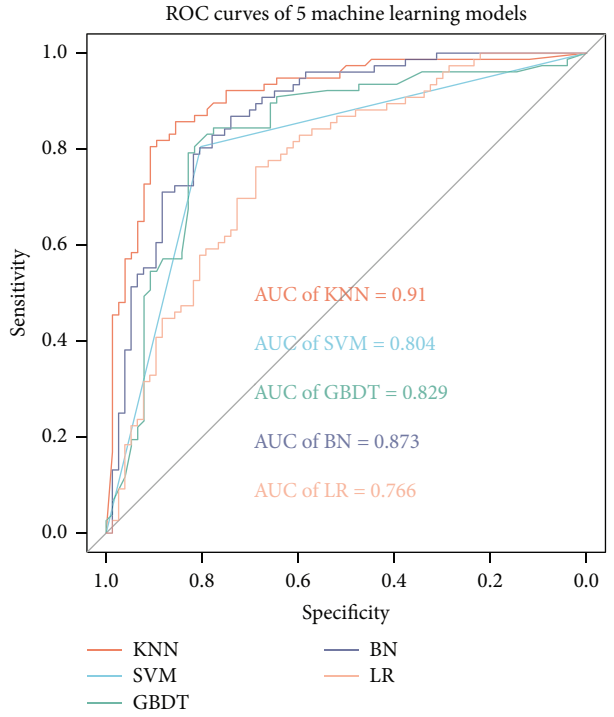

Figure 4: ROC curves of 5 machine learning models.

Table 2: The top 15 effective coupled herbs screened by the KNN model.

Coupled herbs	
Astragali radix	Ophiopogonis radix
Ophiopogonis radix	Schisandrae chinensis fructus
Atractylodis macrocephalae rhizoma	Citri reticulatae pericarpium
Citri reticulatae pericarpium	Poria
Rhizoma pinelliae	Citri reticulatae pericarpium
Radix notoginseng	Ziziphi spinosae semen
Chuanxiong rhizoma	Radix angelicae sinensis
Codonopsis radix	Schisandrae chinensis fructus
Ziziphi spinosae semen	Schisandrae chinensis fructus
Radix paeoniae alba	Atractylodis macrocephalae rhizoma
Rhizoma pinelliae	Poria
Puerariae lobatae radix	Radix notoginseng
Atractylodis macrocephalae rhizoma	Poria
Radix paeoniae alba	Codonopsis radix
Radix notoginseng	Schisandrae chinensis fructus

3.6. Therapeutic Mechanism of the Coupled Herbs. The targets of the core herbs were analyzed by GO and KEGG enrichment analysis, and the pathways in which the number of enriched genes for each herb was greater than the quartile of related genes of the herb were retained.

A total of 215 KEGG signaling pathways are obtained. We established an 18×215-dimensional feather profile of the core pathways. HCT divided the KEGG signaling pathways into 7 parts. As shown in Figure 5, based on the KEGG signaling pathways, 18 herbs were divided into 5 parts, each with similar enrichment results. The reserved coupled herbs screened by the KNN model were 59 in different clusters and 10 in the same cluster. Among the excluded coupled herbs, there were 59 in different clusters and 25 in the same cluster. In the reserved coupled herbs, herbs in different clusters were more abundant ($P = 0.04$). In addition, the number of pathways in which the number of enriched genes was greater than the average number of herbs coupled with herbs in different clusters was larger ($P < 0.01$), indicating that the biological processes of the pairing of herbs in different clusters were more extensive.

For example, Atractylodis Macrocephalae Rhizoma, Ophiopogonis Radix, Radix Paeoniae Alba, Chuanxiong Rhizoma, and Ziziphi Spinosae Semen in K1 regions have fewer enriched genes in the inflammatory pathways, such as the HIF-1 signaling pathway, TNF signaling pathway, NOD-like receptor signaling pathway, NF-kappa B signaling pathway, and 31 coupled herbs related to them; 16 were combined with herbs in the K5 region to supplement the regulation of the inflammatory pathway. At the same time, compared with the K5 region, the K1 region had fewer enriched genes in glucose and lipid metabolism, such as insulin resistance, insulin secretion, cholesterol metabolism, and the regulation of lipolysis in adipocytes, so it was necessary to combine the K5 region herbs. A total of 37.5% of the coupled herbs contained herbs in K2 and K4, and the herbs in K4 were mainly enriched in leukocyte transendothelial migration, the calcium signaling pathway, platelet activation, and other pathways related to the formation of coronary artery plaques.

GO enrichment found that the number of enriched genes in the biological process (BP) category of the KNN-coupled herbs was different from that of the deleted coupled herbs ($P = 0.04$), and the molecular function (MF) and cellular component (CC) categories were not different. From the results of GO enrichment in Figure 6(a), the regulatory effects of the core herbs were mainly cytokines, chemokines, growth factors, and the regulation of cell metabolism. As shown in Figure 6(b), the regulatory proteins of the core herbs and the genes related to hypertension complicated with CHD can be coenriched on the main nodes of the GO term network, suggesting that the paired core herbs can cooperate and complement each other, resulting in the regulation of hypertension complicated with CHD.

4. Discussion

The prescription rule of "Jun-Chen-Zuo-Shi" means that different combinations of herbs in the prescription need to be effective against multiple symptoms of clinical diseases. At the same time, the combined use of herbs is in keeping with the TCM theory which emphasizes that the core herbs enhance the efficacy of specific disease symptoms. Herbs are rich in components and match the network regulation mechanism of the disease. Experiments verification for the total mechanism is tedious and expensive. In recent years, with advances in bioinformatics research and the advent of the concept of multitarget drugs, information on compounds and targets has been extracted and screened in large herb databases and biological databases. Evaluating and predicting the efficacy of herb compound prescriptions and deducing their action mechanism has become a widely used research model [13, 15, 33].

The existing herbal pairing research is based on a single commonly used prescription, establishes a drug-gene-disease network and explores the correlation characteristics between nodes, analyzes the interaction law of herbal combinations after prescription decomposition, and discusses the rationality of its curative effect [34–36]. However, in clinical practice, such prescriptions are often used as "Jun" or "Chen" in patients' prescriptions to regulate major disease

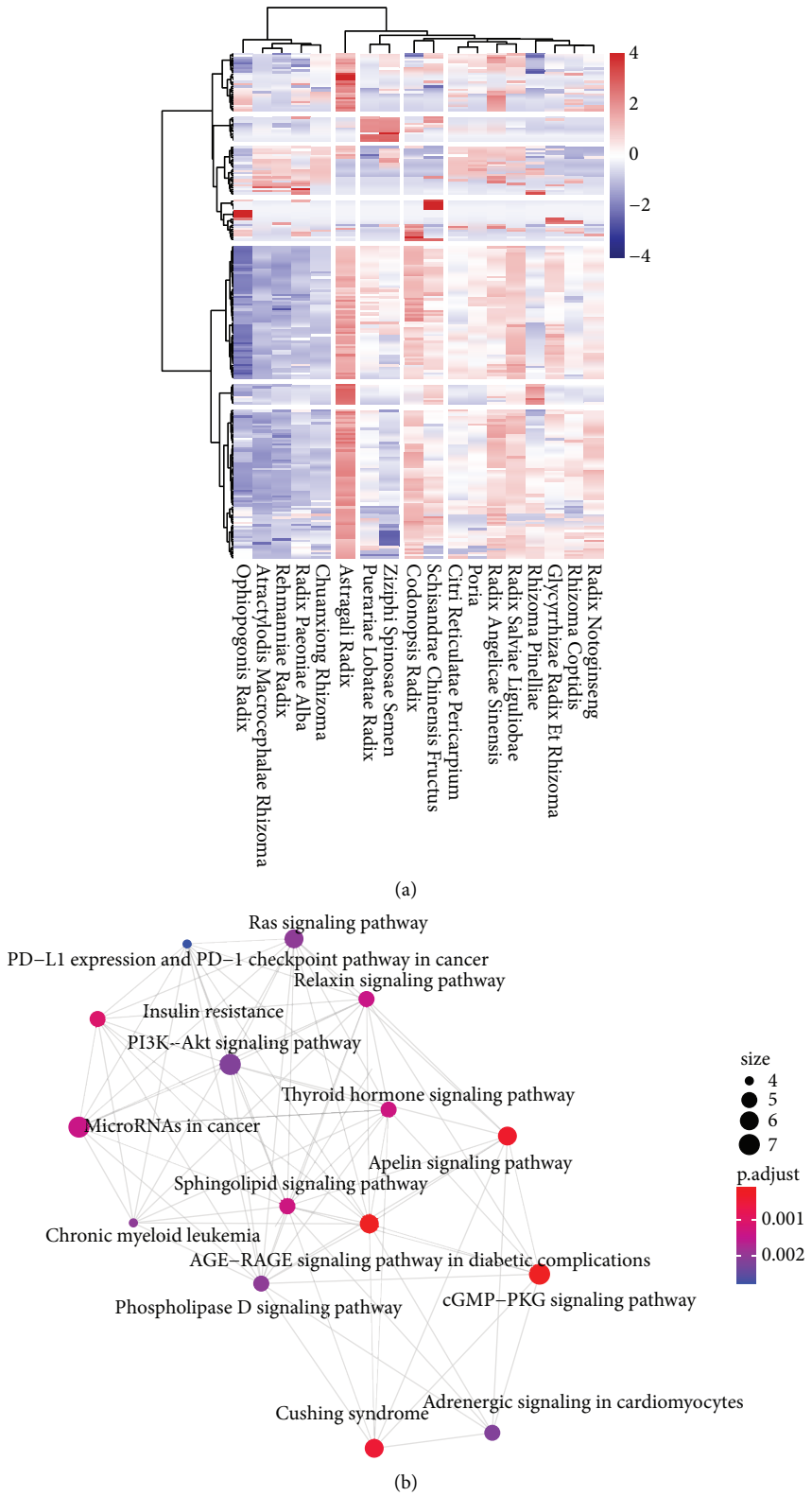

Figure 5: The results of KEGG pathway enrichment: heatmap and hierarchical clustering result of the KEGG signaling pathways (a) and the KEGG pathway network (b).

symptoms, which seriously limits the summary of the findings on the treatment of concurrent diseases and symptoms. Therefore, this study used 5688 EMRs as the data source, extracted the patients' TCM symptoms, and used the hierarchical network extraction algorithm to extract common drugs for the treatment of hypertension complicated

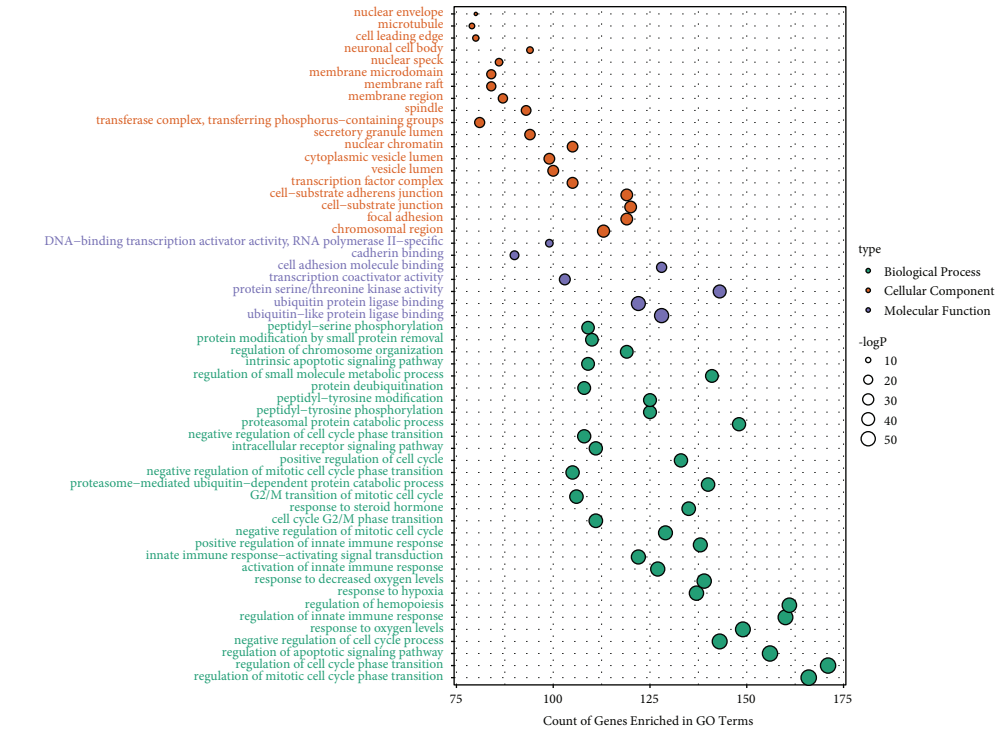

(a)

(b)

Figure 6: The results of the GO term enrichment: (a) is the enrichment result of biological process, cellular component and molecular function. (b) is a network of enriched GO terms represented as pie charts, where pie pieces are color-coded based on the identities of the genes in the herbs and hypertension complicated with CHD. The thicker the line, the more common the targets of the nodes and the closer their interaction.

with CHD in the prescription network, which is not limited to a single doctor or genre. Treatment experience can be widely collected and summarized, but it also increases the heterogeneity of the dataset. To screen out truly effective paired drugs, we established a prediction model for screening the effectiveness of herbs, which integrates different types of information, including the bioavailability of compounds, the degree of association between herbs and the clinical symptoms and the biological functions.

According to previous research [33], the effective coupled herbs in the complete prescriptions of TCM include drugs with different pharmacological directions and application frequencies. Therefore, this study quantifies the effectiveness of coupled herbs on the basis of PPIN. First, we incorporate TCM symptom information into herbal PPIN but, at the same time, it also brings more noise and biological dimensions. By using RWR to amplify the connection information between nodes, the connection probability between herbal targets and disease symptom-related proteins was evaluated, and their closeness was quantified. At the same time, we used Manhattan distance to evaluate the correlation between the two herbs in the clinical application, the Jaccard coefficient to evaluate the similarity between paired herbal symptoms and the disease symptom database, and the OB to determine the bioavailability of the herbs. After calculating the effectiveness of five classical classification machine learning models, the best KNN is selected as the classification model with an AUROC of 91.0%, and when the HN data are used to evaluate the effectiveness of the model, the AUROC is 94.2%. Therefore, according to the best cutoff point of the KNN model, we finally identified 70 effective coupled herbs.

Hypertension and CHD are common cardiovascular diseases with overlapping risk factors. After an increase in blood pressure, the renin–angiotensin–aldosterone system (RAAS) is overactivated, which induces an inflammatory reaction of target organs such as blood vessels, myocardium, and kidney, resulting in the upregulation of inflammatory cytokines. The coronary artery induces vascular endothelial injury, promotes lipids to enter the intima, causes platelet aggregation, and accelerates the growth of plaques [3, 37–39]. To further analyze the therapeutic pathways of coupled herbs, we carried out GO and KEGG enrichment analysis on each herbal target. Finally, we found that coupled herbs can cooperate with each other, directly or indirectly acting on the inflammatory pathway, further assist the body in controlling risk factors by regulating blood lipids, proteins, and carbohydrate metabolism, regulate the expression of various cytokines at the cellular level, and regulate their target proteins to inhibit the inflammatory response and interstitial fibrosis of target organs caused by hypertension.

The analysis results of GO and KEGG enrichment showed that the herbal combinations with synergistic effects could be correctly identified by a machine learning model with the quantitative indicators of herbal effectiveness used in this study, but this study also contains many limitations. First, the herbal-related compounds and target information come from public database. Although we used a variety of models to compare and verify to find the best model, the data deviation of the database may have a potential impact on the research results. Second, although the TCM symptom information of patients has been included in the evaluation system, it fails to make full use of the clinical information of individual differences in EMRS. Third, the sample size for model training is still limited, and information on the interaction between compounds has not been added, so future research needs to improve the performance of the model to design a more effective adjuvant therapy for TCM.

5. Conclusion

This study was based on data from 5688 EMRs of hypertension complicated with CHD in the Affiliated Hospital of Shandong University of Traditional Chinese Medicine from 2014 to 2017, and a patient symptom dataset and prescription dataset were established. Eighteen commonly used herbs were obtained, and their biological network was established. Using the interaction information between nodes in the network, we established quantitative data on the effectiveness of coupled herbs. An effective coupled herb screening algorithm based on a machine learning model was proposed, and a total of 70 coupled herbs were obtained. Based on the analysis of various herbs at the pathway level, they can play a multilevel biological regulatory role in controlling the inflammatory response and regulating energy metabolism for hypertension complicated with CHD and its TCM symptoms. Combined with complex networks and machine learning, this study explored the potential law of herbs in the treatment of hypertension complicated with CHD and predicted the curative effect of coupled herbs, providing a direction for summarizing the TCM EMRs and explaining the TCM rules.

Abbreviations

CVD:	Cardiovascular disease
CHD:	Coronary heart disease
TCM:	Traditional Chinese medicine
RCT:	Randomized controlled trial
RWD:	Real-world data
KNN:	K-nearest neighbor
SVM:	Support vector machine
GBDT:	Gradient boosting decision tree
BN:	Bayesian network
LR:	Logistic regression
EMR:	Electronic medical record
TCMSP:	Traditional Chinese Medicine Systems Pharmacology Database and Analysis Platform
ETCM:	The Encyclopedia of Traditional Chinese Medicine
PPIN:	The protein–protein interaction network
RWR:	Random walk with restart
GO:	Gene ontology
GoSim:	Gene ontology biological process semantic similarity
OB:	Oral bioavailability
HCT:	Hierarchical clustering

Baizhu:	Atractylodis Macrocephalae Rhizoma
Chenpi:	Citri Reticulatae Pericarpium
Gancao:	Glycyrrhizae Radix Et Rhizoma
Banxia:	Rhizoma Pinelliae
Fuling:	Poria
Danshen:	Radix Salviae Liguliobae
Dangshen:	Codonopsis Radix
Huanglian:	Rhizoma Coptidis
Danggui:	Radix Angelicae Sinensis
Huangqi:	Astragali Radix
Baishao:	Radix Paeoniae Alba
Gegen:	Puerariae Lobatae Radix
Chuanxiong:	Chuanxiong Rhizoma
Sanqi:	Radix Notoginseng
Maidong:	Ophiopogonis Radix
Dihuang:	Rehmanniae Radix
Wuweizi:	Schisandrae Chinensis Fructus
Suanzaoren:	Ziziphi Spinosae Semen
ROC:	Receiver operating characteristic
AUROC:	Area under the receiver operating characteristic curve
HN:	Hypertensive nephropathy
Niuxi:	Radix Achyranthis Bidentatae
Maidong:	Ophiopogonis Radix
RAAS:	Renin–angiotensin–aldosterone system.

Data Availability

The TCM prescription data used to support the findings of this study are available from the corresponding author upon request. The data generated by the analysis process can be found in the article databank.

Conflicts of Interest

The authors declare that they have no conflicts of interest.

Acknowledgments

The authors thank the Affiliated Hospital of Shandong University of Traditional Chinese Medicine for its support of this study. This work was supported by The Jinan Science and Technology Bureau Clinical Medical Science and Technology Innovation Program (No. 202019149): based on network pharmacology analysis of the mechanism of real-world core prescriptions for hypertensive renal damage; Shandong Province Medicine and Health Science and Technology Development Project (No. 202103010371): research on the mechanism of ACE2/Ang 1-7/Mas axis regulating hypertensive nephropathy based on proteomics analysis; and the Construction Project of the National Clinical Research Base of Traditional Chinese Medicine for Hypertension (Issued by the State Administration of Traditional Chinese Medicine [2008] No. 23).

Supplementary Materials

1. Apriori: rules of the core herbs obtained for the Apriori algorithm. 2. Features of coupled herbs: The value of Jaccard similarity coefficient, OB, RWR, GoSim, Manhattan distance, and KNN model output of coupled herbs. 3. The main coupled herbs: Seventy coupled herbs for adjuvant treatment of hypertension complicated with coronary heart disease screened by the KNN model. 4. TCM herbs information: the Chinese name, Pinyin name, Latin name, and English name of herbs in this study. (*Supplementary Materials*)

References

[1] T. Unger, C. Borghi, F. Charchar et al., "2020 international society of hypertension global hypertension practice guidelines," *Hypertension*, vol. 75, no. 6, pp. 1334–1357, 2020.

[2] T. B. Olesen, M. Pareek, J. V. Stidsen et al., "Association between antecedent blood pressure, hypertension-mediated organ damage and cardiovascular outcome," *Blood Pressure*, vol. 29, no. 4, pp. 232–240, 2020.

[3] F. Mach, C. Baigent, A. L. Catapano et al., "2019 ESC/EAS guidelines for the management of dyslipidaemias: lipid modification to reduce cardiovascular risk," *European Heart Journal*, vol. 41, no. 1, pp. 111–188, 2020.

[4] D. Ettehad, C. A. Emdin, A. Kiran et al., "Blood pressure lowering for prevention of cardiovascular disease and death: a systematic review and meta-analysis," *The Lancet*, vol. 387, no. 10022, pp. 957–967, 2016.

[5] G. S. Collins and D. G. Altman, "An independent external validation and evaluation of QRISK cardiovascular risk prediction: a prospective open cohort study," *BMJ (Clinical research ed.)*, vol. 339, Article ID b2584, 2009.

[6] R. Conroy, K. Pyörälä, A. P. Fitzgerald et al., "Estimation of ten-year risk of fatal cardiovascular disease in Europe: the SCORE project," *European Heart Journal*, vol. 24, no. 11, pp. 987–1003, 2003.

[7] X. Xiong, P. Wang, Y. Zhang, and X. Li, "Effects of traditional Chinese patent medicine on essential hypertension: a systematic review," *Medicine*, vol. 94, no. 5, p. e442, 2015.

[8] X.-J. Xiong, X.-C. Yang, W. Liu et al., "Therapeutic efficacy and safety of traditional Chinese medicine classic herbal formula longdanxiegan decoction for hypertension: a systematic review and meta-analysis," *Frontiers in Pharmacology*, vol. 9, p. 466, 2018.

[9] X. Xiong, P. Wang, L. Duan et al., "Efficacy and safety of Chinese herbal medicine xiao yao san in hypertension: a systematic review and meta-analysis," *Phytomedicine*, vol. 61, Article ID 152849, 2019.

[10] Z. Shu, Y. Zhou, K. Chang et al., "Clinical features and the traditional Chinese medicine therapeutic characteristics of 293 COVID-19 inpatient cases," *Frontiers of Medicine*, vol. 14, no. 6, pp. 760–775, 2020.

[11] S. Li, "Network pharmacology evaluation method guidance-draft," *World Journal of Traditional Chinese Medicine*, vol. 7, no. 1, pp. 146–154, 2021.

[12] S. Li and B. Zhang, "Traditional Chinese medicine network pharmacology: theory, methodology and application," *Chinese Journal of Natural Medicines*, vol. 11, no. 2, pp. 110–120, 2013.

[13] Y. Yang, K. Yang, T. Hao et al., "Prediction of molecular mechanisms for lianxia ningxin formula: a network pharmacology study," *Frontiers in Physiology*, vol. 9, p. 489, 2018.

[14] Y. F. Wang, J. J. Wang, W. Peng et al., "Identification of hypertension subgroups through topological analysis of symptom-based patient similarity," *Chinese Journal of Integrative Medicine*, vol. 27, pp. 1–10, 2021.

[15] X. Zhou, S. Chen, B. Liu et al., "Development of traditional Chinese medicine clinical data warehouse for medical knowledge discovery and decision support," *Artificial Intelligence in Medicine*, vol. 48, no. 2-3, pp. 139–152, 2010.

[16] J. Ru, P. Li, J. Wang et al., "TCMSP: a database of systems pharmacology for drug discovery from herbal medicines," *Journal of Cheminformatics*, vol. 6, no. 1, p. 13, 2014.

[17] Y. Wu, F. Zhang, K. Yang et al., "SymMap: an integrative database of traditional Chinese medicine enhanced by symptom mapping," *Nucleic Acids Research*, vol. 47, no. D1, pp. D1110–D1117, 2019.

[18] H.-Y. Xu, Y.-Q. Zhang, Z.-M. Liu et al., "ETCM: an encyclopaedia of traditional Chinese medicine," *Nucleic Acids Research*, vol. 47, no. D1, pp. D976–D982, 2019.

[19] D. Szklarczyk, A. L. Gable, D. Lyon et al., "STRING v11: protein-protein association networks with increased coverage, supporting functional discovery in genome-wide experimental datasets," *Nucleic Acids Research*, vol. 47, no. D1, pp. D607–D613, 2019.

[20] N. Rappaport, M. Twik, I. Plaschkes et al., "MalaCards: an amalgamated human disease compendium with diverse clinical and genetic annotation and structured search," *Nucleic Acids Research*, vol. 45, no. D1, pp. D877–D887, 2017.

[21] D. Sinwar and R. Kaushik, "Study of euclidean and manhattan distance metrics using simple k-means clustering," *International Journal for Research in Applied Science and Engineering Technology*, vol. 2, no. 5, pp. 270–274, 2014.

[22] J. Yang, S. Tian, J. Zhao, and W. Zhang, "Exploring the mechanism of TCM formulae in the treatment of different types of coronary heart disease by network pharmacology and machining learning," *Pharmacological Research*, vol. 159, Article ID 105034, 2020.

[23] J. Z. Wang, Z. Du, R. Payattakool, P. S. Yu, and C.-F. Chen, "A new method to measure the semantic similarity of GO terms," *Bioinformatics*, vol. 23, no. 10, pp. 1274–1281, 2007.

[24] G. Yu, F. Li, Y. Qin, X. Bo, Y. Wu, and S. Wang, "GOSemSim: an R package for measuring semantic similarity among GO terms and gene products," *Bioinformatics*, vol. 26, no. 7, pp. 976–978, 2010.

[25] N. Wang, P. Li, X. Hu et al., "Herb target prediction based on representation learning of symptom related heterogeneous network," *Computational and Structural Biotechnology Journal*, vol. 17, pp. 282–290, 2019.

[26] G. Yu, L.-G. Wang, Y. Han, and Q.-Y. He, "ClusterProfiler: an R package for comparing biological themes among gene clusters," *OMICS: A Journal of Integrative Biology*, vol. 16, no. 5, pp. 284–287, 2012.

[27] Y. Zhou, B. Zhou, L. Pache et al., "Metascape provides a biologist-oriented resource for the analysis of systems-level datasets," *Nature Communications*, vol. 10, no. 1, p. 1523, 2019.

[28] Y. Dong, B. Yue, M. Qian et al., "JYYS granule mitigates renal injury in clinic and in spontaneously hypertensive rats by inhibiting NF- κB signaling-mediated microinflammation," *Evidence-Based Complementary and Alternative Medicine*, vol. 2018, Article ID 8472963, 13 pages, 2018.

[29] J. Owoicho Orgah, M. Wang, X. Yang et al., "Danhong injection protects against hypertension-induced renal injury via down-regulation of myoglobin expression in spontaneously hypertensive rats," *Kidney & Blood Pressure Research*, vol. 43, no. 1, pp. 12–24, 2018.

[30] L. Wu, M. Liu, and Z. Fang, "Combined therapy of hypertensive nephropathy with breviscapine injection and antihypertensive drugs: a systematic review and a meta-analysis," *Evidence-Based Complementary and Alternative Medicine: eCAM*, vol. 2018, Article ID 2958717, 17 pages, 2018.

[31] Y. Li, S. Yan, L. Qian, L. Wu, Y. Zheng, and Z. Fang, "Danhong injection for the treatment of hypertensive nephropathy: a systematic review and meta-analysis," *Frontiers in Pharmacology*, vol. 11, p. 909, 2020.

[32] J. M. Huan, W. G. Su, W. Li et al., "Summarizing the effective herbs for the treatment of hypertensive nephropathy by complex network and machine learning," *Evidence-Based Complementary and Alternative Medicine: eCAM*, vol. 2021, Article ID 5590743, 12 pages, 2021.

[33] N. Wang, N. Du, Y. Peng et al., "Network patterns of herbal combinations in traditional Chinese clinical prescriptions," *Frontiers in Pharmacology*, vol. 11, Article ID 590824, 2021.

[34] H. Y. Fang, H. W. Zeng, L. M. Lin et al., "A network-based method for mechanistic investigation of shexiang baoxin pill's treatment of cardiovascular diseases," *Scientific Reports*, vol. 7, Article ID 43632, 2017.

[35] W. Zhou, X. Cheng, and Y. Zhang, "Effect of liuwei dihuang decoction, a traditional Chinese medicinal prescription, on the neuroendocrine immunomodulation network," *Pharmacology & Therapeutics*, vol. 162, pp. 170–178, 2016.

[36] G. Yu, Y. Zhang, W. Ren et al., "Network pharmacology-based identification of key pharmacological pathways of yin–huang–qing–fei capsule acting on chronic bronchitis," *International Journal of Chronic Obstructive Pulmonary Disease*, vol. 12, pp. 85–94, 2016.

[37] D. Chen, M. Liang, C. Jin, Y. Sun, D. Xu, and Y. Lin, "Expression of inflammatory factors and oxidative stress markers in serum of patients with coronary heart disease and correlation with coronary artery calcium score," *Experimental and Therapeutic Medicine*, vol. 20, no. 3, pp. 2127–2133, 2020.

[38] H. Schuett, R. Oestreich, G. H. Waetzig et al., "Transsignaling of interleukin-6 crucially contributes to atherosclerosis in mice," *Arteriosclerosis, Thrombosis, and Vascular Biology*, vol. 32, no. 2, pp. 281–290, 2012.

[39] Q. Su, L. Li, Y. Sun, H. Yang, Z. Ye, and J. Zhao, "Effects of the TLR4/myd88/NF-κB signaling pathway on NLRP3 inflammasome in coronary microembolization-induced myocardial injury," *Cellular Physiology and Biochemistry*, vol. 47, no. 4, pp. 1497–1508, 2018.

Hindawi
Evidence-Based Complementary and Alternative Medicine
Volume 2022, Article ID 5630748, 8 pages
https://doi.org/10.1155/2022/5630748

Research Article

The Fitting Optimization Path Analysis on Scale Missing Data: Based on the 507 Patients of Poststroke Depression Measured by SDS

Xiaoying Lv,[1,2] **Ruonan Zhao**,[3] **Tongsheng Su**,[4] **Liyun He**,[2] **Rui Song**,[4] **Qizhen Wang**,[2] **Xueyun Yu**,[2] **and Yanbo Zhu**[5]

[1]*School of Chinese Medicine, Beijing University of Chinese Medicine, Beijing, China*
[2]*Institute of Basic Research In Clinical Medicine, China Academy Of Chinese Medical Sciences, Beijing, China*
[3]*Xi'an Encephalopathy Hospital of Traditional Chinese Medicine, Shanxi University of Chinese Medicine, Xi'an, China*
[4]*Shanxi Provincial Hospital of Chinese Medicine, Xi'an, Shanxi, China*
[5]*School of Management, Beijing University of Chinese Medicine, Beijing, China*

Correspondence should be addressed to Yanbo Zhu; yanbo0722@sina.com

Received 26 October 2021; Accepted 24 December 2021; Published 13 January 2022

Academic Editor: Xuezhong Zhou

Objective. To explore the optimal fitting path of missing data of the Scale to make the fitting data close to the real situation of patients' data. *Methods*. Based on the complete data set of the SDS of 507 patients with stroke, the data simulation sets of Missing Completely at Random (MCAR), Missing at Random (MAR), and Missing Not at Random (MNAR) were constructed by R software, respectively, with missing rates of 5%, 10%, 15%, 20%, 25%, 30%, 35%, and 40% under three missing mechanisms. Mean substitution (MS), random forest regression (RFR), and predictive mean matching (PMM) were used to fit the data. Root mean square error (RMSE), the width of 95% confidence intervals (95% CI), and Spearman correlation coefficient (SCC) were used to evaluate the fitting effect and determine the optimal fitting path. *Results*. when dealing with the problem of missing data in scales, the optimal fitting path is ① under the MCAR deletion mechanism, when the deletion proportion is less than 20%, the MS method is the most convenient; when the missing ratio is greater than 20%, RFR algorithm is the best fitting method. ② Under the Mar mechanism, when the deletion ratio is less than 35%, the MS method is the most convenient. When the deletion ratio is greater than 35%, RFR has a better correlation. ③ Under the mechanism of MNAR, RFR is the best data fitting method, especially when the missing proportion is greater than 30%. In reality, when the deletion ratio is small, the complete case deletion method is the most commonly used, but the RFR algorithm can greatly expand the application scope of samples and save the cost of clinical research when the deletion ratio is less than 30%. The best way to deal with data missing should be based on the missing mechanism and proportion of actual data, and choose the best method between the statistical analysis ability of the research team, the effectiveness of the method, and the understanding of readers.

1. Introduction

The scale data is filled in by doctors or patients according to the situation and patient feelings at that time. Once it is missing, it is difficult to trace the original case and verify the data [1–3]. However, due to various reasons, such as the privacy and specialty of the scale items, scale data missing often occurs in the process of medical research. For example, some scales involve privacy items, and some patients adopt an avoidance attitude when facing sensitive problems. Some items of the scale may involve traditional Chinese medicine, clinical or other medical terms. Sometimes the patients did not answer because they did not understand the meaning of the question or option—missing data due to the negligence of respondents [4]. However, in previous studies, few researchers have discussed the filling method suitable for scale data missing, and there is no final conclusion on which method is more suitable for fitting scale data. This problem is particularly prominent in

the data of medical, psychological measurement scales. For example, a large prospective cohort study of 71412 women was conducted in France. Data including the center for epidemiological studies depression (CES-D) were collected, of which 45% had missing entries in the scale [5]. A program conducted a questionnaire survey on mental health among 2919 sixth graders in 21 schools across the country, and 86% of the students missed one or more variables [6].

Poststroke depression (PSD) refers to a mood disorder characterized by continuous depression and decreased interest after stroke. It is one of the common complications of a stroke. It is mainly manifested in a series of mental disorders such as depression and slow thinking and even seriously affects the quality of life and rehabilitation of such patients. Zung's Self-rating Depression Scale (SDS) is a 4-level self-rating scale with 20 items, which can directly reflect the subjective feelings of depressed patients and the changes in their depression status in the process of diagnosis and treatment [7]. Therefore, 507 cases of poststroke depression data were selected for fitting study to analyze the optimal path of missing data of the scale.

Data missing mechanisms describe the possible relationship between missing values and observed variables, which can be divided into the following three types: Missing Completely at Random (MCAR), Missing at Random (MAR), and Missing Not at Random (MNAR). Different data fitting methods should be selected according to different missing mechanisms [8]. The contemporary data missing processing methods can make more in-depth and effective use of collected clinical data information to carry out multiple interpolation fitting of missing data, so as to make the data more truly reflect the actual clinical situation. However, in the practical application, the researchers have the problem of blindly applying statistical methods to the treatment, failing to consider the characteristics of the experiment and the possible missing mechanism to make an appropriate analytic strategy in advance in the scheme [9]. Meanwhile, different fitting methods will also draw different conclusions under different missing rates [10]. For example, Van Hulse and Khoshgoftaar believe that when the missing rate reaches more than 40%, the utilization value of data is almost lost [11]. Therefore, based on the data of SDS, this study constructed simulated data sets with different missing mechanisms and different missing rates (5%, 10%, 15%, 20%, 25%, 30%, 35%, and 40%), and compared three interpolation methods: Mean Substitution (MS), Random Forest Regression (RFR), and Predictive Mean Matching (PMM), in the aspect of fitting effects on missing data in the SDS scale, to explore the best fitting optimization path for the missing scale data in clinical research, to make the fitting data close to the real situation of the treatment of patients. Also, to improve the efficiency of statistical tests more accurately and provide methodological support for the fitting of missing data in the scale in the future.

2. Materials and Methods

2.1. Data Information. The study data were derived from complete SDS scale data of 507 stroke subjects collected from more than 10 hospitals in Shandong, Nanjing, and Gansu, from September 2015 to March 2017, including 313 males (61.7%) with an average age of 60.11 ± 0.54, and 194 females (38.3%) with an average age of 62.94 ± 0.63. The study took the above complete data as the training set, and the data set after fitting was called the simulation set.

2.2. Simulation Methods. Based on the training set, the NaControl function in R software was applied to construct the simulation data set. The details are as follows:

① Missing Completely at Random (MCAR): the probability of data missing has no relationship with both observed data and unobserved data [12]. In this study, data were randomly deleted from the training set at the proportions of 5%, 10%, 15%, 20%, 25%, 30%, 35%, and 40%.

② Missing at Random (MAR): the probability of data missing is related to the observed variables but independent of the characteristics of the unobserved data [13]. One study showed a significant increase in the number of missing items on the SDS depression scale in male subjects [14]. In order to facilitate the comparison of the three data missing methods under the eight missing rates, the data of 194 female subjects were randomly deleted at a proportion of 10%, and the data of the remaining 313 male patients were randomly deleted at a certain proportion. The datasets of male and female subjects were transformed into simulated sets with missing ratios of 5%, 10%, 15%, 20%, 25%, 30%, 35%, and 40%, see Table 1.

③ Missing Not at Random (MNAR): the probability of data missing is related to the observed data itself [15]. Zung, the author of the SDS, believed that among depressed patients, the severity of the perception of diurnal change (item 2) was most closely related to the degree of depression [7]. The patients with a score of 3 or 4 in item 2 of the SDS had more severe depression. This study considered the possibility that the more depressed the subjects were, the more likely their data would be missing. Therefore, the data of 108 subjects scoring 1 or 2 points in item 2 were randomly deleted at a proportion of 10%, and the data of 399 subjects scoring 3 or 4 points were constructed according to the proportion of missing data. The two were combined into a simulation set with the above-mentioned missing ratio. See Table 1.

In conclusion, a simulated missing data set was constructed for each training set, and three fitting methods were applied to fitting the data set. Three missing mechanisms (MCAR, MAR, and MNAR, respectively, expressed in C, A, N), eight missing ratios (5%, 10%, 15%, 20%, 25%, 30%, 35%, and 40%, respectively, in 5, 10, 15, 20, 25, 30, 35, and 40), and three interpolation methods (MS, PMM, and RFR, respectively, in M, P, and R) were used to deal with the data sets. For example, the fitting set C10M is a data set that is formed after the simulation set with a missing ratio of 10% is fitted by Mean Substitution under the MCAR mechanism.

Table 1: Missing ratios of the simulation sets.

Mechanism		5 (%)	10%	15 (%)	20 (%)	25 (%)	30 (%)	35 (%)	40 (%)
MAR	MCAR ($n = 507$)	5	10%	15	20	25	30	35	40
	Female ($n = 194$)	10	10	10	10	10	10	10	10
	Male ($n = 313$)	1.90	10.00	18.10	26.20	34.30	42.40	50.50	58.59
MNAR	1-2 points ($n = 108$)	10	10	10	10	10	10	10	10
	3-4 points ($n = 399$)	3.65	10.00	16.35	22.71	29.06	35.41	41.77	48.12

2.3. Missing Value Processing Methods and Some Principles

2.3.1. Mean Substitution. The Mean Substitution refers to that the mean value of nonmissing data of key variables is used as the substitute value of missing data. In the process of filling in the missing values, only one substitute value for missing values is generated. That is, the mean value of the observed data in this sample is used as the substitute value so as to generate a complete data set for analysis [16, 17]. This method applies the HMISC function of R software, and its parameters are set as follows: impute (data, fun = mean).

2.3.2. Predictive Mean Matching. The PMM method is one of the methods to fill in the data of monotone missing continuous variables. This method assumes that there is a linear regression relationship between missing data and nonmissing data. By establishing the regression model of both sides and randomly selecting m parameters from the posterior distribution of regression coefficient estimates, the predicted values are obtained through the calculations of these parameters and used to replace the missing values [18, 19]. This method is suitable for continuous variables in monotone deletion mode. The mice function of R software is used in this method, and the parameters are set as follows: mice (data, $m = 20$, maxit = 5, meth = "pmm," seed = 500).

2.3.3. Random Forest Regression. Random Forest algorithm is an integrated learning algorithm proposed by Breiman in 2001, which is used to solve the problems of classification prediction, regression prediction, and feature selection of high-dimensional nonlinear data. RMR method is an improved algorithm of bagging algorithm. It uses K classification and regression decision trees (CART) as the base learner [20] and takes the average of the predicted values of K base learners as the final result [21, 22]. When dealing with missing data, it is less affected by outliers and has no restrictions on the distribution of data. It can effectively analyze high-dimensional complex data [23]. The missForest function of R software is used in this method, and the parameters are set as follows: missForest (data, ntree = 50).

2.4. Evaluation Methods and Indicators. The evaluation indexes were the root mean square error (RMSE), the width of 95% confidence intervals (95% CI), and Spearman correlation coefficient (SCC) obtained by paired T-test of the total scores of the training set and the simulation set [24]. The smaller the value range of RMSE, the better the fitting accuracy [25]. The narrower the 95% CI, the higher the fitting precision [26]. The bigger the value of the Spearman correlation coefficient, the better correlation of the fitting data [27].

3. The Results

3.1. Number of Missing Items. With the increase of the proportion of data missing in the SDS, the number of missing items and samples gradually increased. When the missing ratio was less than 10%, the number of missing items in most subjects' SDS was concentrated in 1 to 3. When the missing ratio was from 10% to 20%, the result in most subjects' SDS concentrated in 3 to 5. When the data missing ratio reached 40%, the number of missing items in most subjects could be controlled below 10 under the MCAR mechanism, while in the MAR mechanism, 50% subjects' numbers were greater than 10. See Tables 2–4 for more details.

3.2. Comparisons of Fitting Effects

3.2.1. Root Mean Square Error. The RMSE is an indicator of fitting accuracy. The fitting results of the three methods show that, with the increase of the missing ratio, the fitting accuracy becomes lower and lower, and the value of RMSE is between 0 and 0.2. Compared with MS and PMM, the RMSE value of RFR is the lowest under the three deletion mechanisms, especially under the MCAR mechanism, the RMSE is always less than 0.1. When the deletion ratio is greater than 30%, the RMSE of the three methods is greater than 0.1. When the deletion ratio is less than 20%, the RMSE value of RFR is the lowest; under the MNAR mechanism, when the deletion ratio is greater than 30%, the result of RFR is also better. The accuracy of PMM is lower than the other two methods. See Figure 1.

3.2.2. The Width of 95% Confidence Intervals. Usually, the 95% confidence interval stands for the fitting precision. With the increase of deletion ratio, 95% CI width becomes higher and higher, and the value of 95% CI width is between 0.005 and 0.035. Under the MCAR mechanism, when the deletion ratio is less than 15%, the width of 95% CI of MS is the narrowest, and the width 95% CI of MS under the MAR mechanism is also narrower than the other two methods. However, under the MNAR mechanism, the fitting precision of RFR is better than the other two methods. When the deletion ratio is less than 20%, the width of 95% CI of MS and the width of 95% CI of RFR are less than 0.015. For more details; see Figure 2.

Table 2: The item missing conditions of the simulation sets under MCAR ($N = 507$).

Number of missing items (n (%))	5%	10%	15%	20%	25%	30%	35%	40%
0	187 (36.9)[a]	58 (11.4)	17 (3.4)	7 (1.4)	1 (0.2)	1 (0.2)	0 (0)	0 (0)
1	183 (73.0)	146 (40.2)[a]	82 (19.6)	33 (7.9)	12 (2.6)	6 (1.4)	0 (0)	1 (0.2)
2	94 (91.5)[b]	135 (66.8)	101 (39.5)[a]	66 (20.9)	34 (9.3)	12 (3.7)	3 (0.6)	2 (0.6)
3	36 (98.6)	96 (85.7)[b]	134 (65.9)	114 (43.4)[a]	79 (24.9)	38 (11.2)	18 (4.1)	7 (2.0)
4	7 (100.0)	49 (95.4)	85 (81.7)[b]	102 (63.5)	80 (40.6)[a]	59 (22.9)	36 (11.2)	21 (6.1)
5	0 (0)	17 (98.8)	53 (92.2)	92 (81.7)[b]	104 (61.1)	107 (44.0)[a]	60 (23.1)	41 (14.2)
6	0 (0)	5 (99.8)	21 (96.3)	54 (92.3)	88 (78.5)[b]	79 (59.6)	93 (41.4)[a]	57 (25.4)[a]
7	0 (0)	1 (100.0)	9 (98.1)	22 (96.6)	56 (89.5)	92 (77.7)[b]	91 (59.4)	74 (40.0)
8	0 (0)	0 (0)	4 (98.9)	12 (99.0)	29 (95.3)	46 (86.8)	93 (77.7)[b]	83 (56.4)
9	0 (0)	0 (0)	1 (100.0)	4 (99.8)	16 (98.4)	43 (95.3)	56 (88.8)	96 (75.3)[b]
10	0 (0)	0 (0)	0 (0)	0 (0)	6 (99.6)	13 (97.8)	35 (95.7)	60 (87.1)
11	0 (0)	0 (0)	0 (0)	1 (100.0)	2 (100.0)	9 (99.6)	13 (98.2)	42 (95.4)
12	0 (0)	0 (0)	0 (0)	0 (0)	0 (0)	1 (99.8)	8 (99.8)	12 (97.8)
13	0 (0)	0 (0)	0 (0)	0 (0)	0 (0)	1 (100.0)	1 (100.0)	7 (99.2)
14	0 (0)	0 (0)	0 (0)	0 (0)	0 (0)	0 (0)	0 (0)	4 (100.0)

[a]The number of missing samples accounts for 25% of the total. [b]The number of missing samples accounts for 75% of the total.

Table 3: The item missing conditions of the simulation sets under MAR ($N = 507$).

Number of missing items (n (%))	5%	10%	15%	20%	25%	30%	35%	40%
0	225 (44.4)[a]	58 (11.4)	26 (5.1)	18 (3.6)	18 (3.6)	18 (3.6)	18 (3.6)	18 (3.6)
1	146 (73.2)	129 (36.9)[a]	82 (21.3)	64 (16.2)	57 (14.8)	56 (14.6)	56 (14.6)	56 (14.6)
2	71 (87.2)[b]	166 (69.6)	113 (43.6)[a]	76 (31.2)[a]	63 (27.2)[a]	62 (26.8)[a]	58 (26.0)[a]	58 (26.0)[a]
3	46 (96.3)	95 (88.4)[b]	110 (65.3)	81 (47.1)	53 (37.7)	46 (35.9)	43 (34.5)	43 (34.5)
4	12 (98.6)	37 (95.7)	70 (79.1)[b]	69 (60.7)	40 (45.6)	20 (39.8)	13 (37.1)	12 (36.9)
5	4 (99.4)	15 (98.6)	58 (90.5)	66 (73.8)	51 (55.6)	20 (43.8)	8 (38.7)	6 (38.1)
6	2 (99.8)	5 (99.6)	31 (96.6)	58 (85.2)[b]	43 (64.1)	25 (48.7)	15 (41.6)	5 (39.1)
7	1 (100.0)	1 (99.8)	16 (99.8)	33 (91.7)	63 (76.5)[b]	49 (58.4)	19 (45.4)	4 (39.8)
8	0 (0)	1 (100.0)	1 (100.0)	21 (95.9)	58 (88.0)	62 (70.6)	26 (50.5)	10 (41.8)
9	0 (0)	0 (0)	0 (0)	10 (97.8)	34 (94.7)	54 (81.3)[b]	57 (61.7)	27 (47.1)
10	0 (0)	0 (0)	0 (0)	8 (99.4)	14 (97.4)	41 (89.3)	56 (72.8)	45 (56.0)
11	0 (0)	0 (0)	0 (0)	3 (100.0)	9 (99.2)	23 (93.9)	50 (82.6)[b]	45 (64.9)
12	0 (0)	0 (0)	0 (0)	0 (0)	2 (99.6)	24 (98.6)	44 (91.3)	57 (76.1)[b]
13	0 (0)	0 (0)	0 (0)	0 (0)	1 (99.8)	5 (99.6)	24 (96.1)	57 (87.4)
14	0 (0)	0 (0)	0 (0)	0 (0)	1 (100.0)	2 (100.0)	13 (98.6)	30 (93.3)
15	0 (0)	0 (0)	0 (0)	0 (0)	0 (0)	0 (0)	4 (99.4)	17 (96.6)
16	0 (0)	0 (0)	0 (0)	0 (0)	0 (0)	0 (0)	1 (99.6)	13 (99.2)
17	0 (0)	0 (0)	0 (0)	0 (0)	0 (0)	0 (0)	1 (99.8)	4 (100.0)
18	0 (0)	0 (0)	0 (0)	0 (0)	0 (0)	0 (0)	1 (100.0)	0 (0)

[a]The number of missing samples accounts for 25% of the total. [b]The number of missing samples accounts for 75% of the total.

Table 4: The item missing conditions of the simulation sets under MNAR ($N = 507$).

Number of missing items (n (%))	5%	10%	15%	20%	25%	30%	35%	40%
0	171 (33.7)a	61 (12.0)	23 (4.5)	15 (3.0)	15 (3.0)	13 (2.6)	13 (2.6)	13 (2.6)
1	177 (68.6)	146 (40.8)a	76 (19.5)	40 (10.8)	33 (9.5)	31 (8.7)	30 (8.5)	30 (8.5)
2	98 (88.0)b	143 (69.0)	115 (42.2)a	69 (24.5)	40 (17.4)	33 (15.2)	32 (14.8)	32 (14.8)
3	43 (96.4)	91 (87.0)b	112 (64.3)	75 (39.3)a	53 (27.8)a	29 (20.9)	23 (19.3)	19 (18.5)
4	12 (98.8)	43 (95.5)	83 (80.7)b	98 (58.6)	63 (40.2)	36 (28.0)a	15 (22.3)	13 (21.1)
5	2 (99.2)	16 (98.6)	52 (90.9)	84 (75.1)b	83 (56.6)	59 (39.6)	16 (25.4)a	6 (22.3)
6	4 (100.0)	7 (100.0)	32 (97.2)	61 (87.2)	76 (71.6)	82 (55.8)	48 (34.9)	27 (27.6)a
7	0 (0)	0 (0)	11 (99.4)	32 (93.5)	64 (84.2)b	72 (70.0)	59 (46.5)	31 (33.7)
8	0 (0)	0 (0)	2 (99.8)	18 (97.0)	43 (92.7)	57 (81.3)b	78 (61.9)	67 (46.9)
9	0 (0)	0 (0)	1 (100.0)	9 (98.8)	24 (97.4)	43 (89.7)	85 (78.7)b	54 (57.6)
10	0 (0)	0 (0)	0 (0)	3 (99.4)	9 (99.2)	28 (95.3)	43 (87.2)	81 (73.6)
11	0 (0)	0 (0)	0 (0)	2 (99.8)	4 (100.0)	19 (99.0)	37 (94.5)	55 (84.4)b

Table 4: Continued.

Number of missing items (n (%))	5%	10%	15%	20%	25%	30%	35%	40%
12	0 (0)	0 (0)	0 (0)	1 (100.0)	0 (0)	2 (99.4)	16 (97.6)	34 (91.1)
13	0 (0)	0 (0)	0 (0)	0 (0)	0 (0)	2 (99.8)	7 (99.0)	25 (96.1)
14	0 (0)	0 (0)	0 (0)	0 (0)	0 (0)	1 (100.0)	4 (99.8)	16 (99.2)
15	0 (0)	0 (0)	0 (0)	0 (0)	0 (0)	0 (0)	1 (100.0)	1 (99.4)
16	0 (0)	0 (0)	0 (0)	0 (0)	0 (0)	0 (0)	0 (0)	2 (99.8)
17	0 (0)	0 (0)	0 (0)	0 (0)	0 (0)	0 (0)	0 (0)	1 (100.0)

[a]The number of missing samples accounts for 25% of the total. [b]The number of missing samples accounts for 75% of the total.

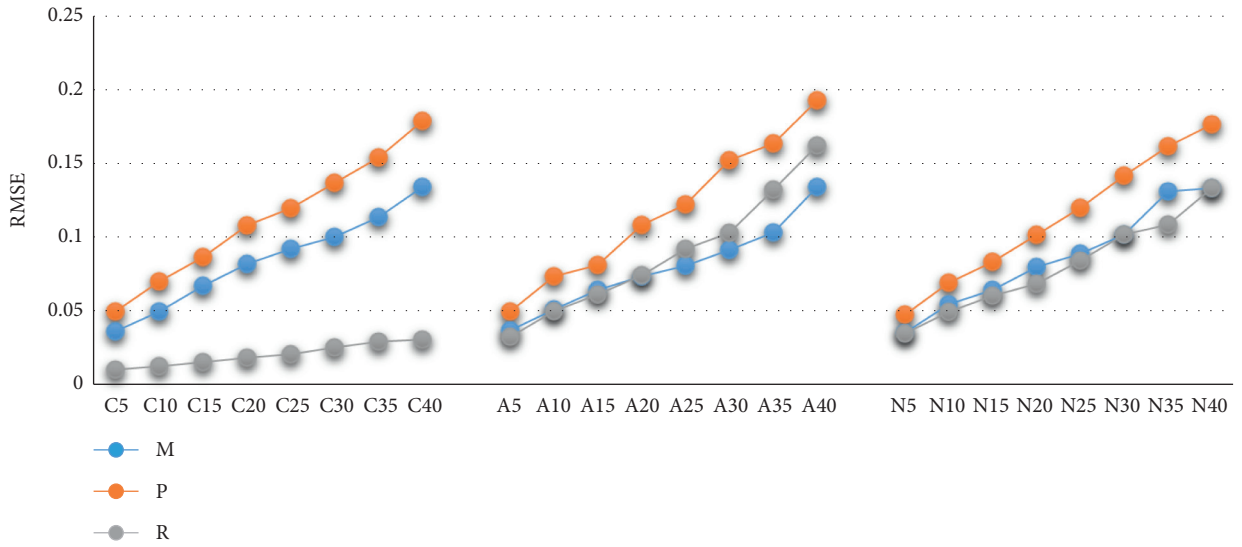

Figure 1: The evaluations of fitting effects by RMSE.

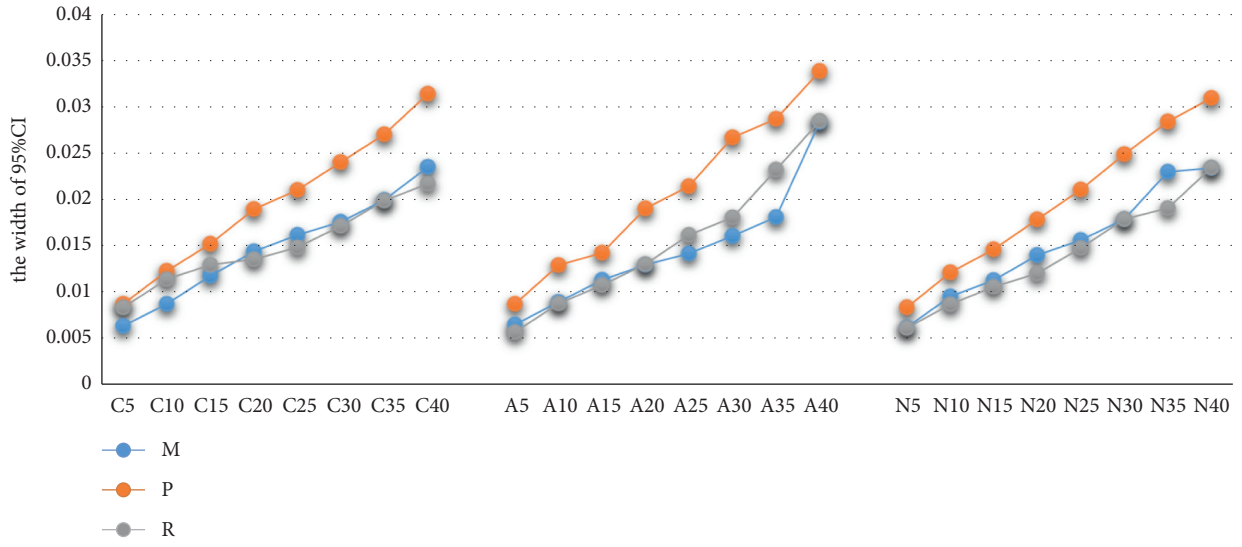

Figure 2: The evaluations of fitting effects by the width of 95% CI.

3.2.3. Spearman Correlation Coefficient. SCC is an indicator representing the fitting correlation. With the increase of deletion ratio, the correlation becomes lower and lower, and the value of SCC is between 1 and 0.85. Under the MCAR mechanism, although the missing ratio reaches 40%, the SCC of the fitting set and the training set can still reach 0.9. When the deletion ratio is less than 20%, the SCC value of the three methods can reach 0.95. When the deletion ratio is

less than 30%, the SCC of RFR can still be greater than 0.95, and the degree of correlation is higher. See Figure 3 for details.

4. Discussion

In this paper, three missing mechanisms, eight missing ratios, and three missing value processing methods (MS, PMM, and RFR) were set to fill the data gaps in the SDS. The SDS has 20 items of self-rating questions and the correlations between items are good, which is easier to lose data due to various reasons such as incomprehension of questions, avoidance of sensitive questions, loss of follow-up, and so on [28]. In addition, the absence of data will cause the reduction of effective data, increase the confidence interval, affect the statistical analysis, and eventually lead to the bias of study results, which may draw conclusions that are not consistent with the facts [4]. Therefore, an effective way to deal with the problem of data missing is in need.

In clinical research, too many missing items on the scale may result in inaccurate or biased estimations. For example, some researchers believed that the validity of statistical analysis would be significantly reduced when one-third of the items in the SF-12 scale was missing [28]. In the study on data missing of the Unified Dyskinesia Rating Scale (UDysRS), some other researchers found that if the number of missing items reached 8 or more, the validity of statistical analysis towards study results would be lost [29], indicating that the missing items of the scale should be controlled within a certain range so as not to affect the final statistical results. In this study, when the missing ratio of SDS was small (5%, 10%), the number of missing items in the SDS for most subjects was below or equal to 5. When the missing ratio reached 30%, the numbers in most patients concentrated in 5 to 8. While, as the proportion increased to 35% or 40%, a small number of subjects even had missing items of 18. Therefore, in the actual research, if the data missing ratio is greater than 30%, attention should be paid to the subjects' responses to the scale items. If there are subjects with many missing items in the scale, researchers should consider removing them from the study to ensure the reliability of the evaluation results as much as possible.

It can be seen from this study that in most simulation scenarios, the fitting result of the RFR algorithm is closest to the training set and has the best fitting effect in terms of fitting accuracy, precision, and correlation, especially under the mechanism of MCAR. The RFR algorithm does not need to consider the distribution of variables. It is a nonparametric estimation algorithm, which is more widely used [30, 31]. Some researchers believe that the fitting effect of the missing forest is worse than other methods, such as the MS method, k nearest distance filling, or Multivariable Interpolation by chained equations (mice) [32, 33].

Furthermore, when the deletion ratio is less than 20%, the RMSE results of MCAR are given, and the results of other RFRs are very close to those of Ms.; however, when the deletion ratio is larger, RFR reflects better fitting accuracy and correlation. Therefore, the RFR algorithm is the most suitable fitting method for the SDS scale in this study. At the same time, it is also found that with the increase of the missing ratio, the accuracy, precision, and correlation of the fitting set decrease. When the missing ratio is less than 30%, RFR or MS can also control results to a relatively good extent (RMSE <1.0, 95% CI width <0.02, SCC >0.95). Therefore, in practical research, we should pay attention to the proportion and mechanism of data loss and select appropriate data fitting methods.

Among the three missing mechanisms, the MCAR, under which the fitting effect of the three interpolation methods was better than that of the other cases, and the smaller the missing ratio, the closer the fitting result was to the actual value, was the optimal one. The case of the MAR was more complex for the simple reason that it is kind of missing was directly related to the missing of other variables and the data simply could not be processed by the straightforward elimination or the method of Single Imputation. Otherwise, it would cause the bias of study results [4]. The RFR algorithm was more suitable for this case. When it comes to the most complicated MNAR mechanism, the results in this paper showed that the fitting effect of the three interpolation methods, in this case, was not as good as that of under the other two mechanisms, but the RFR algorithm also had some good performances under MNAR.

This study had some limitations. The range of the missing ratio of simulation set in this study is 5%~40%, and a specific ratio of simulation data missing is selected at an interval of 5%. According to previous studies, it is found that the proportion of missing data is less than 5%, and more accurate analysis results can be obtained by using the deletion method, while more than 40% of missing data fitting will not get more available results, and more literature use inconsistent fitting methods between 5% and 40%. It is difficult for researchers to choose which fitting method to use, and the results are more accurate [34–37]. In the practical application of the SDS scale, the missing ratio should be regarded as a parameter to determine the missing fitting path. Due to the ideal state of missing ratios and missing mechanisms, the simulated dataset in this paper might be slightly different from that in the actual situation, so the study results might not reflect the data missing patterns in real studies as well as possible. In addition, this study only focused on the SDS and the data missing fitting path is only based on the simulation inference of poststroke depression data, which has not been applied to the actual clinical process. The fitting effect needs to be further verified. In addition, in this study, the fitting results of PMM do not show any advantages over the fitting results of MS and RFR, which may be related to the number of iterations set by PMM. In this study, the number of iterations is set to 5. The results may be better if it is set to 50 or more, but this method costs more than the running time of R software of MS and RFR and is more complex. Therefore, from the perspective of time cost, other methods can be preferred. At last, PMM is suitable for continuous variables in monotone deletion mode. This may also be a reason why the PMM results in this article are not very good.

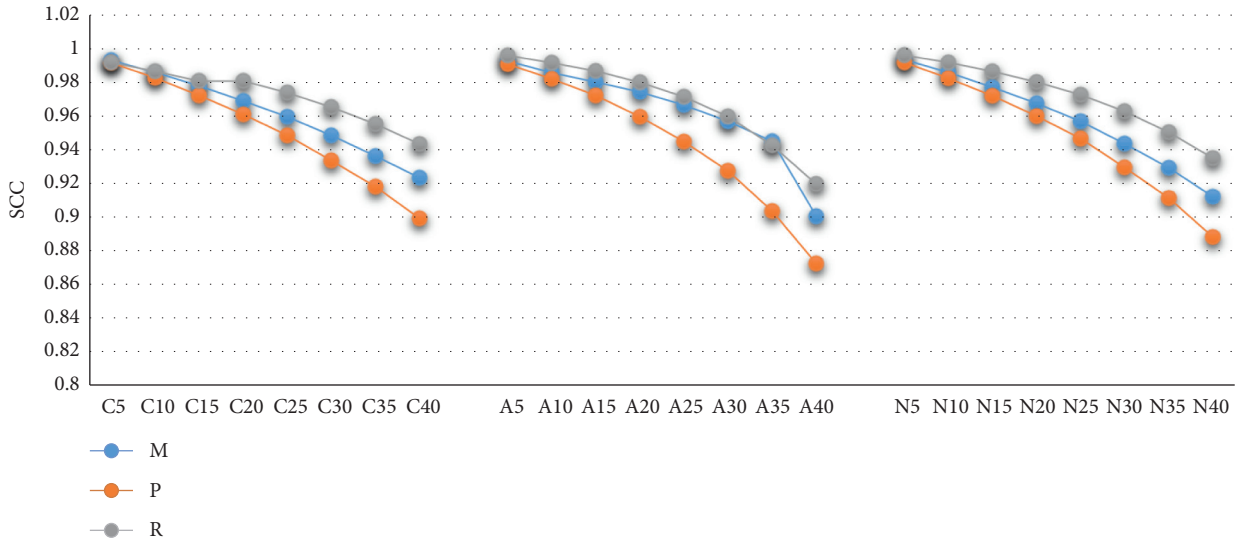

Figure 3: The evaluations of fitting effects by SCC.

5. Conclusions

To sum up, in this study, when dealing with the problem of missing data in scales, the optimal fitting path is ① under the MCAR deletion mechanism, when the deletion proportion is less than 20%, the MS method is the most convenient; when the missing ratio is greater than 20%, the RFR algorithm is the best fitting method. ② Under the Mar mechanism, when the deletion ratio is less than 35%, the MS method is the most convenient. When the deletion ratio is greater than 35%, RFR has a better correlation. ③ Under the mechanism of MNAR, RFR is the best data fitting method, especially when the missing proportion is greater than 30%. In reality, when the deletion ratio is small, the complete case deletion method is the most commonly used, but the RFR algorithm can greatly expand the application scope of samples and save the cost of clinical research when the deletion ratio is less than 30%. The best way to deal with data missing should be based on the missing mechanism and proportion of actual data, and choose the best method between the statistical analysis ability of the research team, the effectiveness of the method, and the understanding of readers.

Data Availability

The datasets used during the study are available from the corresponding author on reasonable request.

Conflicts of Interest

The authors declare that they have no conflicts of interest.

Acknowledgments

This work was supported by The National Natural Science Foundation of China (No. 8170142146) and The Fundatmental Research Funds for the Central Public Welfare Research Institutes (No. ZZ14-YQ-037).

References

[1] A. A. Stone, J. S. Turkkan, C. A. Bachrach, H. S. Kurtzman, J. B. Jobe, and V. S. Cain, *The Science of Self-Report: Implications for Research and Practice*, Lawrence Erlbaum Associates Publishers, Mahwah, NJ, USA, 2003.

[2] G. E. Matt, C. Vázquez, and W. K. Campbell, "Mood-congruent recall of affectively toned stimuli: a meta-analytic review," *Clinical Psychology Review*, vol. 12, no. 2, pp. 227–255, 1992.

[3] S. Shiffman, M. Hufford, M. Hickcox, J. A. Paty, M. Gnys, and J. D. Kassel, "Remember that? A comparison of real-time versus retrospective recall of smoking lapses," *Journal of Consulting and Clinical Psychology*, vol. 65, no. 2, pp. 292–300, 1997.

[4] L. Xia, *The Simulation Studies of Imputation Methods of Missing Data in the Scale*, China Medical University, Taichung, Taiwan, 2018.

[5] L. R. J. D'Agostino, R. D'Agostino, M. L. Cohen et al., "The prevention and treatment of missing data in clinical trials," *New England Journal of Medicine*, vol. 367, no. 14, pp. 1355–1360, 2012.

[6] H. S. Lynn and B. Y. Tsang, "Developing a predictive tool for psychological well-being among Chinese adolescents in the presence of missing data," *BMC Medical Research Methodology*, vol. 11, no. 1, p. 119, 2011.

[7] W. W. K. Zung, C. B. Richards, and M. J. Short, "Self-rating depression scale in an outpatient clinic," *Archives of General Psychiatry*, vol. 13, no. 6, pp. 508–515, 1965.

[8] M. W. Ali and E. Talukder, "Analysis of longitudinal binary data with missing data due to dropouts," *Journal of Biopharmaceutical Statistics*, vol. 15, no. 6, pp. 993–1007, 2005.

[9] J. Wang, J.-J. Han, and Q. Huang, "Statistical considerations on missing data in clinical trials," *The Chinese Journal of Clinical Pharmacology*, vol. 32, no. 05, pp. 469–472, 2016.

[10] K. Wang, H. Yang, and J. Tian, "Comparison of effects of completely random missing data processing methods based on Monte Carlo simulation," *Chinese Journal of Health Statistics*, vol. 37, no. 2, pp. 140–143, 2020.

[11] J. Van Hulse and T. M. Khoshgoftaar, "A comprehensive empirical evaluation of missing value imputation in noisy

software measurement data," *Journal of Systems and Software*, vol. 81, no. 5, pp. 691–708, 2008.

[12] S.-Y. Li, *Study on Multiple Imputation of Missing Data in the Survey Data*, Hebei University of Economics and Business, Shijiazhuang, China, 2015.

[13] D. B. Rubin, "Inference and missing data," *Biometrika*, vol. 3, pp. 581–592.

[14] D., B. Hall, "Data analysis using regression and multilevel/hierarchical models," *Journal of the American Statistical Association*, vol. 104, no. 487, pp. 1275-1276, 2009.

[15] R. J. A. Little and D. B. Rubin, *Statistical Analysis with Missing Data*, Wiley, Hoboken, NJ, USA, 1986.

[16] B. Tian, "Single imputation methods of missing data," *Yinshan Academic Journal (Natural Science Edition)*, vol. 3, no. 25, pp. 19–21, 2011.

[17] K. Wang, H. Yang, J. Tian, C.-H. Li, Q.-H. Han, and Y.-B. Zhang, "Comparison of effects of completely random missing data processing methods based on Monte Carlo simulation," *Chinese Journal of Health Statistics*, vol. 2, pp. 298–301, 2020.

[18] D. A. Paul, *The Missing Data*, Shanghai People's Publishing House, Shanghai, China, 2012.

[19] J. Yan, *Multiple Imputation: Issues and Guidance for Practice*, Chongqing University Press, Chongqing, China, 2017.

[20] L. Rutkowski, M. Jaworski, L. Pietruczuk, and P. Duda, "The CART decision tree for mining data streams," *Information Sciences*, vol. 266, pp. 1–15, 2014.

[21] A. D. Shah, J. W. Bartlett, J. Carpenter, O. Nicholas, and H. Hemingway, "Comparison of random forest and parametric imputation models for imputing missing data using mice: a caliber study," *American Journal of Epidemiology*, vol. 179, no. 6, pp. 764–774, 2014.

[22] A. Pantanowitz and T. Marwala, "Evaluating the impact of missing data imputation through the use of the random forest algorithm," *in Advances in Intelligent & Soft Computing*, pp. 53–62, Warsaw, Poland, 2008.

[23] X. Zhang and Y. Cheng, "Imputation of missing values for compositional data based on random forest," *Chinese Journal of applied probability and statistics*, vol. 33, no. 1, p. 9, 2017.

[24] C. Jenkinson, R. Harris, and R. Fitzpatrick, "The amyotrophic lateral sclerosis assessment questionnaire (ALSAQ-40): evidence for a method of imputing missing data," *Amyotrophic Lateral Sclerosis*, vol. 8, no. 2, pp. 90–95, 2007.

[25] J. E. Galimard, S. Chevret, E. Curis, and M. Resche-Rigon, "Heckman imputation models for binary or continuous MNAR outcomes and MAR predictors," *BMC Medical Research Methodology*, vol. 18, 2018.

[26] A. Pedersen, E. Mikkelsen, D. Cronin-Fenton et al., "Missing data and multiple imputation in clinical epidemiological research," *Clinical Epidemiology*, vol. 9, pp. 157–166, 2017.

[27] C. Jenkinson, C. Heffernan, H. Doll, and R. Fitzpatrick, "The Parkinson's disease questionnaire (PDQ-39): evidence for a method of imputing missing data," *Age and Ageing*, vol. 5, pp. 497–502, 2006.

[28] J. L. Schafer and M. K. Olsen, "Multiple imputation for multivariate missing-data problems: a data analyst's perspective," *Multivariate Behavioral Research*, vol. 33, no. 4, pp. 545–571, 1998.

[29] S. Luo, X. Ren, W. Han, C. G. Goetz, and G. T. Stebbins, "Missing data in the unified dysksinesia rating scale (UDysRS)," *Movement Disorders Clinical Practice*, vol. 5, no. 5, pp. 523–526, 2018.

[30] A. Liaw and M. Wiener, "Classification and regression by randomForest," *R News*, vol. 2, no. 3, pp. 18–22, 2002.

[31] L. Breiman, "Random forests," *Machine Learning*, vol. 45, no. 1, pp. 5–32, 2001.

[32] J.-D. E. M. Yang, "Algorithm and its applications," *Journal of Anqing Normal University (Natural Science Edition)*, vol. 15, no. 4, pp. 30–35, 2009.

[33] L. Shen, G. Hu, and L. Chen, "Application of MissForest algorithm for imputing missing data," *Chinese Journal of Health Statistics*, vol. 31, no. 5, p. 3, 2014.

[34] F. M. Shrive, H. Stuart, H. Quan, and W. A. Ghali, "Dealing with missing data in a multi-question depression scale: a comparison of imputation methods," *BMC Medical Research Methodology*, vol. 6, no. 1, p. 57, 2006.

[35] J. Van Hulse and T. M. Khoshgoftaar, "A comprehensive empirical evaluation of missing value imputation in noisy software measurement data," *Journal of Systems and Software*, vol. 81, no. 5, pp. 691–708.

[36] P. R. Houck, S. Mazumdar, T. Koru-Sengul et al., "Estimating treatment effects from longitudinal clinical trial data with missing values: comparative analyses using different methods," *Psychiatry Research*, vol. 129, no. 2, pp. 209–215, 2004.

[37] L. Hua, N. Shi, Y. Yang, and T. Zhao, "Comparison of different methods in dealing with missing values of missing at random," *Journal of Zhengzhou University (Medical Science)*, vol. 3, pp. 41–44, 2012.

Hindawi
Evidence-Based Complementary and Alternative Medicine
Volume 2022, Article ID 4654793, 16 pages
https://doi.org/10.1155/2022/4654793

Review Article

Efficacy and Safety of "Three Chinese Patent Medicines and Three TCM Prescriptions" for COVID-19: A Systematic Review and Network Meta-Analysis

Shuo Zhang,[1,2] **Zhen Yang**,[3] **Zhen-Lin Chen**,[4] **Zhuo-Ning Li**,[1] **Shi-Jun Yue**,[1] **Jia-Jia Li**,[1] **and Yu-Ping Tang**[1]

[1]*Key Laboratory of Shaanxi Administration of Traditional Chinese Medicine for TCM Compatibility, State Key Laboratory of Research & Development of Characteristic Qin Medicine Resources (Cultivation), Shaanxi Key Laboratory of Chinese Medicine Fundamentals and New Drugs Research, Shaanxi Collaborative Innovation Center of Chinese Medicinal Resources Industrialization, Shaanxi University of Chinese Medicine, Xi'an 712046, Shaanxi Province, China*
[2]*School of Clinical Medicine (Guang'anmen Hospital), Beijing University of Chinese Medicine, Beijing 100029, China*
[3]*School of Public Health, Shaanxi University of Chinese Medicine, Xi'an 712046, Shaanxi Province, China*
[4]*International Programs Office, Shaanxi University of Chinese Medicine, Xi'an 712046, Shaanxi Province, China*

Correspondence should be addressed to Yu-Ping Tang; yupingtang@sntcm.edu.cn

Received 25 September 2021; Revised 7 November 2021; Accepted 14 December 2021; Published 12 January 2022

Academic Editor: Xuezhong Zhou

Objective. To systematically evaluate the efficacy, safety, and precision of TMTP for COVID-19. *Methods*. Randomized controlled trials and retrospective studies were searched in 11 electronic databases. This network meta-analysis included trials using TMTP to treat patients with COVID-19. The traditional pairwise meta-analysis was done by using Stata 15, and Bayesian network meta-analysis was done with WinBUGS. *Results*. 18 trials were included with 2036 participants and 7 drugs. The results showed that LHQW had the most significant effects on improving expectoration, shortness of breath, sore throat, nausea, emesis, inappetence, muscle soreness, and headache, and it could produce the least adverse reactions. XBJ was the best drug for fever, fatigue, and diarrhea, which showed great advantages in lowering WBC levels. XFBD was the most effective drug for cough and chest distress, which had the least exacerbation rate. JHQG was the most effective for rhinobyon and rhinorrhea, while QFPD was the best drug in decreasing CRP levels. *Conclusion*. This study was the first most large-scale and comprehensive research of TMTP for COVID-19. The results showed that LHQW had good efficacy without obvious adverse reactions. Therefore, we believe that it should be firstly recommended for COVID-19 treatment. In addition, XBJ is recommended for patients with a severe fever, fatigue, and diarrhea, and JHQG is recommended for patients with obvious rhinobyon and rhinorrhea; then, XFBD is recommended for patients with cough and chest tightness as the main manifestation. Our findings will help experts develop new COVID-19 treatment guidelines to better guide clinical medication for protecting the health of COVID-19 patients.

1. Introduction

A severe respiratory disease caused by a novel coronavirus infection broke out in late 2019. Since its outbreak, the Corona Virus Disease 2019 (COVID-19) has spread rapidly and enveloped most of the world which is highly contagious and deadly [1]. The increase in the number of pneumonia patients has aroused high vigilance from the World Health Organization (WHO) and China [2] and has been listed as a public health emergency of international concern. As of 8 December 2021, COVID-19 has caused 267534728 confirmed cases and 5290066 deaths worldwide. The COVID-19 pandemic has not only posed a huge challenge to medical workers but also caused social, economic, and political damage. Although a large number of clinical trials have been conducted to study the drugs that were used to treat

COVID-19, no therapeutic approach has been effective in its treatment up to now [3]. Moreover, during the sudden outbreak of COVID-19, there is a lack of effective chemical drugs (CDs) for prevention and control in clinical practice, and the interim screening and development of new drugs may take a long time, making it difficult to apply them in a timely way for clinical treatment. Therefore, the unique advantages of traditional Chinese medicine (TCM) multi-target interventions had become an indispensable systemic approach for patients, and significant progress has been made in China's battle against COVID-19 in China [4].

TCM has been proven to be effective in treating patients with influenza and has very successful experience in the prevention and treatment of infectious diseases. Three Chinese patent medicines and three TCM prescriptions (TMTP) were the key recommended drugs in the *Novel Coronavirus Infection for the Diagnosis and Treatment of Pneumonia* published by the National Health Commission of the People's Republic of China. And the China Administration of Traditional Chinese Medicine pointed out that TMTP had a great clinical advantage in the prevention and control of COVID-19. In addition, three Chinese patent medicines included *Lian-Hua-Qing-Wen* (LHQW), *Jin-Hua-Qing-Gan* (JHQG), and *Xue-Bi-Jing* (XBJ), and three TCM prescriptions included *Qing-Fei-Pai-Du* (QFPD), *Xuan-Fei-Bai-Du* (XFBD), and *Hua-Shi-Bai-Du* (HSBD), which had played an important role in the fight against the epidemic by treating the disease based on syndrome differentiation according to the patient's individuality and seasonal and local conditions. Although TMTP was widely used in clinical practice, there were inconsistent research conclusions due to the different sample sizes, outcome indicators, and unified evaluation criteria in clinical reports, and accurate conclusions cannot be drawn, which made it difficult to grasp its therapeutic effect and clinical advantages. Therefore, we conducted a comprehensive systematic review and meta-analysis to evaluate TMTP efficacy and safety of COVID-19 patients from a variety of clinical symptoms, in order to serve for COVID-19 prevention and control better.

It is a challenging task to comprehensively analyze the present clinical evidence for the efficacy and safety of TMTP for COVID-19 by using traditional meta-analysis methods because there is a lack of head-to-head trials that directly compare certain treatments among existing trials. Bayesian network meta-analysis, also known as a mixed treatment comparison method, is a valuable tool in comparative effectiveness research, which enables the comparison of multiple interventions to incorporate clinical evidence from both direct and indirect treatment comparisons in a network of treatments and associated trials [5], and allows indirect comparison without head-to-head trials to simultaneously compare several treatments by using a common comparator and combined direct and indirect comparisons while retaining randomness in individual trials [6–8].

This study aimed to systematically evaluate the efficacy and safety of TMTP for COVID-19 using Bayesian network meta-analysis, and the competing drugs in each outcome were ranked to obtain the most effective one. The study focused on the diversity of symptoms in patients with COVID-19, which was the most large-scale and comprehensive research on this issue so far. We hope that our study will provide up-to-date information on the treatment of COVID-19.

2. Data and Methods

This systematic review and Bayesian network meta-analysis was conducted and reported following the Preferred Reporting Items for Systematic Reviews and Meta-analyses (PRISMA) with Cochrane methodology [9]. This study has been registered and the PROSPERO number is CRD42021240869.

2.1. Literature Search. From the establishment of each electronic database to November 6, 2021, randomized controlled trials or retrospective studies using TMTP to treat COVID-19 were searched in the following 11 electronic databases: Medline (from 1946 to 2020), Embase (from 1974 to 2020), Cochrane Library (from 1966 to 2020), PubMed (from 1959 to 2020), Web of Science (from 1986 to 2020), SpringerLink (from 1996 to 2020), ClinicalTrials.gov, the Chinese National Knowledge Infrastructure (CNKI, from 1980 to 2020), Chinese Biomedical Literature Database (CBM, from 1978 to 2020), Wanfang Database (from 1998 to 2020), and Weipu Database (from 1989 to 2020). Forward and backward citation searching was conducted for all eligible trials. Following terms were used for searching: ("COVID-19" OR "corona virus disease 2019" OR "coronavirus disease 2019" OR "severe acute respiratory syndrome coronavirus" OR "SARS-CoV-2" OR "novel corona virus" OR "novel coronavirus" OR "2019-nCoV" OR "nCoV-2019") AND ("lianhuaqingwen" OR "lianhua qingwen" OR "lian hua qing wen") OR ("jinhuaqinggan" OR "jinhua qinggan" OR "jin hua qing gan") OR ("xuebijing" OR "xue bi jing") OR ("qingfeipaidu" OR "qingfei paidu" OR "qing fei pai du") OR ("xuanfeibaidu" OR "xuanfei baidu" OR "xuan fei bai du") OR ("huashibaidu" OR "huashi baidu" OR "hua shi bai du") AND ("clinical trial" OR "randomized controlled trial" OR "randomized controlled trial" OR "lin chuang yan jiu" OR "lin chuang shi yan"). And we did not specify the language and status of publications in our literature search. Additionally, we manually searched bibliographies of included trials and related reviews for additional references.

2.2. Criteria for Literature Inclusion

2.2.1. Type of Research. This network meta-analysis included clinical trials using TMTP to treat COVID-19. Trials were excluded if (a) no control group was used; (b) TMTP was not used in the experimental group; (c) there is a combination with other drugs; (d) trials on effective analysis data cannot be obtained; (e) they are reviews, conference paper, case reports, experience sharing, animal trials, etc.; (f) they are repeatedly published articles and plagiarized trials.

2.2.2. Study Subjects. COVID-19 patients who were not restricted by age, gender, or nationality were eligible for inclusion in this study. Please refer to the "New Coronavirus Pneumonia Diagnosis and Treatment Program" (trial seventh edition) for details on COVID-19 criteria [10].

2.2.3. Preventative Measures. The intervention measures in the experimental group should be TMTP single drug combined with CD, and the control group should be CD.

2.2.4. Results. The primary outcomes were defined as clinical effect and CT recovery rate. Clinical effect was evaluated based on the improvement of clinical symptoms of patients before and after treatment, which could better reflect the therapeutic effect of drugs. Symptoms were classified as significant, effective, or ineffective according to the degree of relief. Moreover, CT played an important role in early screening and disease surveillance for COVID-19, and its changes could significantly reflect the therapeutic effect. The secondary outcomes included nucleic acid negative rate, disappearance rate of primary symptoms (fever, cough, fatigue), disappearance rate of respiratory (expectoration, shortness of breath, chest distress, rhinobyon, rhinorrhea, sore throat), gastrointestinal (nausea, diarrhea, emesis, inappetence), and other symptoms (muscular soreness, headache), inflammatory biomarkers such as C-reactive protein (CRP) and white blood cell (WBC), as well as exacerbation rate and adverse reactions.

2.3. Study Selection and Data Extraction. Before starting the screening processes, two researchers who participated in training and calibration exercises independently screened the titles and abstracts of potentially eligible trials that were in duplicate; then, they independently retrieved and reviewed the full text of the possible trials in duplicate based on the inclusion and exclusion criteria and compared their results. If there was disagreement, they agreed through discussion or submitted it to a third party for evaluation. And before the screening process, the third party used a standardized screening form and performed calibration exercises. The screening process was conducted in Endnote X9.

Before the data extraction process began, we conducted various forms of calibration exercises and pilots. Then, according to the inclusion and exclusion criteria mentioned above, the two researchers used standardized tables to independently extract data in duplicate from all eligible trials. In case of disagreement, they agreed through discussion or submitted it to a third party. All the eligible trials were published in English.

For all eligible trials, the researchers extracted data on the following characteristics:

(1) The basic information of the study (author's name, title of the study, year of publication, country/region, and publication status)

(2) Study characteristics (sample size, source of cases, age, diagnostic criteria, and inclusion and exclusion criteria)

(3) Intervention and control measures (dosage form, dose, and duration)

(4) Research methodology (random scheme generation, allocation hiding, blind method, incomplete result data, selective reporting, other biases, and loss of follow-up)

(5) Outcome measures

2.4. Assessment of Literature Quality. The methodological quality of each included study was independently assessed by two reviewers based on 2 tools. The Cochrane collaboration tool has been used to assess the quality of randomized controlled trials, and it comprised the following 7 aspects: random sequence generation, allocation concealment, blind method, incomplete result data, selective reporting, and other biases. The quality assessment results of each item can be divided into three grades: "low risk," "high risk," and "unclear." The risk coefficient is lower because of the more rigorous design and higher methodological quality of each RCT. Newcastle Ottawa Scale (NOS) has been used to assess the quality of retrospective studies. This method includes 3 aspects of evaluation: the selection method, comparability, and contact exposure assessment method of case and control groups. The higher the score is, the greater the quality of the learning is. When necessary, the consensus on this issue was studied with the help of a third party.

2.5. Statistical Analysis. The traditional pairwise meta-analysis was done by using Stata 15 (StataCorp, College Station, TX, USA), and Bayesian network meta-analysis was done with WinBUGS version 14.3 (MRC Biostatistics Unit, Cambridge, UK). Both the continuous and dichotomous outcomes were derived from the included trials without any conversion. The dichotomous outcomes were described by relative risk (RR) and 95% confidence interval (CI); in addition, mean difference (MD) and 95% CI were used to describe the effect value of the intergroup comparison. Heterogeneity was determined according to the results of the I^2 test. $I^2 < 50\%$ indicated the low heterogeneity of interstudy, and the fixed effect model was adopted. Furthermore, the random effect model was adopted when $I^2 > 50\%$ [11], which was also used to generate direct and mixed treatment comparison estimates. Direct estimates of any two interventions were obtained by pooling data from clinical trials that compared the same interventions face to face. And the mixed treatment comparison estimates of interventions were obtained by combining direct clinical trial data for comparative interventions with the indirect estimates between the interventions through a common comparator. Normal prior distributions, noninformative uniform, and 3 different sets of starting values were used to fit the model. At the same time, 4 chains, 2.5 initial values

scaling, 20000 tuning iterations, 50000 simulation iterations, and 10 thinning intervals were used to obtain the posterior distributions of model parameters. Subgroup analysis was used to evaluate the therapeutic effects of different drugs. Inverted funnel plots and Egger's regression test were used to determine publication bias when the number of included studies exceeded 10 in the network meta-analysis [12].

3. Results

3.1. Results of Our Literature Search. Based on the above retrieval strategies, a total of 2796 potentially relevant trials were retrieved from 11 electronic databases, and 632 trials were retrieved after deleting 2164 duplicates. After reviewing the titles and abstracts, 604 articles were excluded because they did not comply with the inclusion criteria, and 28 trials initially met the predetermined requirements for detailed evaluation by reading the full text. Finally, 18 trials were included for meta-analysis [13–30]. The PRISMA flow diagram of the literature retrieval process was shown in Figure 1. All included trials have been published as full articles.

3.2. Basic Characteristics of the Included Studies. Table 1 summarized the basic characteristics of the eligible 18 trials, and a total of 2036 patients with COVID-19 were included. Sample sizes ranged from 12 to 295. In these 18 trials, 10 were randomized controlled trials [13, 15, 18, 19, 21, 23, 24, 27, 29, 30] and 8 were retrospective studies [14, 16, 17, 20, 22, 25, 26, 28]. 7 trials used LHQW *vs.* CD [14, 16, 18, 22, 25–27], 5 trials used XBJ *vs.* CD [13, 17, 21, 23, 29], 3 used QFPD *vs.* CD [19, 20, 28], 1 used JHQG *vs.* CD [15], 1 used XFBD *vs.* CD [24], and 1 used HSBD *vs.* CD [30]. Figure 2 provided the network plot of all the included trials. Table A.1 showed the pooled hazard ratios of different drugs for outcomes. In addition, the specific percentage ranking of competing drugs was revealed in Table A.2, and the drug ranking histogram was shown in Figure A.1.

3.3. Risk of Bias Assessment of the Literature Included in the Study. The methodological quality of 10 randomized controlled trials was summarized in Table A.3, and the criteria in the Cochrane Handbook for Systematic Reviews of Interventions were used to assess the risk of bias in the study. Although randomization was announced in all 10 trials, 5 trials used random number table [15, 18, 21, 23, 27], 1 used the R 3.6.2 software [30], 1 used the method of flip a coin [24], and 3 did not report the method [13, 19, 29]. Moreover, only 1 trial reported allocation concealment [21], and all the trials did not report the blind method. The quality of 8 retrospective studies was assessed by NOS. Table A.4 summarized the NOS scores of each study, all of which were of fair quality. Since fewer than 10 trials were included in each subgroup, publication bias could not be adequately analyzed.

3.4. Outcomes

3.4.1. Clinical Effect. Clinical effect was reported in 6 trials, in which 2 used LHQW *vs.* CD [18, 27], 2 used XBJ *vs.* CD [13, 29], and 2 used QFPD *vs.* CD [19, 20]. Figure 3 provided the forest plots for the network meta-analysis of each relevant drug. The meta-analysis showed that using TMTP to treat COVID-19 could significantly increase the clinical effect (RR, 1.20; 95% CI, 1.10 to 1.31). Compared with CD, LHQW significantly improved the clinical efficacy, which was 1.22 times higher than that of CD (RR, 1.22; 95% CI, 1.10 to 1.35). However, there is no remarkable difference between XBJ and CD (RR, 1.37; 95% CI, 0.94 to 1.99) or QFPD and CD (RR, 1.10; 95% CI, 0.91 to 1.32) on clinical effect. It should be noted that the mixed treatment comparison and drug sequencing were not performed because there was no closed ring in the network plot.

3.4.2. CT Recovery Rate. CT results are of great significance in the diagnosis of COVID-19, which is mainly characterized by ground-glass opacity. The improvement of COVID-19 was determined according to the CT changes before and after treatment in the clinic. A total of 7 trials reported the CT recovery of patients after treatment, in which 4 used LHQW *vs.* CD [14, 18, 25, 27], 2 used XBJ *vs.* CD [17, 29], and 1 used QFPD *vs.* CD [28]. Figure 4 provided the forest plots for the network meta-analysis of each relevant drug. The results exhibited that the CT recovery rate of TMTP was increased significantly more than that of CD alone (RR, 1.24; 95% CI, 1.15 to 1.35). The rates of LHQW, XBJ, and QFPD were 1.22 (RR, 1.22; 95% CI, 1.10 to 1.36), 1.36 (RR, 1.36; 95% CI, 1.06 to 1.75), and 1.26 (RR, 1.26; 95% CI, 1.10 to 1.43) times higher than those of CD. However, because there was no closed ring in the network plot, the mixed treatment comparison and drug sequencing were not performed.

3.4.3. Nucleic Acid Negative Rate. 2 trials reported the nucleic acid of patients before and after treatment [23, 29], all of which used XBJ *vs.* CD. Figure A.2 showed the forest plots. However, compared with CD, XBJ did not show an obvious increasing efficacy on it (RR, 0.97; 95% CI, 0.72 to 1.29).

3.4.4. Disappearance Rate of Primary Symptoms. The primary symptoms of COVID-19 patients were fever, cough, and fatigue. 7 trials reported the improvement of fever and cough after treatment [14–17, 22, 24, 26], and 6 reported fatigue [14, 15, 17, 22, 24, 26]. Figure 5 provided the forest plots for the network meta-analysis of each relevant drug. Compared with CD, the disappearance rates of fever (RR, 1.49; 95% CI, 1.30 to 1.70), cough (RR, 1.72; 95% CI, 1.38 to 2.14), and fatigue (RR, 1.55; 95% CI, 1.25 to 1.93) were greatly increased when using TMTP.

Compared with CD, LHQW showed a significant effect on increasing the disappearance rate of primary symptoms, which were 1.42 (RR, 1.42; 95% CI, 1.22 to 1.65), 1.97

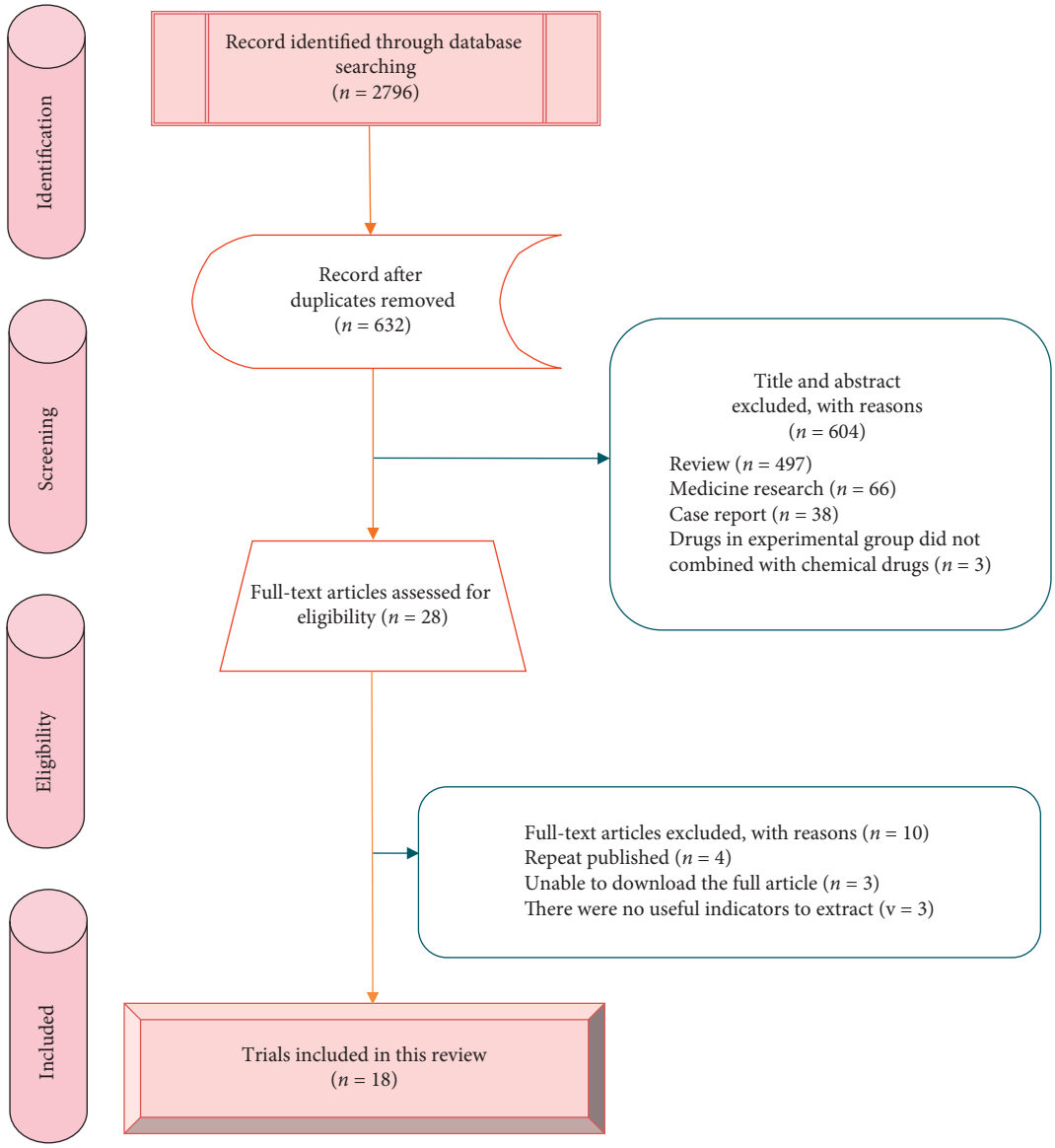

Figure 1: PRISMA flow diagram of literature selection.

(RR, 1.97; 95% CI, 1.45 to 2.68), and 1.52 (RR, 1.52; 95% CI, 1.15 to 2.03) times higher than those of CD in fever, cough, and fatigue respectively. JHQG and XBJ could remarkably improve the fever symptoms of patients, which were 1.51 (RR, 1.51; 95% CI, 1.07 to 2.41) and 15.71 (RR, 15.71; 95% CI, 1.03 to 240.75) times higher than those of CD, but they did not show an obvious advantage in cough and fatigue. A significant improvement of cough was observed by XFBD, whose efficacy was 1.97 times higher than that of CD (RR, 1.97; 95% CI, 1.04 to 3.72). However, there was no remarkable difference in fever and fatigue.

The results of network meta-analysis showed that XBJ was the most effective drug for improving fever, followed by XFBD, LHQW, JHQG, and CD. XFBD was the best drug for cough, followed by LHWE, JHQG, CD, and XBJ. In addition, XBJ was best for fatigue, followed by XFBD, LHQW, JHQG, and CD, while LHQW and JHQG had similar effects on fatigue.

3.4.5. Disappearance Rate of Respiratory Symptoms. The respiratory symptoms of COVID-19 patients mainly included expectoration, shortness of breath, chest distress, rhinobyon, rhinorrhea, and sore throat. Expectoration was reported in 6 trials [14–17, 22, 26], and shortness of breath was reported in 5 trials additionally [14, 16, 22, 24, 26]; then, 4 trials reported chest distress [14, 22, 24, 26], rhinobyon [15, 16, 22, 26], rhinorrhea [15, 16, 22, 26], and sore throat [15, 22, 24, 26]. Figure A.3 provided the forest plots for the network meta-analysis of each relevant drug. Meta-analysis identified that TMTP could significantly improve expectoration (RR, 2.05; 95% CI, 1.28 to 3.30), shortness of breath (RR, 2.27; 95% CI, 1.33 to 3.86), and chest distress (RR, 2.24; 95% CI, 1.47 to 3.41) compared with CD, but it had no obvious advantages in rhinobyon, rhinorrhea, and sore throat.

Using LHQW to treat COVID-19 could obviously increase the disappearance rate of expectoration, shortness of

Table 1: Characteristics of the 18 trials included in the Bayesian network meta-analysis.

Author(s)	Sample size (experimental/control)	Time frame (y)	Contrast drugs	Duration	Outcome measures
Chen et al. (2020)	15/15	2020.1–2020.3	XBJ *vs.* CD	14 days	Clinical effect, CRP, adverse reactions.
Cheng et al. (2020)	51/51	2020.1.1–2020.1.30	LHQW *vs.* CD	7 days	CT, fever, cough, fatigue, expectoration, shortness of breath, chest distress, nausea, inappetence, muscle soreness, exacerbation rate.
Duan et al. (2020)	82/41	2020.2.1–2020.2.5	JHQG *vs.* CD	5 days	Fever, cough, fatigue, expectoration, rhinobyon, rhinorrhea, sore throat, nausea, diarrhea, emesis, muscle soreness, exacerbation rate, adverse reactions.
Fang et al. (2020)	42/41	2020.1.28–2020.3.31	LHQW *vs.* CD	NR	Fever, cough, expectoration, shortness of breath, rhinobyon, rhinorrhea, muscle soreness.
Guo et al. (2020)	16/16	2020.1.20–2020.3.11	XBJ *vs.* CD	NR	CT, fever, cough, fatigue, expectoration, diarrhea, CRP, WBC.
Hu et al. (2020)	142/142	2020.2.2–2020.2.15	LHQW *vs.* CD	14 days	Clinical effect, CT, exacerbation rate, adverse reactions.
Li and Zhang (2020)	6/6	2020.2–2020.3	QFPD *vs.* CD	6 days	Clinical effect, WBC, adverse reactions.
Li et al. (2020)	30/30	2020.1.24–2020.3.7	QFPD *vs.* CD	NR	Clinical effect, exacerbation rate, adverse reactions.
Luo et al. (2021)	29/28	2020.2.16–2020.3.25	XBJ *vs.* CD	14 days	Exacerbation rate, adverse reactions.
Lv et al. (2020)	63/38	2020.1.1–2020.1.27	LHQW *vs.* CD	10 days	Fever, cough, fatigue, expectoration, shortness of breath, chest distress, rhinobyon, rhinorrhea, sore throat, nausea, diarrhea, emesis, inappetence, muscle soreness, headache, exacerbation rate, adverse reactions.
Wen et al. (2020)	20/20	2020.1–2020.3	XBJ *vs.* CD	7 days	NANR, CRP, WBC, exacerbation rate.
Xiong et al. (2020)	22/20	2020.1.30–2020.2.10	XFBD *vs.* CD	7 days	Fever, cough, fatigue, shortness of breath, chest distress, sore throat, nausea, diarrhea, emesis, inappetence, headache.
Xu et al. (2020)	26/26	2020.1.29–2020.2.28	LHQW *vs.* CD	7 days	CT.
Yao et al. (2020)	21/21	2020.1.11–1.30	LHQW *vs.* CD	NR	Fever, cough, fatigue, expectoration, shortness of breath, chest distress, rhinobyon, rhinorrhea, sore throat, nausea, diarrhea, emesis, inappetence, muscle soreness, headache.
Yu et al. (2020)	147/148	2020.2.17–2020.3.6	LHQW *vs.* CD	7 days	Clinical effect, CT, CRP, exacerbation rate.
Zeng et al. (2020)	104/125	2019.12–2020.3	QFPD *vs.* CD	NR	CT, adverse reactions.
Zhang et al. (2020)	22/22	2020.1.21–2020.2.24	XBJ *vs.* CD	7 days	Clinical effect, CT, NANR, adverse reactions.
Zhao et al. (2021)	204/204	2020.2.13–3.7	HSBD *vs.* CD	7 days	Exacerbation rate.

Abbreviations: CD, chemical drugs; CRP, C-reactive protein; HSBD, *Hua-Shi-Bai-Du;* JHQG, *Jin-Hua-Qing-Gan*; LHQW, *Lian-Hua-Qing-Wen*; NANR, nucleic acid negative rate; NR, not reported; QDPD, *Qing-Fei-Pai-Du*; WBC, white blood cell; XBJ, *Xue-Bi-Jing*; XFBD, *Xuan-Fei- Bai-Du*.

breath, and chest distress, whose effects were 2.58 (RR, 2.58; 95% CI, 1.15 to 5.82), 2.79 (RR, 2.79; 95% CI, 1.29 to 6.02), and 2.15 (RR, 2.15; 95% CI, 1.38 to 3.33) times higher than those of CD. However, there was no remarkable difference between LHQW and CD on rhinobyon, rhinorrhea, and sore throat. JHQG could also improve expectoration, and its efficacy was 1.85 times higher than that of CD (RR, 1.85; 95% CI, 1.01 to 3.38), but it did not show good effects on rhinobyon, rhinorrhea, and sore throat. According to the results, there was no obvious difference between XFBD and CD in shortness of breath and chest distress, as well as QFBD and CD in sore throat.

The network meta-analysis exhibited that LHQW and JHQG were the best drugs for expectoration, followed by CD and XBJ. And LHQW was the most effective drug for shortness of breath, followed by XFBD and CD. XFBD was the best one in improving chest distress, followed by LHQW and CD. JHQG was the best drug for rhinobyon and rhinorrhea, in which the former was secondary to LHQW and CD, and the latter was secondary to CD and LHQW.

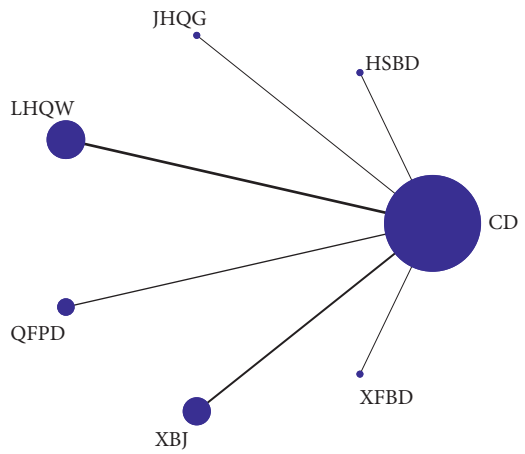

Figure 2: Network plot of the comparisons for the Bayesian network meta-analysis.

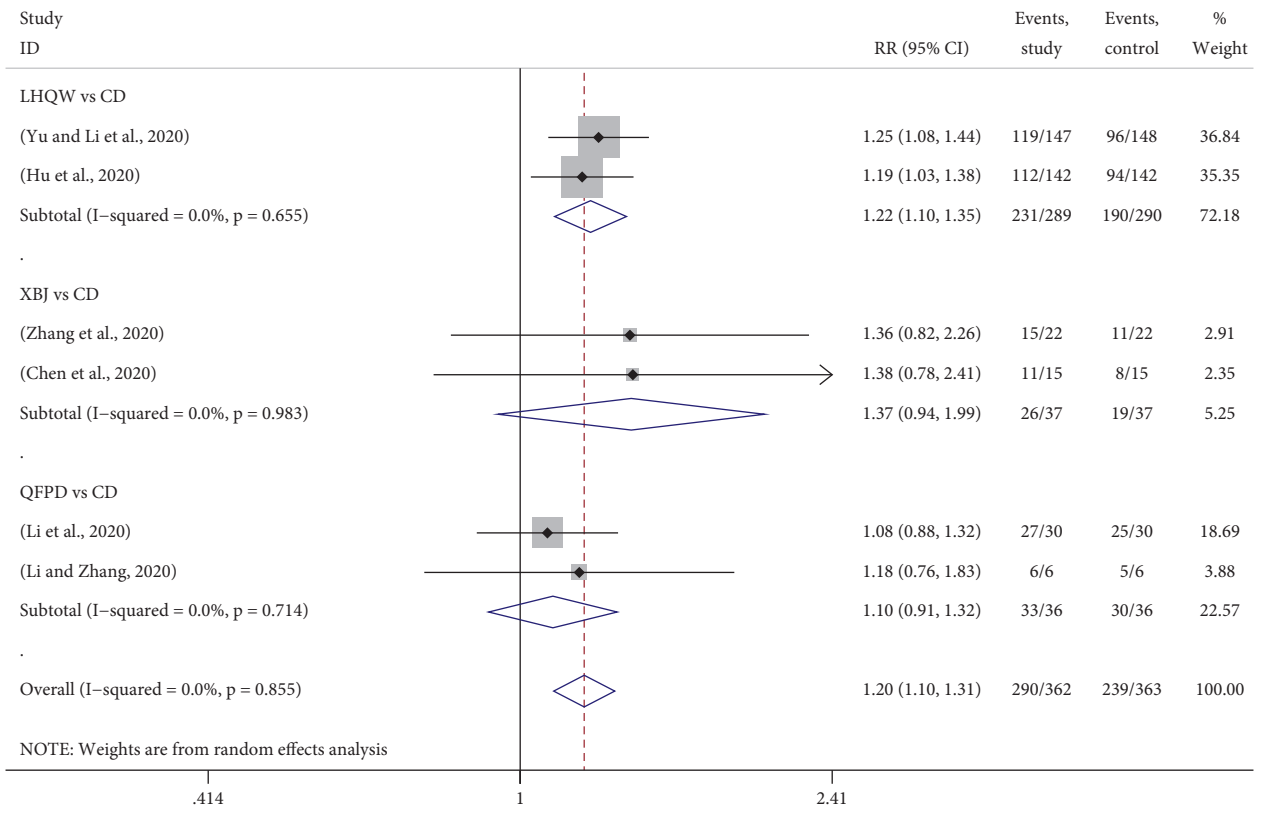

Figure 3: Forest plots for clinical effect by Bayesian network meta-analysis and traditional meta-analysis.

Additionally, LHQW was the most effective for sore throat, followed by JHQG, CD, and XFBD.

3.4.6. Disappearance Rate of Gastrointestinal Symptoms. The gastrointestinal symptoms of COVID-19 patients mainly included nausea, diarrhea, emesis, and inappetence. 5 trials reported nausea [14, 15, 22, 24, 26] and diarrhea [15, 17, 22, 24, 26], and 4 reported emesis [15, 22, 24, 26] and inappetence [14, 22, 24, 26]. Figure A.4 provided the forest plots for the network meta-analysis of each relevant drug. However, the meta-analysis evaluated that there was no significant difference between TMTP and CD in the disappearance rate of nausea, diarrhea, emesis, and inappetence. LHQW and XFBD did not show a remarkable advantage on them, just as JHQG on nausea, diarrhea, and emesis and XBJ on diarrhea.

The results of the network meta-analysis identified that LHQW was the most effective in nausea, followed by JHQG, CD, and XFBD. XBJ was the best drug in improving diarrhea, followed by LHQW, CD, XFBD, and JHQG. For emesis, the drug sorts were LHQW, JHQG, CD, and XFBD. And LHQW was also the best drug for inappetence, followed by XFBD and CD.

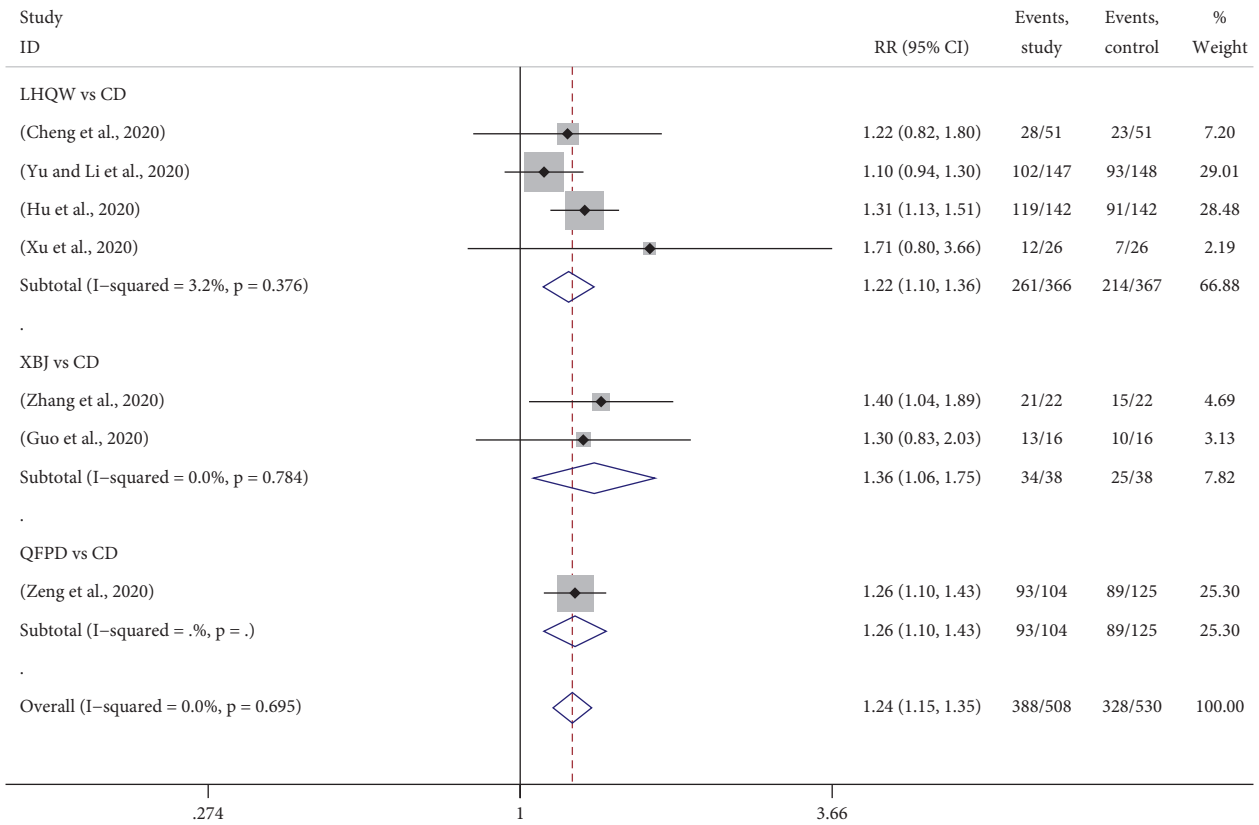

Figure 4: Forest plots for CT recovery rate by Bayesian network meta-analysis and traditional meta-analysis.

3.4.7. Disappearance Rate of Other Symptoms. 5 trials reported muscle soreness before and after treatment [14–16, 22, 26], and 3 reported headache [22, 24, 26]. Figure A.5 provided the forest plots for the network meta-analysis of each relevant drug. Compared with CD, TMTP exhibited significant effects on increasing the disappearance rate of muscle soreness (RR, 1.51; 95% CI, 1.03 to 2.20), but there was no obvious difference between TMTP and CD on headache. 4 trials comparing LHQW with CD reported muscle soreness before and after the intervention. The meta-analysis revealed that LHQW significantly improved its efficacy, which was 1.88 times higher than that of CD (RR, 1.88; 95% CI, 1.05 to 3.36); however, it did not show a remarkable advantage on headache. Either JHQG or XFBD was not more effective than CD in the treatment of muscle soreness and headache.

According to the results of network meta-analysis, LHQW was the best drug for improving muscle soreness and headache, followed by JHQG and CD for muscle soreness, and XFBD and CD for headache.

3.4.8. Inflammatory Biomarkers (CRP and WBC). 4 trials reported CRP level before and after treatment [13, 17, 23, 27] and 3 reported WBC [17, 20, 23]. Figure A.6 provided the forest plots for the network meta-analysis of each relevant drug. Meta-analysis showed that using TMTP could significantly decrease CRP level (MD, −0.94; 95% CI, −1.79 to −0.09); however, there was no obvious difference between TMTP and CD in WBC. The reduction in CRP was remarkably greater for XFBD than that of CD (MD, −0.46; 95% CI, −0.69 to −0.23). But XBJ had no obvious advantages in decreasing the levels of CRP and WBC, and there was no significant difference between QFPD and CD in WBC.

The network meta-analysis results identified that QFPD was the best drug for decreasing CRP levels, followed by CD and XBJ, and XBJ was the best for WBC, followed by CD and QFPD.

3.4.9. Exacerbation Rate. Exacerbation after treatment was reported in 9 trials, in which 4 used LHQW *vs.* CD [14, 18, 22, 27], 2 used XBJ *vs.* CD [21, 23], 1 used JHQG *vs.* CD [15], 1 used QFPD *vs.* CD [20], and 1 used HSBD *vs.* CD [30]. Figure 6 provided the forest plots for the network meta-analysis of each relevant drug. Meta-analysis exhibited that using TMTP to treat COVID-19 could significantly reduce the exacerbation rate of patients (RR, 0.55; 95% CI, 0.42 to 0.73). Compared with CD, exacerbation rates of LHQW and HSBD groups were significantly reduced, which were 0.57 (RR, 0.57; 95% CI, 0.38 to 0.85) and 0.33 (RR, 0.33; 95% CI, 0.012 to 0.88) times than those of CD. However, there was no obvious difference between JHQG, QFPD, XBJ, or XFBD and CD.

The network meta-analysis evaluated that using XFBD to treat COVID-19 had the least exacerbation number, followed by HSBD, JHQG, LHQW, QFPD, XBJ, and CD.

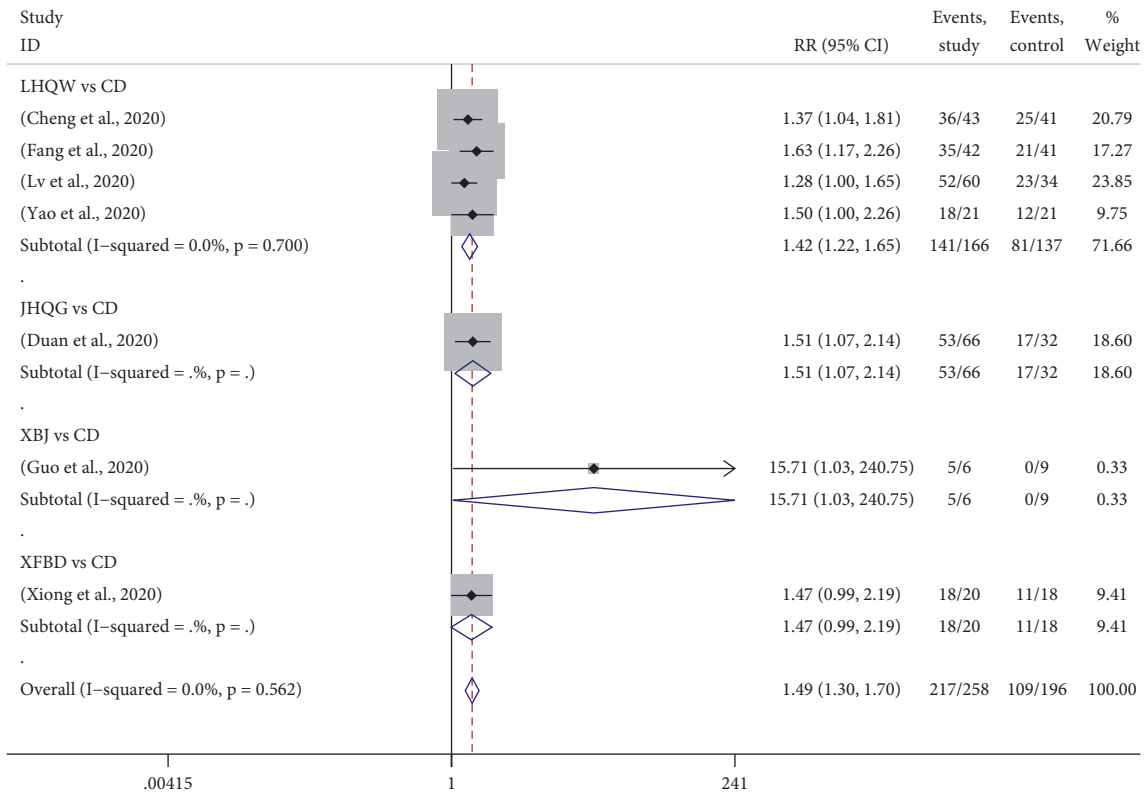

(a)

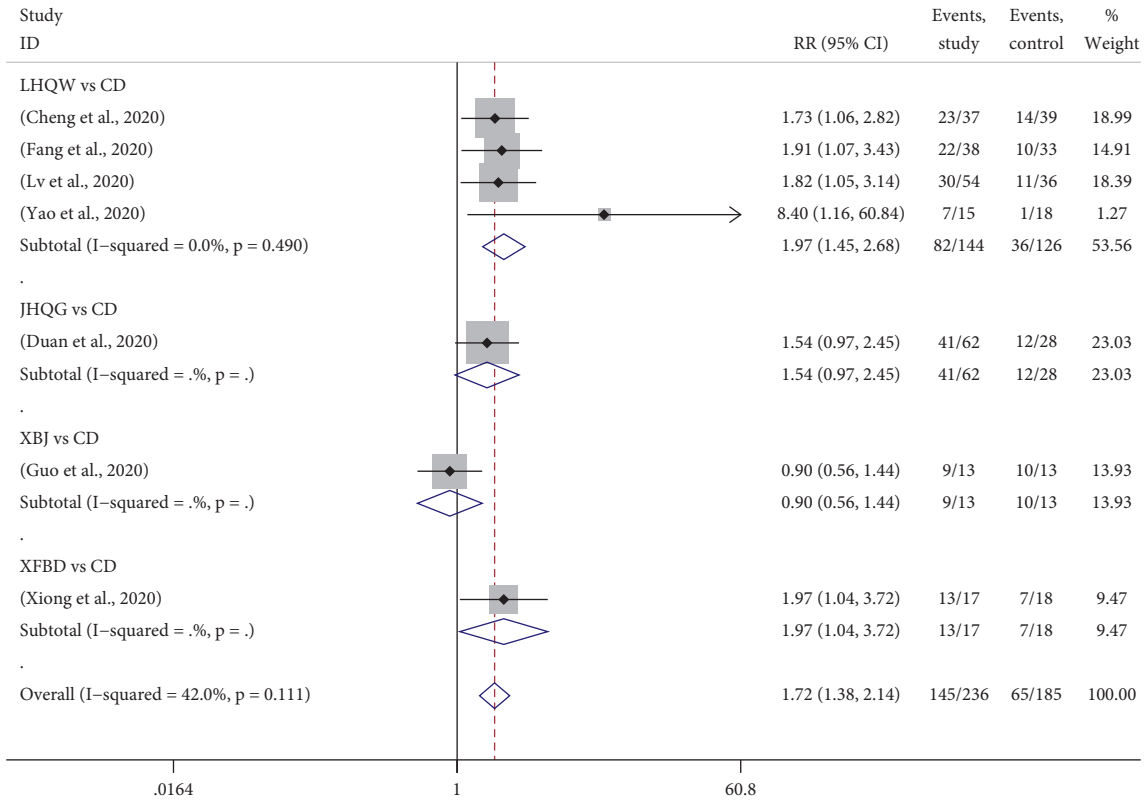

(b)

Figure 5: Continued.

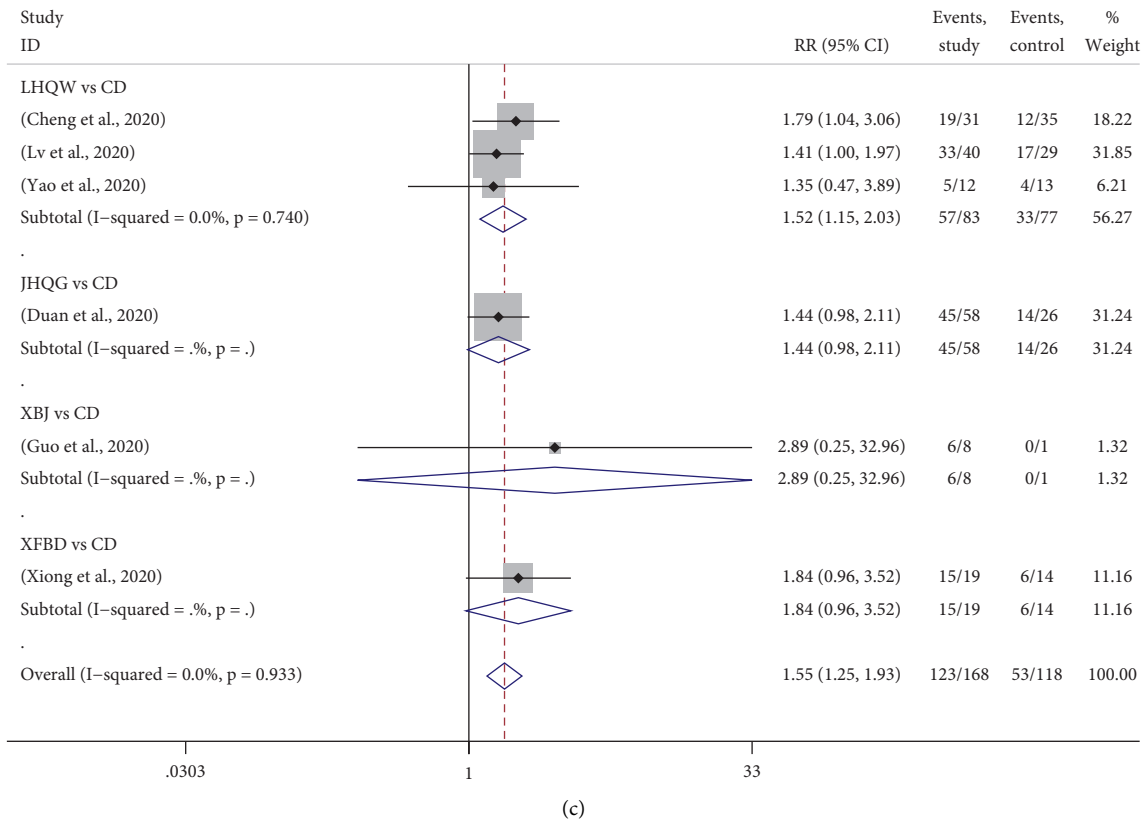

(c)

Figure 5: Forest plots for disappearance rate of primary symptoms by Bayesian network meta-analysis and traditional meta-analysis. (a) Fever. (b) cough. (c) fatigue.

3.4.10. Adverse Reactions. Adverse reactions were reported in 9 trials, in which 3 trials used QFPD *vs.* CD [19, 20, 28], 3 used XBJ *vs.* CD [13, 21, 29], 2 used LHQW *vs.* CD [18, 22], and 1 used JHQG *vs.* CD [15]. Figure 7 showed the forest plots for the network meta-analysis of each relevant drug. Compared with CD, the rate of adverse reaction in the QFPD group was significantly lower, which was 0.72 times that of CD (RR, 0.72; 95% CI, 0.58 to 0.90). However, LHQW and XBJ did not show good advantages in lowering adverse reactions.

The results of network meta-analysis showed that using LHQW to treat COVID-19 could produce the least adverse reaction, followed by QFPD, CD, XBJ, and JHQG.

4. Discussion

The efficacy and safety of TMTP for COVID-19 were evaluated by Bayesian network meta-analysis. 18 trials that contained 2036 participants were included. The traditional meta-analysis exhibited that using LHQW to treat COVID-19 could significantly increase the efficacy, and its clinical and CT effect was 1.22 times higher than that of CD, which could also improve most of the symptoms. Its effects on fever, cough, fatigue, expectoration, shortness of breath, chest distress, and muscle soreness were 1.42, 1.97, 1.52, 2.58, 2.79, 2.15, and 1.88 times those of CD, respectively, and the exacerbation rate was 0.52 times that of CD. The CT effects of XBJ and QFPD were 1.36 and 1.26 times those of CD, and the adverse reaction rate of QFPD was 0.72 times that of CD. The effects of JHQG on the improvement of fever and expectoration were 1.51 and 1.85 times those of CD. The cough effect and exacerbation rate of XFBD were 1.97 and 0.29 times those of CD, and it could also lower than the CRP level. The network meta-analysis identified that LHQW was the most effective drug in improving expectoration, shortness of breath, sore throat, nausea, emesis, inappetence, muscle soreness, and headache of COVID-19 patients, and it could produce the least adverse reactions. XBJ was the most effective in improving fever, fatigue, and diarrhea, and it showed great advantages in lowering WBC levels. XFBD was the best drug in improving cough and chest distress, and it had the least exacerbation rate. JHQG was the best one in improving rhinobyon and rhinorrhea, and QFPD was the most effective drug in decreasing CRP levels.

Some clinical studies have proved the efficacy and safety of TCM in the treatment of COVID-19. It was shown that TCM treatment of COVID-19 could significantly reduce the mortality of patients and delay the progression of the disease, especially in the treatment of severe/critical cases, which showed good advantages [31]. Furthermore, it could significantly improve clinical remission rates and shorten the nucleic acid conversion time and hospitalization time. The combination of HSBD and TCM injection showed obvious superiority in the treatment of COVID-19 [32]. Meanwhile, HSBD alone could also remarkably shorten the fever time of COVID-19 patients, relieve symptoms such as cough,

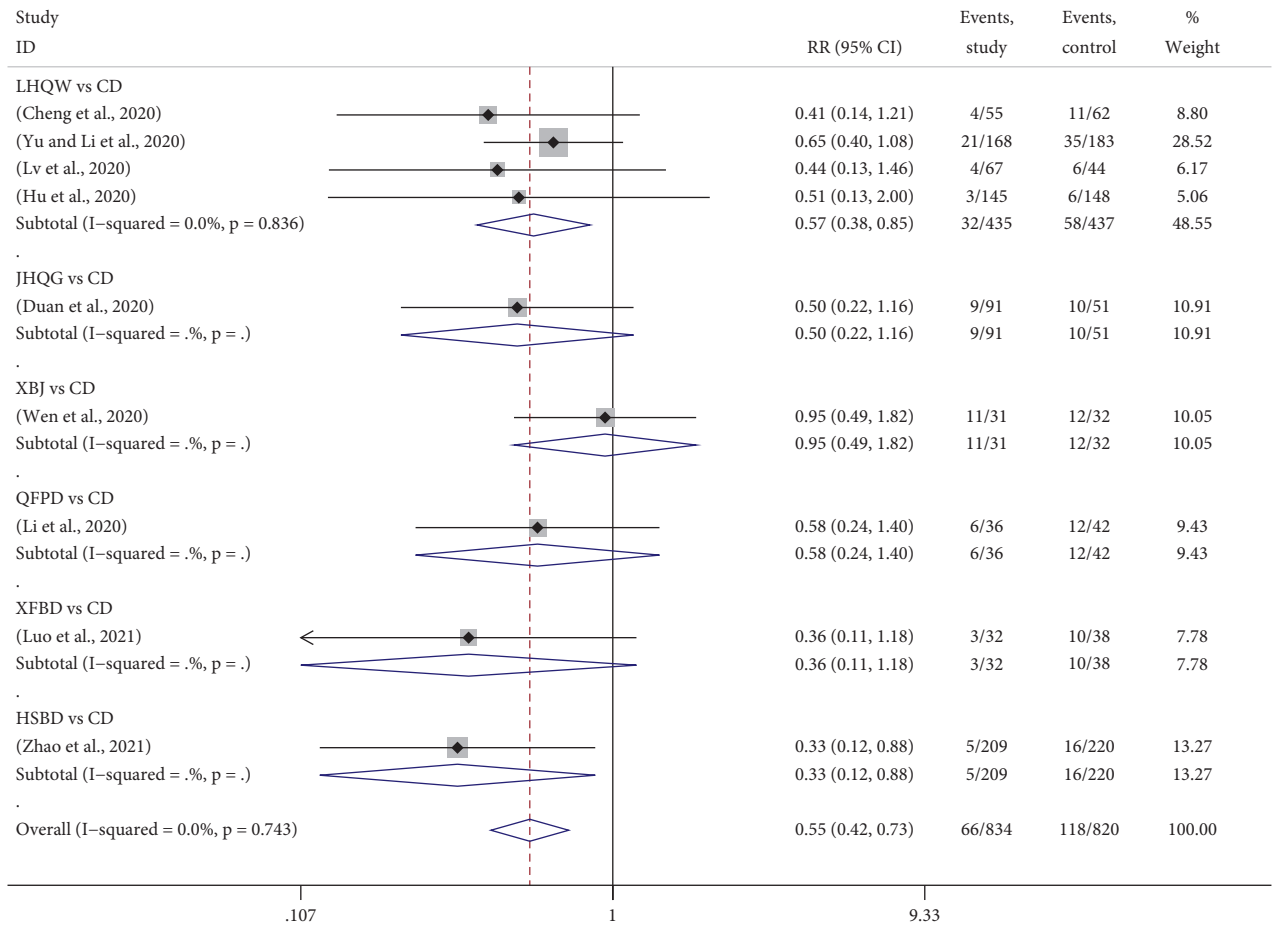

Figure 6: Forest plots for exacerbation rate by Bayesian network meta-analysis and traditional meta-analysis.

fatigue, and chest discomfort, and improve the CT recovery rate [33]. Based on the two indicators of exacerbation rate and adverse reactions, this study showed that TCM could effectively prevent the deterioration and progression of the disease and had good safety. It could not only obviously relieve the multisystem clinical symptoms of COVID-19 patients and reduce clinical indicators but also significantly improve the clinical efficacy, which is a powerful and effective measure for the treatment of COVID-19.

Each prescription in TMTP is a combination of classical and famous formulae, which can play a role in the treatment of COVID-19 through multitarget comprehensive intervention. They can be used clinically in combination with the actual situation of patients and are suitable for the treatment of mild, common, and severe COVID-19 patients.

LHQW is a combination of *Maxing Shigan Decoction* and *Yinqiao Powder*, which is composed of 12 kinds of herbs including Lianqiao (fructus of *Forsythia suspensa* (Thunb.) Vahl), Jinyinhua (floral bud of *Lonicera japonica* Thunb), Mahuang (herb of *Ephedra equisetina* Bge.), Xingren (seed of *Prunus armeniaca* L. var. *ansu* Maxim), Banlangen (root of *Isatis indigotica* Fort), Guanzhong (rhizome of *Dryopteris crassirhizoma* Nakai), Yuxingcao (herb of *Houttuynia cordata* Thunb.), Huoxiang (wrinkled herb of *Agastache rugosus* (Fisch. et Mey. O. Ktze.), Dahuang (radix and rhizome of *Rheum palmatum* L.), Hongjingtian (radix and rhizome of *Rhodiola rosea* L.), Bohe (herb of *Mentha haplocalyx* Briq.), Gancao (radix and rhizome of *Glycyrrhiza uralensis* Fisch.), and a mineral drug Shigao (*Gypsum fibrosum*). Lianqiao and Jinyinhua clear heat-toxicity and dispel wind pathogens; Mahuang disperses lung qi and dissipates phlegm; Shigao clears heat; Xingren improves cough and asthma; Banlangen cools blood to relieve sore throat; Guanzhong and Yuxingxao remove toxicity for eliminating carbuncles; Bohe dispels wind pathogens and relieves sore throat; Huoxiang removes dampness for regulating stomach; Dahuang eliminates heat; Hongjingtian moistens lung for arresting cough; Gancao clears heat-toxicity. Thus, LHQW has the effects of dispelling disease and detoxification, as well as relieving heat in the lung. Studies have shown that LHQW could significantly inhibit the replication of SARS-CoV-2 in Vero E6 cells at the mRNA level and greatly reduce the production of proinflammatory cytokines TNF-α, IL-6, CCL-2/MCP-1, and CXCL-10/IP-10, thus playing a role in the resistance to the virus; furthermore, it has a broad-spectrum effect on a series of influenza viruses by inhibiting virus proliferation and regulating immune function [34], which can not only enhance the body's immunity and inhibit respiratory inflammation [35] but also affect the relevant cytokines and ameliorate lung injury associated with inflammatory cell infiltration [36]. Therefore, LHQW has antibacterial, antipyretic, analgesic, anti-inflammatory, cough relieving, and

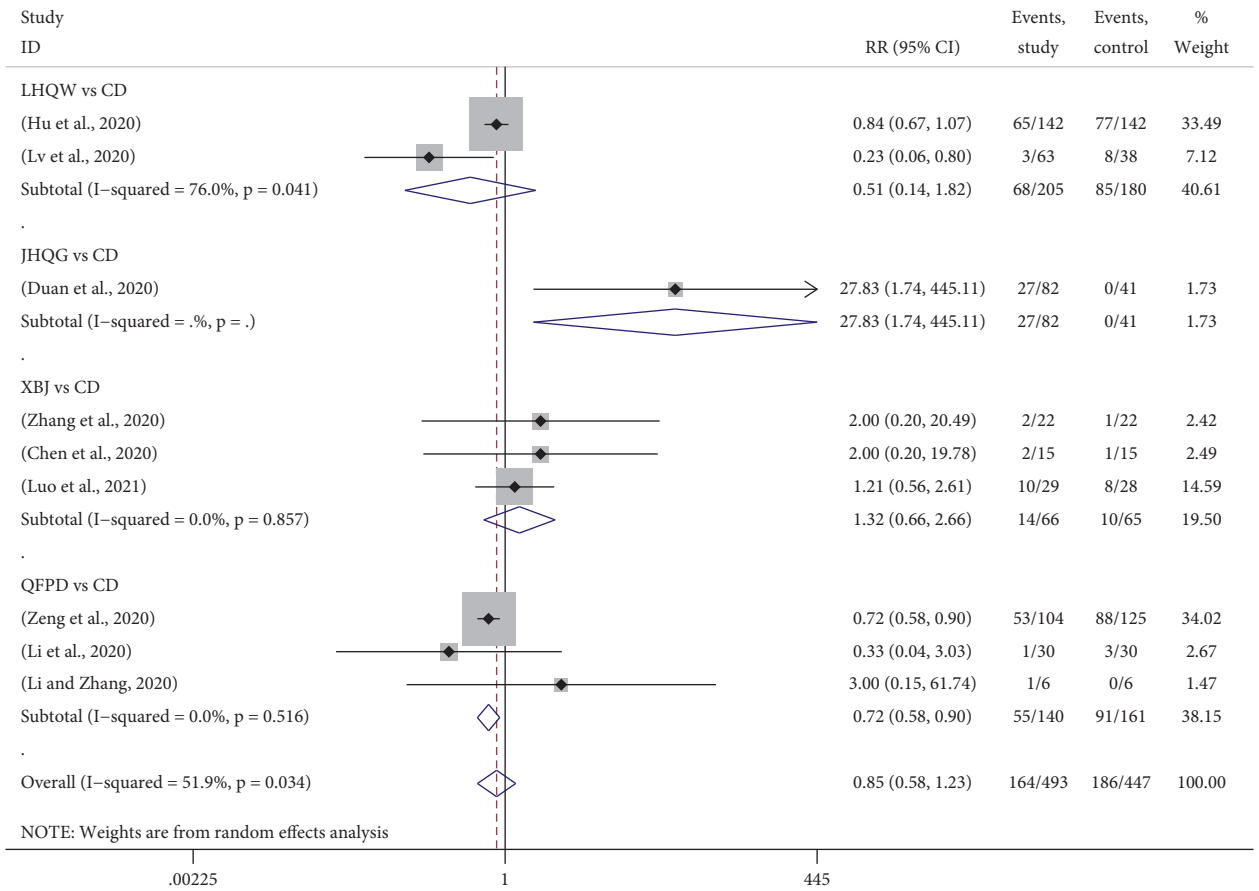

Figure 7: Forest plots for disappearance rate of adverse reaction by Bayesian network meta-analysis and traditional meta-analysis.

expectorant effects [37], which can significantly improve flu-like symptoms such as phlegm, shortness of breath, sore throat, headache, muscle soreness, and inappetite.

JHQG integrates the classic formulae *Maxing Shigan Decoction*, *Yinqiao Powder,* and *Baihu Decoction* into one, which has the effects of dispelling wind and heat pathogens and clearing heat toxicity. It includes Lianqiao (fructus of *Forsythia suspensa* (Thunb.) Vahl), Jinyinhua (floral bud of *Lonicera japonica* Thunb), Mahuang (herb of *Ephedra equisetina* Bge.), Xingren (seed of *Prunus armeniaca* L. var. *ansu* Maxim), a mineral drug Shigao (*Gypsum fibrosum*), Huangqin (radix of *Scutellaria baicalensis* Georgi), Zhebeimu (bulb of *Fritillaria thunbergii* Miq.), Zhimu (rhizome of *Anemarrhena asphodeloides* Bge.), Niubangzi (fructus of *Arctium lappa* L.), Qinghao (herb of *Artemisia annua* L.), Bohe (herb of *Mentha haplocalyx* Briq.), and Gancao (radix and rhizome of *Glycyrrhiza uralensis* Fisch.). Lianqiao and Jinyinhua clear heat-toxicity and dispel wind pathogens; Mahuang disperses lung qi and dissipates phlegm; Shigao clears heat; Xingren improves cough and asthma; Huangqin dispels heat and removes dampness; Zhebeimu reduces phlegm; Zhimu nourishes yin and clears heat; Niubangzi dispels heat pathogens and relieves throat disorder; Qinghao and Gancao clear heat-toxicity; Bohe dispels wind pathogens and relieves sore throat. JHQG could inhibit the replication of the influenza virus, promote virus clearance [38], alleviate rhinobyon, rhinorrhea, and other symptoms through a variety of mechanisms, and shorten the fever time by PTGS2 possibly [39].

XBJ is developed on the basis of *Xuefu Zhuyu Decoction*, including Honghua (floral bud of *Carthamus tinctorius* L.), Chishao (radix of *Paeonia lactiflora* Pall.), Chuanxiong (rhizome of *Ligusticum chuanxiong* Hort.), Danshen (radix and rhizome of *Salvia miltiorrhiza* Bge.), and Danggui (radix of *Angelica sinensis* (Oliv.) Diels), which is used for the mutual syndrome of stasis and poison in warm and hot diseases. XBJ has the function of activating blood circulation and removing blood stasis, which can antagonize endotoxin *in vitro*. It can not only improve a variety of infectious symptoms such as fever and fatigue by anti-inflammatory, antiendotoxin, and the improvement of blood coagulation function and alleviate digestive symptoms such as abdominal pain and diarrhea by reducing the inflammatory response of the body but also shorten the recovery time of white blood cells [40]. Furthermore, it could effectively reduce acute lung injury by regulating the expression of pulmonary inflammatory factors p-p38 MAPK, NF-κB 65, HIF-1α, p-IκB-α, and TGF-β1 [41] and improve dyspnea and hypoxemia in patients with severe COVID-19.

QFPD integrates *Maxing Shigan Decoction*, *Shegan Mahuang Decoction*, *Xiao Chaihu Decoction*, and *Wuling Powder*, which includes Mahuang (herb of *Ephedra equisetina* Bge.), Xingren (seed of *Prunus armeniaca* L. var. *ansu* Maxim), a mineral drug Shigao (*Gypsum fibrosum*), Guizhi

(twig of *Cinnamomum cassia* Presl), Zexie (bulb of *Alisma orientate* (Sam.) Juzep), Zhuling (sclerotium of *Polyporus umbellatus* (Pers.) Frie), Chaihu (radix of *Bupleurum chinense* DC.), Huangqin (radix of *Scutellaria baicalensis* Georgi), Banxia (tuber of *Pineilia ternata* (Thunb.) Breit), Shengjiang (rhizome of *Zingiber officinale* Rose), Ziyuan (rhizome of *Aster tataricus* L. f.), Kuandonghua (floral bud of *Tussilago farfara* L.), Shegan (rhizome of *Belamcanda chinensis* (L.) DC.), Xixin (radix and rhizome of *Asarum heterotropoides* Fr. Schmidt var. *mandshuricum* (Maxim) Kitag.), Shanyao (rhizome of *Dioscorea opposita* Thunb.), Zhishi (fructus of *Citrus aurantium* L.), Chenpi (pericarp of *Citrus reticulata* Blanco), Huoxiang (wrinkled herb of *Agastache rugosus* (Fisch. et Mey. O. Ktze.), and Gancao (radix and rhizome of *Glycyrrhiza uralensis* Fisch.). QFPD has effects of clearing heat toxicity, dispersing lung qi, and dissipating phlegm. It could inhibit proinflammatory cytokines such as IL-6 and IL-1β, increase anti-inflammatory cytokines such as IL-4 and IL-10, or inhibit NF-κB and MAPK signaling pathways, exert an anti-inflammatory and antiviral role, and significantly reduce inflammatory indicators [42, 43].

XFBD is a combination of *Maxingshigan Decoction*, *Maxingyigan Decoction*, *Tinglidazaoxiefei Decoction,* and *Qianjin Weijing Decoction*, including Mahuang (herb of *Ephedra equisetina* Bge.), Xingren (seed of *Prunus armeniaca* L. var. *ansu* Maxim), a mineral drug Shigao (*Gypsum fibrosum*), Yiyiren (seed of *Coix lacryma-jobi* L. *var. mayuen* (Roman.) Stapf), Qinghao (herb of *Artemisia annua* L.), Huzhang (rhizome and radix of *Polygonum cuspidatum* Sieb. et Zucc), Mabiancao (herb of *Verbena officinalis* L.), Lugen (rhizome of *Phragmites communis* Trin), Tinglizi (seed of *Descurainia sophia* (L.) Webb. ex Prantl.), Juhong (pericarp of *Citrus reticulata* Blanco), and Gancao (radix and rhizome of *Glycyrrhiza uralensis* Fisch.). XFBD has the effects of clearing heat toxicity, dispersing lung qi, and dissipating phlegm. It may block inflammatory cytokine storm by inhibiting excessive cytokine production, immune cell activation, and oxidative damage *in vivo*, which is the intervention mechanism after virus invasion [44]. Therefore, XFBD can significantly relieve cough, chest tightness, and other symptoms of patients and inhibit the progression of the disease.

HSBD integrates *Maxingshigan Decoction* and *Tinglidazaoxiefei Decoction* into one, including Mahuang (herb of *Ephedra equisetina* Bge.), Xingren (seed of *Prunus armeniaca* L. var. *ansu* Maxim), a mineral drug Shigao (*Gypsum fibrosum*), Huoxiang (wrinkled herb of *Agastache rugosus* (Fisch. et Mey. O. Ktze.), Houpo (velamen of *Magnolia officinalis* Rehd. et Wils.), Cangzhu (rhizome of *Atractylodes lancea* (Thunb.) DC.), Caoguo (fructus of *Amomum tsao-ko* Crevost et Lemaire), Banxia (tuber of *Pineilia ternata* (Thunb.) Breit), Fuling (sclerotium of *Poria cocos* (Schw) Wolf), Dahuang (radix and rhizome of *Rheum palmatum* L.), Yujin (earthnut of *Curcuma xvenyujin* Y. H. Chen et C. Ling), Huangqi (root of *Astragalus membranaceus* (Fisch.) Bge. *var. mongholicus* (Bge.) Hsiao), Tinglizi (seed of *Descurainia sophia* (L.) Webb. ex Prantl.), Chishao (radix of *Paeonia lactiflora* Pall.), and Gancao (radix and rhizome of *Glycyrrhiza uralensis* Fisch.). HSBD has the effects of dispelling lung heat, preventing asthma, drying damp, strengthening the spleen, and removing blood stasis. It could inhibit the infection, replication, and proliferation of the SARS-CoV-2 virus to some extent, regulate the balance of the RAS system and inflammatory response accordingly, and effectively block the formation of the inflammatory storm after the infection of the SARS-CoV-2 virus [45, 46].

There were some important advantages in this study. Methodologically, our study benefits from rigorous methods, extensive search, repeated and independent screening, meticulous data abstraction process, and comprehensiveness of analytical indicators. In addition, the Bayesian network meta-analysis was used to compare therapies indirectly when no head-to-head trial existed, and more accurate evaluation for efficacy was obtained by jointly assessing direct and indirect comparisons. Moreover, we mapped drug sequencing figures through single and mixed analysis, further ranked the competing drugs, and summed up the best one for that outcome.

The following limitations should be considered in this study. Due to the insufficient sample size, short duration, and partial retrospective study of TMTP in the treatment of COVID-19, the methodological quality had a certain risk bias. In addition, TMTP is mainly used in China because of the limited application of TCM in other countries. The Chinese government has issued health packages to Chinese people all over the world, while the data cannot be calculated and summarized well. Therefore, although TMTP is widely used, the data is limited, which will have a certain impact on the results.

5. Conclusion

In summary, the study focused on the diversity of symptoms in COVID-19 patients, which was the most large-scale and comprehensive research on this issue so far. In this study, multiple outcomes were used to systematically evaluate TMTP efficacy for COVID-19 so as to determine the precise efficacy and safety of each drug for COVID-19 treatment. Bayesian network meta-analysis was used to integrate clinical evidence from direct and indirect treatment comparisons into a network, using a common comparator for indirect comparisons in the absence of head-to-head trials, and the competing drugs in each outcome were ranked. LHQW could significantly reduce proinflammatory cytokines and enhance immunity with antiviral effects. JHQG could inhibit influenza virus replication and promote virus clearance. XBJ could control infectious symptoms and alleviate acute lung injury effectively. QFPD had anti-inflammatory and antiviral effects, which could significantly reduce inflammatory indicators. XFBD could block the inflammatory cytokine storm and intervene in virus invasion. And HSBD could inhibit the infection, replication, and proliferation of the SARS-CoV-2 virus to a certain extent and, obviously, block the formation of the inflammatory storm after infection. As a result, LHQW could improve most symptoms of COVID-19 patients with no obvious adverse reactions. Therefore, we believe that it should be

firstly recommended for COVID-19 treatment, especially for critically ill patients. Patients with severe fever, fatigue, and diarrhea could be treated by XBJ, while patients with obvious rhinobyon and rhinorrhea could choose JHQG. XFBD is recommended for patients with cough and chest tightness as the main manifestation, and HSBD could significantly lower the exacerbation rate. Our findings will help to provide guidance for COVID-19 treatment and future research.

Abbreviations

CD: Chemical drugs
CI: Confidence interval
COVID-19: Coronavirus disease 2019
CRP: C-reactive protein
JHQG: *Jin-Hua-Qing-Gan*
HSBD: *Hua-Shi-Bai-Du*
LHQW: *Lian-Hua-Qing-Wen*
MD: Mean difference
NOS: Newcastle Ottawa scale
QFPD: *Qing-Fei-Pai-Du*
RR: Relative risk
TCM: Traditional Chinese medicine
TMTP: Three Chinese patent medicines and three TCM prescriptions
WBC: White blood cell
WHO: World Health Organization
XBJ: *Xue-Bi-Jing*
XFBD: *Xuan-Fei-Bai-Du*.

Data Availability

The data used to support the findings of this study are available from the corresponding author upon request.

Conflicts of Interest

The authors declare that they have no conflicts of interest.

Authors' Contributions

SZ and YPT were responsible for the conception and design of the study; SZ, ZY, JJL, and ZNL conducted the statistical analysis, drew the tables and pictures, and drafted the manuscript; SZ, SJY, and JJL retrieved the database, screened the trials, extracted the data, and evaluated the methodological quality; and all authors critically revised the manuscript and approved the final version.

Acknowledgments

The authors thank grants from the Key Research and Development Program of Shaanxi (2019ZDLSF04-05) and the National Natural Science Foundation of China (81773882, 81974522, and 81974584). This research was also financially supported by the Subject Innovation Team of the Shaanxi University of Chinese Medicine (2019-YL10).

Supplementary Materials

Supplementary materials provide the methodology quality of included trials and competitive drug sequencing in the study. Forest plots for nucleic acid negative rate and the disappearance rate of respiratory, gastrointestinal, and other symptoms as well as inflammatory biomarkers are also shown. They include pooled hazard ratios for competing drugs in each outcome (Table A1), specific percentage ranking in terms of competing drugs in each outcome (Table A2), methodology quality of the 10 included randomized controlled trials according to the Cochrane handbook (Table A3), rank probability of competing drugs in each outcome (Figure A1), forest plots for nucleic acid negative rate by Bayesian network meta-analysis and traditional meta-analysis (Figure A2), forest plots for disappearance rate of respiratory symptoms by Bayesian network meta-analysis and traditional meta-analysis (Figure A3), forest plots for disappearance rate of gastrointestinal symptoms by Bayesian network meta-analysis and traditional meta-analysis (Figure A4), forest plots for disappearance rate of other symptoms by Bayesian network meta-analysis and traditional meta-analysis (Figure A5), and forest plots for disappearance rate of inflammatory biomarkers by Bayesian network meta-analysis and traditional meta-analysis (Figure A6). (*Supplementary Materials*)

References

[1] H. A. Rothan and S. N. Byrareddy, "The epidemiology and pathogenesis of coronavirus disease (COVID-19) outbreak," *Journal of Autoimmunity*, vol. 109, Article ID 102433, 2020.
[2] C. Wang, P. W. Horby, F. G. Hayden, and G. F. Gao, "A novel coronavirus outbreak of global health concern," *The Lancet*, vol. 395, no. 10223, pp. 470–473, 2020.
[3] H. Wissem and B. L. Nadia, "COVID-19: main therapeutic options," *Tunisie Medicale*, vol. 98, no. 4, pp. 299–303, 2020.
[4] J.-l. Ren, A.-H. Zhang, and X.-J. Wang, "Traditional Chinese medicine for COVID-19 treatment," *Pharmacological Research*, vol. 155, Article ID 104743, 2020.
[5] F. Catalá-López, A. Tobías, C. Cameron, D. Moher, and B. Hutton, "Network meta-analysis for comparing treatment effects of multiple interventions: an introduction," *Rheumatology International*, vol. 34, no. 11, pp. 1489–1496, 2014.
[6] A. E. Ades, M. Sculpher, A. Sutton et al., "Bayesian methods for evidence synthesis in cost-effectiveness analysis," *PharmacoEconomics*, vol. 24, no. 1, pp. 1–19, 2006.
[7] F. Song, D. G. Altman, A. M. Glenny, and J. J. Deeks, "Validity of indirect comparison for estimating efficacy of competing interventions: empirical evidence from published meta-analyses," *BMJ*, vol. 326, no. 7387, p. 472, 2003.
[8] A. Sutton, A. E. Ades, N. Cooper, and K. Abrams, "Use of indirect and mixed treatment comparisons for technology assessment," *PharmacoEconomics*, vol. 26, no. 9, pp. 753–767, 2008.
[9] D. Moher, A. Liberati, J. Tetzlaff, and D. G. Altman, "Preferred reporting items for systematic reviews and meta-analyses: the PRISMA statement," *PLoS Medicine*, vol. 6, no. 7, Article ID e1000097, 2009.
[10] National Health Commission of the People's Republic of China, *Guidelines for the Diagnosis and Treatment of COVID-19 Pneumonia*, National Health Commission of the People's

Republic of China, Beijing, China, 2020, http://www.nhc.gov.cn/.

[11] J. P. T. Higgins and S. Green, *Cochrane Reviewers' Handbook 5.3.0*, Cochrane, London, UK, 2014, https://www.cochranehandbook.org.

[12] P. Sedgwick and L. Marston, "How to read a funnel plot in a meta-analysis," *BMJ*, vol. 351, Article ID h4718, 2015.

[13] L. Z. Chen, H. Liu, and G. L. Xiao, "Therapeutic effect of Xuebijing injection in COVID-19 and its effect on CRP," *Journal of Chiniese Prescription Drug.*vol. 18, no. 10, pp. 10–111, 2020.

[14] D. Z. Cheng, W. J. Wang, Y. Li, X. D. Wu, B. Zhou, and Q. Y. Song, "Analysis of curative effect of 51 patients with novel coronavirus pneumonia treated with Chinese medicine Lianhua Qingwen: a multicentre retrospective study," *Tianjin Journal of Traditional Chinese Medicine*, vol. 37, no. 5, pp. 509–516, 2020.

[15] C. Duan, G. W. Xia, C. J. Zheng et al., "Clinical observation on Jinhua Qinggan Granule combined with conventional western medicine therapy in treating mild cases of coronavirus disease 2019," *Journal of Traditional Chinese Medicine*, vol. 61, no. 17, pp. 1473–1477, 2020.

[16] F. Fang, L. Yang, S. C. Qin, and R. Jiao, "Lianhua Qingwen granule in the treatment of 42 children suspected cases of COVID-19," *Chinese Journal of New Drugs*, vol. 29, no. 24, pp. 2809–2812, 2020.

[17] H. Guo, J. Zheng, G. Xiang et al., "Xuebijing injection in the treatment of COVID-19: a retrospective case-control study," *Annals of Palliative Medicine*, vol. 9, no. 5, pp. 3235–3248, 2020.

[18] K. Hu, W. J. Guan, Y. Bi et al., "Efficacy and safety of Lianhuaqingwen capsules, a repurposed Chinese herb, in patients with coronavirus disease 2019: a multicenter, prospective, randomized controlled trial," *Phytomedicine*, vol. 85, Article ID 153242, 2020.

[19] Y. D. Li and W. J. Zhang, "Evaluation on the clinical effect of traditional Chinese medicine and western medicine regimens on COVID-19," *Guangming Journal of the Chinese Medical Association*, vol. 35, no. 9, pp. 1273–1275, 2020.

[20] K. Y. Li, W. An, F. Xia et al., "Observation on clinical effect of modified Qingfei Paidu Decoction in treatment of COVID-19," *Chinese Traditional and Herbal Drugs*, vol. 51, no. 8, pp. 2046–2049, 2020.

[21] Z. Luo, W. Chen, M. Xiang et al., "The preventive effect of Xuebijing injection against cytokine storm for severe patients with COVID-19: a prospective randomized controlled trial," *European Journal of Integrative Medicine*, vol. 42, Article ID 101305, 2021.

[22] R. B. Lv, W. J. Wang, and X. Li, "Clinical observation on Lianhua Qingwen granules combined with western medicine conventional therapy in the treatment of 63 suspected cases of coronavirus disease 2019," *Journal of Traditional Chinese Medicine*, vol. 61, no. 8, pp. 655–659, 2020.

[23] L. Wen, Z. J. Zhou, D. X. Jiang, and K. Huang, "Effect of xuebijing injection on inflammatory indicators and outcome of patients with severe COVID-19," *Chinese Critical Care Medicine*, vol. 34, no. 4, pp. 426–429, 2020.

[24] W.-z. Xiong, G. Wang, J. Du, and W. Ai, "Efficacy of herbal medicine (Xuanfei Baidu decoction) combined with conventional drug in treating COVID-19:A pilot randomized clinical trial," *Integrative Medicine Research*, vol. 9, no. 3, Article ID 100489, 2020.

[25] X. H. Xu, H. Dong, S. H. Tu et al., "Retrospective analysis of Jinye Budu granule and Lianhua Qinwen capsule in the treatment of common type COVID-19," *Res. Integrated Traditional and Western Medicine*, vol. 12, no. 6, pp. 383–389, 2020.

[26] K. T. Yao, M. Y. Liu, X. Li, J. H. Huang, and H. B. Cai, "Retrospective clinical analysis on treatment of coronavirus disease 2019 with traditional Chinese medicine Lianhua Qingwen," *Chin. Exp. Tradit. Med. Form.*vol. 26, no. 11, pp. 8–12, 2020.

[27] P. Yu, Y. Z. Li, S. B. Wan, and Y. Wang, "Effects of Lianhua Qingwen granules plus arbidol on treatment of mild corona virus disease-19," *Chinese Pharmaceutical Journal*, vol. 55, no. 12, pp. 1042–1045, 2020.

[28] X. H. Zeng, W. H. Ma, and J. Wang, "Effect of Qingfei Paidu decoction on clinical efficacy of COVID-19 pneumonia with Phlegm heat blocking lung," *West China Medical Journal,*vol. 32, no. 12, pp. 1799–1806, 2020.

[29] C. Y. Zhang, Z. H. Li, S. Zhang, W. Wang, and X. Q. Jiang, "Clinical observation of Xuebijing in the treatment of COVID-19," *Chinese Journal of Hospital Pharmacy*, vol. 40, no. 9, pp. 964–967, 2020.

[30] C. Zhao, L. Li, W. Yang et al., "Chinese medicine formula Huashibaidu granule early treatment for mild COVID-19 patients: an unblinded, cluster-randomized clinical trial," *Frontiers in Medicine*, vol. 8, Article ID 696976, 2021.

[31] Z. Shu, K. Chang, Y. Zhou et al., "Add-on Chinese medicine for coronavirus disease 2019 (ACCORD): a retrospective cohort study of hospital registries," *The American Journal of Chinese Medicine*, vol. 49, no. 3, pp. 543–575, 2021.

[32] N. Shi, L. Guo, B. Liu et al., "Efficacy and safety of Chinese herbal medicine versus Lopinavir-Ritonavir in adult patients with coronavirus disease 2019: a non-randomized controlled trial," *Phytomedicine*, vol. 81, Article ID 153367, 2021.

[33] J. Liu, W. Yang, Y. Liu et al., "Combination of Hua Shi Bai Du granule (Q-14) and standard care in the treatment of patients with coronavirus disease 2019 (COVID-19): a single-center, open-label, randomized controlled trial," *Phytomedicine*, vol. 91, Article ID 153671, 2021.

[34] R. F. Li, Y. L. Hou, J. C. Huang et al., "Lianhuaqingwen exerts anti-viral and anti-inflammatory activity against novel coronavirus (SARS-CoV-2)," *Pharmacological Research*, vol. 156, Article ID 104761, 2020.

[35] S. H. Wang, J. F. Liu, Y. L. Zhang, and Z. Dong, "Systematic review of efficacy and safety of lianhua qingwen capsules in treatment of viral influenza," *China Journal of Chinese Materia Medica*, vol. 44, no. 7, pp. 1503–1508, 2019.

[36] Y. Ding, L. Zeng, R. Li et al., "The Chinese prescription lianhuaqingwen capsule exerts anti-influenza activity through the inhibition of viral propagation and impacts immune function," *BMC Complementary and Alternative Medicine*, vol. 17, no. 1, Article ID 130, 2017.

[37] C. Y. Liu, X. Q. Li, and S. Q. Cai Sq, "Pharmacology and clinical research progress of lianhua qingwen capsules," *Pharm. Clin. Chin. Materia. Med.*vol. 26, pp. 84-85, 2010.

[38] C. R. Lupfer, K. L. Stokes, T. Kuriakose, and T.-D. Kanneganti, "Deficiency of the NOD-Like receptor NLRC5 results in decreased CD8(+) T cell function and impaired viral clearance," *Journal of Virology*, vol. 91, no. 17, Article ID e00377-17, 2017.

[39] E. L. R. Sheldrick, K. Derecka, E. Marshall et al., "Peroxisome-proliferator-activated receptors and the control of levels of prostaglandin-endoperoxide synthase 2 by arachidonic acid in the bovine uterus," *Biochemical Journal*, vol. 406, no. 1, pp. 175–183, 2007.

[40] Y. L. Song, C. Yao, Y. M. Yao et al., "XueBiJing injection versus placebo for critically ill patients with severe community-acquired pneumonia: a randomized controlled trial," *Critical Care Medicine*, vol. 47, no. 9, pp. e735–e742, 2009.

[41] M.-w. Liu, M.-x. Su, W. Zhang et al., "Protective effect of Xuebijing injection on paraquat-induced pulmonary injury via down-regulating the expression of p38 MAPK in rats," *BMC Complementary and Alternative Medicine*, vol. 14, no. 1, p. 498, 2014.

[42] T.-L. Si, Q. Liu, Y.-F. Ren et al., "Enhanced anti-inflammatory effects of DHA and quercetin in lipopolysaccharide-induced RAW264.7 macrophages by inhibiting NF-κB and MAPK activation," *Molecular Medicine Reports*, vol. 14, no. 1, pp. 499–508, 2016.

[43] L.-L. Zhang, H.-T. Zhang, Y.-Q. Cai et al., "Anti-inflammatory effect of mesenchymal stromal cell transplantation and quercetin treatment in a rat model of experimental cerebral ischemia," *Cellular and Molecular Neurobiology*, vol. 36, no. 7, pp. 1023–1034, 2016.

[44] H. Wang, H. X. Song, D. F. Wang et al., "Potential mechanism of Xuanfei Baidu formula in treating new coronavirus pneumonia based on network pharmacology and molecular docking," *Journal of Hainan Medical University*, vol. 26, pp. 1361–1372, 2020.

[45] L. Yi, Z. Li, K. Yuan et al., "Small molecules blocking the entry of severe acute respiratory syndrome coronavirus into host cells," *Journal of Virology*, vol. 78, no. 20, pp. 11334–11339, 2004.

[46] H. Liu, F. Ye, Q. Sun et al., "Scutellaria baicalensis extract and baicalein inhibit replication of SARS-CoV-2 and its 3C-like protease in vitro," *Journal of Enzyme Inhibition and Medicinal Chemistry*, vol. 36, no. 1, pp. 497–503, 2021.

Hindawi
Evidence-Based Complementary and Alternative Medicine
Volume 2021, Article ID 7402979, 18 pages
https://doi.org/10.1155/2021/7402979

Research Article

History and Development of TCM Case Report in a Real-World Setting

Hua Zeng,[1] **Yiqi Qiao**,[1] **Xue Luo**,[1] **Xin Chen**,[1] **Zhendong Wang**,[1] **Huafeng Pan**,[1] **Qi Wang**,[1] **and Guo-qing Zheng**[1,2]

[1]*Science and Technology Innovation Center, Guangzhou University of Chinese Medicine, No. 12, Jichang Road, Baiyun District, Guangzhou 510405, China*
[2]*Department of Neurology, The First Affiliated Hospital of Zhejiang Chinese Medical University (Zhejiang Provincial Hospital of Chinese Medicine), No. 54, Youdian Road, Shangcheng District, Hangzhou 310006, China*

Correspondence should be addressed to Huafeng Pan; gzphf@gzucm.edu.cn, Qi Wang; wangqi@gzucm.edu.cn, and Guo-qing Zheng; gq_zheng@sohu.com

Received 14 September 2021; Accepted 17 November 2021; Published 29 December 2021

Academic Editor: Xuezhong Zhou

Objective. The medical record of Chinese medicine is a miniature of the theoretical system of traditional Chinese medicine (TCM), with a time-honored history in a real-world setting and a firm place in medicine. In modern times, people have emphasized the value and standardization of TCM cases. The aim of this study was to explore the historical origins and developments of TCM case records. *Methods*. A chronological narrative style was used to divide the development history of TCM case records into early (1600 BC–220 AD), middle (220–1911 AD), and modern periods (1912–till now). The historical context of the origin and development of TCM case records was analyzed through the evolution of the format and content of the case recording files with the specific documents and distinctive cases. *Results*. From the early to middle period, the development of TCM case record had experienced four periods: the budding, blossoming, maturity, and heyday. In modern times, they presented the following characteristics: A, the establishment and development of the discipline of TCM medical records; B, the standardization of the writing format of TCM medical records; C, a large number of books concentrating on recording and studying TCM medical records, especially those of prestigious veteran TCM doctors; D, the proliferation of TCM case reports published in journals; E, the establishment of TCM medical records databases and application platforms integrating computer programs and artificial intelligence; F, many reporting guidelines have been developed in order to improve the reporting quality of case report in TCM. *Conclusions*. The study analyzed and illustrated the characteristics of TCM case records of different dynasties in terms of writing content and format. TCM case record is a relatively young discipline in spite of its ancient origins. TCM case records still have far-reaching significance for the inheritance and development of TCM theory and clinical experience. From the wisdom of history, its positive impact has just been revalued to be validated and it will continue to develop.

1. Introduction

On the issue of terminology in this study, "case record" is used extensively in various aspects, whereas "case report" is used exclusively in modern medical journals. Case report refers to a detailed description and formal summary of a diagnostic or therapeutic problem experienced by one or several patient(s), such as exposure, symptoms, signs, interventions, and outcomes [1, 2]. The early case records in the west can be found in the ancient Egyptian medicine papyrus records from about 1600 BC [3–5]. In modern times, the case report is a particular form of clinical evidence despite the low-ranking evidence level in the modern evidence hierarchy [6]. It plays important roles in identifying new, rare, or unusual diseases [7]; evaluating the efficacy, safety, and cost of treatments; and improving medical education, patient care, and medical research. Vandenbroucke [8] stated that "case reports and series are highly sensitive to

the discovery of novelty and therefore remain one of the cornerstones of medical progress, providing many new perspectives in medicine."

Traditional Chinese Medicine (TCM) is a unique and integrated medical theoretical system with a long history of several thousand years. Its origin can be traced back to remote antiquity. Historically, case records are a delicate and irreplaceable form of reporting on the comprehensive application of TCM theories [9], a great treasure of TCM heritage, and a product of its long-term development. The possibly earliest TCM case records date back to the Yin and Shang Dynasties (1300-1046 BC). When hieroglyphics were invented, medical records were engraved on cattle bones and tortoise shells [10, 11]. Case records/case reports have been providing evidence for effectiveness and safety of TCM in a real-world setting, which has been accumulated over thousands of years. Its connotations are the following: (1) It originates from clinical practice with integrity and authenticity; (2) it is hands-on, immersive case of treatment; (3) it describes individual syndrome differentiation and treatment, which is the personalized design and application of the TCM theory; and (4) it is clinically instructive and exemplary for future generations [12, 13].

The wisdom of the long history of TCM has blossomed by taking history as an inspiration to guide the future development. For example, the inspiration for artemisinin for malaria came from Ge Hong's (284–346 AD) "A handful of Artemisia annua, soak in two liters of water, wring out the juice and drink it all" from the *Zhouhou Beiji Fang* (*Handbook of Prescriptions for Emergencies*) [14]. *Report to ministers from the Department of Health Steering Group on the Statutory Regulation of Practitioners of Acupuncture, Herbal Medicine, Traditional Chinese Medicine and Other Traditional Medicine Systems Practised in the UK* [15] pointed out that "the recorded history of traditional use over many years should be assessed and incorporated into the evidence base supporting the effectiveness and safety of herbal/traditional medicines and acupuncture" when building an evidence base. The *European Directive on Traditional Herbal Medicinal Products* [16] also noted that "The long tradition of the medicinal product makes it possible to reduce the need for clinical trials insofar as the efficacy of the medicinal product is plausible on the basis of long-standing use and experience" (Directive 2004/24/EC). Thus, it is necessary to explore chronologically the historical origin and development of TCM case records and their contribution to the modern innovations and developments of TCM.

2. Early Period

The early period of TCM case records was from Shang Dynasty (1600-1046 BC) to Han Dynasty (206 BC–220 AD). The summary of their main contributions in the period is shown in Table 1.

During the Shang Dynasty, medical principles were based on myths and legends as well as experience, which were very primitive in form. Inscriptions emerged on oracle bones of buffalo and tortoise shells (Figure 1), some of which described the use of wine and hot water as medicine and stone needles and bronze knives as surgical instruments. Some oracle bones threw light on illnesses, which were divination records about symptoms and signs, disease patterns, etiology, diagnosis, dynamic course of disease development, and interventions. It seemed as the earliest records about medical cases and the embryonic form of TCM case records [17].

Zhou Dynasty (1100-221 BC) was divided into four periods: Western Zhou (1100-771 BC), Eastern Zhou (700-256 BC), Spring and Autumn Period (770-476 BC), and Warring States Period (476-221 BC). TCM achieved in an extent of development during Zhou Dynasty especially in medical organization. The *Zhouli* (*Rites of Zhou*) [18, 19], written by Zhou Gong-dan, is an important document that records the ceremonies and systems from Western Zhou Dynasty to Warring States Period. He played a valid role in the consolidation and development of Zhou Dynasty and in the establishment of national laws and regulations. The book consists of six parts corresponding to six ministries according to ancient cosmology. One part named the celestial ministry, recorded that there was an organized medical system in the Eastern Zhou Dynasty in which the imperial officials received various medical training. TCM doctors were classified into four categories: *shiyi* (dietitian), *jiyi* (physician), *yangyi* (surgeon), and *shouyi* (veterinarian) [20]. Their duties were well defined. The chief doctor was responsible for the administration of all medical matters and the collection of drugs for medical purposes. The doctors' works were examined based on their case records recorded by the chief doctor [21]. Each doctor's salary was fixed according to the case recording results shown at the end of the year. If all cases get well, it is excellent; if there is one failure in ten cases, it is second; if two out of ten, third; three out of ten, fourth; and if four out of ten, it is bad. When any death occurs, the doctor in charge has to record the cause of death and submit the report to the superintendent.

During the early Spring and Autumn Period, *Lvshi Chunqiu* (*The Spring and Autumn of Lv Bu-wei*) [22], an encyclopedic Chinese classic document compiled around 239 BC, had recorded the budding of TCM case record. It recorded the following case of psychotherapy:

> Case 1: King of the Qi state (323-284 BC) suffered from *Wei* (sore and ulcer) during the Warring States Period. Wen Zhi, a proficient TCM physician at the Song state, was invited to treat him. After detailed diagnosis, he said to the prince: "Your father is treatable, but he will kill me after cured." The prince asked: "Why?" Dr. Wen said: "The only treatment method is to infuriate your father. If I do it, I am surely put to execution." However, the prince begged: "I pledge my life and my mother's life for you." Dr. Wen had appointments with the prince to cure the King, but he deliberately broke them numerous times. Consequently, he incurred the wrath of the King. Then, Dr. Wen kept the appointment with King to ignite his fury through the following behaviors:

Table 1: Summary of main contributions of TCM case records in the early period.

Representative books	Author	Time	Contributions to TCM case records
Rites of Zhou	Zhou Gong-dan	—	It recorded the earliest organized medical system in the Eastern Zhou dynasty in which the imperial officials received various medical training. TCM doctors were classified into four categories: *shiyi* (dietitian), *jiyi* (physician), *yangyi* (surgeon), and *shouyi* (veterinarian). The doctors' salary was connected with their medical cases recorded by the chief doctor. The death was needed to record too.
The Spring and Autumn of Lv Bu-wei	Lv Bu-wei	239 BC	It is an encyclopedic Chinese classic document, which had recorded the budding of TCM case record.
The Historical Records	Sima Qian	206 BC-24 AD	There were 25 TCM cases recorded in the biographical section of *The Historical Records*, named *Biography of Bian Que and Cang Gong*, which was probably the earliest extant and relatively complete TCM case records in Chinese historical literature. Cang Gong was the first to record clinical cases through personal observations with the motivation to evaluate the percentage of successes and failures and find a guide for future predictions. The 25 cases of him reflected the change of thinking from passive assessment to active case compilation in the Western Zhou dynasty.

—: not clear; TCM: traditional Chinese medicine.

Figure 1: The oracle bones of buffalo and tortoise shells in Shang Dynasty, which we obtained from the Shandong Museum in Shandong province, China.

he went to King's bed without taking off his shoes and deliberately trampled on King's clothes. Subsequently, Dr. Wen inquired the medical details; however, the King refused to reply. Dr. Wen further intentionally attacked the King with rude language, causing that the King raised the devil. He was so angry that he shouted loudly and sat up. These treatments cured the King's disease.

Comments: It is similar to psychotherapy in modern medicine. Although the case was not recorded by the doctor himself, it already contains three important parts of the case record: the schedule, diagnosis, and treatment of the disease. However, it lacks patient's information and doctor's opinion in detail.

The Han Dynasty (206 BC-220 AD) was a time of innovation with great developments in arts, philosophy, and technology. The ancient Silk Road in Northwest China, a popular communication and trade route, played key roles in promoting the development of TCM. The buds of TCM case records burst into a gorgeous blossom in the Dynasty. In addition, books on the study of ancient Chinese history appeared. For example, the *Shi Ji* (*The Historical Records*) [23], completed by Sima Qian (145-85 BC), was described in detail of China's history from the earliest times to his own days. There were 25 TCM cases recorded in the biographical section of *The Historical Records*, named *Bian Que & Cang Gong Liezhuan (Biography of Bian Que and Cang Gong)*, which was probably the earliest extant and relatively

complete TCM case records in Chinese historical literature [24]. *Cang Gong*, also named Chunyu Yi (215-167 BC), was the only physician going down in history in the Western Han Dynasty [25]. He was the first to record clinical cases through personal observations with the motivation to evaluate the percentage of successes and failures and find a guide for future predictions. He said: "The record of medical cases should be a conscious behavior of TCM physicians to summarize the success or failure and to improve the medical level." The 25 cases of him reflected the change of thinking from passive assessment to active case compilation in the Western Zhou Dynasty. The main characteristics and academic thinking of these cases are as follows: A, it pioneered the writing content and format of TCM case record, which included patient' name, home address, profession, name of disease and name of TCM pattern, main complaint, pulse condition, etiology, pathogenesis, syndrome differentiation, diagnosis, treatment, and prognosis; B, 23 kinds of diseases were recorded, most of them were digestive diseases. Failures as well as successes were noted as they really happened. Fifteen out of 25 patients were successfully cured; C, he ascribed most illnesses to excess sweating or excess sexual life or over-drinking or over-fatigue or exogenous pathogenic factors such as wind or cold; D, he paid much attention to the diagnosis of observation and pulse-taking; E, he was skilled at flexibly using acupuncture, moxibustion, Chinese herbal medicine, cold compress, and other treatment methods. Chinese herbal medicine was used in the form of decoction, powder, medicated liquor, gargle, and even pill. He is thought to be the first person to use pills as a form of drugs, such as pill of Banxia (*Rhizoma Pinelliae*). The following is a case record of his style:

> Case 2: An officer in the Qi state suffered from dental caries. Dr. Chunyu asked him: "Do you rinse your mouth after eating?" The officer said: "No, I do not." Dr. Chunyu asked again: "Will you open your mouth when sleeping?" He said: "Yes, I always do that." "And do you have any other discomfort," Dr. Chunyu inquired. The officer answered: "I have got a wind-cold these days." Dr. Chunyu said: "Ok, I will do moxibustion with your left Yangming meridian, and give you a prescription named Kusen (*Radix Sophora Flavescentis*) decoction, you must gargle it 600 ml a day." The official was confused and asked: "Dear doctor, why do I have cavities?" Dr. Chunyu answered: "I think the causes included that you had attacked with evil-wind, slept with mouth opened, and did not rinse the mouth after eating." Then, the officer did moxibustion every day and rinsed his mouth with Kusen decoction (post-cibum). Several days later, he recovered.
>
> Comments: This case record is more mature in writing style. It is closer to modern guidelines of case record as it contains the patient information, diagnosis, treatment interventions, and the clinical efficacy. It is scientific and advanced at that time to gargle with *Radix Sophora Flavescentis* decoction, which was proved to have a variety of pharmacological activities, such as anti-inflammatory and antiviral in modern [26].

3. Middle Period

The middle period was defined from the Three Kingdoms (220–280 AD) to the Qing Dynasty (960–1911 AD). The development of TCM case records had achieved unprecedented development. There had a huge change took place at the Song Dynasty (960–1279 AD). With the progress of publishing and printing technology and the attention to medicine paid by the Song' government, medicine practice was becoming more reinforced and specialized. Monographs on specialized fields or particular diseases were appeared. At that time, the publications' number and variety transcended the sum of all previous dynasties, many of which were quite original. The summary of main contributions in the period is shown in Table 2.

Xu Shu-wei (1080–1154 AD) was not only an expert on exogenous febrile disease, but also having a greatly influence on the treatment of miscellaneous diseases. One of his great contributions *Shanghan Jiushi Lun* (*Ninety Syndromes of Typhoid Diseases*) [27], written in 1133 AD, was the first existing TCM case records monograph, and the earliest collection of typhoid case records. The book described ninety cases of typhoid, most of which recorded the following aspects: A, patient information: (a) demographic information such as appellation, age, gender, address, occupation, diet, and lifestyle; (b) main symptoms of the patient (his or her chief complaints, tongue, and pulse); B, time line: important dates and times in this case, including time of onset and duration, and time of consultation, as well as the 24 solar terms if related to the case); C, diagnostic reasoning; D, the utilization of herbal formulas and treatment efficacy. The effectiveness was 78 treatable cases and 12 incurable cases. He used 78 prescriptions in total, and 42 out of them were classical TCM prescriptions. His second great contribution was *Puji Benshi Fang* (*Prescriptions of Formularies for Universal Relief*) [28] (1143–1154 AD), the representative formularies that contained a total of 127 cases. It included 113 cases of miscellaneous diseases treated by himself and 14 cases by his peers. The TCM case records were compiled in this book in the form of an appendix. He was the pioneer to record clinical cases behind his prescriptions in order to expound TCM theory, which had an impact on the format of subsequent TCM case record.

Xiao'er Yaozheng Zhijue (*The Appropriate Way of Recognizing and Treating Infant Maladies*) [29] was the earliest extant, well preserved, and complete monograph of paediatric case records in China written by a disciple of Dr. Qian Yi. Qian Yi (1035–1117 AD), an outstanding paediatrician in the Northern Song, was known as the father of TCM paediatrics. This book has a total of three volumes, and the middle volume contains Dr. Qian's 23 case records. He recorded different various kinds of diseases such as fever, vomiting and diarrhea, cough and asthma, skin rash, acute

Table 2: Summary of main contributions of TCM case records in the middle period.

Representative books	Author	Time	Contribution to the TCM case records
Ninety syndromes of typhoid diseases	Xu Shu-wei	1133 AD	It was the first existing TCM case records monograph, and the earliest collection of typhoid case records. The book described ninety cases of typhoid.
Prescriptions of formularies for universal relief	Xu Shu-wei	1143–1154 AD	It was the representative formularies that compiled TCM case records in the form of an appendix. He was the pioneer to record clinical cases behind his prescriptions, which expounded his TCM theory and had an impact on the format of TCM case record.
The appropriate way of recognizing and treating infant maladies	Qian Yi's disciple	1119 AD	It was the earliest extant, well-preserved, and complete monograph of paediatric case records in China written by Qian Yi's disciple. In the view of Dr. Qian's cases, we deduced that he was the pioneer to differentiate the symptoms of diseases.
Han's medical treatment	Han Mao	1522 AD	It was firstly to put forward the specific regulations on TCM case record, including inspection, auscultation, olfaction, inquiry, pulse-taking, palpation, diagnosis, and treatment. These regulations were subdivided into 27 specific items. This was the first time for TCM doctors to put forward the standardized writing structure and elements of TCM case record.
Essence of pulse theory	Wu Kun	1584 AD	It further supplemented and modified the writing structure and elements of TCM case record as "seven aspects and one quotation."
Experience of Chinese medicine	Yu Jia-yan	1643 AD	It contained a specialized chapter about the standardization of writing content and format of TCM case record. It completed the standardization of the items in TCM case record, which played a crucial role in the training of clinical ability, the in-depth discussion of TCM theories, and the improvement of clinical level and also had great practical significance to promotes the development of TCM case record.
Classified medical records of celebrated physicians	Jiang Quan and his son	1549 AD	It collected all of the monographs on medical case records of their predecessors before Ming dynasty, which was the first summary of TCM case records in Chinese history. It provided their pioneering experience for the compilation of TCM case records, which was important work linking the past with the future.
Supplement to classified case records of celebrated physicians	Wei Zhi-xiu and Wang Shi-xiong	1770 AD	It was considered the great work and second summary of TCM case records. It not only provided comprehensive data for his successors to analyze TCM but also lay a foundation for promoting the development of case records. Until now, it was still the largest extant writings of TCM case records, which was of high value in both literature and academic.
Compendium of Materia Medica	Li Shi-zhen	1578 AD	It was the first time to provide corroborative evidence of the efficacy of the medicinal product through attaching the relevant TCM case records below each herbal medicine.
Medical Records as a Guide to Clinical Work	Ye Tian-shi	1764 AD	It has become the most researched, the most numerous edition, and the most reprinted personal medical monograph. Its record content was relatively comprehensive and has rich and profound meaning, which still plays an important role in the enlightenment of later generations to learn about TCM case records.

TCM: traditional Chinese medicine.

or slow convulsion, hemoptysis, dyspepsia, and ascariasis. He was the pioneer to differentiate the symptoms of diseases. When coming down to treatment, Dr. Qian emphasized on the relationship between the onset time of disease and the season.

During the long-term development of the TCM theory, due to the diversity of geography, time, and academics, a medical phenomenon with very distinctive characteristics has emerged, namely, the formation of different academic schools of TCM. Its birth has far-reaching significance in promoting the inheritance and development of TCM theories and TCM case records. Academic schools can be formed actively or passively, and they require specific "soil conditions," that is, development background, such as economic development, cultural prosperity, medical and commercial gathering, and academic exchanges. The main characteristics of TCM academic schools are a unique academic idea or proposition, a specific style of medicine, or a certain treatment technique or characteristic therapy as a heritage, and a self-contained system with a certain historical

influence and recognition. TCM academic schools must have typical representatives and representative works, and a stable inheritance system. Before the Tang and Song dynasties, most of the medical practitioners of all generations referred to the classical Chinese medical works such as *Huangdi's Internal Classic* (*Huang Di Nei Jing*), *Difficult Classic* (*Nan Jing*), *Treatise on Cold Damage Diseases* (*Shang Han Lun*), and *Synopsis of the Golden Chamber* (*Jin Gui Yao Lue*), so they could be passively divided into the School of Medical Scriptures, the School of Scriptures, and the School of Typhoid. However, due to their lack of clear and continuous mentor-apprentice system ("Shicheng" system), some scholars believed that the classical classics should not be considered academic schools. It was not until the Jin-Yuan period, when the four great scholars of Liu Wansu, Zhang Congzheng, Li Dongyuan, and Zhu Danxi each formed a different academic doctrine and a relatively independent academic school that TCM academic schools began to be classified according to strict requirements [30].

In the Jin Dynasty, Liu Wansu started to study the *Plain Questions* (*Su Wen*) at the age of 25. He took the "nineteen articles of pathogenesis" of *Plain Questions* as the theoretical basis, systematically classified diseases according to the five evolution phases and six climatic factors (Five Yun and Six Qi), analyzed the etiology of diseases, and combined his clinical experience and academic thought to explore the inner connection between causes and symptoms, and put forward his own insights in diagnosis and treatment methods. This led to the creation of the book *Plain Questions on Concept of Original Disease Type* (*Su Wen Bing Ji Yuan Bing Shi*), in which he proposed that "six climatic factors can transform fire" and founded the He-Jian School, also known as the Fire-Heat School. He also proposed the principles of cooling the exterior of the body and dipping heat to nourish yin as the treatment of heat-related diseases, which laid the foundation for the formation of the later Warming Diseases School. Zhang Congzheng, a follower of Liu Wansu, founded the Eliminating Pathogenic Factor School, emphasizing the academic idea of "disease is born from pathogenic factors," and developed the method of eliminating pathogenic factors by sweating, vomiting, and coming down methods, which also influenced the Warming Diseases School. He also authored the signature work *Confucians' Duties to Parents* (*Ru Men Shi Qin*). According to Li Dongyuan of the Jin Dynasty, "internal injury to the spleen and stomach leads to all kinds of diseases." He believed that "Inadequate spleen and stomach lead to many diseases." Based on the theory of Huangdi's Internal Classic, he thought that the four seasons are all based on nourishing stomach qi, so his treatment emphasized on regulating the spleen and stomach and raising the middle qi, and he made new formulas such as Buzhong Yiqi decoction. Because he was good at regulating the spleen and stomach with warm tonic methods, later generations called the academic school represented by him the Tonifying Spleen School. The representative work of the Tonifying Spleen School is *Treatise on the Spleen and Stomach* (*Piwei Lun*). In the Yuan Dynasty, Zhu Danxi was the founder of the Nourishing Yin School. He was the third-generation disciple (direct student) of Liu Wansu, the founder of the He-Jian School. He studied the doctrines of the above three schools and created the theory that "Yang is always in excess and Yin is always in deficiency," advocating the nourishment of Yin. He advocated the doctrine of nourishing yin with Yin deficiency and Yang hyperactivity as the core and created the famous formula, Yue Ju Pill. The representative work of the Nourishing Yin School is the *Danxi's Mastery of Medicine* (*Danxi Xinfa*), which was compiled by his disciples and focuses on miscellaneous internal diseases and the Danxi doctrine, discussing in detail the disease name, cause, syndrome, identification, symptoms, and treatment prescriptions. The Nourishing Yin School had an important influence on the formation and development of the later Xin'an school of medicine. In summary, the main characteristics of TCM academic schools in Jin and Yuan Dynasties are shown in Table 3.

During the Ming Dynasty (1368–1644 AD) and Qing Dynasty (1616–1912 AD), the development of TCM case record entered a relatively stable stage. With the increase of records of TCM cases in literature in previous dynasties, the number and variety of TCM case records have increased, and the volume of TCM case record has formed a certain scale, which laid a literature foundation for doctors in Ming and Qing Dynasties to summarize the medical cases of predecessors. The large amount and the standard style of TCM case records have become a symbol of the development of TCM case record towards prosperity. Ming Dynasty is the mature period, and Qing Dynasty was the heyday of the development of TCM case record. The main characteristics in this period were as follows: A, many experts begin to work on the standardization of medical case writing, which is one of the important signs of TCM case record maturity; B, TCM cases were recorded in monographs, collection, and research books. In particular, personal medical cases monographs flourished [31]; and C, TCM case records have become a specific medical literature style, which required not only to record personal clinical experience but also to comprehensively analyze the use of TCM theory.

As the rise of every TCM academic school is closely related to the background of the times, the emergence of the Warm Diseases School was a good example of a product of the call of the times of Ming Dynasty. At the end of the Ming Dynasty, major epidemics broke out in Hubei, Zhejiang, and Shandong provinces, resulting in countless deaths and fatalities. As a result, a physician of Wu Youke wrote the *Treatise on Pestilence* (*Wen Yi Lun*) and founded the Warm Diseases School, which was derived from the Typhoid School and He-Jian School and was known for its research and treatment of warm fever, which laid the foundation for the later development of epidemiology of exopathic diseases in China. The representative figures and works of the Warm Diseases School included Ye Tian-shi's *Treatise on Epidemic Febrile Diseases* (*Wen Re Lun*) and *Guide to Clinical Practice with Medical Records* (*Linzheng Zhinan Yi'an*); Wu Jutong's *Differentiation of Warm Febrile Diseases* (*Wen Bing Tiao Bian*); and Xue Shengbai's *Synopsis on Damp-Heat* (*Shi Re Bing Pian*). Han Mao (1441–1522 AD), an excellent doctor in Ming Dynasty, put forward the specific regulations on TCM

Table 3: Summary of main characteristics of TCM academic schools in Jin and Yuan dynasties.

Academic schools	Representative books	Author	Time	Main theory	Similarities	Differences
He-Jian school (fire-heat school)	*Plain Questions on Concept of Original Disease Type*	Liu Wan-su	1110 AD–1200 AD	According to the "five evolution phases and six climatic factors" principle, he advocated the theory that six climatic factors can transform fire.	The theory was referred to the classical Chinese medical work of Huangdi's internal classic.	1. He used the "nineteen articles of pathogenesis" of plain questions as the theoretical basis, systematically classified diseases according to the five evolution phases and six climatic factors (five Yun and six Qi). 2. He also proposed the principles of cooling the exterior of the body and dipping heat to nourish yin as the treatment of heat-related diseases, which laid the foundation for the formation of the later warming diseases school.
Eliminating pathogenic factor school	*Confucians' Duties to parents*	Zhang Cong-zheng	1156 AD–1228 AD	He emphasized the academic idea of "disease is born from pathogenic factors."	He was a follower of Liu Wansu, who also influenced the warming diseases school.	He developed the method of eliminating pathogenic factors by sweating, vomiting, and coming down methods.
Tonifying spleen school	*Treatise of Spleen and Stomach*	Li Dongyuan	1180 AD–1251 AD	He believed that the internal injury to the spleen and stomach or inadequate spleen and stomach can lead to all kinds of diseases.	His theory was based on the theory of Huangdi's internal classic	He thought that the four seasons are all based on nourishing stomach qi, so his treatment emphasized on regulating the spleen and stomach and raising the middle qi, and he made new formulas such as Buzhong Yiqi decoction.
Nourishing yin school	*Danxi's Mastery of Medicine*	ZhuDan-xi	1281 AD–1358 AD	He created the theory that "Yang is always in excess and Yin is always in deficiency," advocating the nourishment of Yin.	He was the third-generation disciple (direct student) of Liu Wansu and had studied the doctrines of the above three schools.	1. He advocated the doctrine of "nourishing yin" with Yin deficiency and Yang hyperactivity as the core, and created the famous formula, Yue Ju Pill (Yue Ju Wan). 2. *Danxi's Mastery of Medicine* was compiled by his disciples and focuses on miscellaneous internal diseases and the Danxi doctrine, discussing in detail the disease name, cause, syndrome, identification, symptoms, and treatment prescriptions. 3. The nourishing Yin school had an important influence on the formation and development of the later Xin'an school of medicine.

case record in his monograph *Hanshi Yitong* (*Han's Medical Treatment*) [32], including inspection, auscultation, olfaction, inquiry, pulse-taking, palpation, diagnosis, and treatment. And he subdivided these regulations into 27 specific items [33, 34]. This was the first time for TCM doctors to put forward the standardized writing structure and elements of TCM case record.

Wu Kun (1551 AD–1620 AD), a successor of his medical family in Ming dynasty, has been engaged in medicine for nearly 60 years. He has written a total of 6 kinds of medical books, one of which was *Mai Yu* (*Essence of Pulse Theory*) [35]. He further supplemented and modified the writing structure and elements of TCM case record as "Seven Aspects and One Quotation." Seven aspects of case record include the following: A, date of consultation, place, and patient's name; B, age, height, weight, face color, and voice; C, the main symptoms and signs, the onset time and the aggravated time of illness, and disease condition; D, the previous treatment history and clinical effects; E, nature of yin or yang, afraid of cold or heat, diet, sleep condition, and pulse condition; F, name of disease, name of TCM pattern, manifestation and root cause of disease, and chronic or acute; G, treatment method, diagnosis, prescriptions, the modification of prescription, the explanation of Chinese medicine and prescriptions, and contraindication. One quotation indicated that a doctor should sign his name and district at the end of a case record. However, he did not include any specific TCM case in his book.

Yu Jia-yan (1585 AD–1670 AD) was a famous doctor in the south of Yangtze River. His representative works, *Yuyi Cao* (*Experience of Chinese medicine*) [36], recorded more than 60 cases of miscellaneous diseases. Dr. Yu wrote a specialized chapter in the book about the standardization of writing content and format of TCM case record, including date of consultation, place, patient's name, age, height, weight, face color, voice, emotions, disease condition, etiology, the onset time and the aggravated time of disease, the main symptoms and signs, the present syndrome, the previous treatment history and clinical effects, afraid of cold or heat, diet, excretory functions, sleep condition, pulse condition, manifestation and root cause of disease, treatment method, diagnosis, prescriptions, composition of Chinese herbs, analysis of illness, analysis of treatment, and clinical efficacy. He not only ruled the specific contents of four diagnostic methods, but also advocated that we should pay attention to the external and internal environment for patients, at the same time record in detail the happening of the disease, the instant syndrome, and the therapeutic process. What's more, he emphasized that the doctor must write the evidence and principle of prescription clearly, as well as the prognostic situation. Thus, the comprehensive standardization of the items included in TCM case record played a crucial role in the training of clinical ability, the in-depth discussion of TCM theories, and the improvement of clinical level, and also had great practical significance to promotes the development of TCM case record.

Jiang Quan (1522–1566 AD) and his son collected all of the monographs on medical case records of their predecessors before Ming Dynasty and integrated them into *Mingyi Leian* (*Classified Medical Records of Celebrated Physicians*) [37], which was the first summary of TCM case records in Chinese history. The book consisted of 12 volumes, which were divided into 205 chapters with more than 3,300 TCM case records. It provided their pioneering experience for the compilation of TCM case records, which was important work linking the past with the future.

> Case 3: In August 1280 AD, a Judge Zhao of Zhengding County, Shijiazhuang City, Hebei Province, suffered a stroke. His signs and symptoms included loss of consciousness, paralysis on one side of his body, facial redness, deafness, nasal congestion, and slurred speech. Dr. Zhang felt his pulse, which showed stringy and rapid. From these manifestations, the diagnosis was a stroke that apoplexy infringed on the internal organs (zang-fu organs). He believed that a stroke in the five-zang organs would block the nine orifices, whereas a stroke at six-fu organs would stagnate the limbs. Therefore, he used Sanhua decoction as a purgative formula to eliminate blood stasis for regulating *qi* and nourishing limbs, and then used the *Zhibao Dan* (*zhibao mini-pills*) as inducing resuscitation formula to calming heart for tranquillization and resuscitation with aromatics in order to make *zang-qi* ascending and nine orifices resuscitated. After five days, the consciousness and speech turned clear. Dr. Zhang modified the prescription and asked the patient to use a rope to tie the affected low limb for walking aid exercise in order to promote the recovery of motor function. A few days later, the patient's muscle strength improved. During the stroke recovery period, Dr. Zhang performed acupuncture on the meridian points of the twelve regular meridians for dredging meridians and collaterals. The patient's motor function improved rapidly, and he was able to walk several hundred steps without support. It was obvious that the patient was recovering well. Dr. Zhang told him to maintain a good mood and a regular diet every day. At the follow-up visit one year later, the condition and quality of life had basically improved (From *Classified Case Records of Celebrated Physicians*).
>
> Comments: Zhang Yuan-su was a famous doctor in the Jin Dynasty (1115–1234 AD) who specialized in treating stroke. This case is written in a more complete format and content, as it contains symptoms, syndromes, basic information, diagnosis, treatment, and follow-up. It has a time line depicting important dates and times. It also reports the therapeutic method of each treatment and the doctor's own views of the disease. As for the Sanhua decoction used by Dr. Zhang, our modern pharmacological study found that it can alleviate neurological deficits and exert neuroprotection against focal cerebral I/R injury [38].

Wei Zhi-xiu (1722–1772 AD), an eminent doctor, compiled a monumental work of *Xu "Mingyi Leian"* (*Supplement to "Classified Case Records of Celebrated Physicians"*) [39], which was considered the great work and second summary of TCM case records. It initially finished 60 volumes in 1770 AD. Unfortunately, he left his incomplete works since he died suddenly. Wang Shi-xiong, a famous peer, continuously completed the Wei's work and reclassified the book into 36 volumes, 350 chapters. This book collected about 5, 000 TCM case records from 308 famous physicians before the early Qing Dynasty. It takes the case records under the name of disease, and thus, one disease has several case records. The readers could compare mutually and inspire among them. In addition, Dr. Wei's detailed description of the causes of most of the patients includes their previous history, hobbies, dietary habits, body constitution, mental state, and family background. It not only provided comprehensive data for his successors to analyze TCM but also lay a foundation for promoting the development of case records. Until now, it was still the largest extant writings of TCM case records, which was of high value in both literature and academic.

Li Shi-zhen (1518–1593 AD), one of the greatest physicians, pharmacologists, and naturalists, compiled the outstanding medicine monograph *Bencao Gangmu* (*Compendium of Materia Medica*) [40], which is a work on an encyclopedic scale. He attached the relevant TCM case records below each herbal medicine in order to provide corroborative evidence of the efficacy of the medicinal product.

Ye Tian-shi (1667–1746 AD) was considered an eminent doctor in infectious disease in TCM. His followers collected his medical cases in his later years and compiled them into a book named *Linzheng Zhinan Yi-an* (*Medical Records as a Guide to Clinical Work*) [41]. Since its publication in 1764 AD, the book has become one of the most researched, the most numerous editions and the most reprinted personal medical monographs. There are 10 volumes in total, including medical, surgical, gynecological, paediatric, and androgynous diseases and syndromes. All the TCM case records reflected Dr. Ye's academic inheritance and innovation from the predecessors. TCM cases were recorded in chronological order of the symptoms, pathogenesis, dialectical diagnosis, and prescriptions according to the process of before and after treating. Its content was relatively comprehensive and has rich and profound meaning, which still plays an important role in the enlightenment of later generations to learn about TCM case records [42].

In the late Qing Dynasty, Western medicine gradually developed in China, and progressive physicians with a reform spirit in the TCM team realized that both Chinese and Western medicine had their own strengths and tried to converge the two academic disciplines. They put forward a series of views on the convergence of Chinese and Western medicine from theory to clinical practice and gradually formed a convergence trend and the School of Fusion of Chinese and Western Medicine. The School of Fusion of Chinese and Western Medicine was represented by Tang Zonghai, Zhu Peiwen, and Zhang Xichuan, whose representative works include *Records of Chinese medicine and Western Medicine* (*Yixue Zhongzhong Canxi Lu*) and *Five kinds of Chinese and Western Medical Books*. Zhang Xichun, was eclectic, absorbing new knowledge on the basis of traditional medicine and publishing his academic views and his clinical experience in the press continuously, which was widely praised by the medical community and had a great impact on the Chinese and Western medicine, making Zhang Xichun one of the most representative figures of the School of Fusion of Chinese and Western Medicine. This school opened up a new trend of convergence between Chinese and Western medicine and opened up the way for the modern combination of Chinese and Western medicine.

4. Modern Period

The modern period refers to the period from the Republic of China (1912–1949) to the present. Western medical knowledge has been permanently introduced into China [43]. Especially after the Opium War, a large number of missionaries were crowded into China [44], leading to unprecedented challenges in a variety of fields. As a result, many TCM practitioners began to integrate Western medicine into their practice and established medical journals for TCM.

After the establishment of the Republic of China in 1912, the whole governmental system was modeled on a western pattern, including the medical system. Thus, the development of TCM has not last long before because the Republic of China government changed the policy to restrict the medical activities of TCM and even call for abolishing TCM in 1929. TCM case records have also undergone a hard and tortuous course of development. TCM doctors began to vigorously establish medical journals, which can help to exchange medical experience and skill quickly. According to statistics, the number of TCM periodicals created during the Republic of China was at least 378. The spread media of TCM case records have partly turned from the books to journals, which leads to a transformation from case records to case reports in terms of writing format. For example, He Lian-chen (1861–1929), a prominent physician in the modern TCM history, recorded the case of scarlet fever using modern diagnosis and examination tools such as laryngoscope and round mouth plier to help diagnosis in his book *Chongding "Guang Wenre Lun"* (*The Revise of "Treatise on Epidemic Febrile Diseases"*) [45]. He also founded the earliest TCM journal *Acta Medica Shaoxing* in June 1908 [46] and set up a case column that classified the specific items as follows: A, patient information: name, gender, age, and address; B, history of present illness: etiology, onset time of disease, and symptoms. He emphasized the patient's name and clinical effect should be recorded clearly because it is good for later generations to verify the authenticity and accuracy so as to the value of modern medical record. He also pointed out that it is necessary to record the authors' institutions or societies, or any other relevant background information in published clinical case report [47]. He proposed eight requirements for the purpose of regulating writing format of TCM case to a unified style, which

Table 4: The main structure and elements of the format standard of TCM case records from the 5 monographs.

Representative books	Structure and elements
Biography of Bian Que and Cang Gong	Patient' name, home address, profession, name of disease and name of TCM pattern, main complaint, pulse condition, etiology, pathogenesis, syndrome differentiation, diagnosis, treatment, and prognosis
Han's Medical Treatment	Date of consultation, place, height, weight, face color, voice, disease condition, disease location, etiology, the onset time and the aggravated time of illness, afraid of cold or heat, diet, the previous treatment history, pulse condition, manifestation and root cause of disease, diagnosis, severity of illness, treatment method, prescriptions, medication methods.
Essence of Pulse Theory	Date of consultation, place, patient's name, age, height, weight, face color, voice, the main symptoms and signs, the onset time and the aggravated time of illness, disease condition, the previous treatment history and clinical effects, nature of yin or yang, afraid of cold or heat, diet, sleep condition, pulse condition, name of disease, name of TCM pattern, manifestation and root cause of disease, chronic or acute, treatment method, diagnosis, prescriptions, the modification of prescription, the explanation of Chinese medicine and prescriptions, contraindication, the doctor's signature.
Experience of Chinese Medicine	Date of consultation, place, patient's name, age, height, weight, face color, voice, emotions, disease condition, etiology, the onset time and the aggravated time of illness, the main symptoms and signs, the present symptoms, the previous treatment history and clinical effects, afraid of cold or heat, diet, excretory functions, sleep condition, pulse condition, manifestation and root cause of disease, treatment method, diagnosis, prescriptions, composition of Chinese herbs, analysis of illness, analysis of treatment, clinical effect.
Eight Requirements to TCM Case Record and Case Report by He Lian-chen	Patient, name of disease and name of TCM pattern, etiology, TCM pattern, diagnosis, treatment principle, prescriptions, treatment outcomes.

TCM: traditional Chinese medicine.

Table 5: The frequency of structures and elements according to the corresponding attribution principle.

Structure (frequency)	Corresponding attribute element (frequency)	
Patient information (5)	Date of consultation (3), place (3), patient's name (3), age (2), home address (1), profession (1)	
Past medical history (3)	The previous treatment history (2) and the previous clinical effects (3)	
Diagnosis (5)	Inspection (4)	Height (3), weight (3), face color (4)
	Auscultation (3)	Voice (3)
	Inquiry (5)	The main symptoms and signs (2), the onset time of illness (2), the aggravated time of illness (3), afraid of cold or heat (3), diet (3), sleep condition (2), excretory functions (1), emotions (1)
	Pulse-taking (5)	Pulse condition (4)
	Other diagnoses (2)	Name of disease (3), Name of TCM pattern (3)
Treatment (5)	Treatment method (4), treatment principle (1), prescriptions (4), medication methods (1), composition of Chinese herbs (1)	
Analysis of disease (2)	Etiology (4), pathogenesis (manifestation and root cause of disease) (3), nature of yin or yang (1), disease condition (3), disease location (1), severity of illness (1), chronic or acute (1)	
Analysis of treatment (2)	The modification of prescription (1), the explanation of Chinese medicine and prescriptions (1), contraindication (1)	
Outcome assessment (3)	Clinical effect (3)	
Prognosis (1)	Prognosis (1)	
Acknowledgment (1)	The doctor's signature (1)	

TCM: traditional Chinese medicine.

included patient, name of disease and name of TCM pattern, etiology, TCM pattern, diagnosis, treatment principle, prescriptions, and treatment outcomes. Based on the eight requirements, he further selected 371 case records from national prominent veteran TCM doctors and compiled them into a book *Quanguo Mingyi Yanan Leibian* (*Compilation of TCM Case Records from National Prominent Veteran TCM Doctors*) [48] in 1922.

Case column of a journal was gradually germinated and developed. The columns of TCM case report were mainly divided into four categories during the period of the Republic of China: (1) medical cases of famous doctors—the column of medical cases of famous doctors at that time was fresh records of clinical diagnosis and treatment in terms of content. There are also some columns, due to the long-term publication of a certain doctor's experiences, gradually developed into a column to record his or her individual clinical cases, such as *Ding Ganren Yan-an* (*Experienced Treatment Cases of Dr. Ding Ganren*) [49]; (2) ancient medical cases—the column of ancient medical cases reviewed the TCM case records of influential predecessors and put forward their own opinions about the cases, so as to strengthen the understanding and further study of TCM cases, such as *Gujin Yi-an Pingyi* (*Review on Ancient and Modern TCM Case Records*) [50] (written by Dr. Zhang Shanlei); (3) medical cases on quitting opium—the column of medical cases on quitting opium was emerged because Western countries began and smuggle opium into China, such as *Cao Yingfu Yi-an* (*Medical Case Records of Cao Yingfu*) [51]; and (4) medical cases about infectious diseases—due to the changeable climate and the poor sanitary conditions, many TCM journals opened up columns that actively participated in the prevention and treatment of epidemic diseases such as cholera, measles, and encephalitis, and the publications were more than 1,000 articles [52]. Thus, the publication of medical cases on opium cessation and infectious diseases was in line with the trend of that era.

As case records in medical books are still important as before, we summarized the content of the format standard of TCM case records from the 5 monographs, which is related to the format standard of medical cases, and then extracted the structure and elements of TCM case records (Table 4). In addition, according to the writing habit of modern medical cases, we combined the structures and elements obtained by the same category and counted the frequency of structures and elements according to the corresponding attribution principle (Table 5). The results showed that the ancient TCM case records not only included some items of the modern medical records such as the basic information, chief complaint, disease history, diagnosis, and treatment, but also contained the contents such as inspection, listening and smelling, inquiring, and pulse-taking, which can reflect the characteristics of TCM. The TCM case records especially emphasized the content of medical case analysis, which highlighted the essential attribute that case records are the carrier of clinical experience.

Since the People's Republic of China had established on October 1, 1949, the country and government have attached great importance to TCM. The Chairman Mao once said: "Traditional Chinese Medicine is a great treasure-house and should be explored and improved diligently." At present, the economic strength in China has enhanced greatly, and modern science and technology has developed rapidly, providing favorable social, economic, and technological conditions for the development of TCM [53]. The development of TCM case record/report is presented a situation of a hundred flowers bloom as follows: A, the establishment and development of the discipline of TCM medical records; B, the writing format of TCM medical records is standardized; C, lots of books concentrated on recording and studying TCM case records, especially from prestigious veteran doctors; D, a surge of TCM case reports published in journals; and E, establishment of TCM case database and application platform integrating computer program with artificial intelligence.

With the development of TCM case records, the discipline of TCM medical records has been set up [54, 55] for the purpose of analyzing, extracting, and summarizing TCM case record and then deeply studying the law of diagnosis and treatment, the clinical thinking characteristics, academic thought, and corresponding research methods of TCM [56]. As a new branch of TCM disciplines, the discipline of TCM medical records has been developing rapidly. The increasing number of medical schools has compiled the corresponding textbooks for undergraduate and graduate students, such as "*Introduction to Medical Cases of Modern Prominent Veteran TCM Doctors*" [57]. Thus, the discipline of TCM medical records shows a significant role in the education field. On the one hand, case studies have the potential to be highly read and to have a significant impact on subsequent case research [58]. It provides a wide range of subjects, ideas, and methods for graduate students to carry out clinical, experimental, and history literature case research, and also plays a significant role in cultivating graduate students' clinical practice skill and scientific methods [59]. TCM case record can also help students or practitioners to learn relevant information and technology, which may strengthen clinical thinking ability and sense of responsibility [60]. It not only gives readers a chance to confront novel clinical scenarios and reflect upon their own practice [61], but also trains authors to think and write clearly and critically case records [62].

The writing format of TCM medical records become gradually standardized. In 1983, the Department of TCM in the Ministry of Public Health formulated and issued "*The writing format and requirements of TCM medical records (trial)*." In 1991, the *National Administration of Traditional Chinese Medicine* formally formulated the writing regulations of TCM medical records and published the book "*Standards of Writing TCM medical records*" [63]. The regulations include five aspects: A, general rules of writing TCM medical records; B, unified name of TCM medical records; C, sort order and explanation of subjects of TCM medical records; D, writing format of TCM medical records; and E, key points of writing medical records about various TCM departments and set examples of them. In 2002, the *National Administration of Traditional Chinese Medicine* set up "*The general standards of writing medical records of TCM and integrated Chinese and Western medicine (trial)*" [64]. In 2010, the *National Administration of Traditional Chinese Medicine* promulgated "*The general standards of writing TCM medical records*" [65]. These regulations issued by the national administration promoted the development of medical records and gradually transformed the traditional writing format of TCM case records into "modern medical records." These regulations require a complete set of items,

including TCM characteristic diagnosis and treatment information such as inspection, auscultation, smelling, inquiry, and pulse-taking.

Lots of books concentrated on recording and studying TCM case records. One of the representative literature studies is "*ErXu 'Mingyi Leian'*" (*The Second Supplement of 'Classified Case Records of Celebrated Physicians'*)" [66], compiled by Lu et al. in 1996. It was regarded as the second supplement of "*Classified Case Records of Celebrated Physicians*" and the third summary of TCM case records. This book added the medical cases of famous doctors from the Qing Dynasty to the early years of People's Republic of China, with a total of about 15,000 medical cases and more than 200 monographs of TCM case records. In 1990, the *Ministry of Personnel*, *Ministry of Health, and National Administration of Traditional Chinese Medicine* jointly issued the decision on taking emergency measures to inherit the academic experience of prestigious veteran TCM doctors [67]. Due to the urgency to rescue their academic thoughts and clinical experiences, a large amount of case records by prestigious veteran TCM doctors have been compiled and published across China. The first kind is a compilation of medical cases of one famous TCM doctor such as *Medical Records of Pu Fuzhou*, which was first published in 1972 and was regarded as a classic work of TCM medical cases after the founding of the People's Republic of China [68]. The second kind is the book on collecting, organizing, and researching various medical cases of modern TCM doctors such as *The Essence of Medical Records of prestigious veteran TCM doctors*, which was compiled in 1990 and a selection of 146 famous TCM doctors with 1850 cases [69]. It reflected the general scenery of contemporary TCM clinic and played an important role in summarizing and inheriting the clinical experience of old TCM practitioners [70]. The third kind is medical case monographs on specific departments, which are on the rise. *Review and Analysis of Medical Case Reports in Internal Diseases by Famous Doctors* [71], edited by Li et al. [72], took the classification of internal diseases as the outline and the classification of doctors and TCM diseases and syndromes as the order. It compiled the TCM case reports of nearly 100 influential doctors, which promotes the development of TCM case reports of specialized departments. All in all, summarizing, inheriting, and studying the experience and academic thoughts of prestigious veteran TCM doctors can not only enrich the theoretical system of TCM, but also promote the academic progress of TCM [72].

A number of medical journals and columns have set up that focus on case reports. The first international, PubMed-listed medical journal called "*Journal of Medical Case Reports*" was established in 2007 [73]. Up to 2013, thousands of medical journals listed in PubMed have published more than 1.6 million medical cases [74]. At mid-2015, more than 160 journals were set up specifically for reporting case reports [75]. We did electronic searches in the database of Chinese National Knowledge Infrastructure from the inception to December 31, 2018, with the search terms of "subject" containing "case report*" OR "case record*" OR "case series" OR "medical case*" OR "medical record*," excluding "case control" AND "case observation" AND "clinical study" AND "clinical observation" AND "randomized controlled trials," and the literature source set from "Traditional Chinese medicine." A total of 19572 studies were identified, of which 51 studies were excluded because of duplicates. After screening the title and abstract of studies, 4000 studies were excluded because they are observations of clinical efficacy, minutes of conferences, or western medical case records. Five hundred and forty-eight studies were excluded because they are not related to case reports or case records after browsing full text. Finally, there were 14973 TCM case records or case reports left. The process of screening is presented in a flow diagram (Figure 2). The bar chart (Figure 3) shows that the general trend of publishing TCM case reports in journals was growing. It has a well beginning because TCM was used as a symbol for China and considered a national treasure in the years between 1953 and 1959 under the chairman Mao Zedong' government. However, when the Cultural Revolution was launched, traditional culture, thinking, and perspectives were crushed. TCM and TCM practitioners also suffered greatly under this movement. As a result, the number of published TCM case reports was decreased. After the Cultural Revolution was officially ended in 1976, TCM and Western physicians slowly re-emerged into China's society and TCM began to revive, which led to the ascending number of published cases. Since entering the 21st century, TCM has developed rapidly with its strong vitality. Between 2003 and 2012, the number of TCM case reports was nearly twice as much as that of the past decade, and the number of TCM cases reported in the recent five years exceeded the total number of cases reported in the previous ten years. Thus, the situation of publication of TCM case reports has increased rapidly in the past decades, indicating a great interest in the area.

The research methods of TCM case records have been advanced because of the application of computer program and artificial intelligence. With the combination of mathematical and statistical methods, many databases established specifically for TCM case records [76]. For example, Chinese Medical Case Database [77], Statistics and Analysis System for Medical Case Records in Ancient and Modern Times [78], and Database of Ancient TCM Medical Cases [79] resulted in much improvement in the efficiency of consulting case records literature. Computer software of an expert system [67] is an application platform for the purpose of exploring the medical thought and clinical experiences contained in TCM case records, so as to find the laws of clinical diagnosis and treatment of famous TCM practitioners, which can quickly transform doctors' experience into theory and guide clinical practice. According to artificial intelligence, an evidence base of TCM case reported system has been initiated to use in the Donzimeng Hospital of Beijing University of Chinese Medicine. All these high-tech tools serve as a breakthrough in the case record research method [80] help to improve the reporting quality and contribute to inheriting and developing TCM [81].

As for TCM academic school, since the Jin-Yuan Dynasty, they have been flourished and different distinctive schools of Chinese medicine have emerged so far. For

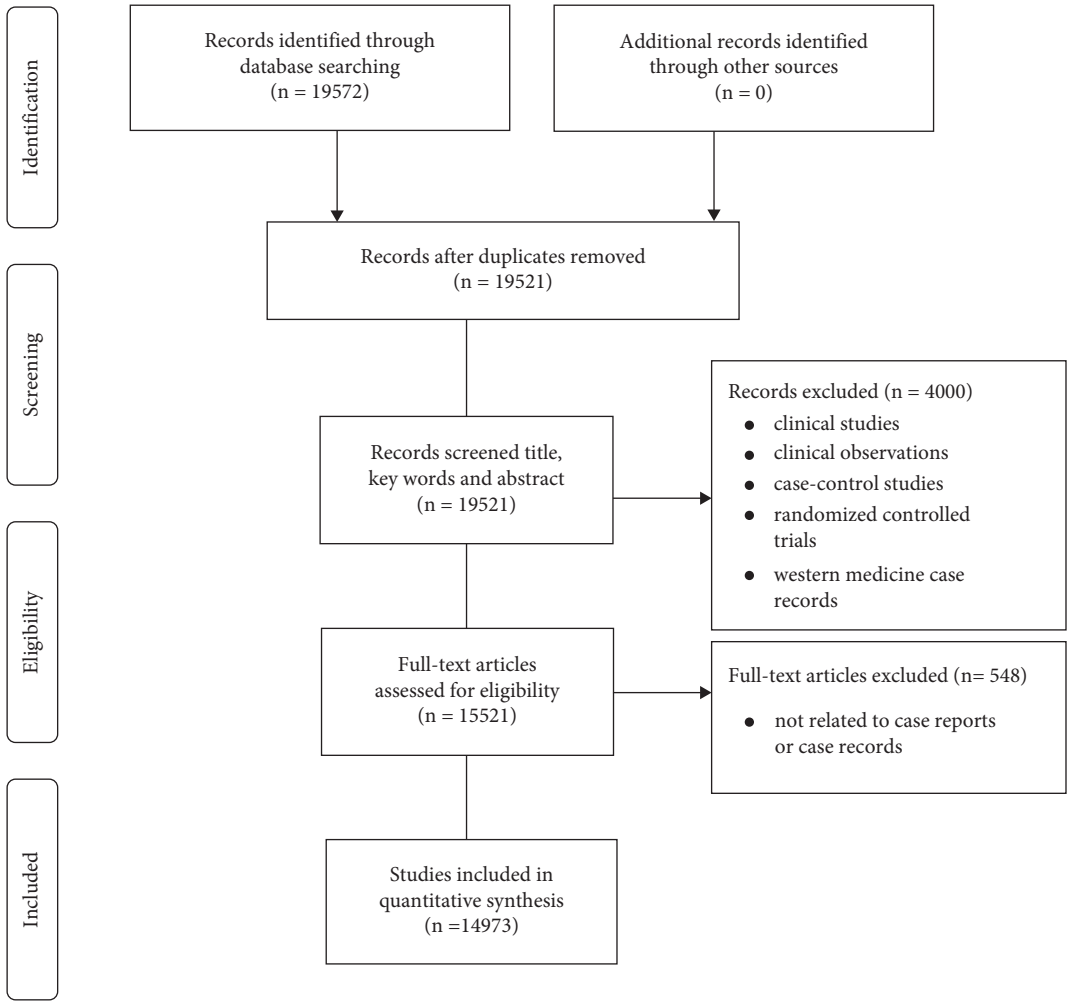

Figure 2: Flow diagram of the included studies.

example, according to the geographical division, there is the Yi-Shui School in the north, the Meng-He school in the south, and other schools such as the Qian-Tang school, Xin-An school, and Long-Sha school, which have flourished and led the way. The Hai School of Chinese Medicine has a history of several hundred years and has been divided into many specific academic schools according to different disciplines.

On July 30, 2013, the kick-off meeting of the national TCM academic school inheritance studio construction project, sponsored by the National Administration of Traditional Chinese Medicine and hosted by the Traditional Chinese Medicine Bureau Of Guangdong Province and Guangzhou University of Traditional Chinese Medicine, was held in Guangdong. The smooth and successful convening of this project kick-off meeting not only beat the gong for the full-scale work of the first batch of 64 TCM academic schools nationwide, but also marked the establishment of the TCM academic schools of TCM Inheritance Promotion Base Office, which is responsible for the daily business guidance and provision of services for the academic schools of TCM inheritance studios. This is conducive to promoting academic exchanges and resource integration among academic schools, realizing the intensification, scale, and specialization of academic school inheritance promotion, promoting the common development and sharing of results among schools, building a service platform for each school studio, promoting exchanges among academic schools, accelerating research, and realizing the transformation of results. With the change of times, there are many problems and challenges in the development of TCM academic schools. For example, there is a single mode and method of training talents of schools, the lack of communication among schools conservatively, the constraints of standardization and standardization of TCM treatment on the development of school inheritance, and the imperfect evaluation and use mechanism of school talent training. The characteristics of TCM clinical treatment are reflected in personalized treatment plans, reliance on doctors' personal experience, and the existence of multiple choices of TCM theories to guide clinical practice, rather than a single standard. Therefore, while implementing the standardization and standardization of TCM clinical and case writing, it is necessary to fully respect the law of TCM's own development, not only to meet the requirements of the accepted TCM theories and technical specifications, but also to reserve enough space for the

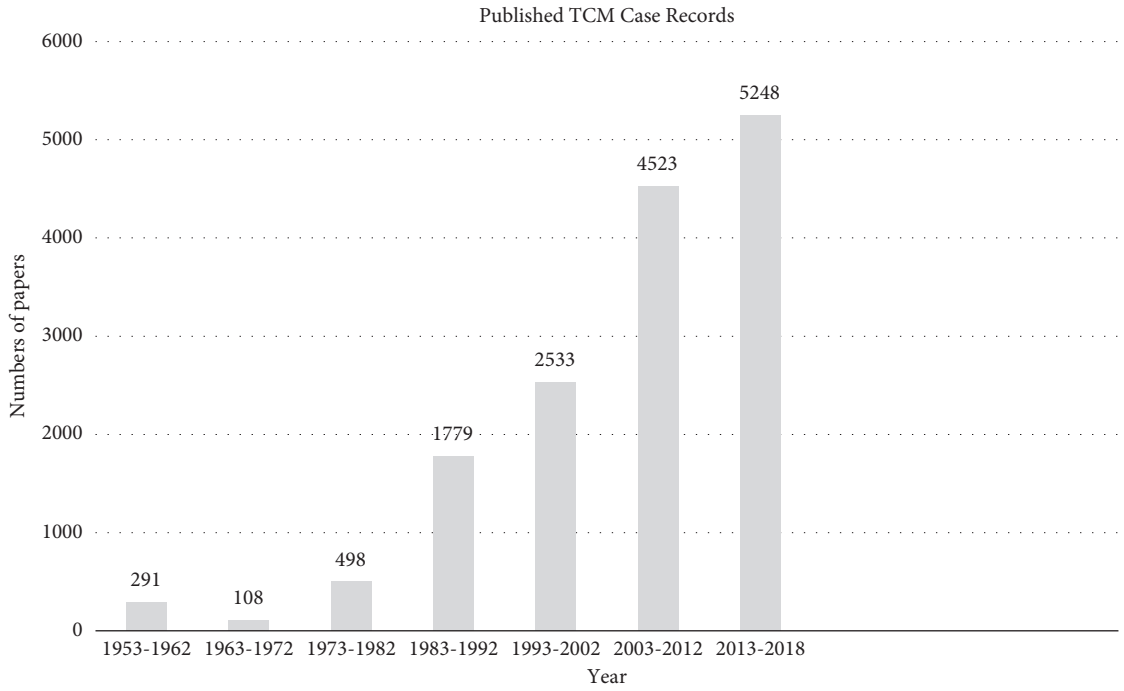

Figure 3: The characteristic of publishing trend of TCM case records (1953–2018).

Table 6: The characteristics of guidelines of TCM case reports.

Title	Theme	Author	Time	Journal	Characteristics
Writing case reports—author guidelines for acupuncture in medicine	Acupuncture	Adrian White	2004	Acupuncture in Medicine	It was a developing guideline for helping authors to write thorough but succinct case reports in a structured manner. The format of acupuncture case report in this guideline includes an abstract, description of the case, literature search, discussion, and summary or conclusions. A patient consent is required before publication.
Towards improving the reporting quality of clinical case reports in complementary medicine: Assessing and illustrating the need for guideline development	Conventional and complementary medicine	R. A. van Haselen	2015	Complementary therapies in medicine	It was presented as a conceptual framework for developing clinical case reporting guidelines for CAM treatments to integrate general guideline with specific quality items of CAM therapy, which practically implemented the development of a reporting guideline for case report in homoeopathy. It will be more clarity in reporting CAM cases because the specific quality items of CAM treatment are determined by the specific characteristics of the clinical case report and the corresponding specific objectives of CAM discipline.

Table 6: Continued.

Title	Theme	Author	Time	Journal	Characteristics
Consensus-based recommendations for case report in Chinese medicine (CARC)	Chinese medicine	FU Shufei	2016	Chinese Journal of integrative medicine	The CARC group established systematic recommendations by reviewing the general reporting quality of case reports. They have an important effect on promoting the development of TCM as it retained the principles of scientific, diversity, and practicability and satisfied the needs of standardization.
Writing a case report an introductory guide for practitioners of herbal medicine	Herbal medicine	Richard Adams	2016	Journal of herbal medicine	It was developed as an introductory guide for practitioners to write a case report about herbal medicine. It suggested a trick that herbal medicine' activity can only be explained in general terms with references of previous clinical observations partly because of inadequacy understanding of many biomedical mechanisms.

TCM: traditional Chinese medicine; CAM: complementary and alternative medicine.

development of unique academic ideas, clinical skills, and treatment characteristics, so that the TCM academic school can not only retain their own characteristics in terms of content, but also keep pace with the times, constantly accommodating and absorbing new elements, and promote their format tends to be standardized and standardized.

4.1. The Standardization of TCM Case Reports. The reporting quality of cases varies considerably in medical journals [82]. One study [83] had evaluated 1,316 case reports, which were published in four emergency medicine journals. The result showed that most case reports had fully reported patient information, types of interventions, and outcomes, whereas 50% case reports had not detailed the specific interventions and 67% case reports had not mentioned adverse events. Thus, in recent years, many experts in journals and organizations have developed reporting guidelines to increase the reporting quality of case report in both conventional western medicine and complementary and alternative medicine (CAM). In 2013, a consensus-based clinical case reporting guideline [84] was proposed through a consensus process in order to improve the completeness and transparency of published case reports. The CAse REport (CARE) guideline was simultaneously published in 7 journals. Up to 2017, this guideline has been translated into 10 languages and endorsed by a number of medical journals [85].

Similarly, the necessary elements of a CAM or TCM case had been continuously proposed for the purpose of providing guidance for publication in a standardized format in a peer-reviewed journal (Table 6). In 2004, the editor-in-chief Adrian White in the journal of "*Acupuncture in Medicine*," had written two articles [86] entitled "*Writing case reports – author guidelines for Acupuncture in Medicine*" in order to help authors to write thorough but succinct case reports in a structured manner. *Guidelines for case reports of adverse events related to acupuncture* had been published in the same year and same journal [87]. In 2008, based on the international requirements for case report writing, Yang et al. [81] integrated with the characteristics of the TCM theory and summarized the key components of TCM case reports, which can be used as a reference for later TCM practitioners to write case reports, and for qualitative quality evaluation of published case reports. In 2009, Wang et al. [88] propounded the recommendations on the publication and process norms of clinical case and determined the writing requirement and traceability from the aspects of brief abstract, background, general information, chief complaint, disease history, diagnosis, treatment, discussion, expert estimate, and reference.

van Haselen [89] presented a conceptual framework in 2015 for developing clinical case reporting guidelines for CAM treatments to integrate general guideline with specific quality items of CAM therapy. This framework has been practically implemented the development of a reporting guideline for case report in homoeopathy. It will be more clarity and transparency in reporting CAM cases because the specific quality items of CAM treatment are determined by the specific characteristics of the clinical case report and the corresponding specific objectives of CAM discipline. It will also greatly contribute to CAM research and education, as well as to improved patient care.

In 2016, a working group of case report in Chinese medicine (CARC) established systematic recommendations by reviewing the general reporting quality of case reports [9]. The CARC recommendations comprised a 16-item checklist, including title, abstract, keywords, English summary, introduction, patient information, clinical findings, diagnosis, treatment, outcome assessment, follow-up, advices and precautions, discussion/comment, acknowledgment, references, and figures/tables. They can not only expound the specialties of TCM, but also can apply to the common

projects in modern health research. Thus, they have an important effect on promoting the development of TCM as it retained the principles of scientific, diversity, and practicability and satisfied the needs of standardization.

In the same year, Adams [90] developed an introductory guide for practitioners to prepare case reports on herbal medicine. The checklists are as follows: title, author(s), addresses and any affiliation, abstract, introduction, case report, literature search, discussion, conclusion, acknowledgments, references and tables, illustrations, photographs, and figures. He points out the important issue that it is not wise to give a biomedical interpretation for the response to your herbal treatment without supporting references. The solution is that we can humbly point out that the activity of herbal medicine can only be explained in general terms by previous clinical observations due to the lack of knowledge and inadequacy understanding of many biomedical mechanisms. By following the recommendations and checklists of these guidelines, the reporting quality of TCM case reports would be greatly improved.

5. Conclusions

TCM case records have a history of several thousands of years and have been continuously inherited and developed. This study analyzed and illustrated the characteristics of TCM case records of different dynasties in terms of writing content and format. In modern times, with the strengthening of China's economic strength and an increase of policy support for TCM, TCM case records have also gained a rapid development in the following aspects: the state attaches great importance to the transmission of academic thoughts of prestigious veteran TCM practitioners; published a large number of medical case monographs; the emergence of a large number of specialized clinical cases both in books and journals; attached importance to standard writing of medical cases; and the application of technological innovation research methods such as mathematical statistics, database, and artificial intelligence. Despite its ancient origins, the discipline of TCM case records is a relatively young discipline. TCM case records remain far-reaching significance for the inheritance and development of TCM theory and clinical experience. From the wisdom of history, its positive impact has just been revalued to be validated and it will continue to develop.

Data Availability

No data were used to support this study.

Conflicts of Interest

The authors declare that they have no conflicts of interest.

Authors' Contributions

Hua Zeng contributed as the principal investigator and author and drafted the manuscript. Yiqi Qiao and Xue Luo helped to correct the grammatical errors in the article. Xin Chen and Zhendong Wang helped to sort and translate TCM case records. Hua-Feng Pan was the senior investigator of this study who refined the study. Guo-Qing Zheng and Qi Wang contributed to the overall design and summarized the feedback and comments. All the authors have read and approved the final version of the manuscript.

Acknowledgments

The authors are grateful to Zhao-Wen Han for providing the picture of oracle bones through the on-site visit to the Shandong Museum in the Shandong province in China. This work was supported by the Science and Technology Innovation Center and Institute of Clinical Pharmacology of Guangzhou University of Chinese Medicine. This work was supported by Key Laboratory Project of Colleges and Universities in Guangdong Province (2019KSYS005) and Guangdong Province Science and Technology Plan International Cooperation Project (2020A0505100052). This study was supported by grants from the National Natural Science Foundation of China (81673627 and 81973918).

References

[1] R. Garg, S. E. Lakhan, and A. K. Dhanasekaran, "How to review a case report," *Journal of Medical Case Reports*, vol. 10, no. 1, p. 88, 2016.

[2] A. G. Florek and R. P. Dellavalle, "Case reports in medical education: a platform for training medical students, residents, and fellows in scientific writing and critical thinking," *Journal of Medical Case Reports*, vol. 10, no. 1, p. 86, 2016.

[3] T. Nissen and R. Wynn, "The history of the case report: a selective review," *JRSM Open*, vol. 5, pp. 2054270414523410–2054270414523412, 2014.

[4] J. Breasted, *The Edwin Smith Surgical Papyrus*, The University of Chicago Press, Chicago, IL, USA, 1930.

[5] R. A. Rison, "Neurology case reporting: a call for all," *Journal of Medical Case Reports*, vol. 5, no. 1, p. 113, 2011.

[6] M. Hauben and J. K. Aronson, "Gold standards in pharmacovigilance," *Drug Safety*, vol. 30, no. 8, pp. 645–655, 2007.

[7] N. C. Dragnev and S. L. Wong, "Do we CARE about the quality of case reports? A systematic assessment," *Journal of Surgical Research*, vol. 231, pp. 428–433, 2014.

[8] J. P. Vandenbroucke, "In defense of case reports and case series," *Annals of Internal Medicine*, vol. 134, no. 4, pp. 330–334, 2001.

[9] S.-f. Fu, C.-w. Cheng, L. Zhang et al., "Consensus-based recommendations for case report in Chinese medicine (CARC)," *Chinese Journal of Integrative Medicine*, vol. 22, no. 1, pp. 73–79, 2016.

[10] L. K. T. Fu, "Pien Chueh, the Chinese god of medicine," *Journal of Medical Biography*, vol. 10, no. 2, pp. 92–99, 2002.

[11] H. Li, X. B. Liu, and J. H. Hu, "A review on the study of ancient case records of traditional Chinese medicine in recent ten years," *Chinese Medical Journal*, vol. 37, pp. 88–90, 2005.

[12] D. J. Pierson, "How to read a case report (or teaching case of the month)," *Respiratory Care*, vol. 54, no. 10, pp. 1372–1378, 2009.

[13] D. A. Grimes and K. F. Schulz, "Descriptive studies: what they can and cannot do," *The Lancet*, vol. 359, no. 9301, pp. 145–149, 2002.

[14] Y. Tu, "The discovery of artemisinin (qinghaosu) and gifts from Chinese medicine," *Nature Medicine*, vol. 17, no. 10, pp. 1217–1220, 2011.

[15] Department of Health Steering Group on the Statutory Regulation of Practitioners of Acupuncture, *Report to Ministers from The Department of Health Steering Group on the Statutory Regulation of Practitioners of Acupuncture, Herbal Medicine, Traditional Chinese Medicine and Other Traditional Medicine Systems Practised in the UK*, Robert Gordon University, Aberdeen, Scotland, 2008, http://hdl.handle.net/10059/176.

[16] The European Parliament and The Council Of The European Union, "Directive 2004/24/EC of the European Parliament and of the Council of 31 March 2004 on amending, as regards traditional herbal medicinal products, Directive 2001/83/EC on the Community code relating to medicinal products for human use," *Orkesterjournalen*, vol. L136, pp. 85–90, 2004.

[17] J. Chen, "Origin and historical development of medical records in ancient China," *Journal of ShaoXing University of Arts and Sciences*, vol. 2, p. 106, 2002.

[18] Z. Y. Xu, *Rites of Zhou (Chang PY Notes)*, Zhonghua Book Company, Beijing, China, 2014.

[19] X. D. Chen, "Brief research on the theory of cold and heat of the foods in "Zhou Li (The rites of Zhou)," *Chinese Medical Journal*, vol. 37, pp. 248–250, 2007.

[20] L. Fu, "Surgical history of ancient China: part 1," *ANZ Journal of Surgery*, vol. 79, no. 12, pp. 879–885, 2009.

[21] S. M. Li and Z. W. Guo, "Origin, development and research overview of medical case reports," *World Journal of Traditional Chinese Medicine*, vol. 10, pp. 809–812, 2015.

[22] Zhonghua Book Company, *The Spring and Autumn of Lv Buwei*, Zhonghua Book Company, Beijing, China, 1981.

[23] W. Susan, "Historical records by Sima Qian; Raymond Dawson," *Journal of the Royal Asiatic Society*, vol. 6, no. 2, pp. 286-287, 1996.

[24] B. C. Zheng, "A pioneer in establishing the tradition of keeping case records," *Journal of Traditional Chinese Medicine*, vol. 7, pp. 231-232, 1987.

[25] Z. Y. Zhen, *History of Chinese Medicine*, Shanghai Science and Technology Press, Shanghai, China, 1997.

[26] W. Wang, R.-l. You, W.-j. Qin et al., "Anti-tumor activities of active ingredients in compound kushen injection," *Acta Pharmacologica Sinica*, vol. 36, no. 6, pp. 676–679, 2015.

[27] S. W. Xu, *Three Books on Typhoid Diseases*, People's Medical Press, Beijing, China, 1993.

[28] S. W. Xu, *Prescriptions of Formularies for Universal Relief*, Shanghai Science and Technology Press, Shanghai, China, 1959.

[29] Y. Qian, *The Appropriate Way of Recognizing and Treating Infant Maladies*, People's Medical Press, Beijing, China, 2006.

[30] K.-j. Chen, Y.-h. Xie, and Y. Liu, "Profiles of traditional Chinese medicine schools," *Chinese Journal of Integrative Medicine*, vol. 18, no. 7, pp. 534–538, 2012.

[31] S. J. Xu and G. W. Wang, "Characteristics and value of TCM case reports," *Beijing University of Traditional Chinese Medicine*, vol. 20, pp. 7–11, 2013.

[32] M. Han, *Han's Medical Treatment*, Jiangsu Science and Technology Press, Jiangsu, China, 1985.

[33] W. K. Fu, "Format history of ancient Chinese medical record," *Knowledge of ancient medical literature*, vol. 4, pp. 30-31, 2003.

[34] D. P. Gao, Y. H. Wang, and R. S. Zhang, "Commentary on standardization of TCM records," *Chinese Journal of Integrative Medicine*, vol. 25, pp. 131–135, 2008.

[35] K. Wu, "Essence of pulse theory," 2019, http://www.360doc.cn/article/61422117_815218883.html.

[36] J. Y. Yu, *Experience of Chinese medicine (Jiao Zhenlian, et al. Notes)*, Shanghai Pujiang Education Press, Shanghai, China, 2013.

[37] Q. Jiang, *Classified Medical Records of Celebrated Physicians*, People's Medical Press, Beijing, China, 1957.

[38] L. Lu, H. Q. Li, J. H. Li, A.-J. Liu, and G.-q. Zheng, "Neuroprotection of Sanhua decoction against focal cerebral ischemia/reperfusion injury in rats through a mechanism targeting aquaporin 4," *Evidence-Based Complementary and Alternative Medicine*, vol. 2015, Article ID 584245, 7 pages, 2015.

[39] Z. X. Wei, *Supplement to Classified Case Records of Celebrated Physicians*, People's Medical Press, Beijing, China, 1957.

[40] S. Z. Li, *Compendium of Materia Medica*, People's Medical Press, Beijing, China, 1975.

[41] T. S. Ye, *Medical Records as a Guide to Clinical Work*, People's Medical Press, Beijing, China, 2006.

[42] F. Zhao, D. Lin, and Y. J. Zha, "Current study on guide to clinical records," *Liaoning University of Traditional Chinese Medicine*, vol. 18, pp. 144–146, 2016.

[43] K. C. Wong and L. T. Wu, *History of Chinese Medicine: Being a Chronicle of Medical Happenings in China from Ancient Times to the Present Period, Book 2*, Tientsin Press, Tientsin, China, 1932.

[44] L. Fu, "Medical missionaries to China and the reformation of anatomy," *Journal of Medical Biography*, vol. 24, no. 2, pp. 169–180, 2016.

[45] L. C. He, *The Revise of "Treatise on Epidemic Febrile Diseases"*, Fujian science and technology Press, Fujian, China, 2005.

[46] J. W. Zhang, Z. P. Wang, and Z. L. Lu, "Research on life and academic thoughts of He Lian-chen," *Journal of Traditional Chinese Medical Sciences*, vol. 11, pp. 18–20, 2004.

[47] F. J. Li, "Observing the standardization of TCM medical records from the view of "compilation of TCM case records from national prominent veteran TCM doctors"," *Journal of Chinese Medicine*, vol. 31, pp. 47-48, 1986.

[48] L. C. He, *Compilation of TCM Case Records from National Prominent Veteran TCM Doctors*, Shanghai science and technology Press, Shanghai, China, 1922.

[49] G. R. Ding, *Experienced Treatment Cases of Dr. Ding Ganren*, People's Medical Press, Beijing, China, 2007.

[50] S. L. Zhang, *Review on Ancient and Modern TCM Case Records*, Shaanxi Science and Technology Press, Xi'an, China, 2013.

[51] Y. F. Cao, *Medical Case Records of Cao Yingfu*, Shanghai Science and Technology Press, Shanghai, China, 2010.

[52] S. L. Bing, Y. S. Duan, and H. L. Ren, "Characteristics and research significance of the TCM periodicals in modern history," *Journal of Traditional Chinese Medical Sciences*, vol. 26, pp. 1029–1032, 2011.

[53] Z. Wang, "Modern opportunities for the development of traditional Chinese medicine," *Democracy Science*, vol. 28, pp. 29–31, 2016.

[54] Y. M. Cui, J. Shi, and L. G. Wang, "Thoughts on the establishment of subject of TCM medical records," *Chinese Medicine Modern Distance Education of China*, vol. 10, pp. 75-76, 2012.

[55] L. L. Chen, S. F. Liu, and C. Zhang, "Research on construction of database and data processing on TCM medical records," *Journal of Traditional Chinese Medical Sciences*, vol. 32, pp. 24–27, 2014.

[56] Y. Bian and J. X. Qiu, "Thoughts on the modernization of TCM medical records," *Chinese Journal of Information and Traditional Chinese Medicine*, vol. 18, pp. 1-2, 2011.

[57] Y. Xiao, *Introduction to Medical Cases of Modern Prominent Veteran TCM Doctors*, Department of Teaching Materials, Guangzhou University of Traditional Chinese Medicine, Guangzhou, China, 2004.

[58] S. Bhattacharrya, J. Miller, and A. H. Ropper, "The case for case reports," *Annals of Neurology*, vol. 76, no. 4, pp. 484–486, 2014.

[59] Al Liu and G. Zhou, "The role of course of TCM medical records in postgraduate training," *Chinese Medicine Modern Distance Education of China*, vol. 10, pp. 58-59, 2012.

[60] R. A. van Haselen, "Homeopathic clinical case reports: development of a supplement (HOM-CASE) to the CARE clinical case reporting guideline," *Complementary Therapies in Medicine*, vol. 25, pp. 78–85, 2016.

[61] C. J. Li, W. Z. Guo, and Y. N. Luo, "Application of case teaching in clinical practice teaching in pharmacy," *Journal of Pharmaceutical Sciences*, vol. 25, pp. 198–200, 2013.

[62] A. J. Martinez Cabán and W. F. Beltrán García, "Advancing medicine one research note at a time: the educational value in clinical case reports," *BMC Research Notes*, vol. 5, p. 293, 2012.

[63] Medical Department of National Administration of Traditional Chinese Medicine, *Standardization of Writing TCM Medical Records*, Medical Department of National Administration of Traditional Chinese Medicine, Beijing, China, 1991.

[64] Ministry of Public Health of the People's Republic of China, National Administration of Traditional Chinese Medicine, *The General Standards of Writing Medical Records of TCM and Integrated Chinese and Western Medicine (Trial)*, Ministry of Public Health of the People's Republic of China, National Administration of Traditional Chinese Medicine, Beijing, China, 2002.

[65] Ministry of Public Health of the People's Republic of China, National Administration of Traditional Chinese Medicine, *The General Standards of Writing TCM Medical Records*, Ministry of Public Health of the People's Republic of China, National Administration of Traditional Chinese Medicine, Beijing, China, 2010.

[66] Z. L. Lu, S. S. Yang, and X. P. Wang, *The Second Supplement of Classified Case Records of Celebrated Physicians*, Liaoning Science and Technology Press, Shenyang, China, 1996.

[67] C. L. Liu, Z. H. Yang, and Y. Xiao, "A survey of the collation and research of TCM case reports from prestigious veteran TCM doctors in modern times," *Forum on Traditional Chinese Medicine*, vol. 24, pp. 50-51, 2009.

[68] T. F. Chen and Q. Q. Liu, "Characteristic studying of medical records of Pu Fuzhou," *Journal of Traditional Chinese Medical Sciences*, vol. 33, pp. 271–273, 2014.

[69] G. K. Feng, "Thoughts after reading the medical records about encephalopathy in the essence of medical records of prestigious veteran TCM doctors," *Liaoning University of Traditional Chinese Medicine*, vol. 14, pp. 38-39, 2012.

[70] J. H. Dong, *Essence of Medical Records of Modern Famous Chinese Medicine Doctors*, Beijing Press, Beijing, China, 1990.

[71] l Li, J. X. Zhao, and Y. X. Tian, "Evaluation on review and analysis of medical case reports in internal diseases by famous doctors," *Hebei Journal of Traditional Chinese Medicine*, vol. 23, pp. 797-798, 2002.

[72] L. F. Yang, "Analysis of the dilemma and countermeasures of famous Chinese medicine cases based on big data technology," *Chinese Journal of Ethnomedicine and Ethnopharmacy*, vol. 27, pp. 120–122, 2018.

[73] M. Kidd and C. Hubbard, "Introducing journal of medical case reports," *Journal of Medical Case Reports*, vol. 1, p. 1, 2007.

[74] US National Library of Medicine, *"Case Reports" Search Results*, http://www.ncbi.nlm.nih.gov/pubmed/?term=case+reports, US National Library of Medicine, Bethesda, MD, USA, 2013, http://www.ncbi.nlm.nih.gov/pubmed/?term=case+reports.

[75] K. G. Akers, "New journals for publishing medical case reports," *Journal of the Medical Library Association: JMLA*, vol. 104, no. 2, pp. 146–149, 2016.

[76] J. Liu, "Establishment of a traditional Chinese medicine data service and application platform," *Modern Traditional Chinese Medicine*, vol. 11, pp. 582–584, 2009.

[77] Z. H. Wang, "Value of case reports and conception of computer prescription selection system for famous experience cases," *Shanxi University of Chinese Medicine*, vol. 29, pp. 16–18, 2006.

[78] Y. G. Ren, X. F. Liu, and J. B. Gao, "Introduction to basic database system of Chinese medicine," *Chinese Medical Journal*, vol. 8, pp. 90-91, 2001.

[79] Z. P. Wu, X. H. He, and X. F. Ke, "Introduction to statistical analysis system for medical case inquiry," *Shanghai Journal of Traditional Chinese Medicine*, vol. 37, pp. 54–56, 2003.

[80] G. Z. Tao, "History and achievements of TCM case study," *Journal of Traditional Chinese Medical Sciences*, vol. 9, pp. 50–53, 2002.

[81] H. Yang, Y. T. Fei, and J. P. Liu, "Reporting methods of clinical medical cases and expert experience in traditional Chinese medicine: case report design," *Journal of Traditional Chinese Medicine*, vol. 49, pp. 215–217, 2008.

[82] D. Moher, K. F. Schulz, I. Simera, and D. G. Altman, "Guidance for developers of health research reporting guidelines," *PLoS Medicine*, vol. 7, no. 2, Article ID e1000217, 2010.

[83] M. Kaszkin-Bettag and W. Hildebrandt, "Case reports on cancer therapies: the urgent need to improve the reporting quality," *Global Advances in Health and Medicine*, vol. 1, no. 2, pp. 8–10, 2012.

[84] J. J. Gagnier, G. Kienle, D. G. Altman, D. Moher, H. Sox, and D. Riley, "The Care guidelines: consensus-based clinical case report guideline development," *Journal of Clinical Epidemiology*, vol. 67, no. 1, pp. 46–51, 2014.

[85] D. S. Riley, M. S. Barber, G. S. Kienle et al., "CARE guidelines for case reports: explanation and elaboration document," *Journal of Clinical Epidemiology*, vol. 89, pp. 218–235, 2017.

[86] A. White, "Writing case reports - author guidelines for acupuncture in medicine," *Acupuncture in Medicine*, vol. 22, no. 2, pp. 83–86, 2004.

[87] E. Peuker, T. Filler, P. Elmar, and F. Timm, "Guidelines for case reports of adverse events related to acupuncture," *Acupuncture in Medicine*, vol. 22, no. 1, pp. 29–33, 2004.

[88] W. Wang, Z. H. Ji, and M. Jiang, "A summary of studies in countries other than China on acupuncture in anesthesia and for postoperative complications," *Journal of Chinese Integrative Medicine*, vol. 32, pp. 797–799, 2009.

[89] R. A. van Haselen, "Towards improving the reporting quality of clinical case reports in complementary medicine: assessing and illustrating the need for guideline development," *Complementary Therapies in Medicine*, vol. 23, no. 2, pp. 141–148, 2015.

[90] R. Adams, "Writing a case report an introductory guide for practitioners of herbal medicine," *Journal of Herbal Medicine*, vol. 7, pp. 47–50, 2016.

Hindawi
Evidence-Based Complementary and Alternative Medicine
Volume 2021, Article ID 6195174, 14 pages
https://doi.org/10.1155/2021/6195174

Research Article

Effects of Qinghuang Powder on Acute Myeloid Leukemia Based on Network Pharmacology, Molecular Docking, and In Vitro Experiments

Ying-jian Zeng,[1,2] Min Wu,[1,2] Huan Zhang,[2] Xin-ping Wu,[2] Lu Zhou,[2] Na Wan,[1] and Zhen-hui Wu[1,2]

[1]*Jiangxi University of Chinese Medicine, Nanchang 330004, Jiangxi Province, China*
[2]*The Affiliated Hospital of Jiangxi University of Chinese Medicine, Nanchang 330006, Jiangxi Province, China*

Correspondence should be addressed to Na Wan; wanna988@163.com and Zhen-hui Wu; wzh77580@163.com

Received 3 July 2021; Revised 23 November 2021; Accepted 30 November 2021; Published 28 December 2021

Academic Editor: Jianan Xia

Qinghuang powder (QHP) is a traditional Chinese herbal medicine. This is a unique formula that is frequently used to treat malignant hematological diseases such as acute myeloid leukemia (AML) in modern clinical practice. An approach of network pharmacology and experimental validation were applied to investigate the pharmacological mechanisms of QHP in AML treatment. First, public databases for target genes known to be associated with AML are searched and compared to the target genes of the active compounds in QHP. Second, AML-associated genes and QHP target genes are compared to identify overlapping enriched genes, and these were used to predict selected target genes that may be implicated in the effects of QHP on AML. Additionally, we conducted functional enrichment analyses, such as gene ontology (GO) and the Kyoto Encyclopedia of Genes and Genomes (KEGG) pathways. The significantly enriched pathway associated with potential target proteins was the PI3K-Akt signaling pathway, suggesting that these potential target proteins and pathways may mediate the beneficial biological effects of QHP on AML. All these following genes were found to occur in the compounds-target-pathway networks: AKT1, MAPK1, MAPK3, PIK3CG, CASP3, CASP9, TNF, TGFB1, MAPK8, and TP53. Then, based on the molecular docking studies, it was suggested that the active compound isovitexin can fit into the binding pockets of the top candidate QHP-AML target proteins (PIK3CG). Subsequently, based on the prediction by network pharmacology analysis, both in vitro AML cells and western blot experiments were performed to validate the curative role of QHP. QHP exerted its antitumor activity on AML in vitro, as it inhibits cells proliferation, reduced the expression of Bcl-2 protein, and downregulated the PI3K-Akt signaling pathway. In conclusion, these results revealed that QHP could treat AML via a "multicomponent, multitarget, multipathway" regulatory network. Furthermore, our study also demonstrated that the combination of network pharmacology with the experimental study is effective in discovering and identifying QHP in the treatment of AML and its underlying pharmacological mechanisms.

1. Introduction

Acute myeloid leukemia (AML) is an aggressive malignancy worldwide with a poor prognosis. It is a relatively rare type of cancer (statistically accounting for 1.1% of all new cancer cases), with an estimated 19, 940 new cases in the United States in 2020, according to the NIH (National Institutes of Health) and SEER (Surveillance, Epidemiology, and End Results) databases. AML is characterized by the rapid proliferation of immature myeloid leukemia cells [1]. Most patients suffering from AML are struggling for life every day because it has the lowest overall survival rate of all cancer, in spite of aggressive treatments with chemotherapy. One of the biggest obstacles in AML treatment is the high relapsing rate despite a positive response to chemotherapy. Many drugs are used to treat AML, including FLT3 inhibitors (midostaurin), IDH inhibitors (ivosidenib and enasidenib), hedgehog pathway inhibitors (glasdegib), Bcl-2 inhibitors (venetoclax), and proteasome inhibitors (bortezomib). However, the action of these drugs can suppress the progression of AML and is associated with several adverse side

effects including neutropenic fever, infections, hyperleucocytosis, and gastrointestinal symptoms [2, 3].

Evolving pharmacological treatment strategies have led to the development of more comprehensive and multistage AML therapies, and patients are now able to use complementary and alternative medicine therapies. Traditional Chinese medicine (TCM) is a commonly used alternative medicine therapy for AML patients [4–12]. TCM has been used widely in China for more than 2,000 years and has gradually gained international recognition due to its outstanding efficacy. For example, the exceptional Chinese scientist Tu Youyou found that artemisinin, a substance extracted from a medicinal plant that was described in the third-century book Emergency Prescriptions to Keep up Your Sleeve (Zhouhou Beiji Fang) as a treatment for malaria, could be developed into a pharmaceutical drug. The work of Dr. Tu and her team eventually led to an effective treatment that saved the lives of millions of people. She along with two other scientists was awarded the Nobel Prize for their research.

Qinghuang powder (QHP, Realgar-Indigo Naturalis formula) was used as a folk Chinese medicine, and this medicine is also described in many ancient medical books, such as Jing Yue Quan Shu, Shi Yi De Xiao Fang, and Qi Xiao Liang Fang. QHP is composed of the Chinese herbs Qing Dai (Indigo Naturalis) and Xiong Huang (Realgar). The compounds of Indigo Naturalis include indigo, indirubin, proteins, tannic acid, and inorganic salts. The constituents of Realgar include arsenic disulfide (As_2S_2), with a small amount of arsenic trioxide (As_2O_3) and other heavy metal salts. QHP has been used to treat malignant hematological diseases including AML, chronic myeloid leukemia (CML), and myelodysplastic syndrome [13–17]. However, very little research on the mechanism underlying the therapeutic effects of QHP in AML has been conducted.

Network pharmacology-based drug discovery is an emerging, cost-effective drug development approach incorporating systems biology, bioinformatics, and poly-pharmacology [18]. Network pharmacology utilizes network structures to discover and analyze multicomponent and multitarget drugs [19, 20]. Chinese herbal medicines such as QHP are potential "drugs" that could be the basis for developing multicomponent and multitarget synergistic AML therapeutics.

In this study, we examined the active components and mechanisms underlying the effects of QHP on AML using network pharmacology analysis in combination with molecular docking and experimental validation. This study was designed using Network Pharmacology Evaluation Method Guidance-Draft [21].

2. Materials and Methods

2.1. Network Pharmacology

2.1.1. Chemical Components Screening. All components of QHP were retrieved from the Symptom Mapping Database [22] (SymMap; http://www.symmap.org/), TCM Systematic Pharmacology Database [23] (TCMSP; https://tcmspw.com/index.php), and TCM Integrated Database [24] (TCMID; http://www.megabionet.org/tcmid/) and supplemented by literature mining. The oral administration of TCM therapeutics must overcome the barriers which come in the form of absorption, distribution, metabolism, and excretion (ADME) processes to be active [25]. In ADME processes, oral bioavailability (OB) and drug-likeness (DL) are the two most important parameters to measure the pharmacokinetic process of drugs in vivo. A good OB for a new drug candidate is of the most essential pharmacokinetic parameters. DL refers to physical and chemical properties such as stability, solubility, and biological properties. High OB is usually a crucial indicator for determining the DL index of active compounds. In the Drug Bank database, the average DL index is 0.18. The compounds with DL index ≥ 0.18 and OB $\geq 30\%$ were regarded as better drugs and were better for the use of humankind [25]. The components meeting the OB $\geq 30\%$ and DL ≥ 0.18 criteria were selected as active compounds in this study.

2.1.2. Establishment of Target Library. The proteins and gene targets of the active compounds and AML-related human genes were collected from multiple databases. Information on target proteins or genes of active compounds was collected from the TCMSP, TCMID, and SymMap databases. For comprehensiveness, we used the Swiss Target Prediction database [26] (https://www.swisstargetprediction.ch/) and TargetNet [27] (https://targetnet.scbdd.com/calcnet/index/) to look for targets for the components Indigo Naturalis and Realgar. These active compounds were uploaded to an online database, the species was restricted to Homo sapiens, and the target data with probability > 0 were downloaded.

AML-related human genes were collected from several databases, namely, DrugBank (https://go.drugbank.com/), DisGeNET (https://www.disgenet.org/search), GeneCards (https://www.genecards.org/), and OMIM (https://omim.org/). All protein target names were identified and converted to names of standard genes via UniProt (https://www.uniprot.org/) [28]. After these were determined, the gene targets of QHP were combined, and repetitive targets were deleted. Similarly, the gene targets of AML from four databases were combined, and the repetitive targets were deleted. A Venn diagram of QHP-AML targets was plotted and visualized with web tools (https://bioinformatics.psb.ugent.be/webtools/Venn/). Finally, the QHP and AML targets that overlapped were collected using R software, and the intersection of overlapped targets was selected as the target library of this study.

2.1.3. Bioinformatic Annotation. The gene ontology (GO) and Kyoto Encyclopedia of Genes and Genomes (KEGG) pathway enrichment analyses were conducted using the R software (version 3.6.0 for Windows). The GO enrichment analyses include biological process (BP), cellular component (CC), and molecular function (MF). The GO enrichment analysis for AML-related targets of QHP revealed remarkably 10 rich terms in BP, CC, and MF. The KEGG pathway enrichment analysis was used to elucidate the potential mechanism of QHP for AML. The bar charts and bubble diagrams were drawn with R-studio software (version 3.6.5 for Windows).

2.1.4. Protein-Protein Interaction. Biological processes involve interaction between multiple body systems are regulated by a complex regulatory network, rather than just a single gene or protein. These interactions include direct (physical) and indirect (functional) associations. STRING (https://string-db.org/) is a database of known and predicted protein-protein interactions [29]. The target proteins were uploaded to the STRING online database, and the organism selected was limited to Homo sapiens sources. We then downloaded the protein-protein interaction (PPI) relationships that we discovered into TSV format and imported the TSV file into Cytoscape software (ver. 3.7.1) to construct the PPI network diagram. In this diagram, each node represents a protein, respectively, and the connection between nodes indicates an interaction between two proteins.

2.1.5. Network Construction. Network construction was achieved with Cytoscape software (ver. 3.7.1). Cytoscape is an open-source software platform for visualizing molecular interaction networks and biological pathways and then integrating these networks with annotations, gene expression profiles, and other data [30]. Based on our previous work, we identified and visualized the compounds-targets-pathways (C-T-P) relationship between QHP and AML. This included 2 networks, named as follows: (1) the active compounds-potential targets network of QHP for targeting AML; (2) active compounds-potential targets-pathways network of QHP for targeting AML.

2.2. Molecular Docking. To further validate the effects of QHP acting on AML, molecular docking technology was applied for screening the active compounds and candidate proteins. Molecular docking technology is an important method for the screening of drugs, which starts from known proteins and small-molecule compounds and identifies them by simulating the geometry and energy matching. We used the RCSB protein data bank (https://www.rcsb.org/) database to retrieve related protein information and downloaded the 3D structure files of the candidate proteins as the receptors. We then modified them using PyMol software (version 1.8) and AutoDockTools software (version 1.5.6) to isolate the original ligands, remove water molecules, add hydrogen, and patch amino acids. The mol2 structure of the active compounds was set to rotatable and saved as a "pdbqt" format file through the Autodock Tools software. Finally, we performed molecular docking using Autodock-vina software (version 1.1.2). The docking results were visualized with PyMol software, and the docking interaction patterns were established.

2.3. Experiment Verification

2.3.1. Reagents and Drugs. Isovitexin (lot no. abs47023192) was obtained from Absin Bioscience Inc. Roswell Park Memorial Institute (RPMI) 1640 (lot no. RHBH8770) and DMSO (lot no. RNBD8012) were purchased from Sigma-Aldrich (Shanghai) Trading Co., Ltd. FBS (lot no. 42F7180 K) was purchased from Gibco Life Technologies Ltd. Cell Counting Kit-8 (CCK-8) kit (lot no. KGA317) was obtained from KeyGEN Biotech Co., Ltd. RIPA lysis buffer (lot no. P0013 B), PMSF (lot no. 020421210524), BeyoECL kit (lot no. P0018AS), SDS-PAGE Sample Loading Buffer 5 × (lot no. 070121210811), and BCA protein quantitation kit (Lot No. 062521210726) were purchased from Beyotime Institute of Biotechnology. BSA (lot no. EZ4567D106) was purchased from Guangzhou Saiguo Biotech Co., Ltd. Anti-PIK3CG (lot no. 5405S) were purchased from Cell Signaling Technology, Inc. Anti-AKT (lot no. CJ38131), anti-Bcl-2 (lot no. CN48171), and goat anti-mouse IgG (lot no. BS12478) were purchased from Bioworld Technology, Inc. Anti-GAPDH (lot no. AB0037) was purchased from Nanjing JinZai Biotechnology Co., Ltd. Anti-Rabbit IgG (lot no. 147832) was purchased from Jackson ImmunoResearch Laboratories, Inc.

2.3.2. Cell Source and Culture. KG1-a cells were gifted from the Southern Medical University. HL-60 cells were purchased from JiangSu Rongtai Biotech Co., Ltd. Both KG1-a cells and HL-60 cells were cultured in RPMI-1640 containing 10% FBS and 1% penicillin-streptomycin at 37 ˚C in an incubator containing 5% CO_2. Once cell confluence reached~80%, these cells were passaged.

2.3.3. Cell Viability Assay. The viability of the KG1-a cells and HL-60 cells was determined using CCK-8 kit. Firstly, KG1-a cells and HL-60 cells were suspended, respectively, in RPMI-1640 (5 × 103 cells/well in 100 μL) and sown in Corning disposable 96-well plates for 24 h. Different concentrations of isovitexin (in 0.024, 0.098, 0.39, 1.56, 6.25, 25, and 100 μmol/L range) were incubated with KG1-a cells and HL-60 cells for 48 h. Then, the culture medium of 96-well plates was added with CCK-8 solution (culture medium: CCK-8 solution = 10 : 1). Lastly, 96-well plates were incubated at 37 ˚C for 1.5 h. The absorbance was read at 450 nm using Multiskan MK3 microplate reader (Thermo Fisher Scientific, Inc.). The half-maximal inhibitory concentration (IC50) of isovitexin was calculated using GraphPad Prism 8.3.0 software.

2.3.4. Western Blot Analysis. Further to study how isovitexin affects these cell signaling pathways, KG1-a cells and HL-60 cells were plated in 6-well plates (1 × 104 cell/well) and treated for 48 h with a variety of isovitexin concentrations (0.39, 1.56, 6.25, and 25 μmol/L). These cells were collected from the 6-well plates followed by the addition of RIPA lysis buffer (containing 1 mM PMSF) and incubated on ice for 15 min. The recovered lysate was centrifuged at 4 ˚C at 14,000 ×g for 10 min. Thereafter, the protein concentration was measured with a BCA Protein Assay Kit. An equal amount of protein (50 μg/lane) was separated by 12 SDS-PAGE and electroblotted onto polyvinylidene difluoride (PVDF) membranes (Millipore). Subsequently, the PVDF membranes were blocked with 5% skim milk for 1 h and incubated overnight with different primary antibodies

against PIK3CG (1 : 1,000 dilution), AKT (1 : 500 dilution), Bcl-2 (1 : 500 dilution), and GAPDH (1 : 3,000 dilution), respectively, at 4 °C. Following 3 washes, the membranes were incubated for 1 h with secondary horseradish peroxidase-conjugated antibody at room temperature. Immunolabeled protein bands were detected with ECL substrate. Semiquantitative analysis was performed using ImageJ software. Target protein levels were normalized against the level of GAPDH.

2.4. Statistical Analysis. Data were expressed as mean and standard deviation (SD) from at least three independent experiments. The statistical significance of differences between the two groups was determined using Student's *t*-test or LSD test. For multiple comparisons, one-way ANOVA was performed with SPSS software (version 22.0; IBM Corp., Armonk, NY, USA). Statistical significance was set at p value < 0.05.

3. Results

3.1. Active Compounds in QHP. The QHP formula contains two Chinese medicinal constituents. They are Indigo Naturalis and Realgar. We identified a total of 48 compounds in QHP through the TCMSP, TCMID, and SymMap databases, 38 of which were contained in Indigo Naturalis and 10 in Realgar. Among the 38 compounds in Indigo Naturalis, 8 (26.3%) met the requirement of OB $\geq$ 30% and DL $\geq$ 0.18 based on the TCMSP database, and the 4 compounds in Realgar also met this criterion based on the TCMID and SymMap databases. Therefore, 14 compounds were chosen as candidate active compounds for further analysis. A detailed list of these compounds is shown in Table 1. Through this process, we found that four of these compounds (As_2O_3, As, AsS, and As_4S_4) do not meet the ADME parameters and were therefore excluded.

3.2. Targets Identification of QHP on AML. Among the 14 active compounds, 319 target genes were retrieved from the TCMSP, TCMID, TargetNet, and SymMap databases. After eliminating duplicates, 261 gene targets were obtained for further study. In total, 947 AML-related human gene targets were collected from OMIM, GeneCards, DisGenet, DrugBank, and SymMap databases. We then extracted all the unique gene targets from each result. The intersection of these two types of gene targets was then collected for further analysis (Figure 1). As a result, we found that 89 gene targets from 13 compounds (bisindigotin was removed as it has no related target genes) in QHP were associated with AML.

3.3. Compounds-Target Network and Analysis. The targets of 13 compounds that were associated with AML were imported into Cytoscape (ver. 3.7.1), and the QHP-AML target network diagram that was constructed is shown in Figure 2. Our analysis of the QHP-AML target network showed that it contains 274 nodes and 434 edges. The yellow node in Figure 2 represents the Chinese herbal medicine formula point, the cyan node represents compound points, and the red node represents target points. These bioactive compounds were associated with multiple AML targets, namely, As (degree = 147), As_4S_4 (degree = 60), beta-sitosterol (MOL000358, degree = 52), As_2O_3 (degree = 46), indirubin (MOL002309, degree = 36), AsS (degree = 23), 5-O-methylvisamminol (MOL001753, degree = 21), indican (MOL011105, degree = 12), indigo (MOL001781, degree = 9), isoindigo (MOL011335, degree = 8), isovitexin (MOL002322, degree = 7), qingdainone (MOL001810, degree = 7), and quindoline (MOL011332, degree = 6). These high-degree compounds in the network were deemed to relate to the essential therapeutic effects of QHP on AML.

3.4. Network of Protein-Protein Interaction. The 89 gene targets shared between QHP and AML were imported into the STRING database (https://www.string-db.org/), and the results were downloaded as a "TSV" file. The TSV file was imported into Cytoscape (ver. 3.7.1), and the diagram of the gene target network was constructed as shown in Figure 3. By analyzing the gene target network, we found that the network includes 89 nodes and 1568 edges, and the degrees represent the number of connected edges (the edges represent relations between two adjacent nodes) of nodes. The average node degree was 35.24, and the average clustering coefficient was 0.74. The higher the degree, the greater the regulatory role of nodes plays in the network. We selected those genes with an above-average node degree. As a result, only 9 targets had good network connectivity characteristics. These 9 targets that may be core genes are shown in Table 2.

3.5. Networks and Enriched Functions in AML-Associated Genes

3.5.1. GO and KEGG. In order to further identify the functional characteristics of putative target genes of QHP on AML in detail, the GO and KEGG pathways enrichment analyses of target genes were performed using the R statistical language. GO enrichment analysis showed that these genes were involved in three aspects of biological functions: biological process (BP), cellular component (CC), and molecular function (MF). The top 10 significantly enriched GO terms in BP, CC, and MF of the potential targets are shown in Figure 4(a). The GO enrichment analysis indicated that the targets of QHP were correlated with the BP of response to molecule of bacterial origin, response to lipopolysaccharide, extrinsic apoptotic signaling pathway, and other processes. The CCs include membrane raft, membrane microdomain, and membrane region. These targets of QHP are also involved in the MF, including cytokine receptor binding, protein serine/threonine kinase activity, and receptor ligand activity. To analyze the underlying KEGG pathways of QHP that may be responsible for its effects on AML, pathway enrichment analysis was conducted. The top 20 significantly enriched KEGG pathways are shown in Figure 4(b). The pathway of PI3K-Akt signaling pathway exhibited the largest number of related gene targets (34 counts).

Table 1: Description of active compounds of QHP.

Number	Molecule	OB (%)	DL	Molecular structure	Herb
MOL011100	Bisindigotin	41.66	0.39	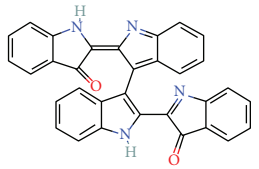	Indigo Naturalis
MOL011105	Indican	34.9	0.23	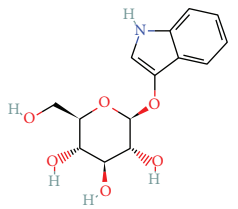	Indigo Naturalis
MOL011332	Quindoline	54.57	0.22	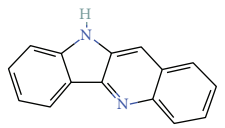	Indigo Naturalis
MOL011335	Isoindigo	94.3	0.26	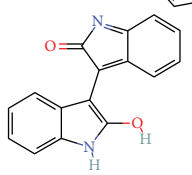	Indigo Naturalis
MOL001753	5-O-Methylvisamminol	37.99	0.25	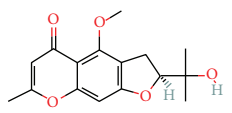	Indigo Naturalis
MOL001781	Indigo	38.2	0.26	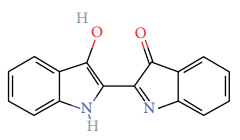	Indigo Naturalis
MOL001810	Qingdainone	45.28	0.89	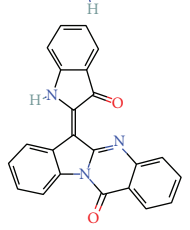	Indigo Naturalis
MOL002309	Indirubin	48.59	0.26	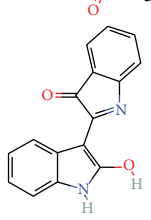	Indigo Naturalis
MOL000358	Beta-sitosterol	36.91	0.75	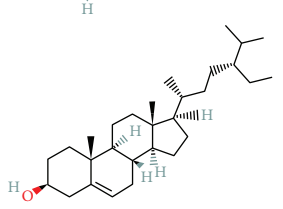	Indigo Naturalis

Table 1: Continued.

Number	Molecule	OB (%)	DL	Molecular structure	Herb
MOL002322	Isovitexin	31.29	0.72	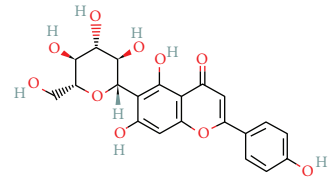	Indigo Naturalis
N/A	As_2O_3	N/A	N/A		Realgar
N/A	As	N/A	N/A	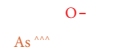	Realgar
N/A	AsS	N/A	N/A		Realgar
N/A	As_4S_4	N/A	N/A		Realgar

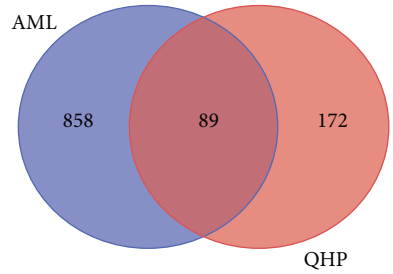

Figure 1: Venn diagram of QHP-AML intersection targets.

3.5.2. Compounds-Target-Pathway Network Analysis. Based on the above GO terms and KEGG pathway enrichment analyses, the compounds-target-pathway network was generated with Cytoscape (version 3.7.2), which connected these compounds, potential targets, and corresponding pathways. The compounds-target-pathway network is shown in Figure 5; it includes 173 nodes (1 Chinese herbal medicine formula node, 13 active compounds nodes, 260 potential target nodes, and 20 pathway nodes) and 799 edges. The yellow diamonds represent compounds, red circles correspond to targets, and cyan rectangles represent pathways.

3.6. Molecular Docking. In order to further validate the ability of the active compounds in QHP to bind with the key targets, molecular docking visualization techniques were used to examine systematic docking. We chose to research these underlying target proteins in the C-T-P network because they were high-degree nodes with multifunctional connections. The top 10 key targets based on degree were as follows: AKT1, MAPK1, MAPK3, PIK3CG, CASP3, CASP9, TNF, TGFB1, MAPK8, and TP53. A total of 13 compounds were selected for docking on the 10 target proteins under the procedure. The thermal map of the lowest binding energy is shown in Figure 6.

Docking analysis successfully predicted docking between QHP and the binding pockets of 10 target proteins. The most active compound in QHP based on docking results was isovitexin. The value of binding affinity (kcal/mol^{-1}) was below −7.0, indicating good binding activity between the compound and the protein [31]. The lower the binding affinity value, the better the docking effect. Isovitexin bounds to PIK3CG via hydrogen bonds with Val851 (3.06 Å) and Lys802 (2.86 Å, 2.88 Å) and had multiple hydrophobic interactions with residues Asp805, Ala775, Lys776, Ser774, Ile932, Met772, Met922, Val850, Glu849, Ile800, Ile848, and Asp933. Similarly, isovitexin was predicted to dock tightly into the protein binding pocket of JUN via hydrogen bonds with Ile32 (2.82 Å) and Glu109 (2.59 Å), and hydrophobic interactions with residues Gln117, Asn114, Ile86, Met108, Ala53, and Leu168. Lastly, isovitexin was also predicted to dock tightly into the protein binding pocket of CHEK1 via hydrogen bonds with Tyr20 (3.24 Å, 3.16 Å), Lys132 (3.09 Å), and Cys87 (3.04 Å, 3.09 Å), and hydrophobic interactions with residues Glu134, Asp148, Gly18, Lys38, Ala36, Val23, Glu85, Tyr86, Leu15, Leu137, and Glu91. The results of molecular docking are shown in Figure 7. The docking pattern for each protein and its components is divided into three subplots: *a*, *b*, and *c*. In our schema, "a" shows the binding position of the small-molecule compound (sticks model) on the associated protein (cartoon model) as a

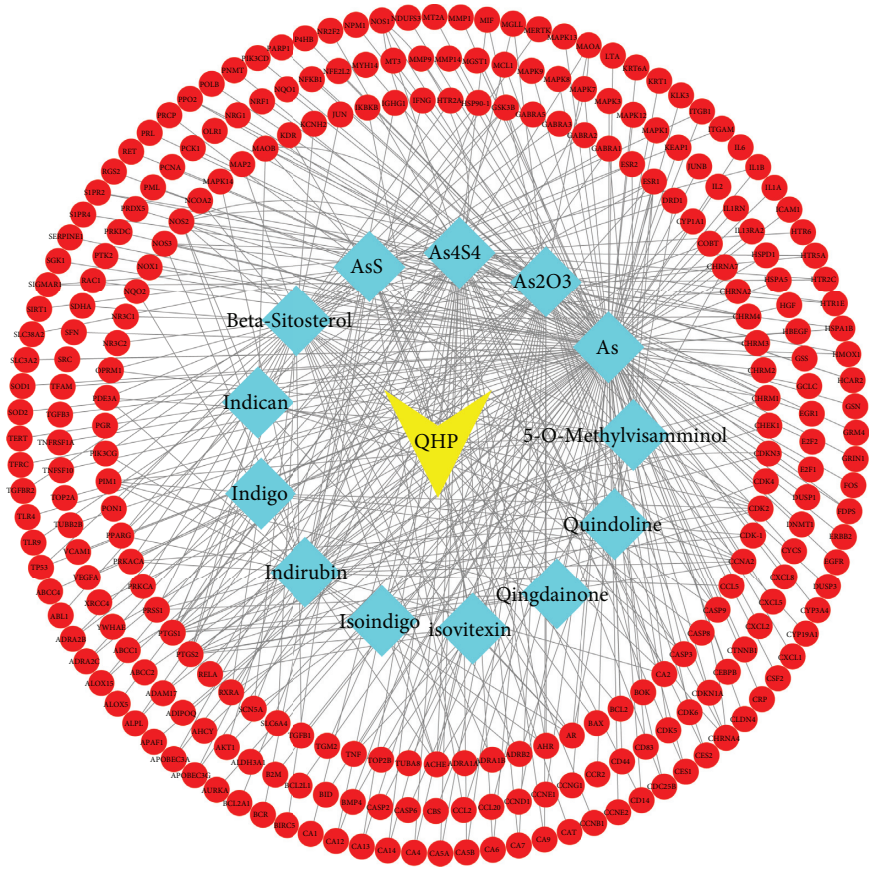

Figure 2: The compounds-target network for QHP on AML. The red node represents the target point, the yellow node represents the Chinese herbal medicine formula point, and the cyan node represents compound points.

whole; "b" shows the interaction between the small molecule (green) and the key residue (grey) on the protein of interest, which facilitates the observation of the spatial stacking between the compound and the protein; and "c" shows a two-dimensional view of the hydrogen bonding and hydrophobic (stacking) interactions between the compound and protein residues.

3.7. Inhibition of Isovitexin on KG1-A and HL-60 Cells. In comparison to the control group, different concentrations of isovitexin had inhibitory effects on KG1-a cells and HL-60 cells in a dose-dependent manner. As shown in Figure 8(a), the isovitexin' IC50 was found to be 0.973 μmol/L (KG1-a cells) and 1.258 μmol/L (HL-60 cells). These results suggest that isovitexin can inhibit AML cell growth.

3.8. Isovitexin Regulated the PI3K-AKT Signaling Pathway in AML Cells. Based on the "3.5.1 GO and KEGG" pathways analyzed and "3.6 Molecular Docking" docking results, the PI3K-AKT signaling pathway was selected for experimental validation as a major tumor-related signaling pathway. As shown in Figure 8(b), 8(c), after 48 h treatment with different concentrations of isovitexin (0.39, 1.56, 6.25, 25 μmol/L), the protein levels of PIK3CG, AKT, and BCL-2 in KG1-a cells and HL-60 cells were decreased in a dose-dependent manner ($^{*}p < 0.05$, $^{**}p < 0.01$, and $^{***}p < 0.001$ compared with the control group). Taken together with the results of cell viability measurement, the anti-acute myeloid leukemia activities of isovitexin seem to be mediated by inhibition of the cell growth and regulation of the PI3K-AKT signaling pathway.

4. Discussion

AML is a highly complex cancer in terms of its molecular and cytogenetic architecture, which are involved with multiple genes or signaling pathways during the development and progression of the disease [32]. Because TCM herbal formulas are composed of multiple compounds, they are generally assumed to work through "multitarget and multipath effects". Previous research has shown that formulas generally have synergistic effects that may regulate multiple biological processes and pathway networks in the body [8, 33]. However, the characteristic of TCM makes in-depth research on the underlying mechanisms quite challenging. Accordingly, there is an urgent need for new approaches to systematically and comprehensively study the mechanisms of actions of single and compound medicinal substances used in clinical practice in TCM. With the rapid development of systems biology and silicon technologies, network pharmacology and molecular docking have become an emerging approach to clarifying the molecular and

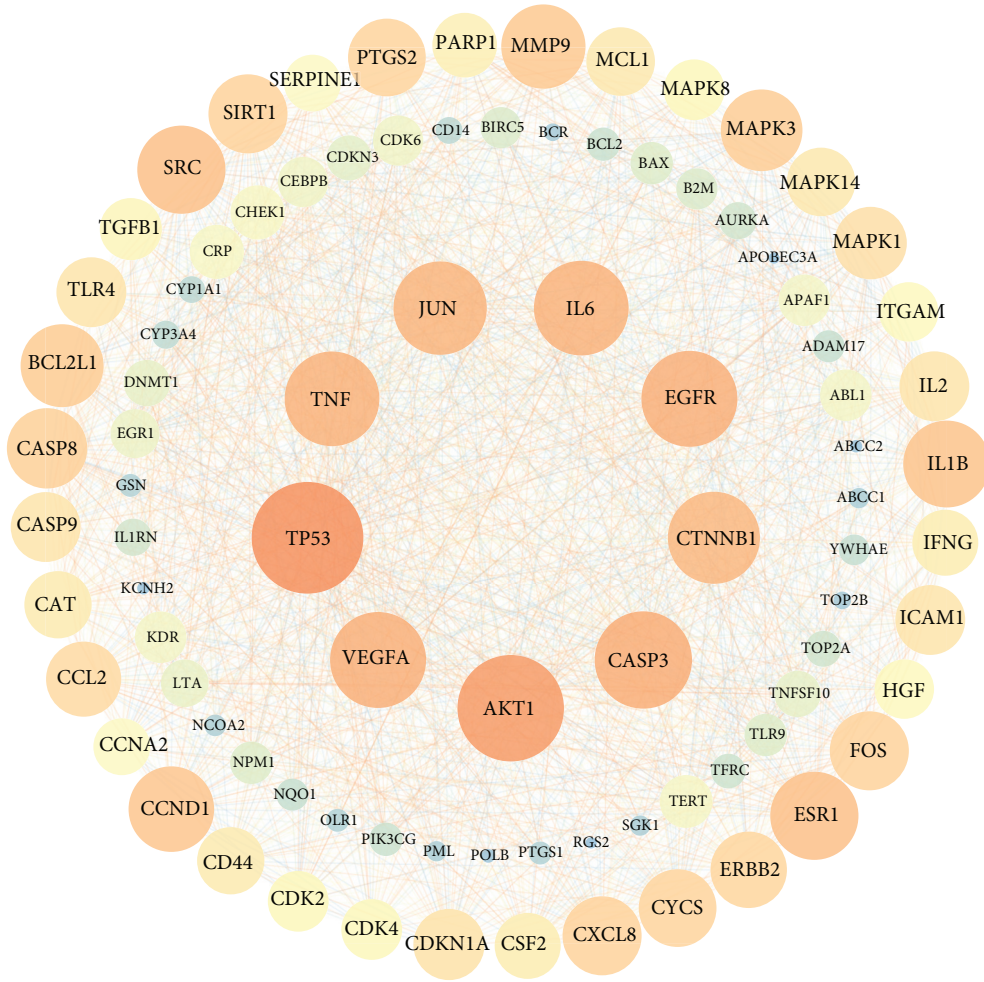

Figure 3: The node size and color shade are positively correlated with the degree.

Table 2: Topological analysis of QHP-AML target network.

Protein name	Gene name	ASPL	BC	CC1	CC2	Degree
Cellular tumor antigen p53	TP53	1.114	0.075	0.898	0.463	78
RAC-alpha serine/threonine-protein kinase	AKT1	1.159	0.046	0.863	0.496	74
Caspase-3	CASP3	1.250	0.021	0.800	0.576	67
Vascular endothelial growth factor A	VEGFA	1.250	0.020	0.800	0.594	66
Epidermal growth factor receptor	EGFR	1.250	0.029	0.800	0.540	66
Interleukin-6	IL6	1.261	0.024	0.793	0.578	65
Tumor necrosis factor	TNF	1.261	0.023	0.793	0.572	65
Transcription factor AP-1	JUN	1.284	0.020	0.779	0.599	64
Catenin beta-1	CTNNB1	1.295	0.020	0.772	0.594	63

ASPL: average shortest path length; BC: betweenness centrality; CC1: closeness centrality; CC2: clustering coefficient.

underlying pharmacological mechanisms of TCM [34, 35]. In the current study, our team used this approach to systematically study the pharmacological mechanisms by which QHP can alleviate AML.

Some compounds did not exhibit pharmacokinetic properties that could allow them to be delivered to target organs to generate biological activities. In modern integrated drug development, these compounds with OB $\geq$ 30% and DL $\geq$ 0.18 were seen as good pharmacokinetically active compounds [36]. There is no relevant data on As_2O_3 and As_4S_4 that could be retrieved from the TCMSP database including OB and DL values. However, there is increasing evidence to associate both As_2O_3 and As_4S_4 with the AML pathological process [37–39]. Moreover, it is clear that As_4S_4 and As_2O_3 are the primary bioactive compounds in QHP [40]. In this study, isovitexin was the most significantly active compound, followed by qingdainone, isoindigo, indigo, indirubin, and quindoline. Isovitexin was shown to have anti-inflammatory and antitumor effects via inhibiting the production of nitric oxide, manganese superoxide

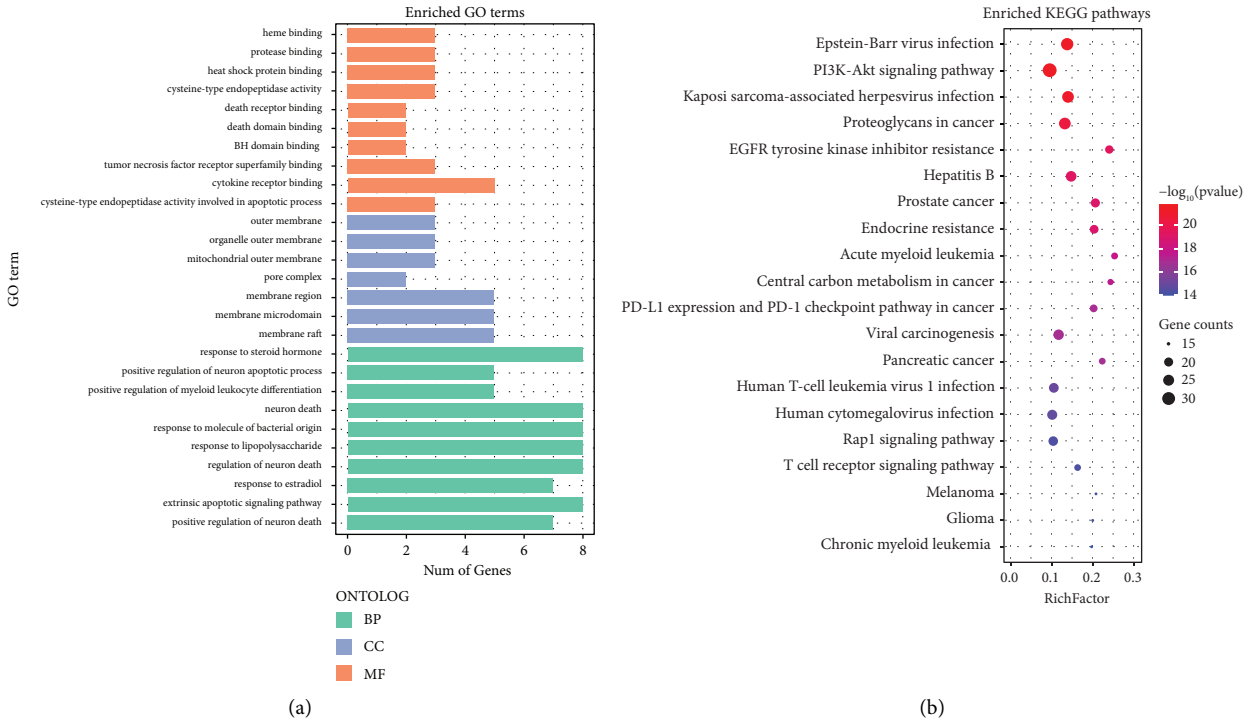

FIGURE 4: The top 10 significance of enriched GO terms (a) and top 20 significance of enriched KEGG pathways (b) analysis of therapy target genes of QHP on AML.

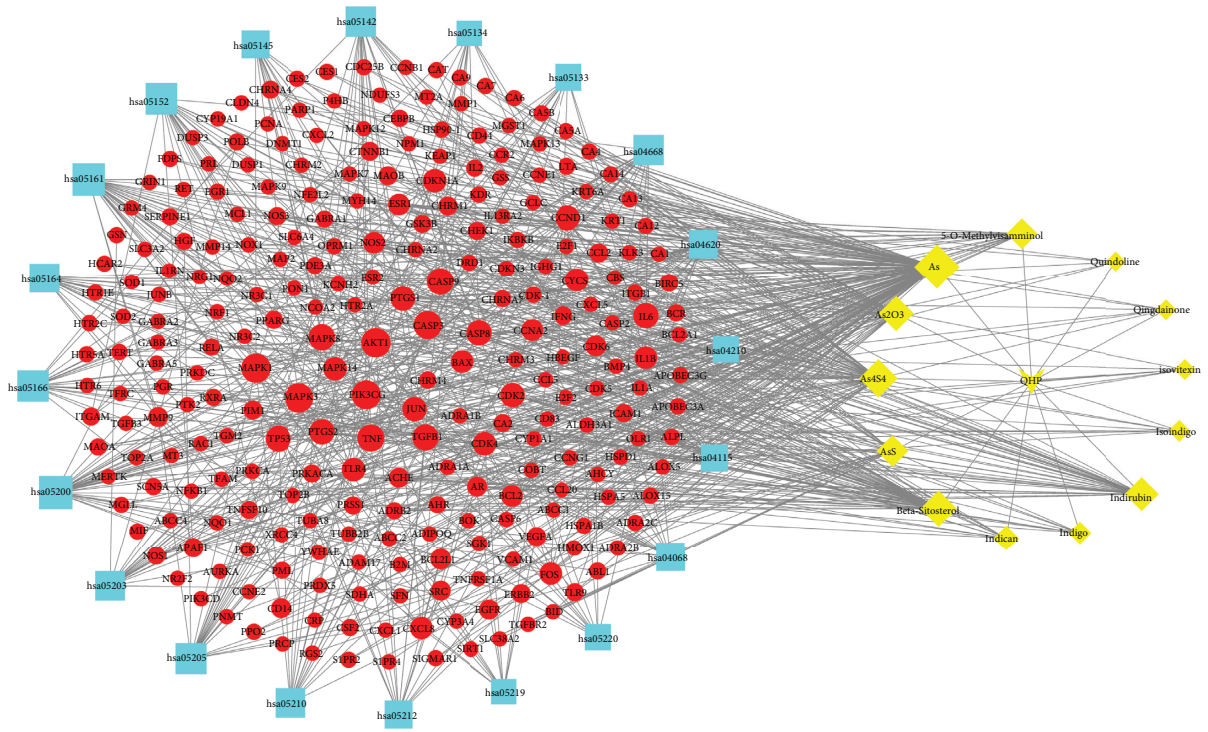

FIGURE 5: The compounds-target-pathway network. The cyan node represents pathways; the red node represents targets, and the yellow node represents compounds. The edges represent the interactions between compounds, target, and pathway, and node size is proportional to their degree.

	AKT1	MAPK1	MAPK3	PIK3CG	CASP3	CASP9	TNF	TGFB1	MAPK8	TP53	CASP8	CHEK1	ESR1	JUN	PTGS2
Beta-Sitosterol	−3.73	−3.51	−2.95	−3.76	−2.72	−2.91	−3.71	−3.28	3.86	−3.00	−3.12	−3.70	−6.12	−5.58	−4.52
Indirubin	−4.94	−5.69	−5.25	−6.73	−4.80	−4.18	−6.46	−5.17	−7.22	−4.33	−4.70	−6.61	−7.07	−6.77	−8.52
Indican	−7.23	−5.75	−5.97	−7.33	−4.99	−6.18	−5.80	−4.49	−6.18	−4.65	−4.91	−5.93	−7.80	−6.53	−7.45
5-O-Methylvisamminol	−5.59	−5.63	−5.21	−7.90	−4.97	−4.33	−5.86	−4.84	−8.02	−3.84	−4.73	−7.14	−6.59	−6.85	−7.64
Indigo	−4.87	−5.51	−6.22	−7.77	−4.08	−4.74	−5.99	−4.32	7.62	−3.97	−3.91	−6.71	−6.90	−6.72	−8.61
Qingdainone	−4.87	−4.98	−5.64	−8.33	−4.00	−2.94	−6.03	−4.57	−8.09	−4.13	−5.00	−7.79	−4.43	−8.54	−4.76
Quindoline	−5.21	−5.13	−7.40	−7.07	−4.46	−3.66	−5.75	−4.50	−6.64	−3.89	−4.30	−5.69	−6.40	−7.51	−8.14
Isoindigo	−5.56	−5.34	−5.51	−7.46	−4.52	−5.04	−6.75	−4.69	−8.24	−4.15	−6.56	−5.28	−7.53	−8.47	−8.38
Isovitexin	−6.12	−5.90	−8.12	−9.14	−4.51	−5.42	−7.24	−4.16	−6.44	−3.43	−4.92	−8.29	−5.33	−8.65	−3.85
As	−4.13	−4.55	−4.05	−4.15	−2.95	−4.10	−2.59	−3.66	−4.22	−4.07	−3.81	−3.99	−2.96	−3.51	−4.31
AsS	−4.81	−5.26	−4.72	−4.82	−3.52	−4.77	−3.12	−4.29	−4.90	−4.74	−4.46	−4.65	−3.53	−4.13	−5.00
As_2O_3	−4.96	−5.46	−4.86	−4.97	−3.54	−4.92	−3.10	−4.39	−5.07	−4.88	−4.58	−4.79	−3.56	−4.21	−5.17
As_4S_4	−5.03	−4.85	−4.52	−4.03	−4.12	−3.59	−4.03	−4.03	−4.84	−4.06	−3.88	−4.12	−3.85	−4.06	−3.78

Binding Affinity (kcal/mol)
<−8
−6~−8
−4~−6
>−4

FIGURE 6: Heat map of the respective lowest binding energy value distribution of key targets and related components by molecular docking.

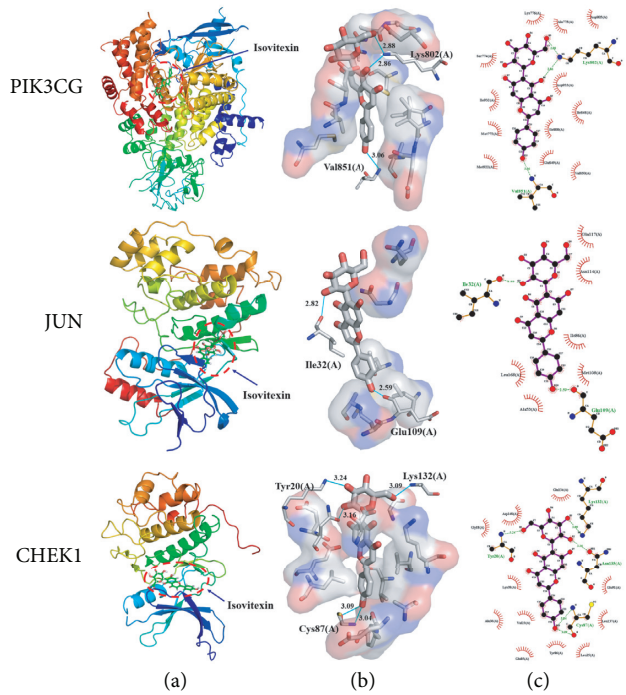

FIGURE 7: The binding pattern of the key targets of the network and the lowest component of their binding affinity. (a) Overall view of docking, with proteins represented by cartoon models; (b) three-dimensional detail of the docking interaction, with the small molecule represented by green sticks; (c) two-dimensional detailed view of the hydrophobic interactions between small molecules and protein residues.

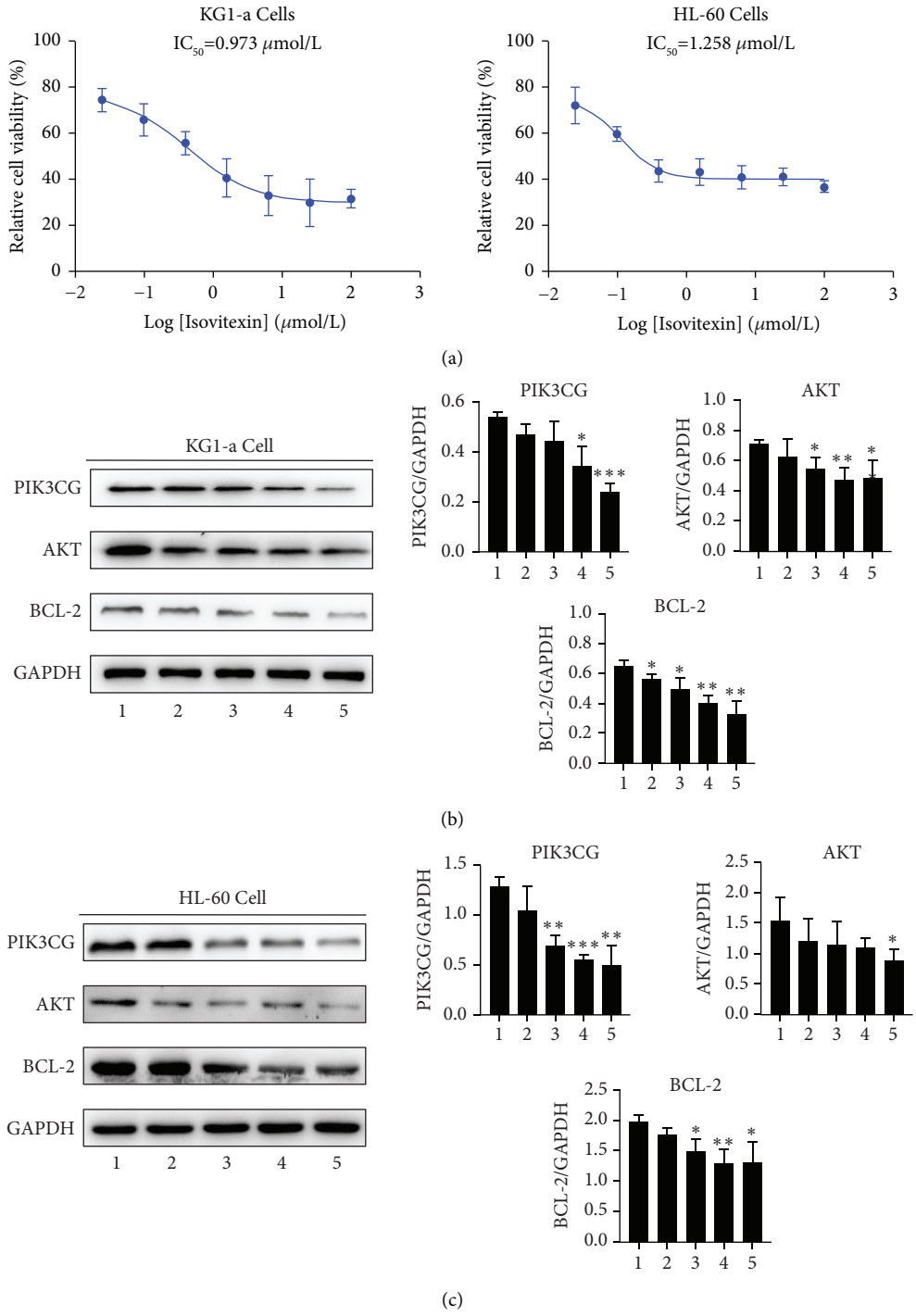

Figure 8: Experimental verification against AML activity of isovitexin in vitro. (a) Isovitexin inhibits the growth of KG1-a cells and HL-60 cells. (b) In KG1-a cell, isovitexin regulated the PI3K-AKT signaling pathway and reduced the expression of Bcl-2. (c) In HL-60 cell, isovitexin regulated the PI3K-Akt signaling pathway and reduced the expression of Bcl-2 in a dose-dependent manner. 1: control group; 2: 0.39 μmol/L; 3: 1.56 μmol/L; 4: 6.25 μmol/L; 5: 25 μmol/L. GAPDH was used as an internal loading control.

dismutase, and ameliorating the bleeding [41, 42]. More specifically, the antileukemia actions of isovitexin, isoindigo, and indirubin were confirmed by in vitro and in vivo models, which enhanced G1/G0 arrest and PML-RARα degradation [43, 44]. Meanwhile, our experimental studies also implicated that isovitexin significantly inhibits the proliferation of KG1-a cells and HL-60 cells. But, we still need to conduct further studies on the antileukemia effects of QHP.

In the process of anticancer drug discovery, the search for key targets that are linked together is a major focus of research. One drug can be linked to many genes and proteins

in complex relationships. Similarly, one gene or protein can be linked to many drugs. At the same time, there are more and more online analysis tools that can be used in network pharmacology studies. In this study, 89 potential target genes related to QHP and AML were identified with TCMSP, TCMID, SymMap, OMIM, GeneCards, DisGenet, and Drugbank database analysis. After that, 89 potential target genes were analyzed based on the STRING database. In order to comprehensively understand their biofunctional annotation information, GO terms, and KEGG pathway enrichments, they were analyzed with R language. According to the analysis of BP terms, QHP is closely related to aging, peptidyl-serine modification, peptidyl-serine phosphorylation, protein autophosphorylation, reactive oxygen species metabolic processes, and so on. These results may be related to targeting AML effects of QHP [45, 46]. What's more, 5 of the first 20 enriched KEGG pathways are related to PI3K-Akt signaling pathway, Epstein-Barr virus infection, Kaposi sarcoma-associated herpesvirus infection, proteoglycans in cancer, and EGFR tyrosine kinase inhibitor resistance. These results suggest that QHP may have antiviral and anticancer effects and that the relevant pathway is the PI3K-Akt signaling pathway.

In addition, we made a C-T-P network diagram. In this network, nodes with high-degree may be considered to represent the major therapeutic effects of QHP on AML. Compared to macromolecular compounds, the molecular weights of As_4S_4 and As_2O_3 are small. Despite their high degree, the binding effects of As_4S_4 and As_2O_3 with proteins are not as strong as that of macromolecules. Moreover, it is significant that these target genes with high-degree are closely related to the PI3K-Akt signaling pathway. Biological studies showed that the dysregulation of the PI3K-Akt signaling pathway in AML may cause the activation of downstream signal molecules, regulate tumor cell proliferation, apoptosis processes, and mediate tumor cell resistance to radiotherapy and chemotherapy [47, 48]. Dysregulation of the PI3K-Akt pathway in AML has become the focus of drug research and development. Thus, targeting the PI3K-Akt pathway in AML may be a potential therapeutic approach [49, 50]. Simultaneously, the molecular docking results showed that the PIK3CG, JUN, and CHEK1 proteins had a good binding affinity with isovitexin. Combined with the results of molecular docking analysis, our western blot analysis results clearly demonstrated that the anti-AML effects of isovitexin were exerted mainly via regulating the PI3K-Akt pathway.

In this study, network pharmacology techniques were used to elucidate the potential antileukemia effects of QHP, and these effects were visualized by molecular docking for verification. This systematic theoretical research provides a fundamental methodology for future pharmacological research designed to further explore the mechanism of action of QHP in the treatment of AML. However, this study has some shortcomings that require further research. Firstly, the public web database selected for this study is characterized by real-time updates, so the results of this study can only partially elucidate the molecular mechanism of QHP against AML. Secondly, only molecular docking and in vitro experimental validation were performed in this study, and a multidimensional validation should be performed subsequently in combination with animal models and clinical trials. Thirdly, studies on the quantitative determination of the content of 14 compounds in QHP are currently not yet perfect. Moreover, isovitexin, though determined as the mainly important bioactive compound of QHP against AML, could not completely stand for QHP. Thus, additional study is required to further explore the underlying molecular mechanism of QHP in the treatment of AML in vitro and in vivo.

5. Conclusion

Based on the network pharmacology, molecular docking analysis, and experimental validation, the underlying mechanism of QHP in AML therapy involves the regulation of signaling pathways and targets. In this study, we identified that isovitexin might be the underlying compounds responsible for the therapeutic actions of QHP. The anti-AML effects of QHP seem to be mediated by inhibition of the AML cells growth and Bcl-2 protein expression, and regulation of the PI3K-Akt signaling pathway. Overall, the obtained results suggested that QHP might be used as a promising therapeutic agent for AML and provide additional evidence for the promotion of the wide use of QHP in the clinic for the treatment of AML diseases.

Data Availability

Data will be obtained from the corresponding author upon reasonable request.

Conflicts of Interest

All authors declare no conflicts of interest.

Authors' Contributions

Yingjian Zeng, Min Wu, Xinping Wu, and Lu Zhou wrote the first draft of the manuscript. Huan Zhang, Na Wan, and Zhenhui Wu corrected the manuscript. All authors read and approved the final manuscript.

Acknowledgments

This work was funded by the Natural Science Foundation of Jiangxi Province (Grant no. 20192BAB205100), Health and Family Planning Commission of Jiangxi Province (Grant no. 20195334), and Science and Technology Planning Project of Administration of Traditional Chinese Medicine of Health and Family Planning Commission of Jiangxi Province (Grant nos. 2020A0184 and 2021B651).

References

[1] N. J. Short, M. E. Rytting, and J. E. Cortes, "Acute myeloid leukaemia," *The Lancet*, vol. 392, no. 10147, pp. 593–606, 2018.

[2] C. M. Csizmar, D.-H. Kim, and Z. Sachs, "The role of the proteasome in AML," *Blood Cancer Journal*, vol. 6, no. 12, p. e503, 2016.

[3] S. Bertoli, S. Tavitian, A. Huynh et al., "Improved outcome for AML patients over the years 2000-2014," *Blood Cancer Journal*, vol. 7, no. 12, pp. 635–638, 2017.

[4] D. Wu, W. Wang, W. Chen et al., "Pharmacological inhibition of dihydroorotate dehydrogenase induces apoptosis and differentiation in acute myeloid leukemia cells," *Haematologica*, vol. 103, no. 9, pp. 1472–1483, 2018.

[5] C. Rong, W. Wei, and T. Yu-Hong, "Asperuloside exhibits a novel anti-leukemic activity by triggering ER stress-regulated apoptosis via targeting GRP78," *Biomedicine & Pharmacotherapy*, vol. 125, pp. 0–6, Article ID 109819, 2020.

[6] Y. F. Shi, L. Liu, L. L. He et al., "Combining triptolide with ABT-199 is effective against acute myeloid leukemia through reciprocal regulation of Bcl-2 family proteins and activation of the intrinsic apoptotic pathway," *Cell Death & Disease*, vol. 11, no. 7, Article ID 555, 2020.

[7] R. Gu, M. Zhang, H. Meng, D. Xu, and Y. Xie, "Gallic acid targets acute myeloid leukemia via Akt/mTOR-dependent mitochondrial respiration inhibition," *Biomedicine & Pharmacotherapy*, vol. 105, no. 473, pp. 491–497, 2018.

[8] Q. Lu, Y. He, Y. Wang et al., "Saponins from Paris forrestii (Takht.) H. Li display potent activity against acute myeloid leukemia by suppressing the RNF6/AKT/mTOR signaling pathway," *Frontiers in Pharmacology*, vol. 9, no. 673, pp. 1–11, 2018.

[9] Z. Y. Nie, M. H. Zhao, B. Q. Cheng et al., "Tanshinone IIA regulates human AML cell proliferation, cell cycle, and apoptosis through miR-497-5p/AKT3 axis," *Cancer Cell International*, vol. 20, no. 1, pp. 1–12, 2020.

[10] W. Liu, K. Xiao, L. Ren et al., "Leukemia cells apoptosis by a newly discovered heterogeneous polysaccharide from Angelica sinensis (Oliv.) Diels," *Carbohydrate Polymers*, vol. 241, Article ID 116279, 2020.

[11] S. K. Heo, E. K. Noh, J. Y. Kim et al., "Rhein augments ATRA-induced differentiation of acute promyelocytic leukemia cells," *Phytomedicine*, vol. 49, pp. 66–74, 2018.

[12] H. Y. Ma, C. Q. Wang, H. He, Y. Zan Yang, and T. Yao, "Ethyl acetate extract of Caesalpinia sappan L inhibited acute myeloid leukemia via ROS-mediated apoptosis and differentiation," *Phytomedicine*, vol. 68, 2020.

[13] T. Fan, R. c. Quan, W. y. Liu et al., "Arsenic-containing qinghuang powder (青黄散) is an alternative treatment for elderly acute myeloid leukemia patients refusing low-intensity chemotherapy," *Chinese Journal of Integrative Medicine*, vol. 26, no. 5, pp. 339–344, 2020.

[14] X.-M. Hu, B. Yuan, S. Tanaka et al., "Arsenic disulfide-triggered apoptosis and erythroid differentiation in myelodysplastic syndrome and acute myeloid leukemia cell lines," *Hematology*, vol. 19, no. 6, pp. 352–360, 2014.

[15] A.-X. Zhou, Z.-W. Cheng, R. Ma, and C. S. Den, "Clinical investigation of treatment with Qinghuang powder for 86 patients with chronic myelogenous leukemia," *Journal of Leuk. Lymphoma*, vol. 19, no. 11, pp. 655–657, 2010.

[16] J. Ming, W. Yi Liu, H. Yan Xiao, X. Yong gang, and M. Rou, "Oral arsenic-containing qinghuang powder (青黄散): a potential drug for myelodysplastic syndromes," *Chinese Journal of Integrative Medicine*, vol. 1, pp. 1–7, Article ID 100091, 2020.

[17] S. Xu, R. Ma, X.-m. Hu et al., "Clinical observation of the treatment of myelodysplastic syndrome mainly with Qinghuang Powder (青黄散)," *Chinese Journal of Integrative Medicine*, vol. 17, no. 11, pp. 834–839, 2011.

[18] G. B. Zhang, Q. Y. Li, Q. L. Chen, and S. B. Su, "Network pharmacology: a new approach for Chinese herbal medicine research," *Evidence-based Complement Alternative Medicine*, vol. 2013, 2013.

[19] M. Yang, J. Chen, L. Xu et al., "A network pharmacology approach to uncover the molecular mechanisms of herbal formula ban-xia-xie-xin-tang," *Evidence-based Complementary and Alternative Medicine*, vol. 2018, no. 489, pp. 22–11, 2018.

[20] S. Li, Z. Q. Zhang, L. J. Wu, X. G. Zhang, Y. Y. Wang, and Y. D. Li, "Understanding ZHENG in traditional Chinese medicine in the context of neuro-endocrine-immune network," *IET Systems Biology*, vol. 1, no. 1, pp. 51–60, 2007.

[21] S. Li, "Network pharmacology evaluation method guidance - draft," *World Journal of Traditional Chinese Medicine*, vol. 7, no. 1, pp. 146–154, 2021.

[22] Y. Wu, F. Zhang, K. Yang et al., "SymMap: an integrative database of traditional Chinese medicine enhanced by symptom mapping," *Nucleic Acids Research*, vol. 47, no. D1, pp. D1110–D1117, 2019.

[23] J. Ru, P. Li, J. Wang, L. Bohui, and H. Chao, "TCMSP: A database of systems pharmacology for drug discovery from herbal medicines," *Journal of Cheminformatics*, vol. 6, no. 1, pp. 1–6, 2014.

[24] R. Xue, Z. Fang, M. Zhang, Y. Zhenghui, and W. Chengping, "TCMID: Traditional Chinese medicine integrative database for herb molecular mechanism analysis," *Nucleic Acids Research*, vol. 41, no. D1, pp. 1089–1095, 2013.

[25] W. Guo, J. Huang, N. Wang et al., "Integrating network pharmacology and pharmacological evaluation for deciphering the action mechanism of herbal formula Zuojin Pill in suppressing hepatocellular carcinoma," *Frontiers in Pharmacology*, vol. 10, pp. 1–21, 2019.

[26] A. Daina, O. Michielin, and V. Zoete, "SwissTargetPrediction: updated data and new features for efficient prediction of protein targets of small molecules," *Nucleic Acids Research*, vol. 47, no. W1, pp. W357–W364, 2019.

[27] Z.-J. Yao, J. Dong, Y.-J. Che et al., "TargetNet: a web service for predicting potential drug-target interaction profiling via multi-target SAR models," *Journal of Computer-Aided Molecular Design*, vol. 30, no. 5, pp. 413–424, 2016.

[28] R. Apweiler, "UniProt: the universal protein knowledgebase," *Nucleic Acids Research*, vol. 32, pp. 115D–119, Article ID 90001, 2004.

[29] D. Szklarczyk, A. L. Gable, D. Lyon et al., "STRING v11: protein-protein association networks with increased coverage, supporting functional discovery in genome-wide experimental datasets," *Nucleic Acids Research*, vol. 47, no. D1, pp. D607–D613, 2019.

[30] D. Otasek, J. H. Morris, J. Bouças, A. R. Pico, and B. Demchak, "Cytoscape Automation: empowering workflow-based network analysis," *Genome Biology*, vol. 20, no. 1, pp. 1–15, Article ID 185, 2019.

[31] A. Allouche, "Software news and updates gabedit — a graphical user interface for computational chemistry softwares," *Journal of Computational Chemistry*, vol. 32, no. 2, pp. 174–182, 2012.

[32] J. L. Carter, K. Hege, J. Yang et al., "Targeting multiple signaling pathways: the new approach to acute myeloid leukemia therapy," *Signal Transduction and Targeted Therapy*, vol. 5, no. 1, pp. 288–316, 2020.

[33] Y. Chen, H. Hui, H. Yang et al., "Wogonoside induces cell cycle arrest and differentiation by affecting expression and subcellular localization of PLSCR1 in AML cells," *Blood*, vol. 121, no. 18, pp. 3682–3691, 2013.

[34] A. L. Hopkins, "Network pharmacology: the next paradigm in drug discovery," *Nature Chemical Biology*, vol. 4, no. 11, pp. 682–690, 2008.

[35] Q. D. Xia, Y. Xun, J. L. Lu et al., "Network pharmacology and molecular docking analyses on Lianhua Qingwen capsule indicate Akt1 is a potential target to treat and prevent COVID-19," *Cell Proliferation*, vol. 53, no. 12, Article ID e12949, 2020.

[36] X.-Q. Shi, S.-J. Yue, Y.-P. Tang et al., "A network pharmacology approach to investigate the blood enriching mechanism of Danggui buxue Decoction," *Journal of Ethnopharmacology*, vol. 235, pp. 227–242, 2019.

[37] M. Tan, Q. Zhang, X. Yuan, Y. Chen, and Y. Wu, "Synergistic killing effects of homoharringtonine and arsenic trioxide on acute myeloid leukemia stem cells and the underlying mechanisms," *Journal of Experimental & Clinical Cancer Research*, vol. 38, no. 1, pp. 308–322, 2019.

[38] N. Russell, A. Burnett, R. Hills et al., "Attenuated arsenic trioxide plus ATRA therapy for newly diagnosed and relapsed APL: long-term follow-up of the AML17 trial," *Blood*, vol. 132, no. 13, pp. 1452–1454, 2018.

[39] Q. Ma, C. Wang, X. Li, H. Guo, and J. Meng, "Fabrication of water-soluble polymer-encapsulated As4 S4 to increase oral bioavailability and chemotherapeutic efficacy in AML mice," *Scientific Reports*, vol. 6, pp. 1–12, Article ID 29348, 2016.

[40] H.-H. Zhu, J. Hu, F. Lo-Coco, and J. Jin, "The simpler, the better: oral arsenic for acute promyelocytic leukemia," *Blood*, vol. 134, no. 7, pp. 597–605, 2019.

[41] X. Cao, L. Liu, Q. Yuan et al., "Isovitexin reduces carcinogenicity and stemness in hepatic carcinoma stem-like cells by modulating MnSOD and FoxM1," *Journal of Experimental & Clinical Cancer Research: Climate Research*, vol. 38, no. 1, pp. 264–281, 2019.

[42] K. Ozawa, D. Mori, A. Hatanaka et al., "Comparison of the anti-colitis activities of Qing Dai/Indigo Naturalis constituents in mice," *Journal of Pharmacological Sciences*, vol. 142, no. 4, pp. 148–156, 2020.

[43] N. H. Tung, T. Uto, A. Sakamoto et al., "Antiproliferative and apoptotic effects of compounds from the flower of Mammea siamensis (Miq.) T Anders on human cancer cell lines," *Bioorganic & Medicinal Chemistry Letters*, vol. 23, no. 1, pp. 158–162, 2013.

[44] L. Wang, G.-B. Zhou, P. Liu et al., "Dissection of mechanisms of Chinese medicinal formula Realgar-Indigo naturalis as an effective treatment for promyelocytic leukemia," *Proceedings of the National Academy of Sciences*, vol. 105, no. 12, pp. 4826–4831, 2008.

[45] A. J. Robinson, G. L. Hopkins, N. Rastogi et al., "Reactive oxygen species drive proliferation in acute myeloid leukemia via the glycolytic regulator PFKFB3," *Cancer Research*, vol. 80, no. 5, pp. 937–949, 2020.

[46] J. U. Kazi and L. Rönnstrand, "FMS-like tyrosine kinase 3/FLT3: from basic science to clinical implications," *Physiological Reviews*, vol. 99, no. 3, pp. 1433–1466, 2019.

[47] M. Estruch, K. Reckzeh, C. Vittori et al., "Targeted inhibition of cooperative mutation- and therapy-induced AKT activation in AML effectively enhances response to chemotherapy," *Leukemia*, vol. 35, no. 7, pp. 2030–2042, 2021.

[48] C. Zhou, J. Du, L. Zhao, H. Liang, and P. Fang, "GLI1 reduces drug sensitivity by regulating cell cycle through PI3K/AKT/GSK3/CDK pathway in acute myeloid leukemia," *Cell Death & Disease*, vol. 12, no. 3, 2021.

[49] S. Darici, H. Alkhaldi, G. Horne, H. G. Jørgensen, S. Marmiroli, and X. Huang, "Targeting PI3K/Akt/mTOR in AML: rationale and clinical evidence," *Journal of Clinical Medicine*, vol. 9, no. 9, Article ID 2934, 2020.

[50] A. M. Martelli, M. Nyåkern, G. Tabellini et al., "Phosphoinositide 3-kinase/Akt signaling pathway and its therapeutical implications for human acute myeloid leukemia," *Leukemia*, vol. 20, no. 6, pp. 911–928, 2006.

Hindawi
Evidence-Based Complementary and Alternative Medicine
Volume 2021, Article ID 4961738, 12 pages
https://doi.org/10.1155/2021/4961738

Research Article

Using the Symptom Patient Similarity Network to Explore the Difference between the Chinese and Western Medicine Pathways of Ischemic Stroke and its Comorbidities

Lunzhong Zhang,[1] Shu Han,[2] Manli Zhao,[1] Runshun Zhang,[3] Xuebin Zhang,[4] Jing Zhang,[2] Xiaoqing Liu,[2] Yuyao He,[2] Zhao He,[2] Yunfang Dong,[2] Xiaoying Hou,[2] Zijun Mou,[4] Liyun He,[4] Hong Zhou,[1] Jie Yang,[5] Xingyan Huang,[5] Yanjie Hu,[5] Yuefeng Zhang,[5] Lili Zhang,[5] Zhengguang Chen,[2] Xiaozhen Li,[2] Yan Tan,[6] Kegang Cao,[2] Wei Meng,[2] and Liqun Zhong[2]

[1]*Neurology Department, Weifang Traditional Chinese Hospital, Weifang 261041, China*
[2]*Dongzhimen Hospital Affiliated to Beijing University of Traditional Chinese Medicine, Beijing 100700, China*
[3]*Guanganmen Hospital, China Academy of Chinese Medical Sciences, Beijing 100053, China*
[4]*Institute of Basic Research in Clinical Medicine, China Academy of Chinese Medical Sciences, Beijing 100700, China*
[5]*Beijing Zhong Teng Bai Mai Medical Technology Co., Ltd., Beijing, China*
[6]*School of Life Sciences, Beijing University of Chinese Medicine, Beijing 100029, China*

Correspondence should be addressed to Lunzhong Zhang; zhanglunzhong@163.com and Liqun Zhong; zhongliqun@sina.com

Received 3 September 2021; Revised 25 October 2021; Accepted 29 October 2021; Published 1 December 2021

Academic Editor: Xuezhong Zhou

Background and Objectives. The development of network medicine provides new opportunities for disease research. Ischemic stroke has a high incidence, disability, and recurrence rate, and one of the reasons is that it is often accompanied by other complex diseases, including risk factors, complications, and comorbidities. Network medicine was used to try to analyze the characteristics of IS-related diseases and find out the differences in genetic pathways between Chinese herbs and Western drugs. *Methods*. Individualized treatment of traditional Chinese medicine (TCM) provides a theoretical basis for the study of the personalized classification of complex diseases. Utilizing the TCM clinical electronic medical records (EMRs) of 7170 in patients with IS, a patient similarity network (PSN) with shared symptoms was constructed. Next, patient subgroups were identified using community detection methods and enrichment analyses were performed. Finally, genetic data of symptoms, herbs, and drugs were used for pathway and GO analysis to explore the characteristics of pathways of subgroups and to compare the similarities and differences in genetic pathways of herbs and drugs from the perspective of molecular pathways of symptoms. *Results*. We identified 34 patient modules from the PSN, of which 7 modules include 98.48% of the whole cases. The 7 patient subgroups have their own characteristics of risk factors, complications, and comorbidities and the underlying genetic pathways of symptoms, drugs, and herbs. Each subgroup has the largest number of herb pathways. For specific symptom pathways, the number of herb pathways is more than that of drugs. *Conclusion*. The research of disease classification based on community detection of symptom-shared patient networks is practical; the common molecular pathway of symptoms and herbs reflects the rationality of TCM herbs on symptoms and the wide range of therapeutic targets.

1. Introduction

Ischemic stroke (IS) is not only a disease with high morbidity, high mortality, and high disability, but also has a great risk of recurrence [1, 2]. An important reason for these characteristics is that patients with IS are often accompanied by a variety of complex diseases, including risk factors, comorbidities, and systemic complications after stroke. The existence of these complex diseases has significantly increased the difficulty and cost of treatment, causing a higher risk of death. Therefore, there is an urgent need for a method to solve the complexity and heterogeneity of IS-related diseases to guide the management of early IS patients.

Thanks to plummeting costs of genetic testing, rapid advances in computational power, massive, linked databases, and new targeted therapies, making it increasingly possible to prevent or treat illnesses based on an individual patient's characteristics, the era of precision medicine is high [3–5]. Recent gene discovery efforts have expanded the number of known single-gene disorders associated with stroke and have linked common variants at approximately 35 genetic loci to stroke risk, which have highlighted novel mechanisms and pathways implicated in stroke related to large artery atherosclerosis, cardioembolism, and small vessel disease and defined shared genetic influences with related vascular traits. [6] In China, traditional Chinese medicine (TCM) has a significant effect on the treatment of acute IS, and its typical individualized medical treatment model also reflects the connotation of precision medicine, but the underlying mechanism has not been fully studied [7]. Therefore, detecting the clinical subtypes of IS in the real-world clinical settings by integrating both TCM and biomedical features would be an interesting research task.

Network medicine, which aims to gain an understanding of human disease from the perspectives of network science, has offered a new platform for identifying novel disease mechanisms and predicting drug efficacy, disease-phenotypic associations, and novel disease taxonomy [8–10]. Symptom-shared patient similarity networks (PSNs) have been established to study many complex diseases, such as hypertension [11] and liver diseases [12]. Li et al. have investigated the correlations between symptoms and TCM herbs and finally found that there are strong positive correlations between symptom similarity and herb similarity [13]. But so far, there is no report about the relationship between TCM herbs and potential molecular pathways in acute IS using symptom-shared PSN. For this purpose, the symptom-shared PSN, which is originated from Shu et al. [12], was used to clarify the characteristics of IS subgroups and compare the molecular enriched pathways between Chinese herbs and Western drugs.

2. Materials and Methods

2.1. Subjects

2.1.1. Diagnostic Criteria. Diagnosis of "cerebral infarction" is referred to the "Guidelines for Diagnosis and Treatment of Acute Ischemic Stroke in China 2014" [14] formulated by the Cerebrovascular Disease Group of Neurological Branch of Chinese Medical Association in 2014 and the "Guidelines for the Early Management of Patient With Acute Ischemic Stroke 2019" [15] issued by AHA/ASA in 2019.

2.1.2. Inclusion Criteria. Inclusion criteria were defined as follows: (1) the first Western medicine diagnosis is consistent with the "acute cerebral infarction"; (2) MRI report suggests a new responsible focus for ischemia; (3) both initial acute stroke and recurrent acute stroke are included; and (4) EMRs with more than or equal to 5 positive symptoms are obtained.

2.1.3. Exclusion Criteria. Exclusion criteria were defined as follows: (1) the first Western medicine diagnosis included "cerebral hemorrhage"; (2) key content of the medical record is missing, such as chief complaint, symptoms, and history of present illness.

2.2. Data Extracting and Preprocessing. EMR data extraction uses "the Clinical Research Information Sharing System of TCM" [16]. Cases of all the inpatients from 2016 to 2018 in Weifang Hospital of traditional Chinese medicine in Shandong Province in China were collected and the diagnosis by "cerebral infarction (ICD-10 code I63)" as a keyword was retrieved. A total of 7170 EMR data were finally screened out, including gender, age, diagnosis, symptoms, herbs, and drugs.

The extracted data of diagnosis, symptoms, drugs, and herbs were standardized. According to ICD-10, the disease diagnosis level is standardized to subcategories. After manual review by physicians with rich clinical experience in TCM, referring to the Unified Medical Language System (UMLS) [17], 362 standardized symptoms were finally obtained.

Referred to the Anatomical Therapeutic Chemical (ATC) developed by the WHO Collaborating Centre for Drug Statistics Methodology and "Catalogue of Chinese Listed Chemical Drugs" published by the China Food and Drug Administration (CFDA), 459 generic names were unified, and then, their genetic target information was obtained using the DrugBank database [18–22]. 351 names of TCM herbs were standardized using Chinese Pharmacopoeia 2015 (CHPH, 2015 Edition) and using TCMSP [23] to obtain the information of corresponding genetic targets.

To better study the characteristics of the disease, the diagnosis has been divided into three categories based on the following principles: risk factors, including various metabolic syndrome and coronary heart disease, are the potential causes of ischemic stroke; the remaining diseases that have no exact causal relationship with ischemic stroke are called comorbidity [24], while complications refer to the diseases involving multiple systems that appear based on ischemic stroke and have an indirect relationship with it [24]. Furthermore, risk factors were divided into eight categories according to the related systems: (1) hypertension; (2) diabetes/impaired glucose tolerance; (3) hyperlipidemia; (4)

hyperuricemia/gout; (5) heart disease including rheumatic heart disease, coronary heart disease, dilated cardiomyopathy, and all other heart diseases; (6) arteriosclerosis, arterial occlusion and stenosis, and arteriovenous malformations called as vascular diseases; (7) polycythemia vera, thrombocytosis, thrombocytopenia, and coagulation defects classified as blood diseases; and (8) fatty acid metabolism disorder, amyloidosis, glycoprotein metabolism disorder, and sulfur-loaded amino acid metabolism disorder (hyperhomocysteinemia) collectively referred to as other metabolic diseases.

2.3. Integration of Symptom-Gene Data. With 362 normalized symptom terms as keywords, part of symptom-gene information was obtained in the SymMap database [25]. Symptoms whose genetic information was not found were searched through the MalaCards database [26] to obtain the corresponding disease information, and then, the genetic information was obtained with disease as the keyword, so as to integrate the corresponding relationship between symptom and gene data.

2.4. Construction of Patient Similarity Network. The Jaccard coefficient [27] was used to calculate the similarities of patients based on their symptom phenotypes and constructed the patient similar network, which is defined as follows: $\text{Jaccard}'\text{sim}(A,B) = P(A \cap B)/P(A \cup B)$, and this means that if two patients have more intersected symptom phenotypes, they would have higher symptom similarity. In particular, the symptom similarity of two patients would be 1 if they have identical symptom phenotypes. Supposing that patient A has 5 symptoms, patient B has 8 symptoms, and 2 of them are common, then the $\text{Jaccard}'\text{sim}(A,B) = (P(A \cap B)/P(A \cup B)) = (P(A \cap B)/P(A) + P(B) - P(A \cap B)) = (2/5 + 8 - 2) = (2/11)$ Then, the edges were filtered by weight ≥ 0.5, which means that only the patient links with almost identical chief symptoms were kept while remaining most of the cases included at the same time. The Jaccard coefficient is a commonly used similarity measure, especially in network medicine research [28–31].

2.5. Community Detection Method to Identify the Patient Subgroups. Patients should be divided into some subgroups with more clear boundaries; thus, a nonoverlapping community detection method is more applicable for PSN [12]. An efficient community detection algorithm, namely, BGLL [32], was applied to obtain the patient subgroups from the whole networks. BGLL is an iterative algorithm based on modularity measurement, by continuous division to get the maximum gain of modularity, combines local optimization and multilevel clustering, and is extremely fast, which has linear complexity on typical and sparse data. Modularity proposed by Newman [33, 34] was designed to measure the strength of division of a network into subgroups. Networks with high modularity (ranges from 0 to 1 and usually appears between 0.3 and 0.7 in actual) have the better effect of community division. In this study, all the results were obtained by setting resolution limit = 1.0 and randomize value on.

2.6. Phenotype Enrichment Analysis. Relative risk (RR) is a classical statistical method, which is the ratio of the probability of an event occurring, in an exposed group that a certain condition is present versus a nonexposed group that lacks the condition [35]. In this study, RR was used to evaluate the specificity of diseases in the patient subgroups. The patient in a specific module was treated as an exposed group, and the left patient cases were regarded as the nonexposed group and a disease as an event. So, RR is defined as follows:

$$\text{RR} = \frac{\left(C_{ij}/C_i\right)}{\left(\left(C_j - C_{ij}\right)/\left(N - C_i\right)\right)}, \tag{1}$$

where C_i is the number of patients in module (patient subgroup) i, C_j is the number of patients with disease j, C_{ij} represents the number of patients in module i and with disease j, and N is the total number of patients in the study. If RR > 1.5, it indicates that the distribution of disease j in module i is higher than the distribution in the whole. A similar method is used to identify the significant symptoms, drugs, and herbs in each patient subgroup. In addition, the true significant disease symptom, drug, or herb is filtered by the chi-square test (with P value <0.05), which is a statistical hypothesis test whose result is evaluated by reference to the chi-square distribution [36].

2.7. Pathway Enrichment Analysis. Pathway analysis of the gene data of symptoms, drugs, and herbs has been carried out. The KEGG pathway database is the main database in the Kyoto Encyclopedia of Genes and Genomes (KEGG), and it consists of manually drawn reference pathway maps together with organism-specific pathway maps [37]. The enriched KEGG pathways were obtained using the database for annotation, visualization, and integrated discovery (DAVID), which is a Web-based online bioinformatics resource that aims to provide tools for the functional interpretation of large lists of genes/proteins. Enriched medicines (drugs or herbs) were selected with P values less than 0.05 as the specific medicines of the module, and then the medicines target as the genes of the module, and the significant pathway through Fisher's exact test [38] was finally found. The Jaccard coefficient [27] was used to calculate the similarity between the pathways of drugs and herbs.

3. Results

3.1. Basic Statistical Characteristics of the 7170 Ischemic Stroke Disease Inpatient Cases. In this study, 7170 patients (3913 males and 3257 females) with IS were included, of which 54.22% were males and 45.78% were females. The proportion of patients with ischemic stroke in different age groups is different. It gradually increases with age to 40 years and decreases after 60 years. The proportion of the 60–79 years of age group was the highest, and it was irrelevant to gender (Figure 1(a)).

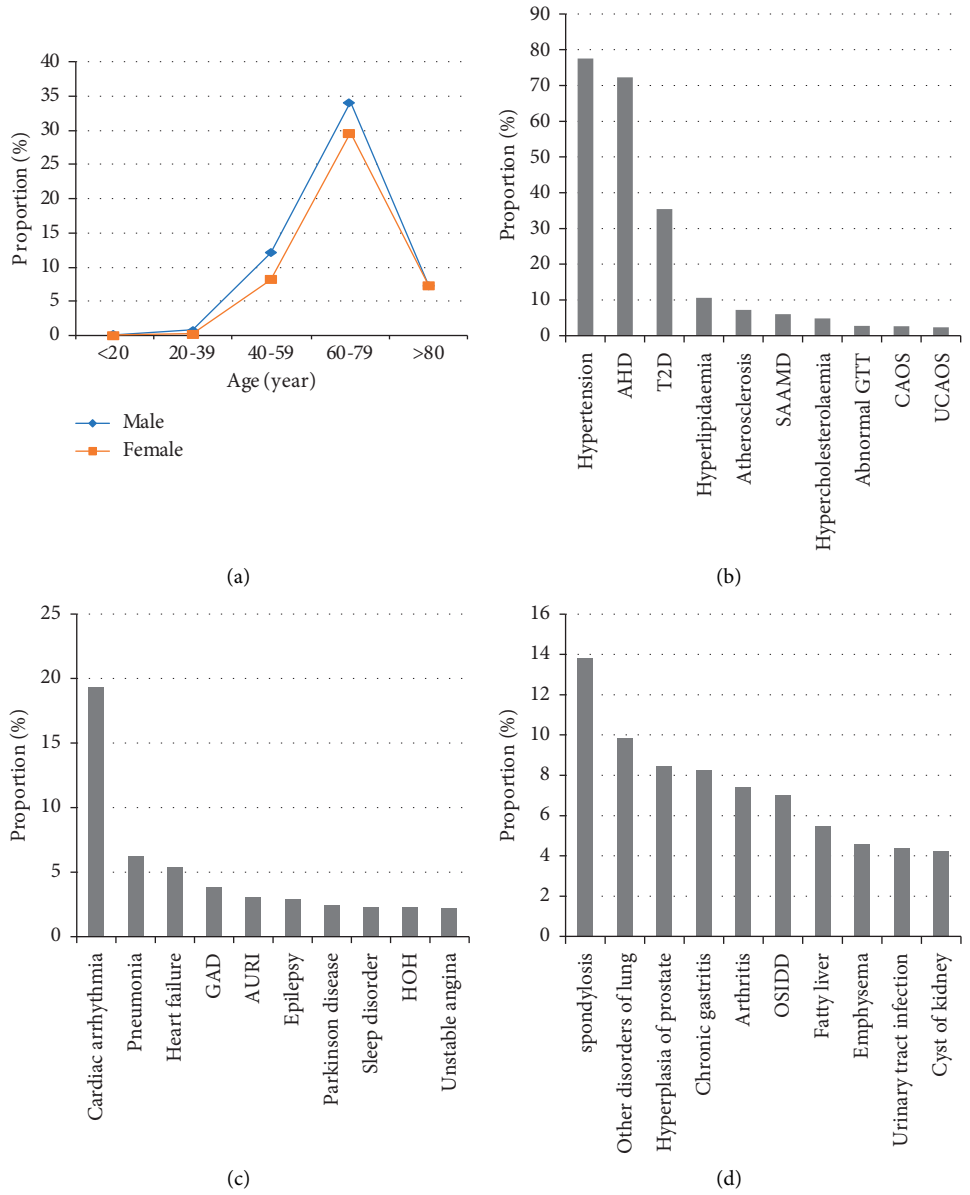

Figure 1: Basic clinical characteristics of 7170 patient cases. (a) The proportion of patients with age and gender in hospitalization. (b) The proportion of patients in the top 10 risk factors. AHD: atherosclerotic heart disease; T2D: type 2 diabetes mellitus; Atherosclerosis: atherosclerosis of other arteries; SAAMD: disorders of sulfur-bearing amino acid metabolism; Hypercholesterolemia: pure hypercholesterolemia; Abnormal GTT: abnormal glucose tolerance test; CAOS: occlusion and stenosis of carotid artery; UCAOS: occlusion and stenosis of unspecified cerebral artery. (c) The proportion of patients in the top 10 complications. GAD: generalized anxiety disorder; AURI: acute upper respiratory infection; HOH: hypoosmolality and hyponatremia. (d) The proportion of patients in the top 10 comorbidity diseases. The proportion in (b–d) means the percentage of patients with this disease in the total population.

Analysis of the risk factors for IS shows that the incidence rates of hypertension, arteriosclerotic heart disease (AHD), type 2 diabetes (T2D), and hyperlipidemia are all greater than 10%, among which the incidence rate of hypertension was up to 77.56%; AHD, as the main risk factor for long-term recurrence of IS [39], has the second highest incidence rate (72.30%); and T2D ranked third with an incidence rate of 35.38% (Figure 1(b)).

In IS complications, incidence rate of cardiac arrhythmia (including bradycardia, atrial fibrillation and flutter, ventricular premature beat, atrial premature beat, tachycardia) is 19.35% higher than others; incidence rates of pneumonia and heart failure are greater than 5% (Figure 1(c)). Among comorbidity diseases, spondylosis (ICD-10 code M47.9) is the most common, with an incidence rate of 13.82% ranking first. The incidence rate of other disorders of lung, hyperplasia of prostate, chronic gastritis, arthritis, other specified intervertebral disc displacement (OSIDD), and fatty liver rank second to seventh, all higher than 5% (Figure 1(d)).

3.2. Patient Similarity Network of Ischemic Stroke. To identify the subtype of patients with ischemic stroke, by calculating the degree of the shared symptom phenotypes between patient pairs, a PSN with 6996 nodes (patients, and 174 of 7170 patients with low similarity have been eliminated) and 397775 edges was constructed. On this basis, a high-performance community detection method (see Materials and Methods) was used to explore the subgroup of ischemic stroke disease population. Finally, 34 modules (modularity: 0.478) were obtained, in which the numbers of patients for each module ranged from 2 to 2046. These modules represent the subgroup of stroke patients, among which 7 modules (such as M3 and M2) have 124 or more cases, accounting for 98.48% of all cases, and 27 modules have 20 or fewer cases, accounting for 1.52%. Considering a more comprehensive study of the diversity of ischemic stroke subgroups, we used four large modules (M3, M2, M1, and M5) and three small modules (M0, M29, and M4), which accounted for 85.09% and 13.39% of all cases, respectively, to illustrate the characteristic phenotype and genotype of ischemic stroke subgroups (Figure 2). The cases of the 7 subgroups were as follows: M3 ($n = 2046$, 29.25%), M2 ($n = 1570$, 22.44%), M1 ($n = 1265$, 18.08%), M5 ($n = 1072$, 15.32%), M0 ($n = 615$, 8.79%), M29 ($n = 198$, 2.83%), and M4 ($n = 124$, 1.77%).

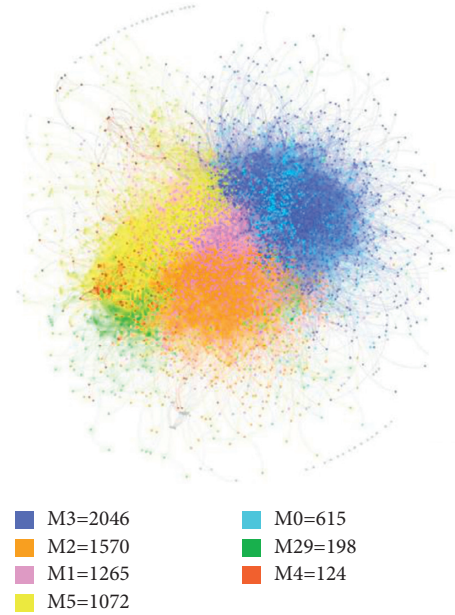

Figure 2: Patient similarity network. Different colors refer to different modules (modules with less than 100 patients are indicated in grey).

3.3. Significant Disease of the Ischemic Stroke Subgroups. The characteristic diseases in 7 subgroups ($P < 0.05$, $RR > 1.5$, Figure 3(a), Supplementary Materials—Table S1) were divided into three categories according to risk factors, complications, and comorbidities, as shown in Figure 3(b). In Figure 3, it shows that M5 has the most disease among the seven subgroups, with 63 diseases in total, and M1 has the least, with only 12 diseases. The proportion of risk factors in each subgroup is below 50%, among which M1 and M0 are more than 30% (33.33% and 31.58%, respectively), and the rest subgroups are less than 20%; the largest proportion of comorbidities is M3, which is as high as 84.48%, and it is more than 50% in M2, M1, and M0 (53.33%, 50%, and 57.89%, respectively), while the other three subgroups are all under 50%; the complications accounted for less than 50% in each subgroup as well, of which M5, M29, and M4 accounted for more than 40% (46.03%, 43.59%, and 44.44%, respectively), and the remaining subgroups are less than 30%. In addition, the number of complications and comorbidities in M5, M29, and M4 is relatively average.

As a whole, the disease characteristics of each module are analyzed in more detail. It can be found that the types of diseases in M3, M2, M5, M29, and M4 are very complex, involving more than 10 systems. Among them, patients in M2, M5, M29, and M4 are more susceptible to neurological diseases, and patients in M3 are more likely to suffer from digestive system diseases, while patients in M1 and M0 have a small number of selected diseases, not many systems are involved, and their characteristics are not obvious.

The results of 8 categories of risk factors are shown in Table 1. It can be seen that M3 patients were more likely to be associated with impaired glucose tolerance, hyperlipidemia, vascular factors, and other metabolic diseases; patients in M2 were more likely to be associated with hypertension, diabetes, vascular factors, and blood diseases; M1 patients were more likely to have gout, vascular factors, blood diseases, and other metabolic diseases; M5 patients were more prone to be associated with hyperlipidemia, heart disease, blood diseases, and other metabolic diseases; M0 is more likely to be related to hyperlipidemia, heart disease, vascular factors, and other metabolic diseases; M29 is more likely to be related to heart disease, vascular factors, and other metabolic diseases; and M4 is more likely to be related to hyperuricemia, heart disease, and vascular factors.

The results of the characteristic comorbidities of each subgroup can be seen in Figure 4(a). It shows that patients in M2 are more likely to have nervous system diseases; patients in M3, M0, and M29 are more likely to have digestive system diseases; patients in M5 and M4 are more likely to have respiratory system diseases; and patients in M1 are more likely to have the digestive system and orthopedic diseases. In addition, compared with other subgroups, patients in M3 are more likely to have thyroid and otorhinolaryngologic diseases, and patients are more likely to have tumors in M29.

The results of complications analysis are shown in Figure 4(b). Patients in 5 subgroups except M1 and M0 were more likely to have nervous system diseases. Compared with other subgroups, M3 is most prone to syncope; M2 is most prone to skin sensory abnormality; M5 is most prone to epilepsy prone; M0 is most prone to autonomic nervous system disease; M29 is most prone to hydrocephalus; M4 is most prone to quadriplegia; M1 is most likely to be complicated with arrhythmia and mental disorder; and M0 is most likely to be complicated with nutritional anemia. In addition, bedsore and pneumonia of M29 were also more significant than that of other subgroups.

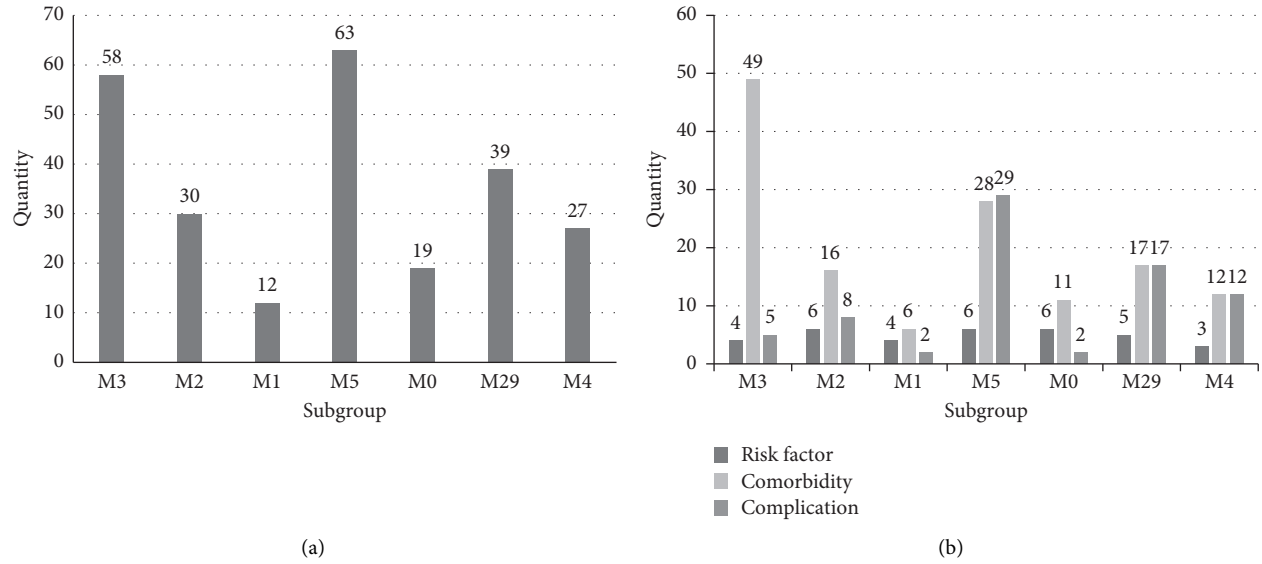

Figure 3: Quantitative statistics of diseases. (a) Total number of selected diseases in each subgroup. (b) Differential count of selected diseases in each subgroup.

Table 1: Risk factors for each subgroup.

Risk factors	M3	M2	M1	M5	M0	M29	M4
Hypertension		√					
Diabetes/impaired glucose tolerance	√	√					
Hyperlipidemia	√			√	√		
Hyperuricemia/gout			√				√
Heart disease				√	√	√	√
Vascular factors	√	√	√		√	√	√
Blood diseases		√	√	√			
Other metabolic diseases	√		√	√	√	√	

3.4. Characteristics of Pathways Specific to the Subgroups. After data preprocessing of the 7170 clinical cases, 362 symptoms, 459 drugs, and 351 herbs with their standard terminologies have been obtained. In enrichment analysis, the specificity of symptoms, drugs, and herbs of 7 subgroups was evaluated by calculating RR (Supplementary Materials—Table S2). Taking the largest module as an example, the top 10 significant symptoms, herbs, and drugs enriched in M3 are listed in Table 2.

Then, genetic pathways of symptom, drug, and herb specific to each of the 7 subgroups were identified by pathway analysis (Supplementary Materials—Table S3). By statistical analysis of the number of pathways, it can be found that the number of drug pathways is significantly smaller than that of symptom or herb pathways in the 7 subgroups ($P < 0.01$). The number of symptom pathways in M2 ($n = 47$) and M4 ($n = 59$) is less than the average ($n = 94$); the number of drug pathways in M1 ($n = 28$), M0 ($n = 8$), and M4 ($n = 31$) is relatively small, which is less than the average of 34, while the number of herb pathways is large than that of symptom and drug pathways, which is not significantly different in each subgroup (coefficient of variation, CV≈6.18) (Table 3).

Comparisons had been made between the pathways of symptom, drug, and herb, one and any of the others. It can be found that the number of symptom-herb pathways shared the most pathways in all subgroups (Figure 5, Table S3). Most of the pathway functions focus on cancer: pathways in cancer, microRNAs in cancer; infectious diseases such as hepatitis B and toxoplasmosis; and signal transduction such as c-AMP signaling pathway and PI3K-Akt signaling pathway. Subgroup M3 was selected with the largest number of common symptom-drug-herb pathways ($n = 16$), and the top 20 enriched pathways of symptom genes and the corresponding P values of drug and herb genetic pathways are shown in Table 4. It can be seen that, for the same symptom pathway, the number of herb pathways with statistical significance is significantly more than that of drug pathway.

4. Discussion

Through the reliable symptom-shared PSN, we found significant quantitative differences between TCM herbs and Western medicine-enriched genetic pathways in acute IS subgroups.

All the data were collected from EMRs of "the Clinical Research Information Sharing System of TCM." From the overall data, the basic characteristics are consistent with the general IS population. For example, the distribution of age and sex is consistent with the report of China Stroke Statistics 2019 [40]. From the perspective of the 7 subgroups, the risk factors, comorbidities, and complications showed distinct characteristics, which are in accord with the heterogeneity of complex diseases. Patients in M29 were more likely to be associated with heart disease and vascular factors, together with bedsore and pneumonia, consistent with the report [40], while their comorbidities were prone to be

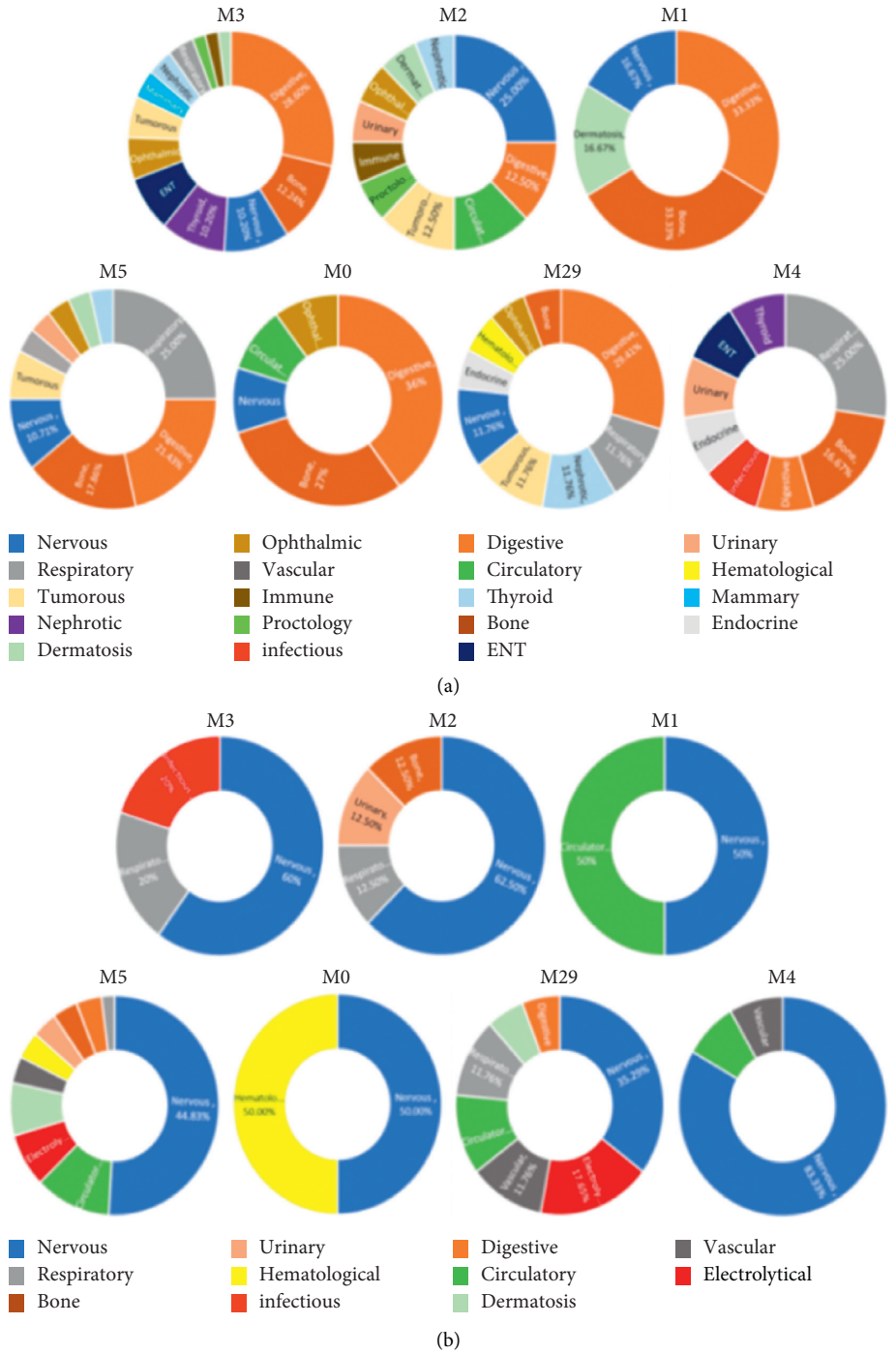

FIGURE 4: Characteristics of comorbidities and complications in each subgroup. (a) System distribution of comorbidities in each subgroup. (b) System distribution of complications in each subgroup.

digestive system diseases and tumors. The top 5 pathways are all about cancer, particularly lung cancer (microRNAs in cancer, pathways in cancer, non-small-cell lung cancer, small-cell lung cancer, proteoglycans in cancer, in Table S3). It obviously reflected the correlation between clinical manifestations and molecular mechanisms of the diseases [41], and the inherent consistent features showed the symptom-shared PSN is practical.

The most interesting subgroup is M3, conforming to the clinical practice in Western medicine and highly consistent with TCM theory as well. Through the enrichment analysis, the main symptoms in M3 are dizzy, headache, vertigo, tinnitus, etc., which are mainly differentiated as "liver Yang hyperactivity syndrome" (LYHS) in the theory of TCM [42]. And the prescription is Tian-Ma-Gou-Teng-Yin, composed of Tianma, Shijueming, Gouteng, Shouwuteng,

Table 2: Top 10 significant symptoms, drugs, and herbs in M3 ($P < 0.01$, RR > 1.5).

		P value	RR
Symptoms	Dizzy	0	2.211773
	Sleep disorder insomnia	2.8E-154	2.213527
	Headache	1.4E-146	4.808182
	Queasy	8.3E-114	3.840246
	Vertigo	3.62E-98	7.746588
	Impaired sensations	9.88E-92	6.330342
	Stiffness muscle	1.36E-87	3.562796
	Palpitation	5.51E-57	1.758678
	Tinnitus	1.34E-39	3.047759
	Dream	4.04E-26	3.584229
Herbs	Tianma	2.44E-81	1.735151
	Shijueming	1.78E-75	3.024194
	Gouteng	1.3E-67	2.307379
	Shouwuteng	4.39E-50	2.812062
	Zhizi	1.81E-49	2.345902
	Gegen	2.39E-48	2.461614
	Huangqin	1E-43	1.749792
	Suanzaoren	1.53E-43	2.478363
	Hujisheng	1.59E-36	2.304421
	Duzhong	2.24E-31	2.475248
Drugs	Betahistine hydrochloride	1.63E-78	3.213303
	Gastrodin injection	2.72E-46	1.852636
	Betahistine mesylate	9.66E-28	2.628823
	Flupentixol	9.6E-22	2.049731
	Promethazine hydrochloride	2.87E-21	2.658477
	Flunarizine hydrochloride	1.72E-20	3.739003
	Ginseng glucose injection	6.07E-11	1.786732
	Vinpocetine	5.06E-09	1.808967
	Levothyroxine sodium	7.79E-09	3.400174
	Homogenin hydrobromide	1.77E-08	2.520161

Table 3: Statistics of symptom, drug, and herb pathways of each subgroup.

Subgroup	Symptom pathway	Drug pathway	Herb pathway	Drug-herb-shared pathway	Drug-herb Jaccard coefficient
M3	115	38	146	20	0.12
M2	47	55	158	40	0.23
M1	117	28	145	14	0.09
M5	118	41	146	21	0.13
M0	100	8	158	3	0.02
M29	102	38	129	15	0.10
M4	59	31	145	20	0.13
Means	94	34.14	146.71	19	—
SD	26.94	13.32	9.07	—	—
CV	28.66	39.03	6.18	—	—

Note: symptom pathway, drug pathway, and herb pathway are, respectively, the number of pathways with P value less than 0.01 for symptom, drug, and herb; the drug-herb-shared pathway is the number of the same pathways with P value less than 0.01 for drug and herb pathway; drug-herb Jaccard coefficient reflects the similarity of drug and herb pathways in the same subgroup; SD: standard deviation; CV: coefficient of variation.

Zhizi, Huangqin, Hujisheng, Duzhong, etc., which are in accord with most of the herbs detected in M3. The above consistent results are in perfect agreement with the "symptom-syndrome-prescription correspondence" principle in TCM theory [43]. Enriched drugs such as hydrochloride, betahistine, promethazine, and flunarizine are also the correct drug to treat the symptoms above. The symptom is a vital basis for clinical diagnosis and treatment as well as disease classification [41]. Meanwhile, TCM syndromes and their corresponding prescriptions heavily depended on symptoms [44, 45], which also bring us the enlightenment of classifying complex diseases according to the symptom phenotype. Considering the consistency between symptoms and medicine in M3, it proves again that the detected subgroups based on symptoms are in line with clinical practice.

On the other hand, we can infer the potential molecular pathway of LYHS from the result of pathways analysis. Using a systems biology approach with the combination of computational analysis and animal experiment, Li et al. [46] have found that "Cold ZHENG" and "Hot ZHENG" have their own corresponding genetic pathways. Zhai et al. [47] found

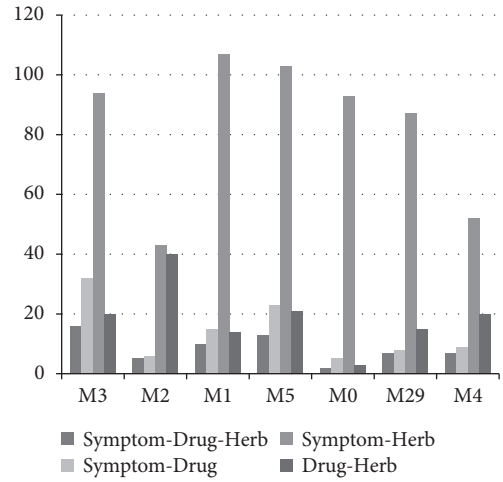

Figure 5: Number of symptom-drug-herb common pathway of each subgroup ($P < 0.01$).

Table 4: Top 20 enriched pathways of symptom genes in M3.

Symptom pathway in M3	Symptom pathway P value	Drug pathway P value	Herb pathway P value
AGE-RAGE SP in diabetic complications	3.3876E-17	ns	2.00999E-29
Neuroactive ligand-receptor interaction	1.32395E-16	9.33419E-48	ns
Alzheimer's disease	3.67245E-16	5.1187E-06	5.56899E-05
Calcium signaling pathway	5.41417E-16	7.04619E-24	ns
Amyotrophic lateral sclerosis (ALS)	3.09577E-15	0.000130295	3.13695E-10
Pathways in cancer	4.09088E-15	ns	1.4964E-32
Hepatitis B	3.44822E-14	ns	1.61268E-31
Bladder cancer	2.22937E-13	ns	7.08838E-17
Proteoglycans in cancer	3.97422E-13	ns	3.49664E-17
Malaria	4.0587E-13	ns	3.28241E-16
Pancreatic cancer	8.48407E-13	ns	4.62234E-21
cAMP signaling pathway	1.77595E-12	4.10807E-14	7.44568E-05
Colorectal cancer	1.48163E-11	ns	5.75226E-16
HIF-1 signaling pathway	2.86538E-11	ns	4.7202E-19
EGFR tyrosine kinase inhibitor resistance	3.02218E-11	ns	3.82288E-17
Endocrine resistance	3.49548E-11	ns	3.29809E-23
MicroRNAs in cancer	9.68694E-11	ns	9.46322E-11
Prostate cancer	3.02359E-10	ns	1.5772E-23
FoxO signaling pathway	3.21659E-10	ns	5.3789E-25
Glioma	4.70998E-10	ns	2.33281E-14

AGE-RAGE SP in diabetic complications: AGE-RAGE signaling pathway in diabetic complications; ns: not significant.

that 46 genes were involved in the Qi deficiency and blood stasis syndrome of both stroke and coronary heart disease (CHD) by means of data mining, which also supported the existence of biological basis under TCM syndrome ("ZHENG" in Chinese). In our study, as mentioned before, the symptoms in M3 have corresponding syndrome LYHS and prescriptions in the theory of TCM. Therefore, it can be inferred that the potential molecular pathways of LYHS are possibly related to the enriched symptom pathways in M3 (Table 4). It is expected to predict more potential pathways of other acute IS syndromes through network methods in the future, strengthen the understanding of the underlying mechanism of TCM treatment of stroke, and provide ideas for TCM syndrome research.

Moreover, through pathway enrichment analysis, we distinguished the feature of genetic pathway of TCM herbs in 7 subgroups (Supplementary Materials—Table S3). In each group, the quantity of herb pathways was more than that of symptom and drug pathways (Table 3, $CV \approx 6.18$). The number of symptom-herb common pathways was larger than that of symptom-drug-shared pathways in all subgroups; in the same subgroup (such as M3), to the same symptom pathway ($P < 0.01$), the number of statistically significant pathways of herbs is obviously more than that of drugs. This may be due to the fact that Chinese herb is different from Western medicine with a single chemical composition, and the complex composition leads to a significantly richer number of herb pathways. It indicates that Chinese herbs play a more comprehensive role in the treatment of IS by acting on multiple targets. The key nodes of disease-herb-target network can be mined through network pharmacology methods to explain the mechanism of multicomponent and multitarget of herbs

and provide ideas for solving the problems such as unclear active ingredients and mechanism of action of herbs [48]. Network pharmacology methods have been used by some scholars [49] to investigate the underlying molecular mechanisms of Lian Xia Ning Xin formula, a Chinese prescription, to treat CHD and disease phenotypes. In the future, on the basis of determining specific Chinese medicines or prescriptions, it may be possible to predict the TCM herb targets for the treatment of stroke.

There are several potential limitations in our research. First of all, the patients in this study were all from one hospital, which might induce sample bias. Actually, "the Clinical Research Information Sharing System of TCM" used in the study has been deployed in 60 Chinese medicine hospitals across China and has been used in studying the mechanism of TCM diagnosis or treatment of many diseases, such as CHD [45, 50], AECOPD [51, 52], and COVID-19 [53]. With appropriate designing strategies, we could integrate these data from the multiple resources to perform a large-scale retrospective cohort study with more reliable results. Secondly, due to the limitations of retrospective research, genetic testing could not be performed to clinically verify the results. Meanwhile, personalized medicine will increasingly rely on EMRs to store vast amounts of genomic data [54]. Supported by the sharing system, we will have the opportunity to carry out multicenter research to obtain more universal conclusions.

5. Conclusions

To our knowledge, this is the first study to demonstrate the utility of symptom-shared PSN for the classification of ischemic stroke and it can be used for other complex diseases as well. The distinct diseases of each subgroup and the underlying biological pathways of its diseases indicate that it is possible to further explore the molecular network mechanisms of complex diseases using this clinical disease subtyping approach. Meanwhile, the inherent consistency on symptom and TCM herb from both clinical and molecular features reflects the rationality of TCM on symptoms and the wide range of therapeutic targets.

Data Availability

The datasets used during the current study are available from the corresponding author on reasonable request.

Disclosure

Lunzhong Zhang and Shu Han, as co-first authors

Conflicts of Interest

The authors declare that they have no financial and personal relationships with other people or organizations that can inappropriately influence our work.

Authors' Contributions

Lunzhong Zhang and Shu Han contributed equally to this work.

Acknowledgments

The authors appreciate Beijing Zhong Teng Bai Mai Medical Technology Co. Ltd. very much for data processing. This study was partially supported by the 2017 National Key R & D Program (nos. 2017YFC1703500 and 2017YFC1703502).

Supplementary Materials

Table S1: enriched diseases of each subgroup. Table S2: enriched symptoms, herbs, and drugs of each subgroup. Table S3: pathways of each subgroup. (*Supplementary Materials*)

References

[1] E. J. Benjamin, P. Muntner, A. Alonso et al., "Heart disease and stroke statistics-2019 update: a report from the american heart association," *Circulation*, vol. 139, no. 10, pp. e56–e528, 2019.

[2] R. Luengo-Fernandez, N. L. M. Paul, A. M. Gray et al., "Population-based study of disability and institutionalization after transient ischemic attack and stroke," *Stroke*, vol. 44, no. 10, pp. 2854–2861, 2013.

[3] F. S. Collins and H. Varmus, "A new initiative on precision medicine," *New England Journal of Medicine*, vol. 372, no. 9, pp. 793–795, 2015.

[4] E. S. Lander, "Cutting the gordian helix—regulating genomic testing in the era of precision medicine," *New England Journal of Medicine*, vol. 372, no. 13, pp. 1185-1186, 2015.

[5] A. R. Weil, "Precision medicine," *Health Affairs*, vol. 37, no. 5, p. 687, 2018.

[6] M. Dichgans, S. L. Pulit, and J. Rosand, "Stroke genetics: discovery, biology, and clinical applications," *The Lancet Neurology*, vol. 18, no. 6, pp. 587–599, 2019.

[7] X. Zhou, Y. Li, Y. Peng et al., "Clinical phenotype network: the underlying mechanism for personalized diagnosis and treatment of traditional Chinese medicine," *Frontiers of Medicine*, vol. 8, no. 3, pp. 337–346, 2014.

[8] E. K. Silverman and J. Loscalzo, "Network medicine approaches to the genetics of complex diseases," *Discovery Medicine*, vol. 14, no. 75, pp. 143–152, 2012.

[9] X. Zhou, L. Lei, J. Liu et al., "A systems approach to refine disease taxonomy by integrating phenotypic and molecular networks," *Ebiomedicine*, vol. 31, pp. 79–91, 2018.

[10] A. L. Barabási, N. Gulbahce, and J. Loscalzo, "Network medicine: a network-based approach to human disease," *Nature Reviews Genetics*, vol. 12, no. 1, pp. 56–68, 2011.

[11] Y. F. Wang, J. J. Wang, W. Peng et al., "Identification of hypertension subgroups through topological analysis of symptom-based patient similarity," *Chinese Journal of Integrative Medicine*, vol. 27, no. 9, pp. 656–665, 2021.

[12] Z. Shu, W. Liu, H. Wu, M. Xiao, and X. Zhou, "Symptom-based network classification identifies distinct clinical subgroups of liver diseases with common molecular pathways," *Computer Methods & Programs in Biomedicine*, vol. 174, 2018.

[13] Y. B. Li, X. Z. Zhou, R. S. Zhang et al., "Detection of herb-symptom associations from traditional Chinese medicine clinical data," *Evidence-Based Complementary and Alternative Medicine*, vol. 2015, Article ID 270450, 11 pages, 2015.

[14] Neurology CSo and Society CS, "Guidelines for the diagnosis and treatment of acute ischemic stroke in China 2014,"

Chinese Journal of Neurology, vol. 48, no. 4, pp. 246–257, 2015, in Chinese.

[15] W. J. Powers, A. A. Rabinstein, T. Ackerson et al., "Guidelines for the early management of patients with acute ischemic stroke: 2019 update to the 2018 guidelines for the early management of acute ischemic stroke: a guideline for Healthcare professionals from the american heart association/ American stroke association," *Stroke*, vol. 50, no. 12, pp. e344–e418, 2019.

[16] B. Y. Liu, X. Z. Zhou, R. S. Zhang et al., "Basic requirements of TCM electronic medical record system in medical treatment and clinical scientific research information sharing system," *China Digital Medicine*, vol. 7, no. 10, pp. 57–60, 2012, in Chinese with English abstract.

[17] O. Bodenreider, "The unified medical language system (UMLS): integrating biomedical terminology," *Nucleic Acids Research*, vol. 32, pp. D267–D270, 2004, Database issue.

[18] C. Knox, V. Law, T. Jewison et al., "DrugBank 3.0: a comprehensive resource for omics research on drugs," *Nucleic Acids Research*, vol. 39, pp. D1035–D1041, 2011, Database issue.

[19] V. Law, C. Knox, Y. Djoumbou et al., "DrugBank 4.0: shedding new light on drug metabolism," *Nucleic Acids Research*, vol. 42, no. D1, pp. D1091–D1097, 2014, Database issue.

[20] D. S. Wishart, Y. D. Feunang, A. C. Guo et al., "DrugBank 5.0: a major update to the DrugBank database for 2018," *Nucleic Acids Research*, vol. 46, no. D1, pp. D1074–D1082, 2018.

[21] D. S. Wishart, C. Knox, A. C. Guo et al., "DrugBank: a knowledgebase for drugs, drug actions and drug targets," *Nucleic Acids Research*, vol. 36, no. suppl_1, pp. D901–D906, 2008, Database issue.

[22] D. S. Wishart, C. Knox, A. C. Guo et al., "DrugBank: a comprehensive resource for in silico drug discovery and exploration," *Nucleic Acids Research*, vol. 34, no. 90001, pp. D668–D672, 2006, Database issue.

[23] J. Ru, P. Li, J. Wang et al., "TCMSP: a database of systems pharmacology for drug discovery from herbal medicines," *Journal of Cheminformatics*, vol. 6, no. 1, p. 13, 2014.

[24] Y. Liu, "Understanding and significance of the concept of primary disease, comorbidities, complication and secondary disease," *Chinese Journal of Coal Industry Medicine*, vol. 14, no. 07, pp. 1093-1094, 2011, in Chinese.

[25] Y. Wu, F. Zhang, K. Yang et al., "SymMap: an integrative database of traditional Chinese medicine enhanced by symptom mapping," *Nucleic Acids Research*, vol. 47, no. D1, pp. D1110–D1117, 2019.

[26] N. Rappaport, M. Twik, I. Plaschkes et al., "MalaCards: an amalgamated human disease compendium with diverse clinical and genetic annotation and structured search," *Nucleic Acids Research*, vol. 45, no. D1, pp. D877–D887, 2017.

[27] S. Niwattanakul, J. Singthongchai, E. Naenudorn, and S. Wanapu, "Using of jaccard coefficient for keywords similarity," in *Proceedings of the Iaeng International Conference on Internet Computing & Web Services; 2013*, vol. 2202, pp. 380–384, Hong Kong, China, March 2013.

[28] M. Guo, Y. Yu, T. Wen et al., "Analysis of disease comorbidity patterns in a large-scale China population," *BMC Medical Genomics*, vol. 12, no. Suppl 12, p. 177, 2019.

[29] Y. Y. Ahn, J. P. Bagrow, and S. Lehmann, "Link communities reveal multiscale complexity in networks," *Nature*, vol. 466, no. 7307, pp. 761–764, 2010.

[30] X. Zeng, Z. Jia, Z. He et al., "Measure clinical drug-drug similarity using electronic medical records," *International Journal of Medical Informatics*, vol. 124, pp. 97–103, 2019.

[31] J. I. F. Bass, A. Diallo, J. Nelson, J. M. Soto, C. L. Myers, and A. J. M. Walhout, "Using networks to measure similarity between genes: association index selection," *Nature Methods*, vol. 10, no. 12, pp. 1169–1176, 2013.

[32] V. D. Blondel, J. L. Guillaume, R. Lambiotte, and E. Lefebvre, "Fast unfolding of communities in large networks," *Journal of Statistical Mechanics Theory & Experiment*, vol. 2008, 2008.

[33] M. E. Newman, "Fast algorithm for detecting community structure in networks," *Physical Review E, Statistical, Nonlinear, and Soft Matter Physics*, vol. 69, no. 6 Pt 2, Article ID 066133, 2004.

[34] M. E. J. Newman, "Modularity and community structure in networks," *Proceedings of the National Academy of Sciences*, vol. 103, no. 23, pp. 8577–8582, 2006.

[35] M. C. Ouimet, B. G. Simons-Morton, P. L. Zador et al., "Using the US national household travel survey to estimate the impact of passenger characteristics on young drivers' relative risk of fatal crash involvement," *Accident Analysis & Prevention*, vol. 42, no. 2, pp. 689–694, 2010.

[36] L. Pirhaji, M. Kargar, A. Sheari et al., "The performances of the chi-square test and complexity measures for signal recognition in biological sequences," *Journal of Theoretical Biology*, vol. 251, no. 2, pp. 380–387, 2008.

[37] M. Kanehisa, M. Furumichi, M. Tanabe, Y. Sato, and K. Morishima, "KEGG: new perspectives on genomes, pathways, diseases and drugs," *Nucleic Acids Research*, vol. 45, no. D1, pp. D353–d361, 2017.

[38] X. Jiao, B. T. Sherman, D. W. Huang et al., "DAVID-WS: a stateful web service to facilitate gene/protein list analysis," *Bioinformatics*, vol. 28, no. 13, pp. 1805-1806, 2012.

[39] W. Fang and Y. Zhiping, "Study on the related factors of 5-year recurrence in patients with cerebral infarction," *China Medical Herald*, vol. 15, no. 02, pp. 67–70+82, 2018, in Chinese with English abstract.

[40] Y. J. Wang, Z. X. Li, H. Q. Gu et al., "China stroke statistics 2019: a report from the national center for healthcare quality management in neurological diseases, China national clinical research center for neurological diseases, the Chinese stroke association, national center for chronic and non-communicable disease control and prevention, Chinese center for disease control and prevention and institute for global neuroscience and stroke collaborations," *Stroke and Vascular Neurology*, vol. 5, no. 3, pp. 211–239, 2020.

[41] X. Zhou, J. Menche, A. L. Barabási, and A. Sharma, "Human symptoms-disease network," *Nature Communications*, vol. 5, no. 1, p. 4212, 2014.

[42] Z. Zhong Ying, *Internal Medicine of Traditional Chinese Medicine*, China Traditional Chinese Medicine Press, Beijing, China, 2nd edition, 2007.

[43] M. Xie and Z. Ran, *Formulaology*, People's Medical Publishing House, Beijing, China, 2nd edition, 2012.

[44] M. Jiang, C. Lu, C. Zhang et al., "Syndrome differentiation in modern research of traditional Chinese medicine," *Journal of Ethnopharmacology*, vol. 140, no. 3, pp. 634–642, 2012.

[45] Y. Zhao, X. Yu, X. Cao et al., "Cluster analysis for syndromes of real-world coronary heart disease with angina pectoris," *Frontiers of Medicine*, vol. 12, no. 5, pp. 566–571, 2018.

[46] S. Li, Z. Q. Zhang, L. J. Wu, X. G. Zhang, Y. D. Li, and Y. Y. Wang, "Understanding ZHENG in traditional Chinese medicine in the context of neuro-endocrine-immune network," *IET Systems Biology*, vol. 1, no. 1, 2007.

[47] X. Zhai, X. Wang, L. Wang, L. Xiu, W. Wang, and X. Pang, "Treating different diseases with the same method-A traditional Chinese medicine concept analyzed for its biological basis," *Frontiers in Pharmacology*, vol. 11, p. 946, 2020.

[48] M. Fan Cui and T. Li Da, "Challenges and prospect in research of Chinese materia medica network pharmacology," *Chinese Traditional and Herbal Drugs*, vol. 51, no. 08, pp. 2232–2237, 2020, in Chinese with English abstract.

[49] Y. Yang, K. Yang, T. Hao et al., "Prediction of molecular mechanisms for lianxia ningxin formula: a network pharmacology study," *Frontiers in Physiology*, vol. 9, p. 489, 2018.

[50] Z. Gao, S. Li, Q. Shang et al., "Complex networks approach for analyzing the correlation of traditional Chinese medicine syndrome evolvement and cardiovascular events in patients with stable coronary heart disease," *Evidence-Based Complementary and Alternative Medicine*, vol. 2015, Article ID 824850, 6 pages, 2015.

[51] H. Jinliang, L. Suyun, Z. Xinghong, Y. Haibin, C. Guorong, and L. Zhen, "Study on syndrome distribution and Chinese medicine composition of AECOPD based on complex networks," *World Science and Technology/Modernization of Traditional Chinese Medicine and Materia Medica*, vol. 17, no. 06, pp. 1268–1273, 2015, in Chinese with English abstract.

[52] H. Jinliang, L. Suyun, Y. Haibin et al., "Correlation analysis of syndromes and symptoms of TCM AECOPD based on clinical research information sharing system," *World Science and Technology/Modernization of Traditional Chinese Medicine and Materia Medica*, no. 7, pp. 1596–1599, 2013, in Chinese with English abstract.

[53] Z. Shu, Y. Zhou, K. Chang et al., "Clinical features and the traditional Chinese medicine therapeutic characteristics of 293 COVID-19 inpatient cases," *Frontiers of Medicine*, vol. 14, no. 6, pp. 760–775, 2020.

[54] N. S. Abul-Husn and E. E. Kenny, "Personalized medicine and the power of electronic health records," *Cell*, vol. 177, no. 1, pp. 58–69, 2019.

Hindawi
Evidence-Based Complementary and Alternative Medicine
Volume 2021, Article ID 2337924, 10 pages
https://doi.org/10.1155/2021/2337924

Research Article

Traditional Chinese Medicine Text Similarity Calculation Model Based on the Bidirectional Temporal Siamese Network

Jigen Luo,[1] **Wangping Xiong**,[1] **Jianqiang Du**,[1] **Yingfeng Liu**,[2] **Jianwen Li**,[1] **and Dingxing Hu**[1]

[1]*School of Computer, Jiangxi University of Chinese Medicine, Nanchang 330004, Jiangxi, China*
[2]*Qihuang Academy, Jiangxi University of Chinese Medicine, Nanchang 330004, Jiangxi, China*

Correspondence should be addressed to Jianqiang Du; jianqiang_du@163.com

Received 29 August 2021; Accepted 1 November 2021; Published 29 November 2021

Academic Editor: Xuezhong Zhou

The text similarity calculation plays a crucial role as the core work of artificial intelligence commercial applications such as traditional Chinese medicine (TCM) auxiliary diagnosis, intelligent question and answer, and prescription recommendation. However, TCM texts have problems such as short sentence expression, inaccurate word segmentation, strong semantic relevance, high feature dimension, and sparseness. This study comprehensively considers the temporal information of sentence context and proposes a TCM text similarity calculation model based on the bidirectional temporal Siamese network (BTSN). We used the enhanced representation through knowledge integration (ERNIE) pretrained language model to train character vectors instead of word vectors and solved the problem of inaccurate word segmentation in TCM. In the Siamese network, the traditional fully connected neural network was replaced by a deep bidirectional long short-term memory (BLSTM) to capture the contextual semantics of the current word information. The improved similarity BLSTM was used to map the sentence that is to be tested into two sets of low-dimensional numerical vectors. Then, we performed similarity calculation training. Experiments on the two datasets of financial and TCM show that the performance of the BTSN model in this study was better than that of other similarity calculation models. When the number of layers of the BLSTM reached 6 layers, the accuracy of the model was the highest. This verifies that the text similarity calculation model proposed in this study has high engineering value.

1. Introduction

The calculation of text similarity is a basic research in the field of natural language processing. It compares the similarity between two texts through a certain strategy to obtain a quantified similarity [1]. This technology is widely used in information retrieval [2], intelligent question and answer [3], and article plagiarism detection [4]. With the development of Chinese medicine, the government, hospitals, and universities are all carrying out the informatization, modernization, and industrialization of Chinese medicine. The electronic cases archived in hospitals have attracted more and more attention. The excavation of medical diagnosis information from the electronic cases is of great benefit to inheriting the experiences of Chinese medicine diagnosis and treatment. Text similarity calculation has important applications in the recommendation of Chinese medicine prescription, question point identification of intelligent question and answer models, and adjuvant therapy.

TCM text condenses the wisdom and experience of various Chinese medicine clinicians, but it requires refinement in expression. Therefore, the formed text has many characteristics, such as short sentence length, strong contextual relevance, and rich semantics [5]. Therefore, the results of some common basic natural language processing tasks, such as named entity recognition extraction, entity relationship extraction, and text similarity calculation, are poor. This is a great challenge faced by researchers in Chinese medicine. Using the traditional text similarity calculation model, we obtained highly similar sentence feature vectors for "can bone metastases of breast cancer be cured?" and "breast cancer skin metastasis can be cured."

However, the semantics of the two sentences are completely different. In order to solve the problem of low accuracy of TCM text similarity, we need to find a method to extract all the semantic information of sentences, reduce feature dimension and sparsity, and improve the accuracy of text similarity calculation. It is better applied to other tasks of natural language processing.

In this study, Section 2 reviewed the literatures on text similarity, Section 3 focused on the text similarity calculation model of TCM based on BTSN. In Section 4, the new method was tested and analyzed on two sets of data. Comparing with several existing algorithms, the effectiveness and feasibility of the new method were further verified. Finally, it was summarized and analyzed in Section 5.

2. Literature Review

At present, there are more and more methods to calculate text similarity, but most of the research on text similarity focuses on the public domain. Due to characteristics of short sentence length and strong semantic relevance, the research of TCM diagnostic text is slow. With the rapid development of natural language technology, scholars have proposed many methods to calculate the semantic similarity of text. The methods accepted by researchers are divided into the following three categories:

(1) The methods based on large-scale domain knowledge or rules: the method based on knowledge rule matching [6] and the method based on syntactic analysis [7]. It is necessary to define grammatical rules in advance to build a large-scale dictionary, conceptual ontology, or knowledge base. Although it is efficient, it has a large investment in preliminary preparation. It is difficult to increase and update rules and knowledge base, which are dependent on the professional knowledge of linguists.

(2) The method based on machine learning: the traditional vector space model (word bag model) [8], latent Dirichlet allocation (LDA) based topic model [9], BM25 algorithm for evaluating the correlation between text and keywords [10], FastText model [11], and so on. Typically, Yulianto et al. [12] used the Rabin–Karp algorithm for string matching and used the Jaro–Winkler algorithm to calculate the similarity of two short text sequences. The text similarity method based on traditional machine learning is more suitable for datasets with few samples. By establishing the quantitative relationship between text and feature vector, we can find the appropriate calculation method of vector and distance, so as to achieve the text similarity. However, these methods cannot fully express the semantic information of sentences in the feature vector part, and the feature dimension is high. These results show that accuracy of the model was insufficient.

(3) The text similarity calculation method based on deep learning is the research direction in recent years [13]. This method trains distributed word vectors through the deep neural network. The feature vector dimension of the traditional bag-of-words model is high and sparse [14]. We can map words to low-dimensional space through distributed word vector. This not only sets word meaning vector value to words but also vectorizes the semantic differences between words to make them more distinguishable. Zeng et al. [15] proposed an emotional word embedding (ewe) model for subsequent tasks such as text classification and text similarity calculation.

Kusner et al. proposed the word move distance (WMD) text similarity calculation method based on deep learning [16]. Xie et al. [17] proposed a deep semantic structured model (DSSM) to calculate the vectorization of each document and then took the cosine value of the two text vectors as the similarity. Ruan et al. [18] calculated similarity by the embedding method. Li et al. [19] proposed a similarity calculation method based on the word meaning vector model. Li et al. [20] tried to combine the structural information and semantic information of sentences and simplified the processing of sentences into feature vectors by the Word2Vec model. Then, they inputted the syntactic structure of LTP to form the features of the sentence similarity calculation model. Later, scholars focused on the twin network, which was first proposed by Chopra et al. [21]. It is widely used in target tracking and face recognition. It is a neural network structure based on a group of networks with the same parameters. The twin network has the good modeling ability for texts with the same structure because of the symmetry from the same parameters. Subsequently, more and more scholars used the twin neural network to act on the text similarity tasks. They used the neural network shared by two weights to extract effective features through nonlinear mapping. Zhao et al. [22] pointed out that the use of asymmetric twin neural network for case correlation analysis is essentially to calculate the similarity of text cases.

The text similarity calculation in TCM is mainly used for the task of prescription recommendation. Li et al. [23] used the complex network to mine the core formula and calculated the similarity between the two formulas by the Jaccard similarity coefficient. Zhu et al. [24] explored the implicit relationship of prescription syndrome components by the LDA topic model. They transformed prescription component into two probability distributions of prescription syndrome type and syndrome component and used KL distance to calculate the similarity. The results showed that the TCM text similarity calculation model has made outstanding contributions.

In order to solve the problems of short sentences, inaccurate word segmentation, strong semantic correlation, high dimension of feature vector matrix, and sparse features of TCM text, we proposed a similarity calculation model of TCM text based on the bidirectional temporal Siamese network (BTSN). The pretrained language model ERNIE was used in this model to train the character vector instead of the word vector to solve the problem of inaccurate word segmentation in TCM. The BTSN structure was used to map the text pair to be tested into two low-dimensional vectors.

The BLSTM was used to replace the traditional fully connected neural network to capture the context semantic information of the current word. It is helpful to extract more semantic information of sentences.

3. Bidirectional Temporal Siamese Network (BTSN)

The similarity calculation model of TCM text based on BTSN converts the similarity calculation into the classification task. When the similarity of the two texts to be tested is large, it is a positive class; otherwise, it is determined as a negative class. The model is divided into two parts. In the whole model structure, Siamese network framework is used to replace the traditional fully connected network in the weight-sharing network with BLSTM, so as to capture more text deep features and context semantic information. The model structure is shown in Figure 1.

The pseudocode of the algorithm of the TCM text similarity calculation model based on BTSN is as follows (Algorithm 1).

We will introduce the three basic parts of the BTSN model, which are character embedding, Siamese network, and LSTM network.

3.1. Character Embedding. The neural network model cannot directly process text data, so it needs to convert text type data into a numerical vector. There are two ways of text vectorization: one hot and distributed representation. Since distributed vector representation can reduce the dimension of vectors and effectively represent the association between semantics, this study adopts the distributed representation method for text vectorization. Before entering the model, the text was embedded at the character level. In this study, the text was converted into the character vector through the pretrained language model, called the ERNIE model [25]. We took the multiinformation entities in the knowledge map as external knowledge to improve the language representation and enhance the representation of the pretrained language model of bidirectional encoder representations from transformers (BERT) [26].

The input sentence is S, the set of words contained in this sentence is $W(w_1, w_2, w_3, \ldots, w_m)$, and m is the sentence length. The word vector of the t word is $w_t^* \in R^d$, where the dimension of the feature vector in the above equation is d. The input text is

$$S = \left[w_1{}^*, w_2{}^*, \ldots, w_m{}^*\right] \in R^{T\times d}. \tag{1}$$

In Figure 1, the input text X_1 and X_2 are similar text sentence pairs that will be tested. After character embedding, the input text entered the bidirectional LSTM neural network model with shared weights. The overall framework was the Siamese network, and the internal fully connected neural network was replaced by bidirectional LSTM. The LSTM network is improvement of the recurrent neural network (RNN). Its main purpose is to solve the problem of gradient disappearance or gradient explosion and make full use of context information to mine more hidden features.

3.2. Siamese Network. The Siamese network is a connected neural network with weight sharing. It was first published in 2005 for judging facial similarity. The Siamese neural network has two input terminals. In specific tasks, two data are input into the neural network with weight sharing. Through nonlinear mapping to the new space, we calculated loss function in the new space to measure the similarity between the two input data. The framework of the Siamese network is shown in Figure 2.

In Figure 2, X_1 and X_2 are the two input similarity samples that will be tested. Through the traditional neural network shared by the two weights, the feature can be transformed into another feature space through nonlinear mapping, and two output vectors can be obtained to evaluate whether the two input samples are similar, $G_W(X_1)$ and $G_W(X_2)$. In the Siamese network, the energy function $E_W(X_1, X_2)$ is used to compare the outputs of two weight-sharing networks. The energy function is

$$E_W(X_1, X_2) = \left\|G_W(X_1) - G_W(X_2)\right\|. \tag{2}$$

The loss function is related to the input and parameters, and the loss function of the Siamese network is

$$\begin{aligned} L\left(W, (Y, X_1, X_2)^i\right) &= (1-Y)L_G\left(E_W(X_1, X_2)^i\right) \\ &\quad + YL_I\left(E_W(X_1, X_2)^i\right), \\ K(W) &= \sum_{i=1}^{p} L\left(W, (Y, X_1, X_2)^i\right), \end{aligned} \tag{3}$$

where $(Y, X_1, X_2)^i$ represents the i^{th} sample, which is composed of a pair of test similarity text and its label. L_G is the loss function of text pairs of the same category, L_I is the function of text pairs of different categories, and p is the total number of training samples. By designing different loss function expressions, we can reduce the energy of the same category pair and increase the energy of the different category pair.

3.3. LSTM Network. We replaced the traditional neural network by LSTM in Siamese because of its strong memory ability. In addition, it can accurately grasp the overall semantic information of sentences and has strong feature expression ability. The difference from the RNN is the neuron. The neural unit of the LSTM neural network is joined with gate structure, and the neural unit of the LSTM neural network is shown in Figure 3.

There are three gates in the structure diagram of LSTM unit: input gate, output gate, and forget gate. Due to its special structure, LSTM can solve the problem of long-distance dependence to some extent.

At time t, the component update status of each LSTM unit is

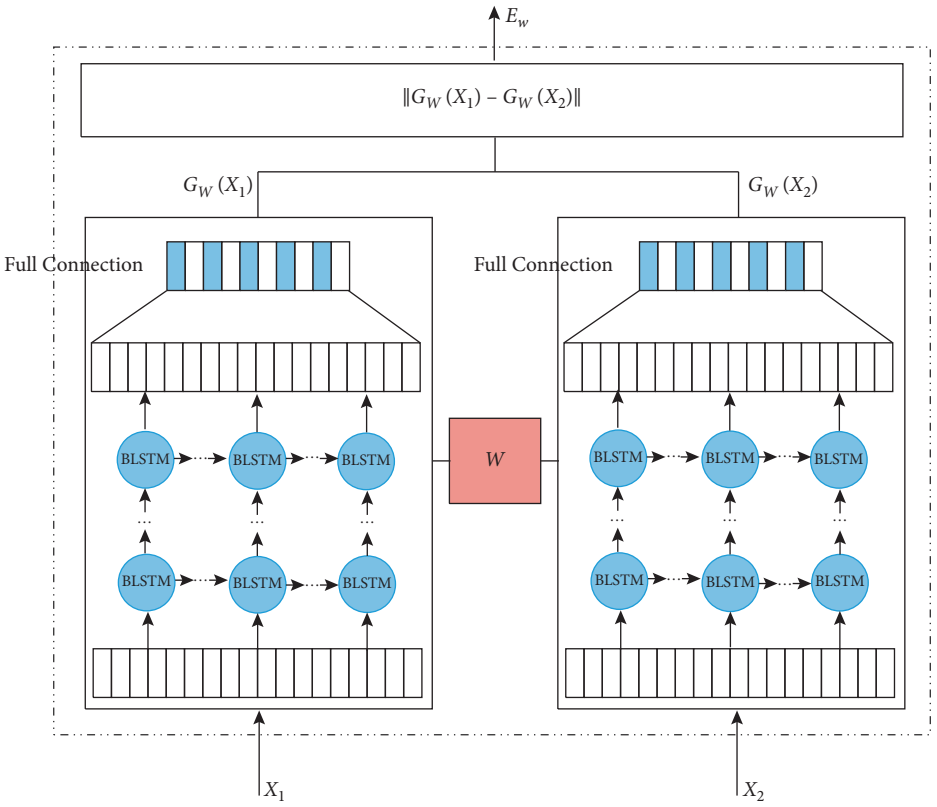

Figure 1: Text similarity calculation model based on BTSN.

(1) Input: dataset D
(2) Process:
(4) The dataset D is divided into training set and test set according to 7 : 3
(5) Import the pretrained language model ERNIE to obtain the dynamic character vector. The similarity calculation model is obtained through the training set.
(6) Forward$_{\text{-LEFT}}$ = LSTM$_{\text{-LEFT}}$ (vector); forward$_{\text{-RIGHT}}$ = LSTM$_{\text{-RIGHT}}$ (vector);
(7) Backward$_{\text{-LEFT}}$ = LSTM$_{\text{-LEFT}}$ (vector); backward$_{\text{-RIGHT}}$ = LSTM$_{\text{-RIGHT}}$ (vector)
(8) H$_{\text{-LEFT}}$ = connect (Forward$_{\text{-LEFT}}$, Backward$_{\text{-LEFT}}$); H$_{\text{-RIGHT}}$ = connect (Forward$_{\text{-RIGHT}}$, Backward$_{\text{-RIGHT}}$);
(9) Siamese (H$_{\text{-LEFT}}$, H$_{\text{-RIGHT}}$)
(10) Return similarity calculation model
(11) Use the test set to get various evaluations
(12) End

Algorithm 1: Bidirectional temporal Siamese network (BTSN).

$$\begin{aligned} f_t &= \sigma\left(W_f \cdot [h_{t-1}, x_t] + b_f\right), \\ i_t &= \sigma\left(W_f \cdot [h_{t-1}, x_t] + b_i\right), \\ \tilde{c}_t &= \tanh\left(W_c \cdot [h_{t-1}, x_t] + b_c\right), \\ c_t &= f_t \circ c_{t-1} + i_t \circ \tilde{c}_t, \\ o_t &= \sigma\left(W_o \cdot [h_{t-1}, x_t] + b_o\right), \\ h_t &= o_t \circ \tanh\left(c_t\right), \end{aligned} \tag{4}$$

where σ represents the activation function sigmoid, $\circ$ is the element multiplication, x_t is the input vector of LSTM at the time t, h_t represents the implied state, W_f, W_i, W_c, and W_o represent the weight matrix of forgetting gate, input gate, memory unit, and output gate, respectively, b_f, b_i, b_c, b_o represent the bias of forgetting gate, input gate, memory unit, and output gate, respectively, f_t i_t, c_t, and o_t represent the forgetting gate, input gate, memory unit state, and output gate, respectively.

In order to make full use of context information of sentences, we mined more implied features to effectively solve the problem of feature extraction. In this study, we used BLSTM to replace the Siamese ordinary neural network structure. This method is composed of two opposite direction LSTM network. The model structure is shown in Figure 1. $\overrightarrow{h_t}$ is the LSTM, prior to the output of the neural

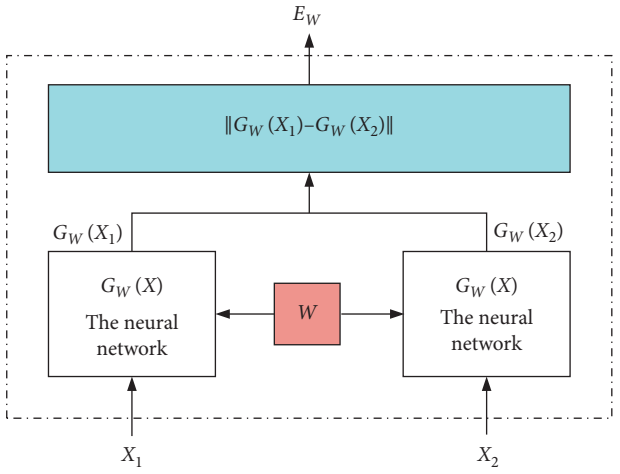

Figure 2: The framework of the Siamese network.

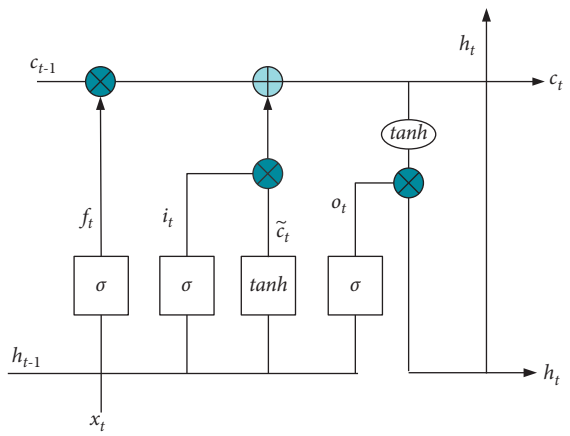

Figure 3: LSTM unit structure.

network in t time, and $\overleftarrow{h_t}$ is after the LSTM output at time t. Therefore, the output for the first time t back to joining together is $h_t = [\overrightarrow{h_t}, h_t]$.

4. Experiment and Analysis

4.1. Experiment. In order to verify the feasibility and effectiveness of the improved text similarity calculation model proposed in this study, we compared experiments on two sets of data of TCM and finance through the TCM text similarity calculation model based on BTSN. The example of TCM text similarity dataset is given in Table 1.

The experimental evaluation index in this study is the accuracy on the training set and the test set. In order to give the formula of the accuracy more intuitively, the required confusion matrix is given in Table 2.

Based on the confusion matrix in Table 2, the accuracy is

$$\text{Accuracy} = \frac{TP + TN}{TP + FN + FP + TN}. \quad (5)$$

In order to comprehensively verify the advantages of the improved text similarity calculation model proposed in this study, we set three comparative experiments. Experiment 1 is a comparative experiment of training character vector and word vector with various pretrained language models as the input of the network. The purpose is to verify which language model was selected in the embedding layer and whether character level or word level vector has been selected as the network input; the second experiment is the experimental comparison between BTSN and other algorithms. This verifies that BTSN is more scientific than other text similarity algorithms; experiment 3 is an in-depth network depth experiment of BTSN to find the optimal number of network layers.

4.2. The Comparison of Character and Word Input Vectors of Different Pretrained Models. In experiment 1, three pretrained language models, Word2Ver, BERT, and ERNIE, were selected to train character vector and word vector as the input of the BTSN model. Word2Vec training word vector was the input of BTSN (WW-BTSN), Word2Vec was used to train the character vector as the input of BTSN (WC-BTSN), BERT training word vector was the input of BTSN (BW-BTSN), BERT training character vector was the input of BTSN (BC-BTSN), ERNIE training word vector was the input of BTSN (EW-BTSN), and ERNIE training character vector was the input of BTSN (EC-BTSN). In experiment 1, the input vector dimension was uniformly set to 300 dimensions, the epoch was uniformly set to 20 times, and the network depth was 2 layers. The model results are given in Table 3.

Comparing the word and character vectors trained by the pretrained model on the two sets of data in Table 3, we found that the effect of the ERNIE model was significantly better than that of the other pretraining models. ERNIE added knowledge information from entities on the basis of the original semantic information of the BERT model. However, the Word2Vec model is a static word embedding model. It is highly limited in expressing semantic information.

Comparing character input vector with word input vector, we found that character vector as the input of the text similarity calculation model is better than word vector input. In the financial training dataset, the accuracy of EC-BTSN was 0.8328. It was 1.15% greater than that of the EW-BTSN model. In the financial test set, the accuracy of the EC- BTSN model was 0.8311. It was 2% greater than that of the EW-BTSN model, reached 0.8102.

In the training set of TCM, the accuracy of the EC-BTSN model was 0.7967. It was 2.36% greater than that of EW-BTSN, reached 0.7731. In the TCM test set, the accuracy of the EC-BTSN model was 0.7827. It was 2.19% greater than that of EW-BTSN. In addition, the effect of using character vector as the input of the neural network model was remarkable.

The results of above six groups of comparative experiments show that selecting character vector as model input can improve the accuracy of evaluation indicators to varying degrees. This is because the mainstream word segmentation tools have serious inaccurate word segmentation problems

Table 1: Samples of the TCM data.

Sentence 1	Sentence 2	Similarity label
Hypertension, coronary heart disease how to treat	Can hypertension give birth to children?	0
Can people with diabetes drink yoghurt	Diabetes drink yoghurt line	1
What are the symptoms of breast cancer terminal?	What are the symptoms of early breast cancer?	0
Is breast hyperplasia and breast cancer related?	What is the incidence of breast cancer?	0

Table 2: Confusion matrix.

	The prediction is a positive class	The prediction is negative
The actual is class	Is actually positive and predicted to be TP	It is actually positive and it is predicted to be negative (FN)
The actual negative class	The actual value is negative and the prediction is FP	It is actually negative, and it is predicted to be negative (TN)

Table 3: The comparison of experimental results of word vector.

	Financial data		TCM data	
	Training set accuracy	Test set accuracy	Training set accuracy	Test set accuracy
WW-BTSN	0.7054	0.6764	0.6283	0.5986
WC-BTSN	0.8170	0.7861	0.6661	0.6503
BW-BTSN	0.7634	0.7276	0.7023	0.6891
BC-BTSN	0.8192	0.7943	0.7483	0.7239
EW-BTSN	0.8213	0.8102	0.7731	0.7608
EC-BTSN	**0.8328**	**0.8311**	**0.7967**	**0.7827**

Bold values indicate the best record in the comparative test.

in TCM. Due to a large number of terminology in TCM, it is impossible to achieve accurate word segmentation through stuttering word segmentation and other tools. For example, in TCM terminology, "yin-yang deficiency syndrome" will be divided into yin-yang, two, and deficiency syndrome through the stuttering word segmentation tool. In TCM, this phrase should be taken as a whole and cannot be separated.

4.3. The Comparison of Different Similarity Calculation Models. In experiment 2, we set up six groups of comparison models, represented by term frequency-inverse document frequency (TF-IDF) feature, to calculate the cosine distance of the similarity text [27]. Word2Vec was used to represent the character level vector. After weighted average of all characters in the sentence, the similarity was determined by the cosine distances [28]. The Siamese-LSTM model is for text vector extraction using straightaway LSTM. We replaced the fully connected network in Siamese with the CNN and paid more attention to local information of sentences in the Siamese-CNN model; The sentence semantic information and extract the Siamese-RNN model of sentence overall features were captured by RNN. The forward and backward semantic information of sentences was captured by the bidirectional LSTM neural network. The overall features of sentences were extracted through the BTSN model; the comparison results of six groups are given in Table 4 and Figures 4 and 5.

The experimental results of the BTSN text similarity calculation model and other five models are given in Table 4 and Figures 4 and 5. The improved algorithm BTSN proposed in this study has better results on two sets of data.

The TF-IDF model constructs feature vectors based on the sentence word frequency statistics, without the semantic information between words. It has the disadvantages of high feature dimensions and sparseness. Therefore, the result of similarity calculation is not good enough. The accuracy in the financial training dataset was 0.7042 and that in the test set was 0.7102. The accuracies in the training set and test set of TCM were 0.5967 and 0.5510, respectively. There is still a lot of room for improvement.

In order to solve the shortcomings of the TF-IDF model, we mapped high-dimensional features to heterogeneous space in the Word2vec model. This further reduced feature dimensions and ensured strong semantic relationship between characters. The accuracies of this method in the financial training set and test set were 0.7242 and 0.6954. Compared with the TF-IDF model, the accuracy in the training set was improved by 2%, and the accuracy in the test set was reduced by 1.148%. However, the experimental effect on the TCM dataset was significant. The accuracies of the training set and test set were 0.6441 and 0.6013, which was nearly 5% greater than that of the TF-IDF model. This indicates that considering the semantic information of sentences has more advantages over the text similarity calculation model.

The text similarity calculation model based on Word2vec weighted the average vectors of all characters in the sentence after character embedding, without the nonlinear

Table 4: The comparison of different similarity calculation models.

Datasets	Financial data		TCM data	
Models	Training set accuracy	Test set accuracy	Training set accuracy	Test set accuracy
TF-IDF	0.7042	0.7102	0.5967	0.5510
Word2vec	0.7242	0.6954	0.6441	0.6013
Siamese-LSTM	0.8156	0.7886	0.6574	0.6103
Siamese-CNN	0.8273	0.8097	0.7517	0.7502
Siamese-RNN	0.8039	0.7830	0.7383	0.7129
BTSN	**0.8328**	**0.8311**	**0.7967**	**0.7827**

Bold values indicate the best record in the comparative test.

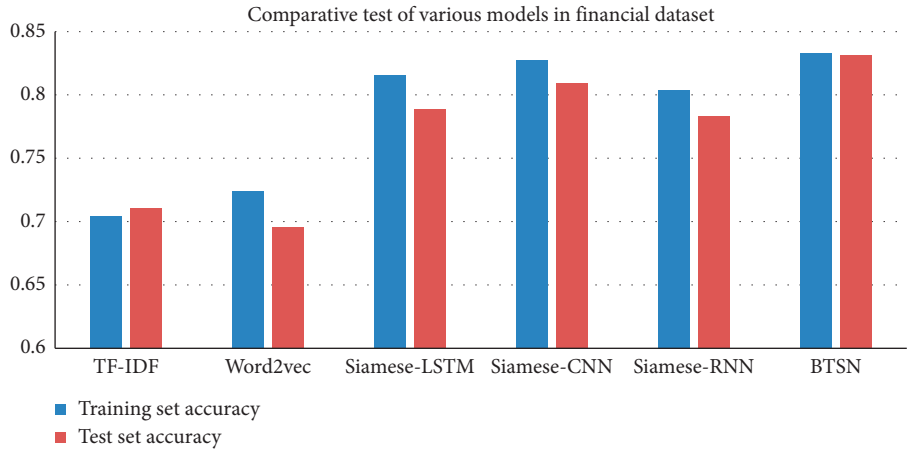

Figure 4: Histogram of accuracy of each model in the financial dataset.

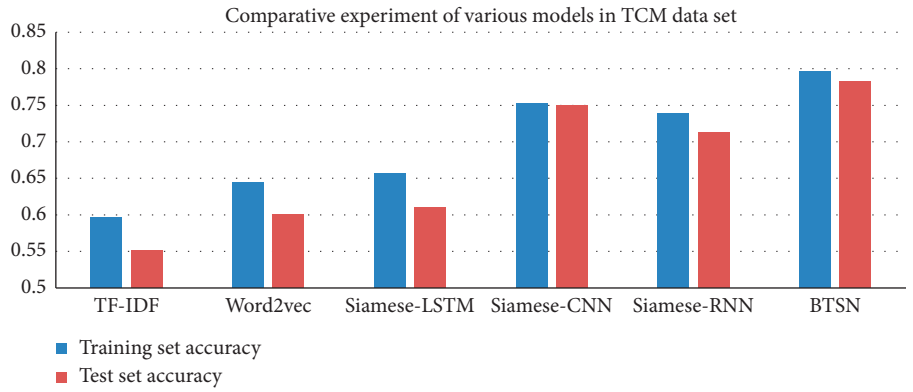

Figure 5: Histogram of accuracy of each model in the TCM dataset.

relationship between character vectors. In order to solve this problem, this study proposed a text similarity calculation model based on Siamese-LSTM. In Table 4, the effect of the Siamese-LSTM model on two sets of datasets has been greatly improved. The accuracies of the Siamese-LSTM model on the financial training set and test set were 0.8156 and 0.7886, respectively. They were 9% greater than that of the Word2Vec model. The accuracy of the Siamese-LSTM model on the training set and test set of TCM was 0.6574 and 0.6103, respectively. They were 1% greater than that of the Word2Vec model.

Considering the local information of sentences extracted by the CNN, this study proposed a text similarity calculation model based on the Siamese-CNN. In Table 4, on the financial data training set, the accuracy of the Siamese-CNN was 0.8273, which is 1% greater than that of the Siamese-LSTM model. In contrast, on the financial test set, the accuracy of the Siamese-CNN was 0.8097, which was also greater than that of Siamese-LSTM. The accuracies of the Siamese-CNN for the training set and test set of TCM were 0.7517 and 0.7502, respectively. They were 9.43% and 13.99% greater than that of the Siamese-LSTM model. Local features

sentences play an important role in the text similarity calculation model.

We set the Siamese-RNN model to verify the advantages of LSTM over the RNN model. We found that there are many advantages of LSTM from the two groups of test data of the Siamese-LSTM and Siamese-RNN. The accuracies of financial data and TCM data have been improved to a certain extent. Furthermore, the experiments also verified that the gate structure provided by LSTM can alleviate the problem of gradient disappearance or gradient explosion. In addition, we can mine more hidden features through the full use of context information.

Finally, based on the Siamese-LSTM model, a layer of reverse LSTM neuron structure was added to form a Siamese network with bidirectional LSTM structure, that is, BTSN. The purpose is to capture more context information of sentences based on the nonlinear transformation. In Table 4, the experimental results show that context information of sentences is very important for feature extraction. The accuracies in the financial training set and test set were 0.8328 and 0.8311, respectively. They were greater than that of other algorithms. However, the experimental effect on the TCM dataset was more significant. The accuracies of the improved model in its training set and test set were 0.7967 and 0.7827, respectively. They were 4.5% and 3.25% greater than that of the Siamese-CNN model. The improved BTSN model proposed in this study has the better experimental effect on text similarity calculation. The bidirectional LSTM network can extract useful features. It has a better and significant effect on the text of short sentences in TCM.

4.4. The Comparison of Different Network Layers. In experiment 3, we set different depths of the BLSTM networks to find the optimal number of network layers. In this experiment, the layers of BTSN models were from layer 1 to layer 7. The experimental results of each layer are given in Table 5 and Figures 6 and 7.

According to the graphs of the network layer experiment, the accuracy of the BTSN text similarity calculation model on the two sets of datasets was increased, with the increasing depth of the BLSTM. When the depth of the network was 6 layers, the accuracies of the training set and the test set of the financial dataset were 0.8361 and 0.8314, respectively. The accuracies of training set and test set of TCM data were 0.8125 and 0.8014, respectively. After that, with the continuous increase of network depth, the effect of the model was decreased, and the training time was increased. Therefore, when the network depth of the BTSN text similarity calculation model is 6 layers in this experiment, the experimental effect is the best.

Finally, this study proposes a TCM text similarity calculation model based on BTSN, with certain advantages. It can overcome the problems of short sentences, inaccurate word segmentation, strong semantic correlation, high dimension of feature vector matrix, and sparse features of TCM diagnosis text. We comprehensively considered the semantic time series information of the sentence context and

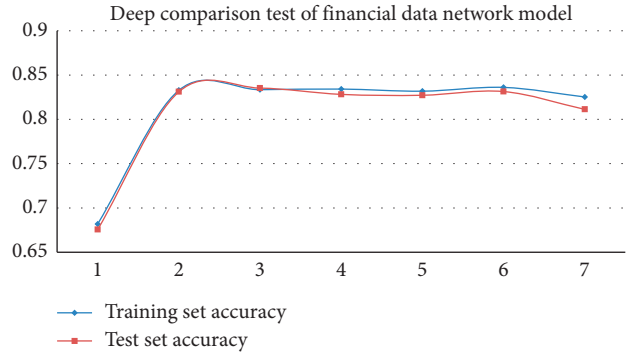

Figure 6: The experimental diagram of network layers of the financial dataset.

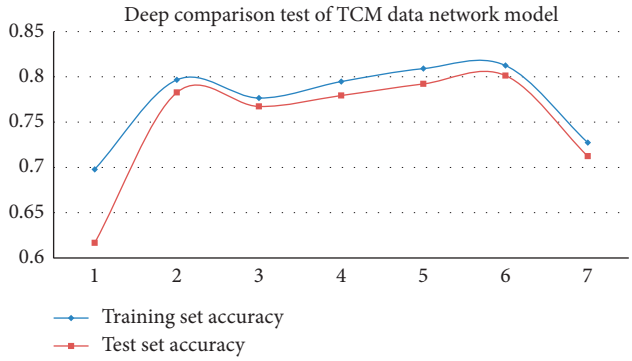

Figure 7: The experimental diagram of network layers of the TCM dataset.

Table 5: The number of layers in the BTSN model network.

Network layers	Financial data		TCM data	
	Training set accuracy	Test set accuracy	Training set accuracy	Test set accuracy
1 network layer	0.6819	0.6756	0.6979	0.6166
2 network layers	0.8328	0.8311	0.7967	0.7827
3 network layers	0.8335	0.8353	0.7766	0.7673
4 network layers	0.8342	0.8282	0.7948	0.7794
5 network layers	0.8318	0.8272	0.8091	0.7922
6 network layers	**0.8361**	**0.8314**	**0.8125**	**0.8014**
7 network layers	0.8253	0.8113	0.7274	0.7124

Bold values indicate the best record in the comparative test.

improved the accuracy of the model. The experimental effect is more scientific.

5. Conclusions

Due to the sentence characteristics of TCM text, the higher and sparse dimension of the vector matrix in constructing sentence features, we comprehensively considered the time sequence information of sentence context and proposed a TCM text similarity calculation model based on the bidirectional temporal Siamese network (BTSN). The model uses the ERNIE pretrained language model to train character vectors instead of traditional word vectors to solve the problem of

inaccurate word segmentation in TCM; the traditional fully connected neural network was replaced by the deep BLSTM network in the Siamese to capture the context timing information of the current word. This is conducive to extract more semantic information of sentences. Through experiments on two sets of datasets of TCM and financial, it is proved that the BTSN model has certain advantages over other models. When the depth of the BLSTM network is 6 layers, the accuracy of the two sets of data can reach the best. This can be well applied to the calculation of text similarity. For the feature extraction of TCM short text, we will further increase the effective features related to sentence expression through external knowledge base or domain knowledge map.

Abbreviations

TCM: Traditional Chinese medicine
BERT: Bidirectional encoder representations from transformers
ERNIE: Enhanced representation through knowledge integration
LSTM: Long short-term memory
CNN: Convolutional neural network
RNN: Recurrent neural network.

Data Availability

The datasets generated and/or analyzed during the current study are available from the corresponding author upon request.

Conflicts of Interest

The authors declare that there are no conflicts of interest.

Acknowledgments

This research was supported by National Key Research and Development Program of China (2019YFC1712301), the National Natural Science Foundation of China (61562045 and 82160955), the Natural Science Foundation of Jiangxi Province (20202BAB202019), the Science and Technology Research Project of the Department of Education of Jiangxi Province (GJJ190683), and Jiangxi Province First-Class Discipline Construction Scientific Research Initiation Fund Special Project (SYLXK-ZHYI060).

References

[1] C. L. Wang, Y. H. Yang, and F. Deng, "Review of text similarity approaches," *Information Science*, vol. 37, no. 3, pp. 158–168, 2019, in Chinese.
[2] J. P. Wang and Y. H. Dong, "Measurement of text similarity: a survey," *Information*, vol. 11, no. 9, 2020.
[3] W. H. Du, J. W. Ge, X. C. Liu, and J. J. Ai, "Convolutional neural network model based on text similarity for customer service," *Journal of Physics: Conference Series*, vol. 1550, no. 3, 2020.
[4] E. Y. Puspaningrum, B. Nugroho, A. Setiawan, and N. Hariyanti, "Detection of text similarity for indication plagiarism using winnowing algorithm based K-gram and jaccard coefficient," *Journal of Physics: Conference Series*, vol. 1569, no. 2, Article ID 022044, 2020.
[5] B. Liu, J. Q. Du, and B. Nie, "Part-of-speech tagging of traditional Chinese medicine diagnosis ancient prose based on second-order HMM," *Computer Engineering*, vol. 43, no. 07, pp. 211–216, 2017, in Chinese.
[6] Y. Y. Dong, W. H. Li, and H. Yu, "Hierarchical relation mining of Chinese text based on mixed cosine similarity," *Application Research of Computers*, vol. 34, no. 5, pp. 1406–1409, 2017, in Chinese.
[7] S. P. Zhai, Z. Z. Li, and H. Y. Duan, "Sentence semantic similarity method based on multi feature fusion," *Computer Engineering and Design*, vol. 40, no. 10, pp. 2867–2873+2884, 2019, in Chinese.
[8] X. H. Dong, "Classification algorithm for Chinese product reviews tendency based on emotion eigenvector space model," *Computer Applications and Software*, vol. 40, no. 10, pp. 2867–2873, 2019, in Chinese.
[9] L. J. Zhao, "Modified LDA model based on semantic similarity for topic analysis of text," *Computer Engineering and Design*, vol. 40, no. 12, pp. 3514–3519, 2019, in Chinese.
[10] Y. Li and B. Liu, "Research on text snippet mechanism in document retrieval," *Journal of Frontiers of Computer Science & Technology*, vol. 14, no. 4, pp. 578–589, 2020, in Chinese.
[11] J. Choi and S.-W. Lee, "Improving FastText with inverse document frequency of subwords," *Pattern Recognition Letters*, vol. 133, pp. 165–172, 2020.
[12] M. A. Yulianto and N. Nurhasanah, "The hybrid of jaro-winkler and rabin-karp algorithm in detecting Indonesian text similarity," *Jurnal Online Informatika*, vol. 6, no. 1, p. 88, 2021.
[13] B. G. Chang and Q. X. Liu, "Similarity analysis of CT report of chronic liver disease based on deep learning," *Computer Applications and Software*, vol. 35, no. 8, pp. 289–294, 2018, in Chinese.
[14] X. J. Hu, X. J. Chen, N. Zhao, and W. Xue, "PSO_BFA optimized bag of words model and prediction of protein subcellular localization," *Computer Engineering and Applications*, vol. 56, no. 01, pp. 165–171, 2020, in Chinese.
[15] Q. Zeng, X. Zhao, and X. Hu, "Learning emotional word embeddings for sentiment analysis," *Journal of Intelligent and Fuzzy Systems*, vol. 40, no. 4, pp. 1–13, 2021.
[16] M. Kusner, Y. Sun, and N. Kolkin, "From word embeddings to document distances," in *Proceedings of the 32nd International Conference on Machine Learning*, pp. 957–966, ACM, New York, NY, USA, July 2015.
[17] Z. W. Xie, Z. Zhao, G. Y. Zhou, and W. J. Wang, "Topic enhanced deep structured semantic models for knowledge base question answering," *Science China Information Sciences*, vol. 60, no. 11, 2017.
[18] H. Ruan, Y. Li, and Wang, "A research on sentence similarity for question answering system based on multi-feature fusion," in *Proceedings of the 2016 IEEE/WIC/ACM International Conference on Web Intelligence (WI)*, ACM, Omaha, NE, USA, October 2016.
[19] X. T. Li, S. J. Shu, and W. Chen, "An algorithm of semantic similarity between words based on word single-meaning embedding model," *Acta Automatica Sinica*, vol. 46, no. 8, pp. 1654–1669, 2020, in Chinese.
[20] X. Li, H. Xie, and L. J. Li, "Research on sentence semantic similarity calculation based on Word2vec," *Computer Science*, vol. 44, no. 9, pp. 256–260, 2017, in Chinese.
[21] S. Chopra, R. Hadsell, and Y. Lecun, "Learning a similarity metric discriminatively, with application to face verification,"

in *Proceedings of the 2005 IEEE Computer Society Conference on Computer Vision and Pattern Recognition (CVPR'05)*, IEEE, San Diego, CA, USA, June 2005.

[22] C. D. Zhao, J. J. Guo, and Z. T. Yu, "Correlation analysis of news and cases based on unbalanced siamese network," *Journal of Chinese Information Processing*, vol. 34, no. 03, pp. 99–106, 2020, in Chinese.

[23] X. L. Li, Y. Liu, L. Zhou et al., "Prescription similarity-based analysis of core formulas and medicinals and related indications through data mining:taking insomnia as an example," *Journal of Traditional Chinese Medicine*, vol. 62, no. 2, 2021.

[24] Z. P. Zhu, J. Q. Du, Y. F. Liu, F. Yu, and J. G. Luo, "Similarity calculation of traditional Chinese medicine prescriptions based on LDA topic model," *Application Research of Computers*, vol. 34, no. 6, 2017, in Chinese.

[25] Z. N. Li and J. T. Ren, "Fine-tuning ERNIE for chest abnormal imaging signs extraction," *Journal of Biomedical Informatics*, vol. 108, 2020.

[26] J.-S. Lee and J. Hsiang, "Patent classification by fine-tuning BERT language model," *World Patent Information*, vol. 61, Article ID 101965, 2020.

[27] S. D. Ma, *Research on the Method of Microblog Text Similarity Calculation Based on Weighted Word2Vec*, Xidian University, Xi'an, China, 2019, in Chinese.

[28] J. Y. Wang, W. H. Xu, W. H. Yan, and C. X. Li, "Text similarity calculation method based on hybrid model of LDA and TF-IDF," in *Proceedings of the Computer Science and Artificial Intelligence*, New York, NY, USA, December 2019.

Hindawi
Evidence-Based Complementary and Alternative Medicine
Volume 2021, Article ID 6095476, 11 pages
https://doi.org/10.1155/2021/6095476

Research Article

Correlation between TCM Syndromes and Type 2 Diabetic Comorbidities Based on Fully Connected Neural Network Prediction Model

Yifei Wang,[1] Runshun Zhang,[2] Min Pi,[3] Julia Xu,[4] Moyan Qiu,[1] and Tiancai Wen[5,6]

[1]*Wangjing Hospital, China Academy of Chinese Medical Sciences, Beijing, China*
[2]*Guang'anmen Hospital, China Academy of Chinese Medical Sciences, Beijing, China*
[3]*Shenzhen Traditional Chinese Medicine Hospital, Shenzhen, Guangdong, China*
[4]*The University of Melbourne, Melbourne, Australia*
[5]*Data Center of Traditional Chinese Medicine, China Academy of Chinese Medical Sciences, Beijing, China*
[6]*Institute of Basic Research in Clinical Medicine, China Academy of Chinese Medical Sciences, Beijing, China*

Correspondence should be addressed to Tiancai Wen; wentiancai@ndctcm.cn

Received 16 August 2021; Accepted 8 November 2021; Published 20 November 2021

Academic Editor: Mohammad Hashem Hashempur

Objective. To predict the major comorbidities of type 2 diabetes based on the distribution characteristics of syndromes, and to explore the relationship between TCM syndromes and comorbidities of type 2 diabetes. *Methods*. Based on the electronic medical record data of 3413 outpatient visits from 995 type 2 diabetes patients with comorbidities, descriptive statistical methods were used to analyze the basic characteristics of the population, the distribution characteristics of comorbidities, and TCM syndromes. A neural network model for the prediction of type 2 diabetic comorbidities based on TCM syndromes was constructed. *Results*. Patients with TCM syndrome of *blood amassment in the lower jiao* were diagnosed with renal insufficiency with 95% test sensitivity. The patients with *spleen deficiency* combined with *ascending counterflow of stomach qi* and *cold-damp* patterns were diagnosed with gastrointestinal lesions with 92% sensitivity. The patients with TCM syndrome group of *spleen heat* and *exuberance of heart fire* were diagnosed as type 2 diabetes complicated with hypertension with a sensitivity of 91%. In addition, the prediction accuracy of combined neuropathy, heart disease, liver disease, and lipid metabolism disorder reached 70~90% in TCM syndrome groups. *Conclusion*. The fully connected neural network model study showed that syndrome characteristics are highly correlated with type 2 diabetes comorbidities. Syndrome location is commonly in the heart, spleen, stomach, lower *jiao*, meridians, etc., while syndrome pattern manifests in states of *deficiency*, *heat*, *phlegm,* and *blood stasis*. The different combinations of disease location and disease pattern reflect the syndrome characteristics of different comorbidities forming the characteristic syndrome group of each comorbidity. Major comorbidities could be predicted with a high degree of accuracy through TCM syndromes. Findings from this study may have further implementations to assist with the diagnosis, treatment, and prevention of diabetic comorbidities at an early stage.

1. Introduction

Type 2 diabetes mellitus (T2DM) is a chronic and progressive disease with multiple etiologies over a long course. It seriously affects the quality of life of patients and increases the risk of early death [1]. IDF estimated that approximately 4.2 million adults will die as a result of diabetes and its complications in 2019. Globally, 11.3% of deaths are due to diabetes. Almost half of these deaths are in people under 60 years of age [2]. Studies have found that more than 40% of diabetics suffer from comorbidities [3]. Comorbidity is an important factor affecting the prognosis of diabetics, and some comorbidities are also major causes of disability and death.

Type 2 diabetes develops mainly due to insulin resistance and relative insulin insufficiency and usually manifests as a glycolipid metabolism disorder [4, 5]. As diabetes progresses over time, various comorbidities may develop. In recent

years, many studies have shown that complementary and alternative medicine therapies including traditional Chinese medicine (TCM) have good efficacy in improving insulin resistance and regulating glycolipid metabolism with a high degree of safety [5–8]. At the same time, the application of relevant complementary alternative medicine therapies is of great significance in improving the quality of life of diabetic patients and preventing the occurrence and development of diabetes-related comorbidities. However, long-term hyperglycemia in diabetics affects multiple organs over time. Therefore, in the treatment of diabetes with complementary and alternative medicine, we must first accurately diagnose diabetes mellitus according to a theoretical system.

TCM is a common and important model of complementary and alternative medicine. It is the crystallization of thousands of years of medical experience and wisdom of the Chinese nation [9]. TCM has unique insights into the diagnosis and treatment of diabetes and its comorbidities and has been shown to effectively control the progression of diabetes, as well as diagnose, prevent, and treat diabetes mellitus at an early stage. TCM emphasizes the concepts of "holism" and "syndrome differentiation and treatment". "Syndrome differentiation" is the essence of TCM diagnosis and treatment of disease. TCM views that disease symptoms reflect the nature of a particular internal and external environment at a certain stage of the disease or the individual patient at the time. It manifests in corresponding patterns observed in the tongue, pulse, shape, color, and complexion. Patterns can also reveal aspects of pathogenesis such as etiology, disease location, disease nature, and disease status to various degrees, providing a basis for syndrome differentiation and treatment [10]. Different diseases contain different progression patterns of syndromes [11]. Syndromes usually reflect the current state of the disease. Being able to clarify the relationship between syndromes and various comorbidities will assist with the diagnosis of type 2 diabetes comorbidities based on syndrome characteristics, which is important for early treatment and prevention. Based on real clinical medical records, this study analyzed the relationship between TCM syndromes and comorbidities. A prediction model of "TCM syndrome-comorbidity" based on a neural network was also constructed to provide a reference for the diagnosis of diabetes comorbidity.

2. Data and Methods

2.1. Data Sources. The data for this study was obtained from the electronic medical records of T2DM patients, which were collected in the database of the Data Center of Traditional Chinese Medicine, China Academy of Chinese Medical Sciences. Data screening rules were as follows: (1) the primary diagnosis being type 2 diabetes, (2) at least one secondary diagnosis, (3) age ≥18 years, and (4) complete information about TCM and Western medicine diagnosis and TCM syndrome diagnosis. To protect privacy, all personal information such as patient names and phone numbers was desensitized prior to the study, and medical record numbers were used to identify each patient. Data regarding patient ID, gender, age, frequency of visit, course of the disease, disease diagnosis, and syndrome diagnosis was extracted. This study was approved by the Ethics Committee of the Institute of Basic Research in Clinical Medicine, China Academy of Chinese Medical Sciences (approval number: 2016 No.11-01).

2.2. Data Standardization and Classification. In cases where disease names were not standardized (terms have different semantic expressions), medical professionals matched the original data with the standard disease names in the *International Classification of Diseases 10th edition* (ICD-10) [12]. For example, cerebral infarction (lacunar) was standardized as lacunar infarction. Next, the standardized disease names were classified for statistical analysis. For example, bile duct stones, bile duct dilatation, and cholangitis were categorized into bile duct disease.

There were problems with the standardization of the TCM syndrome diagnosis such as classification confusion and different names of the same syndrome. In these circumstances, the compound syndrome was divided into two or several single syndromes and standardized according to *Clinic terminology of traditional Chinese medical diagnosis and treatment • Syndromes (GB/T16751.2- 1997)* [13] and *syndrome element syndrome differentiation (SESD)* [14]. For example, the "*qi and yin deficiency with blood stasis*" syndrome was divided into *qi deficiency*, *yin deficiency,* and *blood stasis*.

2.3. Data Analysis

2.3.1. Descriptive Analysis. Microsoft Excel 2019 was used to count the gender, age, distribution of visits, and frequency of comorbidities of all patients in the included case data. Continuous variables with normal distribution were represented by mean ± standard deviation (SD) and the continuous variables with nonnormal distribution were represented by median and interquartile ranges (M (Q1, Q3)). Categorical variables were described by frequency and percentage (n (%)).

2.3.2. Construction of Neural Network Model. In this study, Python 3.6 was used to construct a fully connected neural prediction model from TCM syndromes to comorbidities. A fully connected neural network is the oldest data mining model, which has the most network parameters and the largest amount of computation. It consists of an input layer, hidden layer, and output layer, and the "neurons" in each layer are interconnected with the neurons in the next layer in a fully connected mapping model [15]. The input layer is the independent variable. The output layer is the dependent variable. The hidden layer and the number of nodes determine the complexity of the network model. The neural network first randomly assigns weights to the independent variables and then compares the predicted results with the known results. The prediction error of the hidden nodes in the upper layer is estimated by the prediction error of the output layer, and the error is back-propagated to the input

layer from back to forward layer by layer, so as to adjust the link weight and find the best diagnostic model.

In this study, a four-layer fully connected neural network model was adopted. Descriptive analysis results were used to select representative syndromes and comorbidities. Label encoding of TCM syndrome diagnosis information was taken as the input layer and main diabetic comorbidities as the output layer, and the hidden layer was set as 2 layers (Figure 1).

In order to adapt to the neural network model, the relationship data of "multiple syndromes-multiple comorbidities" in the original data was split to form the data tables of "single syndrome" and "single comorbidity" in this study. The two tables were then fully joined to form the "syndrome-comorbidity" data table (Figure 2). The single syndrome corresponds to the neural network's input layer, and the single comorbidity corresponds to the neural network's output layer.

When the neural network model was trained, more than 80% of samples were randomly selected from the "syndrome-comorbidity" data set as the training set, and the rest of the data selected as the test set. The training was considered complete when the calculated results of the model loss function became relatively stable. Finally, a neural network model for predicting the comorbidities of diabetes was established using TCM syndrome patterns. The calculation results of the final model in the prediction set were taken out to calculate the predictive probability of different syndrome groups for comorbidities.

3. Results

3.1. General Information. A total of 3413 medical records of 995 T2DM patients were included in this study, which comprised 158 types of diabetic comorbidities and 188 types of TCM syndromes. Of all patients, 470 were male (47.24%) and 525 were female (52.76%). In terms of age, the patients were mainly distributed in the range of 40 to 80 years old, including 465 (46.73%) aged 40–59 years and 374 (37.59%) aged 60–79 years. The number of visits ranged from 1 to 36, with a median of 2 (1–4) visits, and the number of patients with 1–3 visits was the largest. Patients were mainly complicated with 1-2 diseases and were mostly associated with 1-2 syndromes (Table 1).

The top 10 comorbidities included hypertension, renal insufficiency, disorder of lipid metabolism, liver disease, neuropathy, heart disease, gastrointestinal disease, cerebral infarction, retinopathy, and biliary tract disease, accounting for 82.36% of all comorbidities (Figure 3). Compared with other age groups, there were more patients with liver diseases and gastrointestinal diseases in the 18–39 age group, and the number of patients with cardiovascular and cerebrovascular diseases increased significantly with age (Figure 3(a)). In terms of gender distribution, there were far more males than females in patients with liver disease (Figure 3(b)). The most common TCM syndromes included *blood stasis*, *yin deficiency, qi deficiency*, *fire or heat*, *stomach heat*, *phlegm*, spleen deficiency, liver constraint, dampness, and damp-heat (Figure 4). The syndrome manifestations of patients aged 18–39 years were mainly excess syndromes, such as blood stasis, fire or heat, stomach heat, phlegm, and liver constraint. The elderly over 80 years old showed obvious qi deficiency, yin deficiency, and blood stasis (Figure 4(a)). Female patients with qi deficiency, yin deficiency, and blood stasis were slightly higher in number than males with those symptoms (Figure 4(b)).

3.2. Syndrome Characteristics of Different Comorbidities. This study conducted a statistical analysis on the syndrome distribution characteristics of the top 10 comorbidities (Figure 5). It was found that there were obvious differences in the distribution characteristics, location, and nature of syndromes of different diseases. For example, in patients with diabetes mellitus complicated with hypertension, patterns of *deficiency* and *excess* were present in their syndrome manifestations. *Deficiency syndromes* were mainly *yin deficiency* and *qi deficiency*. The *excess syndromes* were *fire or heat*, *blood stasis*, *phlegm,* and *yang hyperactivity*. The syndromes of patients with renal insufficiency were mainly *qi deficiency*, *blood stasis*, *yin deficiency,* and *fire (heat)*. At the same time, the syndrome characteristics of *turbidity*, *toxin*, *dampness,* and *water retention* were highlighted. Patients with liver disease mostly had liver and stomach organ lesions. The main syndrome characteristic was the disorder of *qi* movement in the middle *jiao*, and the syndrome manifestations included *stomach heat*, *liver constraint*, *fire or heat*, *phlegm*, and *qi stagnation*. Patients with neuropathy mainly showed *deficiency syndrome* and *stasis syndrome*, including *qi deficiency*, *blood stasis*, *yin deficiency*, and *coldness*. The disease location of combined heart disease was mainly in the heart, and the main syndromes included *qi deficiency*, *yin deficiency*, *blood stasis*, and *yang deficiency*.

3.3. Evaluation of "Syndrome-Comorbidity" Neural Network Model. There was a total of 4375 "syndrome-comorbidity" data cases for diabetes, with 188 syndrome diagnoses, which formed a 4375×188 label-encoding characteristic matrix. The top 10 comorbidities of diabetes were selected as the output label Y, forming a 4375×10 Label-encoding matrix. The original data was divided into a training set and a test set. 3875 cases of data were randomly selected from the feature matrix X as the training set and the remaining data as the test set. After repeated training of the model, convergence was reached at 1400 runs (Figure 6).

MSE is the mean square error, which is the average value of the square of the distance between the predicted value $f(x)$ of the model and the real value y of the sample. It is a type of loss function which is used to evaluate the degree of inconsistency between the predicted value $f(x)$ of the model and the real value y.

3.4. "Syndrome-Disease" Predictive Relationships for Major Comorbidities. Through detailed analysis of the prediction results of the model, it was found that the accuracy of the model in predicting the seven comorbidities of renal insufficiency, gastrointestinal disease, hypertension,

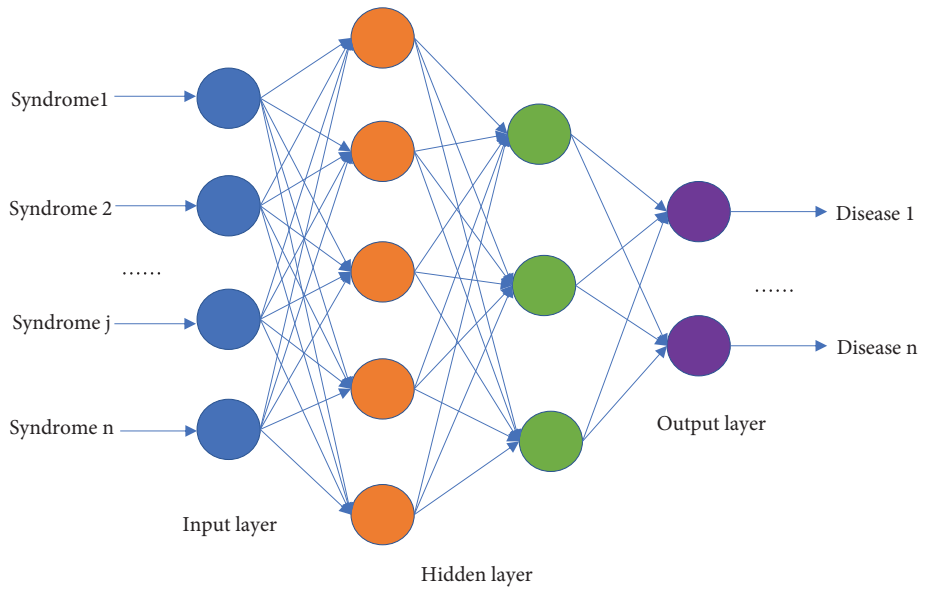

Figure 1: Neural network model of predicted TCM syndromes and comorbidities.

ID	TCM syndromes	Comorbidities
625	qi deficiency, yin deficiency, yang hyperactivity, dampness	renal insufficiency, retinopathy, neuropathy

ID	TCM syndromes
625	qi deficiency
625	yin deficiency
625	yang hyperactivity
625	dampness

×

ID	Comorbidities
625	renal insufficiency
625	retinopathy
625	neuropathy

ID	TCM syndromes	Comorbidities
625	qi deficiency	renal insufficiency
625	qi deficiency	retinopathy
625	qi deficiency	neuropathy
625	yin deficiency	renal insufficiency
625	yin deficiency	retinopathy
625	yin deficiency	neuropathy
625	yang hyperactivity	renal insufficiency
625	yang hyperactivity	retinopathy
625	yang hyperactivity	neuropathy
625	dampness	renal insufficiency
625	dampness	retinopathy
625	dampness	neuropathy

Figure 2: Example of "syndrome-comorbidity" construction process.

neuropathy, heart disease, liver disease, and lipid metabolism disorder could reach 70~90%, while the prediction accuracy for cerebral infarction was about 50%, and the prediction accuracy for retinopathy and biliary tract disease was below 50% (Figure 7). The results showed that different characteristic syndrome groups could be used to predict the corresponding comorbidities.

Renal insufficiency was the most predictive comorbidity. Patients with TCM syndrome of *blood amassment in the lower jiao* were diagnosed with renal insufficiency with 95% accuracy. Patients with syndrome groups of *kidney qi deficiency, turbid, toxic,* and *obstruction in meridians and collaterals* were diagnosed with renal insufficiency with a sensitivity of 87%. It could also be seen from other TCM syndrome groups that the syndrome was dominated by *interior patterns*, and patients with *turbidity*, *toxin*, *stasis,* and *deficiency* of the kidney and spleen had a higher probability of being diagnosed with combined renal insufficiency.

The gastrointestinal disease was also comorbidity with characteristic syndrome groups and high accuracy of prediction. Patients with *spleen deficiency* combined with *ascending counterflow of stomach qi* and *cold-damp* patterns were diagnosed with gastrointestinal lesions with 92% sensitivity. The syndrome group of *ascending counterflow of stomach qi* and *deficiency-coldness of the spleen and stomach* were diagnosed with diabetes combined with the gastrointestinal disease with 91% sensitivity. It could also be observed from the other TCM syndrome groups that the main locations of disease were in the stomach, spleen, and middle *jiao*, and patients with the syndrome groups of *deficiency*, *qi counterflow*, *coldness,* and *blood stasis* had a high probability of being diagnosed with diabetes complicated with gastrointestinal disease.

For patients with hypertension, the probability of the syndrome group predicting the comorbidity was also relatively high. 92% of patients with TCM syndrome group of *spleen heat* and *exuberance of heart fire* were diagnosed with type 2 diabetes complicated with hypertension. 89% of patients with the syndrome group of *liver wind*, *ascendant hyperactivity of liver yang*, *liver yin deficiency,* and *kidney yin deficiency* were diagnosed with diabetes combined with hypertension. 86% of patients with TCM syndrome group of *liver yin deficiency*, *kidney yin deficiency*, *disharmony of the*

Table 1: General information of type 2 diabetes patients with comorbidity.

Variable	Value
Gender, *n* (%)	
Male	470 (47.24)
Female	525 (52.76)
Age (years), M (Q1, Q3)	56 (46, 65)
Age (years), *n* (%)	
18–39	130 (13.06)
40–59	465 (46.73)
60–79	374 (37.59)
≥80	26 (2.61)
Frequency of visit, M (Q1, Q3)	2 (1,4)
Frequency of visit, *n* (%)	
1–3	717 (73.31)
4–6	144 (14.72)
7–9	42 (4.29)
≥10	75 (7.67)
Comorbidity, *n* (%)	
1-2	3019 (86.82)
3-4	396 (11.39)
≥5	62 (1.78)
TCM syndrome, *n* (%)	
1-2	2562 (75.17)
3-4	829 (24.33)
≥5	16 (0.47)

M: median; Q1: lower quartile; Q3: upper quartile.

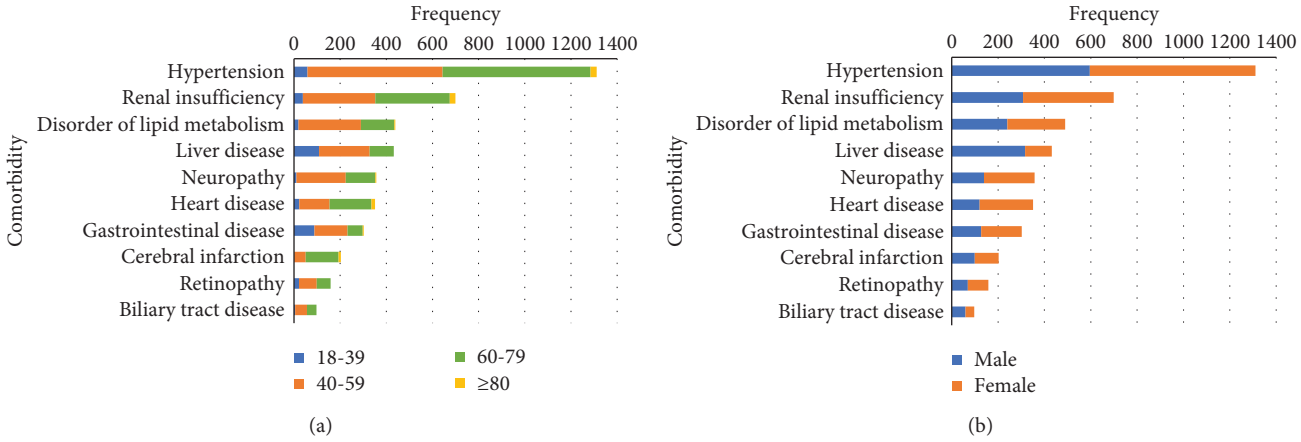

Figure 3: Distribution of comorbidities. (a) Age. (b) Gender.

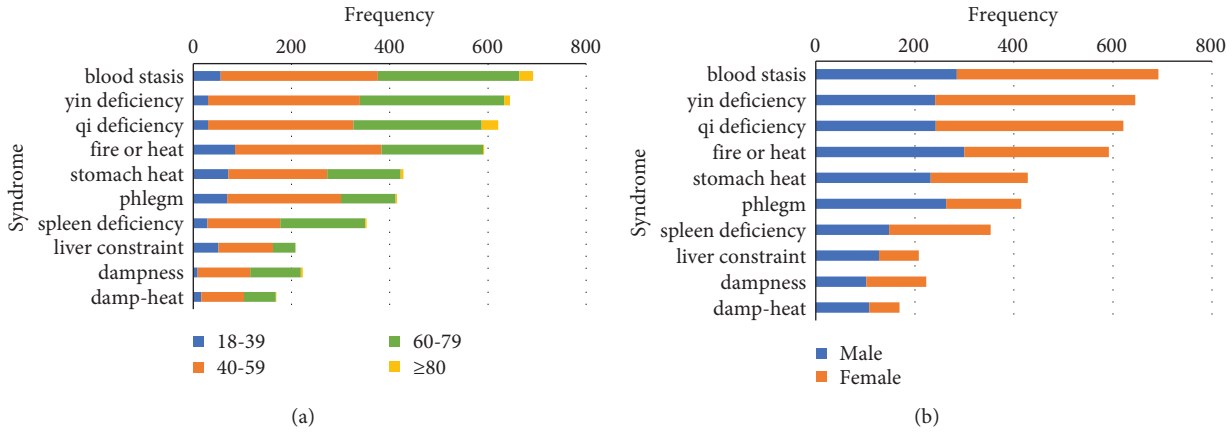

Figure 4: Distribution of syndromes. (a) Age. (b) Gender.

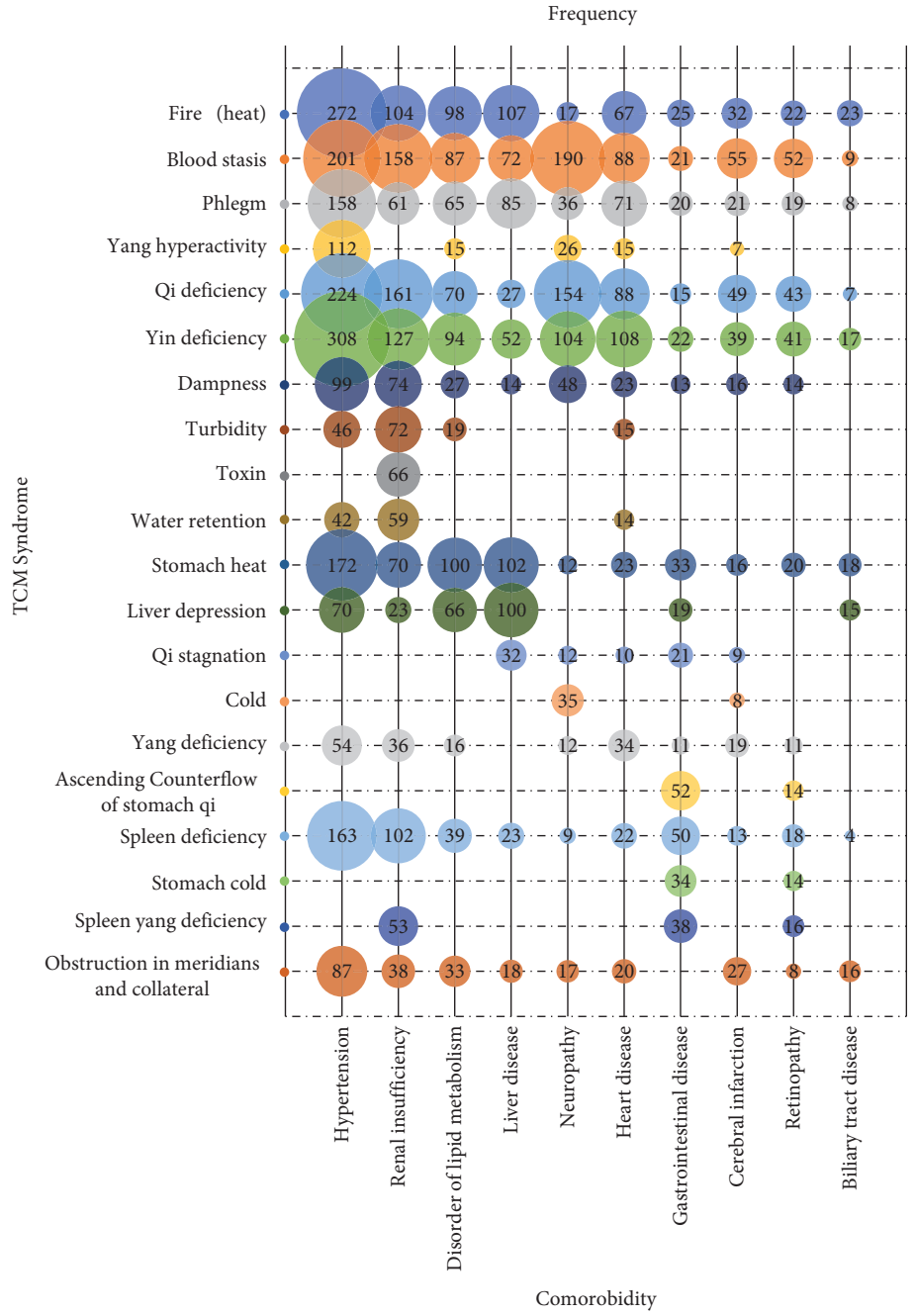

Figure 5: Syndrome distribution of comorbidities.

chong and ren mai, and *yang floating* were diagnosed with hypertension. It could also be seen from the other TCM syndrome groups that a portion of patients with liver or kidney as the main location of disease and *deficiency* or *wind* as the main nature of disease were diagnosed as diabetes complicated with hypertension.

The results of this study showed that different syndrome groups could predict corresponding comorbidities. The syndromes of *fire or heat*, *qi stagnation*, *blood stasis,* and *damp-heat* were associated with the diagnosis of diabetes complicated with liver disease. A high portion of patients who had a location of disease mainly in the heart and *kidney,* nature of the disease being *deficiency* and *coldness,* were diagnosed with diabetes complicated with heart disease. Those with *blood stasis*, *coldness,* and *deficiency* as the main syndrome manifestations were diagnosed with type 2 diabetes complicated with neuropathy with high sensitivity. *Damp retention in the middle jiao* was the characteristic symptom in the diagnosis of type 2 diabetes mellitus combined with lipid metabolism disorder. However, among all TCM syndrome groups, the probability of being diagnosed with diabetes combined with cerebral infarction, retinopathy, and biliary tract disease was relatively low, and no syndrome group with a prediction rate of more than 60% was found. 59% of those with TCM syndrome of *kidney essence*

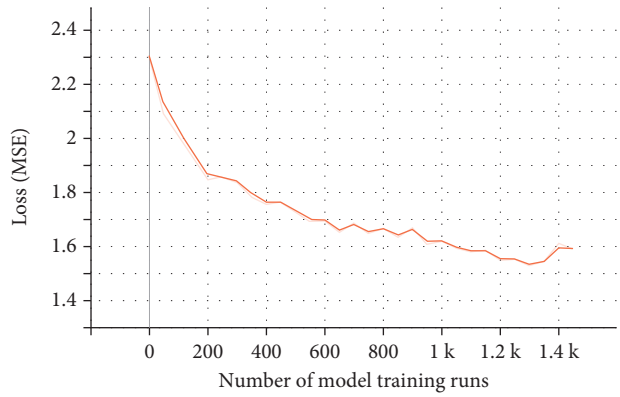

Figure 6: Evaluation of predictive neural network of TCM syndromes and comorbidities in diabetic patients.

deficiency and *cerebrospinal damage* were diagnosed with cerebral infarction, and 56% of patients with the independent syndrome of *wind* were diagnosed with diabetes mellitus combined with cerebral infarction.

4. Discussion

4.1. Distribution Characteristics and Overall Relationship between Diabetic Comorbidities and TCM Syndromes. The results of this study showed that the common syndromes of diabetic patients with comorbidity were a combination of *deficiency* and *excess*. *Excess syndrome* mainly consists of *heat syndrome*, *blood stasis syndrome,* and *phlegm syndrome*. *Qi deficiency* and *yin deficiency* were the main patterns of the *deficiency syndrome*. The number of younger diabetic patients with digestive system diseases was higher in comparison to the elderly, who were more likely to be complicated with cardiovascular and cerebrovascular diseases. In terms of syndrome manifestation, younger patients showed a higher incidence of the *excess syndrome*, while the elderly patients showed a higher incidence of *deficiency syndrome* and *blood stasis*. In terms of gender distribution, male patients were more likely to be complicated with liver diseases, while patients with *qi deficiency*, *yin deficiency,* and *blood stasis syndrome* were mostly female. According to TCM, diabetes is a chronic progressive disease, and the pathogenesis is a *deficiency-excess* complex. The core pathogenesis of diabetes is "*deficiency*, *heat,* and *blood stasis*" [16, 17]. At the same time, *phlegm* is also an important pathological factor in diabetes mellitus [18]. This is consistent with the results of this study. In addition, *constraint-heat* is the main pathogenesis in the early stage of diabetes and gradually progresses to the stage of *deficiency* and *detriment* with the development of the disease [19]. The influence of age on the distribution of diseases and syndromes is related to the modern living and working environment, physique, course of the disease, and other factors. Gender distribution is a dividing factor that may relate to physiology and living environment differences.

The results of this study showed that there were obvious differences in the syndrome distribution characteristics of different comorbidities, and the prediction result of the neural network showed that the prediction of comorbidities by characteristic syndrome group had high accuracy. Studies have shown that untreated type 2 diabetes is prone to various acute or chronic complications when the body is in a high glucose state for a prolonged period of time [20], and with the progression of the disease, the distribution characteristics and symptoms change accordingly [21]. This shows that there is a close correlation between different comorbidities and TCM syndromes. Different pathogenesis often leads to the occurrence of different comorbidities, the characteristics of the comorbidities are significant in the manifestations of TCM syndromes, and there will be some syndrome groups with very obvious characteristics in different diabetic comorbidities. Characteristic syndrome groups can be an important factor in distinguishing the corresponding comorbidities.

4.2. Syndrome Characteristics of Different Comorbidities

4.2.1. Hypertension. The results of this study showed that hypertension was the most common comorbidity. Its TCM syndromes were characterized by *liver wind*, *fire or heat*, *yin deficiency,* and *disharmony of the chong and ren mai*, and the location of the disease was mainly reflected in the kidney and liver. Patients with TCM syndrome group of *spleen heat* and *exuberance of heart fire* were diagnosed as type 2 diabetes complicated with hypertension with a sensitivity of 91%. TCM considers "*liver-kidney yin deficiency*" as the root (the mean) and the "*wind*, *fire*, *phlegm,* and *blood stasis*" as the branch (the secondary) in terms of hypertension pathogenesis [22–24]. Dating back to as early as in *The Yellow Emperor's Inner Classic: Basic Questions*, there was a description of the pathogenesis of hypertensive vertigo: "*All wind with vertigo is ascribed to the liver*". Meanwhile, *disharmony of the chong and ren mai* is also a common symptom of hypertension in perimenopausal women [25, 26]. With the increase of blood glucose, diabetes patients usually suffer from hunger, weight loss, constipation, frequent urination, and other symptoms, which is the main manifestation of "*Stagnancy of Er Yang*", just like what is described in *The Yellow Emperor's Inner Classic*: "*Disorder of Stomach may be Affected by Disorders of the Heart or Spleen*" [27]. *Exuberant heat* in the heart and spleen combined with emotional depression leads to the *binding constraint of liver*

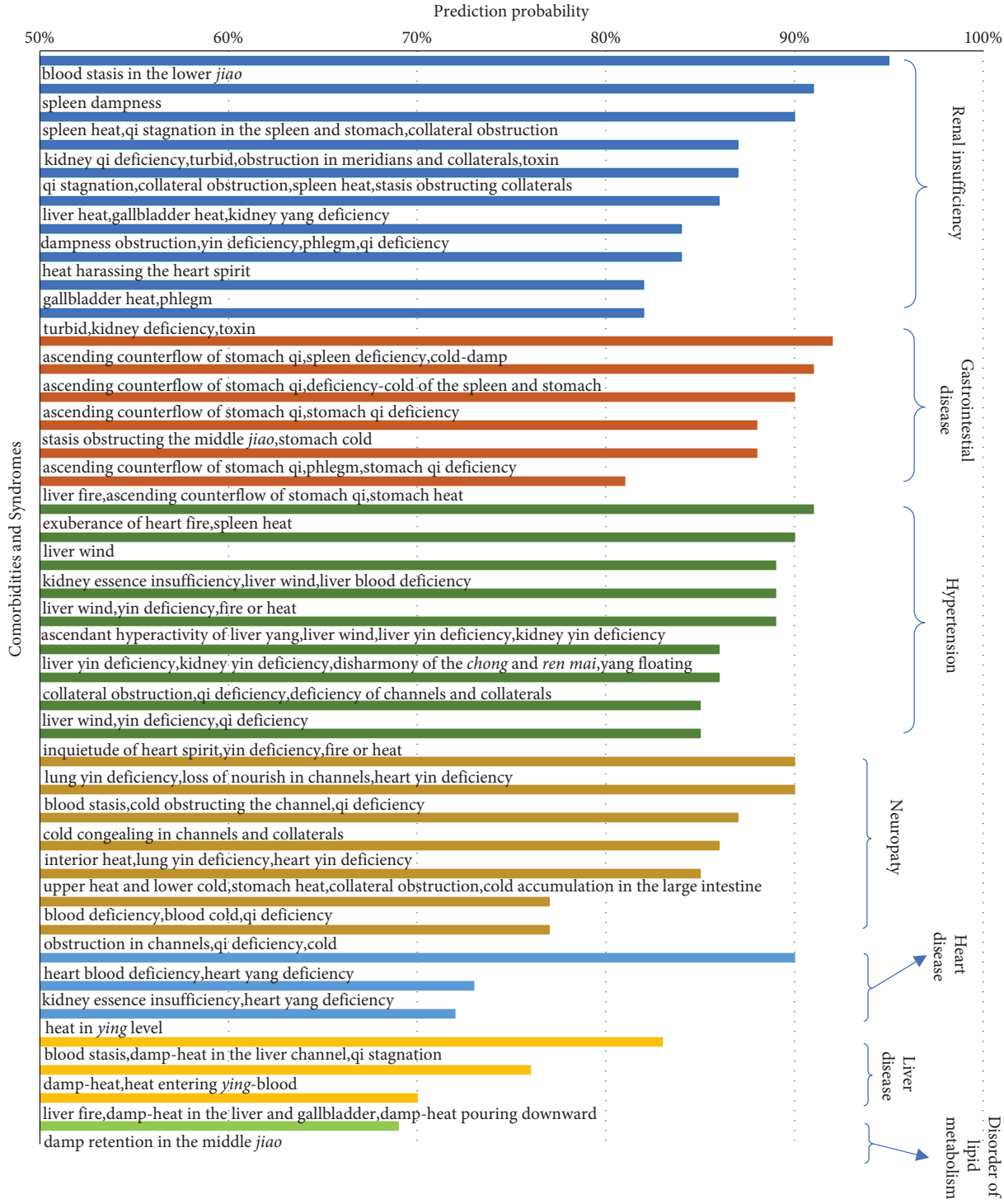

Figure 7: Probability of predicting comorbidity by different syndrome groups.

qi and induces *ascendant hyperactivity of liver yang* and results in the occurrence of hypertension. The prediction results of hypertension in this study are consistent with Traditional Chinese medicine theory and clinical practice.

4.2.2. Renal Insufficiency. Renal insufficiency is also common comorbidity of diabetes. The results of this study showed that in addition to the syndrome of "*blood stasis, heat,* and *deficiency*", the syndromes of *turbidity*, *poison,* and *dampness* were also associated with renal insufficiency. At the same time, patients with TCM syndrome of *blood amassment in the lower jiao* were diagnosed with renal insufficiency with 95% sensitivity. Those with the syndrome group of *kidney qi deficiency*, *turbid*, *toxic*, and *obstruction in meridians and collaterals* were diagnosed with diabetes complicated with renal insufficiency with a sensitivity of

87%. The kidney is located in the lower *jiao*. With further development of the disease, kidney essence is damaged, causing the failure in *qi* transformation, which creates difficulty in distinguishing the clear and metabolic turbidity, leading to the *accumulation of turbid pathogens* and *water-dampness* and formation of *turbid-toxin*. *Turbid-toxin* obstruction in the collateral and consequent unsmooth blood circulation results in *water retention* which then leads to edema and eventually results in kidney disease [28]. Meanwhile, *turbidity-toxin* is closely related to glucose toxicity and lipid toxicity in diabetes mellitus [29]. *Removing turbidity and resolving toxins* are also important priorities in treating diabetic nephropathy [30–32]. The occurrence of related diseases can be actively prevented according to the symptoms, which is also of great significance in controlling the progression of diabetes.

4.2.3. Neuropathy. The characteristic syndromes of diabetes complicated with neuropathy were *malnutrition of channels* and *coldness coagulation in the meridians and collaterals*. The syndrome group of "*blood stasis*, *qi deficiency*, and *cold coagulation in meridians and collaterals*" could predict diabetic neuropathy with an accuracy of 90%. In the early stage of diabetes, "*heat syndrome*" is the main syndrome, whereby the pathogenic *heat* damages the essential *qi* of zang-fu organs, especially the spleen. *Spleen yang deficiency* cannot reach the end of the limbs, resulting in a counterflow coldness in the four limbs. The *coldness congealment* leads to *blood stasis*, which results in *blood bi* and *coldness coagulation in meridians and collaterals* [33]. This is also consistent with the understanding of diabetes complicated with neuropathy in TCM. It is believed that the location of this disease is mainly in the channels and collaterals, involving the liver, kidney, and spleen. *Qi and blood deficiency* are considered as the root of pathogenesis and the *blood stasis obstructing collaterals* as the branch [34].

4.2.4. Other Comorbidities. In addition, there was also a close relationship between TCM syndromes and other comorbidities. Different comorbidities have their own syndrome groups with obvious characteristics. For example, the syndrome characteristics of liver diseases are *damp-heat*, *qi stagnation,* and *blood stasis*. *The binding constraint of liver qi* and *liver-gallbladder damp-heat* are two new syndromes that have evolved in modern life, while *stasis syndrome* is often the key to disability and life-threatening diabetic complications [35]. The syndrome characteristics of combined heart disease are mainly *heart qi deficiency* or *heart yang deficiency*. The characteristic syndromes of patients complicated with gastrointestinal disease were *ascending counterflow of stomach qi*, *stomach qi deficiency,* and *stomach coldness*. The syndrome of disorder of lipid metabolism is characterized by *dampness obstruction in the middle jiao*. It can be seen that with the progression of diabetes, the TCM syndromes also evolve correspondingly, and the TCM syndromes show different manifestations during the occurrence of different comorbidities, indicating that the comorbidities are closely related to the TCM syndromes. It is of great practical significance to be able to predict the associated comorbidities through characteristic syndromes in the diagnosis, treatment, and prevention of diabetes mellitus.

5. Conclusion

In summary, this paper introduced a fully connected neural network approach to the study of the association between type 2 diabetic comorbidities and TCM symptoms with the construction of a "TCM symptom-comorbidity" prediction model. Different kinds of comorbidities were characterized by "*deficiency*, *heat*, *phlegm*, and *blood stasis*" in the viscera of diabetic patients, such as the heart, spleen, stomach, and kidney. According to the characteristics of the disease, different syndrome elements were combined to form characteristic syndrome groups. The corresponding comorbidities of diabetes were predicted based on the characteristics of the syndrome groups with a high degree of accuracy. The construction of the "TCM syndrome-comorbidity" prediction model may be very helpful in assisting the early diagnosis of diabetic comorbidity. However, due to the limitations of the data, only ten common comorbidities were included in this study. The data volume will be expanded in the future to further determine the relationship between type 2 diabetic comorbidities and different TCM syndromes.

Data Availability

The data used to support the findings of this study are included within the article.

Conflicts of Interest

The authors declare that there are no conflicts of interest.

Acknowledgments

This study was supported by the National Natural Science Foundation of China (No. 81774158), China Academy of Chinese Medical Sciences Innovation Fund (No. CI2021A00509), and "Three Famous Project": Method Innovation of Clinical Appraisal of Chinese Medicine, Acupuncture, and Moxibustion by Team of Liu Baoyan, Principal Researcher of China Academy of Chinese Medical Sciences (SZSM201612001).

References

[1] T. Zhang, Q. He, Y. Liu, Z. Chen, and H. Hu, "Efficacy and safety of resveratrol supplements on blood lipid and blood glucose control in patients with type 2 diabetes: a systematic review and meta- analysis of randomized controlled trials," *Evidence-Based Complementary and Alternative Medicine*, vol. 2021, Article ID 5644171, 15 pages, 2021.

[2] International Diabetes Federation, *IDF Diabetes Atlas 9th*, International Diabetes Federation, Brussels, Belgium, 2019, https://www.diabetesatlas.org.

[3] J. N. Struijs, C. A. Baan, F. G. Schellevis, G. P. Westert, and G. A. van den Bos, "Comorbidity in patients with diabetes mellitus: impact on medical health care utilization," *BMC Health Services Research*, vol. 6, no. 1, p. 84, 2006.

[4] A. Manoharan and M. Santhanakumar, "Anti-diabetic evaluation of hydro alcoholic extract of herbal plant oorithal thaamarai chooranam (Otc) on streptozotocin (STZ) induced Type 2 diabetes mellitus in wistar albino rats," *Journal of Traditional and Integrative Medicine*, vol. 4, no. 2, pp. 519–525, 2021.

[5] N. Nayebi, A. Esteghamati, A. Meysamie et al., "The effects of a *Melissa officinalis L.* based product on metabolic parameters in patients with type 2 diabetes mellitus: a randomized double- blinded controlled clinical trial," *Journal of Complementary & Integrative Medicine*, vol. 16, no. 3, 2019.

[6] M. Seyed Hashemi, N. Namiranian, H. Tavahen et al., "Efficacy of pomegranate seed powder on glucose and lipid metabolism in patients with type 2 diabetes: a prospective randomized double- blind placebo-controlled clinical trial," *Complementary Medicine Research*, vol. 28, no. 3, pp. 226–233, 2021.

[7] K. Eqbal, M. A. Alam, M. A. Quamri, G. Sofi, and M. D. Ahmad Bhat, "Efficacy of Qurs-e-Gulnar in ziabetus (type 2 diabetes mellitus): a single blind randomized controlled trial," *Journal of Complementary and Integrative Medicine*, vol. 18, no. 1, pp. 147–153, 2021.

[8] M. A. Morowatisharifabad, M. Asadpour, M. A. Zakeri, and M. Abdolkarimi, "The effect of integrated intervention based on protection motivation theory and implementation intention to promote physical activity and physiological indicators of patients with type 2 diabetes," *BioMed Research International*, vol. 2021, Article ID 6637656, 8 pages, 2021.

[9] National Center for Complementary and Alternative Medicine National Institutes of Health, *What is Complementary and Alternative Medicine?*, https://nccam.nih.gov/health/whatiscam, 2021.

[10] T. T. Deng, *Criteria for TCM Syndromes*, Guangdong Science and Technology Press, Guangzhou, China, 1990.

[11] R. H. Zhang and B. Li, "The connotation and academic viewpoints of the essence of syndrome," *Chinese Journal of Integrated Traditional and Western Medicine*, vol. 29, no. 04, pp. 375–378, 2009.

[12] World Health Organization, *International Statistical Classification of Disease and Related Health Problems*, Tenth Revision (ICD-10). World Health Organization, Geneva, Switzerland, 1992.

[13] The State Bureau of Quality and Technical Supervision, *Clinic Terminology of Traditional Chinese Medical Diagnosis and Treatment*, Standards Press of China, Beijing, China, GB/T 16751.2-1997, 1997.

[14] W. F. Zhu, *Syndrome Element Syndrome Differentiation (SESD)*, People's Health Publishing House, Beijing, China, 2008.

[15] K. Y. Hsu, H. Y. Li, and D. Psaltis, "Holographic implementation of a fully connected neural network," *Proceedings of the IEEE*, vol. 78, no. 10, pp. 1637–1645, 1990.

[16] J. Zhao, X. Feng, X. Tong et al., "TCM core pathogenesis and basic therapeutic methods for diabetes," *Beijing Journal of Traditional Chinese Medicine*, vol. 38, no. 01, pp. 3–6, 2019.

[17] Y. Yang, Z. X. Hu, and J. H. Liu, "Research on the Analysis of the pathogenesis of type 2 diabetes based on evaluating syndrome by drug intervention," *Clinical Journal of Traditional Chinese Medicine*, vol. 33, no. 01, pp. 11–16, 2021.

[18] P. Zhang, F. Sun, S. Wang et al., "Pang guoming's experience in treating type 2 diabetes from phlegm," *Journal of Traditional Chinese Medicine*, vol. 60, no. 18, pp. 1546–1549, 2019.

[19] Diabetes Branch of Chinese Medical Association, "Chinese guidelines for prevention and treatment of type 2 diabetes (2020 edition)," *Chinese Journal of Endocrinology and Metabolism,*vol. 37, no. 4, pp. 311–398, 2021.

[20] W. Liang, L. Kang, X. Meng et al., "Research progress on the relationship between intestinal microflora imbalance and complications of type 2 diabetes mellitus," *Shandong Medical Journal*, vol. 57, no. 29, pp. 107–109, 2017.

[21] Y. Xing, M. Pi, R. S. Zhang, and T. Wen, "Study on the TCM syndromes evolution and Chinese herbal characteristics of type 2 diabetes patients with different courses of disease in TCM heat stage: a real-world study," *Evid Based Complement Alternative Medicine*, vol. 2021, Article ID 1282957, 12 pages, 2021.

[22] Y. Deng, L. Chang, F. Qi, S. Li, and Y. Cui, "Thinking about curing the hypertension illness through wind-phlegm and blood stasis blocking the collaterals," *Chinese Archives of Traditional Chinese Medicine*, vol. 29, no. 04, pp. 750-751, 2011.

[23] L. F. Cui, J. H. Luo, and Z. Y. Li, "Qiu baoguo's experience in treating refractory hypertension," *Acta Chinese Medicine*, vol. 29, no. 10, pp. 1447-1448, 2014.

[24] B. Du, G. Zhao, J. Cheng, and J. Qu, "Effect and mechanism of liu-wei-di-huang pill on vertigo in hypertensive patients with yin deficiency of liver and kidney," *Journal of Chinese Medicinal Materials*, vol. 06, pp. 1509–1513, 2021.

[25] L. Su, H. Jin, L. Zheng, Z. Liu, and S. Liu, "On the disharmony of thoroughfare vessel and conception vessel is the key to the pathogenesis of perimenopausal hypertension," *Traditional Chinese Medicinal Research*, vol. 30, no. 01, pp. 1–3, 2017.

[26] Y. M. Wang, F. J. Liang, and X. J. Feng, "Efficacy of TCM syndrome differentiation in treatment of primary hypertension," *Chinese Journal of Integrative Medicine on Cardio-Cerebrovascular Disease*, vol. 14, no. 17, pp. 2028–2030, 2016.

[27] Q. Fu, S. Wang, Y. Xiao et al., "Exploration of professor lv renhe's academic thoughts on treating diabetes mellitus by staging treatment," *World Chinese Medicine*, vol. 12, no. 01, pp. 21–24, 2017.

[28] X. W. Zhang, H. F. Liu, and X. H. Zhang, "Analysis of pathogenesis level and treatment differentiation of diabetic nephropathy," *Journal of Traditional Chinese Medicine*, vol. 58, no. 05, pp. 390–393, 2017.

[29] S. T. Wu, "On the relevance of turbidity-toxin to glucotoxicity and lipotoxicity in diabetes mellitus," *Journal of Traditional Chinese Medicine*, vol. 09, pp. 647–649, 2004.

[30] L. Peng, Q. Tang, J. Liang, and Q. Xu, "Experience in the treatment of early type 2 diabetes mellitus from a discussion of turbid toxins trapped in the spleen," *Global Traditional Chinese Medicine*, vol. 13, no. 12, pp. 2111–2113, 2020.

[31] X. Wei, L. Yan, J. Lv, W. Xu, and D. Li, "Example of professor li diangui in treating chronic kidney disease by using zhuodu theory," *Chinese Medicine Modern Distance Education of China*, vol. 13, no. 15, pp. 40–43, 2015.

[32] S. Chen and S. T. Wu, "Overview of the treatment of diabetic nephropathy from the perspective of turbid toxicity," *Hunan Journal of Traditional Chinese Medicine*, vol. 35, no. 04, pp. 168-169, 2019.

[33] X. Zhao, Q. Yu, Y. Liu et al., "Tong xiaolin's experience in the management of diabetic peripheral neuropathy," *Journal of Traditional Chinese Medicine*, vol. 54, no. 10, pp. 882-883, 2013.

[34] G. M. Pang, Y. Yan, P. Zhu et al., "Clinic draft specification of traditional Chinese medicine about diabetic peripheral neuropathy," *China Journal of Traditional Chinese Medicine and Pharmacy*, vol. 35, no. 02, pp. 260–264, 2010.

[35] Z. Q. Liu, "Experience of TCM syndrome differentiation and treatment of type 2 diabetes," *Journal of Sichuan of Traditional Chinese Medicine*, no. 11, pp. 20–22, 2006.